EUROPEAN COMMISSION

RESEARCH WORKSHOP

Proceedings

ORIGIN, MECHANISMS AND EFFECTS OF SALTS ON DEGRADATION OF MONUMENTS IN MARINE AND CONTINENTAL ENVIRONMENTS

Scientific Editor Fulvio Zezza

March 25-27, 1996
Bari (Italy)

**Environment
and Climate**

**University C.U.M. School
Monument Conservation**

**Protection and Conservation
of the European Cultural Heritage
Research Report n° 4**

EUROPEAN COMMISSION RESEARCH WORKSHOP

Proceedings

ORIGIN, MECHANISMS AND EFFECTS OF SALTS ON DEGRADATION OF MONUMENTS IN MARINE AND CONTINENTAL ENVIRONMENTS

Scientific Editor Fulvio Zezza

Protection and Conservation
of the European Cultural Heritage
Research Report n° 4

March 25–27, 1996
Bari (Italy)

PREFACE

This volume contains the papers presented at the E.C. Workshop "Origin, Mechanisms and Effects of Salts on Degradation of Monuments in Marine and Continental Environments" held in Bari (Italy) in March 1996. The contributions are divided into the following different aspects: 1) the fundamental scientific acquisitions in the framework of the E.C. Project "Marine spray and polluted atmosphere as factors of damage to monuments in the Mediterranean coastal environment"; 2) the achieved results, presented by invited speakers and participants, of the most recent researches on the degradation of monuments regarding neoformation soluble salts.

At present the researches on weathering, overcoming the limits imposed by the sectorial studies, benefit from the new stimulation given by the interdisciplinary approach to the problems of conservation and the perfecting of analysis methodologies. Also the aspects treated by each specific sector of the research are considered on a large scale so as to establish correlations and deduce appropriate conclusions. In these frameworks there are the scientific contributions of the Workshop which as regards the coastal marine environment and pollution have provided specific results regarding the pilot monuments located in different geographical position along the east–west axis of the Mediterranean Basin, equipped with stations for the environmental monitoring which has been carried out by recording the indoor and outdoor environmental parameters. The comparison of real situations with the equilibrium conditions also represents an important means to estimate the probability of the occurence in the stones of salts of marine origin. This method of planning the research represents without doubt a new step towards a more realistic modelling and forecast of spatio–temporal pure salts occurences in a monitored monument which will contribute also to a better understanding of their mechanisms in the weathering processes.

The knowledge of the occurences of salts present in the stone is of great interest for

the correlation of the microclimate conditions in indoor environment with the behaviour and response of walls, on the basis of the acquisition of more reliable models of crystallization and solution cycles. On the other hand, the elaboration and correlation of the data regarding the environmental monitoring with the analyses performed on stone materials exposed to weathering have shown there is a clear relation between the chemical composition of the aerosols, of wet and dry depositions and weathering forms. This method of planning scientific research represents a promising basis for the creation of a model for the prediction of the susceptibility of stone to sea–salt decay in coastal environment which is also effected by atmospheric pollution due to anthropic activities. In this regard the "cementitious" encrustations on the stones of the monuments, completely different from the well known black crusts and formed above all by Al–silicates and heavy metals in relation to the presence of an extremely high level of air pollution, represent a precise element distinguishing polluted areas.

The present trend sees also employed the researchers in the experimentation of non–destructive control methodologies, alternative to those which are destructive, able to identify stone decay in qualitative and quantitative forms on the basis of which the most suitable techniques of conservative interventions can be adopted. Also in this field in the framework of this Workshop results have been presented of researches which permit the determination of the state of conservation of stone materials exposed to atmospheric agents and to evaluate the rate of weathering in time.

The content of the contributions offered by invited speakers is directed to the above objectives and has ranged over: 1) the nature and distribution of salts on the architectonic surfaces; evolution of a salt system through origin, transport, evaporation, concentration, precipitation, crystallization and disruption; 2) expert chemical models able to assess the risks of the actual environmental conditions with reference to salt damage in porous materials; 3) role of salts crystallization on decay of stones exposed to different environmental conditions; 4) the relationship between climate and weathering in terms of

increased dampness and time of wetness, equilibrium pressure in solutions, effects of sea–salt on freezing–thawing cycles.

The communications and posters by the participants reflect the same approach presenting extremely advanced elaborations, approaches and analytical procedures regarding both the crystallization processes of salts and their mixtures, the decay form and the simulated degradation of stones under marine aerosol. Also biodeterioration has been emphasized not only as an agent in the weathering, but also as a phenomenon which must be considered with great interest in the researches on weathering. Finally, the preservation techniques for stones have been dealt with at the Workshop to increase scientific knowledge if, as is to be hoped, there will be more collaboration and new approaches between researchers and technicians which will undoubtedly facilitate experimentations and interventions carried out in the appropriate way.

The objective of the Workshop was not only to review the results of research projects funded by the European Commission, but also the state of the art in the European Union and beyond, and to promote networking between these projects and other researchers involved in the same field. On examining the results it seems that the objective has been achieved and for this reason I am grateful to the authors and the participants for their support of the Workshop.

In particular I wish to express my most sincere appreciation to Ms. Julia Acevedo, scientific officer for DG XII of the European Commission, who for years has been striving to stimulate and promote collaboration in the framework of scientific researches in the various projects of the European Community for the safeguarding of monuments, and who has encouraged the organization of this Workshop and has given a great contribution of knowledge and experience essential for the good outcome.

Fulvio Zezza

Fulvio Zezza

The E.C. Project
"Marine spray and polluted atmosphere as factors of damage to monuments in the Mediterranean coastal environment": objectives and results

The E.C. Project "Marine spray and polluted atmosphere as factors of damage to monuments in the Mediterranean coastal environment": objectives and results

Fulvio Zezza
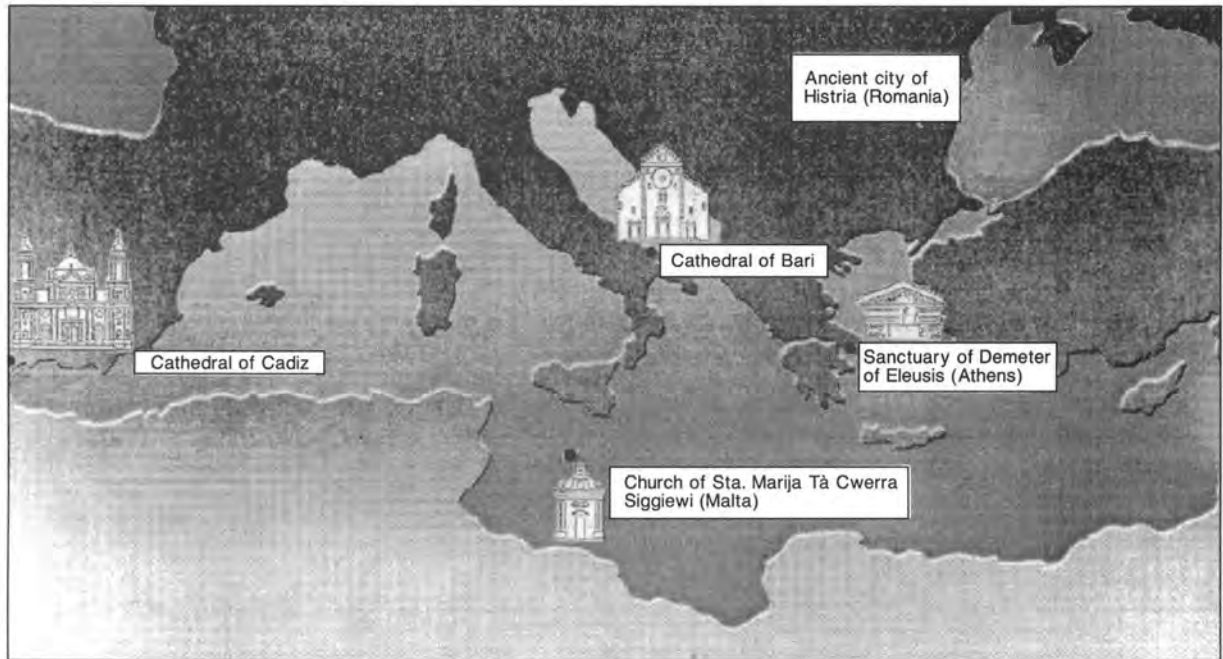
Scientific coordinator

1. Background

The motivation for the Project emerges from the consideration that the phenomenon of stone decay on the coasts is so widespread and intense, and so little is still known about its dynamics. The suggestion was that it would be of great value for the scientific community to take advantage of the opportunity of research in the context of the Environment Programme of the EC. At the same time, as the historic–architectonic heritage is concentrated along the coasts of the Mediterranean, the selected area of study and experimentation concerns a Basin which contains the monuments of the great civilizations of the past. This cultural heritage represents also an economic reality of common interest to all, and not only to the Mediterranean countries. A further reason for the research lies in the fact that the analysis of the complex interrelationships between stone materials exposed to weathering, climatic conditions and micro–environmental parameters, involves the transfer of techniques, methodologies and data to those who study and work to prevent further damage due to the effects of decay.

The Project was the first European project with the objective of analysing organically the influence of the marine aerosol and environmental conditions of the Mediterranean on the processes of weathering on monuments. The project has involved the cooperation of 10 Institutions from 6 different EC countries and also from Malta and Rumania, all of which have actively collaborated in integrating data and experiences.

Four pilot monuments were selected along the East–West axis of the Mediterranean (Fig.1) on which monitoring activities were programmed and advanced analytical procedures and non destructive techniques were applied. While these monuments had in common the lithotypes with which they were built (marbles, limestones and calcarenites), so that correlations can be made between them, they are also exposed to different conditions from a morpho–climatic point of view and in terms of air pollution and exposure to the sea–spray of the areas in which they are located. Also, the lithotypes, in common with many other monuments, because these stone materials have been widely used in the whole Basin, have been exposed to weathering for a time which varies between 200 and 2000 years up to the present day.

In the extreme west, almost at the entrance to the Mediterranean, stands the Cathedral of Cadiz; this monument of the 18th century, in baroque–rococò and neoclassical style, is built with different stone materials, above all an oolitic limestone of the Mesozoic and a quaternary calcarenite. The Church of Sta. Marija Ta' Cwerra at Siggiewi (Malta), occupies a central position in the southern Mediterranean; it is of the 18th century and was constructed entirely of miocenic calcarenite, known as "Globigerina Limestone". The Cathedral of Bari (Italy), is a 12th century construction located in the central area of the Mediterranean. It is built of Cretaceous limestone while the portals are in marble. The Cathedral, built on foundations of the early 11th century, was destroyed in 1146, and in the course of

E.C. PROJECT: "MARINE SPRAY AND POLLUTED ATMOSPHERE AS FACTORS OF DAMAGE TO MONUMENTS IN THE MEDITERRANEAN COASTAL ENVIROMENT"

Ancient city of Histria (Romania)

Cathedral of Bari

Cathedral of Cadiz

Sanctuary of Demeter of Eleusis (Athens)

Church of Sta. Marija Tà Cwerra Siggiewi (Malta)

LOCATION OF THE PILOT MONUMENTS ALONG THE E–W AXIS OF THE MEDITERRANEAN BASIN

Cathedral of Cadiz (XVIII Cent.)

Church of Sta. Marija Tà Cwerra in Malta (XVIII Cent.)

Cathedral of Bari (XII Cent.)

Sanctuary of Demeter in Eleusis (VI Cent. B.C. – Roman period)

Fig. 1

The E.C. Project "Marine spray and polluted atmosphere as factors of damage to monuments in the Mediterranean coastal environment": objectives and results.

5

time has experienced numerous interventions of reconstruction and restoration. The Sanctuary of Demeter in Eleusis (Greece) is a monument built between the 6th century B.C and the Roman period, which occupies a more easterly position on the axis of the Basin examined.

The ruins of the ancient sanctuary are formed mainly of Triassic marbles, which include pentelic marble, and there are also remains of structures in limestone of upper Triassic–Jurassic age and in quaternary calcarenite.

In addition, another pilot monument located on the Black Sea coast was added in the framework of the Programme for Cooperation in Science and Technology with Central and Eastern European Countries, for the correlation between the effects of marine spray and pollution in the Mediterranean Sea and in the Black Sea, which has lower salinity.

2. Objectives

The Project was characterized by two main objectives (Figs. 2 and 3):

1 *In situ and laboratory analysis of marbles, limestones and calcarenites common to the four pilot monuments, exposed to weathering and representative of different conditions and effects due to marine spray and atmospheric pollution.*

2 *The perfecting of non–destructive methodologies able to identify stone decay in qualitative and quantitative terms, can assist the understanding of the phenomena and consequently suggest the most appropriate techniques of study applied to conservative interventions to adopt.*

3. Cooperation partners and their tasks.

The following institutions were involved in the project:

• *C.U.M. University School Monument Conservation – Istituto di Geologia Applicata e Geotecnica, Facoltà di Ingegneria, Politecnico di Bari, Bari–Italy.*

Leading researcher: Fulvio Zezza

– *Scientific coordination of the Project, monitoring data sampling, mapping of weathering forms by non–destructive computerized analysis, investigation by electron microscope, microbiological investigations.*

• *Universidad de Sevilla, Facultad de Quimica, Departamento de Cristalografia, Mineralogia y Quimica Agricola, Sevilla–Spain.*

Leading researcher: Emilio Galan

– *Monitoring data sampling, mineralogical, petrographical and chemical analysis on stone.*

• *National Technical University of Athens, Department of Chemical Engineering, National Sciences and Technology Sector, Athens– Greece.*

Leading researcher: Theodor Skoulikidis

– *Environmental parameters sampling, mineralogical and chemical analysis of stone and mortars, salt spray tests and sulfation tests.*

• *University of Malta, Institute for Masonry and Construction Research, Malta.*

Leading researcher: JoAnn Cassar

– *Monitoring data and environmental parameters sampling.*

• *University of Antwerp, Department of Chemistry, Antwerp–Belgium.*

Leading researcher: René Van Grieken

– *Chemical, trace and microanalysis on crusts, stone, atmospheric aerosols, wet and dry depositions, correlation analysis.*

• *Aristotle University of Thessaloniki, Laboratory Engineering Geology–Hydrogeology, Department of Geology and Physical Geography, School of Geology, Thessaloniki–Greece.*

Leading researcher: Basiles Christaras

– *Mineralogical and petrographical analysis, physico–mechanical investigations.*

• *Rheinisch–Westfälische Technische Hochschule, Geologisches Institut, Aachen–Germany.*
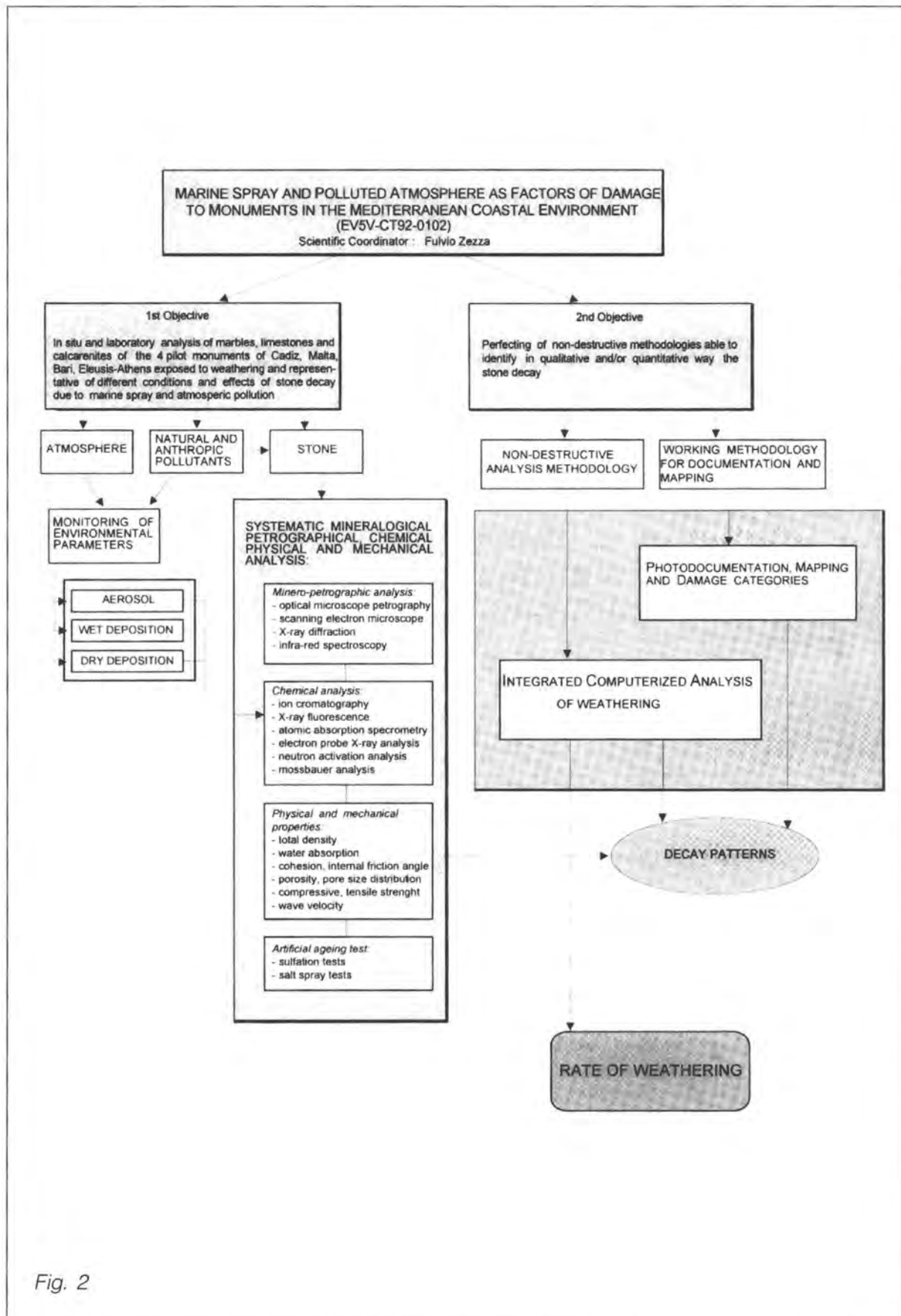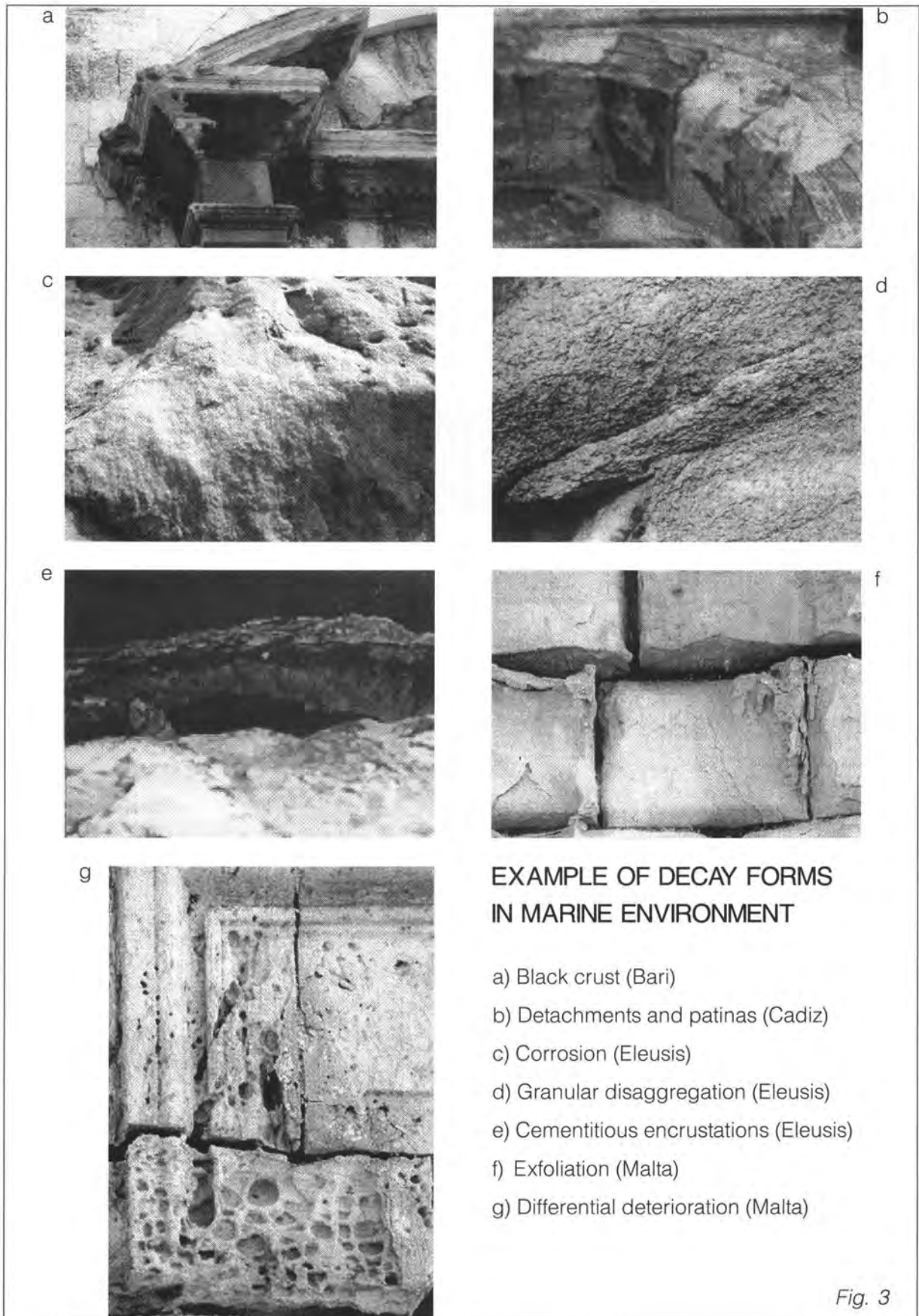
MARINE SPRAY AND POLLUTED ATMOSPHERE AS FACTORS OF DAMAGE TO MONUMENTS IN THE MEDITERRANEAN COASTAL ENVIRONMENT (EV5V-CT92-0102)
Scientific Coordinator : Fulvio Zezza

1st Objective

In situ and laboratory analysis of marbles, limestones and calcarenites of the 4 pilot monuments of Cadiz, Malta, Bari, Eleusis-Athens exposed to weathering and representative of different conditions and effects of stone decay due to marine spray and atmospheric pollution

2nd Objective

Perfecting of non-destructive methodologies able to identify in qualitative and/or quantitative way the stone decay

ATMOSPHERE

NATURAL AND ANTHROPIC POLLUTANTS

STONE

NON-DESTRUCTIVE ANALYSIS METHODOLOGY

WORKING METHODOLOGY FOR DOCUMENTATION AND MAPPING

MONITORING OF ENVIRONMENTAL PARAMETERS

SYSTEMATIC MINERALOGICAL PETROGRAPHICAL, CHEMICAL PHYSICAL AND MECHANICAL ANALYSIS:

AEROSOL

WET DEPOSITION

DRY DEPOSITION

Minero-petrographic analysis:
- optical microscope petrography
- scanning electron microscope
- X-ray diffraction
- infra-red spectroscopy

Chemical analysis:
- ion cromatography
- X-ray fluorescence
- atomic absorption specrometry
- electron probe X-ray analysis
- neutron activation analysis
- mossbauer analysis

Physical and mechanical properties:
- total density
- water absorption
- cohesion, internal friction angle
- porosity, pore size distribution
- compressive, tensile strenght
- wave velocity

Artificial ageing test:
- sulfation tests
- salt spray tests

PHOTODOCUMENTATION, MAPPING AND DAMAGE CATEGORIES

INTEGRATED COMPUTERIZED ANALYSIS OF WEATHERING

DECAY PATTERNS

RATE OF WEATHERING

Fig. 2

The E.C. Project "Marine spray and polluted atmosphere as factors of damage to monuments in the Mediterranean coastal environment": objectives and results.

7

EXAMPLE OF DECAY FORMS
IN MARINE ENVIRONMENT

a) Black crust (Bari)

b) Detachments and patinas (Cadiz)

c) Corrosion (Eleusis)

d) Granular disaggregation (Eleusis)

e) Cementitious encrustations (Eleusis)

f) Exfoliation (Malta)

g) Differential deterioration (Malta)

Fig. 3

Leading researcher: Bernd Fitzner

- *Microstructural analysis of the porous stone system, working methodology of building mapping.*

• *Instituto Superior Tecnico, Laboratorio de Mineralogia e Petrologia, Lisbon–Portugal.*

Leading researcher: Luis Aires Barros

- *Mineralogical and chemical analysis of stone, data treatments of monitoring parameters.*

• *Laboratorio Scientifico della Soprintendenza ai Beni Artistici e Storici di Venezia and Dipartimento di Chimica–Fisica, Facoltà di Scienze, Università di Venezia–Italy;*

Leading researcher: Vasco Fassina

- *Mineralogical and chemical analysis on stone, crusts and efflorescence and on wet and dry depositions.*

• *Technical University of Cluj–Napoca, Faculty of Architecture, Cluj–Napoca–Rumania.*

Leading researcher: Cornelia Elena Berindan

- *Data collecting on the ancient site of Histria on the Black Sea.*

4. Research strategies and results

For each of the pilot monuments analytical studies were carried out on the stone materials, on the monitoring of indoor and outdoor environment, on the atmospheric aerosols, on the neoformation salts, on the weathering forms, on the mapping of the stone decay, on the perfecting of non–destructive techniques for the evaluation of the weathering rate and on experimentations useful for conservative interventions (Fig.2).

In discussing the role of the effect of the marine aerosol and of pollution on the natural processes of weathering in the Mediterranean region it should be recalled, in the first place, that among the particulate which enters the atmosphere every year, the marine aerosol has

the greatest concentration with estimates of annual formation of between 10^9 and 10^{10} tons.

The marine aerosol includes a variety of particles, known as film drops, jet drops, sea–water drops, brine drops, hygroscopic salt drops, sea–salt nuclei and sea–salt particles, the names of which indicate the conditions of formation on the surface of the sea or their physical conditions. The formation of marine aerosol derives from the immission in the atmosphere of minute drops of sea–water. These drops originate from the bursting of bubbles following the breaking of waves in the areas of the sea where there are whitecaps in which a large amount of air is mixed with the water of the sea. The bubbles produced vary greatly in size from many millimeters down to less than 100 μ(many of which are less than 200 μ), and below the surface of the sea, with winds of 10–13 m/s, their concentration decreases from 4.8×10^5 m^3 to 1.6×10^4 m^3 passing from a depth of 0.7 to 0.4 m. Jet drops and film drops evaporate and enter the atmosphere. In the marine atmosphere the concentration of aerosol varies with altitude and with wind speed. Significantly, however, there is a clear change (salt inversion) at the base of the clouds.

The main sources of pollution in the Mediterranean Basin are domestic sewage, industrial wastewater and fluvial drainage. Domestic sewage and industrial wastewater are well known contributors of such pollution but the amount of pollutants carried by river or introduced through atmospheric fallout still remain undetermined components of the total waste which the Mediterranean has to absorb. In the heavily polluting industrial sector four major categories are present: a) leather tanning and finishing; b) iron and steel basic industries; c) petroleum refineries and oil terminals; d) organic and inorganic chemical production. Many industrial complexes are situated on the shores of the Mediterranean.

This pronounced industrial activity in the Mediterranean area is sufficient to qualify this

The E.C. Project "Marine spray and polluted atmosphere as factors of damage to monuments in the Mediterranean coastal environment": objectives and results.

9

area as a prime emitter of pollutants, on a par with many of the industrialized countries of Northern Europe, and the main atmospheric pollutants normally associated with damage to cultural property are produced, including sulphur dioxide, nitrogen oxides, carbon monoxide and carbon dioxide, low molecular weight hydrocarbons and ozone. In addition, other pollutants such as hydrogen sulphide, ammonia, hydrochloric and hydrofluoric acids are also emitted.

In the context of the reactions of the rock–environment binomy, the marine aerosol and pollution determine an aggressive system in which the effect of the former (marine aerosol) accumulates with the latter (pollution) in a circulation regime typical of sea–breeze. It is well known that in coastal areas during the daylight hours, when the warming of the land surface is greater than that of the water, the breeze regime originates. On contact with the land the sea–air forms an unstable layer which becomes increasingly deep as it advances inland. The contaminants of anthropic origin produced in the coastal areas are driven inland and then rise upwards according to the laws of thermal air circulation so that the convective currents return the polluted atmospheric layers towards the sea. With the repetition of the cycles of circulation of the sea–breezes, multilayered structures develop above the surface of the sea in such a way that it is possible that pollutants emitted on the coast in the course of periods of sea–breezes return with the subsequent breezes even after a number of days. This indicates the aggressiveness of the coastal environment on the monuments, not only due to the continuous effect of the marine aerosol carried directly from the sea by strong winds and storms, but also to the circulation of pollutants, produced on the coastal belt and carried by the circulation cells of the area in the sea-breeze regime.

The monitoring stations of the project have given interesting results in this regard. Along the Mediterranean coasts the salts of marine origin, such as chlorides and sulphates,

are especially abundant during the winter, while those of continental origin (carbonates and silicates) are the predominating components in the atmospheric particulate which is deposited in the summer. It is also observed that in the winter the chlorides originate in jet drops and film drops which, once they enter the atmosphere, evaporate and form particles of dimensions of less than 5 μm while, for their part, the sulphates are in particles of between $1 \div 50$ μm. During the summer the particulate contains chlorides and sulphates with dimensions prevalently within two granulometric classes: $0.5 \div 5$ μm e $50 \div 100$ μm.

Together with the particulate of marine origin also dust, smoke and mists are the products of pollution effecting the stone in monuments with which this particulate matter suspended in the atmosphere interacts. In the monitoring stations of the four pilot monuments different acidity levels of depositions have revealed that H^+ (0.025 μmol) contents are higher where there are polluting anthropogenic activities resulting from the presence of large urban centres with refineries as well as heavy industries, as is the case of Eleusis near Athens; they are lower ($H^+ = 0.0002$ μmol) in the case of Malta, in the centre of the Mediterranean Basin, and intermediate ($H^+ = 0.01$ μmol) at Cadiz and Bari.

Also the comparison between the composition of the dry and wet deposition through the calculation of the average concentrations has provided interesting data for the pilot monuments. The pH is almost always around 7; especially high $(8.1 \div 11)$ pH levels can be explained by the neutralization through soil dust which is carried by the currents of air which cross the Mediterranean from north to south and the Ca^{++} of the rocks of the monuments themselves.

The relationship of the concentrations of the different ions present in the wet and dry depositions with the Na^+ concentrations of the sea water has also allowed the evaluation and detailing of the influence of different types of

sources. In the case of Eleusis a close relationship has been established with the Cl⁻ as a result of which the sea cannot be the only source. This high concentration of Cl⁻ could be linked with processes of coal burning in the nearby industrial area. In the monitoring stations of Bari, Malta and Cadiz two groups of ions can be distinguished (Fig.4): a first group of NO_3^- and SO_4^{2-} of clear anthropic origin, and a second group, of marine origin, formed by Na^+, Mg^{2+} e Cl^-.

The content of the soil dust, evaluated in the concentrations of the elements of which the aerosol is comprised, has also indicated that the aerosol is enriched by elements such as S, Cl, K e Ca with respect to the composition of the soil dust. An enrichment in V is found at Malta and Eleusis and in Mn at Eleusis. Fe, Cu and Zn also contribute to enriching the aerosol of each pilot monument, being especially abundant at Eleusis, Malta and Cadiz, and to a lesser degree at Bari.

The micro–climatic monitoring system installed in the indoor environment of three of the pilot monuments (the site of Eleusis is characterized only by an outdoor environment) involved the collection of data regarding thermo–hygrometric parameters. These parameters are the temperature of the stone surface, the air temperature, the relative humidity of the air, and the chemical composition of the condensation waters. The collection of this information was required in order to establish:

1) the thermal stratification in indoor environment of the monuments;

2) the boundary conditions relative to humidity and temperature for the verification of the conditions which favour condensation and evaporation;

3) the determination of the frequency of the conditions which provoke stone decay through processes of solution–crystallization of the soluble neo–formation salts.

It is of particular note to observe that in the indoor environment of these monuments, with the flow of warm air towards the upper parts, the aerosols are deposited in greater quantities on the cold surfaces of stone materials which they reach first and on which they stagnate, roofs, narrowing areas (eg. the bases of domes), overhanging capitals and cornices thereby become the sites of greatest condensation. The Cathedral of Bari is an emblematic case where not only the humidity levels in the internal stone facing of the dome but also the distribution of soluble salts in the same parts of the building confirm this interesting reconstruction which was verified with on site tests by means of microbores for the sampling of powders for analyses (fig. 5).

The soluble neo–formation salts, common to the four pilot monuments, which are responsible for the intense degree of stone decay, are halite and gypsum which, on the basis of the existence of two groups of ions recurring in the wet and dry deposition (Ca^{++}, SO_4^-, NO_3^- and Na^+, Mg^{++}, Cl^- and K^+) are to be attributed to the effects of anthropic pollution and the marine aerosol. At Cadiz other salts have also been identified such as thenardite and trona in accordance with the higher Na^+ contents which have been found at this site than at the others. At Malta, where the action of the marine aerosol is more significant, thenardite is present associated with other chlorides such as sylvite. At Bari, K^+ found in the highest ionic concentrations of the site contributes to the formation of syngenite. At Eleusis nitrates and oxalate appear to depend on the higher ionic concentrations found in the composition of the total deposition.

Biocolonization was also an argument considered by the Project and the relative researches have been based on microscopical observations and cultural investigations performed on samples representative of outdoor environment, as at Eleusis and Malta, and have allowed further results to be obtained in the context of biodeterioration. The environment of the Mediterranean Basin favours the growth of micro–organisms resistant to solar radiation and to variations of humidity (dematiaceous funghi and cyanobacteria) which contain pig-

DISTRIBUTION OF IONS OF MARINE ORIGIN (Cl–, Na++, Mg++) AND
ANTHROPIC ORIGIN (SO4––, NO3–) COLLECTED BY THE MONITORING
STATIONS AT THE PILOT MONUMENTS.
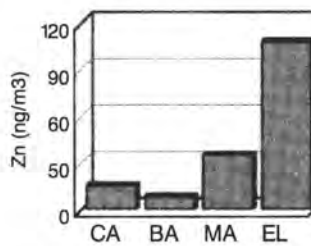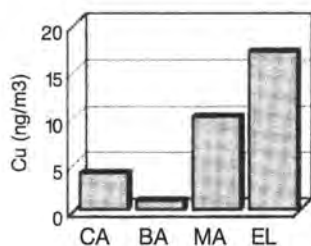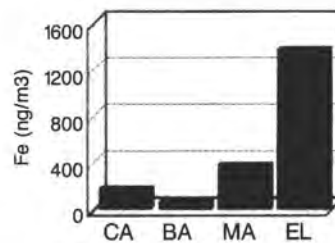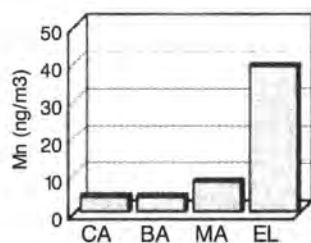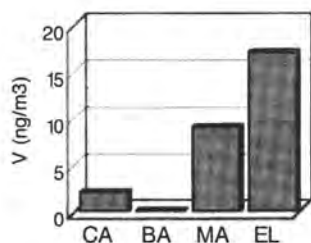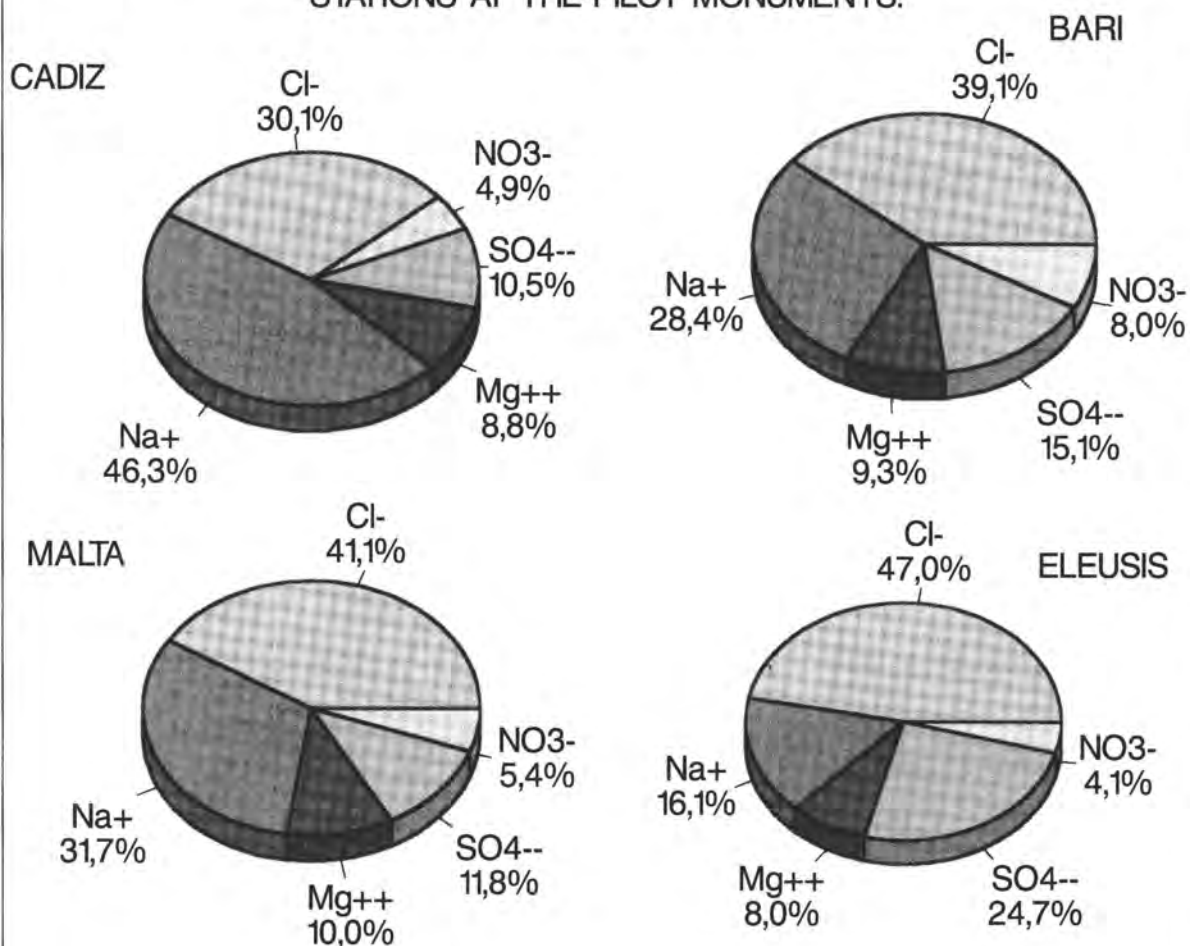
DISTRIBUTION OF METALLIC
IONS IN THE AEROSOL
SAMPLES COLLECTED BY
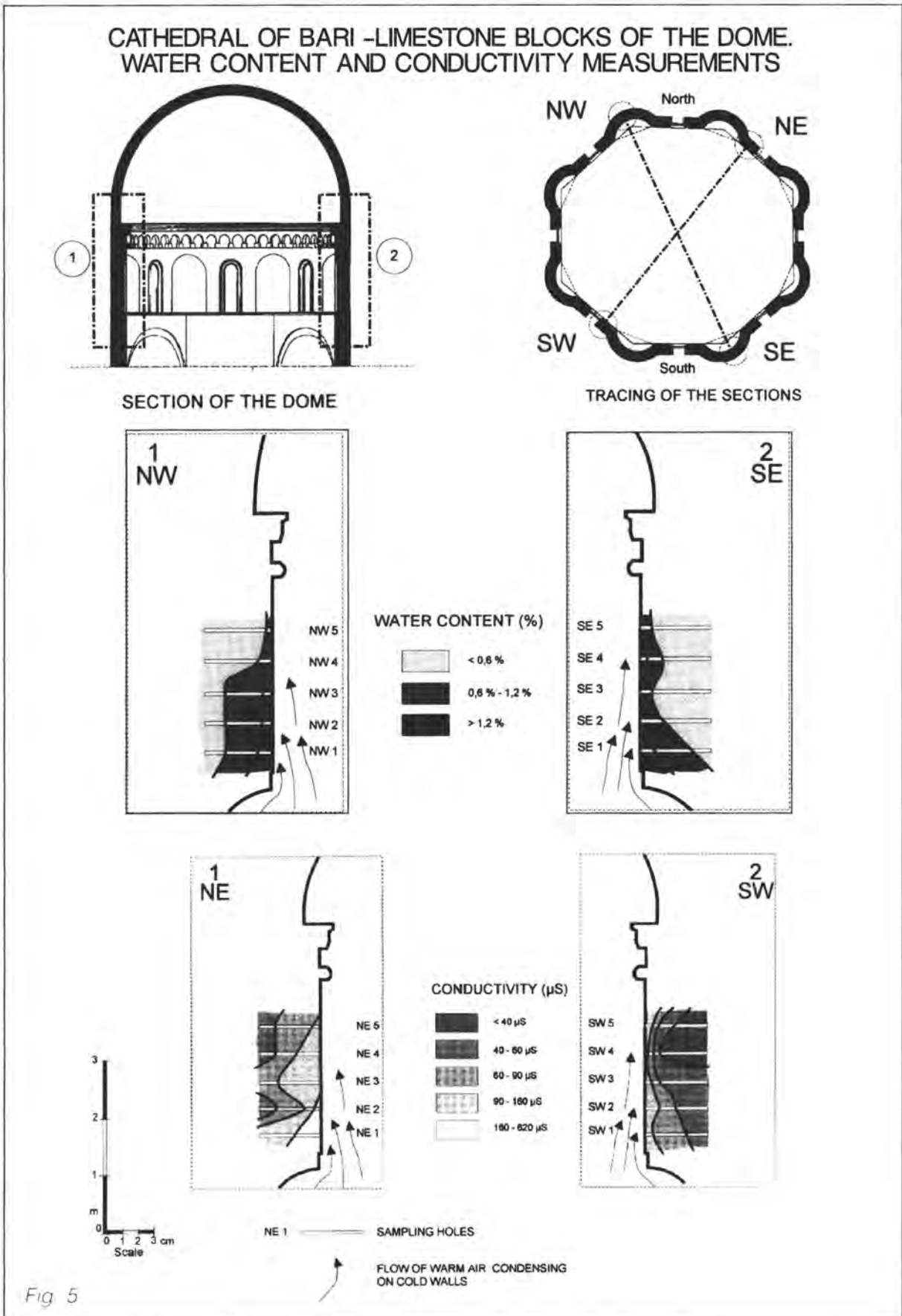THE MONITORING STATIONS
AT THE PILOT MONUMENTS

Fig. 4

**CATHEDRAL OF BARI -LIMESTONE BLOCKS OF THE DOME.
WATER CONTENT AND CONDUCTIVITY MEASUREMENTS**

SECTION OF THE DOME

TRACING OF THE SECTIONS

WATER CONTENT (%)

	< 0,6 %
	0,6 % - 1,2 %
	> 1,2 %

CONDUCTIVITY (μS)

	< 40 μS
	40 - 60 μS
	60 - 90 μS
	90 - 160 μS
	160 - 620 μS

NE 1 ———— SAMPLING HOLES

FLOW OF WARM AIR CONDENSING
ON COLD WALLS

Fig. 5

ments (melanins and carotenoids) that protect them from the effects of these two factors (Fig. 6). Also the bacteria, such as Geodermatophilus, present in black crusts of the marbles are malanin–producers and live in "extreme" habitats such as desert areas where they are closely linked to the so–called "desert varnish" on rock surfaces. Apart from lichens, the micro–organisms colonizing the rock surface are distributed as clusters of cells diffused along the surface and in microcracks, occupying cavities due to a biopitting phenomenon; colonization in inter and intra–crystalline cracks causes decohesion among crystals and their detachment. The bacteria colonies present on limestone and marble are mainly represented by Bacillus, Streptomyces, Micrococcus; among fungi Cladosporium, Ulocladium, Cephalosporium and Phoma are also found.

The acquisitions outlined so far here are contained within the arguments which make up the first objective of the project; the second objective includes the results regarding the mapping of the stone decay and the perfecting of a technique of non–destructive control applied to the forms of weathering.

Considering the weathering behaviour of lithotypes of the pilot monuments, the porosity characteristics, such as total porosity, pore surface and pore size distribution, control decisively the effectiveness of the weathering processes related to the influence of marine spray and polluted atmosphere and thus the extent of weathering damages. With regard to the monument mapping, the detailed documentation and evaluation of the weathering damages has contributed in a fundamental way to the characterization of the complex interrelations between stone types, monument characteristics (location, exposition, architectural structure) and environmental parameters. This is in relation to the achievement of a precise and reproducible characterization, documentation and evaluation of the weathering damages at the pilot monuments according to phenomenologies and geometric criteria.

With regard to the perfecting of a non–destructive technique, within the project the *I.C.A* (Integrated Computerized Analysis) *for Weathering* has been elaborated as an alternative to the traditional methods in order to realize a characterization of stone materials exposed to weathering; it allows the evaluation of the degree of stone decay. In "severe" conditions of exposure, such as those found along the coastal zone of the Mediterranean, fairly high levels are found for the thicknesses of the decayed layers, while for its part the factor of time is found to have affected the rate of weathering. By means of *I.C.A. for Weathering* important objectives are achieved through the comparative examination of the stone materials in the four pilot monuments (Fig.7). The weathering rates of the white marbles of the Sanctuary of Demeter in Eleusis and of the portals of the Cathedral of Bari show that on the sheltered surfaces the thickness of the decayed layers is undoubtedly due to the different lengths of exposure time to the agents of weathering (Sanctuary of Demeter from 6th century. B.C. – Roman period to the present day and the Cathedral of Bari from the 12th century); however an important role is to be attributed to the environmental conditions of the two sites, one of which (Eleusis) is influenced by the cumulative effects of marine spray and anthropic pollution while the other (Bari) especially by sea–spray.

The elaboration of the results obtained with the same techniques on the limestones of the internal walls of the Cathedrals of Cadiz (18th century) and of Bari (12th century), which present frequent detachments of chips, indicates that in reality "very severe" microenvironmental conditions of exposure due to marine aerosol produce larger and more frequent detachments from the blocks of the walls on which stone decay has reached greater thicknesses in relatively short periods of time (Cadiz). A further comparison, referred to the calcarenitic lithotypes exposed for equal periods of time in indoor environment to the influence of the marine aerosol in the Church of
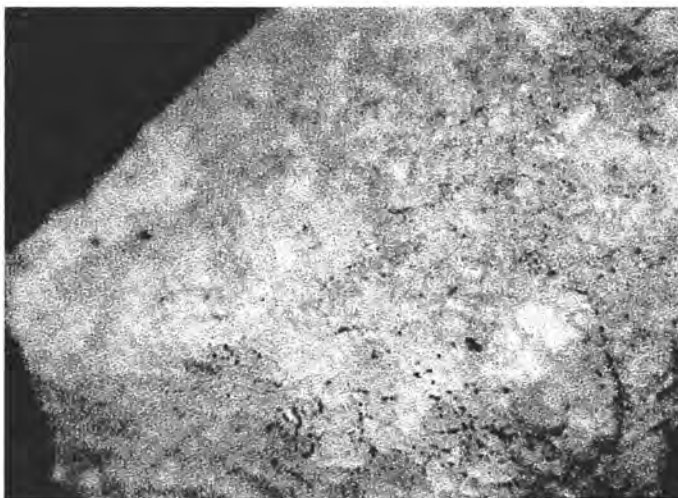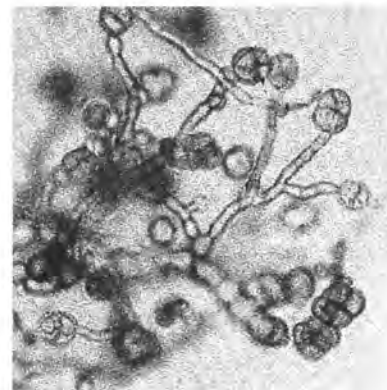
BIODETERIORATION
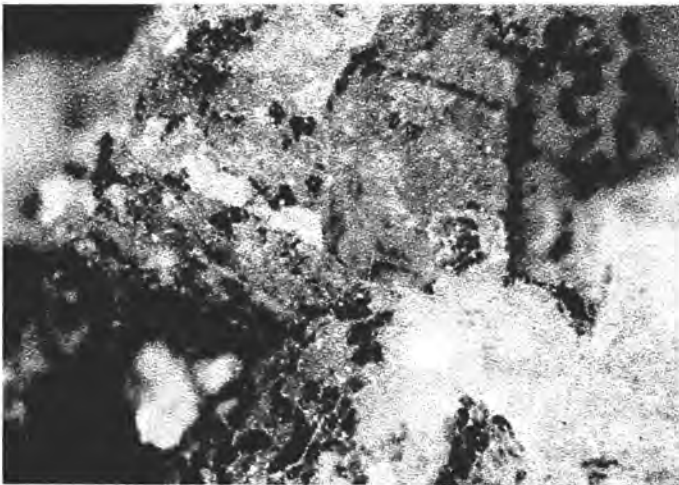
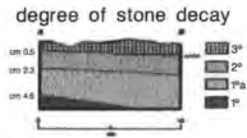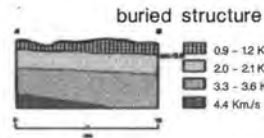Massive algal colonisation on surface of marble (a) and in the intercrystalline contacts (b). Intercrystalline DEMATIACEOUS fungi colonisation (c). Detail of more representative fungal genus (d):ULOCLADIUM (isolated in BR II+ 10% NaCl).
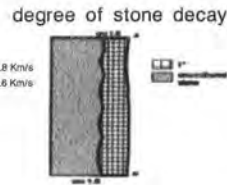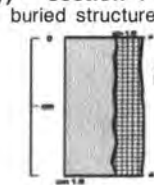
a

b

c

d

Fig. 6

RATE OF WEATHERING

MARBLES - *black crust*

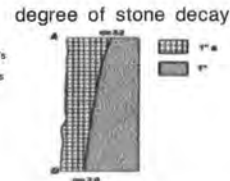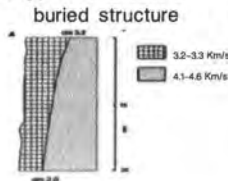### Eleusis Sanctuary of Demeter (from VI cent. B. C. to Roman period) – section 6

buried structure

degree of stone decay

BARI Cathedral (XII century) – section 4
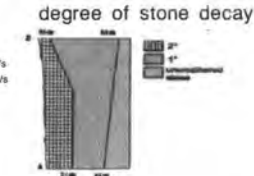
buried structure

degree of stone decay

LIMESTONES - *detachments*

CADIZ Cathedral (XVIII century) – section 2

buried structure

degree of stone decay

BARI Cathedral (XII) century) – section 2

buried structure

degree of stone decay
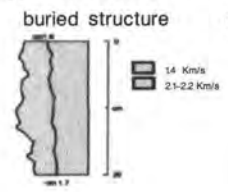
CALCARENITES - *differential deterioration and efflorescences*

CADIZ Cathedral (XVIII century) – section 5

buried structure

degree of stone decay

SIGGIEWI Malta Church of Sta. Marija Ta' Cwerra (XVIII century) – section 1

buried structure
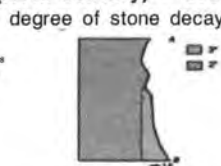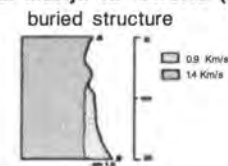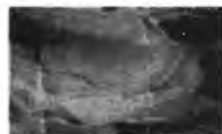
degree of stone decay
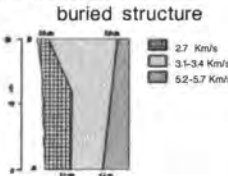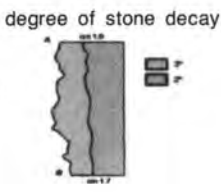
Fig. 7

Siggiewi (Malta, 18th century) and the Cathedral of Cadiz (18th century), demonstrates that the thicknesses reached by decayed parts are substantially similar.

Finally, the Project has involved accelerated ageing tests on the marbles, limestones and calcarenites of the four pilot monuments. The salt spray tests used a sodium chloride solution in a 5% concentration and were performed on untreated, protected and consolidated specimens, as well as consolidated and/or protected.

The weight loss was measured and the concentration of Ca^{++}, Mg^{++} and Fe^{++} in the solution was collected: variations of weight loss were detected according to the type of protective employed. Measurements of the point mechanical resistance on consolidated and samples gave values around 39 MPa as opposed to 30 MPa for unconsolidated samples. Finally, SO_x accelerated attack was carried out to test the efficiency of the protection employed.

The results of the Project have allowed the publication of the following works in the course of Symposia, Congresses and meetings, including this Workshop.

5. Publications produced in the course of the project

1   ZEZZA F. "Marine spray and polluted atmosphere as factors of damage to monuments in the Mediterranean coastal environment". *Proceedings of the 3rd International Symposium on the Conservation of Monuments in the Mediterranean Basin,* Venice 22–25 June 1994, pp 269–273, (1994).

2   ZEZZA F. "Stone decay diagnosis and control of treatments by computerized analytical techniques", *Proceedings of the 3rd International Symposium on the Conservation of Monuments in the Mediterranean Basin,* Venice, 22–25 June 1994, pp 77–82 (1994).

3   FASSINA V., ROSSETTI M., ODDONE M., MAZZOCCHIN S. & CALOGERO S. "Marine spray and polluted atmosphere as factors of damage to monuments in the Mediterranean Coastal Environment: an analytical study of some samples from the Sanctuary of Demeter in Eleusis (Athens)". *Proceedings of the 3rd International Symposium on the Conservation of Monuments in the Mediterranean Basin,* Venice, pp 287–294 (1994).

4   MOROPOULOU A., ZEZZA F., AIRES BARROS L., CHRISTARAS B., FASSINA V., FITZNER B., GALAN E., VAN GRIEKEN R., & KASSOLI-FOURNARAKI A. "Marine spray and polluted atmosphere as factors of damage to monuments in the Mediterranean coastal environment – a preliminary approach to the case of Demeter Sanctuary in Eleusis". *Proceedings of the 3rd International Symposium on the Conservation of Monuments in the Mediterranean Basin,* Venice, 22–25 June 1994, pp. 275–285, (1994).

5   ZEZZA F. & MACRI' F. "Marine aerosol and stone decay". *The Science of the Total Environment,* 167, pp.123-143 (1995).

6   ZEZZA F., MOROPOULOU A., URZI' C., MACRI' F., & ZAGARI M. "Indagine microanalitiche e microbiologiche di patine e croste presenti su pietre calcaree e marmi esposti all'aerosol marino e all'inquinamento atmosferico" *Scienza e Beni Culturali,* vol. XI, pp. 293–303 (1995).

7   AIRES BARROS L., & MAURICIO A., "Forecast of spatio–temporal probability of salt efflorescence occurences on monuments stone". *Memòrias* n.4 161–167. Univ.do Porto, Porto, (1995).

8   MOROPOULOU A., BISBIKOU K., CHRISTARAS B., KASSOLI-FOURNARAKI A., ZOUROS N., MAKEDON TH., FITZN-

ER B., & HEINRICHS K., "Examination of building stones of Demeter Sanctuary in Eleusis. Origin, petrography and physical, mechanical and microstructural properties". *Bolletino Geofisico*, 18, 1, pp37–38, (1995).

9 CHRISTARAS B. "Physical and mechanical properties of stones in the protection of monuments". *Proceedings of 3rd Course CUM University School "Monument Conservation*, Limone–sul–Garda, 4–9 September 1995, (1995).

10 MOROPOULOU A., KOUI M., THEOLAKIS P., KOURTELI CH., & ZEZZA F. "Digital Image Processing for the environmental impact assessment on architectural surfaces". *Journal of Environmental Chemistry and Technology, n.1*, pp 23–32, (1995).

11 ZEZZA F. "Azione dell'aerosol marino sui monumenti del Bacino mediterraneo: stato delle ricerche e grandi programmi internazionali". *2nd European Intensive Course "Sciences and Materials of Cultural Heritage"*. European University Center for Cultural Heritage, Ravello, Italy, (1995) (in the press).

12 MOROPOULOU A.& BISBIKOU K. "Environmental monitoring and damage assessment at the Ancient Sanctuary of Demeter in Eleusis, Greece". *Materials Issues in Art and Archaeology IV*, edited by J.R. Druzik and P.B. Vandiver, Pub. Materials Research Society, (in the press).

13 FITZNER B., HEINRICHS K., & VOLKER M. "Stone deterioration at monuments of Malta". LCP Congress, 25–29 September, 1995, (in the press).

14 MOROPOULOU A., BISBIKOU K., VAN GRIEKEN R., TORFS K., ZEZZA F. & MACRI' F., "Origin and growth of deteriorating crusts on ancient marbles in *industrial atmosphere*". *Atmospheric Environment* (in the press).

15 ZEZZA F. "Integrated Computerized Analysis of Weathering. Perfecting and experimentation on pilot monuments damaged by marine aerosol and pollution" *Proceedings E.C.Workshop "Non–destructive testing to evaluate damage due to environmental effects on historic monuments"*, 15–17 February 1996, Trieste (in the press).

16 CHRISTARAS B. "Non–destructive methods for investigation of some mechanical properties of natural stones in the protection of monuments" *Bull. IAEG* (in the press).

17 VAN GRIEKEN R. "Atmospheric aerosols and deposition near historic buildings". E.C. Workshop *Origin, Mechanisms and Effects of Salts on Degradation of Monuments in Marine and Continental Environments*, 25–27 March 1996, Bari (1996).

18 FASSINA V. "Neoformation decay products on the monuments surface due to marine spray and polluted atmosphere in relation to indoor and outdoor climate". E.C. Workshop *Origin, Mechanisms and Effects of Salts on Degradation of Monuments in pMarine and Continental Environments*, 25–27 March 1996, Bari (1996).

19 AIRES BARROS L. "Monitoring of some meteorological variables related with hygroscopic products occurring at monuments of the Mediterranean Basin". E.C. Workshop *Origin, Mechanisms and Effects of Salts on Degradation of Monuments in Marine and Continental Environments*, 25–27 March 1996, Bari (1996).

20 GALAN E., AIRES BARROS L., CHRISTARAS B., KASSOLI–FOURNARAKI A., FITZNER B., ZEZZA F. "Representative stones from the Sanctuary of Demeter in Eleusis (Greece), Sta.Marija Ta' Cwerra

of Siggiewi (Malta) and Bari (Italy) and Cadiz (Spain) Cathedrals: petrographic characteristics, physical properties and alteration products". E.C. Workshop *Origin, Mechanisms and Effects of Salts on Degradation of Monuments in Marine and Continental Environments,* 25–27 March 1996, Bari (1996).

21 SKOULIKIDIS TH. "Salt spray tests on untreated and treated marble and stones". E.C. Workshop *Origin, Mechanisms and Effects of Salts on Degradation of Monuments in Marine and Continental Environments,* 25–27 March 1996, Bari (1996).

22 ZEZZA F. "Decay patterns of weathered stones in marine environment". E.C. Workshop *Origin, Mechanisms and Effects of Salts on Degradation of Monuments in Marine and Continental Environments,* 25–27 March 1996, Bari (1996).

23 BENEA M. "Representative stones and weathering forms at Histria Fortress, Rumania". E.C. Workshop *Origin, Mechanisms and Effects of Salts on Degradation of Monuments in Marine and Continental Environments,* 25–27 March 1996, Bari (1996).

24 CHRISTARAS B., KASSOLI-FOURNARAKI A., GALAN E., AIRES BARROS L. "Origin and stone material characteristics in the protection of monuments. The case of the archaeological site of Eleusis, in Athens". E.C. Workshop *Origin, Mechanisms and Effects of Salts on Degradation of Monuments in Marine and Continental Environments,* 25–27 March 1996, Bari (1996).

25 TORFS K., VAN GRIEKEN R., GARCIA N., MACRI' F., ZEZZA F. "Study of environmental effects of deterioration of monuments: case study the Cathedral of Bari". E.C. Workshop *Origin, Mechanisms*

and Effects of Salts on Degradation of Monuments in Marine and Continental Environments, 25–27 March 1996, Bari (1996).

26 TORFS K., VAN GRIEKEN R., CASSAR J. "Environmental effects on deterioration of monuments: case study the Church of Sta. Marija Ta'Cwerra, Malta". E.C. Workshop *Origin, Mechanisms and Effects of Salts on Degradation of Monuments in Marine and Continental Environments,* 25–27 March 1996, Bari (1996).

27 FITZNER B., HEINRICHS K., VOLKER M. "Monument mapping a contribution to monument preservation". E.C. Workshop *Origin, Mechanisms and Effects of Salts on Degradation of Monuments in Marine and Continental Environments,* 25–27 March 1996, Bari (1996).

28 FITZNER B., HEINRICHS K., VOLKER M. "Porosity properties and weathering of natural stones". E.C. Workshop *Origin, Mechanisms and Effects of Salts on Degradation of Monuments in Marine and Continental Environments,* 25–27 March 1996, Bari (1996).

29 CHRISTARAS B. "Particularities in studying the physical and mechanical properties of stones in monuments". E.C. Workshop *Origin, Mechanisms and Effects of Salts on Degradation of Monuments in Marine and Continental Environments,* 25–27 March 1996, Bari (1996).

30 MAURICIO A., AIRES BARROS L., FASSINA V., CASSAR J., TORPIANO A. "Multivariate data analysis applied to salt efflorescences occuring at Sta. Marija Ta'Cwerra Church (Malta). E.C. Workshop *Origin, Mechanisms and Effects of Salts on Degradation of Monuments in Marine and Continental Environments,* 25–27 March 1996, Bari (1996).

The E.C. Project "Marine spray and polluted atmosphere as factors of damage to monuments in the Mediterranean coastal environment": objectives and results.

19

31 FITZNER B., HEINRICHS K., VOLKER M. "Model for salt weathering at Maltese Globigerina Limestones". E.C. Workshop *Origin, Mechanisms and Effects of Salts on Degradation of Monuments in Marine and Continental Environments*, 25–27 March 1996, Bari (1996).

32 KOUI M., BISBIKOU K. "Use of liquid crystals as deterioration indicators on marble surfaces at the archaeological site of Eleusis". E.C. Workshop *Origin, Mechanisms and Effects of Salts on Degradation of Monuments in Marine and Continental Environments*, 25–27 March 1996, Bari (1996).

33 ZEZZA F., CALOGERO S. "A neutron activation analysis study of limestone of the Cathedral of Bari". E.C. Workshop *Origin, Mechanisms and Effects of Salts on Degradation of Monuments in Marine and Continental Environments*, 25–27 March 1996, Bari (1996).

34 NEAGOE I., BERINDAN C. "Types of chemical and biochemical degradation found as developed at Histria Fortress – Romania". E.C. Workshop *Origin, Mechanisms and Effects of Salts on Degradation of Monuments in Marine and Continental Environments*, 25–27 March 1996, Bari (1996).

35 BERINDAN C. "Some specificities in assessment of environmental risk factors in the weathering process at Histria Fortress Wall – Romania". E.C. Workshop *Origin, Mechanisms and Effects of Salts on Degradation of Monuments in Marine and Continental Environments*, 25–27 March 1996, Bari (1996).

36 MOROPOULOU A., BISBIKOU A., STAGAKIS M., VAN GRIEKEN R., TORFS K. "Environmental outdoor impact assessment on ancient monuments: the case of the Sanctuary of Demeter in Eleusis".E.C. Workshop *Origin, Mechanisms and Effects of Salts on Degradation of Monuments in Marine and Continental Environments*, 25–27 March 1996, Bari (1996).

37 GALAN E., GUERRERO M.A., VASQUEZ M.A., CARRETERO M.I., ORTIZ P. "The Cathedral of Cadiz (Spain). Environmental study and stone damage evaluation". E.C. Workshop *Origin, Mechanisms and Effects of Salts on Degradation of Monuments in Marine and Continental Environments*, 25–27 March 1996, Bari (1996).

38 FASSINA V., MIGNUCCI A., NACCARI A., STEVAN A., CASSAR J., TORPIANO A. "Investigation on the moisture and salt migration in the wall masonry and on the presence of salt efflorescences on stone surface in the Church of Sta. Marija Ta'Cwerra at Siggiewi (Malta)". E.C. Workshop *Origin, Mechanisms and Effects of Salts on Degradation of Monuments in Marine and Continental Environments*, 25–27 March 1996, Bari (1996).

39 ZEZZA F., GARCIA N., MACRI' F. "Microclimate of Bari Cathedral. The influence of outdoor factors in the indoor microevironment". E.C. Worckshop *Origin, Mechanisms and Effects of Salts on Degradation of Monuments in Marine and Continental Environments*, 25–27 March, Bari (1996).

40 FASSINA V., MOROPOULOU A., RATTAZZI A. "Principle decay patterns on the archaeological site of Demeter Sanctuary in Eleusis: weathering mechanism". E.C. Workshop *Origin, Mechanisms and Effects of Salts on Degradation of Monuments in Marine and Continental Environments*, 25–27 March 1996, Bari (1996).

R. Van Grieken
K. Torfs

Atmospheric aerosols and deposition near historic buildings: chemistry, sources, interrelations and relevance
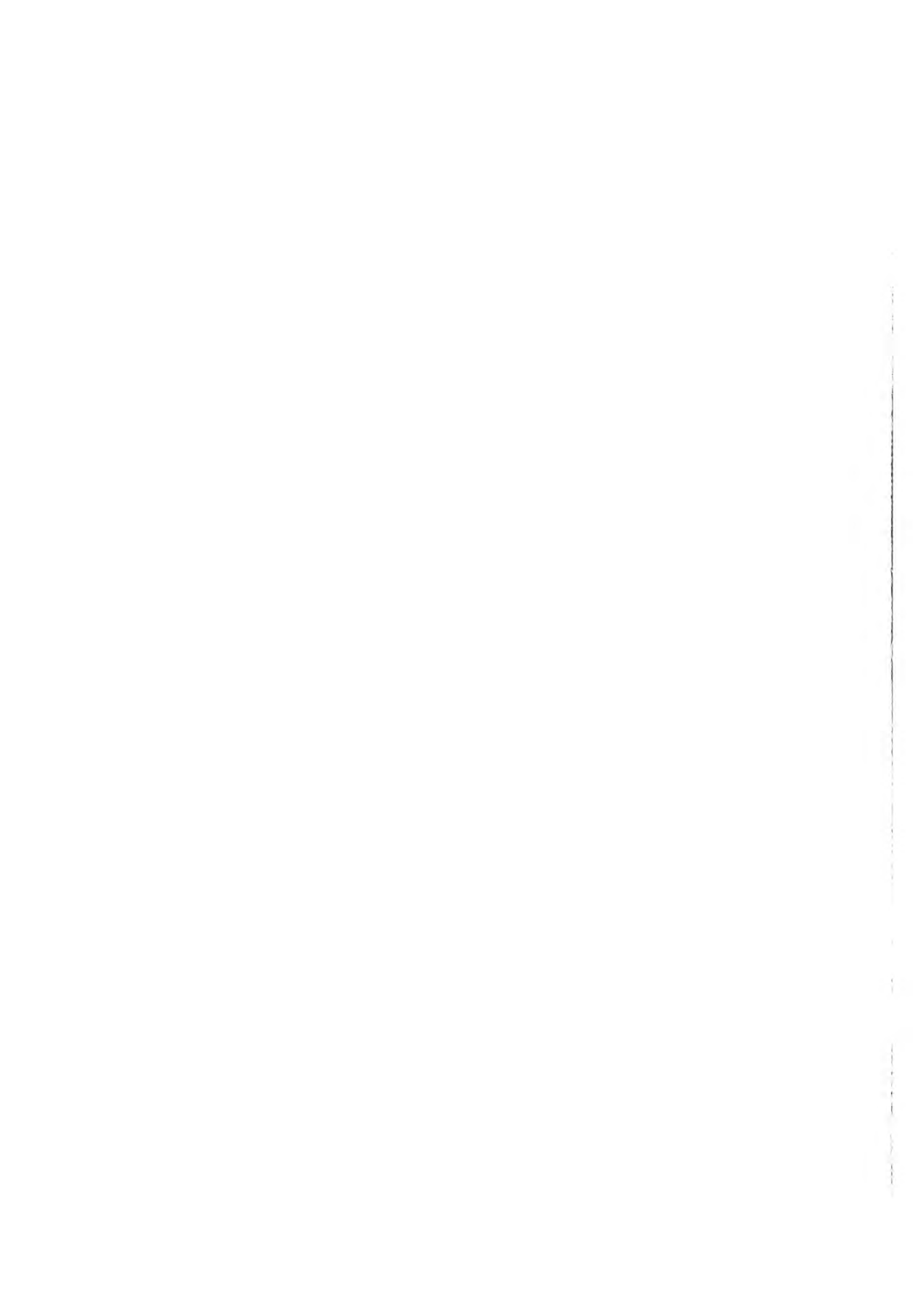
Atmospheric aerosols and deposition near historic buildings: chemistry, sources, interrelations and relevance

R. Van Grieken, K. Torfs

Dept. of Chemistry, University of Antwerp (U.I.A.), Belgium

Abstract

To evaluate the effects of the environment on weathering of historical buildings, an extensive study has been carried out at four pilot monuments in the Mediterranean Basin, with specific interest to the action of marine salts and air pollution. The composition of the atmosphere around the monuments has been studied by characterizing the deposition and the aerosols near the monuments. These results are combined with the stone decay phenomena to explain the stone deterioration at the respective sites.

1. Introduction

Studies on the effects of environmental conditions on the deterioration of monuments have been carried out regularly. Mostly, attention has been focused on the effects of anthropogenic induced decay [1,2]. It is only in relative recent times that the effects of marine aerosols on the stone decay process have attracted the attention of researchers [3]. Not only air pollution causes decay, the unfavourable marine environment, in e.g. Venice, enhances it also [2]. The building materials deteriorate under the action of environmental weathering factors, which are, in Mediterranean cities, the presence of salts in combination with movement and evaporation of water which forms solutions of soluble salts in the stone [4].

In the present study, four monuments have been selected along the east–west axis of the Mediterranean Basin. The different position of the monuments reflects different conditions of salinity, state of marine and atmospheric pollu-

tion and physicographical aspects of the areas. The monuments which have been studied are: the Cathedral of Cadiz (Spain), situated at the furthest limits of Mediterranean Spain, near Gibraltar, significantly influenced by the Atlantic climatic conditions; the Cathedral of Bari (Italy), located in the central part of the southern coast of Europe, exposed to a marine environment influenced by anthropogenic activity; the Church of Santa Marija Ta' Cwerra in Siggiewi (Malta) in the centre of the Mediterranean, far away from any industrial activity; the Demeter Sanctuary of Eleusis (Greece), located near the sea in a typical urban centre of intense and diversified industrial activity [5].

The cathedral of Cadiz is situated in the south of the city, separated from the sea by a promenade. In view of the characteristics of this open space, the problems presented by traffic pollution become negligible in comparison with those produced by the scourge of marine winds, saturated with aerosols and water droplets. The building has been constructed in the 18th century. Different lithological stone types have been used: oolitic limestone, black, red and white marble and calcarenite. The vaults of the Cathedral are loosing an important part of their stone section through fissures, fractures and fragmentation. The foundations and the crypt, which are of porous stone, are acting as sponges to sub–soil humidity.

The Cathedral of Bari is situated in the centre of the old city, at a distance of 300 metres from the sea. The building contains elements of

a paleo–christian church, the cathedral built at the beginning of the 11th century by Byzantius, the cathedral which was dedicated in 1292 and the subsequent restorations. The cathedral is constructed of limestone and marble. The phenomena of stone decay belong mainly to corrosion of the exposed surface (alveolization and crumbling), exfoliation, efflorescence, granular disaggregation, detachment, pulverization, fissuring and black crust on the external facade.

The church of Sta. Marija Ta' Cwerra is located in the south west of the island Malta at a distance of 3 km from the sea. The building was constructed in the 17th century. The church is built entirely of limestone. The four external walls of the church show severe deterioration. The middle courses are deteriorated in the form of alveolar weathering as well as powdering of several areas. Most of the mortar has been lost from the joints. At the inside of the building, the plaster has fallen away revealing powdering and flaking stone underneath.

The Demeter Sanctuary of Eleusis is located in an area, which had been a rural site for years, but in the post–war period has become increasingly industrialised, with key manufacturing sectors, basically metallurgical and chemical ones. According to the Homeric Hymn to Demeter, the first temple of Demeter and the Eleusinian Sanctuary were founded in the reign of the legendary King Celeus in the Late Helladic period (1500–1425 BC). During the Roman Period, the Triumphal Arches and the Greater and Lesser Propylea were added. The Sanctuary was largely destroyed in 395 during the invasion of the Visigoths. Pentelic marble has been applied mostly in the Sanctuary. Some limestone has been used in the Eastern Triumphal and the surrounding walls. The main decay phenomena are as follows: pitting of the marble surfaces, black crust formation, chromatic alterations of the white marble, granular disintegration and detachment and biological decay [6].

2. Experimental

2.1. Sampling

Samples of stones, weathering layers and efflorescence were taken at the four monuments. In the cathedral of Cadiz 5 samples have been taken at the inside, namely from the vaults, which lose stone sections, and from the efflorescence on the foundations of the crypt and the ceiling. In Bari, the major part of the samples (7) has been taken at the inside of the cathedral from stones with a coating layer, efflorescence and powders. Two black crust samples have been taken at the outside of the cathedral, one on limestone and one on marble. In Malta, three samples have been taken at the outside of the building, from the deep destruction of the stones. At the inside, two efflorescence samples have been collected. In the ruins of the Demeter Sanctuary 13 samples are taken of washed out areas, black crust, cementitious crust, dust depositions and disintegrated areas on limestone and marble.

The total deposition is sampled at the four sites by using a funnel with an inner diameter of 20 cm, attached to a 1 L polyethylene bottle. A metal ring is placed around the funnel, a bit away from it, to avoid contamination by bird droppings. The system is kept well clear of overlooking structure to avoid micro–climatic interference, such as shadow, windage, etc. To prevent growth of algae and mould, 1 mL of formaldehyde is added to the collection bottle. The samples are collected every week. The funnel is rinsed then with exactly 50 mL of deionised water to remove the dry deposition in the funnel. This rinsing water is added to the collection bottle to ensure a new sample every week. More than 200 total deposition samples were collected during almost two years. In Bari and Cadiz, a rain water collector is installed to sample the wet deposition; in Bari the equipment permits to sample the dry deposition as well, by rinsing the bucket which is opened during dry periods, with 50 mL water every week.

Aerosol sampling is carried out near the four

pilot monuments. In Malta and Cadiz monitoring takes place at the inside and the outside of the building, while in Bari and Eleusis monitoring is performed at the outside only. To collect outdoor aerosols, a filter unit in cascade geometry provided with a top–hat inlet is used, to avoid the collection of rain and large droplets. Polycarbonate filters (Nuclepore filters) with a diameter of 47 mm and a pore–size of 2 µm and 0.4 µm are placed behind each other in order to collect coarse and fine particles separately. The indoor sampling takes place using only one Nuclepore filter with a pore–size of 0.4 µm. A gas flow meter is placed behind the pump and measures the exact volume of air that is pumped through the filters. A low volume pump is used, to provide a flow rate of around 20 L/min. The sampling is carried out during one week in Malta and in Cadiz. In Eleusis the sampling periods are only a few hours. In Bari the sample is obtained by sampling 4 days during a week. In this way 150 aerosol samples have been collected during one year.

2.2. Analysis

To determine the bulk chemical composition of the stone, the samples are crushed and the powder is dispersed in demineralised water. After filtration of the suspension, the filtrate is analyzed for soluble compounds using ion chromatography (IC), atomic absorption and atomic emission spectrometry (AAS/AES). A few millilitres of the wet ground suspension is brought on a Mylar foil. The foil is dried and analyzed using energy dispersive X–ray fluorescence (EDXRF). To analyze the stone composition in depth by scanning electron microscope analysis with energy dispersive X–ray attachment (SEM–EDX), the sample is imbedded in a resin, cut perpendicularly to the weathered crust and polished without water.

The volume of the total deposition sample is determined. The sample is filtered over a Whatman 41 filter and the total suspended particulate

mass (TSP) is measured. The pH of the filtrate is determined potentiometrically, the HCO_3^- content is determined by titration with HCl, the end point is determined using methyl–orange indicator. The analyses of Ca^{2+}, Mg^{2+}, Na^+ and K^+ are carried out with AAS and AES and Cl^-, NO_3^- and SO_4^{2-} are determined using IC.

The Nuclepore filters, containing the aerosols, are first analyzed by EDXRF. Afterwards, the samples are leached in exactly 25 mL of deionised water, the suspension is filtered and the filtrate analyzed using IC, AAS and AES.

IC is used for Cl^-, NO_3^- and SO_4^{2-} determinations; a Dionex 4000i instrument, equipped with a AS11 separator column is installed; 20 mM NaOH is used as eluent.

Ca^{2+} and Mg^{2+} are determined by means of AAS, whereas Na^+ and K^+ are measured by AES, both by means of a Perkin Elmer 3030 spectrometer. The samples are acidified to pH 2 with HCl and 100 µL 10% La^{3+} solution is added to the samples to avoid interferences.

EDXRF analyses are carried out using a Tracor Spectrace 5000 instrument. The instrument is equipped with a Si(Li) detector and a low power X–ray tube with a Rh target, controlled by an IBM computer. The X–ray spectra are accumulated for 3000 s and analyzed using the AXIL software [7]. The calculation of the concentrations in the stones has been checked with soil standards: IAEA Soil 5 and BCR 142. The AXIL program calculates the concentration of the aerosols on the Nuclepore filters in $\mu g/m^2$. Since the surface of the filters and the sampled volume are determined, the concentrations of the elements can be expressed in ng/m^3.

A JEOL–JSM 6300 Scanning Microscope is used to study the stone composition on micrometer scale. The samples are excited with an electron beam of 1 nA and an electron energy of 15 keV. By recording energy dispersive X–ray spectra of subsequent small areas, perpendicular to the exposed surface, depth profiles are obtained, showing the elemental distribution through the sample, when proceeding from the outer surface layer towards the unaffected inner part.

3. Discussion of the results

3.1. Characterization of the stone composition

Table 1 summarizes the bulk composition of the leachates of the stones, that is determined after leaching the stones.

The SO_4^{2-} concentration is highest in the samples from Eleusis. The black crust samples from Bari present also high SO_4^{2-} concentrations. Scanning electron microscopy confirms these results: gypsumneedles are visible in the decay layers. In the samples from these two sites, fly–ash particles, originating from different burning processes are found. In the samples from Malta and Cadiz no such particles have been observed. The Na^+ concentration is very high in the efflorescence samples from Cadiz and Malta and also in the stone samples at the outside of the church in Malta. In Cadiz, the efflorescence consists mainly of Na_2CO_3, while in Malta, Na_2SO_4 and NaCl are

the most abundant salts. In Malta, a significant difference is observed in the efflorescence composition, depending on the sampling height : less soluble sulphates dominate in the lower courses, while chloride dominates in the upper courses, in agreement with the results of Arnold and Zehnder [8]. The efflorescence samples from the cathedral in Bari contain mainly sulphate.

Table 2 summarizes the results of EDXRF analysis. Generally the concentra–tion of heavy metals is highest in Eleusis, followed by Malta. The Pb concentration, however, is lowest in Malta. As this element is the characteristic tracer for motor vehicles, these results indicate high deposition levels of particles emitted by gasoline combustion in Eleusis. V is a tracer for the aerosol emitted by fuel oil combustion and Zn is characterizing for refuse incineration. These elements are most abundant in the stone samples from Eleusis. The enrichment factors of various elements with respect to carbonate rock have been calculated to identify

Table 1 Average stone composition (expressed in weight % of leachable material).								
	Cl^-	SO_4^{2-}	NO_3^-	CO_3^{2-}	Ca^{2+}	Mg^{2+}	Na^+	K^+
Cadiz inside: efflorescence	1	0.5	0.2	30	0.5	0.1	15	0.5
Cadiz inside: stone	3	1	0.2	6	5	0.2	2	0.3
Bari inside: efflorescence	2	12	1.5	–	8	2	1	1
Bari outside: black crust	0.9	31	0.5	–	18	0.7	0.6	0.5
Malta inside: efflorescence	30	15	0	–	1.3	0	18	0.1
Malta outside: stone	10	2	5	–	12	0.3	16	1
Eleusis: black crust	0.1	40	0	–	20	0.1	0.1	0
Eleusis: dust	0.5	61	1.4	–	22	0	8	2

the component due to the deposition of atmospheric gases and aerosol on the stone surfaces. The following formula has been used [9]:

$$EF_{carb.\ rock}\ (X) = \frac{(X/Ti)_{black\ crust}}{(X/Ti)_{carb.\ rock}}$$

where X and Ti are the concentrations of element X and titanium, respectively. The elemental composition of carbonate rock, reported by Mason [10], was used in the denominator. Results are presented in Table 3.

Enrichments to carbonate rock have been found for Cl, S, Na and Pb. Pb seems, however, not to be enriched in Malta and is most enriched in Eleusis. The enrichment of S is lowest in the stones from Cadiz and Malta, and highest in Eleusis and the efflorescence samples from Malta. Na is highly enriched in the stones from Malta and Cadiz.

To estimate the importance of sea derived elements on the stones, the enrichment factor of the ions to the average sea water composi-

Table 2   Average concentration of stone samples, measured by EDXRF (ppm).

	Si*	Ti	V	Cr	Mn	Fe	Ni	Cu	Zn	Br	Pb
Cadiz	2	150		10	50	100		5	15		30
Bari		200			40	1200		10	25	6	40
Malta	4	400		15	80	2000	15	7	20	5	15
Eleusis	2	1500	20	100	200	9000	40	40	300	10	300

* : concentration expressed in %

Table 3   Enrichment factors of damaged layer vs. carbonate rock (Ti as indicator element).

	Cl	S	Ca	Mg	Na	K	Si	Mn	Fe	Sr	Pb
Cadiz inside: efflorescence	110	1.5	0.0	0.0	610	2.2	6.6	0.2	0.7	0.4	7.5
Cadiz inside: stone	300	6.0	0.5	0.1	60	1.9	0.0	0.2	0.1	0.3	14
Bari inside: efflorescence	270	35	0.4	0.2	63	6.9	0.0	0.1	1.6	0.7	18
Malta inside: efflorescence	9300	210	0.2	0.0	2200	1.8	2.7	0.0	0.4	0.4	0.0
Malta outside: stone	660	3.5	0.4	0.1	440	3.3	2.1	0.1	0.6	0.7	1.8
Eleusis: black crust	25	170	0.9	0.0	7.1	0.6	1.9	0.4	1.3	0.5	29
Eleusis dust	20	50	0.3	0.0	1.2	0.0	2.8	0.1	1.4	0.1	13

tion has been determined, using an analogous formula with Na as indicator element. The results are summarized in Table 4. SO_4^{2-} and Ca^{2+} are the components with the highest enrichment factors. Ca^{2+} in the crust originates from the underlying carbonate rock, while SO_4^{2-} is mainly deposited on the surfaces as both gaseous SO_2 and sulphate particles, not originating from the sea. In the samples from Malta and Cadiz, K^+ may originate from the sea, while on the black crusts from Eleusis and Bari, deposition of sea salt particles does not seem to be the most important source for K^+. Mg^{2+} and Cl^-, found in the damage layer, may originate from the sea at all sites (enrichment factors close to 1). The samples from Eleusis and the black crust samples from the Cathedral of Bari present the highest concentrations of sulphur containing alteration products, while in Cadiz and Malta sea salt derived elements dominate. Sulphate, present in the weathering crust from Bari and Eleusis, is not sea salt derived, while in Cadiz and Malta the weathering layer is less enriched relative to the average sea water composition.

3.2. Evaluation of the deposition around the monuments

Since the average deposition around the four monuments reflects better the real deposition on the monuments, than the concentrations do, the weekly average total deposition has been calculated (Figures 1 and 2). For Bari, the wet and dry deposition is given separately as well, while for Cadiz, only the wet deposition is presented.

Generally the deposition is highest in Eleusis, although the deposition of sea salt in Cadiz is also very high. Cl^- is the most important anion in the total deposition samples from Malta and Cadiz, while at the other sites HCO_3^- is the most important anion. In Eleusis, the highest SO_4^{2-} amount is found, but the difference with the other sites is not very large. Na^+ is the most important cation in Cadiz,

Table 4 Enrichment factors of damage layer vs. sea water (Na as indicator element).

	Cl^-	SO_4^{2-}	Ca^{2+}	Mg^{2+}	K^+
Cadiz inside efflorescence	0.03	0.08	0.58	0.05	0.55
Cadiz inside stone	1.30	5.33	200	1.21	11.5
Bari inside efflorescence	1.23	17	200	10.7	18.1
Bari outside black crust	0.80	200	840	1.16	22.6
Malta inside efflorescence	0.75	3.91	2.15	0.01	0.2
Malta outside stone	0.75	0.43	47	0.4	5.4
Eleusis black crust	0.75	870	2800	2.79	20.1
Eleusis dust	3.62	1500	5800	3.25	5.05

while, at the other sites, Ca^{2+} is more important. For all elements, the contribution of the wet deposition is bigger than the dry deposition in Bari. In Cadiz the wet and dry deposition are more of equal importance. In comparison with results obtained in Belgium [11], the Ca^{2+} concentration is much higher due to the vicinity of the monuments. This phenomenon is accompanied by higher pH values, caused by the neutralizing effect of calcite particles, released by the monument. There is therefore no direct attack on the stones of acids in rain water. The Na^+ and Cl^- concentrations are quite high, even higher than observed near the Belgian coast, while the SO_4^{2-} concentration is comparable.

The seasonal variation in the deposition of the volume and ions has been investigated by grouping the different sampling periods according to the season they were part of (Figure 3). In Cadiz the summer season reveals the minimum deposition for all ions, except for NO_3^-, which may be due to enhanced photochemical oxidation of NO_x during this season.
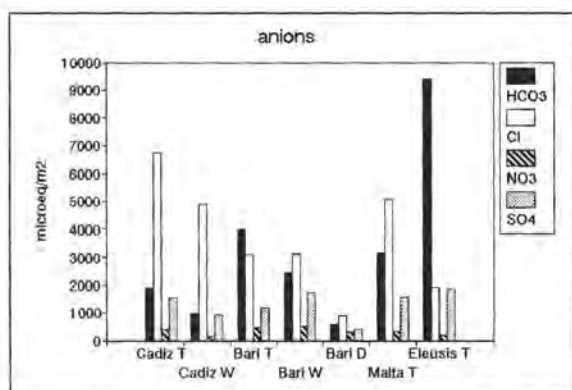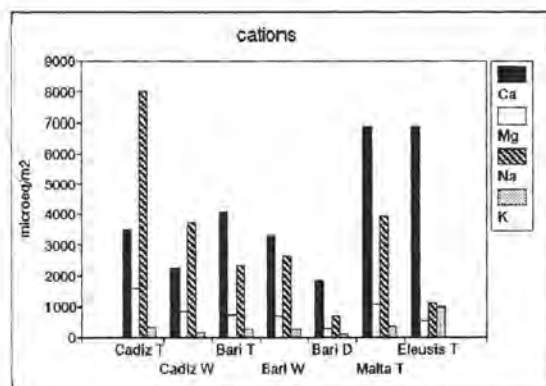
Figure 1 Weekly average anion deposition.

Figure 2 Weekly average cation deposition.

The rainfall volume is highest during winter and spring; this is also true for most ions (H^+, Mg^{2+} and Na^+ maximum during winter, NH_4^+ maximum during spring). In Bari, the highest deposition is seen during spring, except for H^+, which is maximum during winter. Ca^{2+}, K^+, NO_3^- and HCO_3^- are almost not collected in the winter season, while NO_3^- and K^+ are maximum during summer. Contrarily to

Cadiz and Bari, the highest volume in Malta is obtained during autumn. The summer is clearly the season, during which less ions are collected. The high volume during autumn is accompanied by high deposition of Ca^{2+} and HCO_3^-, while in winter the deposition of H^+, Na^+, Mg^{2+} and Cl^- dominates. NO_3^- and K^+ are again the only ions with a still significant deposition during summer. In Eleusis most of
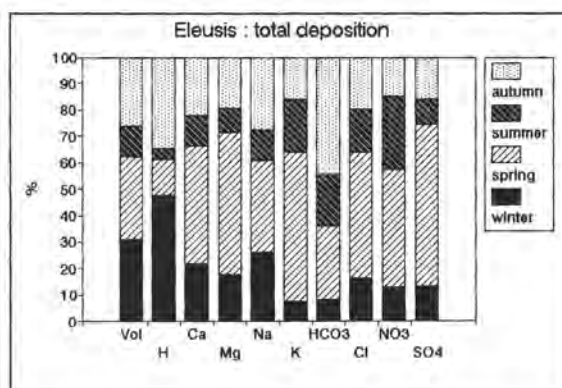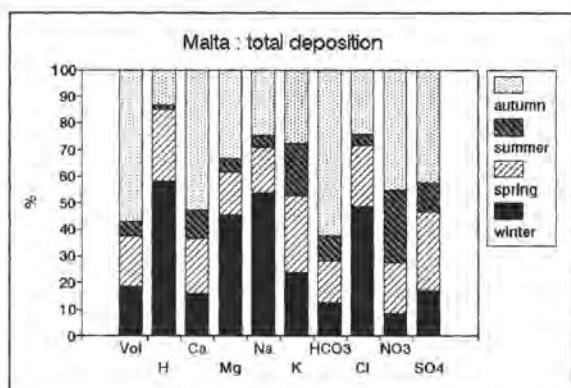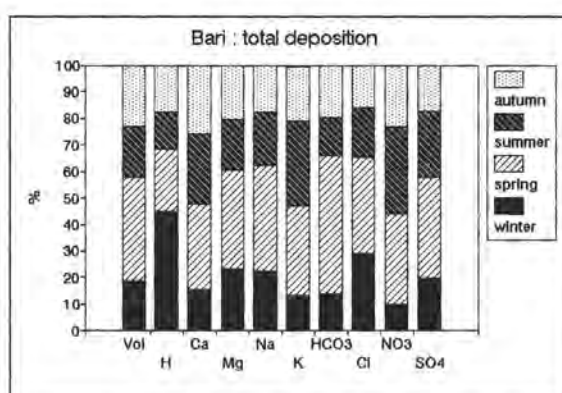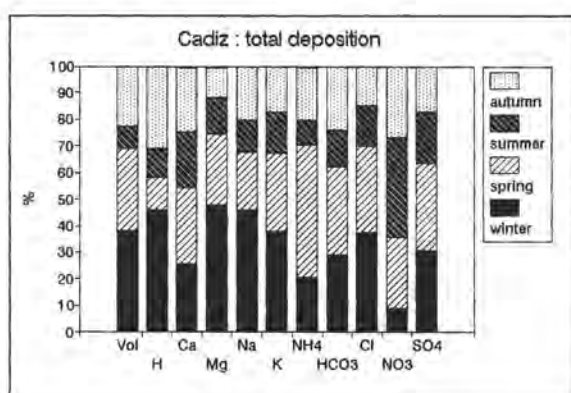

Figure 3 Seasonal variation in the total deposition.

the volume is collected during autumn, winter and spring. The acidity is, like at the three other sites, highest during winter. For the other ions, it seems that they are collected mostly during spring, except HCO_3^- which dominates during autumn. The highest volumes are collected during autumn, winter and spring. Small local variations are observed: in Bari most of the volume is collected during spring, while in Malta autumn is the wettest season. For all ions deposition is less during summer, except for NO_3^- and K^+, which reveal then high depositions.

An estimation of the contribution of sea water to the ion concentrations in the total deposition has been performed by evaluating the ionic ratios of Cl^-, K^+, Mg^{2+}, Ca^{2+} and SO_4^{2-} to the Na^+ concentration in precipitation with this ratio in sea water, obtaining so called enrichment factors. For Cl^- and Mg^{2+} almost no other sources are present. For Ca^{2+}, SO_4^{2-} and K^+ some other sources must be present. Ca^{2+} may be due to Saharan soil dust [12] and particles from the monument [13]; this is especially the case for the dry deposition in Bari and for the ruins of Eleusis. For SO_4^{2-}, some anthropogenic sources are present; for K^+ some other natural or anthropogenic source must be present, especially in Eleusis.

The relationship between two variables is considered by use of the concept of the correlation coefficient. This coefficient may be viewed as providing a measure of the mutuality of relationship between two variables.

At all sites, except Eleusis, a high correlation has been observed between Na^+, Mg^{2+} and Cl^- (r=0.9). Ca^{2+} and SO_4^{2-} are correlated in Eleusis and Bari (r=0.8), while in Malta, Ca^{2+} is correlated with HCO_3^- (r=0.8). The meteorological data present only low correlations with the deposition: only the temperature is slightly negative correlated with the ion amounts.

In Malta and Bari, the acidity (H^+) is correlated with salts (Na^+ and Cl^-)(r=0.7), while in Cadiz the acidity is correlated with the volume

Table 5 Enrichment factors of the deposition vs. sea water (Na as indicator element).

	Cl^-	K^+	Ca^{2+}	Mg^{2+}	SO_4^{2-}
Cadiz	0.72	1.96	10.9	0.90	1.59
Bari	1.13	5.46	43.7	1.40	4.27
Malta	1.11	4.46	44.2	1.23	3.33
Eleusis	1.46	43.1	151	2.16	13.4

(r=0.8). In Eleusis the acidity is correlated with the volume and the Na^+ content. Alaimo et al. [14] suggested the action of two sources: a marine source (Cl^-, Na^+ and Mg^{2+}) and a source influenced by anthropogenic activities (Ca^{2+} and SO_4^{2-}).

Principal component analysis (PCA) is a statistical technique to reduce the dimensionality of a large data set, without loosing information. The original correlated variables are transformed into new uncorrelated variables, which are linear combinations of the original data set. Each principal component is composed of the product of a score vector and a loading vector plus an error term. The loading plot shows the correlation between the variables. If a group of variables correlate with each other and reflect the operation of a single process, the variables will be represented as a cluster in the loading plot.

Variables that are situated close to theorigin of the plot do not contribute to the model.

For the total deposition in Cadiz, the first factor is composed of Cl^-, SO_4^{2-}, Mg^{2+}, N^{a+}, K^+ and Ca^{2+}. These variables form one cluster in the loading plot and are therefore related to the same source: they reflect the combination of sea derived elements and anthropogenic
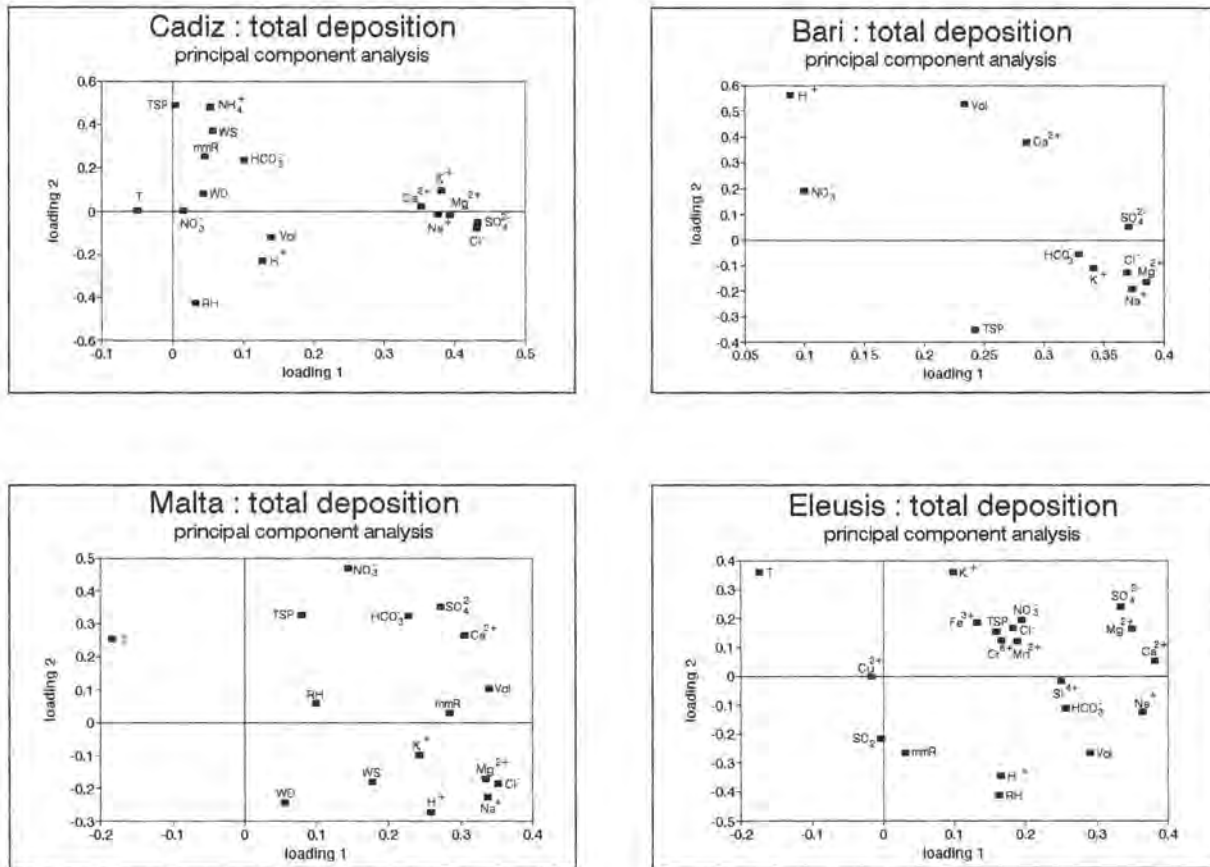
Figure 4   Loading plots of the deposition.

derived elements. The second factor is composed of TSP and NH_4^+ and negatively of the relative humidity. The temperature is slightly negatively correlated with the deposition of most ions. In Bari the first factor is composed of Mg^{2+}, Na^+, Cl^- and SO_4^{2-}. Na^+, Cl^- and Mg^{2+} form one cluster in the loading plot and reflect the action of one source: a marine source, while it seems the SO_4^{2-} originates from another source. The second factor is explained by H^+ and the volume. The first factor of the loading plot for Malta is formed by the volume, Cl^-, Na^+, Mg^{2+} and Ca^{2+}, the second factor is explained by NO_3^-. Na^+, Mg^{2+}, and Cl^- form one cluster, while HCO_3^-, SO_4^{2-} and Ca^{2+} form another cluster of variables. The temperature seems to be negatively correlated with Cl^-, Na^+ and Mg^{2+} (the lower the temperature the higher the deposition of these elements). The seasonal variation of Na^+, Cl^- and Mg^{2+} had already indicated that their deposition is highest during winter. In Eleusis the first factor is ex-

plained by Ca^{2+}, Na^+, SO_4^{2-} and Mg^{2+}. The second factor is composed of the temperature and K^+ content and negatively of the relative humidity and acidity. Ca^{2+}, Mg^{2+} and SO_4^{2-} form one cluster. This is the only sampling site where no cluster of Na^+, Mg^{2+} and Cl^- is found. Fe^{3+}, Cr^{6+}, Mn^{2+}, Cl^-, TSP and NO_3^- form one cluster of variables. Cu^{2+} seems not to be of any importance in the data matrix (close to the origin).

Generally the first factor is composed of Na^+, Mg^{2+}, Cl^- and Ca^{2+} and SO_4^{2-}, which are for some sites present in two clusters. This implies that these elements explain most of the variance in the data matrix, but they do not reflect the action of one source. For Bari, Malta and Eleusis, the acidity explains the second factor (together with the volume of the deposition in Bari). In Malta the second factor seems to be explained by some meteorological factors and NO_3^-. The first four factors explain around 60 to 70 % of the data sets.

3.3. Composition of aerosols

The average aerosol concentrations are given in Table 6.

For the outside aerosol samples, the sum of the 2 and 0.4 μm pore size filter is given. In Eleusis and Malta, concentrations are much higher than in Cadiz and Bari; the higher concentration level in Eleusis may be explained by the higher pollution level there. In Malta and in Cadiz the inside concentration is more or less the same as the outside concentration for most elements. At all sites, Cl, Ca, S, Fe and Si are the most abundant elements. The concentration of heavy metals is highest in Eleusis. When compared with the average aerosol composition near the cathedral in Mechelen (Belgium) [1], it seems that S and Pb are more abundant in Mechelen than in the Mediterranean region.

The contribution of sea salt and mineral dust to each element is assumed to be presented by the concentrations of indicator elements, which are Na and Al, respectively [15]. The extent to which the aerosol is affected by mixing with sea salt and crustal material is estimated using enrichment factors (Table 7 and 8).

Mg, Cl, S, K (for Cadiz), Br and Sr seem to originate mainly from the sea. Schneider [15] also observed that a part of Sr is sea salt derived. In Eleusis and Bari, Ca seems to be originated by sea water for the small particles, while for the large particles Ca is enriched to sea water. At the outside in Cadiz, Ca seems to originate from sea salt, while the aerosols at the inside are enriched to sea salt.

Si, Mg, Fe and Ti behave as non enriched elements to crustal concentrations, while the other elements are enriched to a variable extent. For most elements, the enrichment factors are larger for the small particles than for the large particle fraction. For Mg, K and Cr in Malta, the particles with a size bigger than 2 μm seem to originate from soil dust, while the small particles are enriched relative to soil dust. Correlation coefficients have also been calculated for the aerosols. At the inside of the cathedral in Cadiz, no correlation between elements, derived from the sea (Na^+, Mg^{2+} and Cl^-) is found. In Malta, to the contrary, this correlation is present (r=0.8). At all sites Na^+, Mg^{2+} and Cl^- are highly correlated in the aerosols, collected at the outside. This correlation is found in both fractions. Al and Si are correlated with other elements, derived from the soil (Ti, Fe, K) in the coarse fraction of the aerosols. In the fine fraction, to the contrary, this correlation is less observed.

	NO_3^-	Na^+	Mg^{2+}	Al	Si	SO_4^{2-}	Cl^-	K^+	Ca	Ti	V	Cr	Mn	Fe	Ni	Cu	Zn	Br	Sr	Pb
Cadiz : in	209	620	60	30	70	2090	900	80	680	5	3	1	4	107	1	11	14	3	1	16
out	603	2400	210	30	140	2050	2620	200	460	9	2	1	4	164	1	5	26	8	2	12
Bari : out	220	270	27	12	42	810	400	113	250	1	0	3	5	54	0	2	9	6	1	9
Malta : in	2400	4280	381	76	493	8080	6730	2290	5560	17	4	19	6	293	4	16	53	52	10	95
out	1510	3290	395	213	503	7470	4000	1400	6750	38	9	7	9	379	6	13	37	19	17	43
Eleusis : out	2650	1780	256	326	876	6500	2620	1350	6890	48	17	46	47	1390	17	20	115	26	17	89

Table 6   Average concentration of the aerosols (ng/m3).

Table 7	*Enrichment factors of aerosols vs. sea water (Na as indicator element).*							
	NO_3^-	Mg^{2+}	SO_4^{2-}	Cl^-	K^+	Ca	Br	Sr
Cadiz in	71	0.76	13	0.80	3.6	30	0.85	1.2
out	53	0.73	3.4	0.60	2.4	5.1	0.52	0.5
out 2	52	0.82	3.4	0.60	1.9	6.2	0.57	0.7
out 0.4	55	0.37	3.2	0.57	4.3	0.9	0.36	0.1
Bari out	210	0.90	13	0.79	13	29	3.1	3.5
out 2	270	1.0	13	0.65	11	34	1.8	3.2
out 0.4	77	0.65	14	1.1	19	2.1	3.9	2.1
Malta in	130	0.82	7.6	0.91	15	42	2.3	2.9
out	100	1.1	7.9	0.81	10	60	1.3	4.6
out 2	110	1.1	7.6	0.74	4.4	58	0.87	4.0
out 0.4	60	0.84	10	1.3	58	18	3.6	4.1
Eleusis out	320	1.2	14	1,8	22	100	2.4	7.9
out 2	560	1.6	24	19	20	170	3.3	9.0
out 0.4	110	0.82	12	2.1	25	2.7	2.2	8.7

Table 8	*Enrichment factors of aerosols vs. soil dust (Al as indicator element).*										
	Mg	Si	K	Ca	Ti	V	Cr	Mn	Fe	Ni	Sr
Cadiz in	7.3	0.75	18	150	3.1	95	11	13	8.3	57	9
out	26	1.41	42	95	5.3	55	11	14	12	49	15
out 2	23	1.39	27	92	5.3	55	7.9	14	12	49	15
out 0.4	0	0	0	0	0	0	0	0	0	0	0
Bari out	5.9	1.2	44	99	2.3	29	89	35	8.1	48	18
out 2	5.6	1.2	30	98	2.3	20	55	31	7.6	33	14
out 0.4	65	0.90	930	110	0	330	1300	190	28	620	160
Malta in	16	2.0	140	430	4.5	56	95	7.1	7.8	61	44
out	6.4	0.88	32	190	3.4	42	14	3.7	3.9	30	22
out 2	6.8	0.82	14	190	3.5	40	6.0	3.7	3.9	27	20
out 0.4	22	3.0	760	250	1.7	100	280	5.0	5.8	130	85
Eleusis out	2.8	0.78	25	130	2.6	44	58	14	9.1	59	14
out 2	2.7	0.87	16	140	3.0	38	33	11	8.7	40	12
out 0.4	85	1.8	1300	150	0	210	3800	260	40	2900	710

PCA has been performed on the data set. In Bari, the first factor is composed of Ca, Fe, Si and Al, material of terrestrial origin, while the second factor consists of sea salt (Na, Cl, Br). In Eleusis the first factor is explained by Ti, Ca, Ni, Al, Fe and Mn. The second factor is formed by Ca^{2+}, Cl^-, SO_4^{2-} and NO_3^-. For the aerosols at the inside of the church in Malta the first factor is composed of Fe, Si and K. The second factor is explained by Na, Cl, Mg and K. For the outside aerosol samples the first factor may be explained by Mn, Fe, K, Ca, Al, Si, Ti and Sr. The second component is explained by the temperature and negatively by Cl^-, Na^+ and NO_3^-. Again 60 to 70 % of the data matrix is explained by the first four factors.

The results can be generalized as follows: for most sites, the first factor contains for most sites elements originated from soil, mixed with elements from anthropogenic activities, while the second factor, which explains less of the variance, is composed of marine elements. In Bari and at the inside of the church in Malta, the first factor is composed of almost only terrestrial elements. Only in Eleusis the second factor is not formed of sea derived elements. Eleusis is the only site where concentrations of most elements are negatively correlated with the relative humidity and the rain fall amount (mmR).
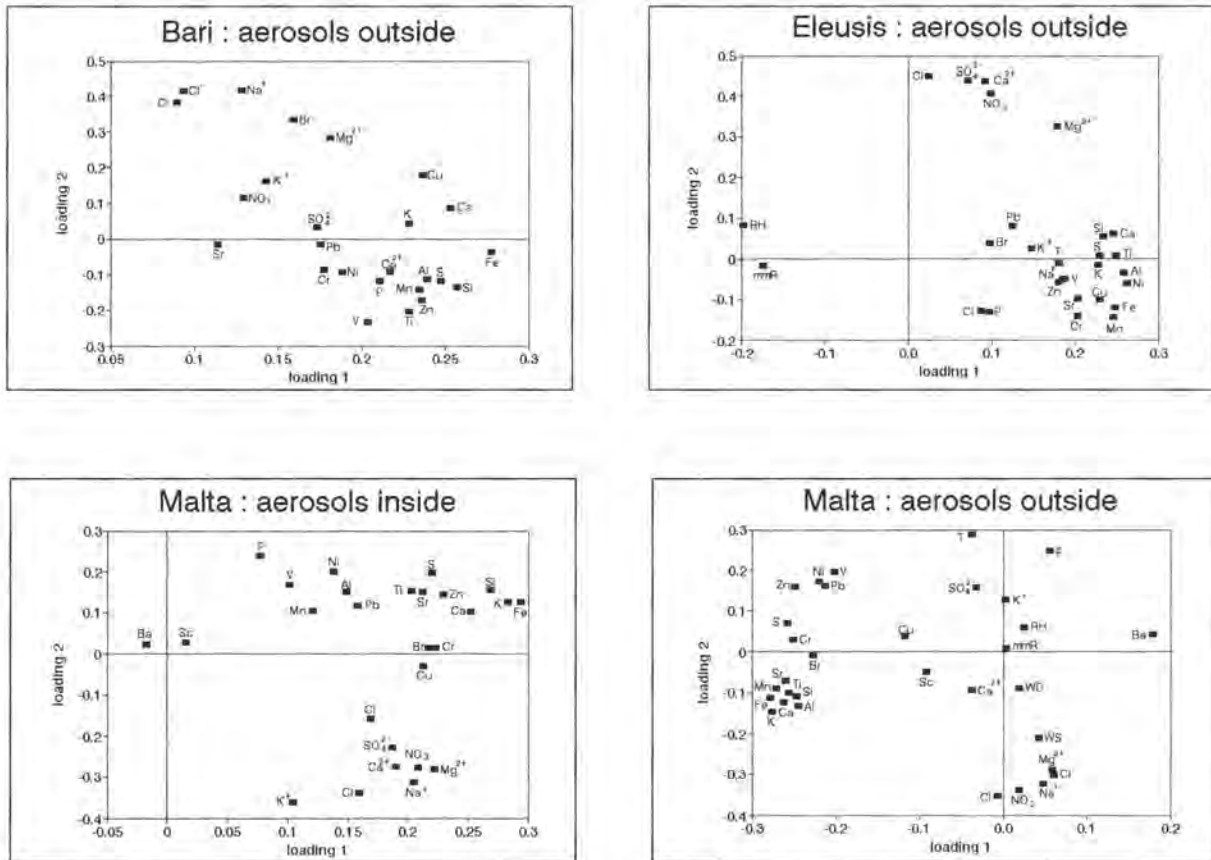
Figure 5 *Loading plots of the aerosols.*

4. Conclusions

The spatial trends in concentrations of ions in the total deposition samples and aerosols are for some elements similar. The Na⁺ concentration is highest in Malta for both the aerosol and total deposition samples, the highest SO_4^{2-} concentration is observed for aerosols and total deposition in Eleusis. Malta and Eleusis have highest Ca^{2+} concentration in aerosols and deposition. The highest deposition of Na⁺ and Cl⁻ is found in Cadiz, while for the aerosols Na⁺ and Cl⁻ are highest in Malta and only second highest in Cadiz. Pratt and Krupa [16] also observed that only selected components were significantly correlated between wet deposition and aerosols.

The results of the stone crusts analyses can be compared with the results of the deposition and aerosol composition at the respective sites. The highest Na⁺ concentration in the stone samples reflects also the highest Na⁺ concentration in the total deposition samples: Cadiz and Malta. The highest Cl⁻ deposition has been found in the total deposition in Malta and Cadiz; in Malta the stone samples contain high Cl⁻ concentration as well; while in Cadiz the stone samples did not show high Cl⁻ content. The highest SO_4^{2-} deposition is found in the total deposition in Eleusis; at this site, the stone crust is highly enriched in SO_4^{2-}. In the crust samples from Bari, a high SO_4^{2-} content has been observed as well; this corresponds, however, not to a high SO_4^{2-} content in the deposition samples. The sulphate in the stone

may be formed under influence of gaseous SO_2. Very high concentrations of Ti, V, Cr, Mn, and especially Fe were found in the crust samples from Eleusis. These elements are also most present in the aerosol samples at that site. In the stone samples from Malta, a high concentration of Fe was observed in comparison with the stone samples from Bari and Cadiz; in Malta also a quite high concentration of Fe was found in the aerosol samples. Cl and Na are present at high concentration in the stone samples from Malta and also in the aerosol samples at that site. SO_4^{2-} concentration is highest in the stone samples from Bari and Eleusis, for the aerosol samples the highest SO_4^{2-} concentrations were found in Malta and Eleusis. This can be explained by the fact that not aerosols, containing SO_4^{2-}, are the most important factors causing gypsum formation on the stone, but gaseous SO_2.

The enrichment factors to estimate the sea water contribution for the stone samples indicate that Ca^{2+}, K^+ and SO_4^{2-} are not generated by the sea. For the stones, aerosols and deposition samples it is observed that the Cl^- and Mg^{2+} content mainly originate from the sea.

The stones from Malta and Cadiz show the highest influence from the sea, although the church in Malta is situated 3 km from the coast, while the stone samples from Bari and especially Eleusis seem to be more affected by anthropogenic emissions. The surrounding atmosphere explains quite well the observations of the stones analyses.

5. Acknowledgement

6. References

1 Leysen L., Roekens E. and Van Grieken R., Air–pollution-induced chemical decay of a sandy–limestone cathedral in Belgium, Sci. Tot. Env. 78, 263–287, 1989.

2 Fassina V., A survey of air pollution and deterioration of stonework in Venice, Atmos. Environ. 12, 2205–2211, 1978.

3 Zezza F. and Macri F., Marine aerosol and stone decay, Sci. Tot. Env. 167, 123–143, 1995.

4 Moropoulou A., Theoulakis P. and Chrysophakis T., Correlation between stone weathering and environmental factors in marine atmosphere, Atmos. Environ. 29, 895–903, 1995.

5 Zezza F., Marine spray and polluted atmosphere as factors of damage to monuments in the Mediterranean coastal environment, European Cultural Heritage Newsletter on Research vol. 7 no. 1–4, 49–52, 1993.

6 Zezza F. (Ed.), 1st Semestrial Report ; "Marine spray and polluted atmosphere as factors of damage to monuments in the Mediterranean coastal environment", R & D Programme in the Field of Environment, Contract No EV5V–CT92–0102, 79 pp., 1993.

7 Van Espen P., Janssens K. and Nobels J., AXIL–PC software for the analysis of complex X–ray spectra, Chemometrics and Intelligent Laboratory Systems 1, 109–114, 1986.

8 Arnold A. and Zehnder K., Salt weathering on monuments. Proc. 1st International Symposium on The Conservation of Monuments in the Mediterranean Basin, Ed. F. Zezza, Grafo, Bari, 31–58, 1989.

9 Sabbioni C., Contribution of atmospheric deposition to the formation of damage layers, Sci. Tot. Env. 167, 49–55, 1995.

10 Mason B., Principles of Geochemistry, 3rd Ed., p. 329, J. Wiley & Sons, New York, 1966.

11 Vleugels G., Weathering of bare and treated limestone under filed–exposure conditions in Belgium: study of the runoff water from micro–catchment units, Ph.D. dissertation, University of Antwerp, 1992.

12 Loye–Pilot M.D., Martin J.M. and Morelli J., Influence of Saharan dust on the acidity and atmospheric input to the Mediterranean, Nature 321, 427–428, 1986.

13 Roekens E., Komy Z., Leysen L., Veny P. and Van Grieken R., Chemistry of precipitation near a limestone building, Water, Air and Soil Pollution 38, 273–282, 1988.

14 Alaimo R., Deganello S., Di Franci L., Montana G., Caratteristiche composizionali del partiolata solido atmosferico e chimismo delle acque di precipitazione nell'area urbana di Palermo. Proc. 1st International Symposium on The Conservation of Monuments in the Mediterranean Basin, Ed. F. Zezza, Bari, Grafo, 369–377, 1989.

15 Schneider B., Source characterization for atmospheric trace metals over Kiel Bight, Atmos. Environ. 21, 1275–1283, 1987.

16 Pratt G. and Krupa S., Aerosol chemistry in Minnesota and Wisconsin and its relation to rainfall chemistry, Atmos. Environ. 19, 961–971, 1985.

Vasco Fassina

Neoformation decay products on the monument's surface due to marine spray and polluted atmosphere in relation to indoor and outdoor climate

Neoformation decay products on the monument's surface due to marine spray and polluted atmosphere in relation to indoor and outdoor climate

V. Fassina
Laboratorio Scientifico–Soprintendenza ai Beni Artistici e Storici di Venezia
Canaregio 3553, Venice, Italy

1. Introduction

As the Coordinator explained in his introductory communication the project was focused mainly on the role of marine spray and atmospheric pollution in the processes of weathering on monuments of the Mediterranean Basin.

The project considered four pilot monuments located along the east–west axis of the Mediterranean. The monuments concerned show different problems of weathering related to their different geographical and topographical position.

In order to obtain some general common informations it was decided to make an environmental monitoring by recording internal and external air temperature and relative humidity in three sites (Santa Marija Ta' Cwerra church in Malta, Cathedral of Cadiz, Cathedral of Bari) which presented similar problems.

In order to evaluate the influence of marine spray and pollution on the decay of stone internally and externally on the pilot monuments, it was thought essential for the objectives of the project, to correlate the microclimate with decay phenomena taking place on the surface and in the interior parts of the stone. The internal climate of the buildings plays a fundamental role in the conservation of a monument. It is determined by local meteorological and climatic factors, by the characteristics of morphology and construction and by the urban environment in which the monument is located.

A thorough knowledge of the stone decay phenomena was obtained through the continuous monitoring of the atmospheric parameters that affect the conservation of monuments. In this way it is possible to determine the duration of the situations that are correlated with the phenomena of deterioration. In order to deduce the interactions between the indoor atmosphere and the stone surface, measurements were carried out in the air layer close to the wall surface. Changes in the characteristics of the air near the wall surface are caused both by the interaction between masonry surface and indoor environment and by mixing with the external air. Carefully positioned probes were therefore taking precise measurements in the air layer close to the wall surface for the measurement of the thermo–hygrometric parameters of stone surface temperature, air temperature and the relative humidity of the air.

On the contrary in the archaelogical site of Eleusis, being an open site, it was not necessary to record temperature and relative humidity.

As regards total deposition from the atmosphere it was decided to install in all four pilot monuments an equipment consisting of a polyethene collection bottle, funnel and metal supporting stand provided by the team of Antwerp. Rainwater in the polythene bottle was collected on a weekly basis.

In the case of Bari Cathedral it was realized a continuous wet and dry deposition sampler ad hoc studied by the team of Venice. The sequential apparatus was collecting dry deposition during dry period and when started to rain the device allowed to take different rainwater samples during meteoric event by separating different rainwater fractions according

to the volume collected. Data obtained for each fraction show us the evolution of chemical composition during each event. The different concentration measured during each event of precipitation allow us to establish the variability of rainwater composition with previous meteorological conditions and wind direction provenance.

2. Description of sites

The Cathedral of Cadiz is situated at the furthest western limits of the Mediterranean area, affected by Atlantic conditions similar to those found in the western part of the Mediterranean. The Cathedral is built by three types of stone: Mesozoic oolitic limestone, quaternary calcarenite and marble.

The latter is suffering a marked decay. The urban and geographical position of the city of Cadiz, the absence of polluting chemical industry or excessively congested traffic and the exposed position of the Cathedral on the sea presents an example of a monument which suffers above all the effects of marine aerosol. The vaults of the building were suffering severe fissures and detachments due to salt crystallisation.

The Cathedral of Bari is exposed to a marine environment influenced by prevailing winds from the north and south–east. The monument suffers above all from the effects of chemical and physical factors, in particular the corrosion of the exposed surface (alveolization), efflorescences, exfoliation of sculptured parts and black crust formation on the external facade.

The church of St. Maria Ta' Cwerra is located in the village of Siggiewi in the south–west of Malta, at a distance of 3 Km from the sea at the nearest point. It represents a monument at the centre of the Mediterranean in a typical marine environment at the perimeter of both the northern and southern coasts of the Mediterranean and in a location where there are no signifi-

cant effects due to atmospheric pollution. The church is built in Globigerina limestone. All four walls show severe deterioration on the external parts. In particular, pronounced alveolar weathering is found, as well as powdering of several areas; much of the mortar in the joints has been lost and the blocks have in many cases lost several millimetres from their surfaces. There is also even more severe decay inside the building, to the extent that some of the carvings have almost completely disappeared.

The only site which is located in a typical urban industrial environment is the Sanctuary of Demeter in Eleusis. It is characterised by an intense industrial activity and it is also affected by climatic conditions which favour photochemical pollution in an atmosphere highly charged by suspended particles. Research on this site is therefore indicative of the effect of pollution on stone decay.

3. Experimental procedure

Chemical analysis such as ion chromatography, atomic absorption and emission spectrometry (AAS/AES) and energy dispersive X-ray fluorescence (EDXRF), scanning electron microscopy (SEM) and microanalysis (SEM-EDX) and electron probe micro-analysis (EPMA) on the stone samples from the four pilot monuments were performed.

Ion Chromatography and AAS/AES were used to determine qualitatively and quantitatively the soluble salts present.

SEM–EDS analyses of the weathered stones and crusts were performed to extract conclusions on the environment-materials interactions taking place on the monument surfaces and in depth.

X–ray diffraction analysis was performed in order to check whether an interrelation exists on crystalline phases and possible transformations between dust and suspended particles depositions and surface encrustation (cementitious crusts).

*Neoformation decay products on the monument's surface due to marine
spray and polluted atmosphere in relation to indoor and outdoor climate*

41

4. Discussion of results

The knowledge of the occurrences of salts in the four pilot monuments is of great interest when we intend to correlate inner micro climate conditions with the behaviour and response of walls (and inherent stone decay). In fact to establish boundary conditions based on the large amount of meteorological data gathered implies, among other parameters, to know the crystallisation and dissolution cycles of soluble salts.

The identification and distribution of salts in our four monuments allowed us to identify: sulphates, nitrates, carbonates, chlorides and oxalate. Knowing the behaviour of these salts regarding temperature and relative humidity it is possible to derive some more reliable correlations among crystallisation and solubilization cycles. (fig. 1)
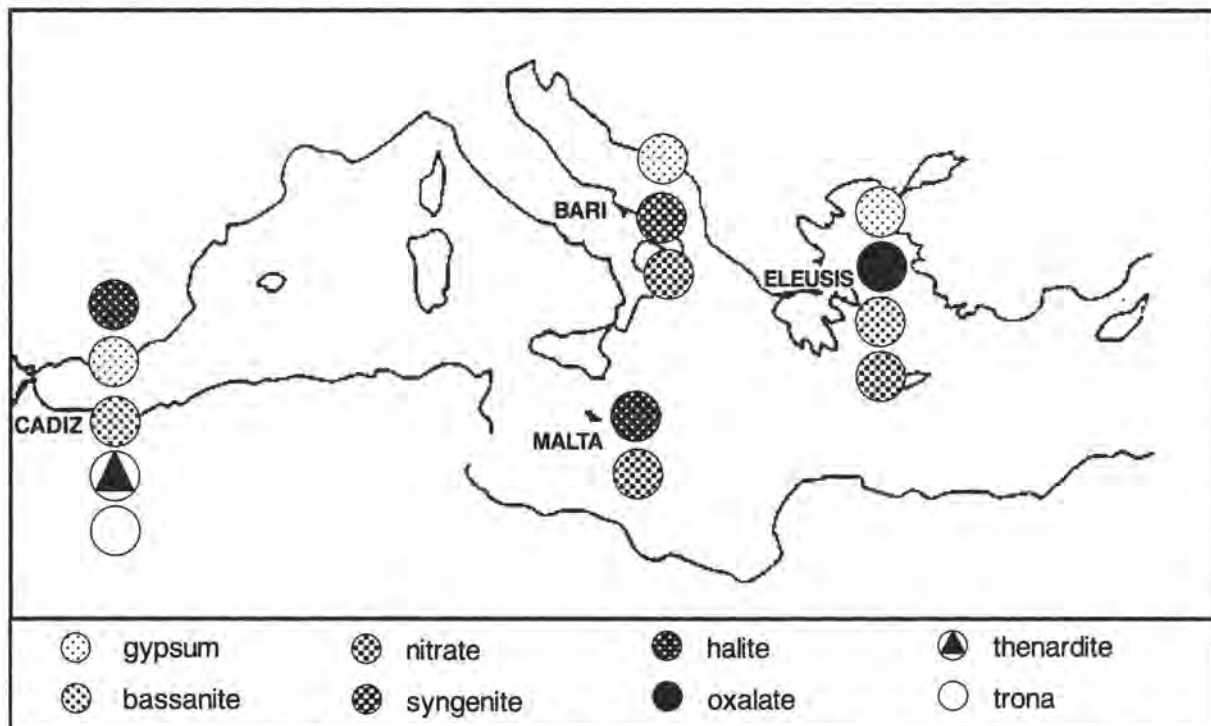
Fig.1 *Salts occurrences in Eleusis (Greece), Cathedral of Bari (Italy), Cathedral of Cadiz (Spain) and in Sta. Marija Ta' Cwerra Church (Malta)*

a) Cathedral of Bari

The phenomena of decay that were observed on the blocks of wall of the Cathedral and on the sculptured surfaces, belong essentially to the following typologies, all linked to chemical and physical factors (six–month report n.1 June 1993):

— *corrosion of the exposed surfaces (alveolization) and crumbling,*

— *detachment of chips and exfoliation,*

— *efflorescence,*

— *exfoliation of layers of scialbatura on the surface of the blocks,*

— *fissuring and detachment of sculptured parts (arches and capitals),*

— *black crusts found on the external facade, especially in correspondence with the marble posts of the portal.*

Samples taken from the Cathedral were characterised by white efflorescence, white powder, white flakes with black deposits, brownish powder, greyish powder, greyish layer covering rock sample.

According to results obtained by Van Grieken team (six–month report n. 3, June 1994) bulk analysis by EDXRF shows that calcium is the most important element in all samples. No high concentrations of ions have been found in the leach ate. Calcium is the main action. Sulphate and chloride are the most important anions. Depth profile analyses from samples 24 and 30 have been measured. Although in the sample description, it has been stated that bacup 24 possibly comes from a recent and bacup 30 from an original block, the crust in sample bacup 24 seems to be thicker than the crust from sample bacup 30. Si, Fe, K, and Al are the most abundant elements in both samples.

According to results obtained by Aires Barros team XRD and IR spectroscopy show the presence of calcite in all samples and gypsum in samples bacup 28, 38, 39 (table 1). Block of limestone show frequently residues of scialbo from previous conservative treatments.

Dry deposition in Bari indicated a good correlation among magnesium, sodium, and chlorides. By comparing these data with the chemical composition of water in the Mediterranean Sea it is possible to ascribe the origin of these ions to water of the sea. As regards calcium and sulphates it seems evident an anthropogenic origin. The acidity is correlated to sulphate.

As regards the micro structure investigation carried out by Fitzner team (six–month report n. 4, December 1994) in porous micritic parts, large pores of irregular shape can be seen, which are probably due to dissolution. Partly sparite has grown in the pores. In micritic limestone halite, partly in the form of octahedral crystals, was not very frequently found (fig.2). Cubic and octahedral halite crystals grown on the surface of the low porosity micrite. Gypsum crystals with inter crystalline porosity in highly porous mortar was found. Halite and Sylvite in highly porous mortar were also found.

Tab. 1

SAMPLE		CALCITE		GYPSUM		SYNGENITE		SILICATES		NITRATES	
	MINERALS & PRODUCTS	XRD	IRS	XRD	IRS	XRD	IRS	XRD	IRS	XRD	IRS
BACUP 28	Global sample	+++	+++	++	++	—	—	v	v	—	v
	Cream flake	++	+	+++	+++	—	—	—	—	—	—
BACUP 29 White efflorescence		+++	+++	—	v	—	—	v Qz	v	—	—
BACUP34 White powder		+++	+++	—	—	—	—	v Qz	v	—	—
BACUP 35 White fine powder		+++	+++	—	—	+	—	—	v	—	—
BACUP 37 White flakes with black crusts		+++	+++	—	—	++	++	v Qz	—	—	v
BACUP 38 Brownish powder		+++	+++	++	+	—	—	v	—	—	—
BACUP 39 Greyish layer		+++	+++	++	—	—	—	—	—	—	++
BACUP 39 Greyish layer covering rock sample		+++	+++	++	+	—	—	—	—	—	++
BACUP 42	White powder	+++	+++	—	+	—	+	—	v	—	—
	Greyish powder	—	+++	—	—	—	—	—	v	—	—
BACUP 43 White powder		+++	+++	—	+	—	—	—	v	—	—
BACUP 44 White spongy powder		+++	+++	—	—	—	—	v Qz	—	—	—
BACUP 45 White powder		+++	+++	—	—	—	—	—	v	—	—
BACUP 46	Yellow powder in fractures	+++	+++	—	+	—	—	+	—	—	v
	Greyish powder on flakes	+++	+++	—	v	—	—	—	—	—	—

+++ very much abundant   ++ abundant   + present   v vestigial

*Neoformation decay products on the monument's surface due to marine
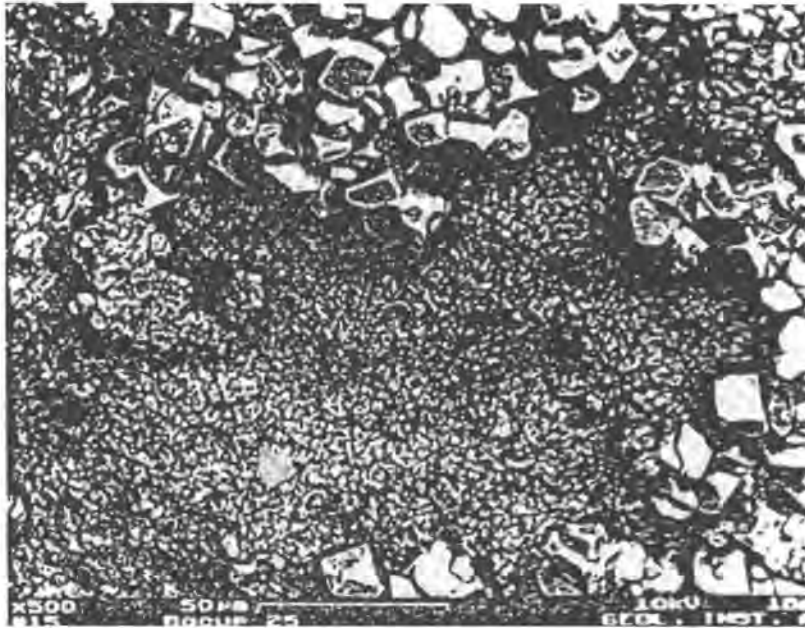spray and polluted atmosphere in relation to indoor and outdoor climate*

43

Image width: 0.23 mm

*Cubic and octahedral halite crystals
grown on the surface of the low
porosity micrite. Larger pores are very
rare.*

Fig.2   Sample: BACUP 25, Limestone

According to Fitzner computerised analysis of
the different decay forms it is possible to make the
following classification: black crusts, granular deseg-
regation, detachments run–off areas, exfoliation.

As regards Bari Cathedral environmental
monitoring the principle objective was to study
condensation phenomena and the deposition of
aerosols. The system installed comprises a net-
work of probes for measurements of the surface
temperature of stones, of internal air tempera-
ture and relative air humidity and of external
air temperature and relative air humidity. For
this first phase of the environmental monitor-
ing the position chosen for the measurements
points was the vertical left section inside the
Cathedral where the most severe decay phe-
nomena due to humidity were found.

Instead of carrying out the monitoring in
a series of brief periods such as a week in each
season, a continuous monitoring lasting two
years was planned which was enable seasonal
and daily cycles to be recognised. The installa-
tion of the probes in different locations along

the whole vertical section of the Cathedral al-
lows the step by step description of:

— *the stratification of the air in the interior
atmosphere,*

— *the evolution in time of the specific hu-
midity,*

— *the identification of the areas where this
evolution is more evident.*

The distribution of thermo–hygrometric
parameters in a vertical section of the church
allows the evaluation of the thermal behaviour
in different locations, thus showing the occur-
rence and frequency of situations which are
dangerous for the stone decay. As is shown in
fig. 3 the probes were positioned at three dif-
ferent heights:

— *in correspondence with the arch of the left
nave,*

— *in correspondence with the base of the
main arch below the dome,*

— *in the dome, under a window.*

Also concerning the study of the internal
micro climate of Bari Cathedral, seasonal sam-
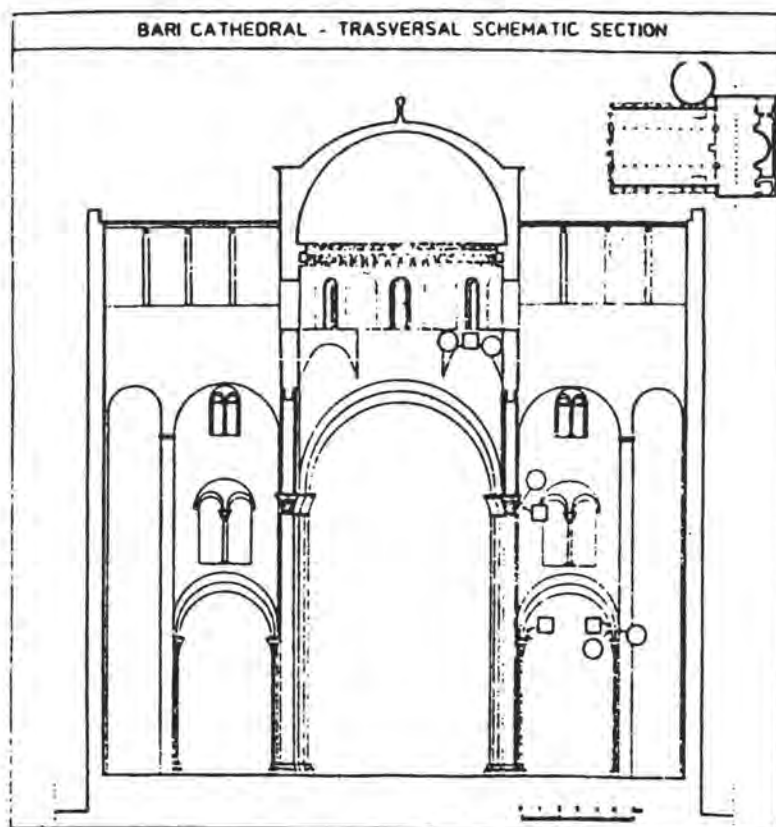
Fig. 3. Position of probes of the microenvironmental monitoring station installed in the Cathedral of Bari

O *Surface temperature probes*

☐ *Air temperature and relative air humidity probes*

Tab. 2

CHEMICAL	DECEMBER 1992			MARCH 1993			JUNE 1993			SEPTEMBER 1993		
PARAMETERS	1 *	2 *	3 *	1	2	3	1	2	3	1	2	3
Specific conductivity (us/cm)	82.7	91.7	68.7	102.9	82.1	99.5	226	96.9	106.1	82.8	73.1	107
Ca++ (mg/l)	7.2930	4.6438	3.5661	12.0411	52.83	5.981	35.8605	8.3821	12.7765	3.642	3.330	16.610
Mg++ (mg/l)	0.4637	0.2406	<0.05	0.337	trances	0.151	2.1098	0.4238	0.3972	abs.	abs	0.071
Na+ (mg/l)	2.0790	2.7465	1.6221	0.033	4.451	3.777	5.5444	2.3456	3.3047	2.905	2.708	1.440
K+(mg/l)	3.7987	4.5853	2.9477	2.987	3.639	4.545	2.8585	1.5934	2.5294	4.096	3.338	1.295
NH4+(mg/l)	4.2097	5.2360	4.3022	5.110	6.855	7.930	5.5873	5.8470	8.3198	5.677	5.200	5.276
HCO3-(mg/l)	44.915	48.378	35.391	56.137	43.933	48.815	84.816	45.764	61.019	34.171	31.730	68.341
CO3-(mg/l)	abs.	abs.	abs.	abs.	abs.	abs.	abs.	abs.	abs.	abs.	abs.	abs.
CI-(mg/l)	3.207	4.311	2.636	4.2069	4.0791	5.4814	7.059	3.0647	5.1288	3.875	3.502	2.037
SO4-(mg/l)	2.648	2.615	1.498	4.5277	2.2971	2.6640	43.4359	3.2272	4.0121	1.801	1.564	1.906
NO3-(mg/l)	0.760	0.609	0.618	0.8129	0.4616	0.6650	2.5355	0.7300	1.0324	0.453	0.544	0.511
NO2-(mg/l)	1.591	1.910	1.915	1.9704	2.3866	2.8562	1.0905	1.1836	1.3718	0.714	1.006	0.276

Neoformation decay products on the monument's surface due to marine spray and polluted atmosphere in relation to indoor and outdoor climate

45

ples have been taken of the condensation waters inside the building in order to study their reactivity in relation to the stone of the internal walls of the Cathedral.

These samples were taken at different heights that are approximately the same as those at which the thermo–hygrometric probes were positioned (table 2).

b) Cathedral of Cadiz

The location of this Cathedral near the sea implies a continuous renewal of air swept in by the wind as well as a strong marine aerosol action originated from the sea and transported by dominant and continuous winds that are always blowing.

According to Galan team (six–month report n. 1, June 1993) the main problem suffering the Cathedral of Cadiz is due to the advanced decay of the vaults which are continuously loosing large fragments of stone due to salt crystallisation. To prevent such "hailstones" a protective net was installed above the cornice, just below the ceiling.

The foundations and the crypt, which are very porous stone, are acting as sponges to sub–soil humidity causing migration of soluble salts by capillary rising damp into the walls. The structure of the very porous "ostionera" stone building represents the second way of access by humidity and salinity.

The third path has been for a long time the roof of the dome without doubt one of the main access routes towards pendentives, arches and smaller walls of the building. The leaching water through the vaults has now been prevented by the restoration work. The ochre coloured lime mortar, which cover the "ostionera" stone of the central dome, was split and loose until the present restoration. The most important salts, because of their high concentrations and roles in the mechanism of alteration, are sodium carbonate and sodium sulphate, the content of the latter increases at ground–levels.

Chlorides are of significant importance on the exterior of the cathedral, but it is estimated that nitrates play a minor role in the alteration. The decay mechanisms are produced by the increase in capillary and interstitial volumes caused by the hydration and crystallisation of salts.

Carbonate as well as sulphate can hydrate with 10 water molecules during moist period, it is at precisely this point of the cycle when the majority of fragments fall into the protection nets.

Different materials show different morphology of decay, in fact limestone suffer much spalling especially near building–block joints, in which the mortar acts as a solution pathways and salt reserves, the vaults, which are continuously loosing material, are the most damaged.

The marble show much chipping and contour scaling, implying a frontal attack. When relative humidity level rises, deliquescence of sodium carbonate deposited in small fissures occurs, crystallising when dehydrated, raising the pressure in stone's pores.

These decay phenomena occurring in the marble affect the whole building, being most serious in the crypt and the plinths and bases of the columns. The bio–calcarenite "ostionera" is preserved well, other calcarenites show grain disintegration by the action of the salts.

Sampling from scaling as well as from salt efflorescence in the crypt were collected by Aires Barros team and studied (six–month report n. 2, December 1993). Three rock samples analysed show the presence of calcite and halite.

Two samples of salt efflorescence from the crypt show the presence of gypsum, bassanite, thenardite and trona (table 3).

Trona is present in aciculate crystals in globular aggregates. The condensation water sampling was carried out at two different levels in the interior of the Cathedral as near as possible from the wall by using a cooled panel.

Table 3   *Efflorescences*

Type of sample	XRD	and	IRS*
CA 3 Grey–greenish sample with layered structure (see representation in Fig. 26 and Fig. III)	CA 3.1 – gypsum (++), bassanite (++), CA 3.2 – calcite (+), gypsum (+), CA 3.3 – gypsum (++), bassanite (++), CA 3.4 – calcite		thenardite (++), calcite (v) calcite (v)
CA 3 White powder (see Fig. III)	Trona in acicular crystals in globular aggregates.		

+++	–	predominant	
++	–	abundant	
+	–	present	
v	–	vestigial	
*	–	see Fig. III	

Salt efflorescences

$$\left\{\begin{array}{lll} \text{gypsum} & - & CaSO_4\text{--}2H_2O \\ \text{bassanite} & - & CaSO_4\text{--}1/2H_2O \\ \text{thenardite} & - & Na_2SO_4 \\ \text{trona} & - & Na_3H(CO_3)_2.2H_2O \\ \text{halite} & - & NaCl \end{array}\right.$$

c) Santa Marija Ta' Cwerra–Malta

According to Cassar and Torpiano (six–month report n. 1, June 1993) the external wall of the church were not plastered, which is quite a usual situation for Malta. However, at some point in the past the lower course were coated with a cement–based mix, probably in an attempt to stop deterioration in this area.

All four walls of the church show severe deterioration on the external faces, for about two–thirds of the height. The lower courses, as already stated, are cemented over and therefore could not be examined. The middle courses are, however, badly deteriorated, mostly in the form of pronounced alveolar weathering of many of the stones, as well as the powdering of several areas; many of the blocks have also lost from the joints area. The uppermost courses, on the other hand, are much better preserved, the stone appearing quite sound, and having developed a red–brown patina quite typical of local building stone. There are, however, areas, particularly in sheltered locations, of black crust formation.

The walls are also severely deteriorated on the interior, up to the height of the cornice. The walls here are plastered, but in several areas the plaster has fallen away revealing powdering and flaking stone underneath. Some of the decorative elements in stone are also badly deteriorated, to the extent that the carvings in some places have almost completely disappeared. In general, the inside of the church appears to be more severely deteriorated than outside, occurring also to a greater height.

In order to ascertain the process of weathering it was decided to survey continuously the internal micro climate to put in relation the interaction of environmental parameters with the stone surface processes of decay which were taking place. Moisture and salt contents in the wall masonry were also investigated to individuate if other phenomena like rising damp were active in the weathering of stone surface. Moreover the nature and origin of efflorescence present on the internal surface was also investigated.

As regards the rising damp phenomenon two sampling campaigns (third and fourth campaign) were carried out in different times. During the third campaign core samples were taken at four levels from the ground floor and at two depths (superficial 0–5 cm, interior 5–15 cm). Moisture content shows a decreasing trend according to the increase of height and it is practically ceasing at 3–4 meters. Comparison of moisture content at each level generally shows higher values for samples taken at 5–15 cm of depth with respect the superficial ones.

Neoformation decay products on the monument's surface due to marine spray and polluted atmosphere in relation to indoor and outdoor climate

47

The highest moisture value measured was 12 % at 50 cm of height and 5–15 cm of depth, in the north wall.

As regards anions in wall masonry sulphate are mainly concentrated in lower parts of the walls, while chlorides and nitrates in upper levels. This is a typical distribution previously observed by other authors in other monuments. Salts, dissolved in the water inside the walls, are transported vertically by capillary rising damp. When water evaporates there is a fractionate precipitation of different salt phases, according to their solubilities.

Sulphates remain at lower levels because they have a low solubility.

The highest amount of anions were found in the south wall:

— *chlorides have their maximum value of 3,57 %, at 2.5 m of height and 0–5 cm of depth,*

— *nitrates reach the maximum of 1,49 % at same level and depth,*

— *sulphates show the maximum value of 1.65 %, at 0.5 m of height and 0–5 cm of depth.*

During fourth campaign only two levels: 0.5 and 2.5 cm from the ground were considered. The highest moisture value was 12,8 %, in the north wall, at 0.5 m of height and from 5 and 15 cm of depth. In both campaigns, for the other walls, the moisture reached maximum values between 8 and 9 % at 50 cm of height. As regards anions, in this campaign their values were generally lower than in the third campaign. This very probably could be ascribed to different meteorological conditions, occurred before sampling campaigns. Chlorides have their maximum concentration of 1,35 % at 250 cm of height and 0–5 cm of depth in the west wall, nitrates reach 0,88 % at the same height and depth of the north wall, sulphates reach 0,24 % at 0.5 m of height and 0–5 cm of depth in the east wall.

As regards nature and origin of efflorescence three campaigns were carried out.

XRD analyses show the presence of halite (NaCl) on the south, east and west walls, while on north wall thenardite (Na_2SO_4) was found. In fourth campaign XRD analyses have been carried out on 16 samples. Calcite was found in all samples due to the stone or mortar presence in the powder analysed. The same origin is ascribed to the quartz, which is present in low amount almost in all samples. Saline efflorescence mainly consist of halite crystals which are of marine origin. Halite is present in 12 samples in small or discrete amount. The other mineralogical phases found are:

— *gypsum which is present in four samples probably due to gypsum plastering;*

— *thenardite which is present in two samples probably from cement;*

— *mirabilite and trona which are present in the same sample (31A/95), are also probably from cement as thenardite.*

Diffractometric results closely correspond to the chromatographic one. Nitrates represent the only problem. In fact nitrates are found even in high percentage (around 4%) with chromatographic analyses, while they are not recognised with diffractometric analyses. This is probably due to the equilibrium relative humidity low values characteristic of nitrocalcite (RH=50.0% at T=25° C) and nitromagnesite (RH=52.9% at T=25° C. Amorosso and Fassina, 1983), which determine the solution of these salts in a higher relative humidity ambient.

With regard to crystallisation pressures, halite is the most dangerous salt. According to Winkler (1975) data, with an hypothetical C/Cs = 2, where C is the actual concentration of the solute during crystallisation and Cs is the concentration of solute at saturation, and T = 0° C, the halite crystallisation pressure is 554 atm, while the gypsum one is 282 atm, the thenardite one is 292 atm and the mirabilite one is 72 atm. On the other hand if
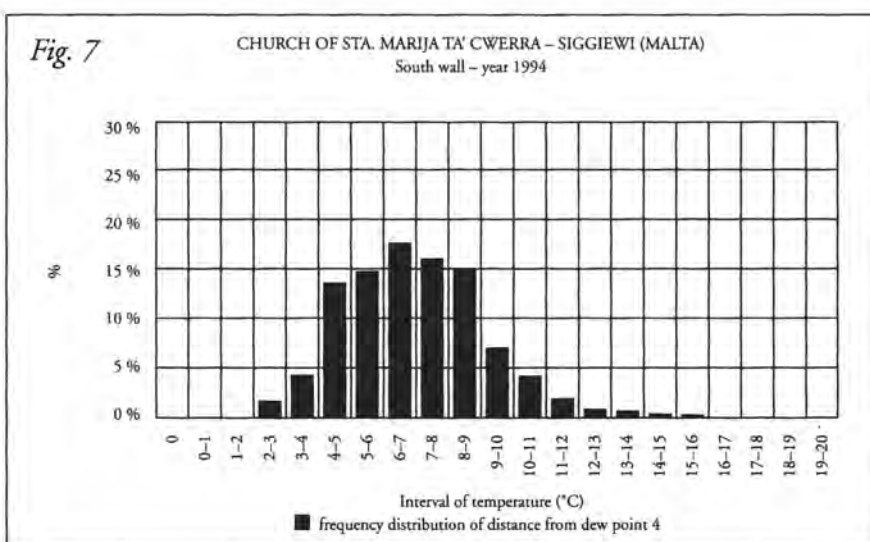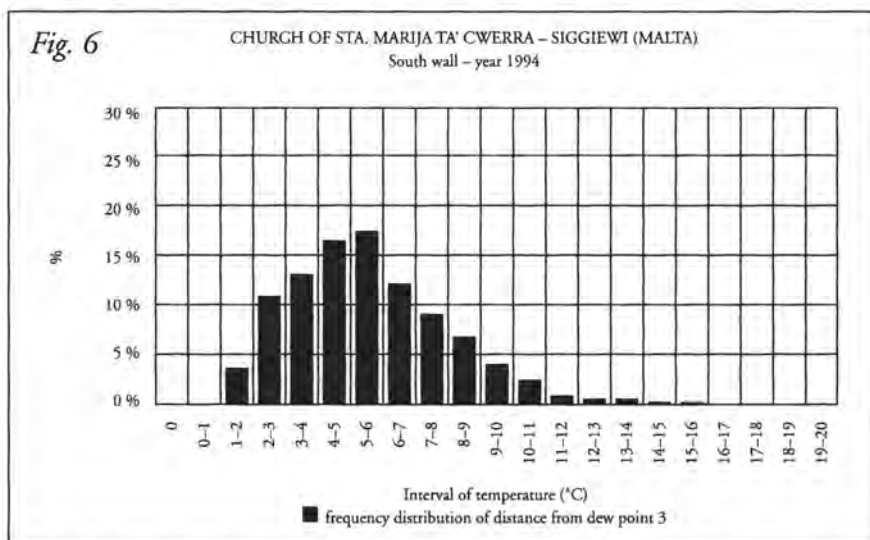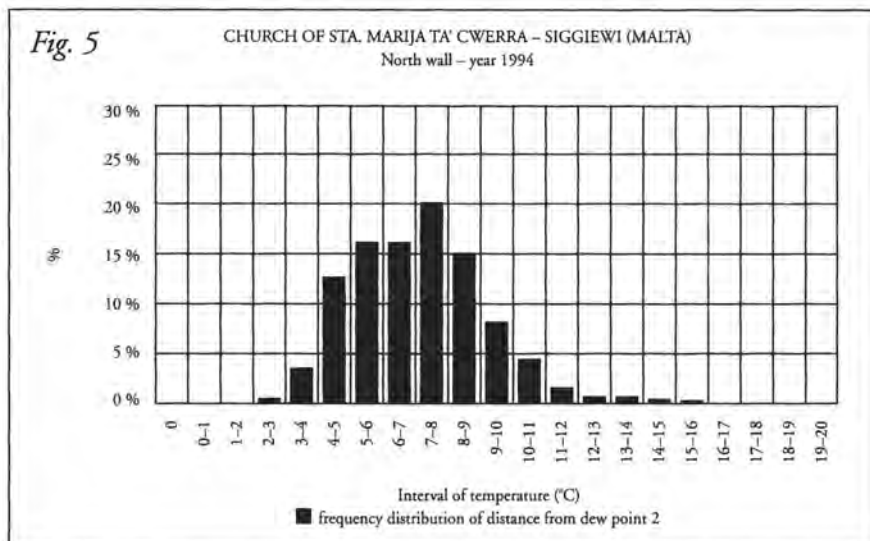
we consider the molar volume, mirabilite with a $Vm = 220$ cm³/mole is the most dangerous salt. Halite has a $Vm = 28$ cm³/mole, gypsum a $Vm = 55$ cm³/mole and thenardite a $Vm = 53$ cm³/mole. In this specific case, moreover, we found mirabilite and thenardite together in the same sample. That would seem to show that phase transitions between the anhydrous and the hydrate forms easily occurs in the stone, producing hydration pressure in the pores that is particularly effective because of the rapidity of the change. The transition of sodium sulphates thenardite to mirabilite is more rapid than hydration of other salts: it takes about 20 minutes at 39° C.

As regards environmental monitoring on south and north wall 4 probes measuring surface temperature were placed at different heights. In correspondence to the same positions 4 couples of probes measuring temperature and relative humidity were installed. By comparing the surface temperature and the air temperature close to the surface it is possible to calculate the probability of occurrence of condensation phenomena (figs. 4,5,6,7). During 1994 year location 3 on the south wall showed most chances to have condensation phenomena. On the contrary on north wall the probability was inferior. In any case the probability to reach condensation is very low. The only possibility could be the presence in the atmosphere of sodium chloride aerosols particles which can cause the formation of solution at relative humidity higher than 75% which is the equilibrium relative humidity of sodium chloride.

For this reason we have calculated the relative frequency distribution of relative humidity at different relative humidity ranges (figs. 8,9,10,11). Also in this case location 3 show a considerable time of liquid phase for sodium chloride thus indicating a higher probability to have more solubilization and crystallisation cycles which represent more destructive conditions with respect the dry conditions of the other location.

Fig. 4   CHURCH OF STA. MARIJA TA' CWERRA – SIGGIEWI (MALTA)
North wall – year 1994

Interval of temperature (°C)
■ frequency distribution of distance from dew point 1

Fig. 5 — CHURCH OF STA. MARIJA TA' CWERRA – SIGGIEWI (MALTA) North wall – year 1994

Fig. 6 — CHURCH OF STA. MARIJA TA' CWERRA – SIGGIEWI (MALTA) South wall – year 1994

Fig. 7 — CHURCH OF STA. MARIJA TA' CWERRA – SIGGIEWI (MALTA) South wall – year 1994

Fig. 8

CHURCH OF STA. MARIJA TA' CWERRA – SIGGIEWI (MALTA)
Frequency distribution of relative humdity on surface 1
North wall – year 1994

Fig. 9

CHURCH OF STA. MARIJA TA' CWERRA – SIGGIEWI (MALTA)
Frequency distribution of relative humdity on surface 2
North wall – year 1994

Fig. 10

CHURCH OF STA, MARIJA TA' CWERRA – SIGGIEWI (MALTA)
Frequency distribution of relative humdity on surface 3
South wall – year 1994

Neoformation decay products on the monument's surface due to marine spray and polluted atmosphere in relation to indoor and outdoor climate

51

Fig. 11 — CHURCH OF STA. MARIJA TA' CWERRA – SIGGIEWI (MALTA) Frequency distribution of relative humidity on surface 4 — South wall – year 1994

d) Sanctuary of Demeter in Eleusi.

The main decay phenomena in relevance to the environmental factors and in the sequence of the frequency that they are observed, are as follows:

- *granular disintegration and detachment, the most general and important weathering, concerning yellowish limestone and biocalcarenites as well as marble, presented at washed out surface areas, or on surface areas facing the sea,*

- *biological attack to the stone,*

- *chromatic alteration from the white of the Pentelic marble to the rusty–yellow colour at the washed out surfaces and mainly where water rebound phenomena occur,*

- *soiling (loose dirt deposits) are frequently present at horizontal top sides of numerous building stones relief in form of micro–karst. The micro–karst are formed by solution processes resulting from accumulation of rain water reacting with suspended particles deposited during long period of dry deposition.*

- *black grey crust formations formed on hollows,*

- *black crust strongly attached at the surfaces often present in unwashed areas,*

- *loose deposition inside hollow*

- *orange–coloured crust very thin and firmly attached to the stone surface.*

A focus was made on a first stage to examine several dust depositions, crusts (Amoroso G., Fassina V., 1983) and encrustation, mainly concerning white marble, in order to investigate the various correlations between the heavily polluted atmosphere and the weathering patterns, as they are discerned / distinguished according to the sampling criteria. The examination of the deposited dust and suspended particles in layers was essential as their evidently observed stratification is governed by natural phenomena, while the crust profiles is driven by physico–chemical mechanisms.

The XRD results (Table 4) give evidence to the high calcitic composition of the dust, while lower percentages of gypsum, quartz, dolomite, mica, chlorite and cementitious compounds are also present. These results are in agreement with EDXRF ones. All the examined samples contain much Si, Ca, Fe, S. The most of the Si and Fe is ascribed to the cement production in the neighbourhood of the archaelogical site. The type of deposition quality could distinguish crusts as well in relation to sampling positions. SEM and depth profiles by EDS performed on surface and cross sections of black–grey crust in comparison with the cementitious encrustation and the rusty yellow patinas of the washed out areas lead to the following results.

Tab. 4

| Sample | Composition | | | | | | | | |
	Cc	Q	Gy	Do	A–Fsp	Mi	Mu	Chl	CSH
E9	+++	+	+		+	+	traces	traces	
E8	++++	++		++	traces				traces
E7	+++	++++	++	++++	traces	+		+	

++++ : 65–90%, +++ : 35–65,% ++ :15–35%, + : 5–15%
Cc   : Calcite (5–0586)
Q   : Quartz (5–0490)
Gy   : Gypsum (6–0046)
Do   : Dolomite (11–78)
A–Fsp   : Alkalifeldspars–Plagioclase (9–466, 10–357)
Mi   : Mica (2–0045, 7–42)
Mu   : Muscovite (7–42)
Chl   : Chlorite (10–412, 17–470)
CSH   : Calcium Silicate Hydrate (3–0248)

The high calcitic composition of the dust is evidenced. Lower percentages of Gypsum, Quartz, Dolomite, Mica, Chlorite and cementitious compounds (Calcium Silicate Hydrate) are also present.

a) *From sheltered areas crusts formation from grey to black were detected. It is possible to distinguish two types of black crust.*

—   *Samples E1 and E14 are very similar they contain a gypsum layer with a constant composition until 140–150 μm together with a few amount of iron oxides. Carbonaceous particles are mainly located on the surface and show a decreasing amount moving towards the inner part of the marble.*

—   *Samples E4 and E7 are very similar and the gypsum layer is more thick than previous samples thus indicating that the sulphation processes have reached a higher rate of formation.*

b) *From sheltered areas grey soiling formation were detected. In this case carbonaceous particles and silicon cementitious particles and gypsum layer are deposited above a brown iron oxide rich layer.*

—   *sample E11 and E15 has the same feature.*

c) *From washed out areas yellow–brown layer were observed.*

Samples E2 and E3 show a thin yellow layer visible above the typical texture of the marble. Small quantities of gypsum are present in the cracks. The yellow–brown feature is due to particulate from soil carried by the winds. Small particles of iron oxides have also been detected by EDAX.

d) *Brown layer with soiling dust from sheltered and washed out areas were observed.*

Samples E10 and E12 were taken respectively from sheltered and washed out areas. They show the same brown superficial deposition of iron oxide and also a silicon increasing amount in the layer underneath the superficial gypsum layer. Sample E10 show an increasing amount of iron oxide moving towards the inner part of the marble. The abundant presence of iron and silicon is ascribed to cement industry.

e) *Red patina composed by iron oxide and silicon like in the E16 sample at the basis of a column.*

f) Grey–black–crust from hollow on the ground floor (sample E5)

This crust is formed by a very thin gypsum layer which is deposited on a very thick silicon rich layer. Carbonaceous particles and iron oxides are present. Silicon is present in large amount together with significant amount of Fe and Al. For the white marble the influence of the heavily polluted atmosphere in a marine environment is varying, resulting in several weathering patterns, mainly in the form of crusts. Rusty, yellow patinas on washed out areas, firmly attached black grey crusts in contact with water and cementitious crusts in hollow ground floor characterise the various material – environment interactions taking place. Dust and deposition analysis give indications for the causes of the various crust formations. In particular, cement industry depositions could be related to the cementitious surface encrustation. Salt crystals embedded give evidence to the characteristic synergy of air pollution, suspended particles deposition and marine spray producing damage to the stone surface. Black crust formed on the hollow are mainly composed by cementitious particles. This type of decay was not generally found and it was ascribed to the deposition of suspended particles emitted from cement industry neighbourhood the archaeological site. The hollow are formed by solution processes resulting from accumulation of rainwater reacting with suspended particles deposited during long period of dry deposition.

5. Acknowledgements

6. References

1   Amorosso G., Fassina V. Stone Decay and Conservation, Elsevier Amsterdam, 1983, pp. 453.

2   Fassina V., Rossetti M., Oddone M., Mazzocchin S., Calogero S. Marine spray and polluted atmosphere as factors of damage to monuments in the Mediterranean Coastal Environment: an analytical study of some samples from the Sanctuary of Demeter in Eleusis (Athens). Proceedings of the 3th International Symposium on the Conservation of monuments in the Mediterranean Basin, Venice, 1994, 287–293.

3   Moropoulou A., Zezza F., Aires Barros L., Christaras B., Fassina V., Fitzner B., Galan E., Van Grieken R., Kassoli–Fournaraki A. Marine spray and polluted atmosphere as factors of damage to monuments in the Mediterranean Coastal Environment – a preliminary approach to the case of Demeter Sanctuary in Eleusis. Proceedings of the 3th International Symposium on the Conservation of monuments in the Mediterranean Basin, Venice, 1994, 275–285.

4   Six–month report n. 1, June 1993.

5   Six–month report n. 2, December 1993.

6   Six–month report n. 3, June 1994.

7   Six–month report n. 4, December 1994.

8   Six–month report n. 5, June 1995.

9   Zezza Fulvio. Marine spray and polluted atmosphere as factors of damage to monuments in the Mediterranean Coastal Environment. Proceedings of the 3th International Symposium on the Conservation of monuments in the Mediterranean Basin, Venice, 1994, 269–273.

Luis Aires–Barros

Monitoring of some meteorological variables related with hygroscopic products occurring at monuments of the Mediterranean basin

Monitoring of some meteorological variables related with hygroscopic products occurring at monuments of the Mediterranean basin

L. Aires – Barros
Lab. Mineralogy, I.S.T.
Technical University of Lisbon

Abstract

Data processing of a large campaign of *in situ* measurements regarding continuous monitoring of some micrometeorological variables in three monuments such as Cathedrals of Cadiz-Spain and Bari-Italy and the Church of Sta. Marija Ta'Cwerra-Malta, is presented.

Some chronograms, of those variables have been derived. These chronograms allow us to see the global behaviour of the meteorological data, to compare them and to evaluate their distribution against time.

Based on real thermohygrometric data from the studied monuments some processing was made to estimate thermodynamic equilibrium conditions of pure salts for real conditions different from the tabulated ones. This processing allowed to obtain phase diagrams for each studied saline mineral. Besides this it was also possible to compare real conditions with the estimated equilibrium conditions and to estimate the probability of pure evaporitic salts occurrences.

This study could be a step forward towards a more realistic modelling and forecast of spatio-temporal pure saline minerals occurrences in a given monitorized monument and it may contribute to a better understanding of their damage mechanisms.

The meteorological variables measured and registered on a hourly basis were: air temperature, air relative humidity, wall temperature, wind speed and direction and solar radiation. Relationships between micro and nanoclimates and hygroscopic salts occurring at these monuments are attempted.

The analysis of the chronograms allows us to criticize the quality of the sampled data and to see the global behaviour along time of the air micro–meteorological values as well as to compare them. Besides it is also possible to plot the frequency distribution of the detrended sampled values, and to characterize their complex origin by their statistic structure. It should be noticed that we present also graphs of the temperature measurements and relative humidities estimations of the atmosphere in contact with walls surfaces. These representations are the results of the calculation of surface relative humidities based on the assumption of thermal equilibrium between the atmosphere nearby the wall and the wall. For these estimations we have used an empirical approximation made by Tetens to the Clausius–Clapeyron equation (MONTEITH & UNSWORTH, 1990).

The chronograms of the differences between wall and air temperatures and of wall and air relative humidities have been derived in order to feel the potential contribution of phoretic effects to dry deposition of airborne pollutants (gases and aerosols) to and from the wall, in the absence of air movement of the atmosphere.

1. Introduction

Data processing of some meteorological variables monitored inside and outside by local people working in the framework of the project at cathedral of Cadiz and Bari and at church of Sta Marija Ta'Cwerra (Malta) is presented.

Data processing of monitorized variables and salt crystallization phenomena

The presence of evaporite minerals contributes significantly to the weathering of monuments stones due to their response to "cycles" of air relative humidity and temperature (RH, T). In fact these "cycles" normally fall within typical ranges of air temperature and relative humidity observed in most temperate climates.

Besides these alternative deliquescent – crystallization transitions, the evaporite minerals could affect the behaviour of gypsum crusts: activation of gypsum crusts in unsheltered areas of the monuments, increase of frequency and intensity of dissolution/recrystallization transitions, modification of hydration state, modification of physical form and structure of the crust.

So it was important to dress up salt hygroscopic equilibrium relative humidity plots of tabulated values taken from the literature (ARNOLD & ZEHNDER 1989) and to derive adequate descriptive continuous functions. As those values are discrete and not abundant we derived a polynomial function that describes them. Tabulated values were adapted for those minerals with very few experimental data. Lagrange polinomies were fitted to the adapted tabulated values. For this purpose it was assumed those functions approach good enough real equilibrium conditions for pure salts studied. Besides it was assumed the kinetics of system transitions is fast enough.

Fig. 1a is a complex representation in which we have together the chronograms of air temperature and air relative humidity of the exterior of the cathedral of Cadiz. In the same graph is represented the equilibrium conditions evolution of halite against time. The Lagrange approximation of the theoretical phase diagram for halite as well as the scatterplot of the observed T *vs* RH conditions are presented in Fig. 1b.

These type of graphs allow us to globally

estimate, during the monitoring time, the probability of occurrence of pure saline products that might occur on the walls surfaces (salt minerals, deliquescent phase and transition conditions). Besides it is possible to visualize the scattering of the observed points on the phase diagram. These scatterplots of micrometeorological variables may allows us to consider the possibility to classify and to characterize their complex origin.

3. Case Studies

3.1. The Cathedral of Cadiz

At cathedral of Cadiz the climate data have been collected from April 1994 to April 1995 by a monitoring station located at the terrace (azotea) as well using sensors positioned on a column, located inside the church (Fig. 2). The four positions where the sensors have been installed have the following characteristics:

A – *on the red limestone, at 0,5 m above the floor*

B – *on the oolitic limestone, at 3,5 m above the floor*

C – *on the oolitic limestone, at 7 m above the floor*

D – *on the oolitic limestone, at 12 m above the floor*

In what concerns the outside microclimate and regarding the presence of halite, we could derive, from the chronograms:

i) *the greater variability along time of the outside air temperature and relative humidity when compared with the same variables taken inside the cathedral (Figs. 1a and 2).*

ii) *it seems that there is no correlation between the variability of outside air temperature and relative humidity along the year. There seems to be yearly and daily seasonalities on temperature chronograms as opposed to relative humidities pseudoperiodicities.*

iii) *Besides, it is easy to follow transition condi-*

Monitoring of some meteorological variables related with hygroscopic products occurring at monuments of the Mediterranean basin

59

tions. From Fig. 1a it could be seen that there are very frequent deliquescent – crystallization transitions along the year. The frequency of these transition states are independent of time. So we could conclude that the mechanical stresses induced by this oscilatory phenomena are similar all over the year.

Taking into account the phase diagram (Fig. 1b) it enables us to have an overall view of the stability fields of saline system (halite crystals as well as deliquescent phase).

Regarding nitrocalcite behaviour, its equilibrium boundary line (Fig. 1d) is not so linear as the halite one.

In the chronogram (Fig. 1c) we could notice a greater variability of boundary conditions during hotter season. This could be explained by higher non–linear behaviour of boundary conditions towards higher temperatures as already said (Fig. 1d).

In what concerns inside nanoclimates and using the data obtained along a column (several heights) we could emphasize (Figs.2a to 2h).

i) *the evolution of thermohygrometric conditions at those several heights shows that at levels A, C and D there are general similarities among them.*
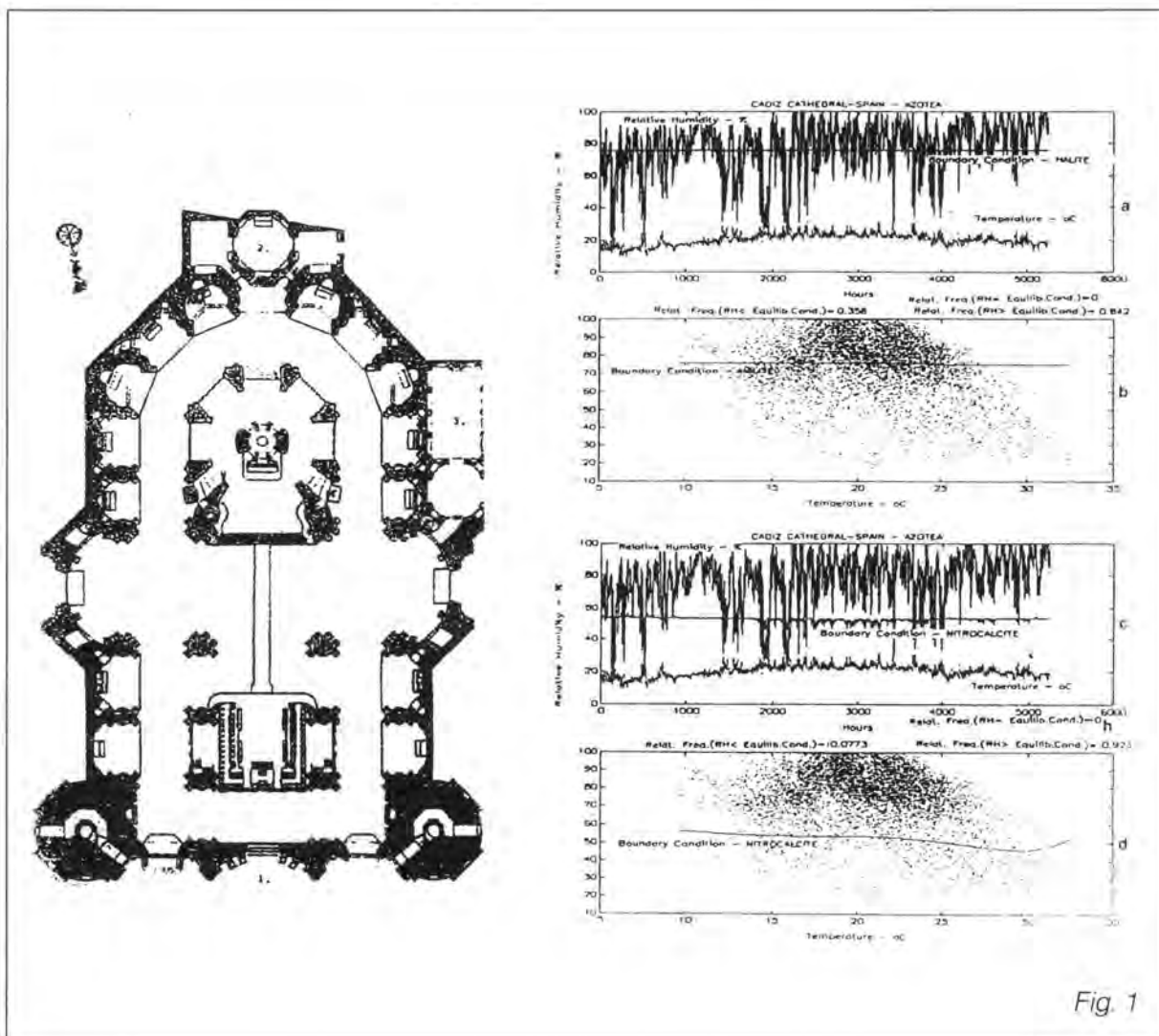
Fig. 1

ii) *at level B the variability along time of the air relative humidity is in general lower than at other levels (heights). We could remark an attenuation of this air relative humidity variability when we move towards Summer time.*

iii) *we should also conclude from the observation of the chronograms, that, for levels A, C and D, the more dangerous period regarding alternative deliquescent – crystallization transitions is final Spring until the Summer/Autumn transition.*

iv) *at level B we have, for halite behaviour, the best thermohygrometric conditions are all the scatterplot develops bellow the equilibrium boundary conditions (air relative humidity curve never crosses the equilibrium conditions line).*

It is evident from the chronograms observation, there is a phase shift in the outside *vs* inside temperature chronograms that corresponds to thermal inertia behaviour, characteristic of heat transfer across church walls.

For nitrocalcite salt, we see that the air relative humidity curves seldom crosses the boundary conditions line at all levels of the monitorized column (Figs. 3a to 3h). This means that nitrocalcite should be almost allways in deliquescent state. We could also see

that the transition states occur at same time at all levels.

In Table I it is synthesized the behaviour of halite and nitrocalcite at the four levels of the studied column of Cadiz Cathedral, in what concerns the relative frequency of air relative humidity (RH) to be above, equal or below equilibrium condions, along time.

The main conclusions, the figures of this table enable us to stress out, are:

I. *For halite*

I.1 *at level B halite is always crystallized.*

I.2 *at level A we encounter the more dangerous site due to the frequencies of the transition states, according to Fig. 2g and (R_1 = 0,38 and R_2 = 0.62). The worst situation regarding mechanical stresses induced by salt crystallizations hould occur where the transition frequency and R_1 or R_2 approaches 0.50.*

II. *For nitrocalcite.*

II.1 *– it seems not to be a mineral salt so dangerous as halite, although the higher non linearity of its equilibrium line. In fact the transition frequency and R_1 and R_2 are far from 0.50 (Table I).*

II.2 *all the column levels have quite similar behaviour against this salt.*

Table I

LEVEL	HALITE		NITROCALCITE	
	R1	R2	R1	R2
D	0.25	0.75	0.98	0.02
C	0.32	0.68	0.96	0.04
B	0.00	1.00	0.96	0.04
A	0.38	0.62	0.98	0.02

R – Relative frequency of RH points being above, equal or below the boundary conditions

R_1 – Relative frequency RH $\geq$ Equilibrium conditions

R_2 – Relative frequency RH < Equilibrium conditions

Fig. 2

Fig. 3

Monitoring of some meteorological variables related with hygroscopic products occurring at monuments of the Mediterranean basin
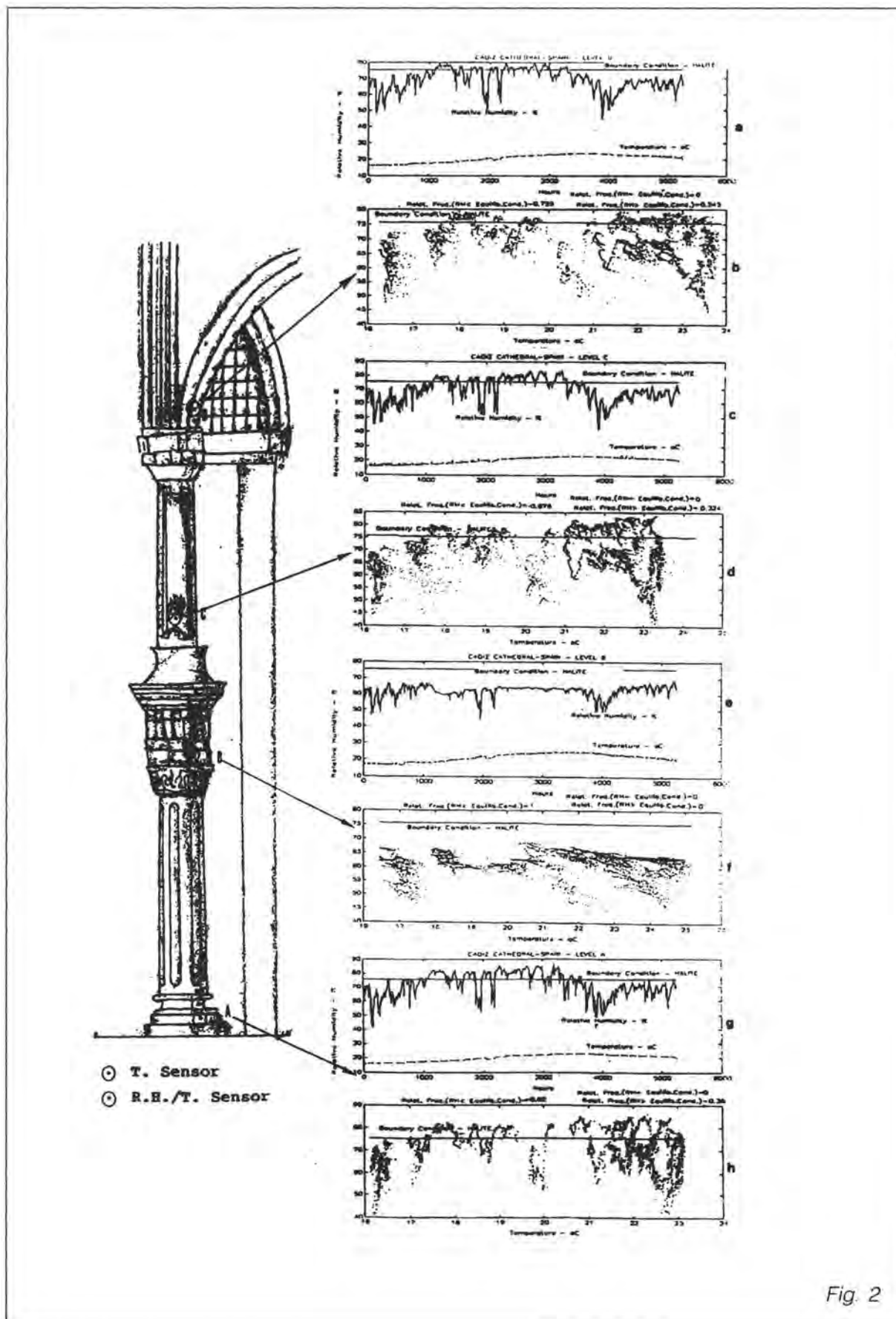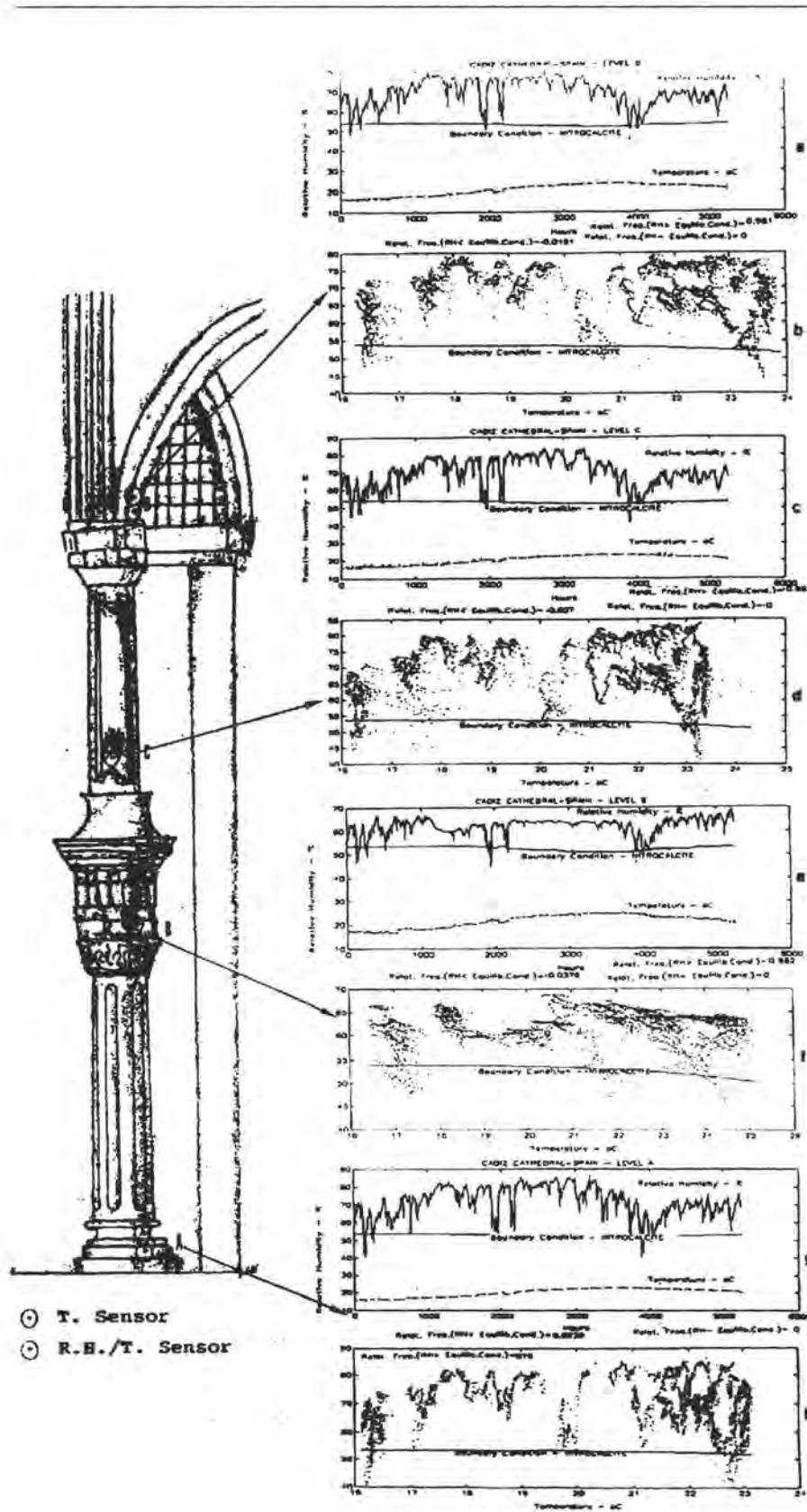
63

3.2. Cathedral of Bari

At Cathedral of Bari the climate data have been collected from October 1993 to October 1994 with a monitor station installed in a terrace facing SE as well as using some probes positioned inside the Cathedral at different heights (Fig. 4).

The system comprises a network of probes for measurements of surface temperature of stones, of internal air temperature and relative air humidity and of external air temperature and relative air humidity.

For this purpose the position choosen for the inside measurement points was the vertical left section inside the Cathedral when the most severe decay phenomena due to humidity are found.

The installation of the probes in different locations along the whole vertical section of this monument allows the step by step description of the nanoclimates occuring and their evolution along time as well as the behaviour of saline products which might occur.

As shown in Fig. 4 the probes have been placed at three different heights:

- *in correspondence with the arch of the left nave, the Arcada level;*

- *in correspondence with the base of the main arch below the dome, the Capitulo level;*

- *in the dome, under a window, the Cupola level.*

In what concerns the outside microclimate and regarding the presence of halite, we could derive from the chronograms:

- *the greater variability along time of the outside air temperature and relative humidity when compared with the same variables taken inside the Cathedral (Figs. 4a to 4h).*

- *it seems that, on average, air temperature and air relative humidity are negativelly correlated. Air temperature shows annual and daily seasonalities while air relative humidity shows a pseudo–periodic oscillatory behaviour.*

- *there are a large number of deliquescent - crystallization transitions along the year which means that there should be severe mechanical strains induced by this oscillatory behaviour.*

The comparision of outside diagrams describing halite and nitrocalcite behaviours show that nitrocalcite equilibrium conditions variability along time is greater than halite ones. Besides this fact the transition state probability is greater for halite than nitrocalcite (Table II, and Figs 4b and 5b).

Analysing inside diagrams we could say:

i) *At Cupola level we have more scattered thermohygrometric conditions than at Capitulo I and Arcada levels.*

The general behaviour of air relative humidity chronograms is quite similar in what

Table II

LEVEL	HALITE		NITROCALCITE	
	R1	R2	R1	R2
Cupola	0.14	0.86	0.87	0.13
Capitulo	0.20	0.80	0.93	0.07
Arcada	0.17	0.80	0.93	0.07

Fig. 4

Monitoring of some meteorological variables related with hygroscopic products occurring at monuments of the Mediterranean basin

65
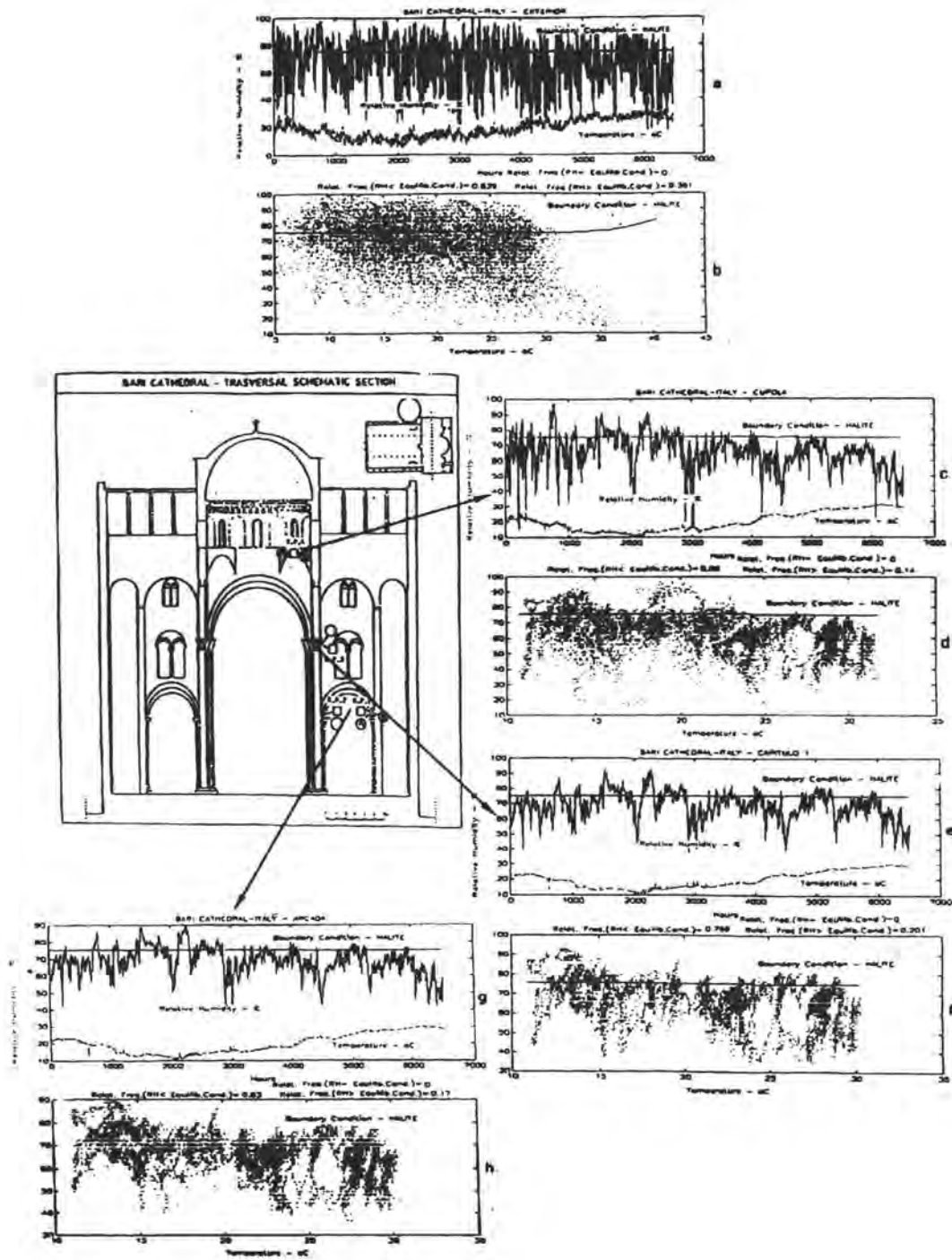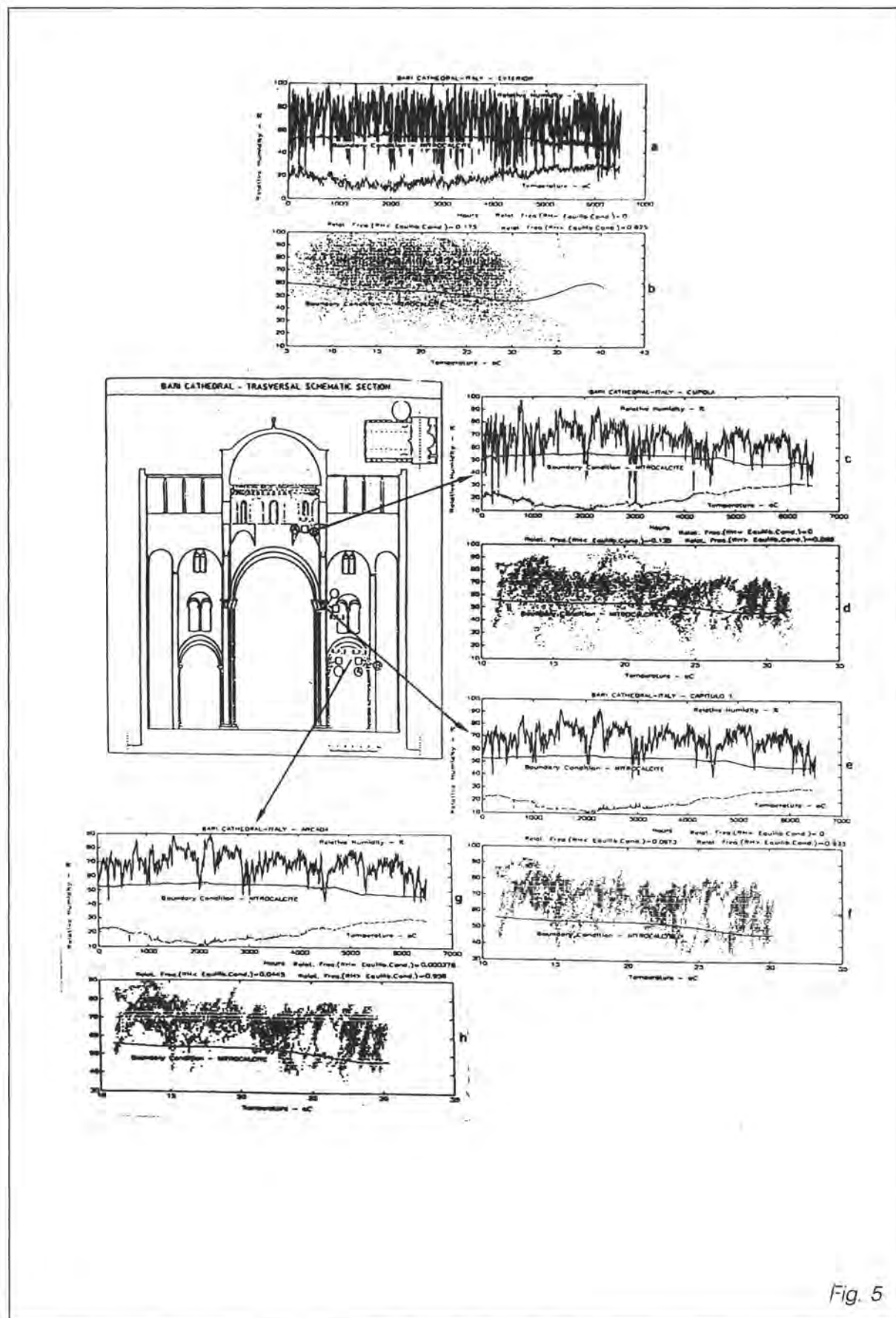
Fig. 5

concerns the pseudoperiodic development of average values.

The air temperature chronograms at the three levels (Figs. 4 and 5) are quite similar. Although the Cupola temperature behaviour shows a more intense daily oscillatory variability

ii) *Outside and inside temperature and air relative humidity chronograms show no time delay behaviour possibly explained by the proximity of site probes to outside conditions (site probes are close to windows). This means inside sites are "short–circuited" in respect to outside conditions.*

In Table II we synthesize the behaviour of halite and nitrocalcite at the three levels studied in the vertical left section inside the Cathedral, regarding relative frequency of air relative humidity (RH).

The main conclusion taken from that table are:

I   – *For halite.*

I.1 – *At Arcada, Capitulo I and Cupola levels the salt system is in solid state during 83%, 80% and 86% respectively of the time.*

I.2 – *By inspection of the three correspondent chronograms it seems the Cupola level shows the more aggressive environmental conditions.*

II   – *For nitrocalcite*

II.1 – *At Arcada, Capitulo I and Cupola levels the salt system is probably in liquid state most of the time: 96%, 93% and 87% respectively. This is the contrary of the halite behaviour.*

II.2 – *Observing the chronograms we see that Cupola level is also the more dangerous site for stone maintenance. It should be*

notice that, at this level, most salt system transitions occur at higher average temperatures.

3.3. The Church of Sta. Marija Ta'Cwerra

At the church of Santa Marija Ta' Cwerra (Malta), from April 1994 to June 1995, four internal air sensors (combined temperature and relative humidity sensors) and two external air sensors (one for temperature and another for relative humidity) were set up as follows:

i) *Interior air sensors*

   North wall – local 2 – 3,5 m

   North wall – local 4 – 0,5 m

   South wall – local 1 – 3,5 m

   South wall – local 3 – 0,5 m

ii) *Exterior air sensors*

Facing South/Southwest, attached to the dome.

In what concerns the outside microclimate, the chronograms show a great disturbance either in the temperature or in the relative humidity developments (Fig. 6). There are oscillations in the average values of temperature corresponding a sharp decrease in the average values of the relative air humidity. Possibly this disturbance is related with an atmosphere modification that lasted about one month. Taking apart this disturbed atmospheric period it seems that there is no correlation between the average values of temperature and air relative humidity.

Regarding the saline systems, for halite (Fig. 6a) we see that, most of the time, the likelihood of transition states is very high sauf during the disturbed period already mentioned. In this period the salin system is in crystallized state.

It should be noticed that the evolution of equilibrium conditions shows much more variability for nitrocalcite than for halite (Figs. 6a and 6b).

Monitoring of some meteorological variables related with hygroscopic products occurring at monuments of the Mediterranean basin

67
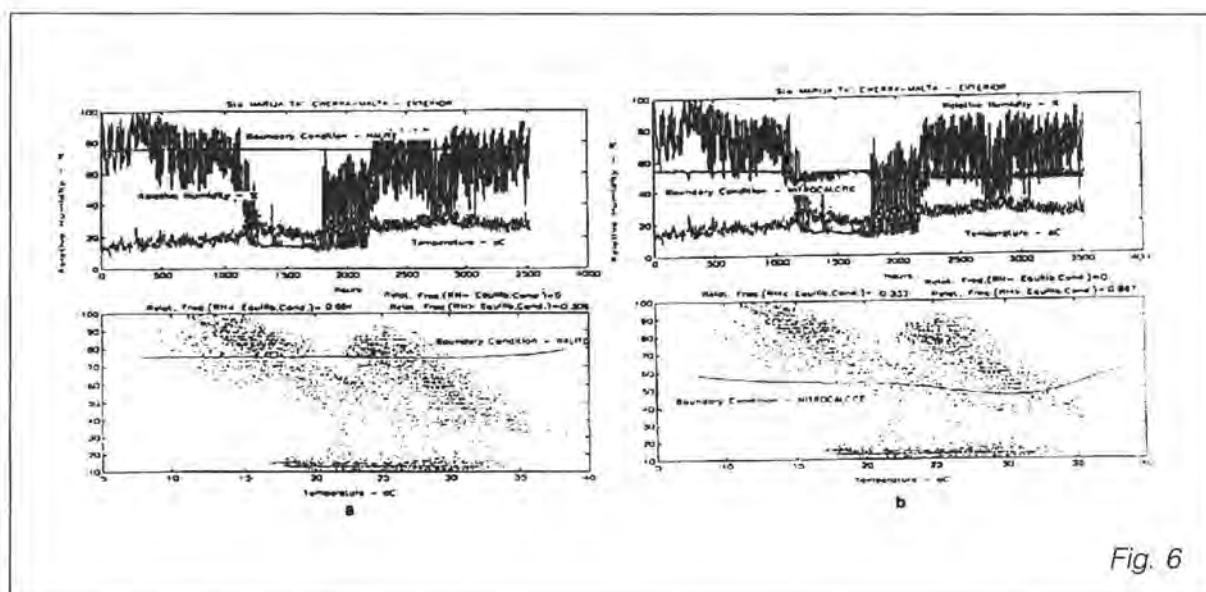
Fig. 6

By comparision with halite behaviour along time, nitrocalcite system does not change state only during part of the "disturbed" period (Fig. 6b). In short, during half monitorized time this system shows a steady behaviour (with a few transition states). In the other half time the probability of transitions increases a lot. This more dangerous period corresponds to warmer average atmosphere temperatures.

Studing inside microclimate of this church we could conclude (Table III and Fig.7). For halite, the more dangerous site is local 4 (North, 0.50 m), where the transition chances are higher than in other places (Rl = 0.51). If we try to dress up a sequence of sites by their weathering potential we could put

$$\frac{\text{local } 4 \rightarrow \text{local } 2 \rightarrow \text{Local } 3 \rightarrow \text{local } 1}{\text{decrease of weathering potential}}$$

For nitrocalcite we see that there is quite no difference between both values taken in north and south walls. Nevertheless south wall is slighly more dangerous.

Table III

LOCAL	HALITE		NITROCALCITE	
	R1	R2	R1	R2
L1 - S 3,5 m	0.06	0.94	0.98	0.02
L2 - N 3,5 m	0.29	0.71	0.99	0.01
L3 - S 0,5 m	0.08	0.92	0.98	0.02
L4 - N 0,5 m	0.51	0.49	≅100	<<0.01
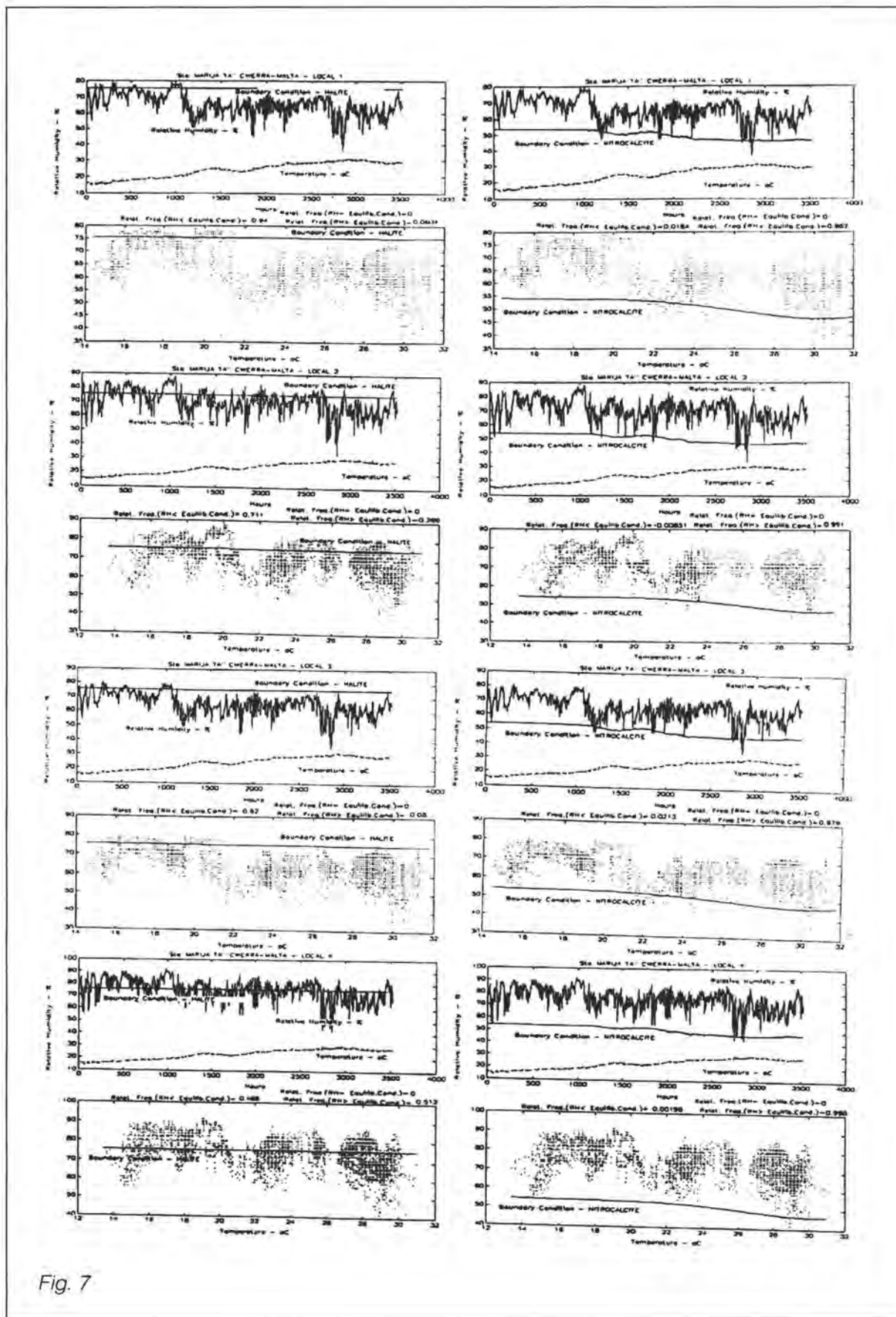
Fig. 7

4. Final remarks

A synthesis of data processing for the three monuments studied is presented in Tables IV, V and VI, where we have the relative frequencies of occurrence of crystallized state for three evaporitic minerals (a chloride, a sulphate and a nitrate), occurring in the monuments studied.

The figures of these tables have been derived from respective chronograms and phase diagrams. For easier under standing of salt behaviour during the monitoring time some diagrams have been derived (Figs. 8). These graphs enable us to have qualitative and quantitative informations about the saline states: deliquescent *vs* crystallized and the estimation of the probability of transitions of system states.

Now an attempt of interpretation derived from those data and diagrams will be dressed.
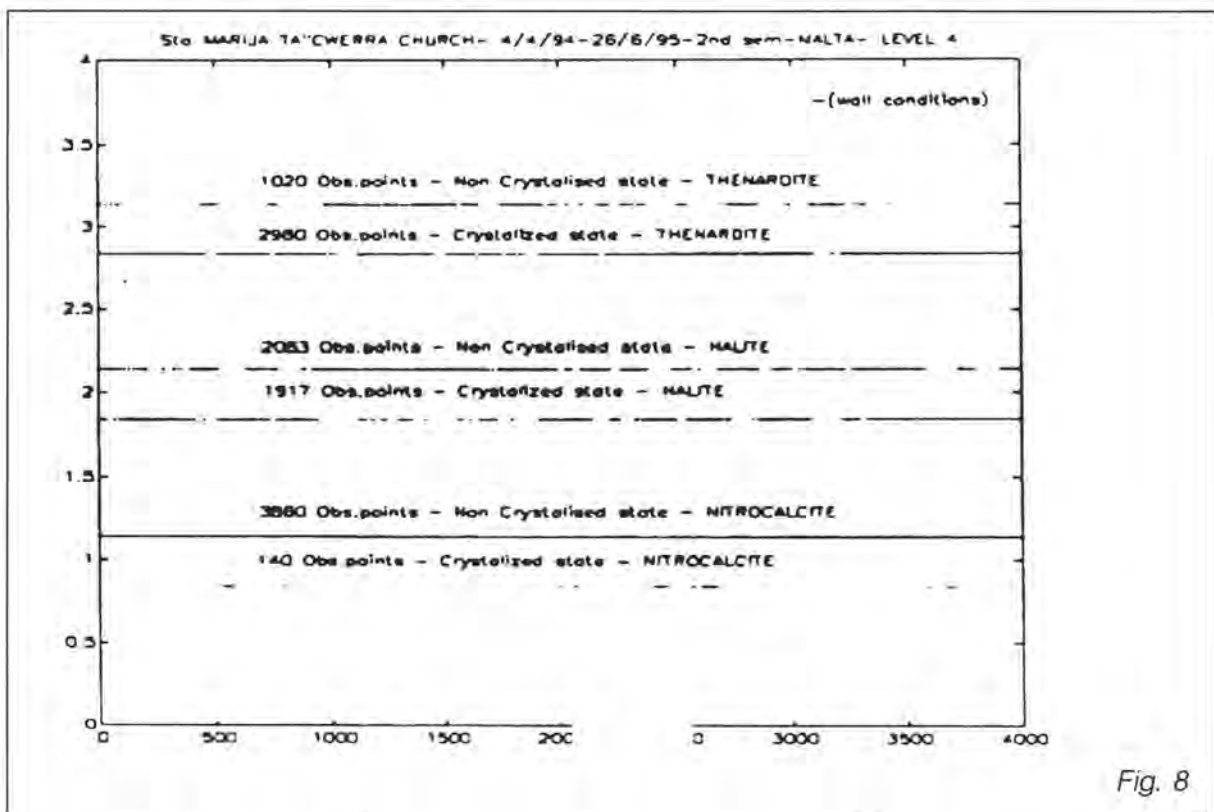
Fig. 8

4.1 The Cathedral of Cadiz

Taking into account Fig. 9 and Table IV we could derive:

i) Comparing profiles along the column studied it is clear the importance to know the temperature values in air and on wall. We could ne several situations when Fig. 9 is studied. So nitrocalcite shows quite similar relative frequency of occurrence of crystallized state *f* in air or on wall. In fact only at level D we have sharp differences for *f* values, mainly on the column.

Nitrocalcite in air and on column shows *f* largely different in respect to halite, in both situations. The same can be said between nitrocalcite, in both situations, in comparison with thenardite behaviour. Thenardite shows *f* values quite similars.

ii) Halite shows the same behaviour at levels A and B where it is always crystallized in both situations. At the other levels it is interesting to follow an increase of crystallization expectation as we go from air to the column.

Thenardite is almost crystallized at all levels.

iii) We could conclude, in general, considering the three salts and the height of the column studied that:

a) *The saline systems at level B have a quite similar behaviour where studied in air or on column.*

b) *Levels A and C show saline systems with behaviours in air and on column relatively.*

c) *At level D, on the column, we get the greatest probability of crystallised state for all saline minerals.*

d) *At level C we encounter a reverse situation regarding what happen at level D.*

Table IV

LEVEL	Relative frequencies of crystallized occurences – f – (%)					
	Nitrocalcite		Halite		Thenardite	
	air	wall	air	wall	air	wall
D	3	14	78	100	100	100
C	5	6	71	82	98	100
B	5	4	100	100	100	100
A	5	6	71	97	98	100

Fig. 9

Monitoring of some meteorological variables related with hygroscopic
products occurring at monuments of the Mediterranean basin

71
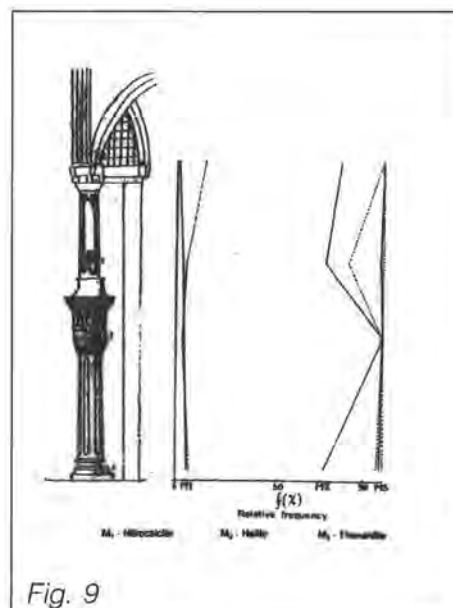
4.2. The Cathedral of Bari

Taking into account Fig. 10 and Table V we could derive:

i) *At Arcada level there are three types of mineral behaviour. Nitrocalcite both at air or on wall is almost always in deliquescent state. Halite system shows at crystallized state during 80% of monitoring time. Finally thenardite system is partically always crystallized.*

Regarding saline systems involved, for nitrocalcite there is an increase in the probability of being crystallized as we move from Arcada to Cupola levels. For halite, at Capitulo level, there is a scattered distribution of f values. Thenardite is almost always crystallized.

ii) *We see that f values increase, for all saline minerals, when we move from wall to air environment. It shonld be noticed that it is the contrary we have at cathedral of Cadiz.*

There are more scattering of nitrocalcite f values than for those refering to halite and to thenardite.

iii) *In general it conld be concluded that the probability of occurrence of crystallized salts increases from below – Arcada level – to the top – Cupola level. Thenardite is almost always crystallized.*

Table V

LEVEL	Relative frequencies of crystallized occurences – f – (%)					
	Nitrocalcite		Halite		Thenardite	
	air	wall	air	wall	air	wall
Cupola I	13	12	86	82	95	94
Cupola II	14	13	86	83	95	95
Capitulo I	7	7	80	76	95	94
Capitulo II	7	7	87	83	97	95
Arcada I	5	4	83	80	97	95
Arcada II	5	4	83	80	97	96
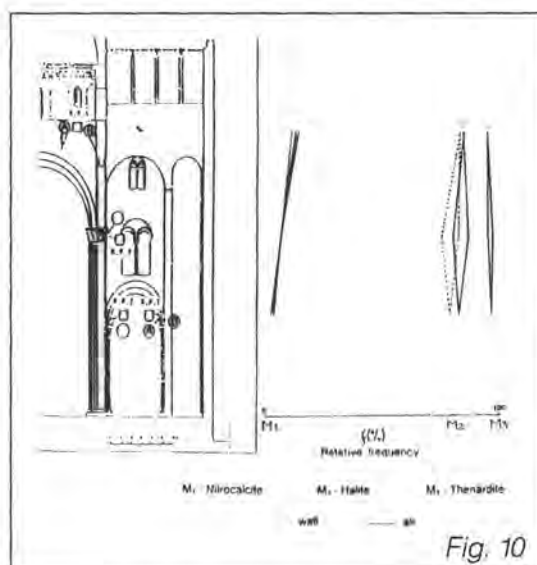
Fig. 10

4.3. The Chucch of Sta Marija Ta'Cwerra (Malta)

For Sta. Marija Ta'Cwerra in Malta island using Fig. 11 and Table VI we could conclude:

i) *For nitrocalcite there are not significant differences between f values obtained on walls or in air for any location (North or South) or height (0.50 or 3.50 m).*

ii) *For halite there is a clear stratification between values according the height of measurement, regardless North or South wall.*

iii) *For thenardite we get the lowest values of -f- in comparison with the correspondent values for the other two monuments. North wall shows the lowest values for all situations (air and wall) and heights.*

iv) *It should be stressed out that halite and thenardite have a more similar behaviour, on average, when compared with nitrocalcite behaviour.*

v) *A general conclusions, regarding the inside behaviour of the walls, is that there is an environmental stratification quite well shown by halite and thenardite -f- values. In fact at 0.50 m level, North or South walls we have lower crystallized states as compared with 3.50 levels. Although nitrocalcite does not show this stratification, thenardite does it.*

A general conclusion that could be taken from this comparative environmental study regards the interest to have values not only of air temperature and relative humidity but also, at least, of wall temperature. This will enable us to estimate air relative humidity on wall.

Table VI

LEVEL		Relative frequencies of crystallized occurences – f – (%)					
		Nitrocalcite		Halite		Thenardite	
		air	wall	air	wall	air	wall
NORTH	3.50 m	3	2	83	81	98	98
	0.50 m	1	2	45	56	73	82
SOUTH	3.50 m	3	2	86	84	$\cong 100$	99
	0.50 m	2	2	62	62	88	87

5. Acknowledgements

6. Bibliography

1 - Arnold, A. –Zehnder, K. – Salt weathering on monuments. Proceedings Ia Int. Symp. Cons. Monuments Med. Basin, pp. 31–58. Bari, (1989).

2 - Monteith, J.L. – Unsworth, M.H. – Environmental physics. E. Arnold. London, (1990).
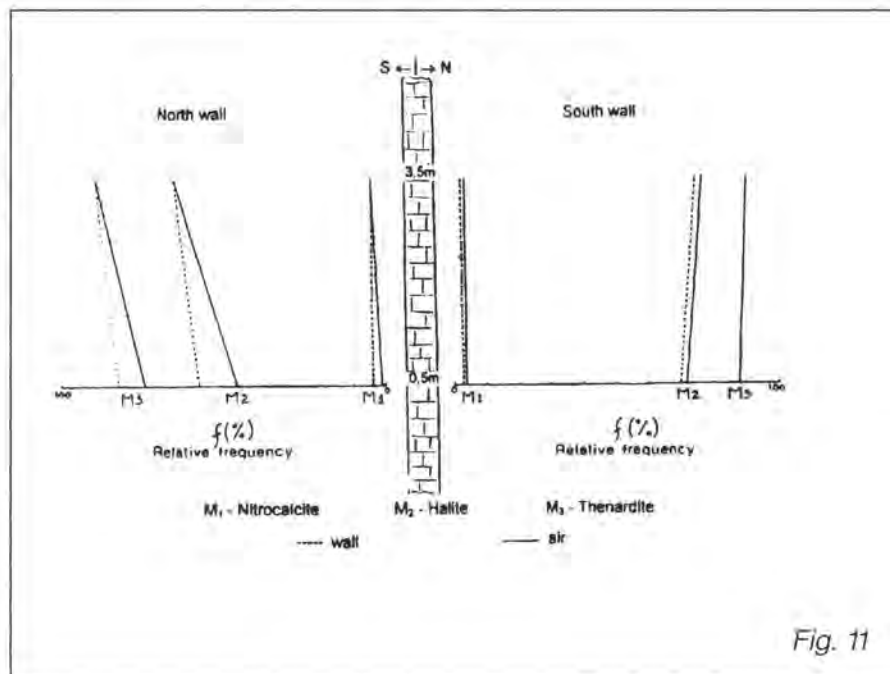
Fig. 11

Emilio Galán
Luis Aires–Barros
Basile Christaras
Anna Kassoli–Fournaraki
Bernd Fitzner
Fulvio Zezza

Representative stones from the Sanctuary of Demeter in Eleusis (Greece), Sta. Marija Ta' Cwerra of Siggiewi (Malta) and Bari (Italy) and Cadiz (Spain) Cathedrals: petrographic characteristics, physical properties and alteration products

Representative stones from the Sanctuary of Demeter in Eleusis (Greece), Sta. Marija Ta' Cwerra of Siggiewi (Malta) and Bari (Italy) and Cadiz (Spain) Cathedrals: petrographic characteristics, physical properties and alteration products

E. Galán – *Departamento de Cristalografía y Mineralogía, Facultad de Química, Universidad de Sevilla (Spain).*

L. Aires–Barros – *Lab. de Mineralogia e Petrologia, Instituto Superior Tecnico, Lisboa (Portugal).*

B. Christaras – *School of Geology, Aristotle University of Thessaloniki, 54006 Thessaloniki, Greece.*

A. Kassoli–Fournaraki – *School of Geology, Aristotle University of Thessaloniki, 54006 Thessaloniki, Greece.*

B. Fitzner – *Geologisches Institut. RWTH Aachen (Germany).*

F. Zezza – *Istituto di Geologia Applicata e Geotecnica. Facoltà di Ingegneria. Politecnico di Bari (Italy).*

Abstract

These four historical monuments of the Mediterranean basin are mainly built up of calcareous rocks, different in age, texture, mineralogy and genesis. Except for the Church of Sta. Marija Ta'Cwerra, more than one lithotype was used, but taking in mind those stones more damaged, a lithotype selection was done for this investigation. Samples from the building, and from quarries in the case of Malta and Cádiz, were petrographically characterized, and two groups of stones can be considered: a) marbles, b) biolimestones.

Marbles and limestones from Eleusis have been mainly degraded by industrial pollution and secondary by marine spray, forming black crusts (in holes and carved blocks) composed of calcite, quartz, mica and gypsum, pink pittings (goethite), and efflorescences (thenardite, halite). The stone from Malta is a very high porosity biosparitic limestone composed of calcite, and glauconite, quartz and iron oxides as accesories, which has been degraded in the building showing less mechanical resistence than that from the quarry stone, and many efflorescences rich in halite with minor nitrate. Also halite was found in quarry stone. Marine spray action is evidenced as the main decay factor for this monument. In Bari Cathedral stones used were low–medium porosity biosparitic/biomicritic limestones, and biomicritic/oomicritic calcarenites. Inside the building, efflorescences on the cupola contain gypsum, singenite and nitrates, which can be the result of marine spray and urban pollution. Finally in Cádiz Cathedral, the Estepa limestone, a technically good construction stone according to its physical properties, presents inside the building many occurrences of efflorescences and crusts with calcite, natron, trona and occasional halite indicating the degradating effect of the close marine environment (marine spray, aerosols, percolation waters and saline rising damp).

The knowledge of building stones (mineralogy, petrography, physical properties) and the characterization of their alteration products are the first step in the research for understanding stone decay phenomena and their causes.

Keywords: limestone, marble, petrography, physical properties, alteration products.

1. Introduction

Historical monuments of the Mediterranean basin are mainly built up of calcareous rocks. The four pilot monuments under study for the Project "Marine Spray and Polluted Atmosphere as Factors of Damage to Monuments in the Mediterranean Coastal Environment" (Contract N°. EV5V–CT92–0102, 1993–96) were also built using marbles and limestones, which are different in age, texture, mineralogy and genesis.

The oldest pilot monument studied, the ruins of the Sanctuary of Demeter in Eleusis (Greece), dated 1500–1400 BC and rebuilt several times during the Ancient times, form now an archeological site of great interest, in which beautiful white marble (Pentelic marble) and white gray marble (from the Attico–Cyclade crystalline complex, Triassic to Upper Cretaceous) are the most representative stones for columns, floor and decorative motives. Also different limestones varieties (micritic, biomicritic and biosparitic) of varied colours (gray, yellow, yellow–brown) of the Pelagonian tectonic unit were used for walls, basements, wells, etc.

The Church of Sta. Marija Ta'Cwerra, located at the village of Siggiewi (Malta), was first built in 1611 and rebuilt in 1742, using the so called "globigerina limestone", Miocene biomicrosparitic limestone from the Mqabba quarry.

Although the Bari Cathedral contains elements of a paleo–christian church (5th–6th centuries), the present building was finished in 1292, using Lower Cretaceous limestones, of "Trani type" as main construction stones, as well as some granite and marble for columns and decorative motives.

Finally, the Cathedral of Cádiz (18th–19th centuries) was built using calcareous stones from many regional quarries (Puerto Real, Antequera, Almayate, Sancti Petri, Morón, Estepa, Medina Sidonia, Mijas, etc.). Main structural stones are Upper Neogene calcarenite ("Ostionera" stone, a sparitic biocalcarenite) and Middle–Upper Jurassic and Miocene limestones (oolitic, micritic and sparitic biolimestones). White marble (dolomite marble) and Triassic black and red "marbles" (sparitic and oolitic limestones), were used as decorative stones.

The aim of this paper is to present the main petrographical, mineralogical and chemical data of the most representative stones of the pilot monuments studied, as well as their characteristic physical properties.

These data were obtained by us within the EC Project mentioned above.

2. Materials and Methods

For this research, representative stones from the four pilot monuments were sampled. In the cases of Bari and Cádiz Cathedrals only the most degraded stones were chosen for the study. The studied samples are the following:

* Temple of Eleusis

   Sample A: gray limestone

   Sample B: white "pentelic" marble

   Sample C: white–gray marble

   Sample D: yellow limestone

   Sample E: gray limestone

   Sample F: yellow–brown limestone

   Sample G: yellow–brown dolomite

   Samples A: and E are Upper Triassic to Upper Jurassic, samples B and C are Triassic to Upper Cretaceous marbles, and samples D and F are Upper Cretaceous.

* Sta. Marija Ta'Cwerra of Siggiewi

   Samples S–1, S–2, S–3: Globigerina limestone (Miocene) from the building (outside).

   Samples 4 and 5: Globigerina limestone (Miocene) from Mqabba quarry.

* Cathedral of Bari

   Eighteen limestone samples from inside the building (Lower Cretaceous).

* Cathedral of Cádiz

   Twenty seven samples including Estepa limestones (Middle–Upper Jurassic), marbles and calcarenites were studied. These samples have been taken from inside the building, and also from quarries in the case of Estepa limestones. Efflorescences, patinas, crusts, flakes and other alteration products were also sampled.

The characterization methodology carried out in this project includes:

* *Petrography by optical microscope (OM).*

* *Mineralogy by X–ray diffraction (XRD), infrared (IR) and optical microscope.*

* *Chemical analysis by atomic absorption (AAS), X–ray fluorescence (XRF) and ultraviolet–visible (UV–V) spectrometries, as well as other conventional techniques (titration, calcimetry).*

* *Microstructural analysis of the porous system by a combination of thin section analysis under optical microscope with image analysis, mercury porosimetry and N_2–sorption.*

* *Physical and mechanical properties: density, water absorption, ultrasonic transmission velocity, abrasion resistance, uniaxial compressive strength, Young's modulus of elasticity, tensile strength, cohesion, angle of internal friction, Schmidt hammer value, following standar methods.*

Nevertheless, this research has been selectively done, specially mechanical properties, by obvious reasons.

Because of the limited extension of this paper, only some data, comparatively shown, will be presented and discussed.

3. Results

All stone materials used in Eleusis are mainly composed of calcite (Fig. 1a), except for the yellow limestone (sample D; calcite and dolomite in approximately equal amounts) and the biomicritic yellow–brown dolomite (sample G), obviously constituted of dolomite. Other minor components are quartz, muscovite, feldspars, zircon, rutile and opaques. Black crusts (in holes and carved blocks), pink patinas and white efflorescences are common on the floor and columns, which are mineralogically composed of calcite, quartz, mica, gypsum and goethite (pink patina), thenardite and halite.

Eleusis rocks usually show low total porosity (2–4 %) formed of large pores (Fig. 2a), and only occassionally (sample D) is higher (≈14 %), constituted mainly by small pores. Water absorption varies between 0.2–0.4 % for marbles and 5 % for yellow limestones (sample D).

Ultrasonic velocity ranges from 6000 m/s for the most compact marble to 5000 m/s for the soft limestone, being the uniaxial compressive strength of about 75–100 MPa for the marbles and ≈50 MPa for the limestones.

"Globigerina limestone" is a Miocene biomicrosparitic limestone composed of calcite, and glauconite, quartz and iron oxides as accesories (Fig. 1b). It contains many bioclasts of planktonic foraminifera and some benthonic ones, and fragments of bivalves. Halite is frequent in all the samples. Salt efflorescences inside the church are mainly composed of halite and calcite, but minor nitrates and silicates have been found by IR.

Total porosity for "globigerina limestone" ranges between 32–37 % (Fig. 2b), formed mainly of small pores with large pores subordinately, and water absorption capacity is around 10–13 %. Values for principal mechanical properties are: UCS of 42–52 MPa and ultrasonic velocity of 2850–3040 m/s for quarry stone, and 21–33 MPa and 980–1600 m/s respectively for building stone.

Studied stone from Bari Cathedral can be grouped in: a)biomicrosparitic (Fig. 1c), and b)biomicritic limestone, both of low porosity of intraparticle and geode type. Calcite is the main constituent (>95 %). Efflorescences and patinas on some limestones located inside the cathedral at the cupola show presence of gypsum, singenite and nitrates. Samples analyzed have a total porosity rather variable, 8–28 % (Fig. 2c), but usually it is around 12–20 %, mainly composed of small pores and showing a low pore area. Water absorption is low, 2–4 %, ultrasonic velocity is around 6000 m/s, and UCS can reach up to 120–180 MPa in quarry stones but is lower for the building ones.

The principal structural stone for the Cádiz Cathedral, the "Ostionera" stone is a sparitic biocalcarenite composed of calcite (40–60 %), quartz (20–40 %), feldspars and micas, and fossil remains. White limestones from Estepa include oolitic, micritic, sparitic and bioclastic varieties, mainly composed of calcite and bivalves or foraminifera remains (Fig. 1d). White and red marbles from Mijas are a dolomite marble and an oolitic limestone with fossil remains respectively. Efflorescences collected from degraded Estepa limestone inside the monument are composed of calcite, natron, trona, and occasional halite.

The Estepa limestone was extensively investigated because it is the most degraded stone inside the building. Concerning porosity there are two varieties, one of 6 % of total porosity (large pore size) and another ca. 13 % (mainly small pores with very small and large pores subordinately) (Fig. 2d). Water absorption is 3 and 4.7 % respectively for these varieties. UCS ranges between 70–100 MPa and ultrasonic velocity varies from 4300 to 5100 m/s.

Tables I and II collect some data of the lithotypes studied from the four monuments.

4. Conclusions

Historical monuments at the coast of the Mediterranean basin are fundamentally built up of limestones and marbles, and degradation is firstly related to the marine spray activity, and locally to the industrial and urban pollution (i.e. Temple of Eleusis and Bari Cathedral). Occasionally saline rising damp and percolation waters could be other degradating factors (i.e. Cádiz Cathedral).

In any case the characterization of building stones, the search of original quarries, and the analysis of their alteration products, are the first step in the research for understanding stone decay phenomena and their causes, to prevent more degradation, if it is possible, and for selecting further conservation treatments.
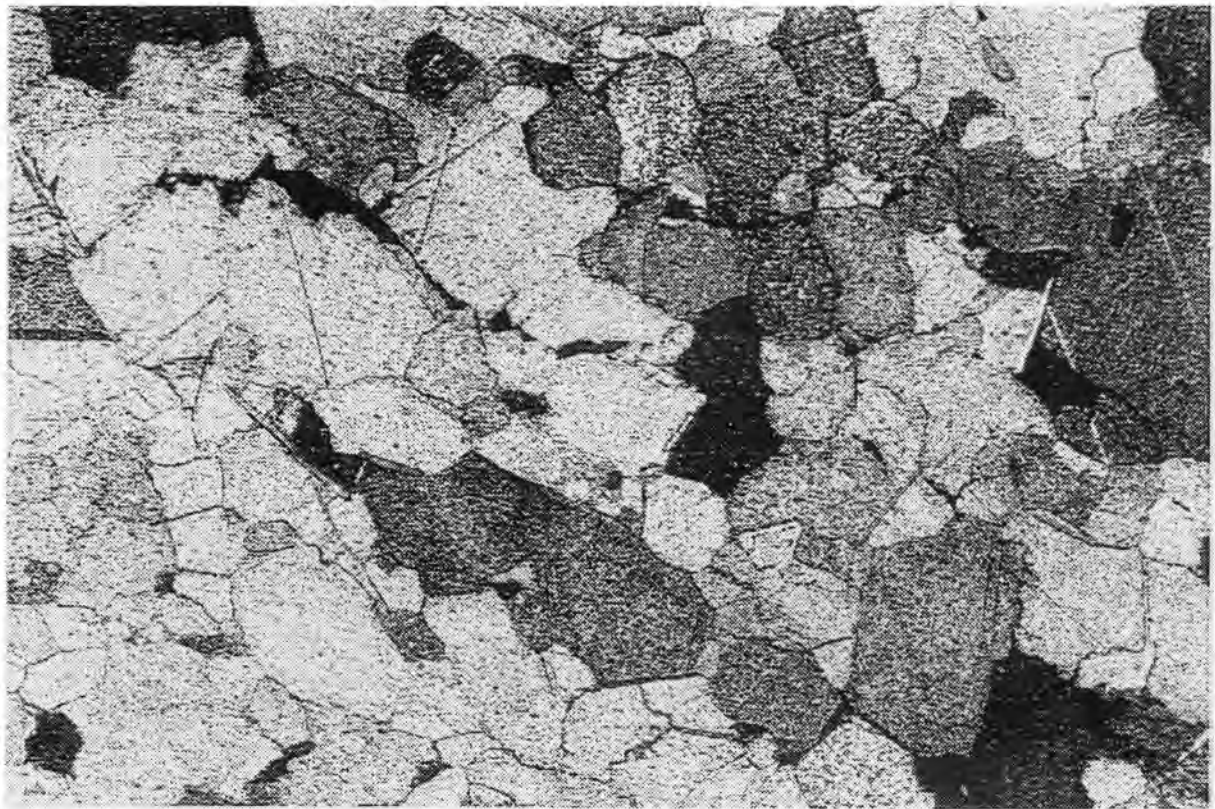
Figure 1a. Pentelic marble. Fissure between calcite grains. (Eleusis) x40. P.N.
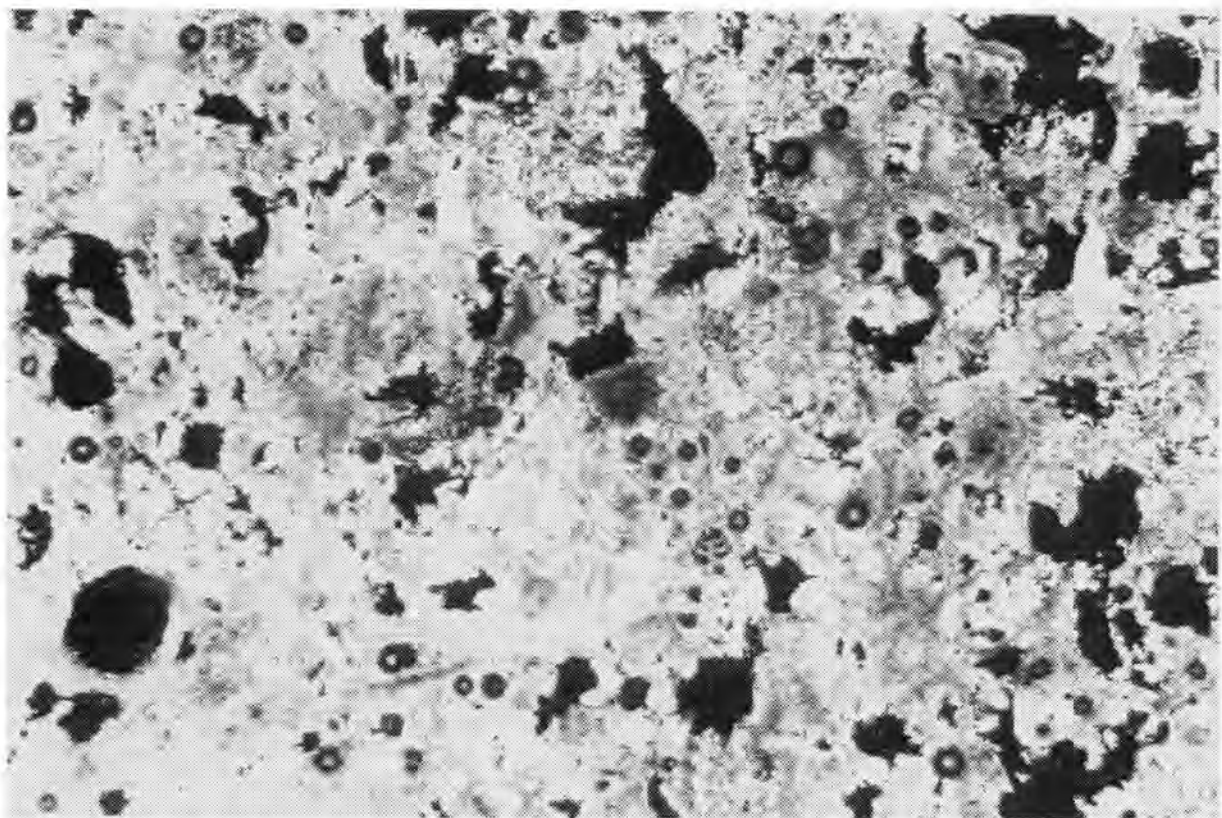
Figure 1b. Glogiberina limestone with some rounded fine grained aggregates of glauconite. (Malta). x92. C.N.
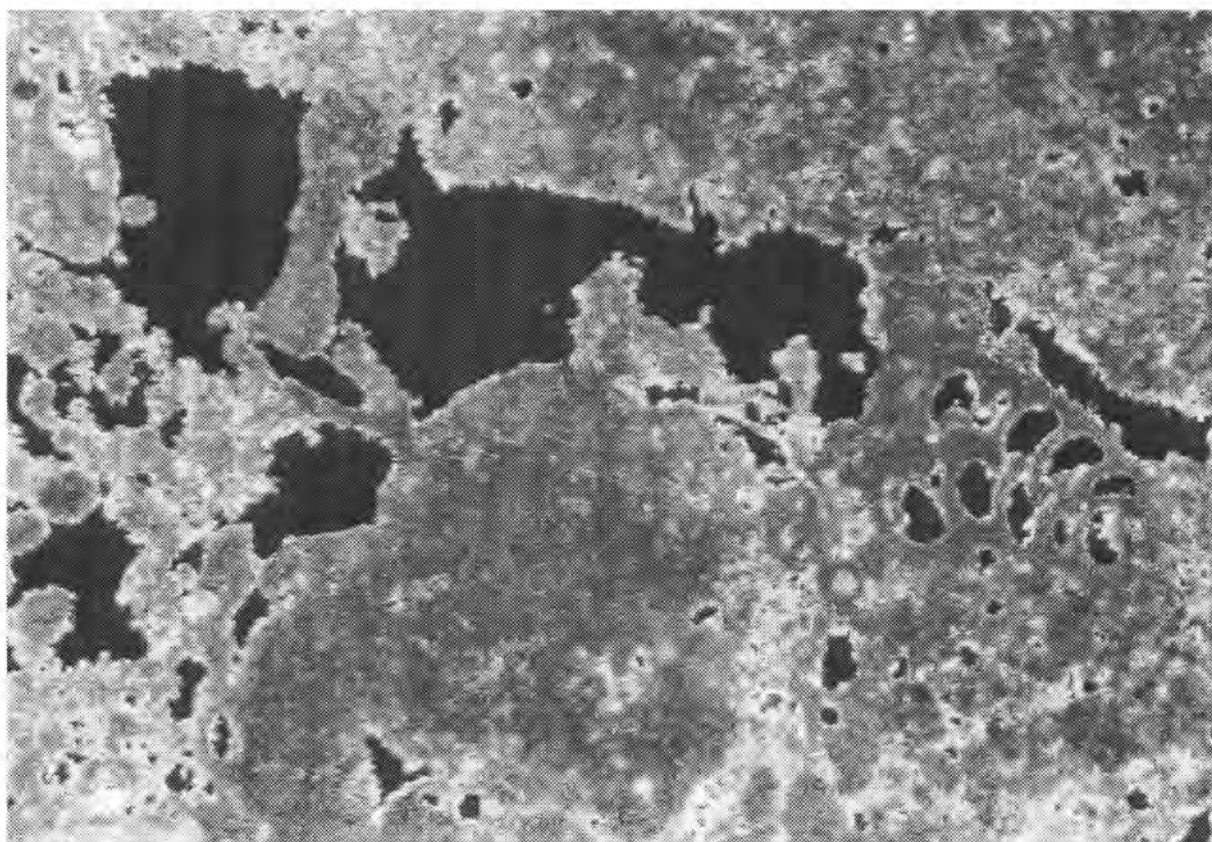
Figure 1c. Biomicrosparitic limestone. Intraparticle and vug porosity. (Bari). x40. C N.
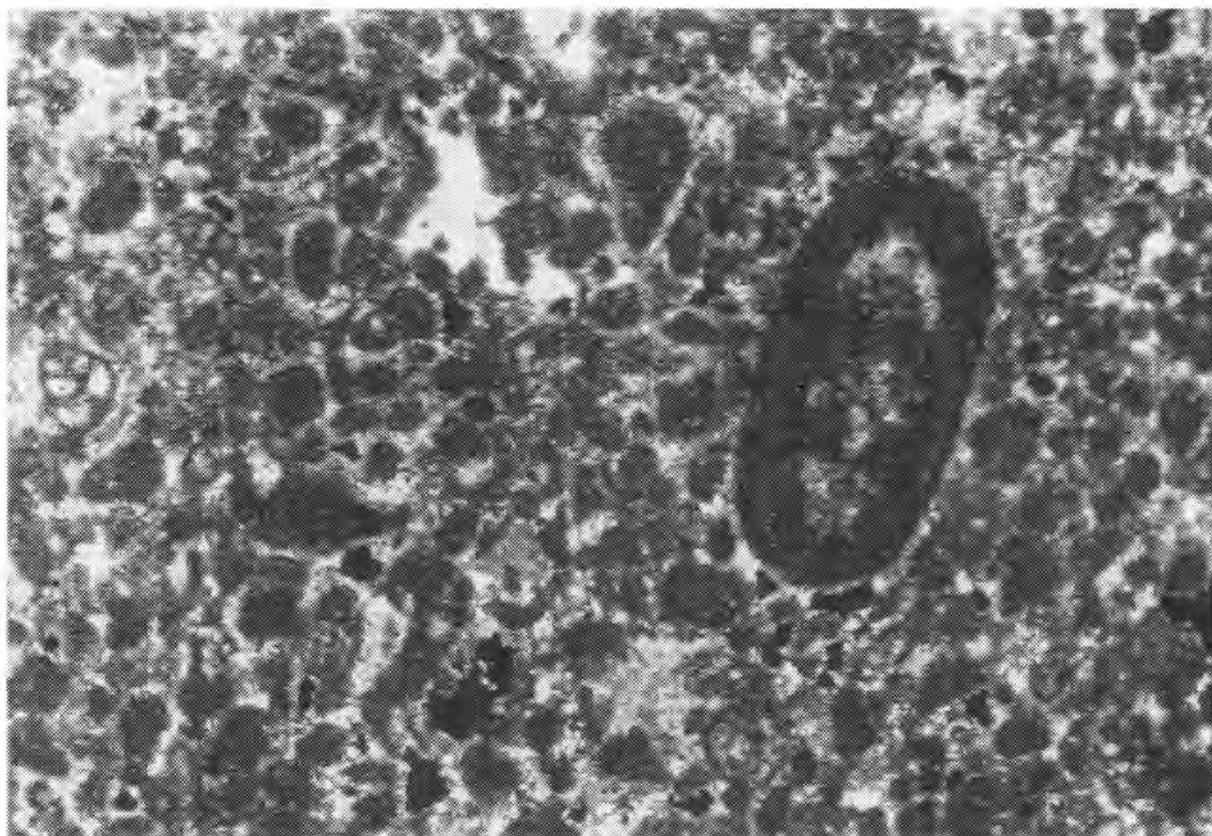
Figure 1d. Oolitic limestone. Bioclasts. Intercrystalline porosity. (Càdiz). x40. C N.
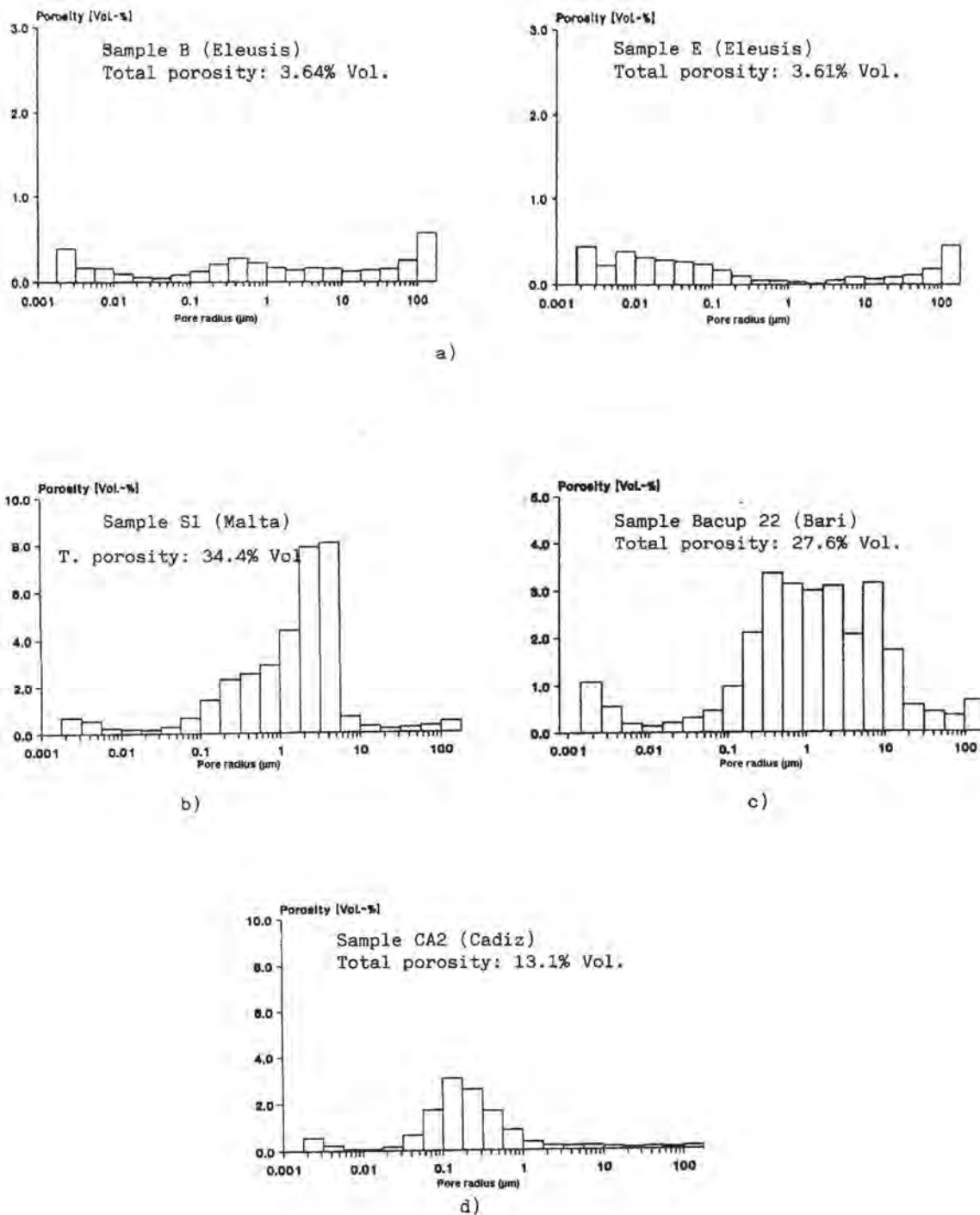
Figure 2 Hg– porosimetry: Pore radii distribution for representative stones

TABLE I

Some Characteristics of Representative Stones

Stone	Age	Description	P (%)	W (%)	U.C.S. (MPa)	P.S. (m²/g)
Pentellic marble White-grey marble (Demeter Snctuary of Eleusis (Greece))	Triassic to Upper Cretaceus	marble	3.5-4	0.2-0.4	75-100	0.04-0.13
Limestones	Triassic-Upper Jurassic and Upper Cretaceus	Micritic/biosparite limestone	2-4	5	≈ 50	0.13-2.22
Church of Sta. Marija (Siggiewi, Malta)	"Globigerina" limestone	Miocene	Biomicrosparitic limestone	32-37	10-13	42-52 (quarry) 21-33 (building)	5.75-7.92 (quarry) 0.53-0.99 (building)
Cathedral of Bari	Limestones	Lower Cretaceus	Biomicrosparitic/ biomicritic limestones	8-28 usually 12-20	2-4	120-180	0.20-0.60 usually <0.35
Cathedral of Cádiz	Estepa limestone	Middle-Upper Jurassic	All varieties	3-15	3-9	60-100	0.04-0.56
			Biomicrosparite	6	3	80-90	---
			Oolitic limestone	13	4.7	70	---

Note: The table columns as read left-to-right: Stone, Age, Description, P (%), W (%), U.C.S. (MPa), P.S. (m²/g). The "Church of Sta. Marija" and "Cathedral of Bari" rows have an additional stone-description subcolumn.

P = Total porosity

W = Water absorption

U.C.S.= Uniaxial compressive strength

P= Pore surface

TABLE II

Chemical data for the representative stones

	Malta	Bari		Cádiz (*)	
	S–1	B–1	B–2	Ca–1	Ca–2
SiO_2 (%)	2.94	—	0.2	0.65	<0.05
CaO (%)	48.88	55.6	55.3	55.06	55.50
Al_2O_3 (%)	0.73	0.02	0.07	<0.05	<0.05
MgO (%)	0.66	0.53	0.31	0.10	0.20
Na_2O (%)	1.00	0.04	0.07	0.13	0.11
K_2O (%)	0.39	0.02	0.03	0.03	<0.01
Fe_2O_3 (%)	0.45	0.03	0.05	<0.01	<0.01
Loss of ignition (%)	44.72	43.6	43.8	44.00	44.00
TOTAL	99.77	99.84	99.83	99.97	99.81

(*) Trace elements

	Pb (ppm)	Zn (ppm)	Sr (ppm)
Ca–1	7	4	34
Ca–2	20	6	99

The following elements have been also determined:

TiO_2 and BaO < 0.01%, Rb and Sb <10 ppm, Co, Cs, Cu, Ni and Cr <5 ppm, and Ag and Cd <1 ppm.

S–1: "globigerina" limestone from building

B–1: biomicrosparitic limestone

B–2: biomicritic limestone

Ca–1: biomicrosparite

Ca–2: oolitic limestone
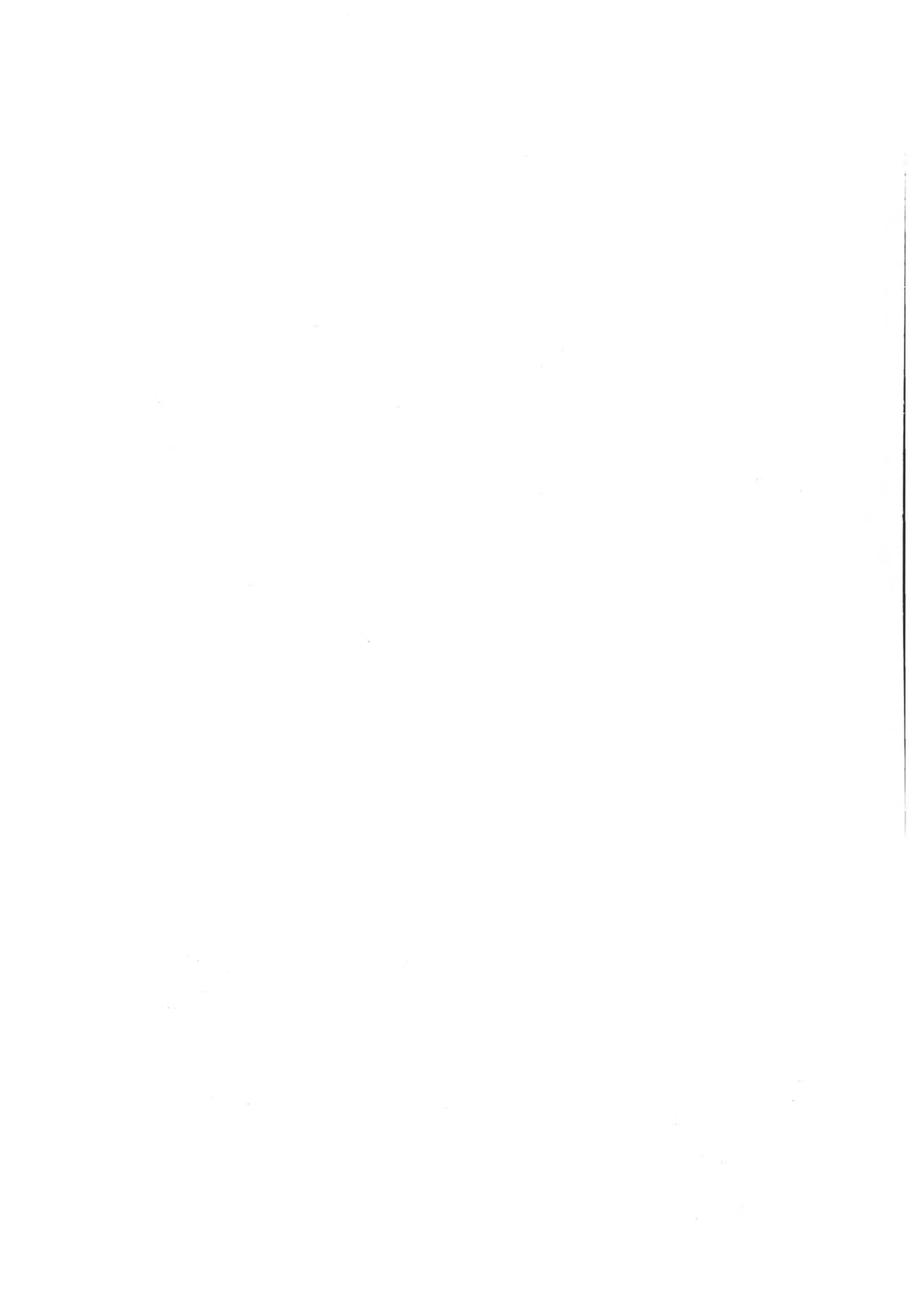
Th. Skoulikidis
E. Kalifatidou
K. Tsakona
M. Evangelatou

Salt spray tests on untreated and treated marble and stones
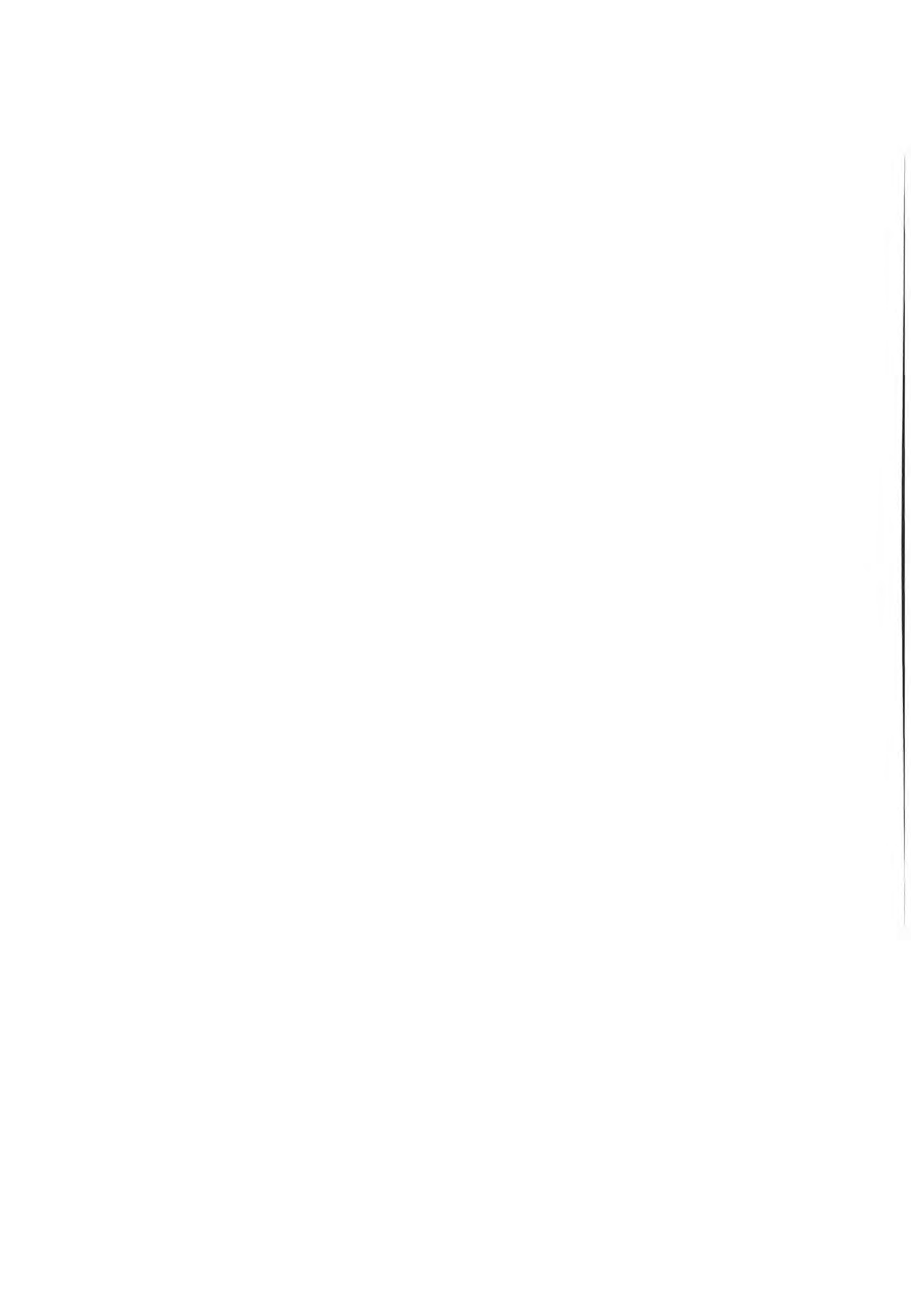
Salt spray tests on untreated and treated marble and stones

Th. Skoulikidis, E. Kalifatidou,
K. Tsakona, M. Evangelatou (*)
National Technical University of Athens, Faculty of Chemical Engineering,
Department of Materials Science and Engineering,
15780 Athens, Greece

Abstract

In order to investigate the damage of pentelic marble, used for the construction of the Acropolis monuments, Eleusis temple and several other monuments in Greece, as well as of several other stones from ancient Eleftherna (Crete, Greece), Cadiz Cathedral (Spain), Church of Sta Marija Ta' Cwerra at Siggiewi (Malta), produced by marine spray, we carried out accelerated salt spray tests on untreated specimens.

Measure of the intensity of the attack was the weight loss of the specimens and the calculated one from the determination by atomic absorption of Ca^{2+}, Mg^{2+} and (in some cases) Fe^{2+} in the solution with which each specimen was washed out in the salt spray chamber.

For untreated specimens the resistance to salt spray is:

Pentelic marble > Cadiz B > Cadiz A > Malta > Eleftherna B > Eleftherna A stones.

The same measurements were carried out on specimens protected by a reversible polymer pigmented or not by n–semiconductor. The same inequality as the above is valid for both types of protection. The resistance of the specimens to salt spray is:

treated with polymer + n–semiconductor > with plain polymer >> untreated.

These results are a proof that the system reversible polymer + n–semiconductor protects marble and stones, not only from sulfation, but also from marine spray.

1. Introduction

In order to investigate the damages produced by marine spray and polluted atmosphere, it is naturally possible to evaluate a synergetic attack of salt spray and acidic attack (f.e. $SO_2 \rightarrow H_2SO_4$ or/and $NO_2 \rightarrow HNO_3$) simultaneously in salt spray chamber. The rate of acidic attack (dissolution of calcareous stones) is much more higher than the salt spray one and the presence of salt in the spraying water does not increase appreciably the rate of dissolution; thus it is necessary to measure separately the salt spray attack. On the other hand salt spray and sulfation can not be measured simultaneously, because in the foam of salt solution the SO_2 will be transformed into H_2SO_4 and the NO_2 into HNO_3 and we will have again acid rain with salt spray. Thus sulfation and salt spray attack must be carried out separately.

In the present work, in order to compare the damages produced on pentelic marble and on several stones from salt attack, after the performed sulfation tests on untreated and protected specimens on the same stones, accelerated salt spray tests were carried out in a ASTM salt spray chamber on untreated specimens and on specimens protected by reversible polymer pigmented or not with n–semiconductor (1–10).

2. Materials, shape and dimensions of specimens

The marble and stone specimens have the following geological description and characteristics (Table 1).

Table 1
Geological description and characteristics of marble and stone

Stone Type	Geological Description
Pentelic marble	White marble, medium grained, well recrystallized, with granoblastic polygonal texture
Cadiz A	Type I: Micritic and and suboolitic limestone: Micritic limestone with some pores and voids, here and there filled by sparry calcite. Sometimes a suboolitic facies develops.
Cadiz B	Type II: Oolitic limestone with sparry calcitic cement: Oolitic limestone rich in spherical and subspherical ooids. Some of them show concentric structure. Mostly show cryptocrystalline calcite composition. Sparry calcite fills the intraooids spaces and voids.
Malta	Limestone from Mqabba quarry: Biomicritic limestone: They are pale yellow micritic foraminifera limestones in which globigerinids are abundant. Glauconite is found usually in rounded fine grained aggregates. Sometimes it is olive coloured, generally it is oxidized to limonite. Iron oxides coated tests and cement grains. Detrital small quartz and zircon grains occur as minor constituents (less than 1%). These rocks are porous with large quantity of voids.
Eleftherna A	Calcite with inclusions of moschovite, kaoline and quartz.
Eleftherna B	Calcite with inclusions of moschovite, kaoline, quartz, potassium nitrate and calcium oxalate.

The specimens were cut from plates of ~ 0.5cm thickness and their dimensions were 4X3cm or 4X1cm.

3. Procedure

The specimens after mechanical treatment, to acquire the above dimensions, were washed with deionised water, dried at 80° C till constant weight and placed in a salt spray chamber.

The continuously sprayed salt solution was 5% w/v and the temperature 30° C. Under each specimen a glass container was placed to collect the solution after washing the specimens (Fig. 1).
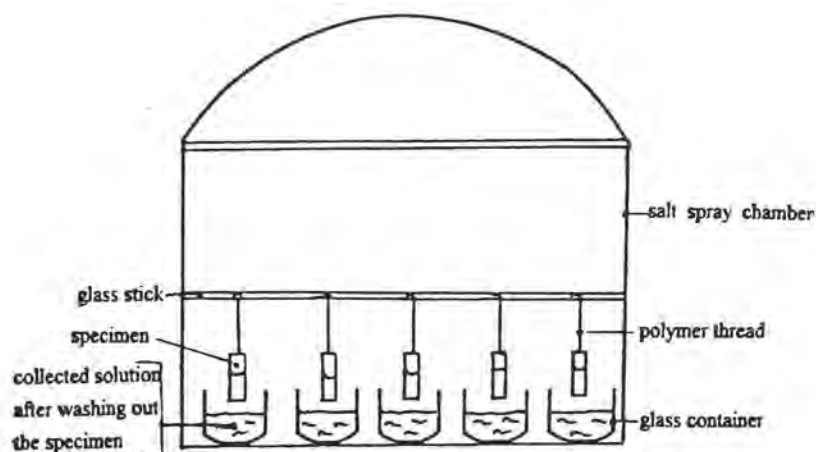
Fig. 1 Arrangement of the specimens in salt spray chamber.

At several time intervals the specimens were removed, washed with deionised water till the removal of all Cl⁻ and dried at 80°C till constant weight; the weight loss was converted to mg/cm². The solution in each glass, with the washing solution of each specimen, were analysed by atomic absorption for Ca^{2+}, Mg^{2+} and (in some cases) for Fe^{2+}. The total loss of each specimen in Ca^{2+}, Mg^{2+} and Fe^{2+} was calculated as $CaCO_3$ + $MgCO_3$ + FeS_2 (or Fe_2O_3) and compared to the weight loss of each specimen. The same specimens were placed back in the salt spray chamber. The specimens used were untreated, treated with reversible polymer (in some cases) and treated with the same reversible polymer coating pigmented with n–semiconductor (doped Al_2O_3) (1–10).

4. Preliminary measurements

First of all the reproducibility of the measurements was checked and it was found that the reproducibility error for the weight loss of specimens was not higher than ±0.5 mg/cm² and for the atomic absorption results ±0.001 mg/cm²

On the other hand, because the weight loss vs time is rectilinear, the correlation coefficient r^2 is not smaller than 0.9.

It is also found that two to four specimens of each type are adequate for reproducibility reasons.

The accuracy and reproducibility of the measurements are independent from the total surface of the specimens: 4 x 3 or 4 x 1.

5. Measurements and results

All types of specimens were placed simultaneously in the salt spray chamber for comparison reasons (same conditions).

The results for weight loss are shown in Figs 2–10.
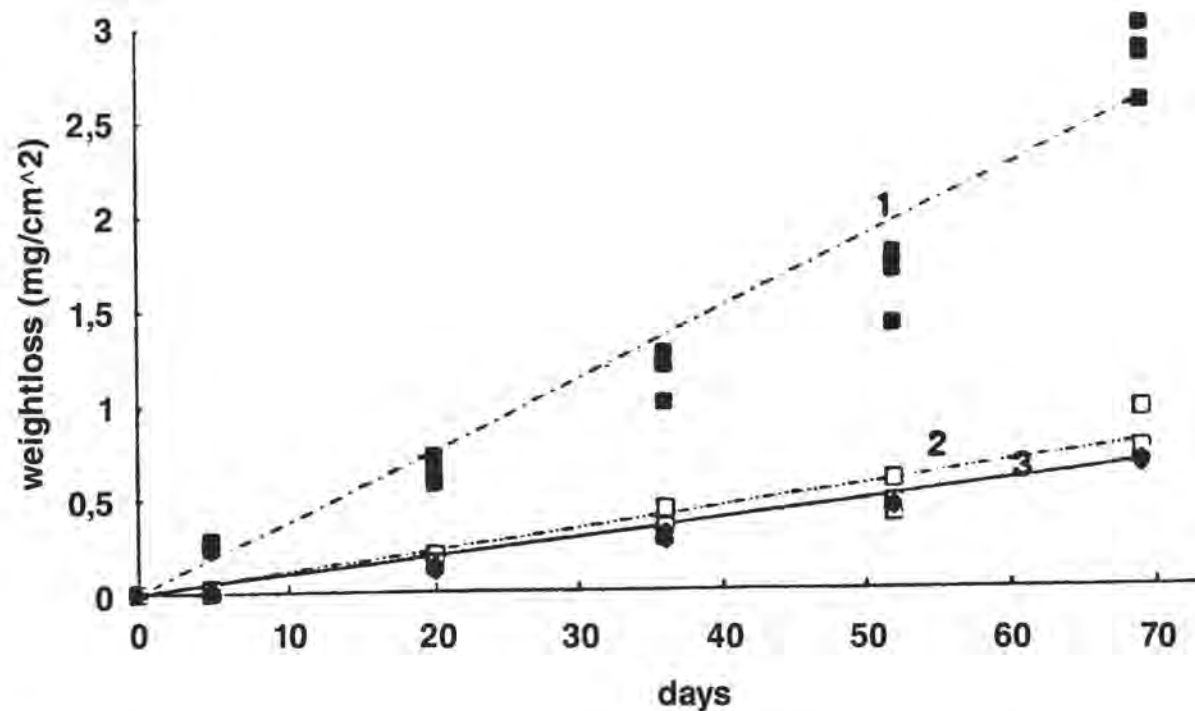
Fig. 2. Salt spray test on unprotected and protected Pentelic marble (1. unprotected, 2. protected with reversible polymer, 3. protected with pigmented reversible polymer).
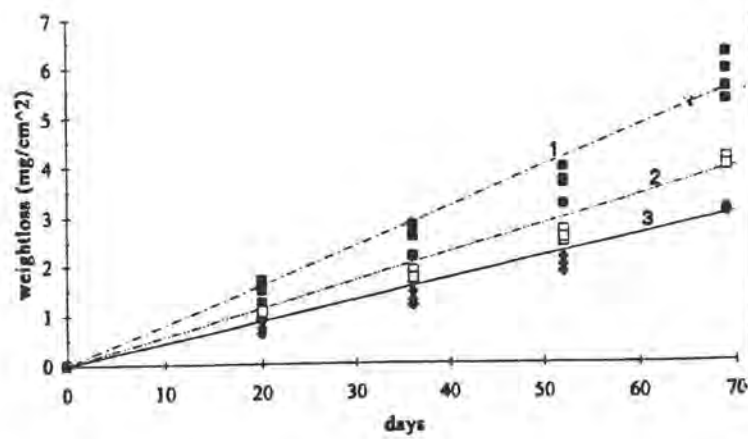
Fig.3.   Salt spray test on unprotected and protected Malta stone (1. unprotected, 2. protected with re-
          versible polymer, 3. protected with pigmented reversible polymer).
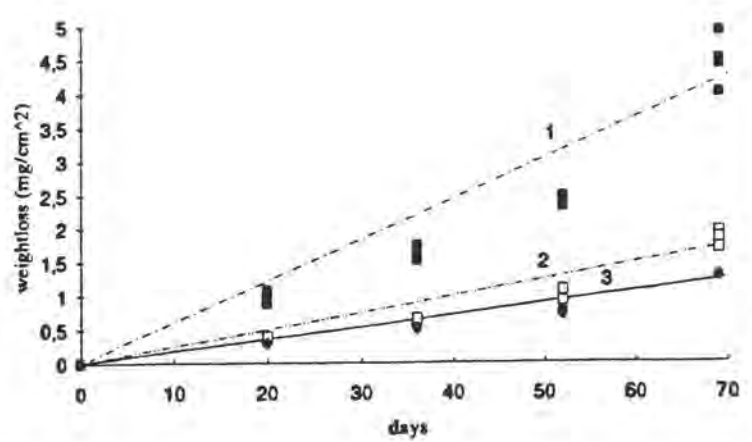
Fig. 4.   Salt spray test on unprotected and protected Cadiz A stone (1. unprotected, 2. protected with re-
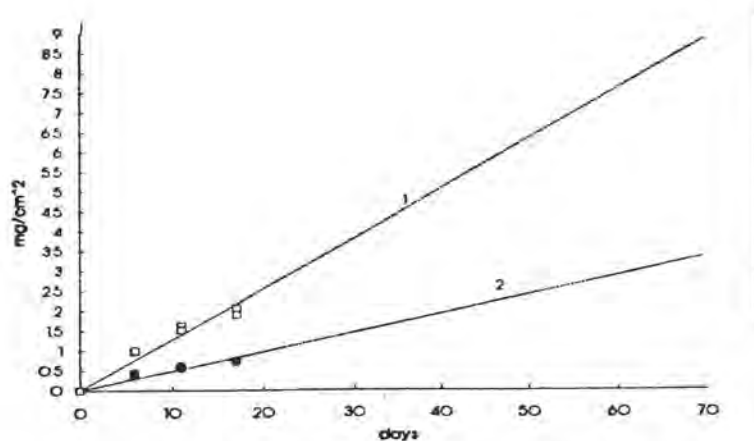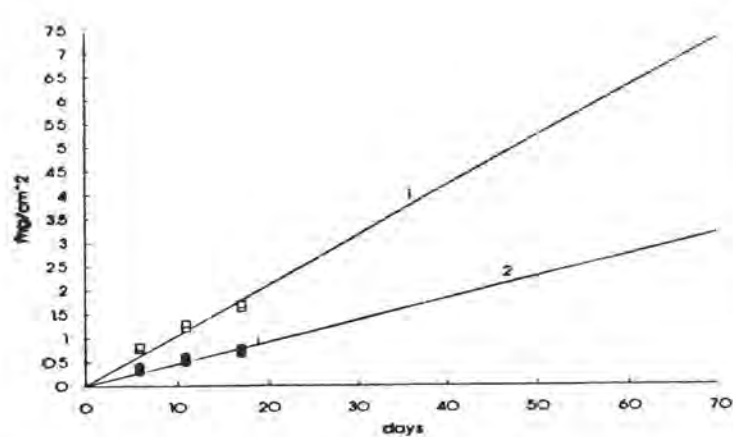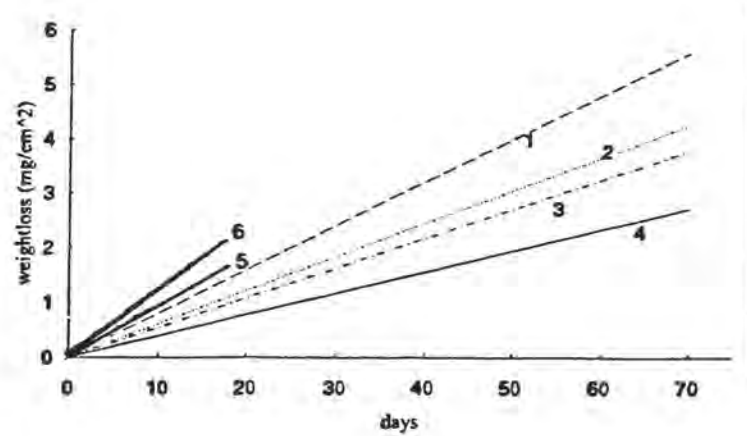   versible polymer, 3. protected with pigmented reversible polymer).
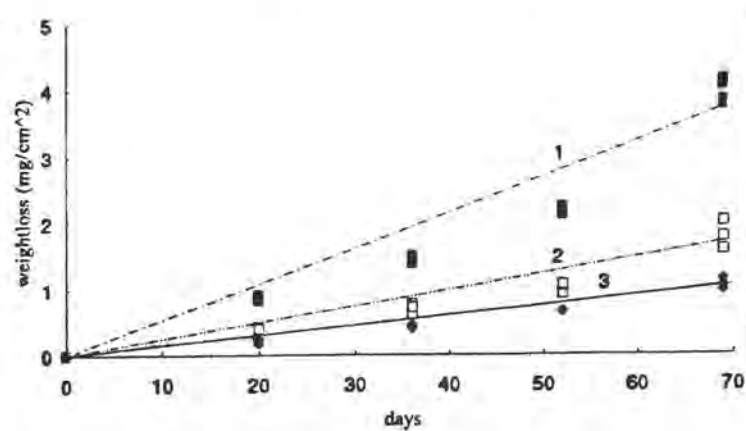
Fig. 5.   Salt spray test on unprotected and protected Cadiz B stone (1. unprotected, 2. protected with re-
          versible polymer, 3. protected with pigmented reversible polymer).

Fig. 6. Salt spray test on unprotected and protected Eleftherna A stone (1. unprotected, 2. protected with pigmented reversible polymer).

Fig. 7. Salt spray test on unprotected and protected Eleftherna B stone (1. unprotected, 2. protected with pigmented reversible polymer).

Fig. 8.   Salt spray test on unprotected stones (1. Malta stone, 2. Cadiz A, 3. Cadiz B, 4. Pentelic marble, 5. Eleftherna A, 6. Eleftherna B stone).
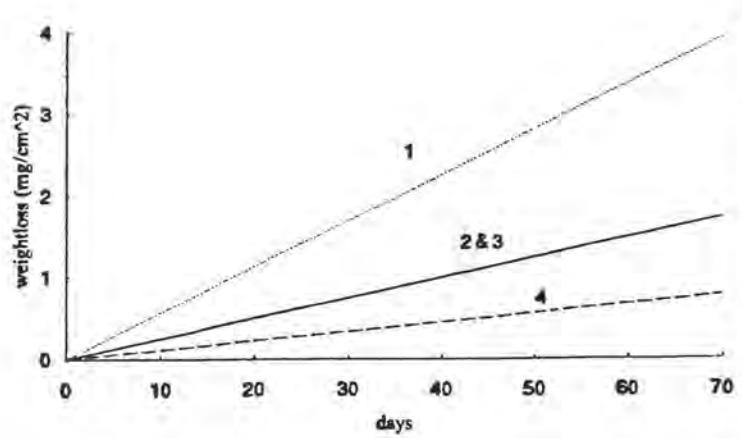
Fig. 9   Salt spray test on stones, protected with reversible polymer (1. Malta stone, 2. Cadiz A, 3. Cadiz B, 4. Pentelic marble).
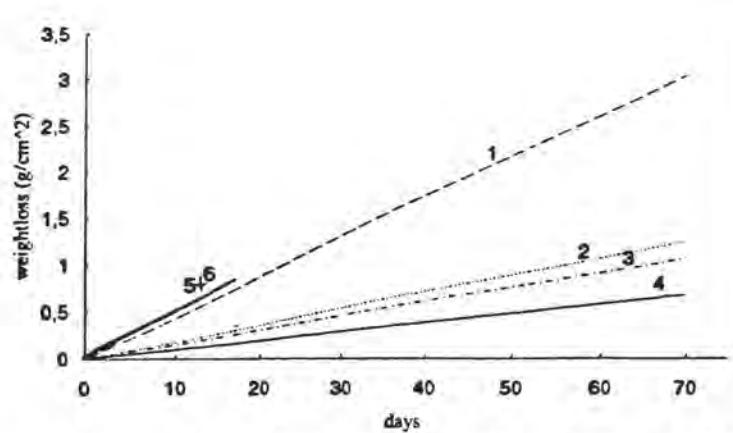
Fig. 10. Salt spray test on stones, protected with pigmented reversible polymer (1. Malta stone, 2. Cadiz A, 3. Cadiz B, 4. Pentelic marble, 5. Eleftherna B, 6. Eleftherna A stone)

In the case of Pentelic marble the collected solutions were analysed by atomic absorption for Ca^{2+}, Mg^{2+} and Fe^{2+}. The results are shown in Figs 11–13.
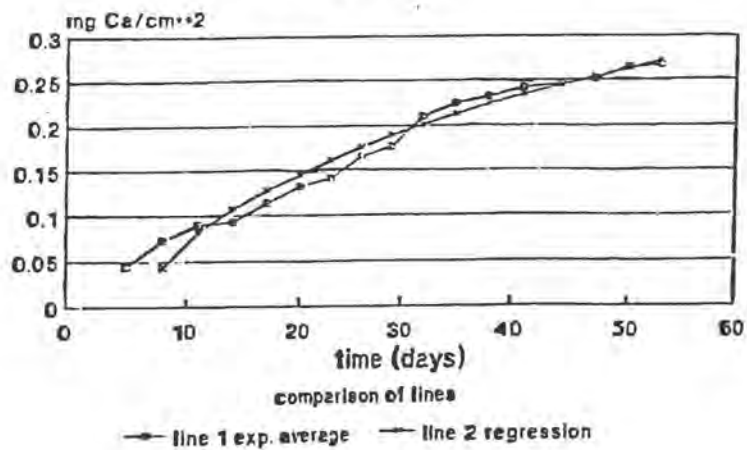
Fig. 11. Ca^{2+} dissolution from Pentelic marble by salt spray.
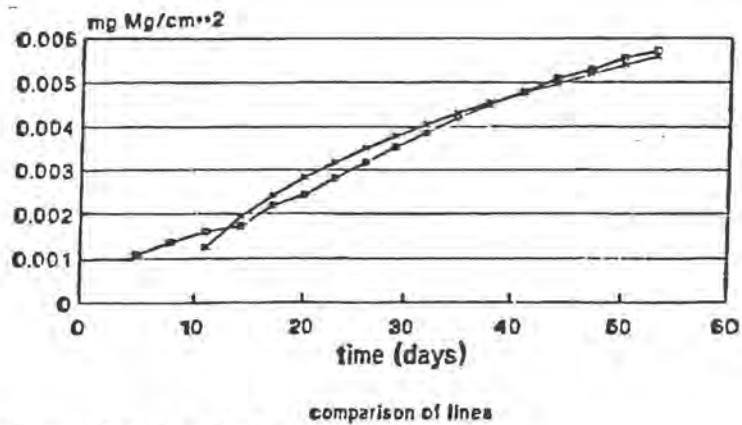
Fig. 12. Mg^{2+} dissolution from Pentelic by salt spray.
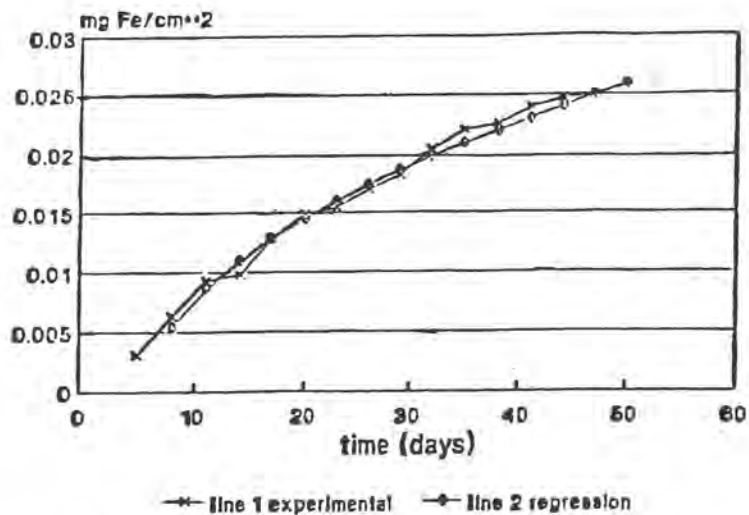
Fig. 13. Fe^{2+} dissolution from Pentelic marble by salt spray.

6. Discussion

From the above mentioned it follows: The weight loss of all types of untreated specimens vs time is rectilinear. The same is valid for the protected with pigmented or not reversible polymer.

The weight loss is approximately proportional to the total porosity of the stones (Table 2).

Table 2
Resistance to salt spray*

Types of stones	Weight loss mg/cm²		
	Unprotected	Protected with polymer	Protected with pigmented polymer
Pentelic marble	2.79	0.79	0.66
Cadiz B	3.95	1.79	1.05
Cadiz A	4.46	1.81	1.28
Malta	5.73	4.03	3.06
Eleftherna B	7.33	–	3.19
Eleftherna A	8.91	–	3.37

* 70 days exposure; for Eleftherna after extrapolation using the rectilinear function (Figs. 6 and 7).

The protection by the reversible polymer is appreciable because it decreases the porosity and changes the pore size distribution of the stones; thus the diffusion of Ca^{2+}, CO_3^{2-}, Mg^{2+}, Fe^{2+} through the pores of the polymer during dissolution is retard, the porosity of polymer being smaller than the one of stones. The protection with n–semiconductor, in comparison with the unpigmented polymer although appreciable, is small because the n–semiconductor does not intervene to the mechanism of dissolution as it is the case for the sulfation (11–20), but it imposes some barrier to the diffusion of positive ions because it has the predisposition to offer electrons and attack them. The n–semiconductors, as pigments in reversible polymers, impose a high protection on stones against sulfation, and, simultaneously protect also stones against marine spray, they do not get exhausted, protect the polymer from U.V. attack, and repulse the suspended particles and some types of microorganisms.

When we calculate the total weight loss for 70 days for Pentelic through the amount of Ca^{2+}, Mg^{2+}, Fe^{2+} (found by atomic absorption in the solution) by conversion of the ions to the corresponding compounds: $CaCO_3$, $MgCO_3$, FeS_2 we found:

Ca : 0.27 mg/cm² $\Rightarrow$ $CaCO_3$: 0.67 mg/cm²
Mg : 0.0058 mg/cm² $\Rightarrow$ $MgCO_3$: 0.02 mg/cm²
Fe : 0.027 mg/cm² $\Rightarrow$ FeS_2 : 0.058 mg/cm²

Total : 0.753 mg/cm²

This does not coincide with the 1.5 mg/cm² total weight loss for the pentelic marble after 70 days exposure in a salt spray chamber. In the bottoms of the glasses, where the solution of NaCl was collected after washing out the specimens, small pieces of stones were found. This was done also for the other stones with the same qualitative results. This means that, beside the dissolution of the compounds $CaCO_3$, $MgCO_3$ and FeS_2 by the salt spray, small pieces detachment from the specimens take place, due the higher sensibility of the grain boundaries in comparison to the grain surfaces.

7. Conclusions

From the above mentioned it follows:

1. Besides other actions the marine spray dissolve the constituents $CaCO_3$, $MgCO_3$, FeS_2 or Fe_2O_3 of calcareous stones and attacking preferentially the grain boundaries follow also to small pieces detachment.

2. The total weight loss is proportional to time.

3. The resistance to salt spray is:

   Pentelic marble > Cadiz A > Cadiz B >

   Malta > Eleftherna B > Eleftherna A

4. If the surface of specimens is spread by a reversible polymer the weight loss is appreciably retard.

5. Further protection is acquired if the polymer is pigmented by n–semiconductor (Al_2O_3).

6. Besides the high protection against sulfation (1–10), the polymer pigmented with n–semiconductor protects also the stones from marine spray: The resistance is: treated with polymer pigmented with n–semiconductor >with unpigmented polymer >> untreated.

References

1. Th. Skoulikidis: "The deterioration of ancient monuments and statues by the atmospheric pollutants and their protection", Intern. Seminar on the Laws Against Pollution, Salonica (Greece), 1980, proc. pp. 349–400. (Invited papers)

2. Th. Skoulikidis: "Presentation of protection methods for marbles against atmospheric pollution", Troisiemes Journees de l' Industrie Minerale, Universite Libre de Bruxelles, Bruxelles, 1981,proc. pp. 839–856, (Invited paper).

3. Th. Skoulikidis, D. Charalambous, E.Papakonstantinou: "New protective coatings for marble against pollution", Intern. Symposium on Engineering Geology as Related to the Study, Preservation and Protection of Ancient Works, Monuments and Historical Sites, Athens, 1988, proc. pp.871–875.

4. Th. Skoulikidis, D. Charalambous, E. Kalifatidou: "New protective coatings for marble against pollution", VIth Intern. Congress on Deterioration and Conservation of Stone, Torun (Poland), 1988, proc. pp. 534–544.

5. Th. Skoulikidis, E. Kritikou: "Protective coating for marble and stones using n–semiconductor as pigments", STREMA Intern. Conference, Seville, 1991.

6. Th. Skoulikidis, E. Kritikou: "Protection of marbles of ancient monuments; method of doped semiconductors", 2nd Intern. Symposium for the Conservation of Monuments in the Mediterranean Basin, Geneva, 1991, proc. pp. 389–396.

7. Th. Skoulikidis, E. Kritikou: "Protective coatings for marbles and stones using polymers pigmented with doped n–semiconductors", 7th Intern. Congress on Deterioration and Conservation of Stones, Lisbon, 1992, proc. Vol. III, pp. 1137–1145.

8. Th. Skoulikidis, P. Vassiliou, D. Charalambous, P. Papakonstantinou, E. Kalifatidou, S. Vlachos, E. Kritikou: "Protection of steel and marbles from pollution based on their similar mechanism of decay", 1st Intern. Exhibition and Conference of Environmental Technology for the Mediterranean Regions (HELLECO), Athens, 1993, proc. pp. 106–115.

9. Th. Skoulikidis, E. Kritikou: "Protective coating for marbles and stones using n–semiconductors as pigments", 3rd Intern. Conference STREMA 93, Bath (U.K.), 1993, proc. pp. 241–249.

10. Th. Skoulikidis, P. Vassiliou, E. Kalifatidou P. Papakonstantinou:, E. Kritikou, D.Charalambous, "Protection of marble against atmospheric pollution, using methods based on the mechanism of decays", Air and Waste Management Association 1993 Annual Meeting, Denver, U.S.A., proc. pp. 146.02, 1–23, Vol. 14.

11. Th. Skoulikidis, D. Charalambous, E. Papakonstantinou, N. Beloyannis: "The mechanism of marble sulfation by SO2 action", 3rd Intern. Congress on the Deterioration and Preservation of Building Stones, Venice, 1979, proc. pp. 439–452.

12. Th. Skoulikidis: "Atmospheric corrosion of the reinforcements of reinforced concrete and of marbles of ancient monuments and statues" Intern. Symposium on Atmospheric Corrosion, Hollywood, Miami, Florida, 1980, proc. pp. 807–825.

13. Th. Skoulikidis, P. Papakonstantinou–Ziotis: "The mechanism of sulfation by atmospheric SO_2 of limestones and marbles of the ancient monuments and statues. I. Observations in situ and measurements in the laboratory; activation energy", Br. Corros. J., 16, 63 (1981).

14. Th. Skoulikidis, D. Charalambous: "The mechanism of sulfation by atmospheric SO_2 of limestones and marbles of the ancient monuments and statues. II. Hypothesis and proofs on the rate determining step; galvanic cell model", Dr. Degree Thesis of D.Charalambous, Br. Corros. J., 16, 70 (1981).

15. Th. Skoulikidis, D. Charalambous, P. Papakonstantinou –Ziotis: "Additional prooves for the galvanic cell model, valid for the marble sulfation", 4th Intern. Congress on the Deterioration and Protection of Building Stones, Louisville, 1982, proc. pp. 307–310.

16. Th. Skoulikidis: "Mechanism of sulfation of marbles by atmospheric SO_2", Symposium on Chemistry and Biology in Service of Research and Preservation of Cultural and Historical Inheritance, Sofia, 1983, proc. pp. 45–53, (Invited paper).

17. Th. Skoulikidis: "Effects of primary and secondary air pollutants and acid depositions on (ancient and modern) buildings and monuments", Symposium on Acid Deposition–A Challenge for Europe, Karlsruhe, 1983, proc. pp. 193–226, (Invited paper).

18. Th. Skoulikidis, D. Charalambous, P. Papakonstantinou –Ziotis: "Mechanism of sulfation by atmospheric SO_2 of the limestones and marbles on ancient monuments and statues. III. Further proofs for the galvanic cell model", Br. Corros. J., 18, 200 (1983).

19. Th. Skoulikidis, D. Charalambous: "Prooves for the galvanic cell model of the mechanism of marble sulfation", Vth Intern. Congress on the Deterioration and Preservation of Stones, Lausanne, 1985, proc. pp. 547–551.

20. Th. Skoulikidis, D. Charalambous, M. Kyrkos: "Further proofs for the mechanism of sulfation (Galvanic cell model) of marbles and orientation for their protection", Conference on the Recent Advances in the Conservation and Analysis of Artifacts, University of London, London, 1987, proc. pp.383–385.

Fulvio Zezza

Decay patterns of weathered stones in marine environment

Decay patterns of weathered stones in marine environment

F. Zezza

Istituto di Geologia Applicata e Geotecnica– Facoltà di Ingegneria–Politecnico di Bari (Italy)

1. The decay patterns of marbles, limestones and calcarenites of the Mediterranean coastal environment have been reconstructed by means of the study methodology *I.C.A. (Integrated Computerized Analysis) for Weathering* to express in qualitative and quantitative terms the phenomenon of stone decay which represents one of the principle objectives of the E.C. Project "Marine Spray and Polluted Atmosphere as Factors of Damage to Monuments in the Mediterranean Coastal Environment".

Four pilot monuments were selected along the east–west axis of the Mediterranean basin in order to determine the effects of marine aerosol and of pollution on stone decay. In the monitoring stations set up at the pilot monuments of Cadiz (Spain), at the entrance to the Mediterranean, Siggiewi (Malta), in the centre, Bari (Italy), and Eleusis, near Athens (Greece), a group of ions (Na^+, Mg^{++}, Cl^-) of clear marine origin is found to be always present in the wet and dry depositions together with metallic elements (V, Mn, Zn, Fe, Cu) of anthropic origin. Different levels of acidity in the depositions are recorded where the polluting anthropogenic activities are intense due to the presence both of urban centres and of refineries, heavy industries and cement factories. In this regard, the most acid deposition is found at Eleusis as opposed to Malta, situated in the centre of the Mediterranean basin. The coastal environment is, therefore, characterized by particularly "aggressive" conditions (fig. 1) which occur in the context of the stone–environment binomy, where the natural and artificial pollutants enter the system on which the process of weathering in the Mediterranean area depends (F. Zezza, 1996).

The stone materials employed for the construction of the pilot monuments taken in consideration are common to all of them and have been exposed to "severe" environmental conditions determined by the agents of weathering for different lengths of time from over 2000 to 200 years ago up to the present.

The non–destructive in situ analyses and the elaborations carried out in the laboratory concerned in particular: a) the classification of weathering forms and mapping of stone decay; b) the thickness of the decay layers and their relative characteristics; c) the rate of weathering in time.

Generally, the study procedures for weathered stone employ mineralogical–petrographic methodologies, techniques and instrumentation involving the electron microscope (transmission and scanning) together with micro analyses (EDAX–EDS, laser, Raman microprobe) IR spectroscopy, mass spectrometry. On the other hand, in the context of non–destructive analyses, various techniques are proposed for the investigation of the structural characteristics of walls and of the stone materials with which they are constructed. The possibility to evaluate at the same time the surface forms of decay and its effects in depth is a relatively recent development (F. Zezza, 1989) while the results of this project involve experimentation to determine the weathering rate suffered by the stones in the course of time and the classification of the decay layers.

In this context, the verification of the re-

sults obtained with the methodology I.C.A. for Weathering was made in experimental form on representative samples of the stone materials investigated (Fig. 2).

2. The weathering forms which affect marbles, limestones and calcarenites in indoor and outdoor environments are apparently those which are frequently found on architectonic and sculptural surfaces, with the exception of the cementitious encrustations at Eleusis (tab. 1).

With respect to the weathering forms found on stone materials in continental environments, these forms are, however, characterized by the significant presence of neoformation salts resulting from the effects of the marine aerosol and atmospheric pollution along the coast. *Halite* is, in fact, present as the principle neoformation mineral on the stone in all the weathering forms. The other salts of marine origin which stand out in a particular way in relation to the microenvironmental conditions are: *thenardite* and *trona* at Cadiz in accordance with the high Na⁺ content of the site; *thenardite* associated with other chlorides such as *sylvite* is linked with the forms of decay at Malta where the action of the marine aerosol is considerable; *syngenite* is present in the limestones and marble of Bari owing to the high K⁺ concentrations of the site.

For their part the stone materials of Eleusis, as a result of the high level of pollution on the site, reveal together with halite the presence of *nitrates* and of *oxalates* as well as cementitious encrustations and pink–yellow Fe based patinas (Figs. 3–7).

3. In order to investigate the stones below the weathered surfaces, non–destructive analysis has been carried out with homeo–surface method.

This method allows the characteristics of the stones to be established through the interpretation of the buried structures. The main information to obtain is the general aspect of the distance–time diagram which includes the number of segments and their reciprocal relations; each linear segment indicates the velocity value of every layer passed through.

The measurement sections selected and referred to the different forms of stone decay and to the different types of stone material studied, allowed examples to be obtained of distance–time diagrams reconstructed using the method of the propagation of ultrasonic pulses to establish the changes in physical conditions of the stone and the depth of weathered layers.

For the marbles exposed in outdoor environment (Eleusis and Bari) different types of diagrams (Fig. 8) were obtained which indicate: a) the presence of parallel and subparallel decay layers where *black crust* and *cementitious encrustations* develop; b) weathered layers with irregular surfaces and irregular buried surfaces where forms of *corrosion* and *selective weathering* are found; in the latter case also vertical diques are found when the homogeneity of the marble is altered by scistosity planes with micaceous veins; c) buried laterally varying structures and change of the dip of sub–surface are characteristics of the marbles effected by *fissuring* and *detachment*. With regard to the number and thicknesses of the decay layers, a first superficial layer is always present which has a millimetric thickness (5–8 mm); this is followed, as is clearly shown by the information obtained from the distance–time diagrams, by two or three other layers the characteristics of which improve, though gradually, in the remaining depth of 2.8–4 cms, or in some cases more.

The elaboration of the distance–time diagrams for the limestones indicates two–layered buried structures with irregular surface and irregular buried surfaces in the case of forms linked to *corrosion* and *selective weathering*, and buried step and irregular surface where *detachments* predominate accompanied by *fissuring* and *granular disaggregation*. The depth of the first external and more decayed layer varies, in

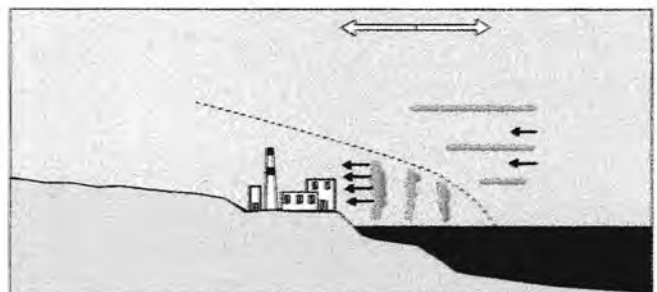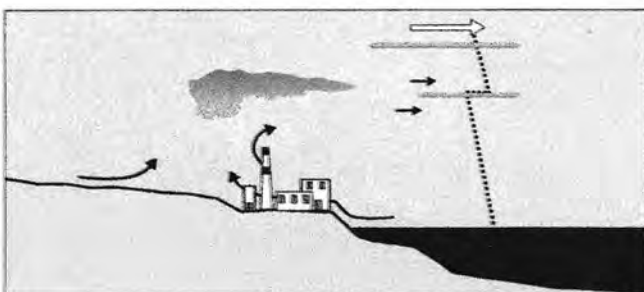# VERTICAL DISTRIBUTION OF SEA - SALT IN THE ATMOSPHERIC LAYERS
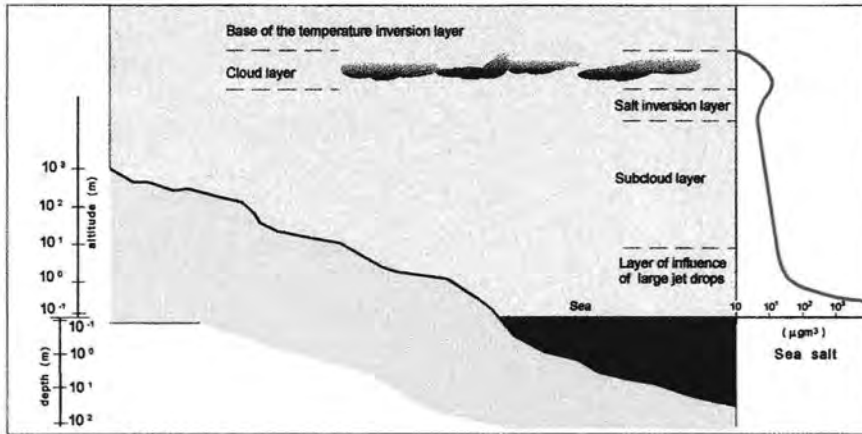
(From Zezza F. - Macrì F., 1995 - modif.)

SCHEME OF THE CIRCULATION REGIEME OF THE SEA-BREEZE ON THE SHORES OF THE MEDITERRANEAN
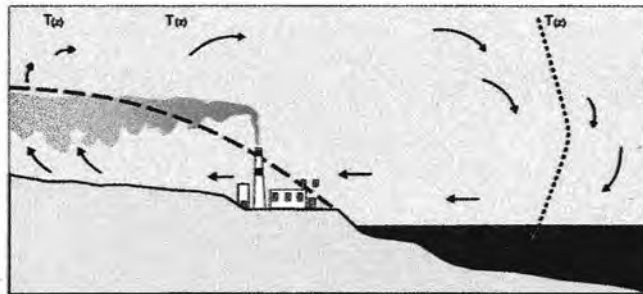
part of the pollutants produced along the coast enter in circulation and are dispersed in the layer of unstable air during periods of breeze to return and reappear many days later with the successive

(From Millan M.M:, 1992 - modif.)

Fig. 1

Fig. 2

Tab. 1
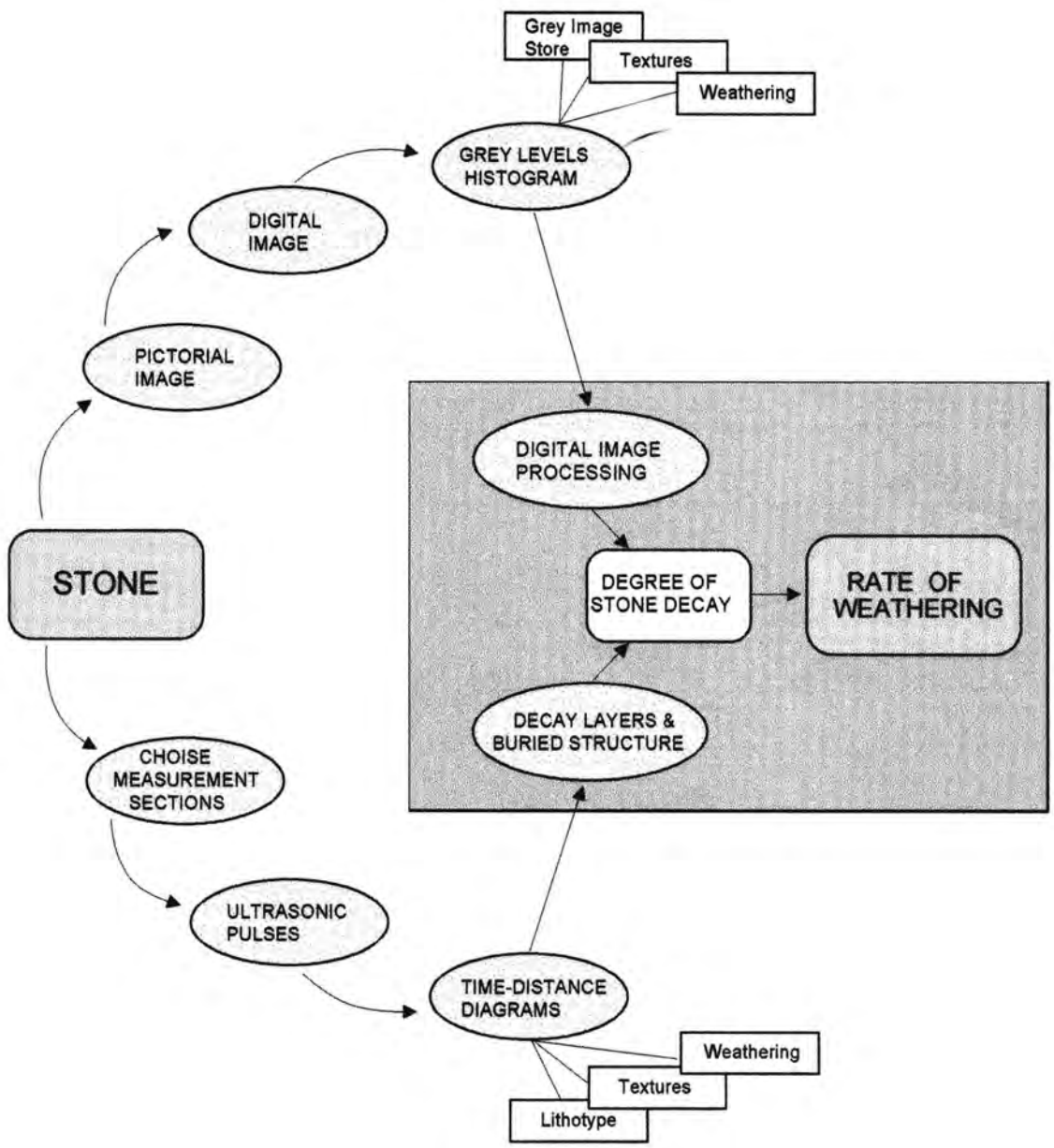
PILOT MONUMENT

WEATHERING FORMS

PILOT MONUMENT	ENVIRONMENT	MARBLE	LIMESTONE	CALCARENITE
CATHEDRAL OF CADIZ, SPAIN XVIII century	Indoor		– Detachment – Granular disaggregation – Patinas – Exfoliation – Efflorescences	– Granular disaggregation – Fissuring – Efflorescences
	Outdoor	– Granular disaggregation – Exfoliation – Black crust	– Granular disaggregation – Black crust – Corrosion – Detachment	
CATHEDRAL OF BARI, ITALY XIII century	Outdoor			– Differential deterioration – Exfoliation – Granular disaggregation
	Indoor		– Granular disaggregation – Corrosion (alveolization) – Pulverization – Efflorescences – Exfoliation – Detachment – Fissuring	
CHURCH OF STA. MARIJA TA' CWERRA, MALTA XVIII century	Indoor			– Detachment – Fissuring – Efflorescences
	Outdoor		– Selective corrosion	– Differential deterioration – Black crust – Detachment – Fissuring
SANCTUARY OF DEMETER ELEUSIS, GREECE VI cent. B.C. - Roman period	Outdoor	– Granular disaggregation – Corrosion – Black crust – Cementitious encrustations – Pink-yellow patinas – Exfoliation – Detachment – Fissuring		

MARBLES - *Weathering forms*

BLACK CRUST DETACHMENTS

SANCTUARY OF DEMETER IN ELEUSIS

Black: black crust
Yellow: detachments
Red, Light red, pink - yellow: patinas

12%
8%
4%
10%
2%
36%

BLACK CRUST - EXFOLIATIONS
GRANULAR DISAGGREGATION
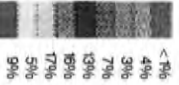
BARI CATHEDRAL

White: exfoliation and granular disaggregations
Violet to Orange: different thicknesses of black crust

< 1%
4%
3%
7%
16%
13%
17%
5%
9%

CEMENTITIOUS ENCRUSTATIONS
CORROSION

SANCTUARY OF DEMETER IN ELEUSIS

Black, Violet, Brown: cementitious encrustations
Yellow: corrosion

23%
6%
9%
4%
2%
56%

CORROSION
GRANULAR DISAGGREGATION

SANCTUARY OF DEMETER IN ELEUSIS

Black: corrosion
Brown granular disaggregation

33%
22%

CORROSION

SANCTUARY OF DEMETER IN ELEUSIS

Light yellow and Yellow: corrosion
Black: alveols due to corrosion

25%
3%
44%

GRANULAR DISAGGREGATION
FISSURING - DETACHMENTS

SANCTUARY OF DEMETER IN ELEUSIS

Colours from Yellow to Brown indicate due progressive intensity of phenomena
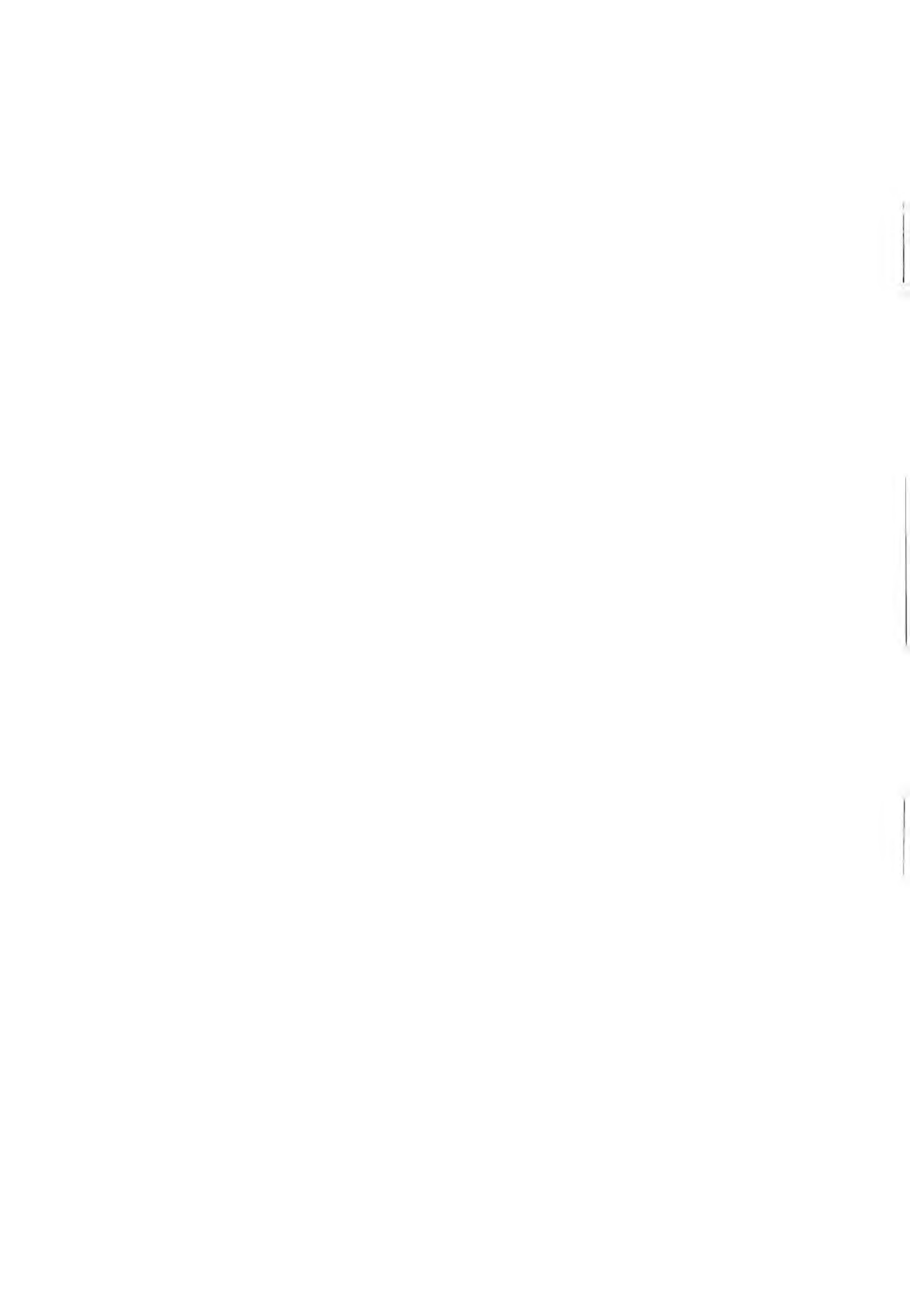
5%
19%
25%
13%
33%

FISSURING
DETACHMENTS

SANCTUARY OF DEMETER IN ELEUSIS

Red fissuring along schistosity plains
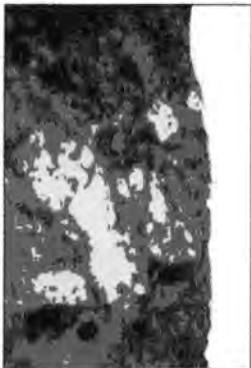Beige to Yellow: progressive intensity of detachments

15%
13%
22%
2%
8%
6%
5%
5%
4%
7%

Fig. 3

LIMESTONES – *Weathering forms*

SELECTIVE CORROSION

SANCTUARY OF DEMETER IN ELEUSIS

Green, Blue: selective corrosion around the smaller clasts

6%
8%
16%
35%
35%

Outdoor environment

BLACK CRUST CORROSION

BARI CATHEDRAL

Black, Violet: black crust
Blue to Orange: areas interested by progressive intensity of corrosion

2%
5%
6%
6%
5%
16%
25%

Outdoor environment BLACK CRUST – GRANULAR DISAGGREGATION DETACHMENTS

BARI CATHEDRAL

Blue, Dark Brown, Black: black crust
Yellow: granular disaggregation, detachments

14%
5%
2%
4%
16%

Indoor environment

GRANULAR DISAGGREGATION

CADIZ CATHEDRAL

Yellow: granular disaggregation
White: detachments

17%
9%
3%

Indoor environment DETACHMENTS PATINAS – EXFOLIATIONS

CADIZ CATHEDRAL

Pinck, Yellow, detachments
Blue, Green, Black, patinas
Red: exfoliations
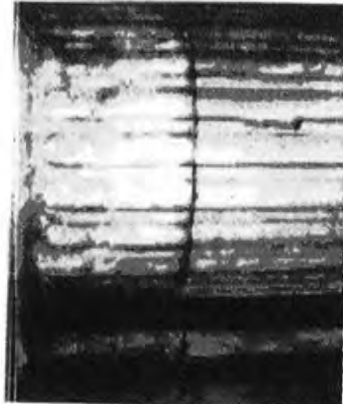
4%
7%
7%
9%
16%
20%
25%
7%

Fig. 4

LIMESTONES – *Weathering forms*

Indoor environment

GRANULAR DISAGGREGATIONS EFFLORESCENCES
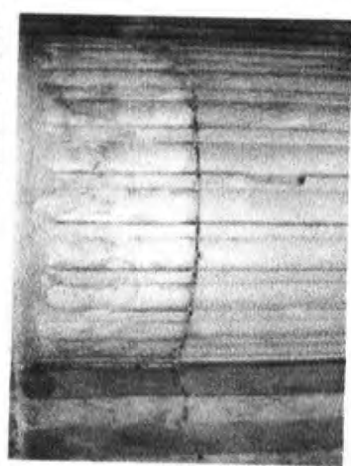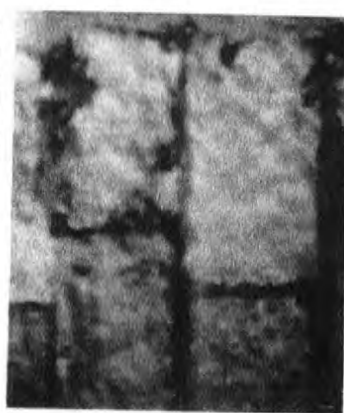

CADIZ CATHEDRAL

White, Yellow: granular disaggregation and efflorescences

17%
7%

DETACHMENTS
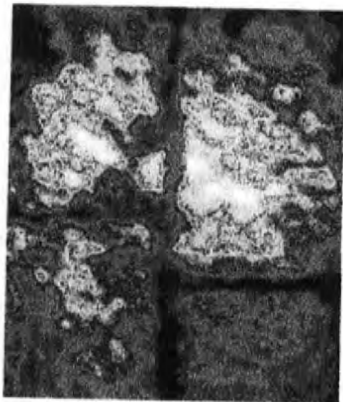
BARI CATHEDRAL

The colours, from dark to light, indicate the detachments from the earliest to the most recent

20%
14%
5%
8%
10%
7%
9%
3%
5%
59%

EXFOLIATIONS PULVERIZATION

BARI CATHEDRAL
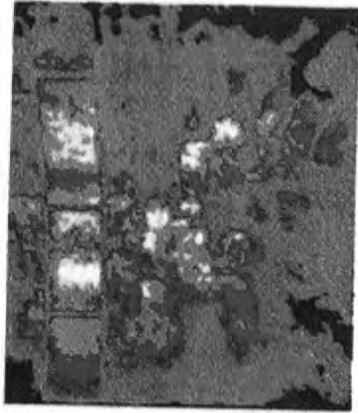
Black to Brown: exfoliations
Yellow to Light Yellow: pulverization

17%
34%
8%
5%
10%
12%
2%
7%
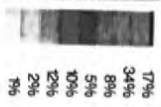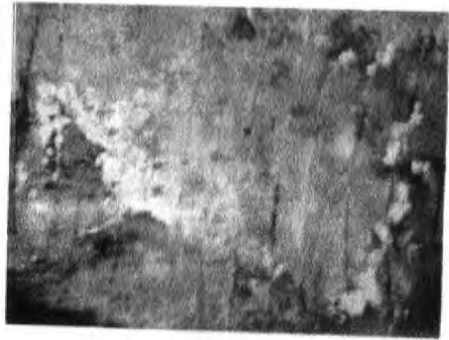
EFFLORESCENCES

BARI CATHEDRAL
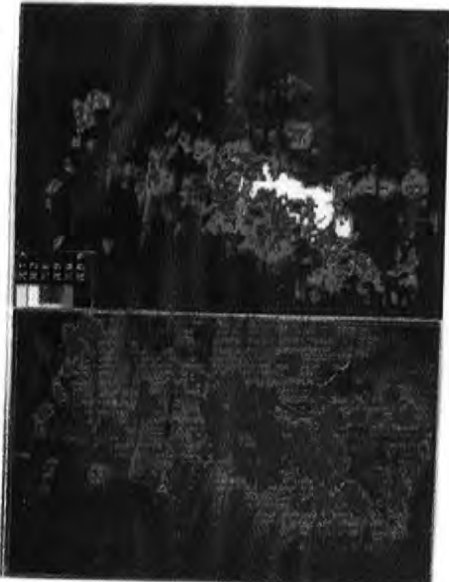
Red to Withe: efflorescences

Purple: humidity sources

Fig. 5

CALCARENITES - *Weathering forms*

Outdoor environment

DIFFERENTIAL DETERIORATION

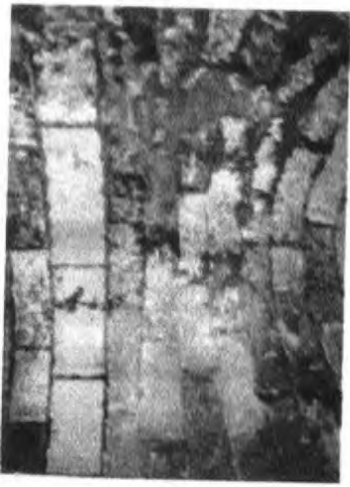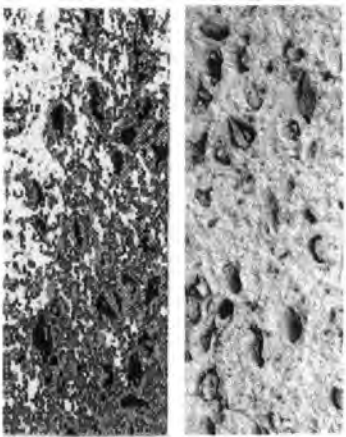SANCTUARY OF DEMETER IN ELEUSIS
Red, Black: selective weathering in correspondence with the fossil cavities

1%
1%
5%
10%
21%
15%
24%
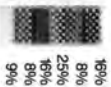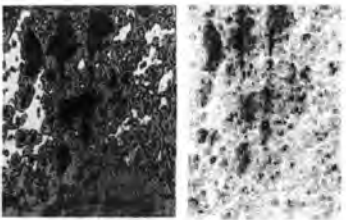
CADIZ CATHEDRAL   Black: selective weathering in correspondence with the fossil cavities

16%
8%
25%
16%
8%
9%

STA. MARIJA TA' CWERRA IN MALTA

DIFFERENTIAL DETERIORATION

Black, Brown, Blue: buried forms (holes) in correspondence of "bioturbations".
Green to Yellow: less weathered rock

1%
8%
7%
1%
2%
2%
7%
73%

BLACK CRUST DIFFERENTIAL DETERIORATION
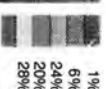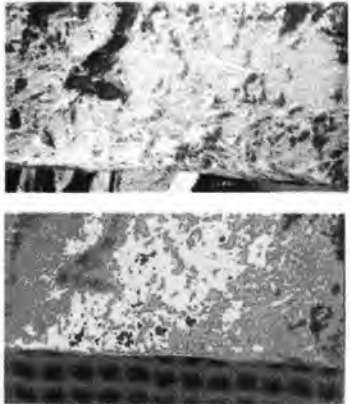
SANCTUARY OF DEMETER IN ELEUSIS
Brown: black crust
Yellow to Orange: differential deterioration

1%
6%
24%
20%
28%

FISSURING DETACHMENTS

SANCTUARY OF DEMETER IN ELEUSIS
Black, Violet: fissuring
Yellow: detachments
Brown: chips close to detachment

30%
7%
11%
21%
24%
4%
2%

DIFFERENTIAL DETERIORATION
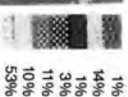
STA. MARIJA TA' CWERRA IN MALTA
Violet to Red: earliest exfoliation
Yellow, light Yellow: areas close to exfoliation

1%
14%
1%
3%
11%
10%
53%

BIOLOGICAL ATTACK

SANCTUARY OF DEMETER IN ELEUSIS
Green: biological attack

24%
7%
1%
7%
7%
41%

Fig. 6

CALCARENITES – *Weathering forms*

Indoor environment

DETACHMENTS   EFFLORESCENCES
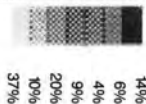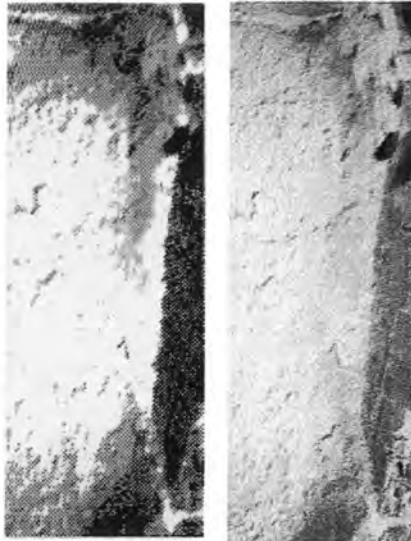
STA. MARIJA TA' CWERRA
IN MALTA

Brown to Orange: areas close to detachment
Yellow efflorescences

14%
6%
4%
9%
20%
10%
37%
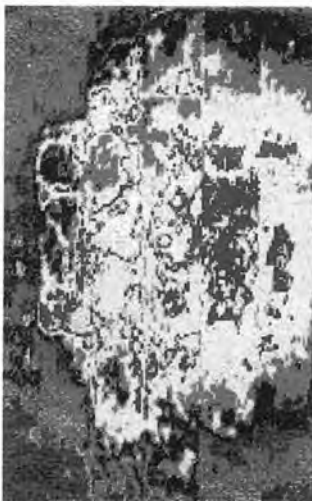
EFFLORESCENCES

CADIZ CATHEDRAL

Blue: efflorescences

12%
8%
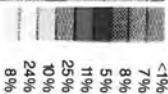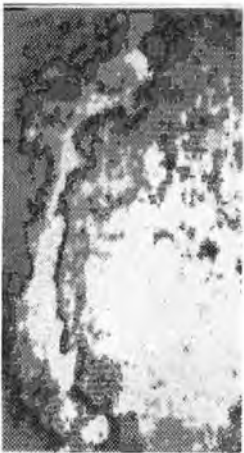
FISSURING

CADIZ CATHEDRAL

Blue: fissuring

<1%
7%
8%
5%
11%
25%
10%
24%
8%
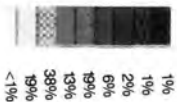
FISSURING

STA. MARIJA TA' CWERRA
IN MALTA

Black, Blue: fissuring

1%
1%
2%
6%
38%
13%
19%
19%
<1%

Fig. 7
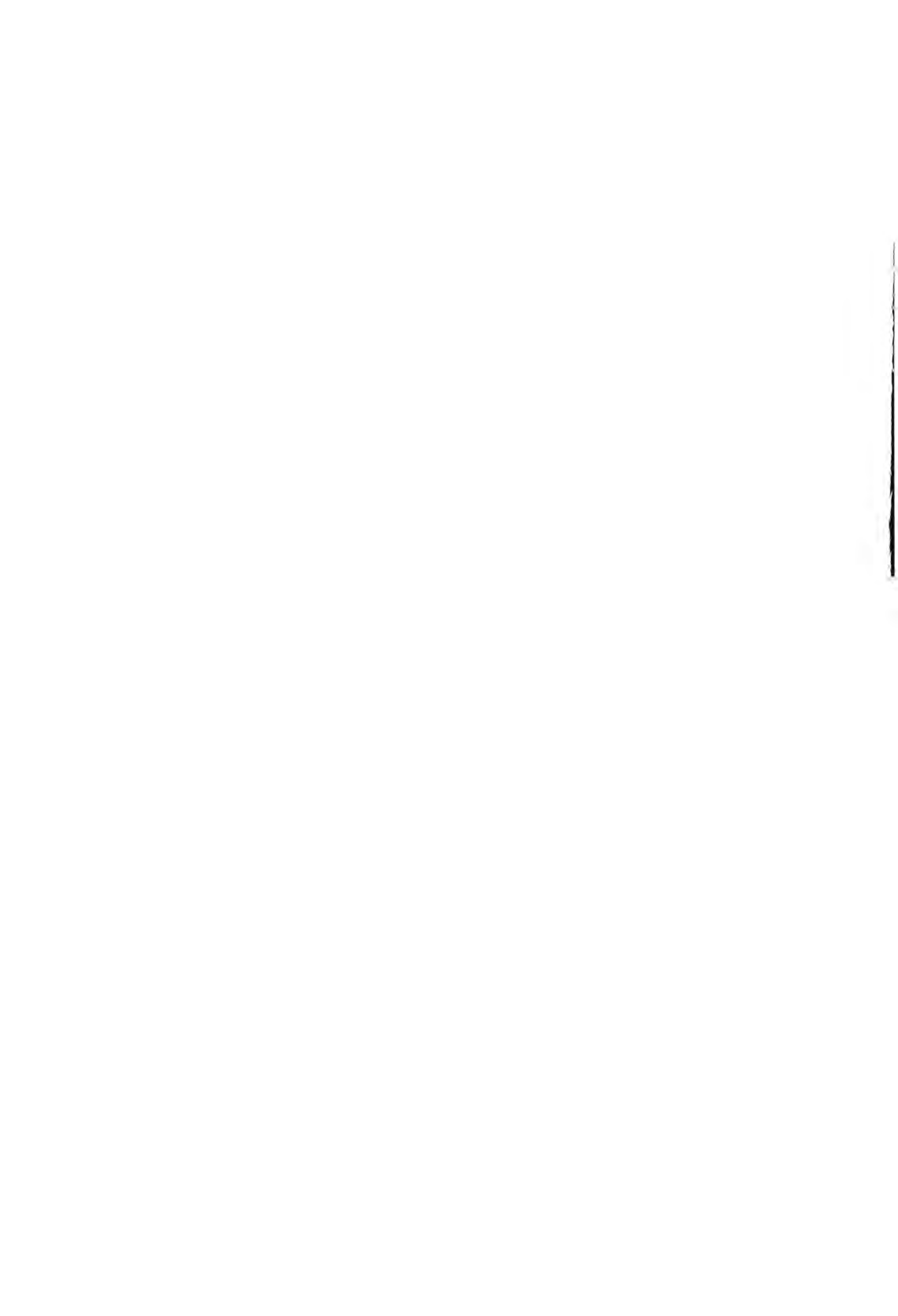
Weathering forms and correlated "buried structures" detected by ultrasonic pulses employing I.C.A. for weathering and analizing lithotypes, structures and stone decay through distance - time diagrams

1 BLACK CRUST
Section 4 EL

Depth scale
0
2 cm

Ultrasonic Velocities
1.4 km/s
4.4 - 5.3 km/s
5.0 - 6.6 km/s

3 CORROSION
Section 2 EL

Depth scale
0
2 cm
4

Ultrasonic Velocities
1.2 km/s
3.3 - 3.5 km/s
5.0 - 6.6 km/s

5 FISSURING and DETACHMENTS
Section 10 EL

Depth scale
0
2 cm
4

Ultrasonic Velocities
0.7 km/s
1.0 km/s
1.6 km/s
3.3 km/s
6.6 km/s

1 BLACK CRUST
Section 6 EL

Depth scale
0
2 cm
4

Ultrasonic Velocities
0.9 - 1.2 km/s
2.0 - 2.1 km/s
3.3 - 3.6 km/s
4.4 km/s

4 SELECTIVE WEATHERING and CORROSION
Section 1 EL

Depth scale
0
2 cm
4

Ultrasonic Velocities
1.2 km/s
2.5 - 2.6 km/s
6.6 km/s
Micaceous vein

5 FISSURING and DETACHMENTS
Section 5 EL

Depth scale
0
2 cm
4

Ultrasonic Velocities
1.2 km/s
4.0 km/s
4.4 km/s

2 CEMENTITIOUS ENCRUSTATIONS
Section 7 EL

Depth scale
0
2 cm
4

Ultrasonic Velocities
1.0 - 1.1 km/s
2.4 - 3.0 km/s
5.1 - 7.2 km/s

5 FISSURING and DETACHMENTS
Section 9 EL

Depth scale
0
2 cm
4

Ultrasonic Velocities
0.6 - 0.9 km/s
1.1 - 1.7 km/s
2.3 - 2.8 km/s

BURIED STRUCTURES IN MARBLES

1 - BLACK CRUST:
Parallel and subparallel decay layers.
Thickness of weathered stone:
1.6 - 4.6 cm and over

2 - CEMENTITIOUS ENCRUSTATIONS:
Parallel decay layers.
Thickness of weathered stone:
1.8 - 2.3 cm.

3 - CORROSION:
Decay layers with irregular surface and irregular buried surface.
Thickness of weathered stone:
2.1 - 4.6 cm.

4 - SELECTIVE WEATHERING and CORROSION:
Decay layers with irregular surface and irregular buried surfaces; vertical slopes due to schistosity plans with micaceous veins.
Thickness of weathered stone:
2.6 cm and over.

5 - FISSURING and DETACHMENTS:
Buried laterally varying structures and change in dip of sub-surface.
Thickness of weathered stone:
2.7 - 5.4 cm and over.

Fig. 8

general, between 0.5 and 1.2 cms in the case of corrosion and selective weathering, and is of about 3.2 cms in the case of detachments.

The distance–time diagrams relative to miocenic and plio–quaternary calcarenites indicate: a) buried structures characterized by irregular surface and changes in dip of surface for the forms linked to *selective weathering* and *detachments;* b) irregular surface and buried irregular surface characteristic of the forms linked to *exfoliations* and *granular disaggregation;* c) parallel layer with irregular surface for *black crust;* d) parallel layer with irregular surface for the *granular disaggregation.* The thicknesses of the first decay layer, which is particularly weathered, vary between 0.5 and 1.8 cms for a) and b) and they increase up to values of between 1.7 and 4.2 cms for c) and d).

The confirmation that the buried structures depend on the weathering emerges from the scanning electron microscope analyses which show that, however the typology of these structures may differ and though in the presence of different thicknesses and relationships of dips between the decayed layers, all the stone materials examined have the common characteristic of planar and undulating cracks, whi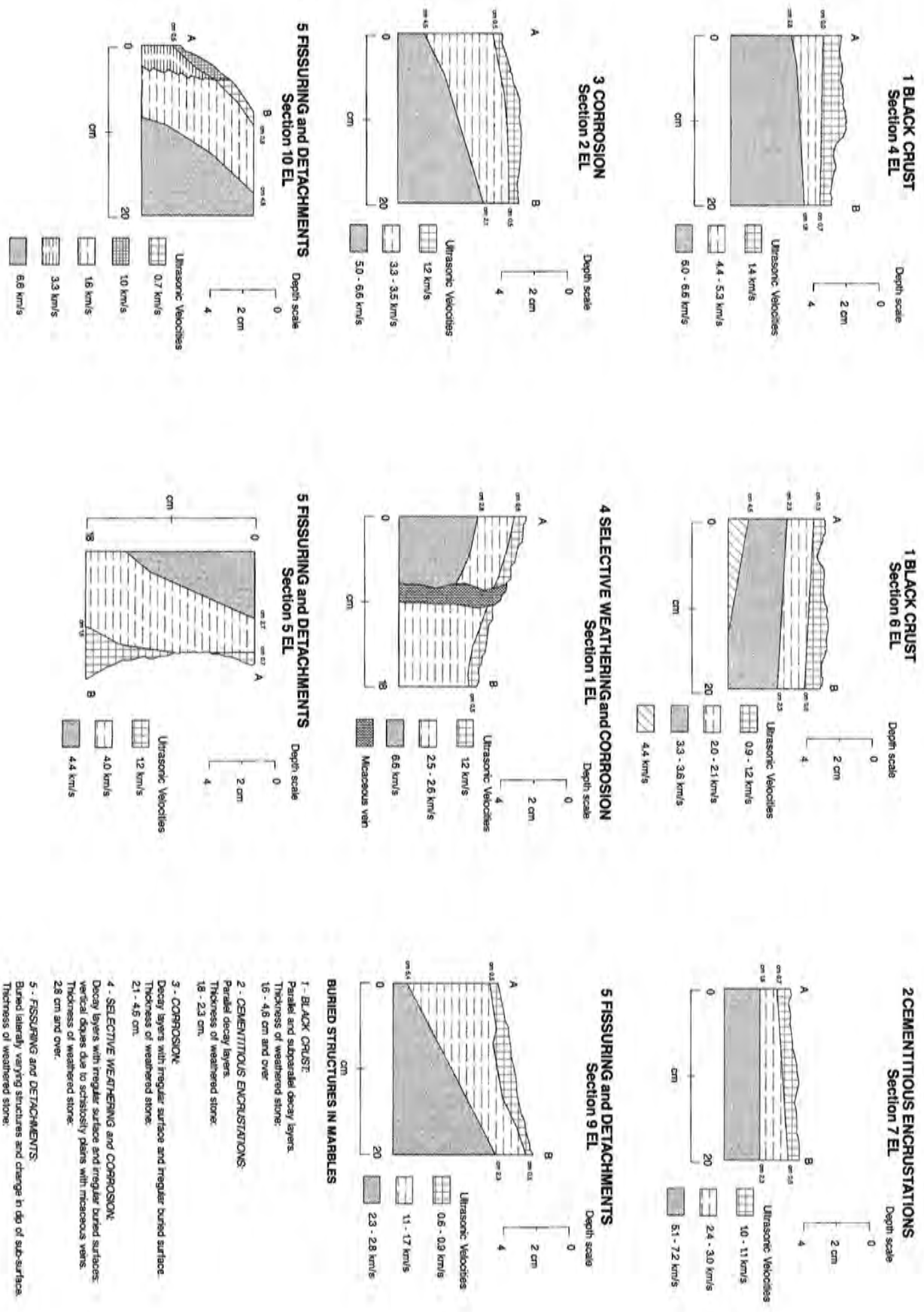ch are also transversal and subparallel to the external surfaces, filled by chlorides as well as by sulphates (Fig.9). The transversal cracks, through which salts penetrate from the external surface, connect the planar cracks distributed at different depths. It is along these cracks that the migration and crystallization of neoformation salts occurs, and these salts tend to concentrate in the form of subefflorescences in the planar and undulating cracks. The depths which are reached by the neoformation salts largely correspond with those of the decay layers indicated in the buried structures. This behaviour under weathering is typical of marbles and of micritic and oo–micritic compact limestones.

In the porous lithotypes, which may be represented by oosparitic limestones and calcarenites of the tertiary *(Globigerina limestone)* and plio–quaternary age *(calcareous tuffs* and *Ostionera stone),* while the same phenomenolgy continues to appear, conditioned by the presence of cracks subparallel to the surfaces, the intergranular pores are affected by the migration of chlorides from the exterior, and the progressive widening of the pores is linked with the forms of granular disaggregation, selective weathering and, in some cases, such as the oosparite and limestone of Cadiz, also the detachment of chips.

The Globigerina limestone of Malta represents a typical example of selective weathering, as also do the Ostionera stone and the calcareous tuffs. For the Globigerina limestone, (Fig. 10) in particular, the different porosities in the stone, in the variety in which the miocenic formation is affected by bioturbations, can determine the evident forms of differential deterioration which, for this reason, are not to be confused with forms of alveolization. The homogeneous variety of Globigerina limestone, on the other hand, is not affected by differential deterioration but only by granular disaggregation and exfoliation provoked by subefflorescences.

With reference to Tab. 2, the correlation between buried structures and ultrasonic pulses by means of indices and physical–mechanical parameters permits the classification of the decayed rock. From this point of view the ICA for Weathering methodology allows the determination of the modification due to the weathering which has been suffered by stone in the course of time, on the basis of mutual relations of interconnection between crystals or granules with cement which determine the degree of compactness related to total porosity and imbibition coefficient, and, in the final analysis, to the mechanical behaviour of the stone.

4. On the basis of the results obtained, the above method of investigation allows the following conclusions to be reached once the comparison has been made between the behav-

iour of similar lithotypes, which have suffered weathering in different areas, and the different lengths of time they have been exposed. The decay of marble is undoubtedly effected by the exposure time, as is shown by the difference in the length of the periods in which the marbles of Eleusis (from the 6th cent. BC to the Roman period) and Bari Cathedral (12th cent.) have been exposed; this difference is certainly responsible for the different thickness of the decayed layers (Fig. 11). It is also certain, however, that the environmental conditions of the two sites, the first influenced both by marine spray and anthropic pollution and the other principally by marine spray, have also had a fundamental role in characterising as "very severe" the condition of exposure at Eleusis. This conclusion is supported by the comparison between the limestones of the Cathedral of Bari (12th cent.) and those of the Cathedral of Cadiz (18th cent.), the latter being laid 600 years later (Fig. 12). In this case, in fact, the "time" factor has a secondary role with respect to the marine aerosol which provokes "very severe" exposure conditions and a consequently more intense degree of stone decay where it acts with greater intensity (Cadiz). On the other hand, in similar micro–environmental conditions the stone materials, and also those which are moderately weak, such as the calcarenites of Malta (18th cent.) and of Cadiz (18th cent., Fig. 13), exposed for similar periods of time to the marine aerosol, show the same behaviour as regards the depth reached by the soluble neoformation salts independently of the decay forms which characterize them. It is well known, in fact, that the development of these forms may depend on the particular petrographic nature of the stone, its structural and textural characteristics (including the size of the pores and the degree of cementation of the grains), as well as the cutting of the stone and its laying in the monument.

SCANNING ELECTRON MICROSCOPE ANALYSIS

a

b

c

d

e

f

g

h

i
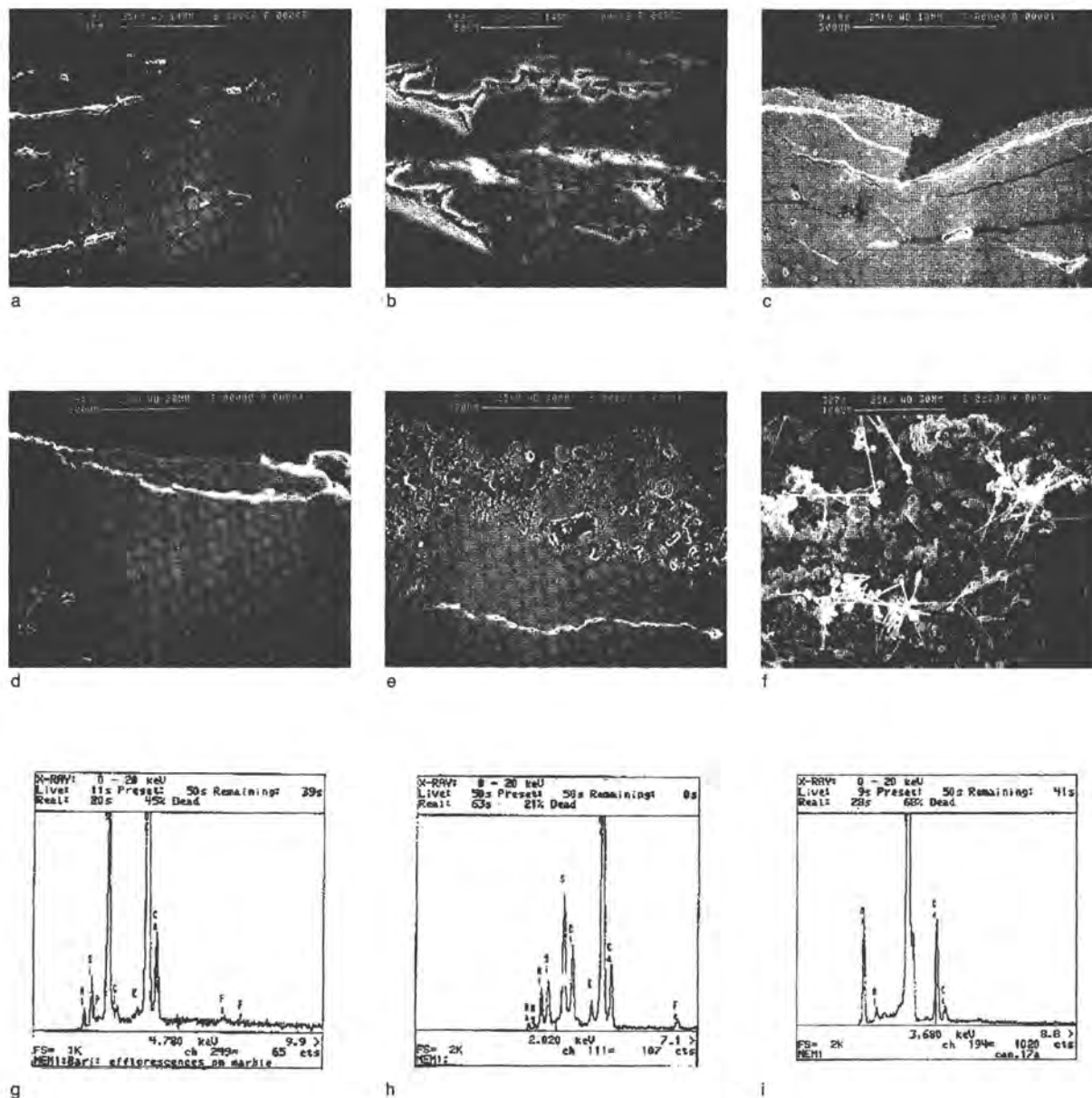
MARBLES and MICRITIC LIMESTONES

Marbles (a, b, e) and Limestones (c, d) present the common characteristic of planar and undulating cracks which are subparallel and transversal to the external surface. Along these cracks the migration and crystallization takes place of neo-formation soluble salts, represented by chlorides and sulphates (h), from the surface to the inner part of the stone. Efflorescences are mainly represented by halite (i) in form of acicular or cubic crystals (f) with gypsum (g).

Fig. 9

SCANNING ELECTRON MICROSCOPE ANALYSIS
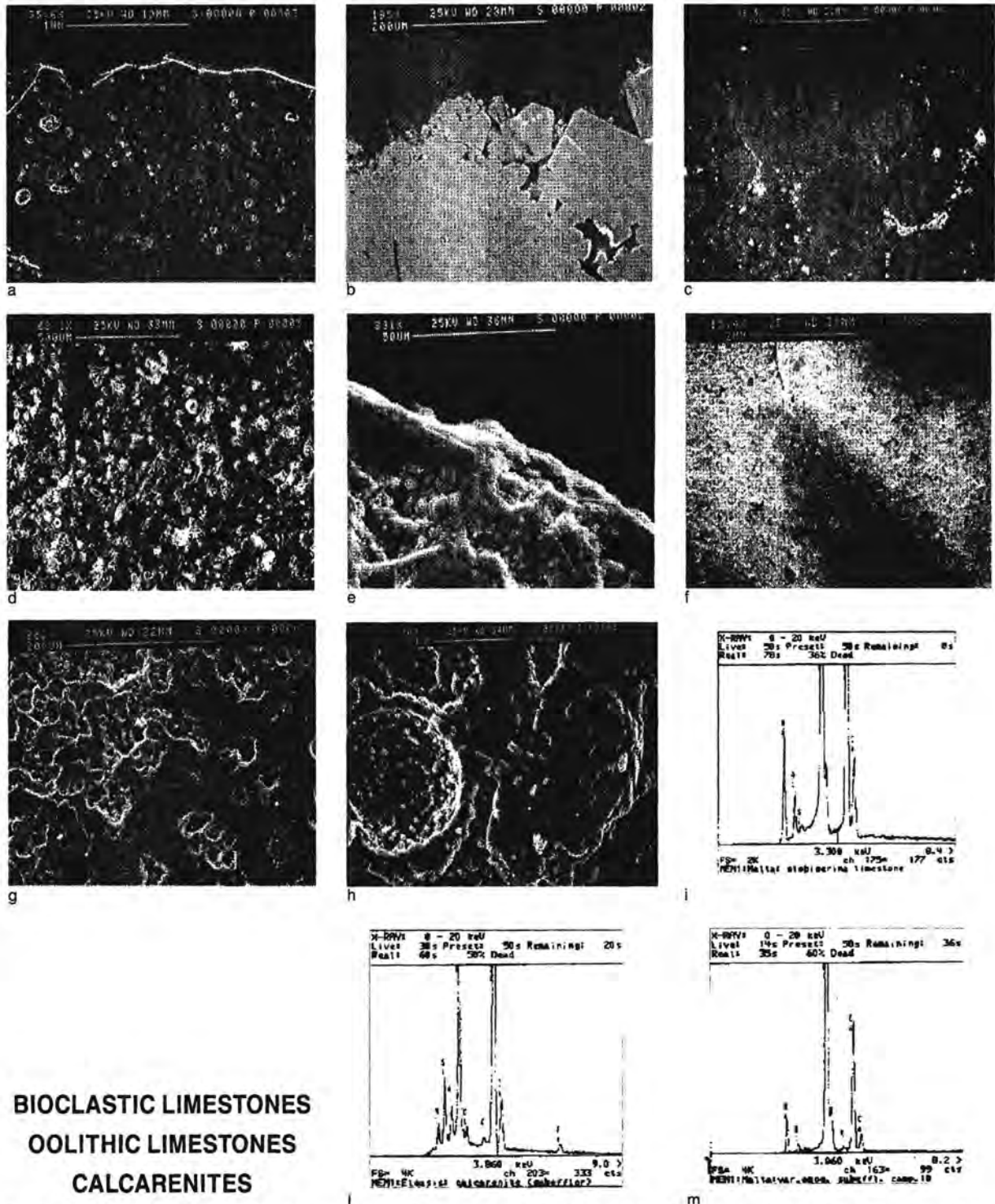
BIOCLASTIC LIMESTONES

OOLITHIC LIMESTONES

CALCARENITES

In the porous lithotypes, such as bioclastic limestones (a), oolithic limestones (b, c) and calcarenites (d–h) the intergranular pores enlarged by weathering (a–c) are the passages through which chlorides and sulphates (i, l, m) migrate to the inner part contributing to cause granular disaggregation (b) and detachment (e). In particular, for the Globigerina limestone of Malta the different porosities of the variety interested by bioturbations (f, g) is responsible for the weathering form of differential deterioration. The homogeneous variety (d), on the contrary, is interested by granular disaggregation and exfoliation provoked by subefflorescences of halite in the form of cubic crystals (h).

Fig. 10

ULTRASONIC VELOCITIES AND DEGREE OF STONE DECAY EXPRESSED BY THE AVERAGE VALUES OF INDICES AND PHYSICAL - MECHANICAL PARAMETERS OF MARBLES LIMESTONE AND CALCARENITES

F. ZEZZA 1996

ULTRASONIC PULSES (Km/sec)	0,6	1,8	3,0	5,0	6,5
STRENGTH (MPa)	1	5	10	50	100
	VERY WEAK	WEAK	MODERATE WEAK	MODERATE STRONG	STRONG / VERY STRONG
COMPACTNESS	0,52	0,59	0,66	0,93	0,97
POROSITY (%)	46	40	34	6	1
IMBIBITION (%)	25	18	13	1,40	0,80
STONE DECAY (degree)	(IV°) WEATHERED ROCK	(III°)	(II°)	(I°) FRESH ROCK	MARBLES LIMESTONES

CALCARENITES

Miocenic calcarenites

Mesozoic limestones and marbles

Miocenic calcarenites and Plio - Quaternary calcarenites
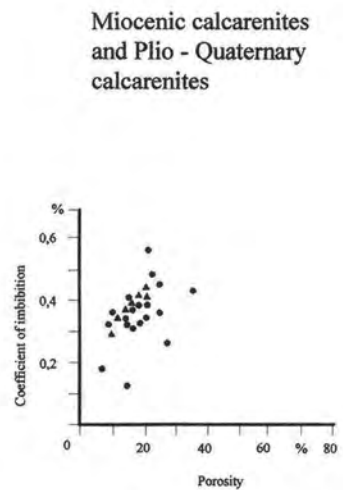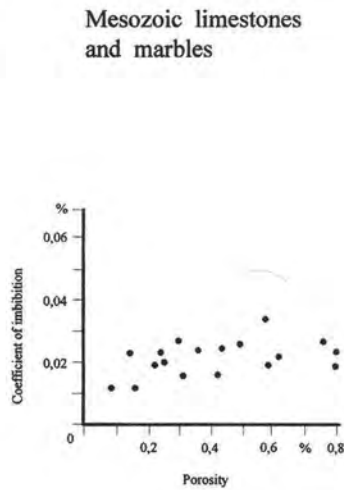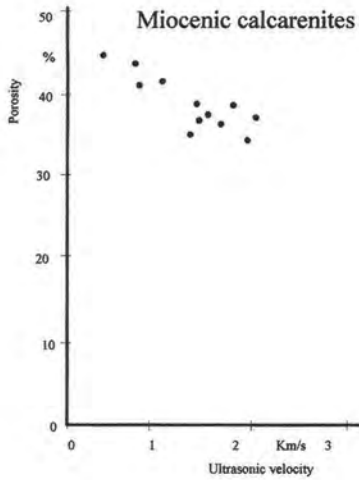
MARBLES - *black crust*

Eleusis Sanctuary of Demeter 1900 - 1600 b.C. - section 6

pictorial image

energy content of grey levels

digital image of stone decay

ultrasonic pulses: diagram distance-time

buried structure

degree of stone decay

F. ZEZZA

BARI Cathedral XII century - section 4

pictorial image

energy content of grey levels

digital image of stone decay

ultrasonic pulses: diagram distance-time

buried structure

degree of stone decay

F. ZEZZA
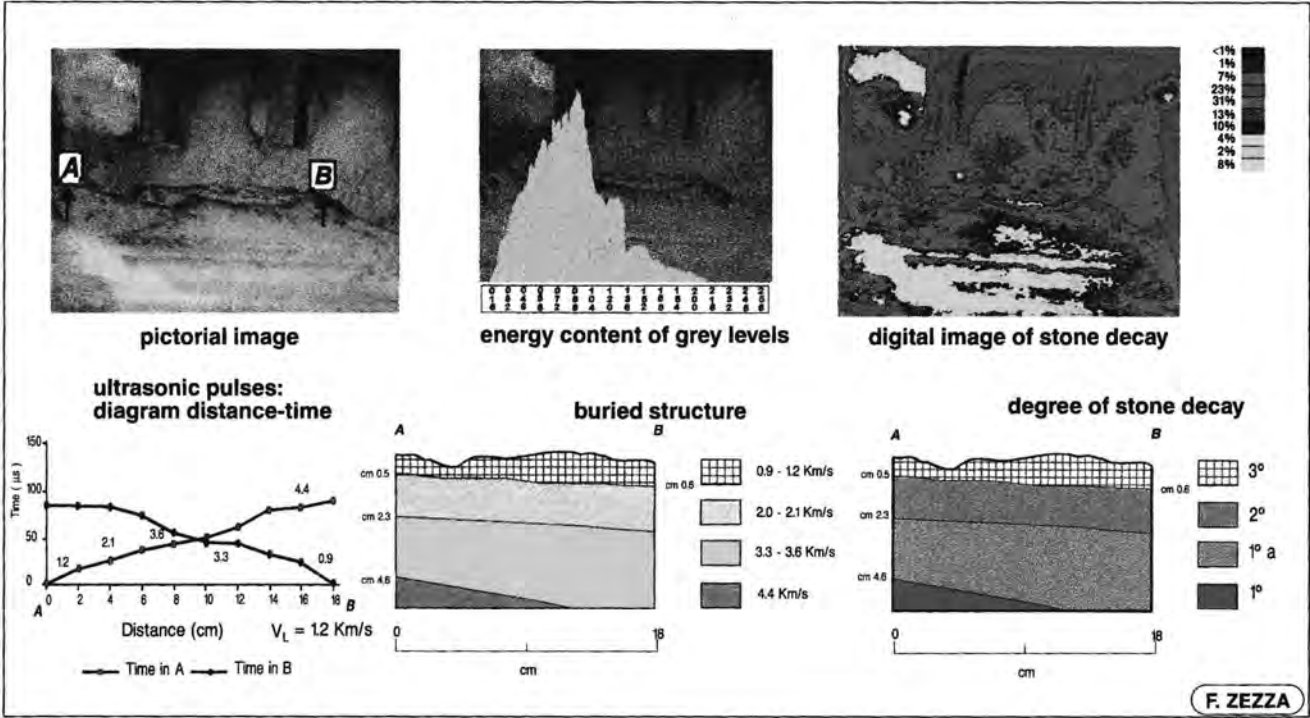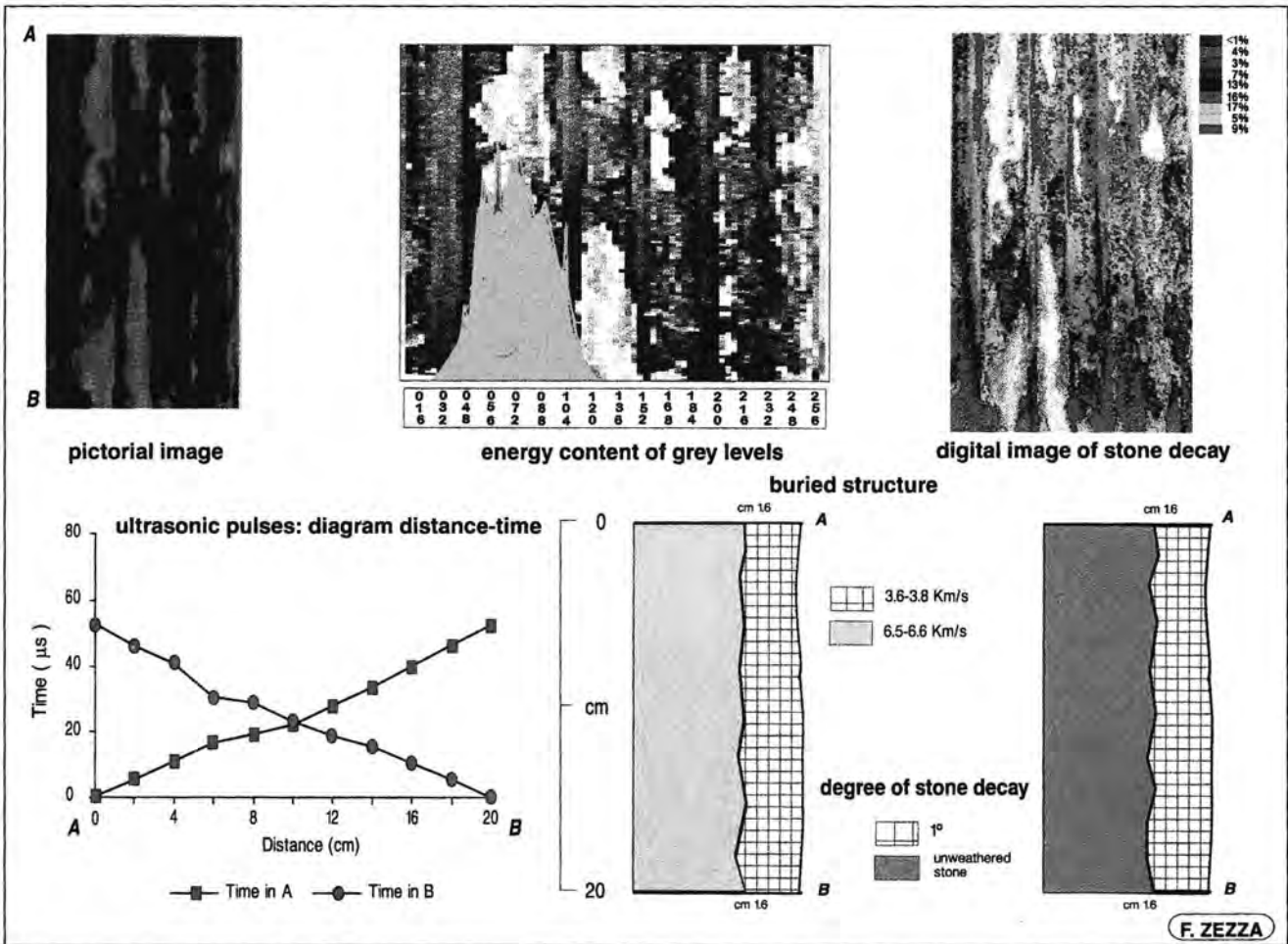
Fig. 11

LIMESTONES - detachments

CADIZ Cathedral, sec. XVIII - section 2

pictorial image

energy content of grey levels

digital image of stone decay

ultrasonic pulses: diagram distance-time

buried structure

3.2 - 3.3 Km/s

4.1 - 4.6 Km/s

degree of stone decay

1° a

1°
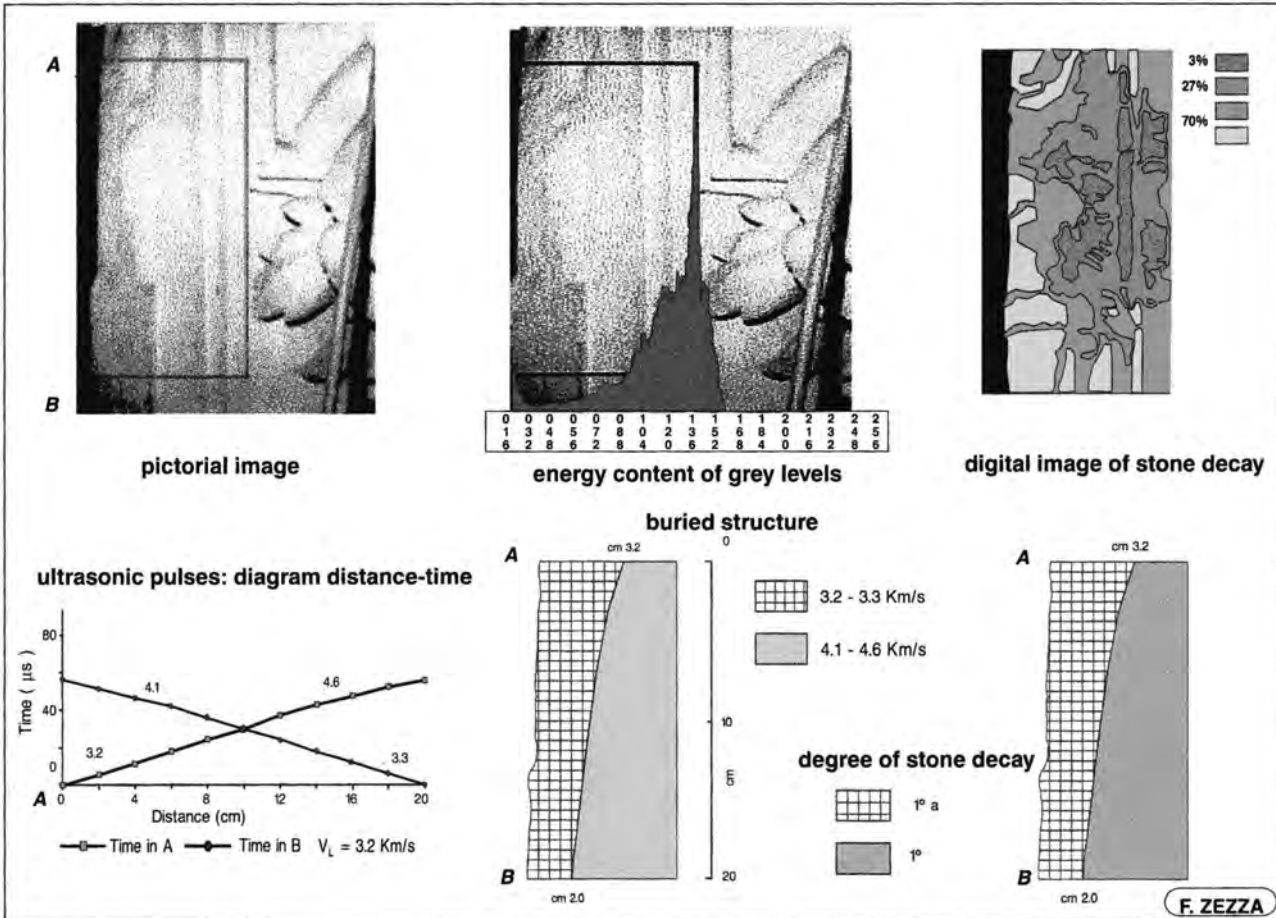
F. ZEZZA

BARI Cathedral sec. XII - section 2

pictorial image

energy content of grey levels

digital image of stone decay

ultrasonic pulses: diagram distance-time

buried structure

2.7 Km/s

3.1 - 3.4 Km/s

5.2 - 5.7 Km/s

degree of stone decay

2°

1°

unweathered stone

F. ZEZZA

Fig. 12

CALCARENITES - *differential deterioration and efflorences*

CADIZ Cathedral XVIII century – section 5

pictorial image   energy content of grey levels   digital image of stone decay

ultrasonic pulses: diagram distance-time

buried structure

1.4 Km/s
2.1 - 2.2 Km/s

degree of stone decay

3°
2°

F. ZEZZA

SIGGIEWI Malta Church of Sta. Marija Ta' Cwerra XVIII century – section 1

pictorial image   energy content of grey levels   digital image of stone decay

ultrasonic pulses: diagram distance-time

buried structure

0.9 km/s
1.4 km/s

degree of stone decay

3°
2°

F. ZEZZA

Fig. 13

References

1. F. Zezza, "Computerized analysis of stone decay in monuments". Proceedings of the 1st International Symposium on the Conservation of Monuments in the Mediterranean Basin, Bari, Italy, 7–10 June 1989.

2. F. Zezza, "Stone decay diagnosis and control of treatments by computerized analytical techniques". Proceedings of the 3rd International Symposium on the Conservation of Monuments in the Mediterranean, Basin, Venice, Italy, 22–25 June 1994.

3. F. Zezza, "Marine Spray and Polluted Atmosphere as Factors of Damage to Monuments in the Mediterranean Coastal Environment". Proceedings of the 3rd International Symposium on the Conservation of Monuments in the Mediterranean Basin, Venice, Italy, 22–25 June 1994.

4. F. Zezza, F. Macri, "Marine aerosol and stone decay". The Science of the Total Environment, Elsevier, 167, 123–143, (1995).

5. F. Zezza, "Integrated Computerized Analysis of Weathering. Perfecting and experimentation on pilot monuments damaged by marine aerosol and pollution". Proceedings E.C. Workshop "Non–destructive testing to evaluate damage due to environmental effects on historic monuments", Trieste, 15–17 February 1996, (in the press).

Andreas Arnold

Origin and behaviour of some salts in context of weathering on monuments

Origin and behaviour of
some salts in context of weathering on monuments

A. Arnold

ETH Zurich

1. Introduction

Salts are a condition of life. All waters circulating in our environment are salt solutions, whose main components are: Na, K, Ca, Mg, NH_4, CO_3, SO_4, NO_3, and Cl.

Deterioration due to the bursting action of salts crystallising in pores and cavities of rocks, stones and other materials is actually considered to be one of the most effective weathering agent. Of course, it concurs with the action of frost, rust bursting, hygric and thermal expansion, chemical and biochemical weathering etc.

The deteriorations due to salts are the product of an evolution of salts systems. In nature and on buildings salts originate *(origin)* from ions leached out from weathering of stones and soils. They are transported *(transport)* by surface and pore waters on buildings but also by ground waters and rivers to lakes and to the sea. Where the water evaporates in lakes, in the sea, and on buildings, salt ions are supported and accumulate *(accumulation)*. When water evaporates, the solutions become more and more concentrated *(concentration of solutes)*. Where and when a particular salt phase in the system becomes supersaturated, it precipitates *(precipitation)*. From multicomponent solutions the different salt phases will precipitate in sequences according to the different solubilities or ion activities; the system fractionates *(fractionation)*. When fractionation occurs in a stationary solution (salt lake or a particular place on a building), one salt phase –or coexisting group of salt phases– after the other may precipitate at one place, forming a *chronological sequence;* if the solution is moving the salt phases will be deposited at different

places, *forming spatial sequences.* When salts dispersed over a large volume concentrate in distinctive areas, they are locally concentrated *(local concentration)*.

The salts being precipitated crystallise either on or beneath the surface of the porous material. When crystallisation occurs on the surface efflorescence is formed. The salts crystallise in a variety of specific forms determined *by the internal atomic and molecular structure* of the crystal lattice. The efflorescences appear in different habits and aggregate forms that depend on the *external environmental conditions* such as supersaturation, composition, impurities and the shape and current of the solution nourishing the growing crystal. These external conditions are important in our context, because they may be influenced for conservation.

Decay occurs when growing salt crystals exert (mostly linear) pressures on the walls of pores and other cavities and thereby disrupt the structures of a material. Being conscious that deterioration due to salts represents one group of the possible interactive decay processes, we may retain the following possibilities to prevent salt crystallisation on walls:

- *eliminate or impede the supply and remove or reduce the salt deposits present (desalination);*

- *avoid or impede the salt crystallisation events by intervening in the humidity balance and the microclimate;*

- *reduce the effects by improving the resistance of materials against salt weathering.*

We now want to enter into the problem of eliminating or impeding the supply of salts at the origin. For that purpose, we need to determine the origin and also the evolution of salt system in the concerned walls. We are living in an environment, where all waters are saline solutions. That creates some problems to define the specific origin of the ions supplying the salt systems of a wall. This also concerns the salts, we may find in the vicinity of the sea and we assume to originate from salt spray. Not all chlorides occurring near the sea are from the sea. In fact, human beings and animals eat and excrete sodium chloride and accumulate it in their environment. A critical determination of the origin of salts should be emphasised in any case we deal with preservation of monuments affected by soluble salts.

2. Origin of salt solution in walls

The salts in walls, are products of the chemical and biogenic weathering of stones and other materials, both in nature and on buildings, and of human activity. Salt accumulations in walls originate from the ions that have been leached out of rocks, soils, stones, and other materials used on buildings, deposited from the compounds of natural and polluted atmosphere, and generated by metabolism of organisms. On buildings the following sources have to be considered: the building stones and mortars, the soils, the materials used for preservation and restoration, the polluted atmosphere, de-icing salts, organisms and further unknown sources. We are interested to know more about the particular origin of the salts occurring in any case for two reasons:

1. *to know more about the evolution of the salt systems,*

2. *to get information for prevention in the individual case.*

We may get information about the origin from the nature and composition of a salt. So *ettringite* [$Ca_6Al_2(SO_4)_3(OH)_{12} \cdot 26\ H_2O$] and

thaumasite [$Ca_3Si\ (OH)_6(CO_3)\ (SO_4)\ \cdot 12H_2O$] are mainly known from concrete, but actually they contribute to the decay of materials on monuments that have been reinforced by means of injections with Portland cement and alkali silicates. The oxalates *whewellite* and *weddellite* [$Ca(C_2O_4)\ \cdot H_2O$] have previously been considered as relics of treatments, but now they are known to form biogenic crusts on monuments as well as on natural outcrops of carbonate rocks. The nitrates are all produced by the metabolism of micro–organisms.

Besides of such clear relationships the determination of the sources of salts may also be very tricky. Let us have a look at several examples.

2.1 Evident sources

Saas Fee, (VS), Switzerland, Kappellenweg [1]

Several of 15 small chapels decorated with statues and wall paintings, having been built in 1707–10 along a mule–track, lean on a rock composed of Triassic dolomite. The restorer found strong damages due to salts on the wall paintings inside of some of the chapels and sent me samples, to determine their origin. The analysed samples turned out to be of *epsomite* [$MgSO_4 \cdot 7H_2O$], what is the main salts that effloresce after any water percolation trough the walls in that region. But the restorer looked only inside the chapels and did not see, that the rock surface behind the chapels, being in contact with their walls, and at a distance of about 1 to 2 meters from the wall painting, was covered with a thick white efflorescence of epsomite. Thus the origin was evident but just not recognised, because the restorer did not look behind the chapel.

Niedergösgen, (SO), Switzerland [2], *nitrate salts.*

The economy building of the small castle has been renovated in 1980. The previous stables have then been transformed into offices for the communal administration. Beneath the stable there was an ancient manure pool, that caused very strong salt encrustation composed

of several centimetre thick crust of *nitrokalite* [KNO₃], that has caused strong deterioration on the wall. The origin is evident. Manure penetrated in the wall and nitrificant bacteria oxidised ammonia to nitrous acid, which then was oxidised to nitric acid by nitroso bacteria and then reacted to the nitrate with the cations present in the wall (Bock 1987)[3].

Instead of making a several meter deep trench and isolations at high costs, it was decided to just apply a new render on the outside as a sacrificial layer and to repair or replace it periodically e.g. every ten years. Until now after 16 years, there is a considerable decay, but the render had not yet to be replaced.

Gypsum from polluted atmosphere

Gypsum crusts generated by the sulphur compounds of the polluted air are characterised by some typical properties. They occur as black crusts on sheltered areas of building materials and not on wetter exposed parts. They show an accumulation zone where the crust is thickened on the border between the weathered and the sheltered zone. The black colour is due to the inclusions of small particles of soot and slag in the form of spheres of metal oxides and sulphides. The origin and the general behaviour are very clear and much studied.

2.2 Not evident sources

Erlacherhof, Bern, (BE), Switzerland, (Zehnder & Arnold 1984) [4]*, formate salts from cleaning*

An arcade of the Erlacherhof (1747–1752) at Bern, built originally in molasse sandstone, has been rebuild in 1977 by a new construction made of concrete and molasse sandstone (Burdigalian). A few years later strong efflorescence accompanied by fast granular disintegration of the new sandstone have been observed. An expert having found some sulphate salts, attributed them to the pollution and he gave the advise to avoid the use of this type of sandstone, because it will not resist anymore to the actually polluted atmosphere.

A more serious investigation showed, that the main salts consisted of *magnesium formate* dihydrate [Mg(CHO₂)₂ ·2H₂O] and *calcium formate* [Ca(CHO₂)₂] and on some parts of *epsomite* [MgSO₄ ·7H₂O] and *thenardite* [Na₂SO₄].

The origin of the main salts, and therefore also all the troubles, did not originate from the pollution, but from the cleaning of the concrete and the sandstones with *formic acid*.

Mythenhof, Genfergasse, Zurich, (ZH), Switzerland, salts from acids and alkaline lye used for cleaning [5].

The facades of the private house, made of a very porous "Savonnières" limestone, showed very strong white veils and efflorescence of salts, after having been cleaned. The salts present could be determined to be of *mirabilite* [Na₂SO₄ ·10H₂O] and *thenardite* [Na₂SO₄]. The owner was convinced, that the firm had first cleaned the facade with *hydrochloric acid* [HCl] and then neutralised the acid with *sodium hydroxide lye* [NaOH]. The firm contested it and declared that the results of the analyses exclude any relationship between the cleaning material and the salt efflorescence.

Our investigation showed, that the water in a puddle on a plastic foil at the base of the facade, was alkaline (pH above 12) and contained high amounts of chloride. This facts supported the declaration of the owner. But the salts being of sodium sulphate, there seemed to be no relationship between the cleaning product an the efflorescence. But this conclusion was not correct.

As a matter of fact, the surfaces of a porous limestone exposed to the polluted atmosphere in the town of Zurich are covered by a *gypsum* crust in sheltered areas and impregnated with *gypsum* in rain exposed parts.

Thus the presence of sodium sulphate was probably produced in the following way:

$$NaOH + HCO_3 + 9H_2O \quad \rightarrow \quad Na_2CO_3 \cdot 10\,H_2O$$
$$natrite$$

$$Na_2CO_3 \cdot 10H_2O + CaSO_4 \cdot 2H_2O \quad \rightarrow \quad Na_2SO_4 \cdot 10\,H_2O + CaCO_3 \downarrow + 2\,H_2O$$
$$natrite \quad + \quad gypsum \quad \rightarrow \quad mirabilite \quad + \quad calcite$$
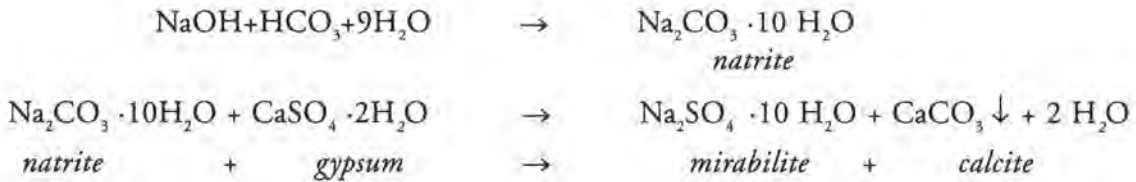
Thus the formation of sodiumsulphate salt can easily be explained by the reaction of sodium lye with *gypsum* present on the stone. Thereby the relationship between cleaning with hydrochloric acid and sodium hydroxide and efflorescence of sodium sulphate became very evident.

Ruin of "Grasburg" Wahlern, Bern, (BE) Switzerland [6], salt from alkaline building material.

The ruin of the mediaeval castle of Grasburg near Schwarzenburg (Switzerland) is situated in rural environment. Originally it was built of local molasse sandstone. During its restoration in the 1930th the uppermost parts of the walls have been replaced with ashlars made of concrete and all the joints have been repared with Portland cement mortars. During our investigation we observed a very strong granular disintegration and heavy salt concentrations and deposits composed of mainly sodium carbonate salts *natrite* [$Na_2CO_3 \cdot 10H_2O$] and *thermonatrite* [$Na_2CO_3 \cdot 10H_2O$], of *mirabilite* [$Na_2SO_4 \cdot 10H_2O$], some *thenardite* [Na_2SO_4], *arkanite* [K_2SO_4] and gypsum, as well as of some Ca, Mg, Cl and NO_3 as solutes in a hygroscopic zone.

We could also observe that crystallisation occurred every day in autumn (late October). Sodium carbonate an sodium sulphate were dissolved during the night, crystallised as hydrated phases *natrite* and *mirabilite* in the morning and then dehydrated to *thermonatrite* and *thenardite* during the day on the parts exposed to sunshine. So in nature the hydrated phases mirabilite and natrite crystallise first and then dehydrate to thenardite or thermonatrite. That is the just the contrary of what is done in the *sodium sulphate test* made in laboratory, where the non hydrated

thenardite crystallises first and then *hydrates to mirabilite* and thereby burst stone structures.

A further interesting fact was observed. A supporting wall made of calcareous tuff stones situated below the ruin is impregnated by the alkaline salts and centimetre thick piles of *natrite* are deposited, looking like snow. The alkaline environment (pH > 12) act as biocide and impede the growth of plants on the affected area.

2.3 Historical aspects

Cloister of the Münster at Basel, (BS), Switzerland [7], tombstones, inherited salts

A number of mainly oil painted tombstones, made of different sandstones and limestones are incorporated on the inside face of the walls within the cloister of the Münster of Basel. The concerned wall was built and rendered first at about 1850 an then rendered again in 1950 with a new lime–cement mortar. Chemical analyses revealed, that several of the strongly deteriorated tombstones, situated at a level of 3.5 to 7 meters above the soil, contained high amounts of chloride and nitrate, as well as of calcium and magnesium and only little sulphate. These salts make the stone become very hygroscopic.

No nitrate and chloride and only some sulphate could be detected within the adjacent masonry and the render of 1950. How to explain the high contents of nitrate and chloride within the stone an not at all in the neighbouring masonry?

The conservator supposed, that the rising damp did supply, transport and concentrate the salts up to a level of 3.5 to 7 meters above the soil and hi aimed to replace the entire "salt contamiated" wall.

The study of the history gave a more plausible explanation. Before 1850 the tombstones where placed on other parts of the cloister within the zone of rising damp just above the ground. They got their concentration and accumulation of chloride, nitrate and of some sulphate from the ground already at that time. Then they have been transferred to the new wall in 1850 together with their concentrated salts. Since then they are in a sheltered position but exposed to the rather polluted and humid microclimate in the centre of the town of Basle. The whole surface of the stones and mortars became gradually impregnated with sulphates (mainly gypsum) since that time. The "inherited" chloride an nitrate salts are now associated with this gypsum. The main climatic events activating salt crystallisation are the changes in temperature and humidity leading to numerous condensation events, that can be observed during the year. These events caused the observed deterioration on the stones.

So, there is absolutely no reason to replace the masonry, because it is neither humid nor exceptionally loaded with salts. For preservation the paint had to be repaired. This now acts a protective layer and avoids further absorption of excess water by condensation and . salt from the polluted air..

The story of the Cleopatra's Needle, New–York City, USA

The long weathering history of the Egyptian Granite Obelisk called "Cleopatra's Needle". of New York City described by Winkler (1980)[8] begins with the excavation of the two obelisks at about 1500 BC. They were than standing at Heliopolis during around 950 years (1449 – 500 BC); than tossed of their plinths by the Persian king and lying on the ground during about 500 years up to 16 BC. They have than been relocated at Alexandria at about 100 feet from the shore of Mediterranean for 1897 years and finally the one called "Cleopatra's Needle" was brought to New York in January 1881, where it stands un-

til now on the humid and polluted climate. The other obelisk was fallen by the earth quake in 1301, but did not brake, and stays at London since 1878.

Winkler ascribes the strong decay unilaterally to hydration of entrapped salt causing a flaking at the base in the first years of exposure to the humid and polluted climate of New York. He attributes the strong decay that happened "since 1880" on its west side, to hydration of salts, that have been taken up during the needle was lying on the ground (500 to 16 BC) at Heliopolis. Then he states that "A hundred years of exposure to ample rain fall has removed all traces of any salt content." That shows, that the assumption on the "salt" history is rather hypothetical. The hieroglyphs of the London needle are also strongly weathered.

Richard Lepsius writes on 16. October 1842. "The two obelisks, from whom the standing one is called *Cleopatra's Needle*, are strongly weathered on the weather exposed sides and the hieroglyphs are partially illegible". (cited in Clayton P.A. 1983)[9]. That documents that both, the standing and the lying obelisk, have already been strongly weathered, while they were in Egypt. The weathering processes on the obelisks and their evolution have probably been more complex, than pure salt hydration wile standing in the polluted atmosphere at new York and London. How ever, we may learn, that conclusion without sufficient knowledge of the history may be erroneous.

Origin of some of the salts in the Egyptian temples.

Very much has been sad about salts in Egyptian monuments. Usually the Nil and the ground water are supposed to be the source and that is certainly true for many salt accumulations. But in the individual cases the origins may be different. The Pharaoh[10] was used to clean the foundation of a new temple by placing a protective layer of *natron* (from Wadi Natron) on the base of the foundation during the founding rite. Such a layer but composed
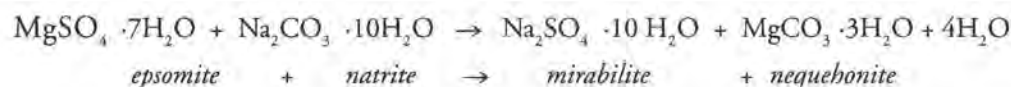
of *halite* [NaCl] could be traced in the stratigraphy of a recent excavation of the, Temple of Merenptah at Qurna, Thebes, near Luxor[11].

3. Conclusion

To sum up, we may state that, we will understand the evolution of salt systems only, if we know where the ions come from and what happened during their evolution i.e. their history. The weathering of a monument has his own history. Measures to prevent salt crystallisation damages can be undertaken in all steps of the evolution of a salt system. A condition to do it, is to know what happens during each step of the evolution i.e.: the origin, the transport in aqueous solutions, the evaporation, concentration, precipitation and the crystallisation and disruption. The complications within the study of the evolution of weathering by salt crystallisation already begin with

the determination of the origin oft the salt actually present system in each individual case. To determine the origin of salts in walls we have to emphasise the general possibilities that are: rocks and soils, stones and mortars, alkaline material used for conservation, polluted atmosphere, de–icing salt an micro–organisms. But the actual building stones may not reflect the composition of their originals salts.

In Eastern Switzerland, we observe a clear predominance of magnesium sulphate salts on molasse sandstones in their natural outcrops, while on building concentrated in towns sodium sulphate clearly predominates. This fact can be explained, when we bear in mind the incredible quantities of alkaline salts brought into the stone constructions during the 19th an 20th century with Portland cement and sodium and potassium silicate. The following reaction may have occurred:

$$MgSO_4 \cdot 7H_2O + Na_2CO_3 \cdot 10H_2O \rightarrow Na_2SO_4 \cdot 10 H_2O + MgCO_3 \cdot 3H_2O + 4H_2O$$

$$\textit{epsomite} \quad + \quad \textit{natrite} \quad \rightarrow \quad \textit{mirabilite} \quad + \textit{nequehonite}$$

In this way magnesium sulphate was probably transformed into sodium sulphate.

Natrite [Na$_2$CO$_3$ ·10H$_2$O], *thermonatrite* [Na$_2$CO$_3$ ·H$_2$O] and *trona* [Na$_3$H(CO$_3$)$_2$ ·2H$_2$O] occur mainly in ultrabasic rocks in nature. Thus there presence indicate, that they originate from alkaline building materials in the regions without ultrabasic building stones. With some exceptions *hydromagnesite* [Mg$_5$(OH(CO$_3$)$_2$)$_2$ ·4H$_2$O] and *nesquehonite* [MgCO$_3$ ·3H$_2$O] crusts can also be traced back to originate from these materials. Greater amounts of NaSO$_4$ salts may also indicate an origing from such alkaline materials.

A final example shows how science may be

far from the reality. While most scientists in Norway have focused their study on weathering by acid rain, some important stone monuments where decaying by alkaline (basic) salts. What happened[12]? An architect having discovered the qualities of Portland cement in Germany in the 19th century has imported it and injected it into the walls of the most important stone buildings in central Norway. Thus the saline solutions are alkaline and not acid, and the main damage not produced by acid rain. All these facts should make us very prudent, when drawing conclusions on the origin of soluble salts. Chlorides near the sea may not be from the sea.

(1) Unpublished internal report, ID–ETHZ (ID–ETHZ = Institute for the Preservation of Monuments and Sites, of the Swiss Federal Institute of Technology).

(2) Unpublished internal reports, ID–ETHZ, 26.2.1980, 14.9.1982.

(3) Bock, E. (1987): Biologisch induzierte Korrosion von Naturstein – starker Befall mit Nitrifikanten.– Baurenschutz / Bausanierung, 10 (1987), H. 1, 24–27.

(4) Arnold, A., Zehnder, K. (1983): Verwitterungsschäden durch Ameisensäure. Eine Fallstudie am Erlacherhof in Bern.– Schweizer Ingenieur und Architekt, 36/83, 841–845.
Zehnder, K., Arnold, A. (1984): Stone damage due to formate salts.– Studies in Conservation, 29, 32–34

(5) Internal report, ID–ETHZ, 29.8.1977.

(6) Internal report, ID–ETHZ, 31.10.1983.

(7) unpublished reports, ID–ETHZ, 1995

(8) Winkler, E. (1980): Historical implications in the complexity of destructive salt weathering – Cleopatras Needle, New York.– APT Bull., 2/80, 94–127.

(9) Clayton, P., A. (1983): Das wiederenteckte alte Ägypten.– Gustav Lübbe Verlag GMBH, Bergisch Gladbach, (ISBN 3–8112–0554–4).

(10) Golvin, J.C. 1990: Karnak Ägypten, Anatomie eines Tempels.– Ernst Wasmuth Verlag, Tübingen, ISBN 3 8030 1037 3.

(11) Personal communication by M. Blödt, restorer.

(12) Personal communication by Per Storemyr, Trondheim, Norway.

Clifford A. Price

An expert Chemical model for determining the environmental conditions needed to prevent salt damage in porous materials

An expert Chemical model for determining the environmental conditions needed to prevent salt damage in porous materials

C. A. Price

Institute of Archaeology, University College London
31–34 Gordon Square, London, UK

1. Introduction

This paper concerns a research project (ENV4 CT95 00135) that has been negotiated with the European Commission as part of the Environment and Climate programme. The project started on 1 April 1996. The paper describes the scientific background to the project, and then sets out the proposed programme of work.

The overall objective of the project is to enable the rate of deterioration of historic stonework and wallpaintings to be reduced, and thereby to conserve an important part of the European cultural heritage. This will be achieved by a new approach to the understanding of salt damage – one of the most common forms of decay in porous materials. The project will predict the behaviour of contaminating salts in stonework. The end–product of the project will be an expert system that will determine the environmental conditions needed to prevent or mitigate salt damage, for any given combination of salts.

2. Salt damage

One of the main causes of decay in porous materials is the growth of salt crystals within the pores, either by crystallisation or hydration. Crystal growth generates stresses which are sufficient to cause disintegration. The material becomes weak and friable, and the surface crumbles away. Once the surface is lost,

the historical and artistic importance is largely lost as well.

Despite its importance, and the exemplary descriptions of salt growth given by Arnold and coworkers (for example, Arnold and Zehnder, 1991), the mechanism of salt damage is not well understood. It is generally assumed that the damage is attributable to volume changes, and there have been a number of attempts to calculate the stresses that may be generated. These are generally related to the work of Correns (1949). What is certain, however, is that salt damage occurs whenever crystals are deposited from solution or when crystals absorb water and are transformed to a higher hydration state. In either case, it is a change in moisture levels that triggers the damage. In an outdoor environment, this can happen as a result of rainfall and subsequent drying. However, damage also occurs in an indoor environment, as a result of changes in the relative humidity (RH) of the air. There are many instances of catastrophic damage to museum objects through long–term storage in an uncontrolled environment. Damage also occurs in the interior stonework of historic buildings and monuments if the relative humidity is not regulated. Control alone is not sufficient, however: the relative humidity must be maintained at an appropriate level.

If a porous material is contaminated with just one salt, then crystallisation damage may be avoided by maintaining the relative humidity of

the air at a value other than the "saturation relative humidity": the relative humidity of air that is in equilibrium with a saturated solution of the salt. If the ambient RH is held above the saturation RH, then the salt remains in solution at all times; if the ambient RH is held below the saturation RH, the salt remains in solid form at all times. Either way, no damage can occur. Similar arguments apply to damage caused by hydration.

Contamination with a single salt is very uncommon, however. Almost invariably, a mixture of salts is present – derived, for example, from air pollution, rising damp or the burial of an object. It is common for stone to be contaminated with sulphates, chlorides, nitrates and a number of other anions; common cations include sodium, potassium, magnesium, calcium and ammonium. This situation is much more complex than the single salt case, and simple considerations of saturation relative humidities no longer apply. However, Price and Brimblecombe (1994) and Steiger (forthcoming), working independently, have recently demonstrated that the thermodynamics of the situation can be analysed and interpreted. It has been shown, for the first time, that it is possible to determine the appropriate environmental conditions in which salt–contaminated materials should be stored, provided that the identity of the salts is known. It has also been shown that damage occurs across ranges of RH, rather than at specific values, and that these ranges can be calculated for known salt mixtures and temperatures.

This project takes the preliminary research much further. It draws on existing thermodynamic models, hitherto used chiefly in geochemistry, and extends them to include some of the highly soluble salts that are often to be found in excavated objects and in buildings. More important, it brings the benefits of advanced thermodynamics into the conservation field, in a way which will be easily used by the non–specialist.

3. Specific objective of the project

The specific objective is to produce a computer program, fronted by an expert system, into which one can input the ionic analysis derived from the object or building under investigation. The computer will then determine the sequence in which specific salts will crystallise or hydrate under the influence of varying relative humidity and temperature. It will determine the total proportion and volume of the salts that exist in the solid form at any given relative humidity, and thereby indicate safe ranges in which the material should be maintained. Many further features are also envisaged. The system will, for example, be capable of analysing data derived from environmental monitoring at the site in question, and of thereby assessing the risks presented by current conditions or by proposed remedial action.

At a superficial level, the program will be extremely easy to use, and will require no knowledge of the thermodynamics on which it was based. The user will merely insert the data requested, and will receive back, for example, the recommended environmental conditions. At a deeper level, the program will be capable of providing more detailed information and back–up, as necessary. The system will be made widely available to the conservation community, both by conventional distribution methods and via the World Wide Web.

4. Project partners

The project partners are:

Dr. Clifford Price, Institute of Archaeology, University College London, UK

Prof. Peter Brimblecombe and Dr. Simon Clegg, School of Environmental Sciences, University of East Anglia, UK.

Dr. Michael Steiger, Institut fur Anorganische und Angewandte Chemie, University of Hamburg, Germany

An expert chemical model for determining the environmental conditions needed to prevent salt damage in porous materials

145

5. References

1. Arnold, A. and Zehnder, K., 1991. Monitoring wall-paintings affected by soluble salts. In *the Conservation of Wallpaintings* (Cather, S, ed.). Los Angeles: J Paul Getty Trust. 103–135.

2. Correns C. W., 1949. Growth and dissolution of crystals under linear pressure. *Disc. Faraday Soc.* 5, 267–271.

3. Price, C.A. and Brimblecombe, P., 1994. Preventing salt damage in porous materials. *Preventive conservation: practice, theory and research.* London: International Institute for Conservation. 90–93.

4. Steiger M., forthcoming. Crystallization properties of mixed salt systems containing chloride and nitrate. Presented at the EC workshop: *Research on the conservation of brick masonry monuments,* 24–26 October 1994, Leuven, Belgium.

Maria Angeles Vicente

The role of salt crystallization in the degradation processes of granite monuments

The role of salt crystallization in the degradation processes of granite monuments

M. A. Vicente

IRNA / CSIC, Apdo 257   37080 Salamanca, Spain

Abstract

The specific role of salt crystallization in the decay processes of granitic (sensu lato) stones, used as building and ornamental materials, in different environmental conditions, is analysed. The results obtained in the STEP program "Granitic materials and historical monuments: Study of the factors and mechanisms of weathering and application to historical heritage conservation" indicates that in granite and similar rocks (heterogeneous, non carbonated) haloclasty is one of the most degradative phenomena and its intensity depends on the intrinsic characteristics of stone material, especially on the characteristic of its pore network and on the environmental and microenvironmental factors, among which humidity and pollution play a crucial role.

1. Introduction

The crystallization of salts in the pore network of stone materials is probably one of the most generalized and degradative processes participating in their decay. Haloclasty (disruption of the rock due to the effect of salts) is not an independent phenomenon but rather quite often plays a simultaneous and synergistic role in the decay of stone together with processes of gelifraction and dissolution of the rock or some of its components. The presence of soluble salts in the fluids impregnating rocks generally increases the degradative potential of these in the zone of drying. However, salts may reduce or even prevent frost weathering by reducing the freezing point of the solution, thus preventing gelifraction.

The participation of soluble salts in decay processes in rocks does not occur only in those used for the purposes of construction. During long episodes of natural weathering, to a large extent responsible for the configuration of landscapes, soluble salts play a relevant role. In a review entitled Frost Weathering of Rocks in the presence of Salts, Williams and Robinson (1991) analyze the problem and make a distinction among the following situations:

- *When dilute solutions are cooled to temperatures that remain above the eutectic but allow freezing, the presence of salts influences ice crystal morphology and dimensions, rates of crystal growth and other factors governing the crystallization pressures.*

- *Crystallization pressures due to the formation of salt crystals (in the absence of ice) as concentrated solutions are cooled at above eutectic temperatures and become saturated.*

- *Crystallization pressures due to the formation of cryohydrates when temperatures fall below the eutectic. Crystals of ice and salt are present within the rock and in intimate admixture.*

- *If the freezing is fast enough and ice cannot escape from the pores and capillaries, there will also be pressures due to the 9% volumetric expansion that accompanies the water ice phase change.*

Access of salts to the rock used as construction and ornamental material may occur

through different routes. There are even open quarries in shore zones that, with storms and even with the high tide, remain covered and the rocks are subject to considerable salt load prior to use.

According to the review carried out by Grossi and Esbert (1994), the salts most frequently appearing in monuments are sulphates and chlorides, followed by carbonates and nitrates and, more rarely, nitrites and oxalates. Among the cations, calcium, sodium, magnesium and potassium are predominant, and sometimes ammonia. The distribution of salts in the different parts of buildings depends on environmental parameters (humidity, temperature, etc.) and on the solubility and mobility of the species present. According Arnold and Zehnder (1989) in a profile in a vertical wall three zones from bottom to top can be distinguished: In the zone closest to the ground, with permanent humidity, no appreciable crystallization of salts is seen; In the zone immediately above, a massive crystallization of salts occurs–above all sulphates, carbonates and nitrates– and this is accompanied by strong phenomena of degradation of the wall in the form of granular disintegration, crumbling, scaling, etc. In the third zone, poorly deteriorated, the presence of nitrates and clorides is detected.

Access of these salts to monuments and their origin could be:

- *The leaching of ions due to the weathering of rocks and other construction materials. Stone for construction and joining mortars and other materials may contain soluble salts that act as weathering agents.*

- *Capillary rise up through walls of waters coming from the ground. Pollution from agriculture, industry or urban activities of the water enhances its ionic charge considerably.*

- *The deposition of atmospheric products occurring especially in polluted atmospheres or zones of maritime influence. In areas very close to the sea, chlorides predominate. Among the atmospheric depositions that give*

rise to salt formation are those that generate sulphates and nitrates.

- *The action of living organisms is also a source of salt-generating ions. Apart from chlorides and nitrates, phosphates, and oxalates may be of biological origin.*

HALOCLASTY occurs through different mechanisms, among which the following could be mentioned due to their destructive effects: crystallization and growth of salt species inside the pore network of rocks and changes in the volume of some species susceptible to crystallizing with different numbers of molecules of water, depending on the environmental humidity. This generates internal stresses bound to the cycles of humidity/dryness. Evidently, the predominance of one factor or another will above all depend on the environmental conditions: frequent cycles of humectacion/drying will favour the passage of anhydrous and hydrated forms and *vice versa*. Long drying times will favour the growth of crystals, etc. Temperature, relative humidity and time, together with the concentration of the salt solutions, will be determinant in the phenomena of haloclasty.

2. Materials

In a project carried out within the STEP framework by two French research teams, one Portuguese team and three Spanish teams, entitled "Granitic Materials and Historical Monuments: Study of the factors and Mechanisms of Weathering and Application to Historical Heritage Conservation", we studied the behaviour of granite *(sensu latu)* materials under different environmental conditions. These were: under a Mediterranean climate of continental trend; areas with a maritime environment, with and without different types of pollution, etc. The problems were studied in buildings in whose construction, different unweathered and naturally weathered granitic facies and non calcareous sandstones have been used.

3. Results

In all cases, study of the results revealed **crystallization of salts** in the pore network of the rock materials as the most aggressive phenomenon in the degradation processes, although in each case the mechanism of salt precipitation and degradation produced was different.

In **Avila** (Spain), which is affected by a continental climate and is unaffected by atmospheric pollution, the building studied (the Cathedral) is built of three varieties of granite with very different petrophysical characteristics. The phenomenon of salt crystallization and associated decay is most pronounced on the lower parts of the buildings, which are affected by capillary humidity. Its destructive effects are further exacerbated by pollution of urban waters (surface and underground). Analyses of the latter (underground water) has revealed the coincidences between the ions contaminating the water and the salt species that are precipitated on the walls. Salt crystallization also appears in zones affected by filtration from roofs and drains and the contamination of roofs (bird droppings) and the effects of soluble and salt generating mortars further enhance the problem. The low relative humidity of the atmosphere in this area increases the drying rate inside the pore network of the stone and hence the amount of efflorescences on the external surface is reduced. The "breaking" effects of the salts are intensified. The result, depending on the case in question, is the appearance of microfractures, plates, flakes and, in some cases, granular disintegration in the affected zones.

The most abundant salt species in the lower parts, affected by humidity arising from capillary ascent, are sulphates, chlorides and nitrates. In the zones in which the salts precipitate from solutions rich in different ions due to the dissolution of old and especially recent cements and mortars, sulphates are the dominant species. In zones affected by contamination arising from bird droppings, phosphates are detected.

Observation with the petrographic microscope of thin layers of a plate from a zone affected by salts due to capillary rise reveals a microfracturing of the rock with the formation of cracks, both inter- and intramineral. The feldspars and plagioclases are highly fractured and the fractures are also filled with salts. A further observation is the opening of biotite crystals due to exfoliation planes and salt precipitation in the spaces thus created. On the outer part of the section, isolated layers of biotite are found to be set inside a saline mass.

Under the Scanning Electron Microscope, a whisker like morphology is seen. Microanalysis indicates an abundance of nitrates and chlorides.

In **Salamanca** (Spain), with environmental conditions similar to those of AVILA and with buildings constructed of Villamayor sandstone – a sandstone whose cement or matrix is mainly formed of smectite and palygorskite – salt crystallization is also the most degradative weathering process. Upon examining specimens of weathered and unweathered rock under the scanning electron microscope in a zone of salt crystallization, the following is observed:

A common finding in the unweathered rock is the presence of pores with a mesh of palygorskite fibres. In the parts where the weathering is mainly due to stresses generated by thermal changes and cycles of expansion/contraction of the smectites, the pores appear empty and the remains of the fractured fibres are readily visible. In zones affected by salt crystallization, the pores are filled with such salts. The most abundant are chlorides and nitrates. The parts affected display a high degree of degradation, unlike what is seen in vertical faces isolated from humidity, in which fine stone work, even after 500 years, is in an excellent state of conservation even though little maintenance work has been carried out. It is common to find façades whose central part is perfectly conserved and in the parts affected by

salt crystallization, either due to capillary rise or filtrations, the deterioration is very pronounced. In view of the special characteristics of this material, any structural defect leading to filtrations may produce great damage in very little time. A curious and interesting case showing how the combined effect of environmental factors is able to change the effect of a process can be found in Salamanca in the building currently housing the Art Nouveau museum. One wall subject to strong humidity from water loaded with a heavy charge of urban pollution shows highly unaesthetic and very hard whitish crusts, whose main components are alkaline and alkaline earth sulphates. When the crusts are removed, the Villamayor sandstone underneath is perfectly conserved, unlike the strong degree of weathering shown by this material in all zones affected by salt crystallization. Between the crust and the stone there is a biofilm formed of a non–lichenized association between a dematiaceous hyphomycete, a coccoid cyanobacterium and a green alga, and the accumulation of different metabolites excreted by these microorganisms. We performed a follow up of the crust in the zone from where we had previously removed it. The first to appear was a biological colonization, followed immediately by saline efflorescences formed of sparingly stable mixed salts. After one year, the crust - whose major components

were sulphates–had been formed.

A microenvironment in which a series of highly particular circumstances participates –(strong access of humidity with waters with a strong ionic charge, a very dry external environment, a biofilm that maintains the surface of the stone humid and does not allow salt crystallization in pores and at the same time acts as a support for salts to crystallize on the exterior, forming a crust)– all this means that although, not aesthetic, the crust is not degradative for the underlying stone.

In **Brittany** (France), a zone affected by a maritime environment (sprays and strong humidity), the most important pathologies appear in churches (at Folguet and Penmarc'h) directly related to salt formation. Both churches studied are constructed of granitic materials and the statuary and some carved architectural elements are made of kersanite. Gypsum and halite appear in the Basilica of Folguet. The presence of these can be detected in the interior up to a height of 2.20 m and outside only up to a height of 1.85 m. Chlorides, more soluble than gypsum, crystallize out at the end of the sequence. Gypsum may also be formed through the oxidation of pyrites.

Thus we have,

$$(\text{Pyrite})FeS_2 + 2\ CaCO_3 + 4H_2O + mH^+ + NO_2 \longrightarrow (\text{gypsum})\ 2CaSO_4\ (2H_2O) + Fe^{3+} + 2CO_2.$$
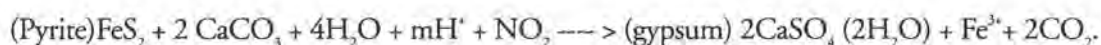
In the church of Penmarc'h salts are very abundant: carbonates (calcite and natron), chlorides (halite and silvite). Gypsum, thenardite and, in lower amounts, nitrates. Gypsum, thenardite and nitrates only appear up to a height of 1.5 m, corresponding to the limit of humidity due to capillary ascent. Carbonates appear throughout the building and it would appear that the solutions they arise from, come from the dissolution of mortars.

The main mechanisms of the action of salts are as follows:

—   *Formation of gypsum and physical degrada-*

tion. The gypsum is formed inside the pores of kersantite, exerting the pressure of crystallization required for rock breakage and appears in black crusts. The advent of sulphates in water due to capillary ascent and the presence of pyrite in the rock are the possible origin of sulphates.

—   *Effect of "sodium carbonate" on the rock. The formation of natron involves an important increase in pH, which may rise to above 10, thus causing dissolution by alkalinolysis of the silicate materials. This has a strong degradative effect. The cause of the forma-*

tion of carbonate is unclear, although the maritime environment and the dissolution of mortars are the most probable causes.

Study of the influence of bacteria in the weathering of granite indicates that the role of autotrophic bacteria in weathering phenomena is to produce large amounts of chemical elements that form strong rock eroding salts. At Penmarc'h, the bacteria of the sulphur cycle may participate in the formation of gypsum, although there is no important microbiological activity at Penmarc'h, with the exception of sugar fermenters on outside faces. At the Basilica of Folguet, the presence of bacteria from the nitrogen cycle is important.

The same result with an even higher amount of nitrifying bacteria has been observed in other areas (coast of Armor), at the chapel of St Malo, the church of Meslin and at the chapel of St Jacques le Majeur.

The influence of the environmental conditions in the degradative potential of salts may be seen in the fact that a strong degree of pollution by NH_3 (of agricultural origin) in some zones of Brittany with the subsequent formation of nitrates is *not* accompanied by an appreciable increase in the degradation of the granitic monuments of the area. The high solubility of nitrates and the elevated rainfall of the zone may account for this, unlike what occurs in a nearby zone subject to a strong degree of pollution by sulphur oxides. Here it is possible to detect a strong increase in the degradation associated with the presence of sulphates.

Regarding one of the monuments studied in **Oporto** in Portugal (Hospital de Santo Antonio), located in a polluted area, important amounts of gypsum or gypsum + halite are characterised on the façades of the building and cause granular disintegration. Apart from the ascent of soluble salts in solution due to capillary ascent from the ground, recent application of Portland cements used for restoration purposes together with the interaction of these with the rainwater are also factors involved in the mechanisms leading to the accumulation of soluble salts.

4. Experimental tests

To experimentally determine the degradative potential of salt crystallization in the granite, three varieties of granite were subjected to salt precipitation cycles following the RILEM procedure (1980). In addition to the standard procedure (drying at 60°C after immersion in the salt solution) a modified one, consisting of heating/cooling cycles (-20°C to 110°C) in a simulation chamber after treatment with the solution, was also applied. Degradation was quantified from changes in the texture of the surface of the blocks, their colour and mass removal.

First, the difference in the behaviour of the different granite facies was detected. Following 20 crystallization cycles, the "Avila Grey" variety, an unweathered facies with a total porosity lower than 0.7%, did not show appreciable losses of mass and the only detectable surface effect was a slight change in colour due to oxidation of the surface biotites. By contrast, a strong degradation together with a loss of material and surface disaggregations occurred after only three cycles in the "ochre" variety. This facies has undergone a strong degree of natural weathering (before its use as a construction material) and has a total porosity greater than 20%.

Treatments following the modified procedure led to an apparently lower degree of surface decay after the first 10 cycles of treatment in the "ochre" variety. However, a sudden and intense fissuration occurred after 13-15 cycles. It is likely that salts would crystallize inside the proof through concentration of the salt solution in the cooling phase and would not reach the surface in massive amounts. As the salt crystals increase in amount and size inside the pore network of the proof, the stress produced gives rise to the haloclasty phenomenon. This is probably compounded by gelifraction, to give rise to total breakage of the proof.

5. Conclusions

– Haloclasty is one of the most degradative phenomena in granite and similar rocks (heterogeneous, non carbonate) used as construction materials.

– The intensity of the phenomenon depends on the conjunction of the characteristics intrinsic to the material and on environmental and microenvironmental factors. The characteristics of the pore network of the stone (amount, shape, homogeneity and interconnection among pores) strongly affect the degradability of a material. Atmospheric pollution and runoff and underground waters, especially if they elicit the formation of sulphates, play an important role in the type and degree of degradation caused by haloclasty.

– The stone decay due to salt crystallization of anhydrous species or species with different degrees of hydratation and the growth and hydration of salt species does not usually act in an isolated way. Its effects are joined to those of thermoclasty, gelifraction, the development of living organisms, dissolutions etc., in general increasing degradation.

– In a few cases, however, the synergistic effect of two or more factors may decrease the aggressiveness of one of them.

Acknowledgements

6. References

1. Arnold, A. and Zehnder, K. Salt weathering on monuments. *The Conservation of Monuments in the Mediterranean Basin,* Bari, 31 58. 1989.

2. Grossi, C.M. and Esbert, R.M. Las sales solubles en el deterioro de rocas monumentales. Revisión bibliográfica. *Materiales de Construcción,* 44, 235, 15 30. 1994.

3. Vicente, M.A. and Brufau, A. Weathering of the Villamayor arkosic sandstone used in buildings, under a continental semi arid climate. *Applied Clay Science,* 1, 265 272. 1986.

4. Vicente, M.A. Granitic Materials and historical Monuments: Study of the factors and mechanisms of weathering and application to historical Heritage conservation Final Report. In: *Degradation and conservation of granitic rocks in monuments.* 1996 (in press).

5. Williams R.B.G. and Robinson D.A.. Frost Weathering of Rocks in the Presence of Salts a Review. *Permafrost and Periglacial Processes,* 2, 347 353. 1991.

Dario Camuffo

The role of climate on stone weathering

The role of climate on stone weathering

D. Camuffo

CNR–ICTIMA, Corso Stati Uniti,4
35127–Padova, Italy

1. Climate, sea salt and stone weathering

Stones weathering is due to a very complex combination of mechanisms, which involve intrinsic properties of the rock, meteorological factors, air pollution, biological life (Winkler, 1994). Stones in coastal areas undergo a more severe weathering which can be attributed to the presence of sea salt, although all the details are not clear. The most known mechanisms that can be considered are:

i.   *the increase of the time of wetness (TOW) which is a consequence of the fact that solutions of hygroscopic salts reach dynamic equilibrium between condensation and evaporation at relative humidity (RH) values lower than that required for pure water (i.e. RH <100%);*

ii. *under usual daily climatic cycles in coastal areas, NaCl crystals become deliquescent during nightime when the RH is very high and crystallises during daytime when the RH drops, possibly exerting mechanical stress as a consequence of the crystals formation and growth;*

iii. *the contamination with sea spray may affect the critical value for deliquescence or hydration of other salts which in turn exert mechanical stresses in the interior of the stone;*

iv. *sea salt contamination lowers the freezing point, and this is a positive factor when dealing with the freezing–thawing cycles, but a negative one when liquid water is utilised for weathering processes, e.g. water and dissolved salts migration, pollutant deposition, chemical reactions, biological life.*

All of these cycles are triggered by the daily and seasonal cycles of the atmospheric variables which are linked to the solar radiation, sea breeze, air temperature and humidity, and so on.

2. Increased dampness and time of wetness

In the case of a non reactive, non–porous surface, condensation occurs when the temperature of the stone surface T_s reaches, or drops below the dew point *(DP)* of the air, i.e. $T_s < DP$, irrespective of both the degree of saturation of vapour *(RH)* and temperature of the air at some distance from the stone. However, for simplicity, herewith it will be assumed that the air and stone have the same temperature, at least in an air layer very close to the material, and the thermodynamic parameters will be referred to this layer in equilibrium with the surface.

Condensation in pores occurs at higher temperatures (i.e. it is in equilibrium with $RH<100\%$) and the departure is mainly affected by the pore radius r as well as, although to a minor extent, by the surface tension of water σ, and the air temperature t (in °C) as it has been discussed in several papers as well as in previous lectures of this course (Camuffo, 1984; 1991; 1994a; 1995). Briefly, the departure can be computed as the critical dew point spread ΔDP which can be calculated after the Kelvin and Magnus equations, i.e.

$$\Delta DP = -\log_{10} \ (\frac{RH}{100}) \ (\frac{237.7 + t}{7.5}) \ = 2.507 \times 10^{-8} \ \frac{\sigma}{r} \ (\frac{237.3 + t}{273 + t}).$$

Also contamination with soluble salts lowers the equilibrium RH (and raises the DP) by a departure which can be calculated with the Wright (1936) or Mason (1971) formulae, as it has been discussed in the above mentioned papers. As a consequence of these two phenomena, condensed water may be found in micropores at usual conditions, and also in relatively dry environments.

In pores with radius $r_p < 0.1$ m the physical (i.e. Kelvin) effect dominates; in pores with $r_p > 1$ m and contaminated by soluble salts, the physico–chemical effect which determines the equilibrium pressure for solutions may also cause condensation at lower *RH*, occurring typically in a marine environment due to contamination with sea salts.

Water supplied by condensation causes dissolution of the rock matrix; condensation–evaporation cycles cause migration of dissolved salts and recrystallisation in other parts, e.g. efflorescences and subflorescences, thus weakening the stone and causing loss of the aesthetic value. Wet materials, e.g. rocks or mortars, may have their mechanical resistance diminished. In other cases, the presence of a film of water may decrease the free surface energy of the material, weakening it (Winkler, 1986).

In certain cases, as for e.g. argillaceous (containing clay minerals) limestone, water may alter the structure of the material, causing expansion, stress and fractures. In fact, the crystal structure is composed of a series of wafers and positive ions are frequently trapped between the wafers. Water is able to penetrate the crystal as it is attracted by the hydroxy groups causing the clay to swell. Of course, this happens only for clay minerals with expanding lattice, e.g. montmorillonite, vermiculite, but not for non–expanding ones, e.g. caolinite, illite, chlorite. When the *RH* decreases, the adsorbed water evaporates, but the structure between the wafers may have changed due to the formation of new crystals. The contraction leads to hysteresis, and in the long run, adsorption–evaporation cycles cause irreversible damage (Torraca, 1981).

Material dampness and air humidity favour biological life and weathering; this negative phenomenon becomes greater and greater when the duration, or the frequency, of *TOW* increases. Inside, the biological activity is limited to some species, e.g. fungi, whereas outside the phenomenon is much more marked with more species, e.g. algae, fungi, lichens, musks. During the time in which the stone is wet, chemical reactions occur between the pollutants deposited and the stone (Laurenzi Tabasso and Marabelli, 1992); the damage is linked to the *TOW*, although no general formula has been yet found to link the damage to the *TOW*.

Condensation is also responsible for increasing the deposition rate of airborne pollutants. This fact is due to two different factors: (i) the particles and the hydrophilic gases that impact on a wet surface stick to it without bouncing, so that the capture efficiency of the surface is increased; (ii) when condensation occurs, near the wet surface several microphysical processes occur, the ultimate result of which is the increased transport of gases and particles towards the surface.

The problem of surface moisture and condensation is very complex, and depends on the chemico–physical characteristics of both the atmosphere and surface. The *RH* within a pore is a function of temperature, mixing ratio, pore geometry, presence and nature of soluble salts, and can be considerably different from pore to pore and from atmospheric *RH*. Total porosity, total pore surface, spatial association of pores that may form pockets and necks, pore size, pore form, and pore radii distribu-

tion are important variables in the weathering of stones. Stones are characterised by a wide variety of pores and necks, with different shapes and sizes, which range from angstroms to millimetres and can be classified in several classes, depending on their properties based on laboratory analysis (Fitzner, 1993). The porosity may change with time, especially in the subsurface layer where migration of salts, leaching, dissolution, erosion, and other physical, chemical and biological attacks occur (Biscontin et al., 1993).

3. Lowering of the equilibrium pressure over a solution

Salts dissolved in the water will lower the vapour pressure of the water because the water molecules are effectively diluted by the presence of the salt, but is useful to discuss some basic results of applied physical chemistry (for further details see Kireev, 1977; Adamson, 1986). The Raoult's law for ideal solutions states that the saturated vapour pressure p_A of the solvent A over a solution is always less than over the pure solvent. The lowering of the vapour pressure is the greater, the greater is the concentration of the solute, i.e. the saturation vapour pressure p_A of the component A over the solution is directly proportional to its mole fraction X_A i.e.

$$p_A = p_o \, X_A$$

where p_o is the vapour pressure of the component A in the pure state, i.e. when $X_A = 1$. However, the concentrations of the solvent A and the solute B, X_B, are linked by the simple relation $X_A + X_B = 1$, so that the previous equation can be rewritten as

$$p_A = p_o \, (1-X_B)$$

which can be rewritten in terms of the difference $\Delta p = p_o - p_A$. Applying the result to the water vapour, the lowering of the partial pressure $\Delta e \, (X)$ of the water vapour in equilibrium with a diluted solution is directly proportional to the mole fraction X of the solute,

$$\Delta e \, (X) = \, e_o X$$

where e_o is the saturation pressure for pure water. The Raoult's law is an ideal, limiting law for complete uniformity of intermolecular forces. A second ideal, limiting law, i.e. the Henry's law, for extremely diluted solutions, states that all the molecules of the solute B are completely surrounded by the molecules of the solvent A and the partial pressure of the solute B becomes proportional to the mole fraction in the limit of zero concentration, i.e. when $X_B \to 0$

$$\lim p_B = k \, X_B$$

where k is a constant with the dimension of pressure and the behaviour of B is determined by the nature of the A–B interactions. In the case of deliquescent salts and concentrate solutions the situation is better described by the Raoult's law.

The lowering of the vapour pressure can be related to the change in free energy of the vapour by

$$\Delta G = \mathcal{R} \, T \, ln \left(\frac{e}{e_o} \right)$$

where ΔG is the change in free energy of the vapour in going from the vapour pressure e to the saturation pressure for pure water e_o. If the water in solution is in equilibrium with the vapour above it, ΔG also represents the change in free energy of the liquid water.

4. Climate cycles, sea spray and salt damage

Salts play an important role in decay because they can precipitate within an aqueous solution when the salt concentration becomes saturated for loss of water due to evaporation, or because some of them are deliquescent and crystallise when the ambient relative humidity drops below certain critical levels, or may change crystalline form or hydrate under some environmental conditions which may be changed by the presence of some contaminants, or may expand for heating. Environmental cycles of temperature or humidity, or

periodic heating due to direct solar radiation may induce salt migration, precipitation, growth, hydration and expansion and trigger disruptive cycles within the pores, causing fatigue or breaking the internal material structure.

If a dilute salt solution within the pores is exposed to a low relative humidity, water will evaporate from the solution and the salt concentration will increase. The higher the concentration, the lower the vapour pressure in equilibrium with it, until a critical limit is reached, i.e. the lowest equilibrium *RH* at which the salt solution reaches saturation. If the ambient *RH* drops below this critical value, the water molecules will continue to evaporate and some salt crystals will begin to precipitate and grow. The mechanism is in some aspects similar to that for freezing. Evaporation begins in medium or large pores which are in contact with the external environment and some precipitation begins. New water is withdrawn from the neighbouring small pores to replace the evaporated moisture. This transport leads empty the smallest pores, whereas the too large cavities remain empty. Arnold and Zehnder (1990; 1991) noted that salt crystals form mainly in pores from 1 to 10 m diameter, and that they follow a sequence: crystallisation continues filling the pores where the crystallisation began, then crystals enter the neighbouring pores; successively small fissures are determined, and crystallisation continues in columnar growth able to lift spalls and detach crusts. The same Authors found also that the crystal morphology is related to the substrate humidity: in the presence of liquid water large crystals grow completely immersed into the solution; on a damp substrate smaller and hygrometric crystals form a granular crust covered with a film of solution; in dryer environment, a humid substrate forms a fibrous crust; on less humid substrates isolated columnar crystals grow; on nearly dry surfaces with localised supply of moisture the crystals are very thin and acicular, hair like, and are called 'whiskers'. New dampness may transform fresh whiskers in a more compact, differently crystallised crust.

Every cycle of *RH* which crosses the critical equilibrium values causes a precipitation/redissolution cycle. In the general case several soluble salts are present inside walls or stones determining a very complex situation for their interactions. However, they precipitate in sequences according to their respective solubilities, whereas the most soluble remains in solution, determining time sequences of crystallisation or space patterns which reflect on vertical layering of the salt front when the source is groundwater capillary rise. In this case Arnold and Zehnder (1991) found that the salts are locally accumulated in a zone from 0.5 to 3 m above the ground level, with this typical sequence from the lower to the higher part: sulphates, nitrates, chlorides. This vertical fractionation was explained considering that, during evaporation, salts with low solubility become supersaturated and are the first to precipitate, while the more soluble salts can continue their rise and will precipitate at upper levels. The more soluble the salts, the more hygroscopic they tend to be (Arnold, 1983). For this reason, the upper layer is characterised by a high concentration of very soluble and hygroscopic salts, which tend to form a humid belt on the top of the rising damp.

When a solution in equilibrium with its environment has reached saturation, every drop of relative humidity causes evaporation, supersaturation and precipitation. Some solutions reach this critical condition at ordinary *RH,* and above the critical equilibrium levels of *RH* only the precipitated salts can be found. A salt which becomes a solute by hygroscopic reaction with humid air is called *'deliquescent'* and several of them can be found, e.g. NaCl at $RH = 75\%$, $NaNO_3$ at $RH = 74\%$, $Mg(NO_3)_2 \cdot 6H_2O$ at $RH = 54\%$, $Ca(NO_3)_2 \cdot 4H_2O$ at $RH = 53\%$, when the temperature is 20°C, but the equilibrium *RH* changes with temperature. Daily microclimate cycles due e.g. to solar heating or room heating may induce crystallisation cycles in walls or monuments.

Some salts are able to exist in two crystalline forms, i.e. anhydrous and hydrate, including some 'water of crystallisation' as part of their structure e.g. gypsum ($CaSO_4 \cdot 2H_2O$) and anhydrite (i.e. $CaSO_4$). In the transition from the anhydrous to the hydrated phase they expand and may damage the stone.

Certain sites are very unfavourable for stone conservation, due to adverse natural conditions determined by climatic cycles and sea spray contamination, worsened by the presence of anthropogenic pollution. Venice is one of them and will be presented here to elucidate the problem with reference to the daily and seasonal values of relative humidity and air temperature (Fig.1).
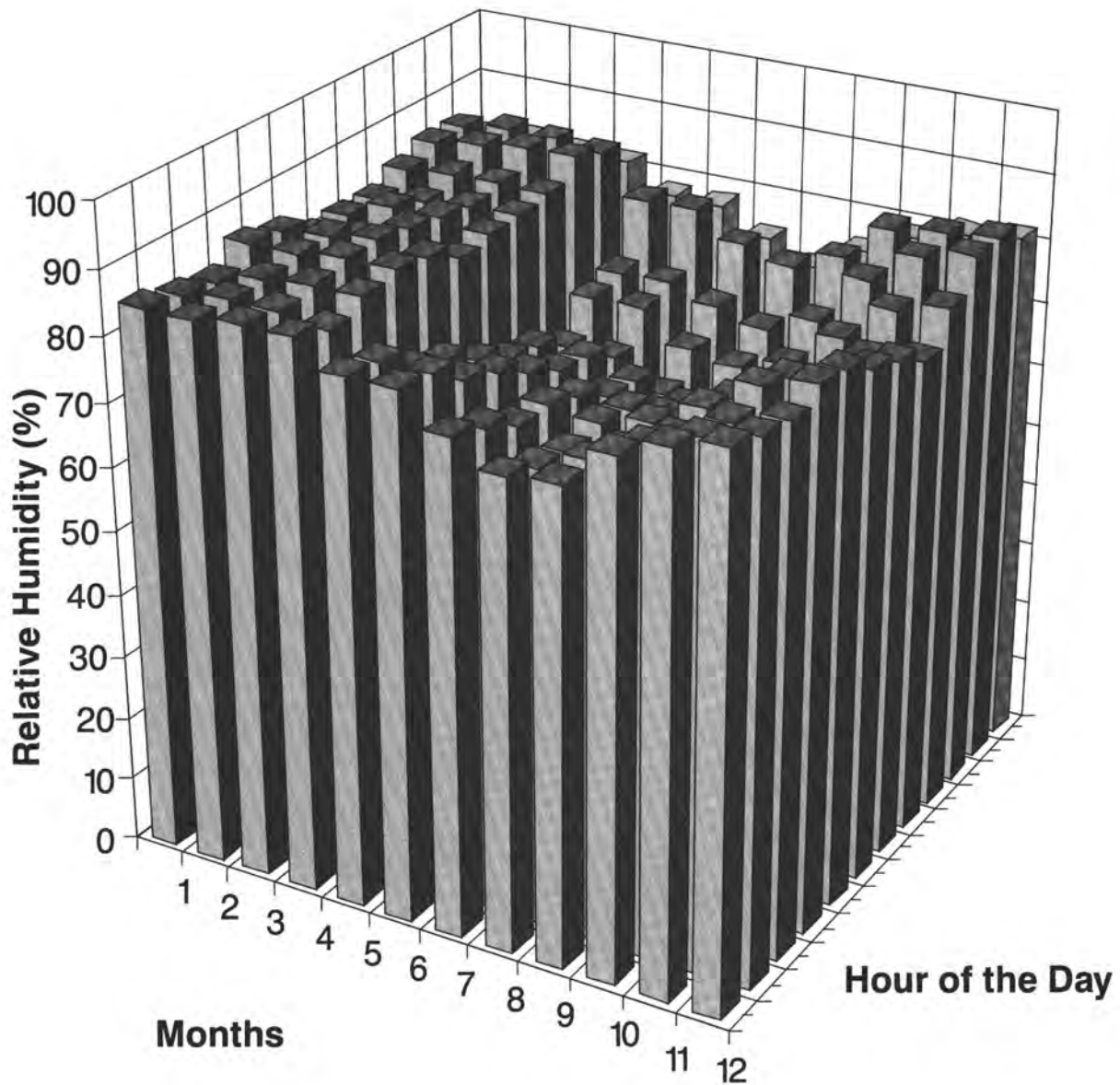

Fig. 1 Daily and seasonal values of relative humidity (RH) and air temperature (T) at Venice

The sea spray contamination increases not only the *TOW,* but also the solubility of some salts, causing many disruptive cycles. Initially the solubility of gypsum increases with the sea spray concentration until it increases by a factor of four when it reaches the maximum, and then decreases again. When a stone is contaminated by sea spray, the NaCl may be either in the crystalline form or in solution with adsorbed water vapour. At ambient *RH* below 75% the NaCl is in form of dry crystals, and at higher *RH* values it will be wet and dilute within the adsorbed water. The solubility of calcium sulphate in aqueous solution of NaCl will begin at *RH* = 75%, will increase until *RH* = 90% and then will fall again as the NaCl concentration decreases, i.e. the *RH* increases. As the maximum solubility is reached at ambient *RH* = 90%, at each transition towards increasing or decreasing *RH* values, some gypsum crystals will form. This cycle studied by Price and Brimblecombe (1994) is extremely important. As every night the saturation is reached in Venice, every day this phenomenon occurs twice. In addition, in the mid seasons and in summer, when the *RH* drops below 75% in the central part of the day, reprecipitation of the dissolved fraction of any soluble salt will occur every morning when the salt solution dries, and a partial dissolution will occur every evening when the ambient *RH* rises above 75% and the contaminated stones begin to wet. However, also in the absence of other soluble salts, the NaCl alone is sufficient to cause severe damage. As not all the stones are in thermal equilibrium with the air, the number of cycles and the damage will vary from exposure to exposure, from building to building, from stone to stone.

The increase of gypsum solubility has another important effect. In the white areas, the gypsum crystals which reprecipitate over the original limestone surface are easily removed in a short time being redissolved by rainfall, leaving unprotected the limestone which is eventually dissolved by acid rainfall.

Another interesting hydration/dehydration cycle determined in coastal sites by temperature changes was determined by Gordon and MacDonald (1953). They found that at 40°C and ordinary pressure gypsum, anhydrite and liquid water can coexist. Above 40°C anhydrite is the most stable form, below gypsum. However, the presence of sea spray lowers the transition temperature: the latter decreases with increasing NaCl concentration. When the solution contains 3 moles of NaCl, the transition temperature is 30°C; at 4 moles 25°C; at 5 moles 21°C; at saturation (i.e. 6.15 moles) the transition occurs at 14°C. This suggests that for most part of the year temperature and humidity cycles induce calcium sulphate crystals to undergo daily hydration/dehydration cycles with continuous expansion and contraction of their volume.

The above examples have considered the presence of only one contaminant, but the real situation is much more complex. Other salts which are deliquescent at ordinary humidity levels, e.g. several minerals derived from nitrogen, extend the *TOW* and the range of ambient *RH* at which crystallisation and hydration take place.

Thermal expansion too may intervene to continue the deterioration mechanism. The formed crystals will have mechanical characteristics different from the porous material. If its the expansion coefficient is greater, the new crystal will come in contact with the internal pore surface and exert pressure when the temperature rises; if is smaller, when the temperature drops.

5. Effect of sea salt on freezing–thawing cycles

When the temperature drops below zero, freezing–thawing cycles develop, and the pressure exerted by the ice crystals in the interior of stones may have disruptive effects. At first sight, one would expect that the greater the size of the pores the greater the force, so that stones characterised by

large pores and high total porosity should be more exposed to risk. However, things are different, and sandstones are quite immune from frost damage despite their low mechanical strength and their coarse pore structure. The maximum pressures expected in sandstone have been evaluated some ten times smaller than in a poor limestone. Poor stones non resistant to frost are characterised by a pore size distribution mainly peaked in the range 0.1 to 0.5 m that are rare in good stone (Everett, 1961). Similarly, Torraca (1981) noted that the damage by frost is more likely to occur in stones which have a prevalence of small pores, i.e. with size between 0.1 and 1 m, although the upper limit is not well defined as freezing damages have been found also in other stones with larger porosity. The problem of the damage caused by frost is rather complex and depends on several factors: the pore size distribution, the geometrical combination of pores and capillaries, the Kelvin effect for water and ice.

Everett (1961) noted that the frost damage to monuments is not associated only with the existence of small pores in the already mentioned range, but with the simultaneous occurrence of pores of a critical size with larger pores. In his detailed study on the thermodynamics of frost damage, he found that the geometrical combination of cavities with different size plays a fundamental role, and that during freezing the excess pressure which can exert in a large pore of radius r_{lp}, connected to a supply of supercooled water at the reference pressure by a capillary or fine pores of radius r_{fp} is proportional to the difference $(1/r_{fp} - 1/r_{lp})$. This difference may be small or large and is much more important than the individual value of each of the two terms. Mechanical failure of the stone occurs if the excess of pressure determined by the above difference exceeds the mechanical strength of the stone.

In addition to the Kelvin effect, also the freezing point depression due to the solution of hygroscopic salts must be considered. Internal evaporation occurs first in the largest cavities and other water with dissolved salts is withdrawn from the finer adjacent pores. Considerable amounts of salts are transported and precipitated in the coarsest pores, and salt crystallisation takes places preferably in large pores because of the energetically favourable lower chemical potential (Ginell, 1994). The crystals are more abundant in the lower part and at the bottom of giant pores, where the solution concentrates during evaporation, becoming saturated and precipitating salt crystals. The greater the pore, the greater the possible amount of salt in the bottom. When the ambient relative humidity increases, the hygroscopic salts hydrate, then become deliquescent and a supersaturated solution forms and grows, until all the salt is dissolved; then the solution start to dilute. Salts can be of atmospheric origin or leached from the soil, or due to constituents of the material, mobilised and transported by meteoric or ground water. In coastal regions NaCl is a very important contaminant, which encourages condensation and lowers the freezing point (Camuffo, 1994b).

These salts lower the freezing point and prevent the mechanical stress due to the formation of ice crystals. The freezing point depression due to the presence of hygroscopic salts can be calculated with the simple formula valid for dilute solutions (for a derivation see Adamson, 1986):

$$\Delta T_f = K_f m$$

where K_f is the freezing point depression constant and for water $K_f = 1.86$ K mol^{-1}; m is the molality of the solute. The formula shows that the value of ΔT_f depends only on properties of the solvent and the molality of the solute.

The freezing point depression ΔT_f is very important for large contaminated pores, as shown in Fig.2 where ΔT_f is plotted versus the percent of anhydrous NaCl weight in water (g

solute /g solution): $\Delta T_f = -20°C$ per 23%; $\Delta T_f = -10°C$ per 14% and $\Delta T_f = -5°C$ per 8% (Weast, 1985). This situation makes extremely difficult freezing in bricks, renders and stones in coastal sites. Apparently this factor is an advantage, as the freezing–thawing cycles are strongly reduced; however, the presence of liquid water has many other negative aspects that the positive ones are largely overcome.
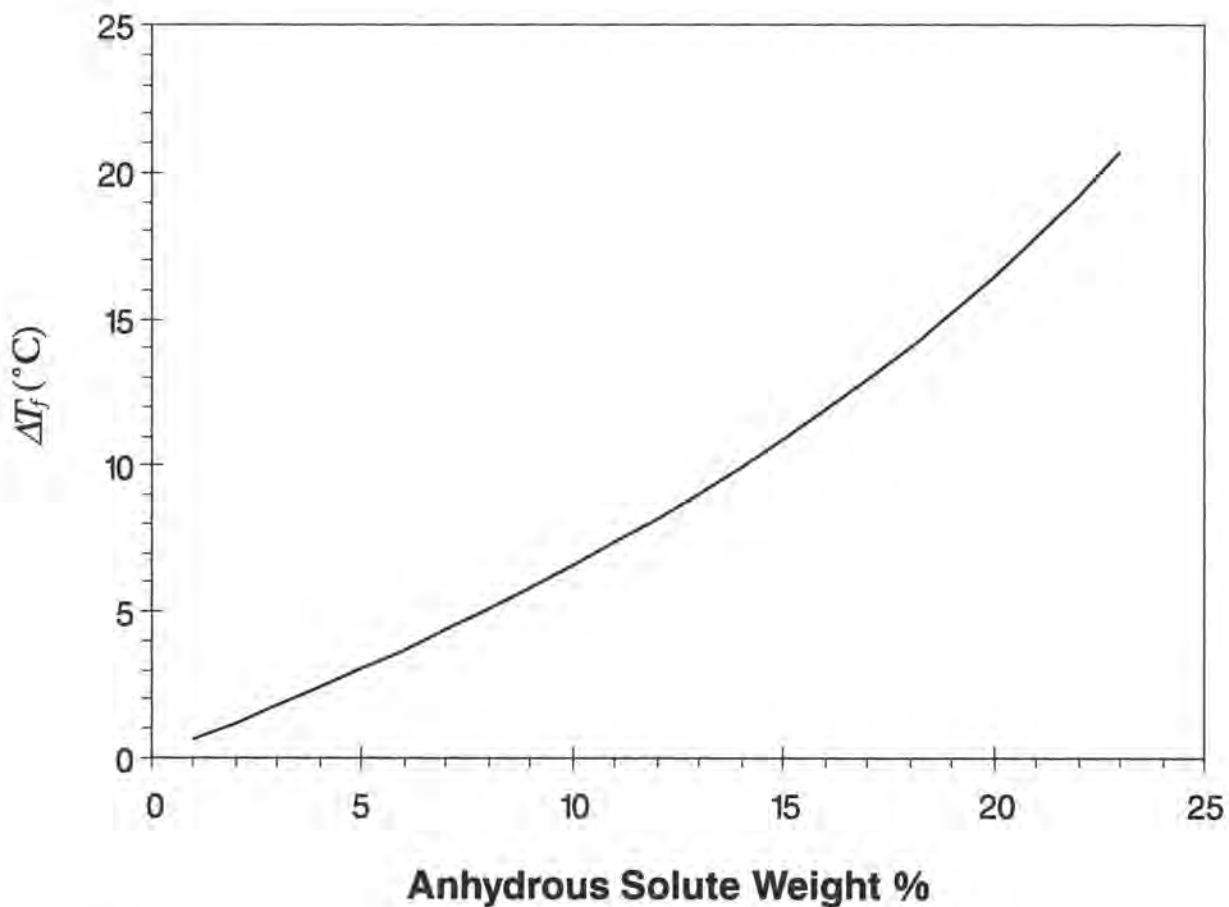
Fig.2 Freezing point depression (ΔT_f) due to the presence of dissolved NaCl at different concentrations (anhydrous solute weight per cent, i.e. g solute/100g solution)

Bibliography

1. Adamson, A..W., 1986: A Textbook of Physical Chemistry, *Academic Press*, San Diego 972 pp.

2. Arnold, A., 1983: Determination of Mineral salts from Monuments. *Studies in Conservation*, 29, 129–138.

3. Arnold, A. and Zehnder, K., 1990: Salt Weathering on Monuments. pp. 31–58 in *F. Zezza (ed.): The Conservation of Monuments in the Mediterranean Basin.* Grafo, Bari.

4. Arnold, A. and Zehnder, K., 1991: Monitoring Wall Paintings Affected by Soluble Salts, pp. 103–135 in *S. Cather (ed.): The Conservation of Wall Paintings*, Paul Getty Trust, Thien Wah Press, Singapore.

5. Biscontin, G., Driussi, G., Maravelaki, P. and Zendri, E., 1993: Physico–Chemical Investigations of Stone Architectonic Surfaces in Venice: the Scuola Grande dei Carmini; pp. 125–136 in G. Biscontin and L. Graziano (ed.s): *Conservation of Architectural Surfaces: Stones and Wall Covering.* Il Cardo, Venice.

6. Camuffo, D., 1984: Condensation–Evaporation Cycles in Pore and Capillary Systems According to the Kelvin Model. *Water, Air and Soil Pollution*, 21, 151–159.

7. Camuffo, D., 1991: Physical Weathering of Monuments, pp. 51–66 in F. Zezza (ed.) *"Weathering and Air Pollution, 1st Course", Community of Mediterranean Universities – C.U.M. University School of Monument Conservation*, Adda, Bari.

8. Camuffo, D., 1994: Pores Capillaries and Moisture Movement in the Stone, pp. 27–42 in F. Zezza (ed.) *"2nd Course on "Stone Material in Monuments: Diagnosis and Conservation", Community of Mediterranean Universities – C.U.M. University School of Monument Conservation*, Adda, Bari.

9. Camuffo, D., 1994: Limits of Stone Sensitivity to Freezing–Thawing Cycles, *European Community Workshop: Degradation and Conservation of Granitic Rocks in Monuments Santiago de Compostela*, 28–30 November.

10. Camuffo, D., 1995: Physical Weathering of Stones. *Science Total Environment* , 167, 1–14.

11. Everett, D.H., 1961: The Thermodynamics of Frost Damage to Porous Solids. *Trans. Faraday Soc.*, 57, 1541–1551.

12. Fitzner, B., 1993: Porosity Properties and Weathering Behaviour of Natural Stones, pp. 43–54 in F. Zezza (ed.): *Stone Material in Monuments: Diagnosis and Conservation, 2nd International Corurse on Monument Conservation*, Adda, Bari, 222 pp.

13. Ginell, W.S., 1994: The Nature of Changes Caused by Physical Factors, pp. 81–94 in W.E. Krumbein, P. Brimblecombe, D.E. Cosgrove and S. Stainforth (ed.s): *Durability and Change*, Wiley, New York, 307 pp.

14. Gordon, J. and Macdonald, F., 1953: Anhydrite–Gypsum Equilibrium Relations. *American Journal of Science*, 251, 884–898.

15. Kireev, V., 1977: Physical Chemistry. Mir, Moscow, 572 pp.

16. Laurenzi Tabasso, M. and Marabelli, M., 1992: Il degrado dei monumenti a Roma in rapporto all'inquinamento atmosferico. *Betagamma*, Viterbo, 169 pp.

17. Mason, B.J., 1971: The Physics of Clouds., *Clarendon Press*, Oxford, 671 pp.

18. Price, C. and Brimblecombe, P., 1994: Preventing Salt Damage in Porous Materials, pp.90–93 in *Proc. Preventive Conservation*, Ottawa.

19. Torraca, G., 1981: Porous Building Materials. *ICCROM*, Rome. 141 pp.

20. Weast, R.C., 1985 CRC Handbook of Chemistry and Physics 1985–86, 66th ed., CRC Press, Boca Raton, Florida, pp.D213–D214.

21. Winkler, E.M., 1986: A Durability Index for Stone. *Bull. Assoc. Engin. Geol.* 23, 344–347.

22. Winkler, E.M., 1994: Stone in Architecture. *Springer Verlag*, Berlin, 313 pp.

23. Wright, H.L., 1936: The Size of Atmospheric Nuclei: Some Deductions from Measurements of the Number of Charged and Uncharged Nuclei at Kew Observatory. *Proc. Phys. Soc.* 48, 675–699.

Johannes Weber
Heinz Leitner
Wolfgang Gaggl
Rafal Szambelan

Crystallization of sulphate salts induced by selective salt extraction by poultices: results from a case study

Crystallization of sulphate salts induced by selective salt extraction by poultices: results from a case study

J. Weber   — *Hochschule fuer angewandte Kunst in Wien, Instituit für Silikatchemie und Archaeometrie Salzgries 14/1, A–1013 Wien, Austria*

H. Leitner   — *Hauptstrasse 3, A–8742 Obdach, Austria*

W. Gaggl   — *Universitaet Wien, Institut fuer Petrologie, Geozentrum Althanstrabe 14, A–1090 Wien, Austria*

R. Szambelan   — *Czerwonych Maków 11, PL–05–806 Komorów, Poland*

Abstract

The paper aims at presenting several sets of salt analyses performed on samples from a 13th century church wall covered by mural paintings. The first set of analyses was made after removal of a paper bulb poultice which had been put onto the wall in order to diminish soluble salts. All relevant ions extracted by the poultice were determined quadrat by quadrat. Further analyses are based on drilling samples from the plaster which were taken during the following years. The attempt to correlate results from both sets of analysis shows some inconsistency due to selective extraction of highly soluble salt species in respect to less soluble ones. When, in addition to the above performed analyses, nature and distribution of surface salt deposits are taken into account, it seems very likely, that in certain zones the poultice treatment had caused sulphate crystallization by reducing salt species of hygroscopic behaviour.

Concerning the encountered datas, the paper draws some general conclusions on the use of water–soaked poultices in restoration.

1. Introduction

Dealing with the determination of content and nature of soluble salts in ancient walls, there is no standardized procedure of investigation, especially in respect to sampling. In many cases, sampling is limited to small pieces from the very surface of the wall or to efflorescences. Sometimes, in–depth sampling is performed using drilling devices or similar procedures. Frequently, big differences between the

ionic content of the pore fluid and the composition of crystalline efflorescences appear, pointing to the necessity of conducting either of the above sampling approaches in parallel. In any case such procedures yield only spotwise informations. A too great number of samples would be required in order to eliminate accidental results due to inhomogeneities .

Whenever restoration work includes salt extraction by means of poultices, a way to obtain information about salt distribution on larger areas may be gained in analyzing salts contained in the poultice material (1). However, this approach lacks of depth information, and the original ion balance is altered by selective extraction of more soluble salt species.

In order to optimize the potentials of the above approaches, in any case they should be accompanied by minute observations in terms of mapping and identification of surface efflorescences. This basic procedure, especially when repeated in certain time intervals, can yield important informations about the distribution of salts all over the wall surface, but of course still largely neglecting what is accumulated behind the surface.

Based on results from a study performed in the church of St. Georgen (Styria, Austria), the present paper will discuss those basic inconsistencies between different methods. A kind of minimum correlation of salt data from poultice analyses with those from plaster analyses and surface salt deposits will be presented. It will be demonstrated that such a correlation can be helpful for the understanding

and interpretation of state and progress of de-
terioration observed in the course of a case
study.

The second part of the paper concerns
about special conclusions drawn from the
above mentioned analyses and observations,
regarding the effects a water–soaked poultice
may exert on the salt system.

In the field of restoration the application
of poultices – either drying or permanently
wet ones – represents a treatment frequently
used in order to minimize salt concentration
within the wall. Many times, however, its use
is not critically evaluated. The ion–selective
nature of the rate of extraction due to different
solubilities of salt species, even if well known
(2, 3), has been frequently neglected as a possi-
ble source of problems. What in particular has
not been discussed sufficiently up to now is
the possibility of sulfate salt cristallization (es-
pecially gypsum) in the aftermath of such a
poultice treatment.

2. The object under investigation

The case study presented in this paper
deals with 13th century mural paintings in the
parish church of St. Georgen ob Judenburg
(Styria, Austria). The paintings are executed as
lime paintings ("*Kalkmalerei*") on plaster upon
a 1.4 m thick wall made of irregular blocks of
stone (predominantely marble, amphibolite
and gneiss).

In December 1987, uncovering of the
paintings from superimposed plaster layers
aided by some local consolidation was per-
formed. On top of that a number of simple
architectural interventions were carried out in
order to diminish capillary rising of moisture
into the wall. In November 1988, desalination
was performed by means of a drying cellulose
poultice, which remained on the wall for
about 4 month. In the course of removal, the
poultice was subdivided into approximatly 135
squares of a size of 50x50 cm with the scope to
analyze the paper bulb for salt ions (fig. 1).

This originally aimed at proving the poultice's
efficiency in respect to salt extraction.

Some months after removal of the poul-
tice, crystallization of magnesium sulphate
whiskers and gypsum was noticed. Crystalliza-
tion of gypsum was visible especially in form
of a whitish veil, most intensively developed
between 2.7 m and 3 m from the ground. In
some places of this area, also gypsum pustules
could be recognized clearly visible by sight. In
addition, increasingly intense dark areas were
observed. They were proved to consist of trans-
parent gypsum crusts at the surface .

Systematic investigations started only on
time of poultice removal. The lack of almost
any information about salt system and mois-
ture before the measures of restoration proved
to be a big disadvantage. Much more informa-
tion could have been gained e.g. if samples had
been taken before uncovering or if removed
material had been collected for futher analysis.

Investigations concentrated upon the
northern wall in the interior of the ro-
manesque steeple where salt deterioration is
most obvious (1, 2).

3. Poultice analyis: methods and results

From each of the poultice quadrats, the
following parameters were detected after ex-
traction of an aliquot in distilled water:

— *total concentration of soluble salt ions by
     means of conductivity of the eluat;*

— *concentrations of chloride, sulphate, nitrate
     and calcium, semiquanitatively by means
     of a commercial analysis set;*

— *concentrations of potassium, magnesium
     and sodium, quantitatively by means of
     atomic absorption (AAS).*

The following considerations are largely
based on just the anions, because the anions
turn out to be more significant when describ-
ing a salt system. The ratio of sulphate versus
the sum of chloride plus nitrate is of major im-
portance for the correlation and interpretation

of datas. This procedure seems to be justified by the well–known crucial differences in the behaviour of the respective salts, as sulphate shows a tendency of crystallizing in form of salts being not or little hygroscopic, while in most cases chloride and nitrate form more or less hygroscopic salts or salt solutions.

Considering the $SO_4:\Sigma(Cl+NO_3)$ ratios in those quadrats where the drilling samples (see section 4) are situated and taking into account the anion distribution over the whole wall (fig. 2), the following trend can be detected:

By means of the poultice analyses, three zones of different composition can be recognized: a sulphate–dominated zone in the lower and a nitrate–chloride–dominated zone in the upper part of the wall, with a zone of transition at a level of about 2.3 m to 2.8 m, where increased amounts of both sulphate and chloride plus nitrate had been extracted. It should be noted that today this transition zone is affected by the crystallization of magnesium sulphate.

The sequence above is in accordance with the frequently reported phenomenon that, due to moisture gradients in a structure afflicted by rising damp, zones of different salts develop (3).

Among the cations, sodium and potassium in the extraction water are concentrated in the chloride–nitrate–zone, i.e. at levels above ca. 2.3 m. The same holds for magnesium, which hence had been to high amounts extracted at a level characterized by today's magnesium sulphate efflorescences.

In the case of calcium, the selective nature of extraction is clearly revealed [see also (4, 5)]: the amount of calcium extracted from the uppermost zone is relatively high compared to that one from the lower, sulphate–dominated zone. However, it is this latter zone where gypsum and hence calcium are predominating the salt system, and there is much evidence that this was true even before the poultice application happened. Thus, interpretation of the poultice analyses tends to be misleading if one does not take into account that gypsum was hardly dissolved by the poultice water, whereas highly soluble calcium nitrate and –chloride, predominating in the upper zone of the wall, was extracted to a high degree.

4. Plaster analyses: methods and results

Between 1992 and 1994, a total of 18 plaster drillings were performed at the northern wall (fig 1). From each of them samples were collected in depth intervals of approximatly 1 cm, comprising a total drilling depth from 1 to 7 cm, depending on the thickness of the plaster layer. The samples were analyzed for their moisture content (gravimetrically) and for the content of sulphate, nitrate, chloride, calcium, magnesium, potassium and sodium (HPLC and IC, respectively). The positions of the drillings are such as that they are roughly arranged on two vertical profiles (profile A on the left side, profile B on the right side of the northern wall).

In general, salt analyses from drilling samples show that salts in the plaster are distributed in a very inhomogeneous way: both the total amount and ion composition of salts in the sample material differ markedly, even if samples have been taken from closely adjacent places. Thus, only certain trends can be detected by this method of sampling. Another general result important to mention is the in–depth gradient of total salt contents in the samples: concentrations are highest in the surface layer of the plaster, i.e. in the outermost centimetre (if one had analyzed even thinner layers of the surface, salt contents would have proved to increase markedly towards the very surface). In contrary to total salt concentrations, the ratio amongst the different ions, however, show no pronounced changes with depth. For this reason and because we do not know up to which depth the salt extraction had developed its dissolving action, it was decided to base all of the following correlations on mean values of all sub–samples of each drilling.

As in the case of poultice analyses, also plaster salt analyses were calculated for the respective ratio of $SO_4:\Sigma(Cl+NO_3)$. Results are marked in the graphs of fig. and discussed in section 6.

5. Visual examination and surface mapping

Probably the most important procedure consists in observing and mapping all kinds of deterioration features at the surface. In the present case, this has been done in repeated intervals over a period of some years, starting about a year after removal of the poultice. It is beyond the scope of this paper to present all results obtained; thus, just those phenomena directly connected to salt crystallization at the surface will be taken into consideration (fig. 3). In this context, it is important to mention that no major altera–tions of efflorescences and no shifting of zones appeared during the whole time span.

Fig. 3 roughly shows three zones in a vertical sequence: from below to above, there is a zone of slight but typical darkening of the paint layer (transparent gypsum crusts on and in the surface layer), further on, at the level called "transition zone" in section 3, a zone of whisker–like efflorescences of magnesium sulphate (epsomite) – in many places connected with flaking of the paint layer –, and finally, at the chloride–plus–nitrate–dominated level of poultice extraction, a zone showing well adhering whitish veils of small gypsum crystalls. At least the two latter zones certainly have formed after salt extraction.

6. Discussion and interpretation of results

To start with methodological aspects, the following critical remarks have to be made:

– *in the case of a rather dry wall system as represented by the present one, drilling samples, even if taken from the vicinity of only a few centimeters from one another, can show highly different compositions of soluble ions.*

A high sampling density would be necessary to overcome this problem, but this is almost never possible both because of economic restraints and conservational aspects.

– *any reasonable interpretation of quantitative results from ion analyses from drilling samples and poultices needs a minute visual study of deterioration features and of the nature and distribution of salt crystalls at the surface.*

– *another factor crucial for the interpretation of salt analyses is the moisture content of plaster and masonry.*

When comparing ratios of sulphate vs. the sum of chloride plus nitrate between poultice and plaster samples, the following can be stated (compare fig. 4):

– *in contrary to the pattern revealed by the poultice analyses, highest sulphate contents in the plaster of profile A are not to be found in the lower part of the wall, but at a level of approx. 2.5 m. These zone is now characterized by whisker–like efflorescences of magnesium sulphate (epsomite).*

– *also samples from profile B show a sulphate maximum at a level of approx. 2.5m. However, this maximum corresponds to the an intense whitish gypsum veil having formed in this area (one profile B plaster sample taken at 1.5m contains both high sulphate and magnesium contents. This points to the presence of magnesium sulphate, which at this level can be sporadically found as epsomite in connection with weathered amphibolites of the masonry.*

– *plaster samples from both profiles show high contents of sodium and chloride at levels of approx. 1.5m which are not reflected by ion analyses from the poultice treatment. This phenomenon can hardly be explained. Even if it is assumed that the height of capillary rise of ground moisture has been highly diminished by architectural interventions carried out in the stage of wall painting*

restauration, causing highly soluble salts to concentrate at lower levels than before, also nitrate should have been accumulated beside chloride. However, this is not the case.

Moisture detected in the drilling samples are generally low, i.e. below approx. 4 weight percent. Even drilling samples from the interior of the wall had no higher amounts of moisture. The above values are very low when compared to data from other historical constructions [see also (6, 7, 8)]. In view of those data it seems obvious that, at the time the study was conducted, the wall was comparatively dry in respect to the situation before restoration. This assumption is supported by today's absence of hygroscopic moisture stains which had been clearly visible in the upper part of wall before the uncovering of the paintings. Otherwise, if the rise of ground moisture would not have been diminished, the originally high content of hygroscopic salts in this zone of the wall should have been reached again in the course of 7 years passed after restoration.

When interpreting the above results, the following facts have to be taken into consideration:

– *formation of calcium and magnesium sulphates in the form of gypsum and epsomite was observed shortly after the poultice had been removed; moisture transport into the wall was strongly reduced in account of the measures accompanying restoration (see above);*

– *today, sulphate concentrations in the plaster are highest in a zone showing heavy formation of gypsum and epsomite (at about 2.5 m from the ground). This zone corresponds to the area where in the poultice the sulphate dominated area overlapped the chloride/nitrate dominated one (2.3 to 2.8 m).*

According to (4) (5) it can be assumed that, by use of water–soaked poultices, the extraction efficiency for chloride and nitrate is

in the range between 70 to 90 %, while for sulphate it is only approx. 10 %. This implies a relative enrichment in sulphate in the pore solution in the course of the extraction. Moreover, the solubility of gypsum is known to be strongly increased by the presence of chlorides and nitrates of sodium, potassium or magnesium (9, 10). A similar influence can be assumed for the solubility of magnesium sulphate.

As to the present case, poultice analyses show high values for all three anions between about 2.3 and 2.8 m ground level. Especially under these conditions, the relative enrichment in sulphate caused by the preferred extraction of chlorides and nitrates is likely to have caused gypsum and epsomite to crystallize, both salts having formerly been dissolved in the pore solution of these hygroscopically highly moist areas.

This conclusion is supported by the visual impression, by the chronological way the damage evolved and by the differences in the ion ratio $SO_4:\Sigma(Cl,NO_3)$ between poultice and plaster analyses.

7. Conclusions

According to all observations and analytical results obtained in the course of the present case study, salt extraction by means of water poultices should be, if ever, applied with special caution whenever the circumstances are as follows:

– *decay is predominately caused by crystallization of sulphate salts of relatively low solubility, and*

– *some portions of the wall show both high sulphate and chloride resp. nitrate contents;*

Considerating above mentioned points, application of water–soaked poultices should be most successful and less dangerous when salts of relatively high solubility, as e.g. sodi-

um nitrate, are recognized as the major factor of deterioration. In such a case, it might be necessary to follow–up with another poultice treatment with better dissolution capacity in respect to sulphates, e.g. ammonium carbonate.

Anyhow it should be critically evaluated, case by case, whether or not salt extraction is necessary in respect to the aim of conservation. One should be aware that salt extraction means to alter a maybe sensible equilibrium and to create a new one – the path from one to the other is necessarily connected to processes some of which might have damage potentials.

Acknowledgements
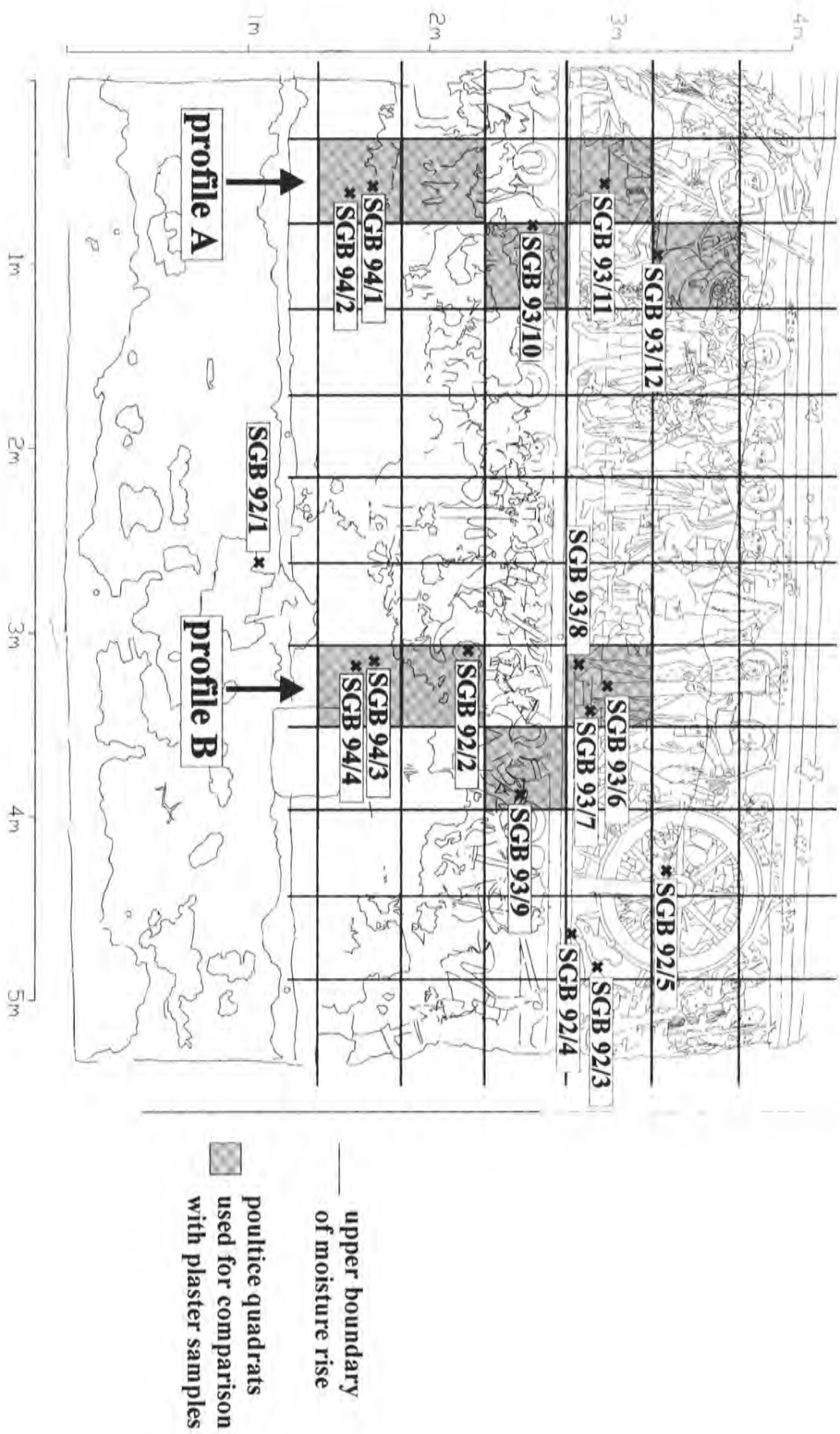
Fig. 1   north wall – position of drilling samples and quadrats from the poultice treatment
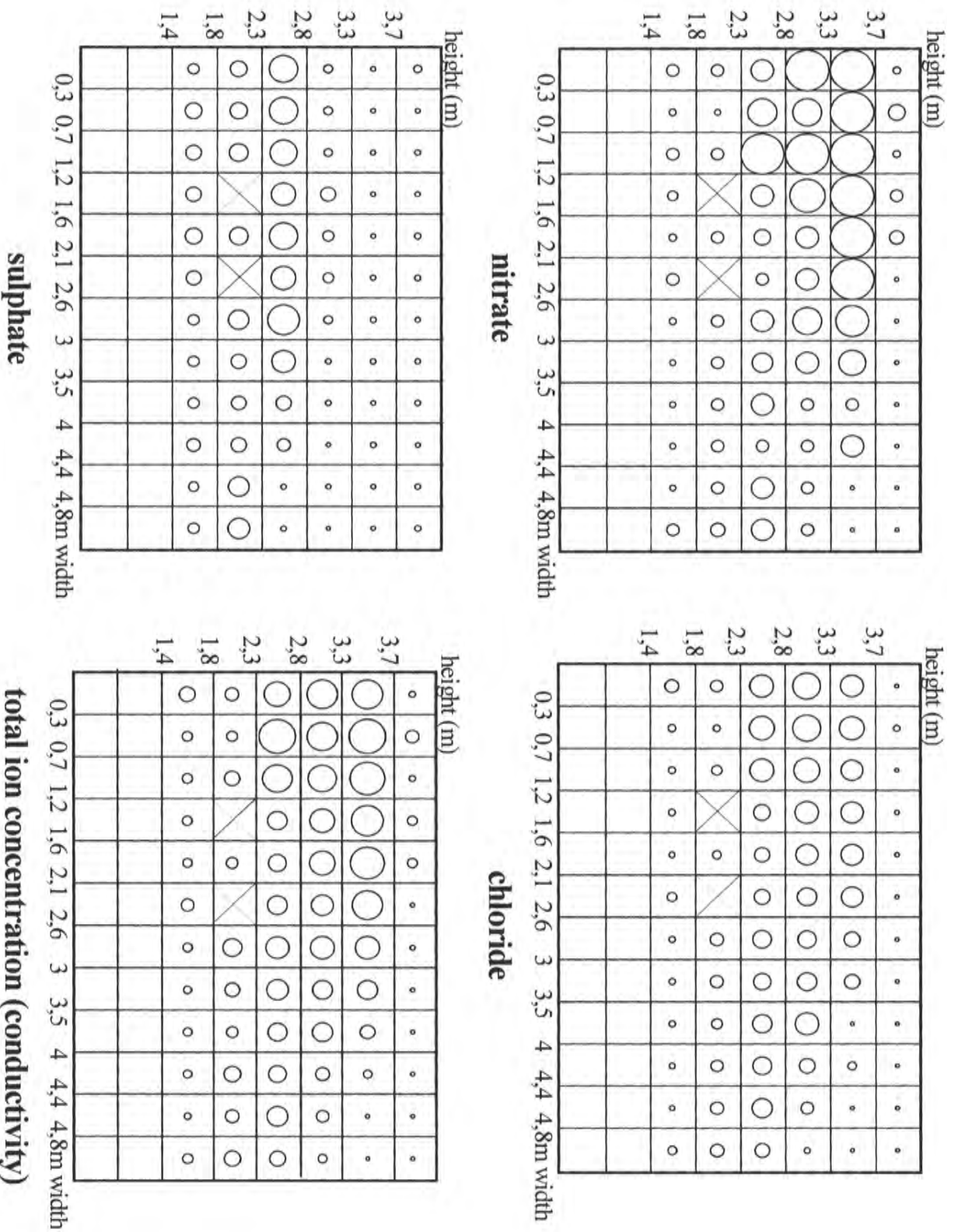
Fig. 2 Anion distribution and conductivity from the poultices on the north wall

Fig. 3 *north wall – surface mapping of salt efflorescences*
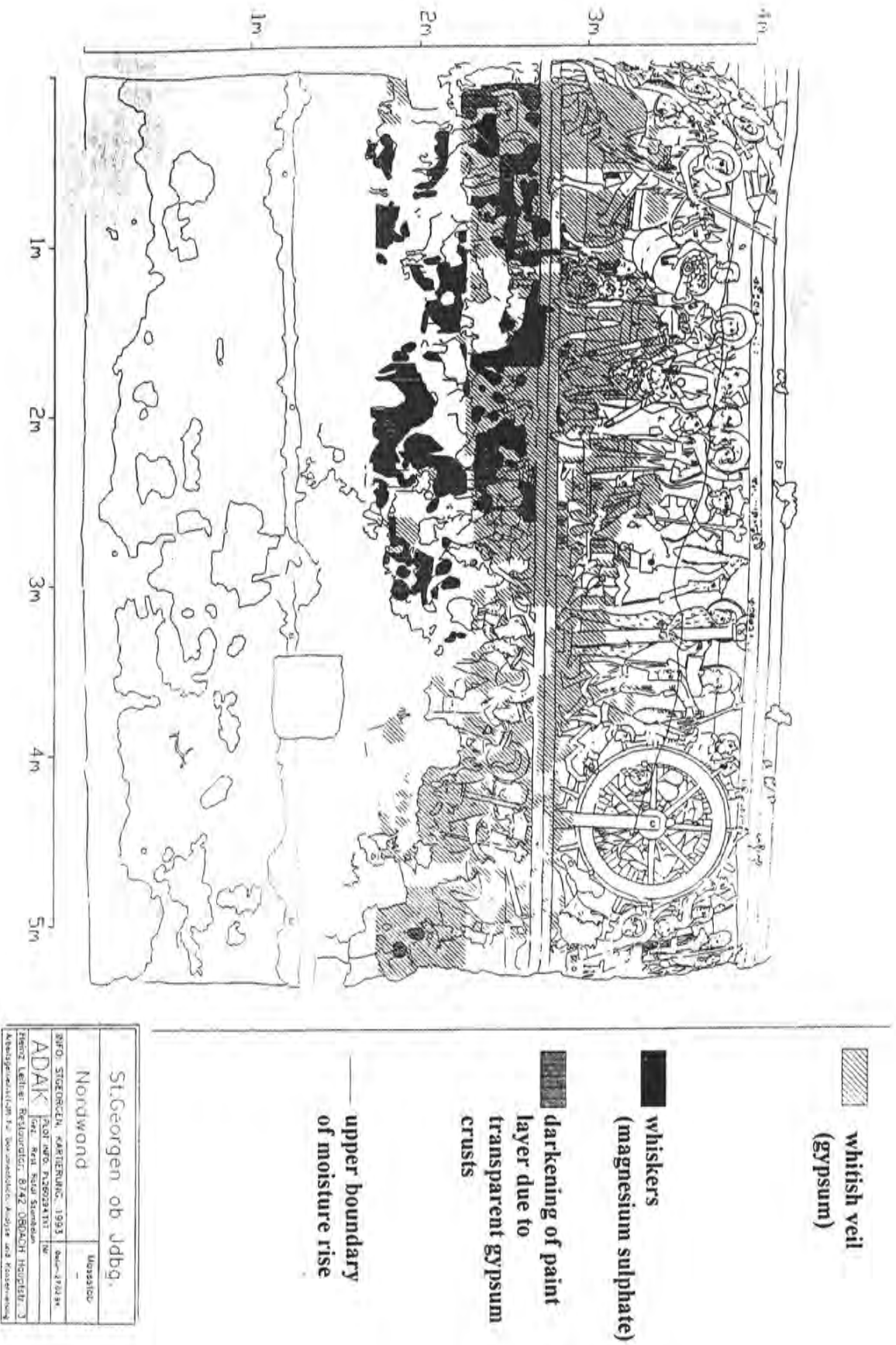
whitish veil
(gypsum)

whiskers
(magnesium sulphate)

darkening of paint
layer due to
transparent gypsum
crusts

—— upper boundary
of moisture rise

St.Georgen ob Jdbg.

Nordwand

Fig. 4A profile A – comparision of ratios between poultices
and plaster drillings (mean values for whole drilling depth)
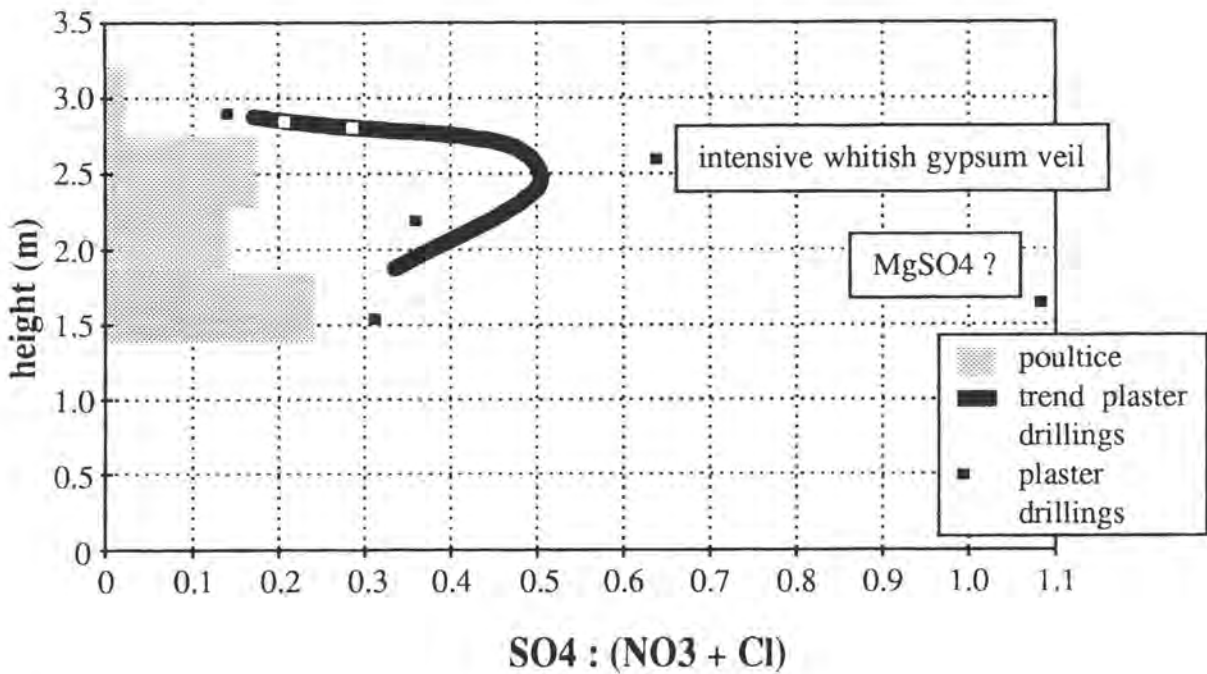
Fig. 4B profile B – comparision of ratios between poultices
and plaster drillings (mean values for whole drilling depth)

References

1.   Weber, J.: Salt–induced Deterioration of Romanesque Wall Paintings in the Church of St. Georgen, Styria, Austria, – Conservation of Architectural Surfaces: Stones and Wall Covering, Int. Workshop Palazzo Labia Venice, 12–14/03/1992, G. Biscontin and L. Graziano eds., pp. 97–104, 1993

2.   Gaggl, W.: Salzschäden an Kulturdenkmälern – Die romanische Wandmalerei in der Kirche St. Georgen ob Judenburg. unpubl. thesis Inst. f. Petrologie Univ. Wien, 1995

3.   Arnold, A.: Rising Damp and Saline Minerals, – Proc. 4th Internat. Congr. on Deterioration and Preservation of Stone, Louisville 7–9/7/1982, K.L.Gauri and J.A.Gwinn eds., Louisville, 1982

4.   Grassegger, G., Grüner, F.: Salzextraktion an Baudenkmälern – Beispiele aus der Praxis und Rahmenbedingungen. – Otto–Graf–Journal 2, pp. 57–71, 1991

5.   Grüner, F., Grassegger, G.: Der Einfluß der Kompressentrocknung auf den Entsalzungseffekt – Laborversuche zur quantitativen Erfassung, – WTA–Berichte 9, pp. 75–86, 1993

6.   Zehnder. K., Arnold, A., Spirig, H.: Zerfall von Wandmalerei durch lösliche Salze am Beispiel der Krypta des Großmünsters Zürich, – 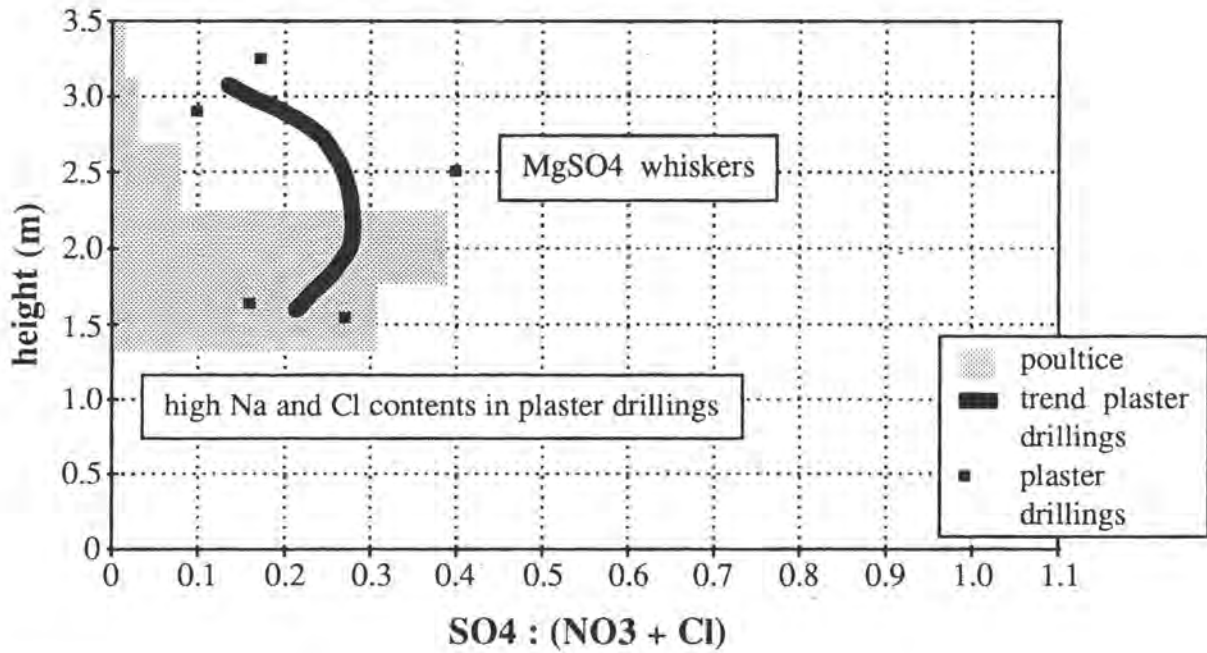Vortragstexte der 3. Fach– u. Fortbildungstagung der Fachkl. Konservierung und Restaurierung, Schule für Gestaltung Bern, 5/6.11.1984, pp. 14–39, Paul Haupt, Bern und Stuttgart, 1985

7.   Rösch, H., Schwarz, H.–J.: Mineralogische und anorganisch–chemische Untersuchungen zur Klärung der Schadensursachen an romanischen Wandmalereien, – Arb.–hefte z. Denkmalpflege in Niedersachsen 11, pp. 104–114, CW Niemeyer, Hameln, 1994

8.   Zenger, R.: Gaderkesee, ev.–luth. Kirche –Untersuchungen von Feuchtigkeits –und Salzsystemen,–Bestandserfassung und Bestandsanalyse an Kulturdenkmälern, 1. Fortbild.–eranst. f. Restaura–toren in Hannover, pp. 60–66, Niedersächs. Landesverwaltungsamt, Inst. f. Denkmalpflege, 1993

9.   Linke, W.F.: Solubilities – Inorganic and Metal–Organic Compounds, Vol. 1. – 4th ed., pp. 680–683, Am. Chem. Soc., Washington, D.C., 1958

10.   Friedel, B.: Gipslöslichkeiten in wässrigen Systemen mit $NaCl$, $MgCl2$, Na_2SO_4 und $MgSO_4$,– Z. Pflanzenernähr. Bodenkde., 141, p. 337–346, 1978

Benita Silva
Teresa Rivas
Beatriz Prieto

Relation between type of soluble salts and decay forms in granitic coastal churches in Galicia (NW Spain)

Relation between type of soluble salts and decay forms in granitic coastal churches in Galicia (NW Spain)

B. Silva, T. Rivas, B. Prieto

Dpto Edafologìa y Quìmìca Agrìcola. Fac. Farmacia
Universidad de Santiago de Compostela

Abstract

We studied seven churches situated on the coast of Galicia (NW Spain) affected by an intense weathering of three different types: plaque shedding, alveolization and sand disaggregation. The last one is particularly severe in sculpted areas.

Petrographic and mineralogical analyses of the rock show that from this point of view, weathering is slight, so alteration is caused by physical mechanisms related to the abundance of soluble salts present. The results appear to indicate that the apparition of one form of decay or another depends on the type of salts most likely to crystallize which, in turn, depends on the specific microclimatic conditions of the affected areas.

1. Introduction

Granitic rocks are considered hard and resistant and really they are in comparison with other rocks traditionally used in the construction of buildings of historical and artistic interest. However sometimes, granitic monuments shows signs of considerable decay. This phenomenon is particular severe in buildings situated on the coast.

To study the mechanisms of alteration and to try to elucidate the reason for the apparition of the diferent forms of decay, we selected seven churches situated on the atlantic coast of Galicia (North West Spain) (Figure 1).

1 Virgen del Camino (Muros)

2 San Pedro de Muros

2 Santa Maria (Finisterre)

4 Buen Suceso (Finisterre)

5 Iglesia Parroquial de Corcubion

6 Santa Maria de Laxe
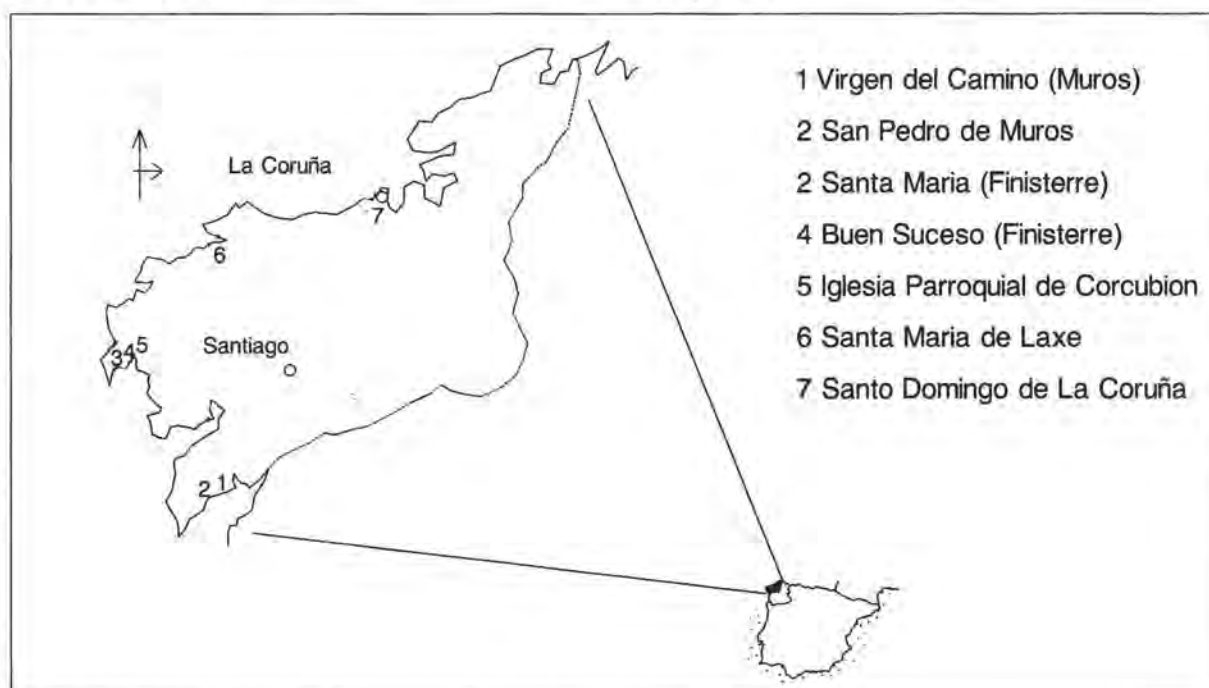
7 Santo Domingo de La Coruña

Figure 1   Situation of the churches selected for the study.

The most frequent forms of decay in these buildings are the following: *Sand disaggregation:* which causes rounding of the edges of the ashlars and erosion which is particularly worrying when it affects sculptures.

Alveolization: which causes deep cavities in the blocks. This form of alteration is uncommon in granitic buildings. From among nearly one hundred monuments studied in previous works in Galicia (Casal, 1989, Guitián Ojea et al., 1993), we have found alveolization only in the churches selected in this study.

Superficial detachments of different dimensions: plaques occupy a big area and they are more than five milimetres thick; plaquettes are similar in area but thinner. Sometimes plaquettes appear one behind another and these we call successive plaquettes. Scales are thinner and smaller in area.

Superficial detachments, which are the commonest form of decay in urban granitic monuments even in semienclosed places such as arcades and cloisters, are not very frequent in coastal churches. In these cases, they are less developed and they are restricted to the lower part of the walls and to the most sheltered areas. Frequently, the stone beneath the superficial detachments is severely disaggregated.

2. Sampling and analytical methods

Samples of the different forms of decay (superficial detachments and sand disaggregation) were taken from the walls at different heights.

In one of the churches (Santo Domingo de La Coruña) we also extracted three cylindrical cores in particular places and collected samples at different depths from its surface. Two of these cores show an intense sand disaggregation. The third one shows a fairly superficial detachment.

The following analyses were performed:

– *x–ray diffraction.*

– *analisys of soluble salt content of aqueous extracts, analyzing cations using atomic absorption spectroscopy and anions using a capillary ion analyzer.*

– *petrographic study of thin sections cut perpendicularly to the surface of the three cylindrical cores.*

3. Results

Petrographic study of the thin section cut perpendicular to the surface of the cylindrical cores, reveals a high intra and transgranular fissuration in the first few milimetres of depth.

Petrographic study and X–ray diffraction analyses show that from a mineralogical point of view the stones are only slightly weathered. Besides the primary minerals only traces of kaolinite were identified in some samples. In some of them we also detected gypsum which was also identified by electron microscopy. Using this technique we also identified halite, but not with x–ray diffraction.

In the case of the core 2 which has superficial scaling, the transgranular fissuration tends to be parallel to the weathered surface.

The negligible mineralogical alteration and the high fissuration which affect the rock, together with the high content of soluble salts detected in the samples, suggest that a physical mechanism related to the presence of soluble salts is implicated in the process of alteration.

The results of the analyses of soluble salts are the following:

• In the areas of the churches with intense disaggregation and alveolization, Cl^- and Na^+ ions are predominat and there is generally a good correlation between both (althought in some cases a better correlation exists between Cl^- and the sum of Na^+, Mg^{+2} and K^+.
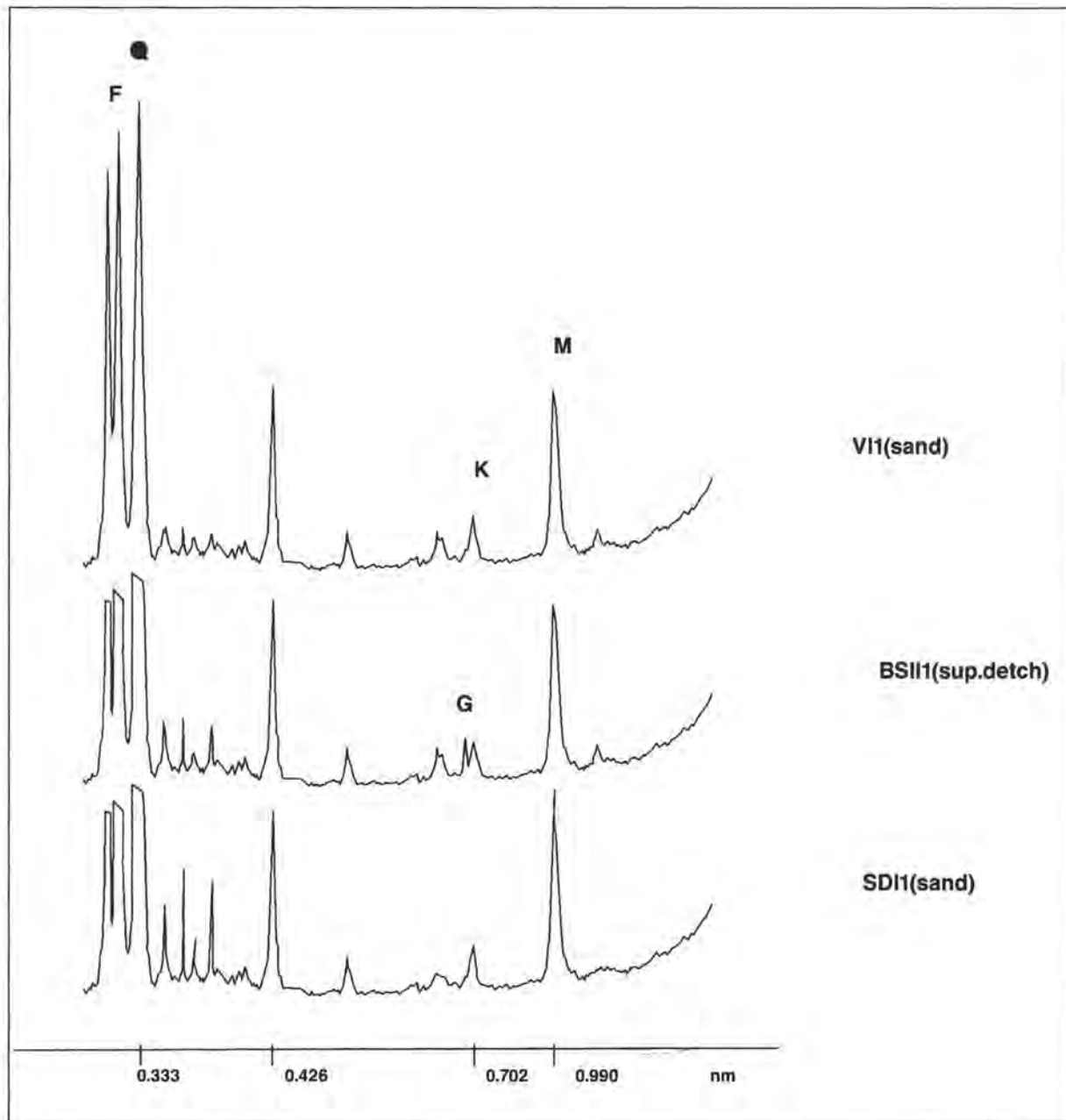
Figure 2   *X–ray diffraction of some samples from the churches. M:Mica; Q:Quartz; F:Feldspars; G:Gyp-sum; K:Kaolinite.*

In the samples of superficial detachments, besides Na^+ and Cl^- we have also found significant quantities of SO_4^{-2} and Ca^{+2} (sometimes they are even more abundant than Na^+ and Cl^-). This is specially evident in some well developed plaques and plaquettes,

although, in some cases, despite SO_4^{-2} being more abundant than Cl^-, the Na^+ ion is present in greater quantity than the Ca^{+2} ion.

This can be seen in San Pedro de Muros, Capilla del Buen Suceso, Santa María de Fisterra y Santa María del Camino (Figure 3).

San Pedro de Muros

Capilla del Buen Suceso
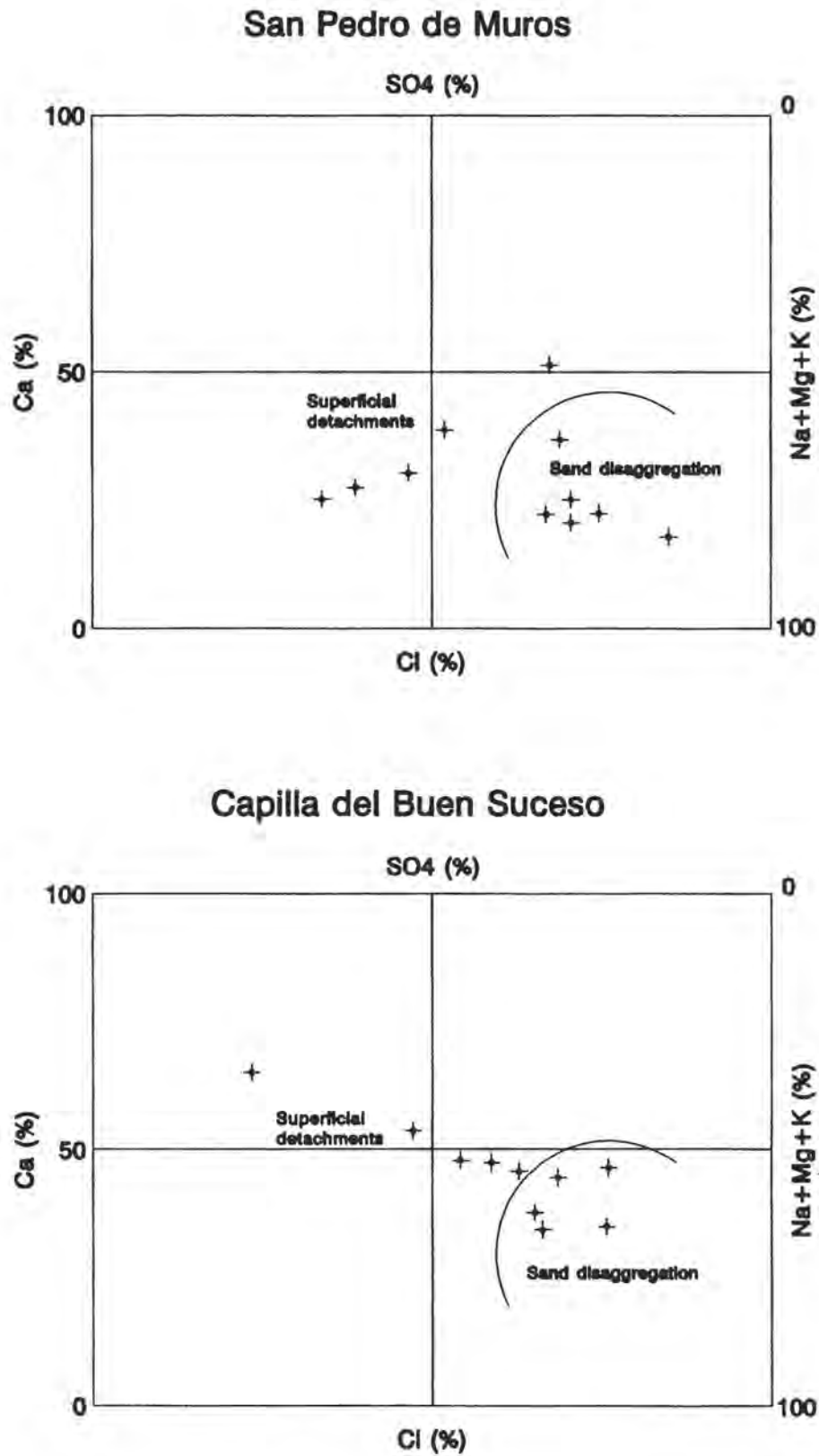
Figure 3   *Langelier–Ludwing diagrams of superficial detachments and sand disaggregation ion contents in samples from San Pedro de Muros and Capilla del Buen Suceso.*

• In the samples taken at different depths from the surface of cylindircal cores, Cl– is present in large and fairly uniform quantities irrespective of depth, whilst SO_4^{-2} tends to concentrate near the surface.

In the two cylindrical cores with superfi-

cial sand disaggregation, Cl⁻ is clearly predominant over SO_4^{-2}, whilst in the third one with superficial scaling, the content of SO_4^{-2} is higher than in the previous cylindrical cores, especially near the surface where it is clearly more abundant than Cl⁻ (Figure 4, 5 and 6).
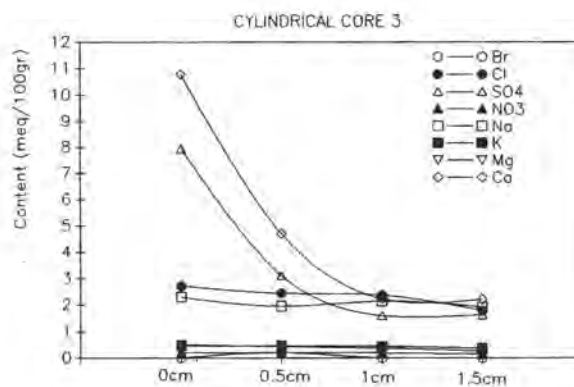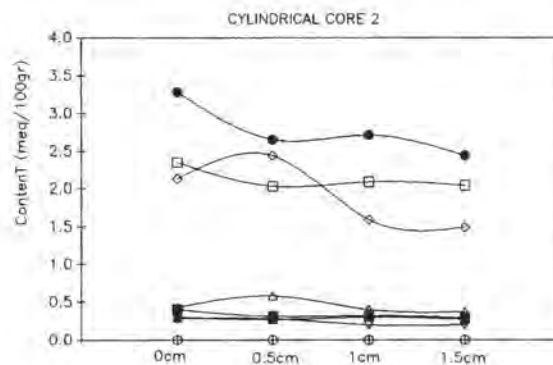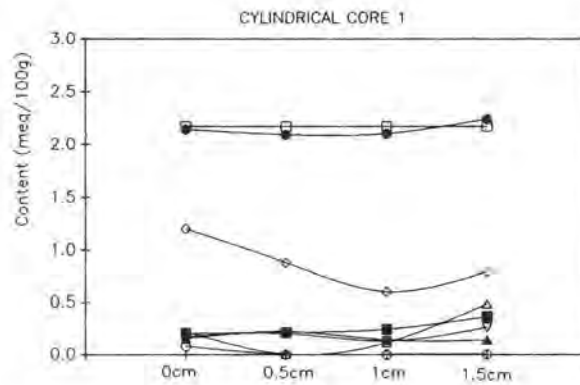
Figure 4,5 and 6 Ion content distribution with depth in the three cylindrical cores.

• On the walls affected by sand disaggregation, Cl⁻ and Na⁺ content do not vary with height; the oscillations sometimes observed have nothing to do with a more intense sand disaggregation, that is to say, there is not a higher level of Na⁺ and Cl⁻ in the most disaggregated areas. SO_4^{-2} and Ca^{+2} are less abundant than Cl⁻ and Na⁺, but their distribution is similar to them.

This can be seen in San Pedro de Muros y Santa María de Iaxe (Figure 7).

On the walls affected by plaque–shedding, SO_4^{-2} and Ca^{+2} are more abundant on the lower parts of the walls coinciding with the presence of superficial detachments. This can be seen in Santo Domingo y en San Pedro de Muros (Figure 7).
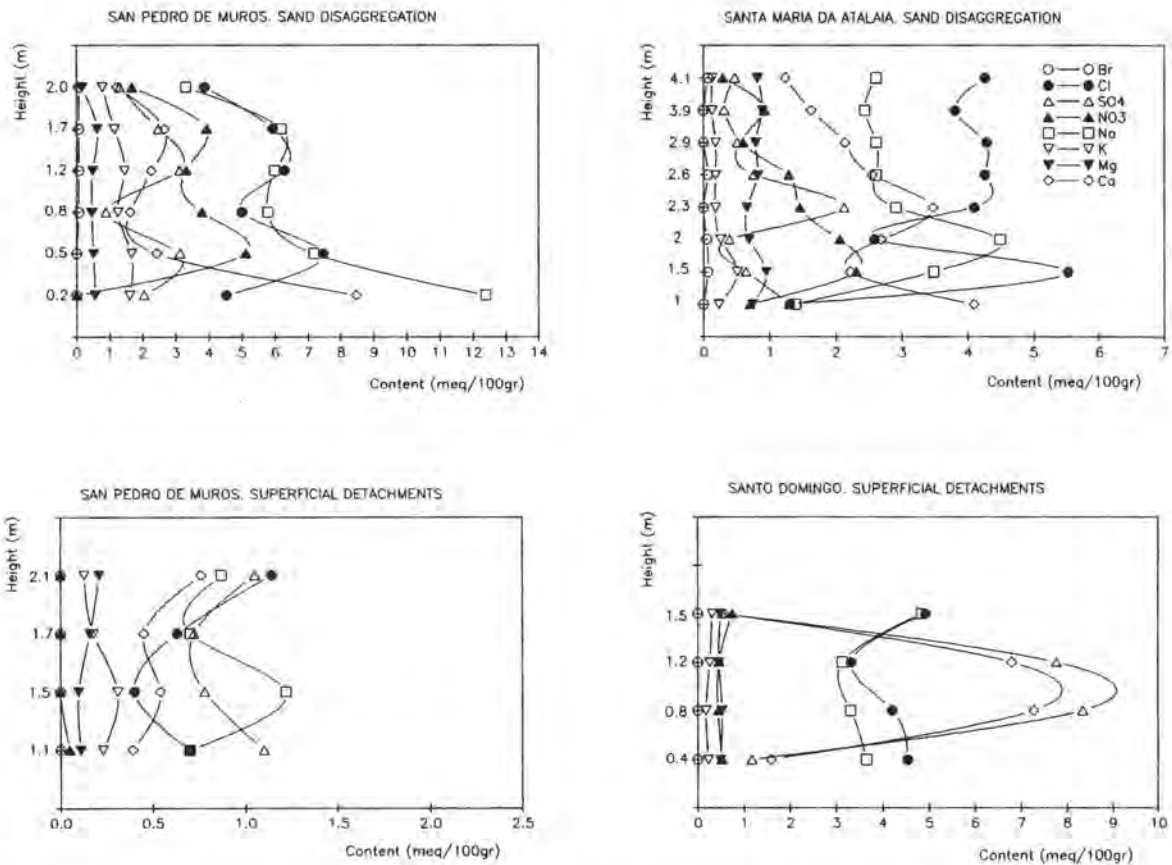
Figure 7   Ion content distribution with height in superficial detachments from San Pedro de Muros and Santo Domingo de La Coruña and in sand disaggregation samples from San Pedro de Muros and Santa Maria de Laxe.

These results appear to indicate that the apparition of one form of decay or another depends on the type of salt most likely to crystallize which, in turn, depends on the specific microclimatic conditions of the affected areas (Silva et al, 1994).

This is suggested by the distribution of the forms of alteration: intense disaggregation and alveolization occur on the highest part of the walls, facing the sea and exposed to the wind.

Superficial detachments, on the other hand, appear exclusively in areas close to the ground and/or areas sheltered from the wind and insolation.

4. Interpretation of the results

We can interpret the results with regards to the formation of differents types of alteration in the following way:

- In the areas which are wet for a longer period of time, the salts most likely to crystallize are the least soluble (whilst the most hygroscopic remain in solution) such as SO_4Ca, and they do so precisely where the loss of water causes the supersaturation of the solution, that is to say, near the surface.

- In the areas exposed to wind, evaporation is greater; crystallization is more frequent and even the most soluble salts crystallize, such as NaCl, causing severe disaggregation. On the other hand, the presence of NaCl considerably increases the solubility of calcium sulphate and, so, an increase in its mobility and its crystallization nearer the surface or even on the surface, and not below the surface as in the previous case.

In this way, SO_4Ca contributes to the process of sand disaggregation as do the most soluble salts.

- In contrast with what happens in buildings situated in urban areas far from the coast in which SO_4^{-2} and Ca^{+2} are clearly correlated, in samples rich in SO_4^{-2} from these coastal monuments, Na+ is frequently present in greater quantity than Ca^{+2}, indicating the possibility that SO_4Na_2 (a salt whose devastating effects are well known) may cristallize.

This salt not only causes sand disaggregation but also plaquette and scale formation in granitic rocks, as we observed in salt crystallization cycles carried out using prismatic granitic samples (Rivas et al, 1994). We have observed that some samples were severed disaggregated on some sides and had plaquettes and scales on other sides.

- With regard to the development of alveolizations, these appear on the monuments studied affecting, on one hand, medium–coarse grained ashlars which also have a heterogeneous texture (presence of nodules, xenoliths, megacrystals or layers of different composition of texture), and, on the other hand, sculpted and carved areas made of medium–fine grained granites.

Both the distribution of alveolizations on the buildings and the fact that in the alveolized areas the salt content is not greater than in disaggregated areas, indicate that for the development of alveolizations in these granitic rocks to take place, two factors are necessary: firstly, the surface of the rock previously affected by salt crystallization cycles must have asperities (be they due to a heterogeneous texture or to chiselling) and secondly it must be directly exposed to the wind.

Thus, the action of salts becomes evident in the least resistant areas of ashlars of an heterogeneous texture and the most resistant areas protude. These protuding areas cause the laminated airflow to break into turbulence airflow which in turn causes erosion at that point and the formation of cavities and hollows in the rock (Quayle, 1992). In the case of sculpted areas, which are more suceptible to the action of salts due to superficial fissuration caused by chiselling (Rivas, 1996), arquitectural mouldings and reliefs and the cavities caused by chiselling may constitute sufficiently important obstacles to modified the airflow and precipitate the formation of hollows.

Superficial detachments-Sand disaggregation
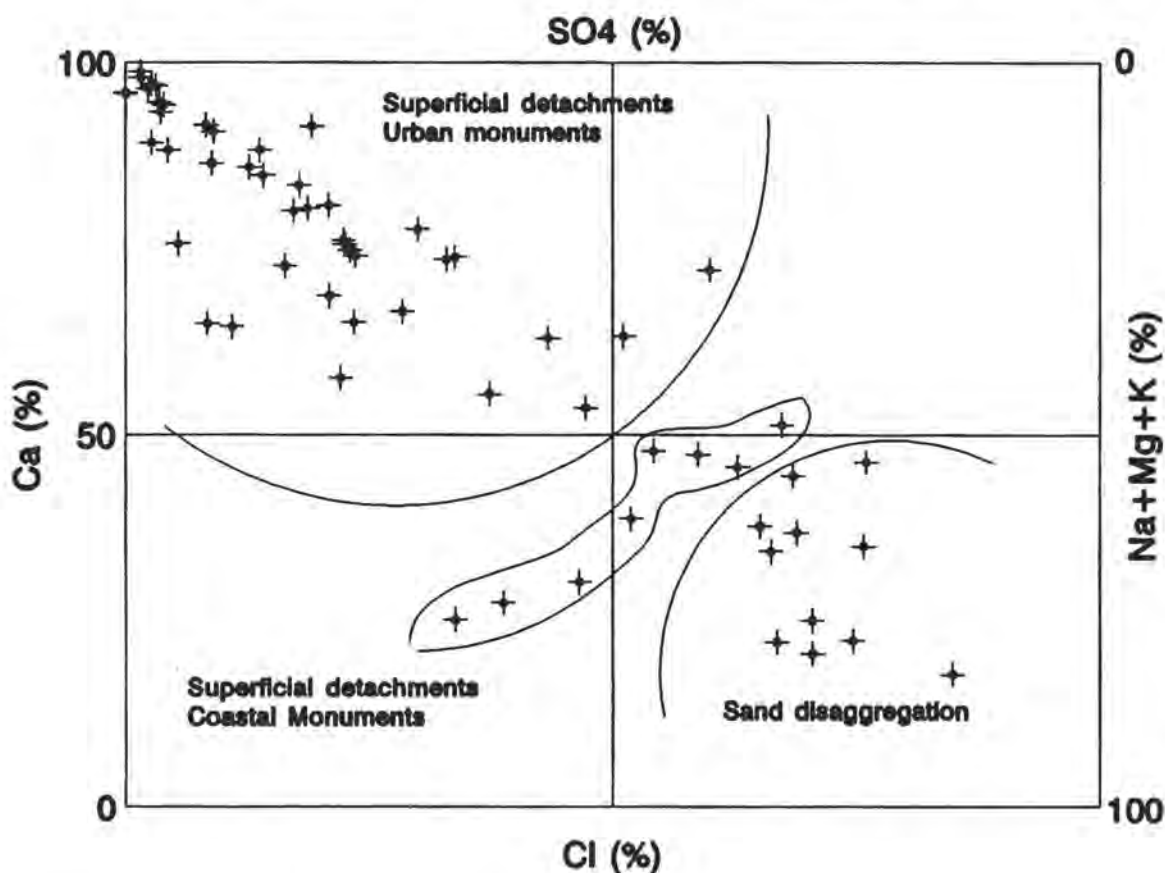
Figure 8   *Langelier–Ludwing of ion content of superficial detachments and sand disaggration of coastal and urban monuments.*

5. References

1. Casal, M. (1989).– *Estudio de la alteración del granito en edificios de interés histórico de la provincia de La Coruña.* Doctoral Thesis. Departamento de Edafología. Universidad de Santiago de Compostela. 1989. 273 pp.

2. Silva, B.; Rivas, T.; Prieto, B.; Delgado, J. (1994).– *A comparison of the mechanisms of plaque formation and sand disintegration in granite in historic buildings.* Abstracts EC Environmental Research Workshop Degradation and Conservation of Granitic Rocks in Monuments, Santiago de Compostela (Spain), 1994.

3. Rivas, T.; Prieto, B.; Silva, B. (1994). – *Salt crystallization test on granited used in the construction of monuments in Galicia. Preliminary results.* Abstracts EC Environmental Re-

search Workshop on Degradation and Conservation of Granitic Rocks in Monuments. Santiago, 1994.

4. Guitián Ojea, F.; Silva, B.; Prieto, B.; Rivas, T. (1993).– *Estudio del estado de conservación de los monumentos más relevantes del Camino de Santiago. Propuesta de intervención.* Monografía (informe no publicado).

5. Quayle, N.J.T. (1992).– *Alveolar decay in stone: its possible origin.* Proc. 7th Int. Symp. Deterioration and Conservation of Stone, vol. 1, 109–118. Lisboa, June, 1992.

6. Rivas, T. (1996).– *Mecanismos de alteración superficial de rocas graníticas usadas en la construcción de moumentos en Galicia.* Tesis Doctoral. Ddto. Edafología y Química Agrícola. Fac. Farmacia. Universidad de Santiago (en preparación).

Anne Chabas
Roger–Alexandre Lefevre

Sea–salt crystallizations from atmospheric aerosols at Delos archaeological site (Cyclades Islands, Greece)

Sea–salt crystallizations from atmospheric aerosols at Delos archaeological site (Cyclades Islands, Greece)

A. Chabas and R. A. Lefevre

Laboratorie Interuniversitaire des Systèmes Atmosphériques (LISA–URA CNRS 1404) Faculté des Sciences de l'Université Paris XII – Val de Marne – F94010 CRETEIL (France)

Abstract

With the aim of studying the salt weathering processes acting on marbles and granites of the archaeological site of Delos island, an intense attention has been paid in determining the chimico–mineralogical composition of liquid and solid particles borne by the atmospheric aerosols coming from the sea.

The aerosols particles were collected by day/night air filtration through Nuclepore membranes (0.4 m in porosity) during a field campaign performed during 20 days in summer (July 1995). The particulate content of the 40 sampled filters was studied by means of two chemico–mineralogical analytical methods:

- *Global analysis by X–Ray Fluorescence Spectrometry (XRFS): day/night variations of the concentrations appear clearly for the following elements: Cl, Na, Mg, and sometimes for S. Weak day/night alternacies were observed for Ca and K. No regular day/night variations were observed for: Al, Si, P, Cl, Ti, Mn, Fe, Zn. Several days periodic variations were observed for V and Cr. Terrigenous and marine characteristic elements have a distinct behaviour: Si, Al, Ti, Fe and Na, Cl, Mg (Ca, K). By means of geochimical calculation it appears that S may have both anthropogenic and marine origins.*

- *Individual chemico – mineralogical characterization by Analytical Scanning Electron Microscopy (ASEM) : 423 microparticles were studied on two filters selected among summer 1995 samples on the basis of their global chemical composition: rich or poor in marine elements. The number, the granulometry, the morphology and the chemical composition of each particle were determined. The main categories of particles are: 1 – Isolated marine particles or homogenous local concentrations originating probably from the evaporation of sea water drops on the filter; 2 – Terrigenous particles (silica, alumino–silicates...); 3 – Mixtures of marine and terrigenous or undetermined particles; 4 – Anthropogenic particles (fly–ash, microsoots, ...); 5 – Biogenic particles.*

The deposition of sea salts on marble and granite surfaces of the Philip Portico, Lions Statues and Column Store, and their successive migrations through the stone porosity in saline solutions, followed by the crystallization of salts during evaporation phases are taken as major factors of deterioration in the marine environment of Delos, besides biodeterioration.

1. Introduction

Since the beginning of archaeological excavations by the Athens French School, in 1873 (Bruneau and Ducat, 1983), materials of the archeological site of Delos island, registered on the UNESCO Humanity Heritage list, undergo an important weathering caused by conjugate action of marine aerosols and littoral organisms. A special attention has been carried here on the characterization of marine aerosol deposits by atmospheric way. The collected aerosol samples were analysed by X–ray Fluorescence Spectrometry (XRFS) and by Analytical Scanning Electron Microscopy (ASEM).

2. Materials and methods

Two field campaigns of atmospheric sampling on the archaeological site of Delos have been carried out during 20 days in March and in July 1995. The samples were collected simultaneously on two special types of Nuclepore membranes of 0.4 m in porosity : the first for XRFS and the second for ASEM. The collection time was 8h–20h and 20h–8h for each sample. The mean flow rate of filtered air was 11 l.min^{-1} (0.66 m^3.h^{-1}). On the whole, 160 filters have been sampled : 80 in March and 80 in July 1995 whose one half for the day and the other for the night.

The whole of the first special type of Nuclepore membranes was analysed by XRFS. This global elementary analysis, reduced to the filtered air volume, has given a g.m^{-3} concentration for each analysed filter. Four of the second special type of Nuclepore membranes were selected per campaign for an ASEM study (JEOL JMS 840A) connected with an Energy Dispersive X–ray Spectrometer (TRACOR TN 5400). The number, the granulometry, the morphology and the chemical composition of each particle encountered in randomly chosen areas have allowed an individual characterization of 423 aerosols particles. Filters are examined and analysed by ASEM, after carbon film coating.

3. Preliminary results on July 1995 filters and discussion

Preliminary results concern global analysis of the 40 filters of July 1995 by XRFS. Two filters (n° 1 and n° 2) are also presented, for an individual chemico–mineralogical characterization of particles by ASEM.

a) Results of global analysis by XRFS

16 elements have been analysed by XRFS: Na, Mg, Al, Si, P, S, Cl, K, Ca, Ti, V, Cr, Mn, Fe, Cu and Zn, on 40 filters according to the described procedure by Quisefit and al. (1994). The examination of the XRFS curves variations in g.m^{-3} versus time shows various behaviours for the different chemical elements:

– *Cl, Na, Mg show slow oscillation of several days cycles and also day/night alternacies of concentration (pl. I, fig. 1), more or less accentuated according to the periods. These day/night concentrations alternacies find some explanations in the winds rating ("meltem") which are, in July, stronger during the day than during the night. The marine aerosols rising follows the same rating (pl. I, fig. 4). It s not a breeze phenomenom because the wind does not inverse systematically the day and the night.*

The less marked character of S day/ night alternacies (pl. I, fig. 2) indicates a not only marine origin. The evaluation of terrigenous (Ter), marine (Mar) and excess (Ex) contributions by means of geochemical calculations (Marchal, 1983) and geochemical models of Mason (1966), for the terrigenous part, and Brewer (1975), for the marine part, has been performed for this element (pl. I, fig.2). "Excess sulphur" has been deduced by difference between the Total sulphur and the Terrigenous and Marine sulphur. It appears that terrigenous contribution is negligible compared to the dominant part of marine and excess sulphur (anthropogenic). This confirms that a part of sulphur inside particles comes from the sea spray and that another is connected to air masses arriving at Delos and bringing a background pollution, at regional scale.

– *Terrigenous elements, like Si, Al (pl. I, fig. 3), Ti and Fe, show simultaneous and non–periodic variations (except at the end of campaign where day/night alternacies appear). These elements are probably dependant on regional air masses as well.*

– *Anthropogenic elements like V and Cr show several days periodic variations.*

b) Results of Analytical Scanning Electron Microscopy (ASEM)

Two filters were chosen for a more detailed analysis by ASEM study (pl. I, fig. 1). The first filter corresponds to a night sampling

showing weak marine elements concentration. The second one corresponds to a day sampling, rich in marine elements. Both are rather poor in terrigenous elements and have mean concentrations in sulphur.(pl. I, fig. 2).

Characteristics and meteorological conditions of sampling during the field campaign of

July 1995 are presented on table 1:

On the filter 1, 210 particles and on the filter 2, 213 particles have been analysed. Their sizes range from 1 to 30 m for the filter 1 (pl. I, fig. 5) and from 1 to 22 m for the filter 2 (pl. I, fig. 6). In fact, the sizes range from 1 to 5 m for 87 % of particles on filter 1, and

Table 1   *Characteristics of the filters 1 and 2 (July 1995) selected for ASEM study and meteorological conditions during the sampling*

N° filter	Date	Time	Filtered air volume (m³)	Wind direction (°)	Wind speed (m/s)	T (°C)	RH (%)
1	16–17/7/95	20h–8h (night)	4,784	350	8	25	73
2	21/7/95	8h–20h (day)	6,049	360	12	26	63

for 92 % of particles on filter 2, with a mediane size of 2 m (pl. I, fig. 5 et 6).

Five categories of particles can be distinguished by ASEM on the studied areas of the two filters. Results are reported and interpreted on table 2 :

1. **Isolated and scattered particles** containing *halite* crystals *(NaCl)* (pl. II, fig. 1), sometimes associated with *Gypsum (CaSO₄ ·2H₂O)* (or *Anhydrite, (CaSO₄)* these two mineralogical species beeing not distinguisable by elemental analysis) (pl. II, fig. 1) and with other undetermined sea–salts containing K, Mg or P. An important group contains only *Gypsum* (or *Anhydrite*) (pl. II, fig. 2), alone or in possible association with *Glauberite (Na₂Ca(SO₄)₂)*, or with undetermined mixture with Na and K, or with *Halite* and *Sylvite (KCl)*. The particle which contains S and Mg could be either *Epsomite (MgSO₄ ·7H₂O)*, or *Kieserite (MgSO₄ ·H₂O)*, or *Hexahydrite (MgSO₄ ·6H₂O)*. All these minerals have been described by Harvie and al. (1980) in sea water evaporation sequences.

These particles are also brought together

in homogenous heap of 25–40 m in diameter. A first group is constituted by *Gypsum* (or *Anhydrite*) crystals (pl. II, fig.3), associated with *Halite* and seldom *aluminosilicates*. A second group is represented by a majority of *Halite* crystals (pl. II, fig. 4), associated with *Gypsum* (or *Anhydrite*), itself combined with probable *Kainite (KMgClSO₄ ·11/4 H₂O)*, *Glauberite* and *aluminosilicates*. These heaps correspond to evapored sea water drops more or less concentrated. This phenomenon had still been described by Storn and al. (1984) on the cascade impactor filters.

All these particles (isolated or in heap) have miscellaneous morphologies: cube, rod shape, squat prism, hexagonal or triangular small plate, round or ovoid particles, efflorescence isolated or developed on previous cubes and prisms. The chemical composition and the morphology confer a **marine origin** for these particles.

2. A second category is formed by Silica (SiO₂) more or less contaminated by Ca, Al or S, Cl, Br and *aluminosilicates* like probable *Illite* (pl. II, fig. 5) and *Kaolinite* which could have a regional origin, and possible *Feldspars, Pyroxene,*
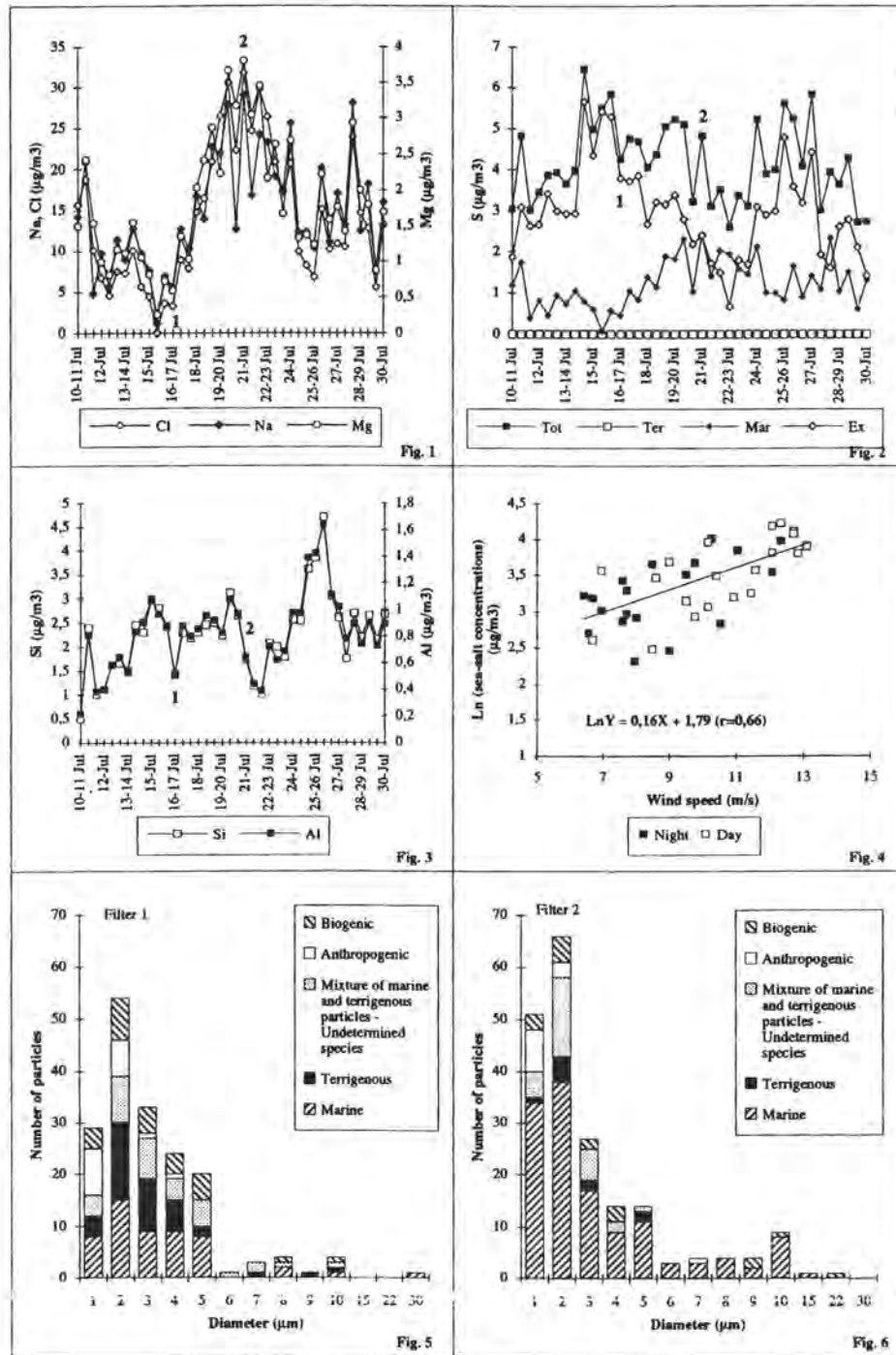
Plate I   *Results of X–Ray Fluorescence analysis of filters sampled all over July 1995 at Delos and granulomet-*
           ric distribution of the two selected samples (number 1 and 2)

Fig.1:   *Variations of Cl, Na and Mg concentration*

Fig.2:   *Variations of S concentration : total (Tot), terrigenous (Ter), marine (Mar) and excess (Ex)*

Fig.3:   *Variations of Si and Al concentration*

Fig.4:   *Sea–salt concentration versus wind speed*

Fig.5:   *Granulometric distribution of sample 1 (night of 16–17 July)*

Fig.6:   *Granulometric distribution of sample 2 (day of 21 July)*

*Table 2 Elementary chemical composition, number, proportion and possible mineralogical nature of analysed particles on the filters 1 and 2 (**Major elements**, minor elements and trace elements)*

ELEMENTARY ANALYSIS	Filter 1 Number of particles 210	Filter 2 213	POSSIBLE INTERPRETATION
	85 (40%)	145 (68%)	1 – Marine particles
	53 (25%)	128 (60%)	*A– Scattered sea-salt particles*
Na Cl	4	91	Halite
Na Cl K Mg S (P)	4	1	Halite + ?
Na Cl S Ca (K Mg)		16	Halite + Gypsum (or Anhydrite)
K Cl	1		Sylvite
S Ca	9		Gypsum (or Anhydrite)
S Ca Na	6		Glauberite
S Ca Na *K*	13		?
S Ca Na Cl	8	1	Gypsum (or Anhydrite) + Halite
S Ca Na Cl *K*	8	18	Gypsum (or Anhydrite) + Halite + Sylvite ?
S Mg		1	Epsomite? Kieserite? Hexahydrite?
	32 (15%)	17 (8%)	*B- Homogenous group of sea-salts (evaporated sea water drops)*
(S Ca Na Cl K) + (Si Al Mg Fe)	9+1		(Gypsum (or Anhydrite) + Halite + ?) + (Aluminosilicates)
(Na Cl) + (S Ca Na Cl) + (S K Mg Cl Na) + (S Ca Na)	19+1+1+1		(Halite) + (Gypsum+Halite) + (Kainite?+Halite) + (Glauberite?)
(Na Cl) + (S Ca *Na Cl Mg K*)		6+4	(Halite) + (Gypsum or Anhydrite + Halite + ?)
(Na Cl) + (S Ca *Na Mg Cl K*) + (Si Al Fe Na Cl)		3+3+1	(Halite) + (Gypsum or Anhydrite+?) + (Aluminosilicates + Halite)
	40 (19%)	10 (5%)	2-Terrigenous particles
Si	6	2	Silica
Si (Al, Ca, S, Cl, Br)	6	2	Silica (+ impurities)
Si Al	2		Kaolinite?
Si Al K (Fe)	9	2	Illite–Muscovite–Orthoclase
Si Al Na (Ca)	2	1	Plagioclase?
Si Al Ca (Fe)	4		Pyroxene-Amphibole?
Si Al Mg K *Fe (Ti)*	7	2	Biotite?
Ca (Si Al S)	4	1	Calcite (+impurities)
	38 (18%)	29 (13%)	3-Mixture of marine and terrigenous particles- Undetermined species
Si AL S Ca	2		Aluminosilicate + Gypsum (or Anhydrite)
Si Al S Ca Na Cl	1		Aluminosilicate + Gypsum (or Anhydrite) + Halite
S Ca Si	2		Gypsum (or Anhydrite) + Silice
S Ca Si Al (K)	2		Gypsum (or Anhydrite) + Illite
Si Al Mg K Fe (Ti) + Na Cl S Ca		18	Biotite + Halite + Gypsum (or Anhydrite)
Si Al + Na Cl S Ca		5	Kaolinite + Halite + Gypsum (or Anhydrite)
Na Cl Si S Ca		1	Halite + Silica + Gypsum (or Anhydrite)
Mg Si Al K Ca Fe	31	5	Undetermind
	18 (9%)	12 (6%)	4-Anthropogenic particles
Si Al (Na Mg K Ca Fe Ti S)	15	10	Fly ash
Background + SCI		1	Microsoot
Fe (Ca S Si Al), Ti (Si Al K Ca Fe)	3	1	Fe-rich debris, Ti-rich debris
	28 (14%)	17 (8%)	5-Biogenic particles
Background + S (P Cl K) (V)	28	17	

Amphibole and *Biotite* (pl. II, fig. 6) which could have a local origin. *Calcite* is also present, pure or contaminated by Si, Al, S. These particles have miscellaneous shapes : irregular, angular, sheet, round ...and are from terrigenous **origin**.

3. The third category consists of **marine and terrigenous Mixture** of *Gypsum* (or *Anhydrite*), *Halite* and various *aluminosilicates*. At this category is associated the group of **Undetermined species** whose composition and origin remain ambiguous.

4. The fourth category consists of typical spherical Si–Al *fly–ash* (pl. II, fig. 7), with fine granulometry (1 m) which reveals a remote origin, carbonaceous *microsoots* agregates (pl. II, fig. 8), wich contain S and Cl, and, at last, *Fe and Ti–debris*. Their origin is anthropogenic (Ramdsen and Shibaoka , 1982).

5. The last category is represented by particles which exibit an important background on X–ray energy dispersive spectrum analyses, expressing a carbonaceous matrix associated with a characteristic peak of S, and rarely P, Cl, K. They have no geometric and regular shape. Their study is out of this present work because they are probably of biogenic origin.

Results given by ASEM confirm those given by XRFS : the first filter, sampled during the night of 16–17 July have less marine particles (40% in total) than the second one, sampled during the day of 21 July (68 % marine particles in total) (pl. I, fig. 8 et 9) . The day sampled particles are rather bigger than the night sampled particles because they are brought by stronger wind (pl. I, fig. 4).

4. Conclusions

The connection of results obtained by XRFS, ASEM and meteorological data can explain the variations of analysed elements concentration and reveals 5 possible origins for particles: marine, terrigenous, mixture of marine and terrigenous particles, anthropogenic and biogenic. Sea–salt particles are observed either as scattered particles (dry deposition) or as heats wich come from evaporated sea water droplets (wet deposition). Their number is dominant, even when the wind is weak. Terrigenous particles have not only a local origin but also a regional one. Sulphur is both of marine and anthropogenic origin. The presence of fly–ash and microsoot particles detected in the atmosphere of Delos shows that, like for S, the impact of anthropogenic pollution is not negligible on the island.

To confirm these data, other filters have to be analysed by ASEM and ATEM (Analytical Transmission Electron Microscopy). The connection between particulate content and climatic and meteorological data (direction and wind speed, air temperature, relative humidity ...) for the same periods have to be precised.

Forms and mecanisms of Delos marbles and granites weathering have to be interpreted taking in account marine aerosols brought by atmospheric way and petrophysical and mineralogical properties of these substrates.
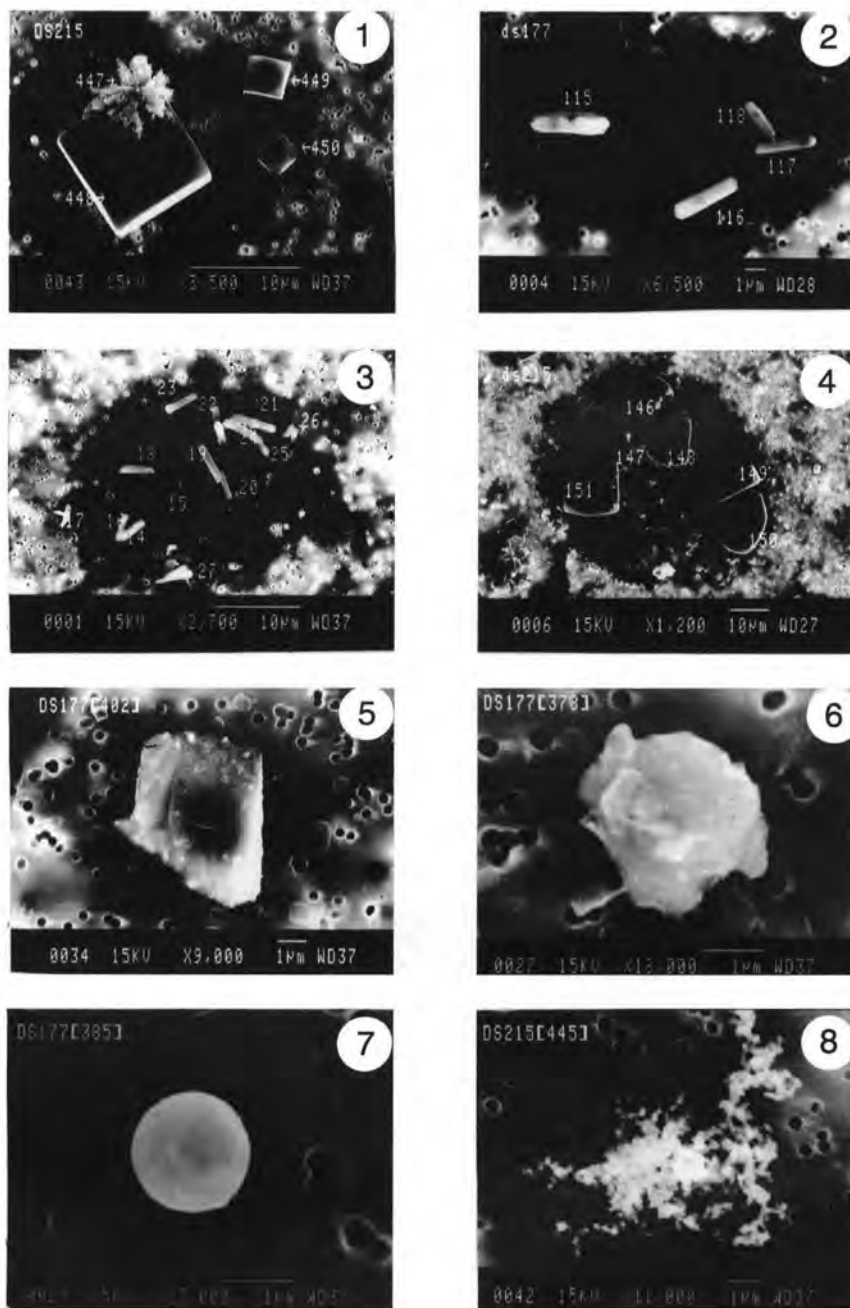
Plate II   Scanning electron micrographs of particles sampled at Delos in July 1995

Fig.1   Isolated cubes NaCl (448, 449, 450) with SCa efflorescence (447)

Fig.2   Isolated rods of SCa particles

Fig.3   Homogenous local concentration of SCa crystals originating probably from the evaporation of a sea wa-
ter drop on the filter

Fig.4   Homogenous local concentration of NaCl crystals originating probably from the evaporation of a sea
water drop on the filter

Fig.5   Angulous and flat fragment of illite

Fig.6   Sheet fragment of biotite

Fig.7   Typical fly ash particle

Fig.8   Typical microsoots agregate

References

1. Brewer P., *Minor elements in seawater,* in Chemical Oceanography, 2nd edition, 1, edited by J. P. Riley and G. Skirrow, 415–496, Academic, New–York, (1975).

2. Bruneau P. and Ducat J.: *Guide de Délos, Edition de Boccard,* Paris, 280 p., (1983).

3. Harvie C. E., Weare J. H., Hardie L. A. and Eugster H. E., *Evaporation of sea water: calculated mineral sequences,* Science, 208, 498–500, (1980).

4. Marchal T., *Contribution à l'étude physico–chimique de l'aérosol atmosphérique en milieu cotier,* Thèse de 3e cycle, Université Paris VII, 138 p., (1983).

5. Mason B., *Principles of geochemistry,* 3rd edition, J. Wiley and Sons, New York, (1966).

6. Quisefit J. P., de Chateaubourg P., Garivait S. and Steiner E., *Quantitative analyses of aerosol filters by wavelength–dispersive X–ray spectrometry from bulk reference samples,* X–Ray Spectrum, 23, 59–64, (1994).

7. Ramdsen A. R.and Shibaoka M., *Characterization and analysis of individual fly ash particles from coal–fired power stations by a combination of optical microscopy, electron microscopy and quantitative electron microprobe analysis,* Atm. Env., 16, 9, 2191–2206, (1982).

8. Storms H., Van Dyck P. and Van Grieken R., *Electron microprobe observations on recrystallization affecting pixe–analysis of marine aerosol deposits,* J. Trace and Microprobe Techniques, 2 (2), 103–117, (1984).

Fernand Auger

Simulated degradation of marbles under marine salt spray

Simulated degradation of marbles under marine salt spray

F. Auger
*Universite de la Rochelle – Laboratoire de
Construction Civile & Maritime
rue de Vaux de Foletier 17026 La Rochelle
Cedex 1 (France)*

It is always very difficult to know the main reason of the degradation of stone on monuments.

Two ways are often purposed

- *Marine salt spray*

- *Air pollution*

but it is not easy to say whether the first or the second is the real cause of the alteration, or even if they work together. If it is so, what is the proportion of each other?

So we decided to test the effects of marine salt spray on different kinds of marbles in an accelerated simulation program.

We tested three different marbles from the mediterranean basin:

- *A French marble from the quarry of "Cases de Pene" in south of France*

- *Carrara from Italy*

- *Pentelikon from Greece.*

The simulator is a special dynamic one of the LCCM. In this apparatus, one day of simulation is nearly the same as one year on a monument situated near the sea–shore.

In fact, it is very difficult to quantify the alteration by a physical process. The most efficient way to estimate the alteration proves to be the visual one. So we get the evolution of the weight of the sample and of the variation of the ultrasonic velocity during the simulation.

But the most spectacular is the variation of the aspect of the samples of rock. The evolution of the surface is very visible on each kind of marble. The alteration is specific of each rock and is reproductible.

So, we demonstrated that marine salt spray is even able to weather marble in a specific way.

The simulator, the petrophysic of rock and the alterations will be described in this paper.

Marcel Benea

Representative stones and weathering forms at Histria Fortress, Romania

Representative stones and weathering forms at Histria Fortress, Romania

M. Benea
"Babes–Bolyai" University Cluj–Napoca,
Department of Mineralogy
1. Kogalniceanu St., RO–3400 Cluj–Napoca,
Romania

Abstract

Histria Fortress is located on the south–west coast of Sinoe Lake (Dobrogea area, Romania). The investigations were carried out only on the building stones of the Late Roman Wall which is made of sedimentary rocks in a proportion of 99 %. Cretaceous lithocalcarenites are the most widespread rocks in the wall. Also, to restore the monument the same rocks were used. This gave us the opportunity to observe the behaviour of the same stone since antiquity. The weathering forms which occur on the wall are mainly represented by granular disintegration, detachment of flakes, scales or solid crumbs. Also, the alteration of the initial colour of the rocks due to red crusts made of gypsum, halite and hematite was noticed.

1. Geological setting

The Dobrogea district lies in the south–eastern part of Romania, between the Danube river and the Black Sea. Histria Fortress lies in Central Dobrogea, on the south–west coast of Sinoe Lake.

Geological, in Dobrogea one can distinguish three main units with a north–west orientation and with different tectonic evolutions. This three units (from north to south) are:

I. *The North Dobrogean Orogen includes strongly folded and slightly metamorphic Palaeozoic formations, intruded by granites and overlain by gentler folded Permian, Triassic and Jurassic formations which in their turn are covered by almost flat lying Upper Albian and Upper Cretaceous (Cenomanian–Coniacian) formations.*

II. *The Central Dobrogean Massif is a distinct structural unit of the Moesian Platform, separated from the adjacent North and South Dobrogea units by deep faults. Its highly folded Precambrian basement (the Green Schists Formation: an Upper Precambrian anchymetamorphic, flysch series) underlies a rather thin sedimentary cover composed of two structural stages: a lower, slightly folded cover encompassing two Middle Jurassic calcareous formations as well as the relatively thick Upper Jurassic Casimcea Formation and an upper, undislocated cover including several scattered patches of Middle and Upper Cretaceous deposits. The Quaternary, rather thick, loess over hides the Jurassic formations and their basement over broad areas. The character of Massif of this unit is given by the rising at the surface of the basement.*

III. *The South Dobrogean Platform consist of Palaeozoic (Silurian, Devonian, Carboniferous), Mesozoic and Tertiary deposits.*

2. Sampling and investigation methods

Twenty nine samples were collected from different parts and levels of the Late Roman Wall, especially from the main gates (the great one and the small one). Standard XRD analysis and microscopic observation of thin sections were carried out in order to establish the mineralogical composition. XRD was performed over powdered samples using a DRON

diffractometer equipped with a broad–focus copper tube. Mineralogical compositions were estimated by comparing the intensities of the strongest diffraction lines diagnostic for the various minerals identified in the sample. Therefore, the results obtained have no absolute value, being only intended for comparative purposes and to check the microscopically observations.

3. Petrography of the building stones

From a petrogenetical point of view, all the samples can be divided in two categories: metamorphic (A) and sedimentary (B) rocks.

A. The metamorphic rocks are represented by different petrographical varieties of the Green Schists Series: graywacke and green pelitic schists.

The most part of the Histria Fortress is sitting directly on the green schists. So, this type of rock was the most available material used in the ancient buildings. But, in the Roman Wall there are very few pieces from such material because of its schistosity.

Macroscopically the rock presents a green, bluish–green colour, sometimes with violet shading. As a result of the weathering the rock becomes a greenish–brown colour. The pyrite crystals are very often, with a typically cube shape and sometimes, as a result of the oxidation, limonite pseudomorph can occur. In thin sections one can observe the schistosity as a consequence of the alternation of chlorite and sericite lamellae and quartz+feldspars grains.

B. The Late Roman Wall is made of sedimentary rocks in a proportion of 99%. On the basis of the fossiliferous content one can perform a distribution depending on the age of the rocks and the petrography.

B.1. Jurassic rocks

The Upper Jurassic age of these rocks was establish on the basis of the echinoids debris (*Collyrites, Rhabdocidaris, Plegiocidaris*). Petrographically, there are white, yellow–white limestones, sometimes with a oölitical appear-

ance. In thin sections the oölitical character is obvious. There are also pelletal structures so, one can describe this rock as a oopelmicrite.

This type of limestones crop out in Central Dobrogea, particularly in the Casimcea Valley (Casimcea Formation, Oxfordian–Kimmeridgian), about 30 km south–west from Histria.

B.2. Cretaceous rocks

On the basis of the paleontological content and the petrographical characters, the most part of the samples were assigned to Upper Cretaceous, respectively to Cenomanian and Turonian–Lower Senonian.

B.2.1. The Cenomanian rocks are represented by microconglomerates with calcitic cement and by lumachellic limestones. This material proceed from a geological formation where the alternation between this two types is very common.

Macroscopically, the microconglomerate presents a brownish–grey colour and a vacuolar aspect. The quartz grains are very abundant, rounded, usually with an undulated extinction and are enclosed in a sparite cement.

In the case of the lumachellic limestones, the vacuolar aspect is given by the presence of a rich bivalves fauna (*Exogyra sp.,* ostreids) which prevail in comparison with the clastic material.

In these calcirudites, the noncarbonatic extraclasts are represented by angular/subangular quartz grains, with normal or undulated extinction, fragments of quartzites, chloritised biotite and glauconite.

B.2.2. Turonian–Lower Senonian

This age of the samples was determined on the basis of different fossils: *Inoceramus labiatus, Globotruncana sp.* and *Pithonella sp.* Petrographically were separated: lithocalcarenites, siliceous nodular limestones and lithic sandstones.

Lithocalcarenites are characterised by yellowish–brown and white–grey colours and sometimes, because of the high clay material content, the rock splits in plates. Under the

microscope, one can observe a calcitic micritic mass in which the clay mixture is abundant. The detritic material reach till to 30–40% and is represented most of subangular quartz grains. Glauconite is a frequent component part (about 6%) and appears like green granules, with a rounded outline and a microcrystalline texture. The bioclasts are represented by echinoderms, sponges and foraminifera debris *(Globotruncana sp., Heterohelix, Hedbergela sp.)*. Macroscopic, on some blocks there are dwelling structures *(Thalassinoides)*.

The siliceous limestones presents usually a yellowish–brown colour and nodular appearance as a result of the non–homogeneous material. This aspect increase in time as a result of the weathering. The shape of the nodules vary considerably from flattened to highly irregular. The mineralogical composition of the nodules is made up mainly of calcedonic and fine grained quartz.

The lithic sandstones with calcitic cement are seldom represented in the Roman Wall (we have only two samples collected). The colour is brown and the aspect is typically sandy. Microscopically, in the calcitic cement occurs angular to subangular quartz grains, quartzite and sericitic schists fragments, muscovite and biotite lamellae, granules of glauconite and opaque minerals. Feldspars are in small amount (about 10%) and are represented by oligoclase and albite.

All these types of Cretaceous rocks are well known in the Babadag Basin (North Dobrogea) where are also nowadays quarried out.

4. Weathering forms

To describe and recording the weathering state of the building stones we have used the classification scheme developed by FITZNER et al.(1992). In this aim carefully observations and colour photos are taken in order to "draw" a weathering map of the wall. All individual weathering forms are exactly registered and by using the abbreviations listed in Table 1, recorded on the photos. Selected examples are shown in Fig.1 to 4.

Table 1 Weathering forms and abbreviations used for the description of the building stones from Histria Fortress, Romania

Weathering forms		Symbols, abbreviations and descriptions
Relief (R)	┇ ┿ ┇	Rr - Rounding / notching
	⊘ ⊙ ⊘	Rc - Weathering of components
Back weathering (W)	▽	Ws - due to loss of scales
	▼	Wo - due to other type of material detachment
Fissures (L)	╲	Li - indipendent of stone bedding
Discoloration (D)	▦	Du - allochtonous discoloration
Soiling (I)	▦	Ix - dirt deposits on the stone surface (soot, dust)
Salt deposits (E)	⊙	Ee - efflorescence
Detachment of material:		
Granular disintegration	▱	G - granular disintegration
Spalling	▱	P - detachment of solid crumbs
Transitional forms	△	FS - flakes to scales
	ᵒ ᵒ ᵒ	GP - granular disintegration to spalling
	▢	GF – granular disintegration to flakes

Fig.1 The left wall of the Small Gate. Map of the weathering forms
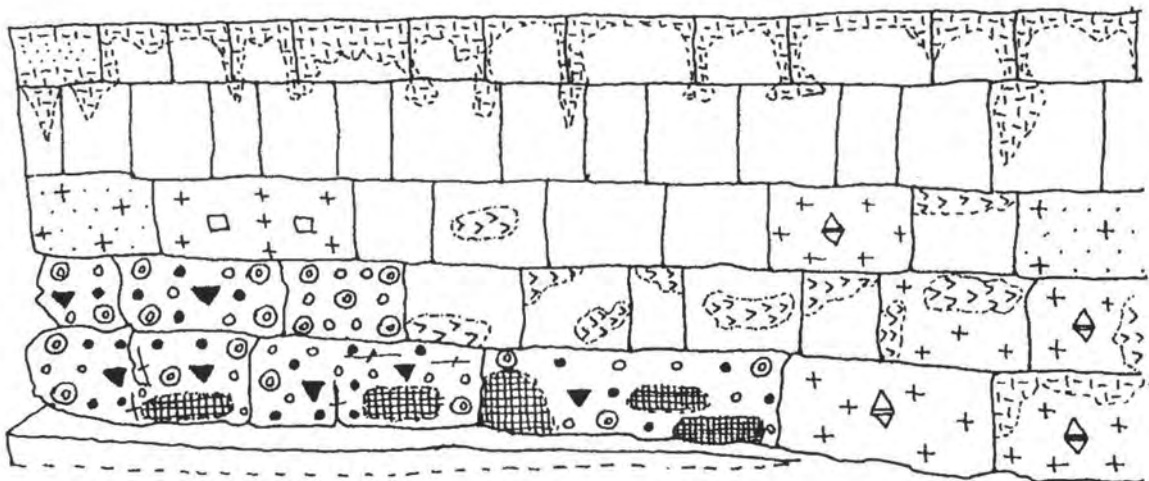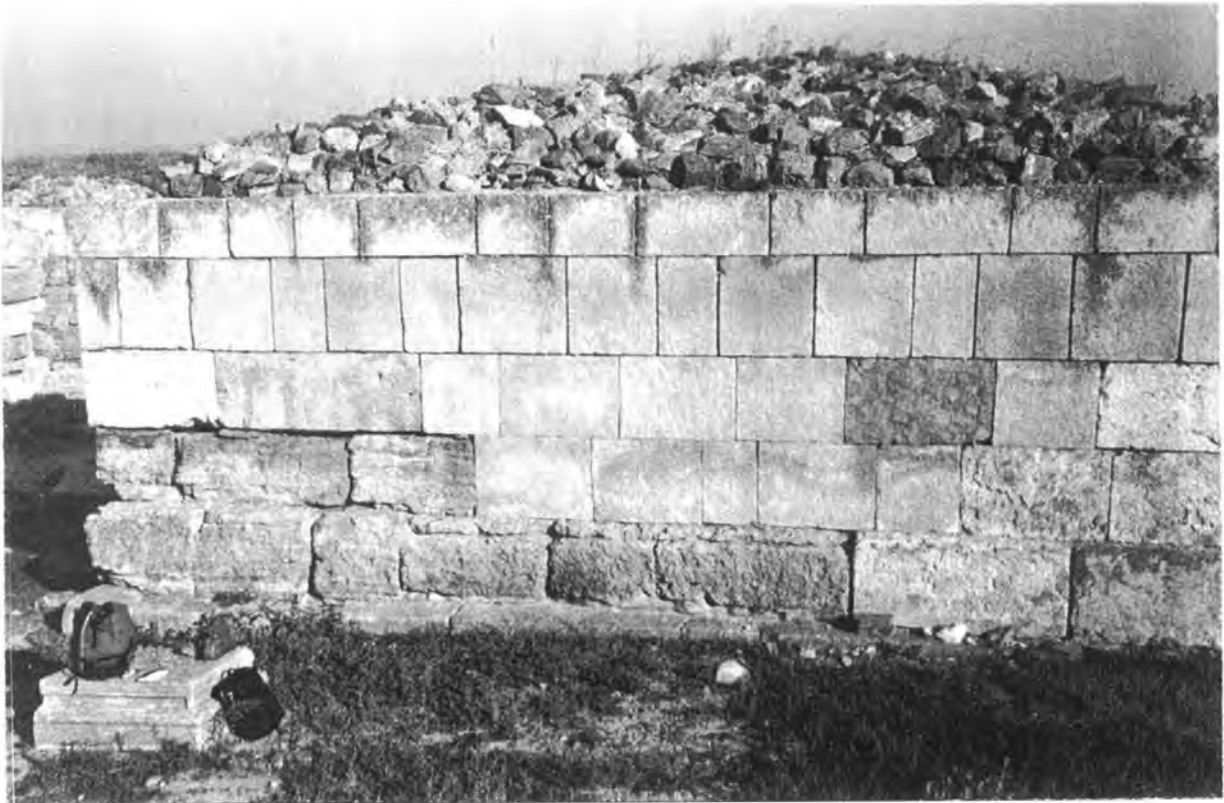
Fig.2 The right wall of the Great Gate. Map of the weathering forms
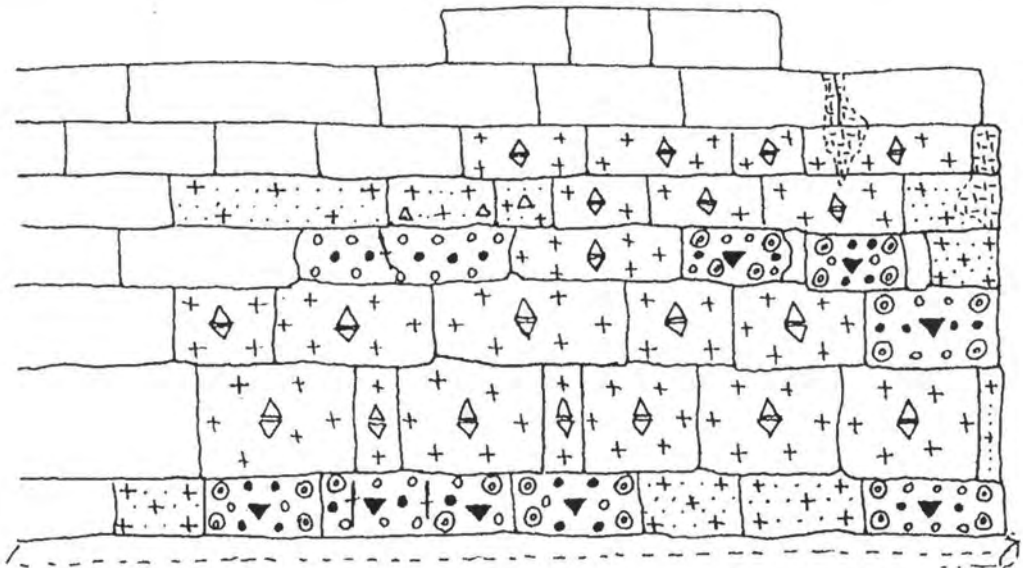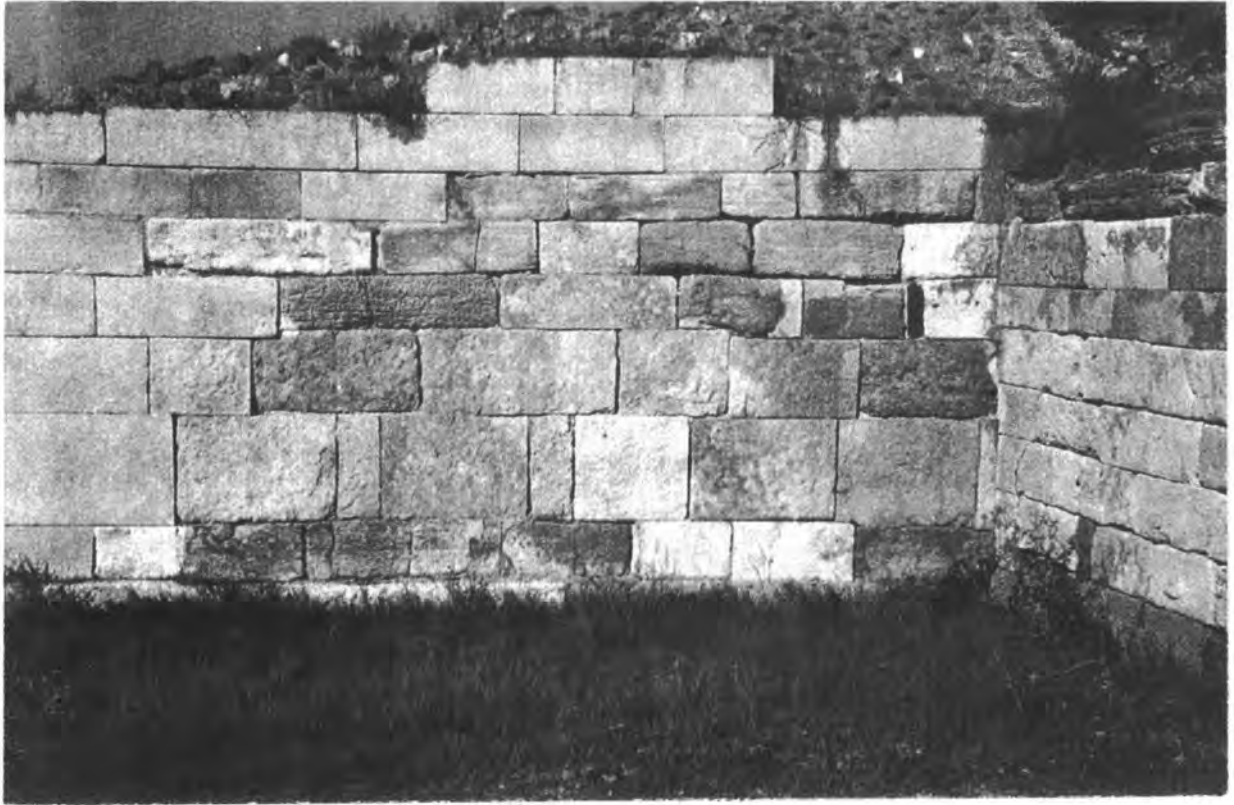
Fig.3 The south side of the I tower. Map of the weathering forms
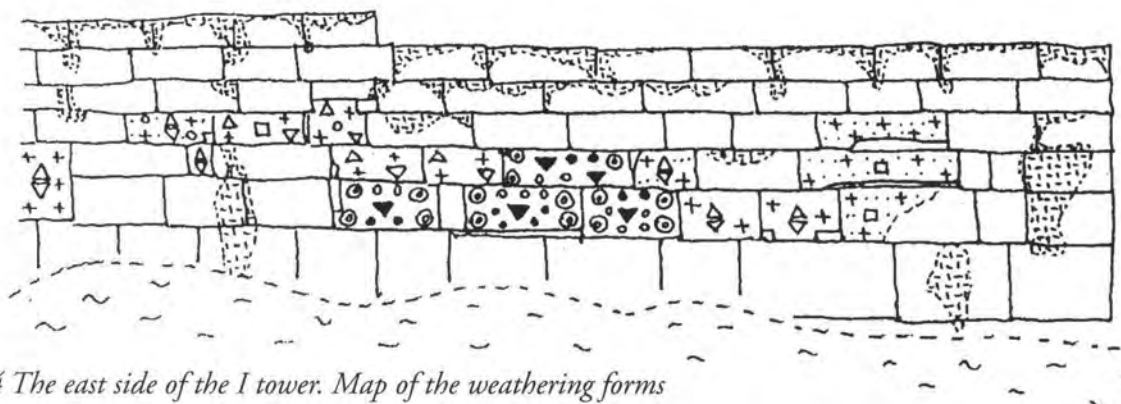
Fig. 4 The east side of the I tower. Map of the weathering forms

Weathering forms		Symbols, abbreviations and descriptions
Relief (R)	⊹	Rr - Rounding / notching
	◉◉◉	Rc - Weathering of components
Back weathering (W)	▽	Ws - due to loss of scales
	▼	Wo - due to other type of material detachment
Fissures (L)	⟍	Li - indipendent of stone bedding
Discoloration (D)	▦	Du - allochtonous discoloration
Soiling (I)	▦	Ix - dirt deposits on the stone surface (soot, dust)
Salt deposits (E)	⬭	Ee - efflorescence
Detachment of material:		
Granular disintegration	⠋⠂⠄	G – granular disintegration
Spalling	•●••	P – detachment of solid crumbs
Transitional forms	△	FS – flakes to scales
	∘∘∘	GP – granular disintegration to spalling
	▫	GF – granular disintegration to flakes

THE LATE ROMAN RAMPART (Z VI)
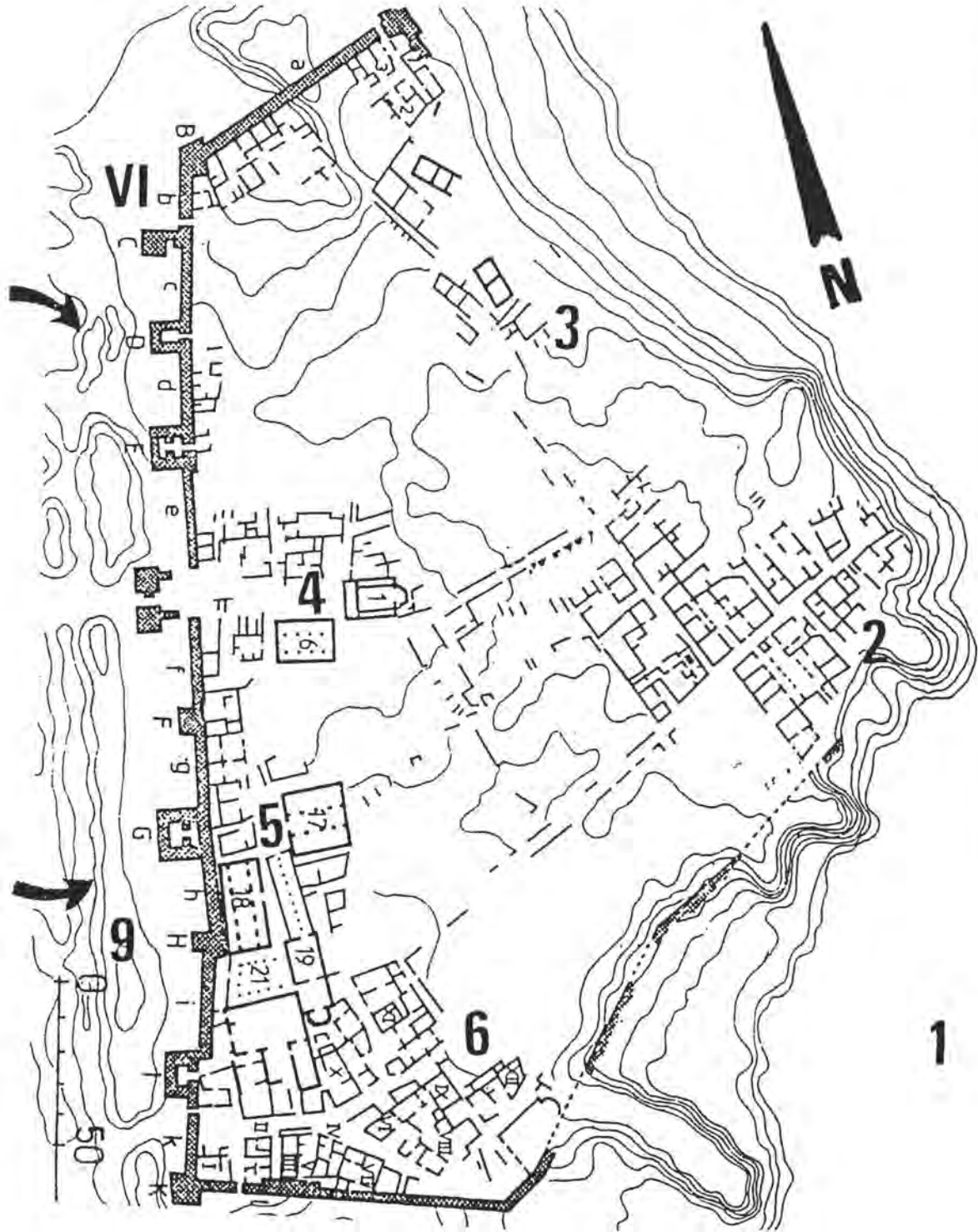
Fig.5   *The Late Roman town – Delimited to west by the Late Roman defensive wall 1.Sinoe Lake; 2.*
Roman–Byzantine Quarter; 3. Sacred Zone; 4. Square; 5. Public buildings; 6. South–west dwell-
ing zone; 7. Late Roman Rampart (Defensive wall, fourth–seventh century); 8. Trading Quarter;
9. "Valum" (Earth Walls)

Taking into account the stone's lithology the following observations were made:

— As we have already presented, the green schists are found in a very low proportion (less than 1%) and was usually used as "filling material" together with mortar, between the big blocks.

— The Jurassic, oölitic limestones are less affected by weathering. The disintegration processes are expressed by fine detachment of material, loss of small grains and selective solubilisation of the contained fossil fauna. The used abbreviations are Rr, G and sometimes GP.

— The initial vacuole aspect of the microconglomerates and of the Cenomanian lumachellic limestones restrains the possibility to determine the new effects of the weathering. It is possible only to say that initial level of the porosity became greater, the gaps enhancing their dimensions. The used abbreviations are Rr, Rc, G, P, GP.

— The Turonian–Lower Senonian calcarenites are showing much visible damages compared to the previsious described stones. Related on their clay content, the rock splits in plates, such phenomena being visible both on the blocks with a vertically or horizontally disposition (concerning the rock bedding). This rocks which are the most widespread in the Roman Wall present concave relief forms, uniform loss of material following the profile of the stone surface and detachment of flakes and scales parallel to the stone surface. In this case, the observations were facilitate by the almost perfect correspondence between the mineralogical and paleontological composition of the original antique blocks and the new ones used in '50 to restore the monument. For the description we have used the notion and abbreviation corresponding to "crust" ("scales"; Ws, Sl) even though "exfoliation" would be more appropriate, but these crusts are not big enough to be considered "foils" (they do not cover all the surface of the block). Used abbreviations: Rr, Rp, Ws, Fl, Sl, FS.

— The siliceous nodular limestones present the most intense effects of disintegration because of the different sensibility of the rock components face to the external environmental conditions (or internal, for the period when the wall was partially buried). The loss of material is high (splits up to 10–15 cm) and the relief of the more resistant components is put in evidence. The alteration of the initial colour of these rocks was also noticed in two areas: on the blocks located in the wall rightward to The Main Gate and on the blocks in the tower Ks. X–ray analysis done on this brownish–red coloured crusts and on the fresh material from inside, have shown the presence of gypsum, halite and hematite (Table 2). In thin sections was also observed fine dispersed limonite in the calcitic mass. The presence of the hematite is accounted on solutions which have migrated from the neighbouring stones, respectively from the green schists in which the iron is present as pyrite. The affected blocks are located at the base of the wall and accounting the long period of time in which they were buried, the migration process of the iron oxides and hydroxides developed itself in optimal conditions. Used abbreviations: Rc, G, P, GP, Du.

Table 2 Diffractometric results of selected samples from Histria Fortress, Romania

Sample	Calcite	Quartz	Muscovite	Gypsum	Glauconite	Halite	Hematite
6	++	+++	tr		+		
6A*	++	+++		++		++	+
8	++	+++	+				
13	+++	++	tr		+		
16	+++						
21	+++	++	tr		+		

6A* = crust collected from the surface of the sample 6
+++ = very abundant; ++ = abundant; + = present; tr = traces

– In the case of the lithic sandstones, the weathering processes are producing loss of material as grains or sometimes fine crusts, parallel to the surface of the block. Used abbreviations: Rr, Ws, G, Sl, GF, FS.

– Beside the salts crust priory mentioned, there were been remarked crusts formed through biologic action, particularly in the shaded area of the wall. The black crusts are mainly visible on the compact grey–white calcarenites and on the white coloured oopelmicrites.

5. Conclusion

In the Late Roman Wall, differences occur regarding the state of deterioration. Obviously these differences are connected to different petrographical character of the building stones. The most intensive damages including also the coloured salts crusts occur on the siliceous nodular limestones. As a rule, the most affected blocks are those ones located on the lower part of the wall. We presume that this is a consequence of ascending ground humidity. The building stones of better quality are the Cretaceous calcarenites and the Jurassic oopelmicrites. To restore the monument the same Cretaceous calcarenites were used. On this blocks the weathering processes are not visible except the very thin and white salt crusts due to marine spray.

6. Acknowledgements

7. References

1.   Ionesi, L.– *Geologia unitătilor de platformă si a orogenului Nord–Dobrogean;* Ed.Tehnică, Bucuresti, 1994

2.   Fitzner, B., Heinrichs, K., Kownatzki, R.–*Classification and mapping of weathering forms;* Proceedings of the 7th International Congress on Deterioration and Conservation of Stone, Lisbon, Portugal, 15–18 June, 1992.

3.   Mirăută, O.–*Stratigrafia si tectonica sisturilor verzi din regiunea Istria–Băltăgesti (Dobrogea Centrală);* D.S. Com. Geol. LI/1 (1963–1964), Bucuresti, 1965.

4.   Muraru, A., Avram, Al.–*Consideratii preliminare asupra pietrei de constructie folosite la Histria; Pontica,* XVI,189–216, Constanta, 1983.

C.M. Grossi
R.M. Esbert
L.M. Suárez del Río

The application of the acoustic emission technique to stone decay by sodium sulphate in laboratory tests

The application of the acoustic emission technique to stone decay by sodium sulphate in laboratory tests

C.M. Grossi, R.M. Esbert and L.M. Suárez del Río
Dept. of Geology. University of Oviedo.
C/Jesus Arias de Velasco S/N 33005 Oviedo (Spain)

Abstract

Acoustic emission was monitored during salt crystallisation cycles in order to study the mechanisms of rock deterioration by sodium sulphate in laboratory tests. Some porous carbonate stones used in Spanish monuments were selected for this study.

The acoustic emission detected during the different stages of the cycles (immersion, drying and cooling) was interpreted to be the result of the salt behaviour inside the stone.

The use of this technique has confirmed that this behaviour depends on salt characteristics (solubility, hydration state and polymorphism of anhydrous sodium sulphate) and stone porosity and pore network.

1. Introduction

Soluble salts are one of the main causes of building stone decay. Therefore they constitute an individual subject of study in the Conservation and Restoration of monuments made of stone. One of current trends in this field is the use of some Non–destructive techniques (NDT) to study the mechanisms and causes of stone decay on–site. For that, the study of the applicability of the acoustic emission/microseismic activity technique (AE/MS) to stone decay by salts was thought to be of great interest, since stresses generated by salts can originate a release of energy in the form of elastic waves (acoustic emission) which can be recorded and analysed (1).

The interpretation of the results obtained by this technique is complex, specially when applied on–site, due to the different processes that can generate acoustic emission.

In this paper, AE was monitored during salt crystallisation cycles in order to study the mechanisms of rock deterioration by sodium sulphate in laboratory tests.

2. Experimental procedure

2.1. Studied Stones

Three carbonate stones from the Spanish monumental heritage with different porosity and pore network have been selected: Vinaixa and Laspra dolomites and Murcia limestone (Table I).

Table I – Pore network characteristics of the studied stones by mercury porosimetry

Stone	open porosity (%)	% pore radius>7.5 m	% pore radius 7.5 m–1 m	% pore radius<1 m	Average pore radius (m)
Vinaixa	15	3.2	76.5	20.3	5
Murcia	30	43.3	24.2	32.5	8
Laspra	31	1.6	4	94.4	0.4

2.2. Methodology

The recommendations of the RILEM (2) for the salt crystallisation ageing test have been followed with some modifications. Each cycle, carried out on 5x5x5 cm cubic specimens, was performed in three stages:

1) *Immersion: 4 hours in a 14% aqueous solution of sodium sulphate decahydrate (at approximately 20°C).*

2) *Drying: 14 hours in an oven with forced ventilation preheated at 60°C.*

3) *Cooling: 6 hours at room conditions (18–20°C; R.H.: 70–75%).*

Acoustic emission rate (in counts/second)

was continuously monitored during each cycle with a Spartan 3000 equipment using a piezoelectric transducer with a resonant frequency of 150 kHz. A 100–300 kHz band-pass filter was employed. Signal recording and processing were carried out using a coupled personal computer.

In order to avoid transducer wetting and heating during the test, it was bonded to the specimen's upper surface during immersion and cooling and placed outside the oven when drying. In this case, the transducer was connected to the stone surface by means of a PYREX glass wave guide. Fig. 1 shows the acoustic emission monitoring during the three stages of each cycle.
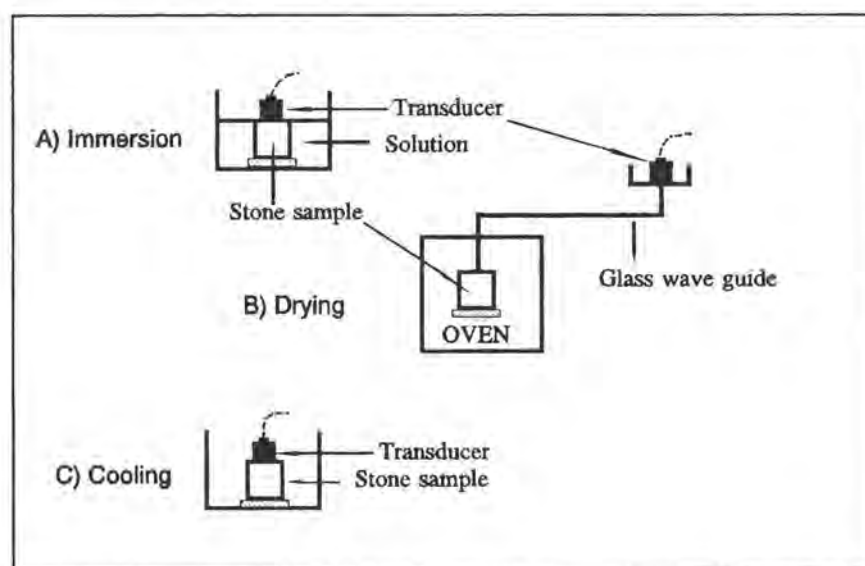
Fig. 1   *Acoustic emission/Microseismic activity monitoring during the different stages of salt crystallisation cycles.*

2.3. Sodium sulphate characteristics

The sodium sulphate characteristics that determine stone decay mechanisms are: its different hydration states, its solubility and the polymorphism of the anhydrous sodium sulphate.

It has two stable phases at room conditions: mirabilite ($Na_2SO_4 \cdot 10H_2O$) and thenardite (Na_2SO_4). The appearance of one or the other depends on humidity and temperature (3, 4, 5).

Sodium sulphate is one of the best known salts in terms of solubility which increases remarkably up to 32.4°C. Above this temperature, solubility slowly decreases as temperature increases. The stable phase under 32.4°C is decahydrate (mirabilite) whereas anhydrous sodium sulphate (thenardite) is the stable phase above this temperature (6). Thenardite and mirabilite solubilities at 20°C are 34.5% and 16% of Na_2SO_4 in water respectively (7).

Another important characteristic is the anhydrous sodium sulphate polymorphism. Five phases are mentioned in the literature: I, II, III, IV and V. Phases III and V can be found at room temperature. At these conditions, Phase V is stable whereas phase III is metastable and tends to slowly revert to phase V (8). Both of them are orthorhombic but they have slightly different densities (6).

Different authors (9,10,11) grew Na_2SO_4 crystals from aqueous solution at different temperatures (40, 50, 60 and 70°C). They obtained crystals mainly of phase III at 60 and 70°C and phase V at 40 and 50°C.

2.4. Results

All the tested stones show a decay throughout the cycles depending on the poros-

ity and pore size distribution (12).

Decay was higher in Laspra dolomite followed by Murcia limestone and Vinaixa dolomite. Weight loss after nine cycles is about 40%, 11% and 1% respectively. Material loss is always produced during immersion.

The monitored AE rate differs from one material to another. In Vinaixa and Murcia stones significant acoustic emission levels appeared mainly during cooling stages. Minor and irrelevant AE was monitored during the first minutes of immersion stages. No AE was monitored during drying. In Laspra stone no AE was detected in any stage.

On the whole, the monitored acoustic emission seams to be higher in Murcia limestone than in Vinaixa dolomite (Figs. 2 and 3).
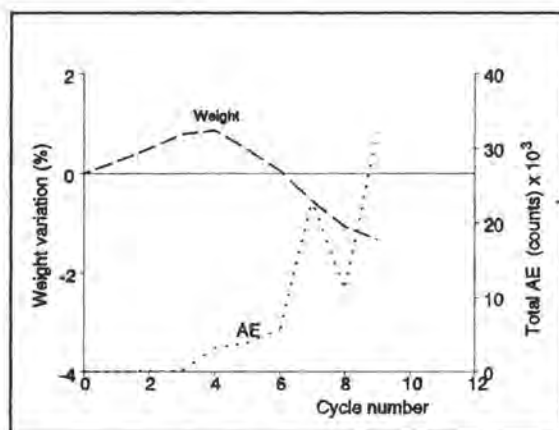
Fig. 2
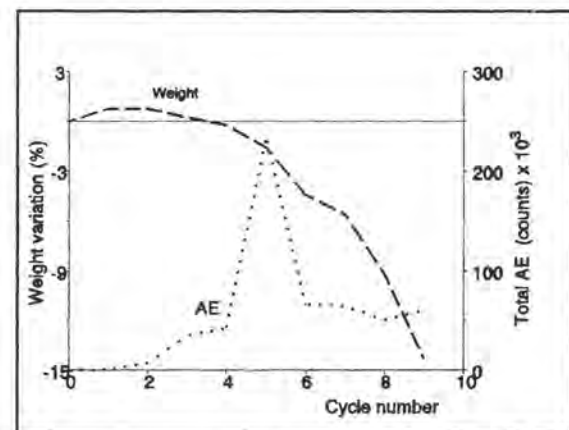
Fig. 3

Figs. 2 and 3   Weight variation and acoustic emission monitored during cooling. Fig. 2   Vinaixa dolomite. Fig. 3   Murcia limestone.

In order to understand the role of the salt on the generation of acoustic emission in this test, sodium sulphate has been precipitated in a PYREX glass vessel from a 14% aqueous solution of sodium sulphate decahydrate during 14 hours of drying at 60°C. Then, the acoustic emission generated by the precipitated salts was monitored during cooling at room conditions.

Depending on the amount of solution,

evaporation and salt precipitation were either complete or partial at the end of the drying stage (60°C).

When precipitation was complete (no solution remains in the vessel) the acoustic emission recorded during cooling was very high. In this case, the salt detected by X Ray Diffractometry was anhydrous sodium sulphate in phase III and V, both at the beginning and at the end of the cooling stage. Moreover, the

higher is the amount of precipitated salts, the higher is the monitored AE rate (Fig. 4).

When precipitation was partial a rest of solution was found at the end of the drying stage which crystallised during the cooling stage.

The AE monitoring was lower than in the previous case.

When a substantial amount of supersaturated solution was found at the beginning of the cooling stage, sodium sulphate decahydrate crystallised and only a minor AE was recorded (13).
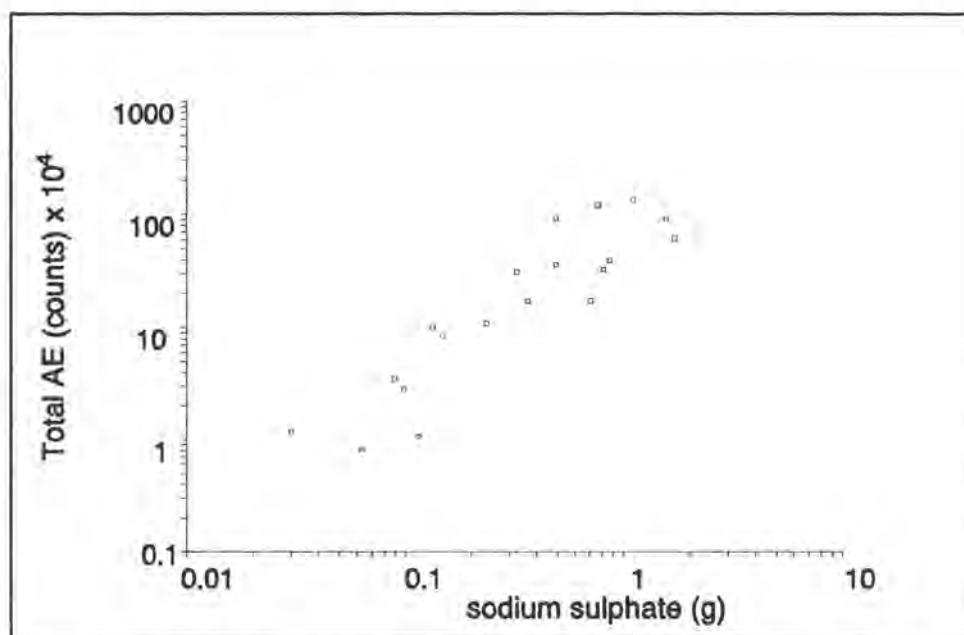
Fig. 4   Acoustic emission monitored during cooling versus amount of sodium sulphate precipitated during drying.

3. *Discussion and conclusions*

From the results obtained in these test conditions, two models of Na_2SO_4–H_2O system behaviour, and thus of decay mechanisms generated by this salt, may be established in relation to stone pore distribution characteristics:

A) Drying stage: If drying is not complete, some solution remains inside the stone.

Cooling stage: Crystallisation of the sodium sulphate decahydrate. No AE is monitored.

Immersion stage: Dissolution of hydrated salt. If supersaturation is reached, sodium sulphate decahydrate crystallises.

B) Drying stage: If drying is complete, anhydrous sodium sulphate precipitates as phases III and V. No solution remains.

Cooling stage: Some changes (crystallographic, textural, microfissuration...) can occur in the precipitated anhydrous salt. AE is detected.

Immersion stage: The anhydrous salt dissolves. If supersaturation in decahydrate sodium sulphate is reached, this salt crystallises, producing a volume increase (14).

These proposed models are only valid for these test conditions (13). Phenomena occurring during crystallisation test are quite complex and strongly dependent on experimental conditions (5, 15, 16, 17).

Both proposed models are conditioned by the stone pore network, that influences the solution absorption during immersion and solution evaporation and salt precipitation during drying. In this way, in Laspra dolomite, with high porosity and very small pore opening

radii, a rest of solution remains at the end of the drying stage. This can lead to the sodium sulphate decahydrate crystallisation during cooling (depending on the test conditions).

This has been demonstrated comparing the weight variation during cooling in Laspra and Vinaixa dolomites (Table II).

In Vinaixa dolomite, with larger pore opening radii, a weight increase is observed. However, in Laspra dolomite, with a high capacity to take water vapour (Table II), a weight decrease occurs suggesting an incomplete precipitation of anhydrous salt during drying.

Therefore, the acoustic emission technique has proved to be useful to interpret the stone decay mechanisms by salts, at least in the performed test conditions.

Table II   Water vapour uptake by Vinaixa and Laspra dolomite under different test conditions.

	Conditions
Weight variation during cooling (%) Vinaixa	Salt crystallisation test. Cycle 6. 3 hours cooling (70%RH; 20°C).
	+0.05
Weight variation during cooling (%) Laspra	Salt crystallisation test. Cycle 6. 3 hours Cooling (70%RH; 20°C)
	-0.24
Weight variation (%) Laspra	Hygroscopic moisture content (23°C; 60%RH) 3 hours.
	+0.7

4. Acknowledgements

5. References

1. Montoto, M.; Esbert, R.M.; Suárez del Río, V.G.; Ruiz de Argandoña, V.G.; Calleja, L. and Grossi, C.M.: "Acoustic emission in stone conservation". Acoustic Emission/Microseismic Activity in Geologic Structures and Materials V. Trans. Tech. Publications, pp. 665–684. 1995.

2. RILEM: "Essais recommandées pour l'altération des pierres et évaluer l'efficacité des méthodes de traitment". Matériaux et Constructions, 13 (75), pp. 216–220. 1980.

3. Arnold, A. "Behaviour of some soluble salts in stone monuments". 2nd International Symposium on the Deterioration of Building Stones, Athens, pp. 27–36. 1976.

4. Sperling, C.H.B. and Cooke, R.U. "Laboratory simulation of rock weathering by salt crystallisation and hydration processes". Earth Surface Processes and Landforms, 10, pp. 541–555. 1985

5. Dohene, E. "In situ dynamics of sodium sulfate hydration and dehydration in stone pores: observation at high magnification using the environmental scanning electron microscope". III International Symposium on the Conservation of Monuments in the Mediterranean Basin. Venice, pp. 143–150. 1994

6. Chrétien, A.; Kohlmuller, R.; Pascal, P. and Rollet, A.P.: "Nouveau traité de chimie minérale". Tome II (Premier Fascicule) "Litium, Sodium". Publié sous la direction de P. Pascal. Edit. Masson et Cie. París. 1966.

7. Braitsch, O.: "Salt deposits. Their origin and composition". Springer, pp. 7–61. 1971.

8. Moffadel, N.; Bouzaziz, R. and Mayer, M.: Le polymorphisme du sulfate de sodium anhydre et les phases intermédiaries, glasérite et aphtitalite, dans le binaire $Na_2SO_4–K_2SO_4$". Thermochimica Acta, 185, pp. 141–153. 1991.

9. Choi, B.K.; Labbé, H.J. and Lockwood, D.J.: "Raman spectrum of Na_2SO_4 (Phase III)". Solid State Communications, 74,2 pp. 109–113. 1990.

10. Choi, B.K. and Lockwood, D.J.: "Ionic conductivity and the phase transitions in Na_2SO_4. The American Physical Society, 40, 7 pp. 4683–4689. 1989.

11. Amirthalingam, V, Karkhanavala, M.D. and Rao, U.R.K.: "Topotaxic phase change in Na_2SO_4". Acta Cryst. A33, pp.522–523. 1977.

12. Grossi, C.M.: "Cristalización de sales en rocas monumentales porosas y su auscultación mediante emisión acústica". Tesis Doctoral, Área de Petrología. Dep. de Geología. Universidad de Oviedo. 1992.

13. Grossi, C,M.; Esbert, R.M.; Suárez del Río, L.M.; Montoto, M. and Laurenzi–Tabasso, M.: "Acoustic emission monitoring to study sodium sulphate crystallisation in monumental porous carbonate stones". Submitted to publication to Studies in Conservation.

14. McMahon, D.J., Sandberg, P., Folliard, K., and Mehta, P.K. "Deterioration mechanisms of sodium sulfate". 7th Int. Congress on Deterioration and Conservation of Stone, Lisbon, pp. 705–714. 1992.

15. Price, C.A.: "The use of sodium sulphate crystallisation test for determining the weathering resistance of untreated stone". International Symposium on Deterioration and Protection of Stone Monuments, Paris, 3.6, 10 p. 1978.

16. Chatterjii, S. Christensen, P., and Ovegaard, G.: "Mechanisms of breakdown of natural stones caused by sodium salts". 3rd International Congress on the Deterioration and Preservation of Stones. Venice, pp. 131–134. 1979.

17. Sperling, C.H.B. and Cooke, R.U.: "Salt weathering in arid environments II. Laboratory Studies". Papers in Geography 9. 1980.

C. Incerti
M. T. Blanco–Varela
F. Puertas
C. Saiz–Jimenez

Halotolerant and halophilic bacteria associated to efflorescences in Jerez Cathedral

Halotolerant and halophilic bacteria associated to efflorescences in Jerez Cathedral

C. Incerti — *Instituto de Recursos Naturales y Agrobiologia, C. S. I. C. Apartado 1052, 41080 Sevilla, Spain*
M.T. Blanco-Varela — *Instituto de Ciencias de la Construccion Eduardo Torroja, C. S. I. C., Apartado 19002, 28080 Madrid, Spain*
F. Puertas — *Instituto de Ciencias de la Construccion Eduardo Torroja, C. S. I. C., Apartado 19002, 28080 Madrid, Spain*
C. Saiz-Jimenez — *Instituto de Recursos Naturales y Agrobiologia, C. S. I. C. Apartado 1052, 41080 Sevilla, Spain*

Abstract

In monuments, halotolerant and halophilic bacteria are common inhabitants of zones of efflorescences, but have traditionally been neglected. The most frequent genera is *Bacillus*, which is also widely distributed in normal and hypersaline soils. The finding of these bacteria opens a way for future research concerning the ecology and physiology of halotolerant and halophilic bacteria in monuments.

rescences of the mural paintings from the monastery of La Rabida (Huelva, Spain), no information exists on the origin, occurrence and distribution of halotolerant and/or halophilic bacteria and fungi in monuments. The present study investigates the halotolerant and halophilic bacteria present in the Chapel of All Souls in Jerez Cathedral, originated by the strong production of epsomite efflorescences.

1. Introduction

Bacteria have adapted to growth in many different niches. One of them, the hypersaline environment is characterized by high concentrations of salts. Usually this refers to waters and the term hypersaline waters defines those which have higher concentrations of salts than seawater. Considerable research has been carried out on halophilic bacteria in relation to these environments (1–3). Comparatively, very little information exists for terrestrial environments.

A general characteristic of hypersaline environments is that they are extreme environments and therefore species diversity is low, and some taxonomic groups are missing. However, a large microbial population was found in hypersaline soils with numbers ranging from 10^3–10^6 per gram of soil. Almost all the organisms isolated were halophilic eubacteria with a remarkable euryhaline response (4).

With the exception of a preliminary report of Saiz–Jimenez and Samson (5) describing the presence of bacteria and fungi in efflo-

2. The Cathedral of Jerez

The building of the cathedral of Jerez was begun in 1695, and finished in 1778. It is located on a hill rising from the Plaza del Arroyo to the Alameda Vieja. The form is a rectangle of 54 m long by 41 m wide, with five naves with gothic–style pilasters bearing brick vaults. The building material is calcarenite from the quarries of Puerto de Santa Maria (also used in Seville Cathedral).

The calcarenite shows alteration phenomena in the west facing parts, with deep cavities in the ashlars. Other, even more obvious alteration phenomena were the mechanical fractures in the stone of the dome due to the pressure of the iron anchors of the railings, and the serious powdering of the calcarenite studied and restored between 1983–86 (6).

The east facing side façade of the Visitation is markedly affected by damp, and bears an abundant vegetation of algae, bryophytes and vascular plants. In the interior is located the stone reredos of the Chapel of All Souls

(now Chapel of the Resurrection), which in the past had a snow–like appearance, being covered by white efflorescences. Although in present times this is periodically cleaned off, it reappears –an extreme case of such formation.

Analysis of the efflorescences by X–ray diffraction revealed that the main component is hexahydrite ($MgSO_4 \cdot 6H_2O$), accompanied by calcite, gypsum and quartz. There are several hydrated phases of magnesium sulphate. The first one, precipiting from a saturated solution and at temperatures below 60°C, is epsomite ($MgSO_4 \cdot 7H_2O$). Dehydratation of epsomite originate hexahydrite. The predominance of one over other depends on the relative humidity. The hexahydrite identified in the studied samples arise from epsomite dehydratation, which could be produced in the cathedral walls or after sampling and transport to the laboratory.

Infrared spectra showed bands of sulphate, a band at 1384 cm^{-1} assigned to soluble nitrates, and two bands in the range 1400–1500 cm^{-1} (corresponding to CO_3-) that cannot exclusively be attributed to calcite, but also to magnesium carbonate.

The 75% of the efflorescence powder is soluble in water, due mainly to hydrated magnesium sulphate. Ion chromatography revealed that, in addition, nitrates amounting for 0.5% and chlorides for 0.3% are present. The X–ray analysis of the 25% insoluble residue indicated the presence of calcite, quartz and poorly crystallized hydromagnesite ($Mg_5(CO_3)_4(OH)_2 \cdot 4H_2O$). Infrared spectrum of the residue matched with those of artificial hydromagnesite (7). SEM–EDX evidenced the presence of two complex sulphates: calcium and potassium sulphate and calcium, magnesium and potassium sulphate, both of similar morphology. The presence of hydrated magnesium carbonate, previously identified by IR spectrum, was confirmed.

In the past, several samples of mortars were analysed and yielded gypsum, calcite, quartz and lower amounts of epsomite, as main components. Concerning the possible

origins of the epsomite, the quarry stone had values of 0.02–0.04% of sulphates (MgO was 0.5%), and the Pliocene bedrock supporting the cathedral foundation contained 0.02% sulphates (6).

Both the narrow street, the east–facing orientation of the external Chapel walls and the fact that the cathedral is built on the bank of a stream contribute to the problem of dampness, although the origin of epsomite should probably be found in the composition of the mortar, with a high amount of magnesium salts. The joints of the ashlars, made with mortar, are completely impregnated with damp due to the hygroscopicity of the soluble salts, evidencing a clear liquid film. The high solubility of magnesium sulphate means that it is readily dissolved in the processes of water recirculation inside the stone and mortar, through the walls of the building.

3. Halotolerant and halophilic bacteria

In monuments not only NaCl is present, but a variety of different hygroscopic salts, including carbonates, chlorides, nitrates, sulphates, etc. can be found. This means that monuments can be considered as extreme or hypersaline environments, at least in the efflorescences zones, but the salinity is not necessarily based on NaCl. In this pecular niche, halotolerant and halophilic bacteria can thrive. Halotolerant bacteria are those which grow better without significant amounts of NaCl in their media, but can also grow with concentrations higher than those of seawater, and can therefore be present in active form in hypersaline environments. Halophilic bacteria, as a whole, are capable of growing over a very wide range of NaCl concentrations. Individual species have more limited salt ranges for growth (8).

The studied cathedral, and particularly, the Chapel of All Souls have a long history in the continuous production of epsomite efflorescences, the higher amounts observed around

the year 1983. Subsequently, the efflorescences were removed periodically in a routine cleaning process. The existence of magnesium salts and their hygroscopicity undoubtely have selected a specific microflora adapted to growth in this high saline environment and it was expected that the bacteria present in efflorescences should mainly be composed of halotolerant bacteria, with a lower, if any, representation of halophilic bacteria.

The existence of a considerable number of bacteria and fungi in efflorescences of monuments was already reported by Saiz–Jimenez (9), the bacteria amounting up to $2 \cdot 10^6$ and the fungi up to $8 \cdot 10^3$ g/sample of the frescoes of the monastery of La Rabida.

In the cathedral of Jerez, bacteria and fungi were isolated from five samples taken from the efflorescences originated in the right side of the Chapel of All Souls. In this paper only data for bacteria are reported. Culture media used in this study were previously described (10). The population obtained in the studied Chapel ranged from 21.6 to 3.8 x 10^3 CFU/g in the absence of salinity, measured after 72 h of inoculation. Salinity concentrations from 0.9 to 5% generally increased the number of CFU. However, the highest salinity ranges reduced the population, except for sample J–5, in which the population obtained with 15% salinity was considerably higher than for other ranges (Table 1). Estimation of the population with increasing ranges of epsomite instead of a mixture of salts showed similar trends, the exception being sample J–3 (Table 2). The estimation of the population using epsomite was considered necessary and complementary of the determination with the mixture of salts because the specific composition of the efflorescences.

Table 1   Colony forming units·10^3/g of efflorescence. Salinity range according to (10).

CFU sample	0% salts	0.9% salts	3% salts	5% salts	10% salts	15% salts	25% salts
J–2	12.7	70.7	12.3	26.3	0	0	0
J–3	3.8	15.3	19.7	8.3	3.3	0	0
J–4	21.6	10.7	22.3	4.0	3.8	3.7	0
J–5	16.3	50.0	37.7	54.3	65.6	28.0	0
J–6	8.7	16.0	8.0	4.3	3.0	1.0	0

Table 2   Colony forming units·10^3/g of efflorescence. Salinity range exclusively with epsomite

CFU sample	0% epsomite	0.9% epsomite	3% epsomite	5% epsomite	10% epsomite	15% epsomite	25% epsomite
J–2	12.7	27.0	18.3	15.7	4.7	9.0	0
J–3	3.8	16.7	20.0	26.6	33.6	11.3	0
J–4	21.6	11.7	13.3	5.8	8.3	3.3	0
J–5	16.3	23.7	20.3	48.3	9.0	6.3	0
J–6	8.7	7.3	5.7	5.7	5.3	2.3	0

Table 3 Distribution of Gram positive bacteria in different media and concentrations

	Salts		Epsomite	
Concentrations	Endospore–forming[1]	Non endospores	Endospore–forming	Non endospores
10%	47.4 (9)	52.6 (10)	56.5 (13)	43.5 (10)
15%	40 (2)	60 (3)	37.5 (3)	62.5 (5)

[1] *in %. Number between brackets indicates the number of isolated strains*

Although after 72 h of incubation do not appeared bacteria at the highest salt concentrations (25%), two isolates were obtained after 15 days, indicating a poor and slow growth, which is normal for such high salt concentration. Some of these and other bacteria isolated from 15% salts had a halophilic behaviour.

Table 3 shows the distribution of Gram positive bacteria isolated from 10 and 15% salt and epsomite concentrations.

The endospore–forming isolates were mainly identified as *Bacillus* species. The genus *Bacillus* is the most abundant in normal and hypersaline soils, amounting for up to 67% and 19%, respectively (4). This genus is virtually absent in hypersaline waters. *Bacillus* encompasses the rod–shaped bacteria capable of aerobically forming endospores that are more resistant than vegetative cells to heat, drying, and other destructive agencies. However, the variable properties of the strains prevent strict adherence to a determined species. Taking into account such variability the isolated endospore–forming Gram positive rod–shaped bacteria from the walls of the Chapel were tentatively identified as *B. circulans, B. licheniformis, B. pumilus,* and *B. sphaericus.*

4. Involvement of halotolerant and halophilic bacteria in the deterioration of monuments

Deterioration of stone begin with calcite

leaching, which is considered one of the most serious consequences of weathering in monumental calcareous stones. This leaching originate the loss of the intergranular binding calcite cement, increases the porosity of the stone, and decreases the mechanical strength. Acid rain contributes significantly to calcite leaching in monuments located in polluted areas and it has also been postulated that microbial growth originated organic acids.

Most of the *Bacillus* species isolated from efflorescences produce organic acids from carbon sources, which could be of interest regarding a possible effect on the calcite cement. However, on the production of acids by microorganisms there is controversy due to extrapolation of data obtained in the laboratory to nature. In fact, the production of metabolites (including organic acids) in artificial culture media might well be considered as pathological, a manifestation of reaction to conditions of nutrition quite foreing to anything the organism encounters under the vicissitudes of survival in nature. It may be said that in the natural complex that is a terrestrial ecosystem, the aerobic inhabitants have evolved to that stage and their metabolism so adjusted through continuous existence in such a jungle, that they are 100 per cent biologically efficient in the utilization of available carbon substrates. Thus it would be that the only products formed are those resulting from perfect biological efficiency, namely cell material, CO_2

and water (11).

Lewis *et al.* (12) suggested that bacteria on stone can be extremely versatile and could maintain their activity during nutrient perturbations, operating at low nutrient levels and utilising what the environment has to offer. As a consequence, bacterial populations may be able to maintain their activity during periods of nutrient flux.

On the other hand, bacteria are able to precipitate calcite and other minerals such as aragonite, struvite, bobierrite, apatite, etc. (13). In this respect, the production of calcite crystals by soil bacteria has been considered a general phenomenon. Many bacteria including *Bacillus pumilus, B. subtilis, B. megaterium, B. cereus, B. bulgaricus, B. globigii, Pseudomonas aeruginosa, P. fluorescens, Serratia* spp., *Citrobacter* spp., *Azotobacter* spp., etc. formed calcite crystals on solid media containing sodium acetate (14).

Rivadeneyra *et al.* (15) found that 26 moderately halophilic strains of *Bacillus* isolated from a saline soil precipitated magnesium calcite, aragonite, monohydrocalcite and dolomite in varying proportions. It has been reported that the formation of calcite is inhibited and aragonite increased as the concentration of magnesium ions in the medium rises (16), however, Rivadeneyra *et al.* considered that the opposite is true with bacteria, and that calcite quantities increase compared to aragonite when the concentration of Mg^{2+} rises, thus supporting the idea that bacteria play an active role in the precipitation of carbonates. Furthermore, the proportion of magnesium in the magnesium calcites increases together with salinity to the extent that at 20% salinity dolomite is formed. The formation of calcium carbonate by some moderately halophilic bacteria was also observed by Del Moral *et al.* (17). Optimum salt concentration for precipitation was 10%, precipitation decreasing at both 20 and 2.5% salt.

To what extent the above reported *in vitro* data can be extrapolated to nature? Could the microbial induced precipitation of calcite consolidate to some extent the weathered stones? Although some studies (13–17) have stressed the precipitation of calcite in culture media by soil and marine bacteria this process needs to be proved *in vivo*, because the conditions used in the laboratory are far from those these bacteria find in their natural habitat. Furthermore, the sources of carbon and energy in culture media probably exceeds those available in nature. As nothing is known about the ecology and physiology of the halotolerant and halophilic bacteria in monuments, the reported data open a way for discussion, and clearly indicates that more research is needed to ascertain the role of these bacteria in monuments.

5. Acknowledgement

6. References

1. Rodriguez–Valera, F. (1988). Halophilic Bacteria. CRC Press, Boca Raton.

2. Javor, B. (1989). Hypersaline Environment: Microbiology and Biogeochemistry. Springer–Verlag, Berlin.

3. Vreeland, R.H. and Hochstein, L.I. (1992). The Biology of Halophilic Bacteria. CRC Press, Boca Raton.

4. Rodriguez–Valera, F. (1988). Characteristics and microbial ecology of hypersaline environments. In: Halophilic Bacteria, F. Rodriguez–Valera (ed.), CRC Press, Boca Raton, pp. 3–30.

5. Saiz–Jimenez, C. and Samson, R.A. (1981) Microorganisms and environmental pollution as deteriorating agents of the frescoes of the monastery of Santa Maria de la Rabida, Huelva, Spain. 6th Triennial Meeting ICOM, paper 81/15/5, 14 p.

6. Rodriguez–Gordillo, J., Martin–Vivaldi Martinez, J.A. and Saiz–Jimenez, C. (1988). Estudio de los procesos de alteración, ensayos de envejecimiento acelerado y respuesta al tratamiento con diversos agentes preservantes, de los materiales pétreos de la cúpula de la Colegiata de Jerez de la Frontera (Cádiz). Congreso Geológico de España, Comunicaciones 2, 341–343.

7. Van der Marel, H.W. and Beutelspacher, H. (1976). Atlas of Infrared Spectroscopy of Clay Minerals and their Admixtures. Elsevier, Amsterdam.

8. Kushner, D.J., Kamekura, M. (1988). Physiology of

halophilic eubacteria. In: Halophilic Bacteria, F. Rodriguez–Valera (ed.), CRC Press, Boca Raton, pp. 109–138.

9. Saiz–Jimenez, C. (1982) Causas del deterioro de los murales de Daniel Vázquez Díaz, Monasterio de Santa María de la Rábida, Huelva. Mundo Científico 18, 1007–1011.

10. Rodriguez–Valera, F., Ruiz–Berraquero, F. and Ramos–Cormenzana, A. (1981). Characteristics of the heterotrophic bacterial populations in hypersaline environments of different salt concentrations. Microbial Ecology 7, 235–243.

11. Foster, J.W. (1949). Chemical Activities of Fungi, Academic Press, New York.

12. Lewis, F.J., May, E. and Bravery, A.F. (1988). Metabolic activities of bacteria isolated from building stone and their relationship to stone decay. In: Biodeterioration 7, D.R. Houghton, R.N. Smith and H.O.W. Eggins (eds.), Elsevier, London, pp. 107–112.

13. Rivadeneyra, M.A., Perez–Garcia, I. and Ramos–Cormenzana, A. (1992). Struvite precipitation by soil and fresh water bacteria. Current Microbiology 24, 343–347.

14. Boquet, E., Boronat, A. and Ramos–Cormenzana, A. (1973). Production of calcite (calcium carbonate) crystals by soil bacteria is a general phenomenon. Nature 246, 527–528.

15. Rivadeneyra, M.A., Delgado, R., Delgado, G., del Moral, A., Ferrer, M.R. and Ramos Cormenzana, A. (1993). Precipitation of carbonates by Bacillus sp. isolated from saline soils. Geomicrobiology Journal 11, 175–184.

16. Cailleau, P., Dragone, D., Girou, A., Humbert, L., Jacquin, C. and Roques H. (1977). Etude experimentale de la precipitation des carbonates de calcium en presence de l'ion magnesium. Bulletin de la Societé Française de Mineralogie et Cristalographie 100, 81–88.

17. Del Moral, A., Roldan, E., Navarro, J., Monteoliva–Sanchez, M. and Ramos–Cormenzana, A. (1987). Formation of calcium carbonate crystals by moderately halophilic bacteria. Geomicrobiology Journal 5, 79–87.

X. Ariño

C. Saiz–Jimenez

A filamentous green alga from aquatic saline environment in mortars and stuccos from archaeological sites of southern Spain

A filamentous green alga from aquatic saline environment in mortars and stuccos from archaeological sites of southern Spain

X. Ariño and C. Saiz–Jimenez
Instituto de Recursos Naturales y Agrobiologia,
C.S.I.C., Apartado 1052, 41080 Sevilla, Spain

Abstract

Marine aerosols have a strong influence on the materials of the Roman city of Baelo Claudia. Salt crystallization processes in the sandstone surface promotes phenomena of abrasion and pulverization, preventing lichen colonization. In addition, the presence of *Ctenocladus circinnatus*, a filamentous green alga typical from saline inland waters and coastal brine pools evidenced the influence of salt accumulation in the colonization of phototrophic microorganisms.

1. Introduction

Cyanobacteria, algae and lichens are common colonizers of building materials. The occurrence of phototrophic microorganisms on stone surfaces does not automatically imply a destructive action, but their presence can be considered as biodeteriogenic, simply because of the aesthetic damage they cause. Apart from the unaesthetic appearance of cyanobacteria and algae, there are references in the literature that point to direct decay mechanisms involving carbonate dissolution and mechanical deterioration of the stone (Ortega–Calvo *et al.* 1993). The combination of chemical and mechanical processes can accelerate the detachment of rock particles and thus the weathering process. On the other hand, the role of saxicolous lichens in the biodeterioration of stone has been recognized (Jones, 1988).

However, there is few information about the factors influencing biological colonization.

Monuments can create different ecological niches between very close places and, when they are built by a variety of materials, even may lead to a species segregation in adjacent materials, for example between mortar and limestone, evidencing the importance of the characteristics of the substrate in the colonization (Puertas *et al.* 1994; Ortega–Calvo *et al.* 1995). Also, the physical and chemical properties of the materials can be altered by environmental agents.

In urban environments, airborne organic and inorganic pollutants accumulate on stone surfaces, influencing, to a great extent, the colonization of microorganisms (Saiz–Jimenez, 1995). In the same way, it is expected that marine aerosols and, consequently, salt accumulation on stone, can acts favouring the colonization of halotolerant microorganisms. The aim of this study is to investigate the relationships between marine aerosols and biological colonization.

2. Material and methods

The study was carried out at the archaeological site of Baelo Claudia (Cadiz, Spain), a Roman city located at 50 m from the sea. The sandstone pavement of the Forum, and the mortars covering the walls of several Temples, appeared relatively well preserved after excavation 25 years ago, although in recent years there has been observed gradual deterioration processes.

To isolate and identify cyanobacteria and algae, enrichment cultures were made in Parafilm–sealed Petri dishes with BBM (Bold Basal Medium), which was modified varying the pH (between 7 and 9) and salt concentration (by adding 1 and 5 g l^{-1} NaCl). Some samples were prepared for transmission electron microscope observations.

3. Results

Only a small number of flagstones of the Forum pavement were covered by lichens. The most abundant are *Caloplaca velana*, *Lecanora albescens*, *Aspicilia contorta* ssp. *hoffmanniana*, *Caloplaca variabilis*, *Verrucaria macrostoma*, *Verrucaria viridula* and *Lecania turicensis*. They are xerophytic species, well adapted to sunny and dry environments.

Major lichen colonization of the pavement of the Forum was restricted to two lines of flagstones at both sides (west and east orientations, which would be indicative of different environmental conditions). In fact, these two lines coincided with the original Roman drainage system of the Forum. The presence of numerous thalli with superficial abrasions, which can lead to the disappearance of the upper cortex or even the medulla of the lichen, is evidence of the aggressive windy environment, confirmed also by the remarkably deteriorated aspect of the surface of the flagstones without lichen cover. In addition, there are some randomly distributed flagstones on which lichen communities have also developed. They are slightly raised from the floor. The other flagstones were free from lichen colonization showing strong physico–chemical weathering patterns (e.g. alveolization, pulverization, exfoliation, etc.) on their surface, and, occasionally, salt efflorescences. One of the main components of the efflorescences is sodium sulfate (thenardite), coming from marine spray.

On the mortars of the walls of the Tem-

ples, lichen were mainly growing on the exposed walls, whilst on the sheltered ones there was an extensive growth of cyanobacteria and algae. Nevertheless, the mortar of the drier walls, affected by long sunlight periods, were also colonized by these phototrophic microorganisms. They were growing inside the stone for protection from the external environment, diminishing the evaporation rates and the excessive radiation. This type of growth, endolithic, was evidenced in sections where a green internal layer, parallel to the surface, at variable depths of 1–1.2 mm could be observed. The community giving rise to this layer was composed of taxa of Cyanobacteria, Chlorophyta and Bacillariophyta. Among these organisms, one of the commonest colonizers in Baelo Claudia materials was *Ctenocladus circinnatus* Borzi. It was observed epilithic and endolithic growth, penetrating into the material through the existing pores and intergranular spaces. Also, it was abundant in the pavement of the Forum.

Ctenocladus circinnatus is a filamentous green–alga with a problematic taxonomic position. The filaments were profusely branched, with a heterotrichous structure. The cells were cylindrical, 3–5 μm broad and 20–150 μm long, uninucleate, with a parietal plastid, and one or more pyrenoids. In unfavorable conditions, cells produced a resistance stage, the akinetes, which were spherical with a diameter of 8–14 μm. In laboratory cultures, better germination and growth was observed when pH was raised to 9, both with crushed mortar or by adding NaOH. Addition of 1 g l^{-1} NaCl gave similar results, but when a concentration of 5 g l^{-1} was supplied, growth of the cells was severely affected and no filamentous thalli developed (the akinetes germinated but rapidly transformed into akinetes again).

The ultrastructural study of *C. circinnatus* evidenced that the vegetative cells and, specially, the akinetes, were surrounded by a thick fibrillar wall, which besides contains a large number of granules, mainly starch and lipids.

4. Discussion

The colonization of the building materials from Baelo Claudia by phototrophic communities of cyanobacteria, algae and lichens is strongly influenced by the environmental parameters, mainly light and water availability. Another factor, salt concentration, which usually are not taken into account, can play an important role, accelerating sandstone disintegration, and increasing osmotic potential and facilitating the development of organisms well adapted to such conditions. The importance of soluble salts, mainly NaCl, is considerable in weathering, and a high correlation is found between salt concentration in stone and sea proximity, concentration increasing as distance decreases. Salt crystallization processes on the flagstones together with the influence of the strong and persistent winds incorporating considerable amounts of airborne sand particles exert an abrasive effect on the surface of stone and lichens.

The colonized flagstones have an air chamber beneath (Figure 1a, 1c), which stabilizes the stone and permits the passage of water and/or salts, avoiding their accumulation and subsequent recrystallization. The remaining Forum flagstones are deposited on a soil with impermeable horizons of loamy clays, producing almost permanent water retention and salt mobility by ascent and descent of capillary water, contributing to deterioration due to dissolution–crystallization processes (Figure 1b). This is especially evident on the flagstone surface, at the stone–atmosphere interface, where there is a maximum evaporation and salt precipitation, even originating efflorescence, frequently associated with descamation processes (Winkler, 1973). This is reflected in the extent of weathering of bare flagstones, and consequently in the difficulty for lichen establishment due to substrate instability, as colonization by lichens depends basically on the existence of stable sites where spores and propagules can install and germinate. When the lichen community is developed, the flagstones do not show evident weathering on their surface, indicating a protective effect of the lichen thallus, buffering the effect of the environment diminishing physical and chemical weathering, mainly wind abrasion, raindrop impacts, water flow, changes in temperature and salt deposi-
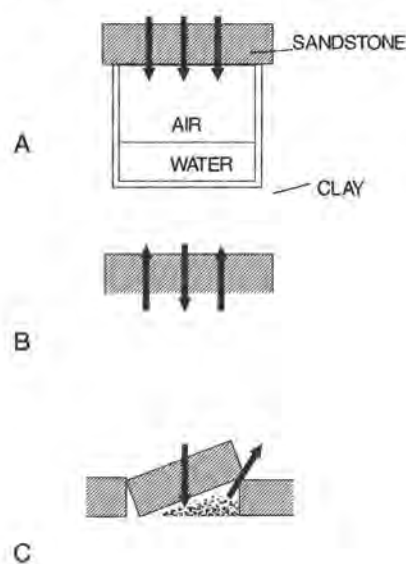
Figure 1 Water and salt movement in the flagstones of the Forum. a) Flagstone on the drainage system, there is a flux of water and salts; b) Flagstone on the clayey soil, which promotes water retention and salt crystallization on the surface; c) In raised flagstones the situation is similar to a).

tion. However, this protective effect is subsequent to the establishment of appropriate conditions for a lichen colonization.

The presence of *Ctenocladus circinnatus* is also noticeable. This alga, considered as typical of saline aquatic environments (Blinn and Stein, 1970), is perfectly capable to growth aerophytically. Its requirements are mainly a high pH and moderate salt concentration. The climatic conditions of the surface – high light intensity and temperature and low water availability – prevented epilithic algal colonization but induced endolithic growth, which is facilitated by the porosity of the material. In spite of the moderate salt concentration detected in the samples, higher values may be located near the surface of the material due to the effect of capillarity, and is in this area where there is the maximum of organisms activity. This fact can contribute to limit the growth of *C. circinnatus* in periods of dryness, when the evaporation accumulates salt in the surface or just beneath it. The ability of *C. circinnatus* to transform rapidly their vegetative cell in akinetes is, undoubtedly, an ecological advantage, permitting the alga to resist long periods of osmotic stress. During the transformation of vegetative cells into akinetes, cells progressively shortened and widened until they became spherical, reducing the ratio between surface and volume and thus the passive loss of water. The resistant stage also involved an increase in cell wall thickness. The growth of *C. circinnatus* in the sandstone and mortars of this archaeological area is facilitated by the alkalinity of the materials. It is suggested that the external input of marine aerosols can be the reason for the abundance of this alga.

5. Acknowledgements

6. References

1. Blinn D.W. and Stein J.R. (1970). Distribution and taxonomic reappraisal of *Ctenocladus circinnatus* (Chlorophyceae, Chaetophorales). Journal of Phycology 6: 101–105.

2. Jones D. (1988). Lichen and pedogenesis. In: M. Galun (ed.) Handbook of Lichenology, vol 3, pp. 109–124, CRC Press, Boca Raton.

3. Ortega–Calvo, J.J., Hernandez–Marine, M. and Saiz–Jimenez, C. (1993). Cyanobacteria and algae on historic buildings and monuments. In: K.L. Garg, N. Garg and K.G. Mukerji (eds.), Recents Advances in Biodeterioration and Biodegradation, vol.1, pp. 173–203, Naya Prokash, Calcutta.

4. Ortega–Calvo J.J., Ariño X., Hernandez–Marine M. and Saiz–Jimenez C. (1995). Factors affecting the weathering and colonization of monuments by phototrophic microorganisms. The Science of the Total Environment 167: 329–341.

5. Puertas, F., Blanco–Varela, M.T., Palomo, A., Ortega–Calvo, J.J., Ariño, X. and Saiz–Jimenez, C. (1994). Decay of Roman and repair mortars in mosaics from Italica, Spain. The Science of the Total Environment 153: 123–131.

6. Saiz–Jimenez, C. (1995). Deposition of anthropogenic compounds on monuments and their effect on airborne microorganisms. Aerobiologia 11: 161–175.

7. Winkler, E.M. (1973). Stone: Properties, durability in man's environment. Springer–Verlag, Vienna.

Michael Steiger

Distribution of salt mixtures in a sandstone monument: sources, transport and crystallization properties

Distribution of salt mixtures in a sandstone monument: sources, transport and crystallization properties

M. Steiger
Institut für Anorganische und Angewandte Chemie,
Universität Hamburg,
Martin-Luther-King-Platz 6, D-20146 Hamburg

1. Introduction

Salts are a major cause of decay in porous materials such as stone, brick, concrete, etc. Severe damage of these materials results when water evaporates and dissolved salts crystallize. Although there might still be a deficit in our understanding of the nature of the underlying processes, which generate high internal pressures and disruptive stress, the deleterious effects of salt crystallization are well established, both, from laboratory experiments and observations at many monuments as well.

Contributions from different sources and transport as pore solutions followed by enrichment due to evaporation of water are characteristic features of complex salt systems evolving in historic monuments over long periods of time. Depending on the nature of the sources and the type of material salt contaminations usually found in historic monuments comprise of many different ions. Typically the chlorides, nitrates and sulfates of sodium, potassium, magnesium and calcium have to be considered. Depending on the temperature and relative humidity (RH) and the solubilities in such multicomponent mixtures, ions may remain in solution or salts may be precipitated and enriched when water evaporates.

Arnold and Zehnder[1] have extensively studied the evolution of salt systems in historic monuments affected by rising damp. They described how the interaction of the different processes results in the accumulation of salts in a zone approx. 0.5–3 m above ground level, where a characteristic vertical profiling due to fractionated crystallization is observed. The same arguments also apply to the upper parts of a facade, where deposition from the atmosphere is often found to be the dominant source for the accumulation of salts, mostly sulfates. Transport of salts in those areas is mainly determined by the capillary uptake of rain water, the formation of surface run–off water and subsequent drying. Again, the interaction of the different processes results in characteristic distributions of salts in a wall[2].

Once that salts are enriched within the pores of stone or any other porous material phase transformations such as crystallization/dissolution, hydration/dehydration or the formation and decomposition of double salts are continuously occurring as a result of temperature and humidity fluctuations of the surrounding environment. These phase transformations are generating the internal pressures responsible for salt damage. The behaviour of a single salt contaminating a porous material can be easily derived from its deliquescence humidity, which is the relative humidity in equilibrium with a saturated solution of the respective salt. At high relative humidities, above the deliquescence humidity, the salt is completely dissolved, at lower relative humidities the salt remains solid. Thus, undesirable dissolution/crystallization cycles do not occur if the ambient humidity does not fluctuate across the deliquescence humidity.

It has been recently shown, however, that this approach does not apply to salt mixtures where phase transformations are continuously occurring within ranges of relative humidity[3, 4, 5]. The same authors have also dem-

onstrated that, in principle, the behaviour of salt mixtures can be analysed using a chemical equilibrium model based on the approach of Pitzer[6].

This paper presents a case study of the salt contamination in a historic sandstone monument. The analytical data obtained from the chemical analysis of drillcores are interpreted with respect to the sources and transport processes determining the distribution and composition of the salt mixture found in the wall. The same thermodynamic model that has been previously used[4,5] is now applied to the experimental data to analyse the hygroscopic and crystallization properties of the salt system.

2. Methods

The north facade of the former convent of Birkenfeld (Northern Bavaria, Germany) founded in the 13th century has been subject to a detailed investigation of concentration and distribution of salts. The building is mainly built of a sandstone rich in clay minerals and feldspar (Schilfsandstein, upper triassic). This sandstone is known to show only poor weathering resistance. It is quite susceptible to salts and moisture. In an earlier study[7] large accumulations of salts have been found in the base of the south wall. In accordance with these findings the mapping of weathering forms at the same wall[8] also revealed that crumbling, flaking and the formation of scales are most pronounced in the base.

Salt contamination had to be also expected when planning the investigation of the north facade. Five drillcores (diameter: 18 mm) have therefore been taken in different heights from 0.65–5.2 m above ground level. In addition, two drillcores from the interior side of the same wall and one drillcore from the south facade have been analysed. The drillcores have been cut into slices of approximately 3 mm near the weathering surface and into 15 – 20 mm pieces in greater

depth. The total lengths of the drillcores have been about 100 mm.

All of the samples obtained in this way were homogenized by grinding to grain sizes <120 μm and subsequently extracted with deionized, bidistilled water (500 mg sample, 25 ml water). The aqueous suspensions obtained were filtered and analysed using ion chromatography (sulfate, nitrate, chloride), atomic spectrometry (sodium, potassium, magnesium, calcium) and photometry (ammonium).

3. Results and discussion

The analytical results confirmed that the base of the north facade of the building is also contaminated with salts. Large concentrations of nitrate, potassium and magnesium have been found. These ions showed pronounced vertical profiles with maximum enrichment at heights of approximately 2–3 m. Their concentrations show only small variations with depth. As an example, the nitrate distribution is presented in Fig. 1. The distributions of sodium, chloride and ammonium are closely matching that of nitrate, their concentrations are much smaller, however.

The sulfate distribution in the wall, is completely different. Strong horizontal concentration gradients can be seen from Fig. 1. The vertical profile is characterized by a shift of the maximum concentrations. Below 2 m maximum concentrations of 2 w.% are found at the stone surface. Penetration to greater depths is observed above 2–3 m. Most of the sulfate is balanced by calcium as the counterion indicating the presence of sparingly soluble calcium sulfate minerals, probably gypsum. Only the drillcores taken above 3 m revealed an excess of sulfate vs. calcium indicating significant contributions of sulfate to the hygroscopic fraction of the salt system.

The salt distributions found can be interpreted as the additive effect of two different sources. The distributions of nitrate, po-
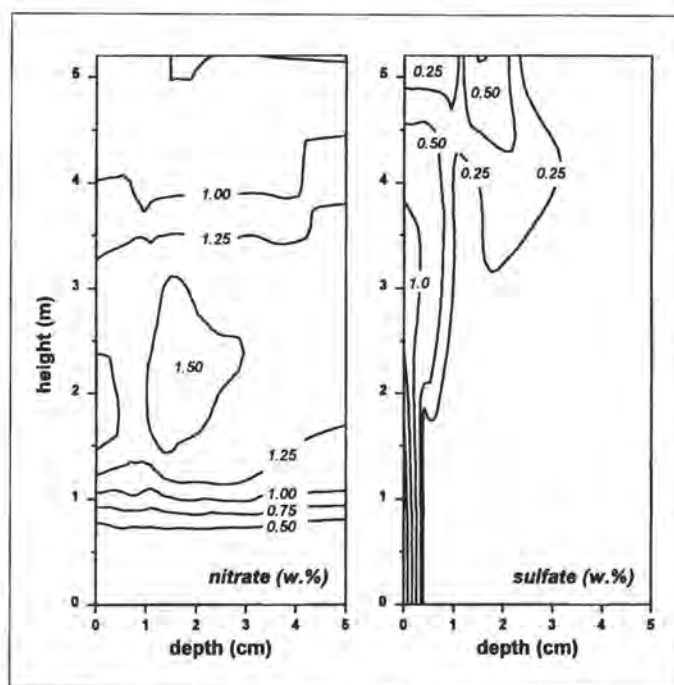
Fig. 1 Distribution of nitrate and sulfate.

tassium and magnesium (also sodium and chloride) can be regarded as being the result of the input of these ions by rising damp.

The zone of maximum enrichment reflects the height of capillary rise of water. Fractionation during the vertical transport is indicated by a shift of the K/Mg ratio, which is significantly higher below the accumulation zone.

On the other hand, the sulfate distribution in the wall indicates that deposition of sulfur dioxide from the atmosphere is the main source of sulfate enrichment. This is also confirmed by the analysis of the indoor drillcores yielding sulfate concentrations approximately an order of magnitude lower than outside. In contrast, the nitrate concentrations are practically identical at both sides of the wall. Finally, the integral sulfate concentrations were calculated up to a depth of 100 mm. The values of 12–43 mg/cm² compare well to those determined at other sandstone monuments also exposed to moderate sulfur dioxide pollution.

To study the crystallization properties of

the salt mixture in the wall the chemical equilibrium model mentioned above has been used. For that purpose the concentrations of the ions in the area of maximum salt enrichment at a height of 3 m have been used as input data. The ionic balances indicated that, within experimental uncertainties, sulfate is completely balanced by calcium at that height. Due to the low solubility of calcium sulfate it can therefore be assumed that practically all of the sulfate and calcium ions remain in solid form (gypsum) at all times. Thus, the influence of calcium and sulfate ions on the properties of the hygroscopic salt fraction can be neglected and the hygroscopic salt fraction can be treated as a mixture of magnesium, potassium, sodium, nitrate and chloride, only. Using the concentrations of these ions as input data the crystallization properties at 25 °C have been calculated. The results are summarized in Fig. 2, which shows the amount of crystalline salts as a function of the relative humidity.

It can be seen that niter (KNO_3) is the first solid to be precipitated from the salt mixture. The crystallization starts if the rela-
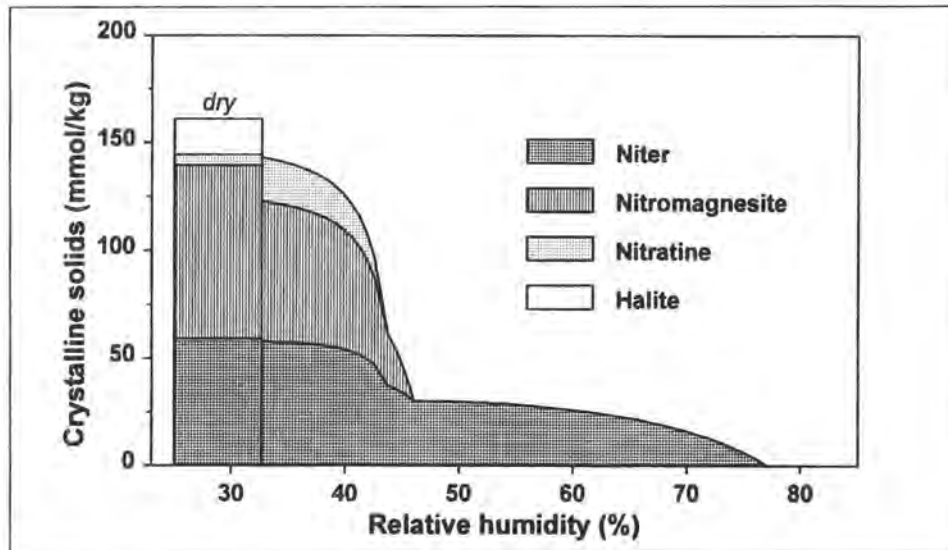
Fig. 2 Crystallization sequences at 25 °C (height: 3m, depth: 0 – 0.3 cm)

tive humidity drops below 77% which is considerably lower than the saturation humidity of pure potassium nitrate (92.7%). Fluctuations of the relative humidity within a range from 47% to 77% cause continuous crystallization and redissolution of niter. Thus, at humidities above 47% all of the sodium, magnesium and chloride and part of the nitrate and potassium ions remain in solution. Decreasing the relative humidity to values below 47% causes the simultaneous crystallization of niter and nitromagnesite $(Mg(NO_3)_2 \cdot 6H_2O)$ and, in addition, below 44% nitratine $(NaNO_3)$ starts to crystallize out. Finally the crystallization end–point is reached at only 32.7% relative humidity with the additional crystallization of halite (NaCl). Thus, after complete evaporation of water there remain four different solids, niter, nitratine, nitromagnesite and halite, respectively.

With respect to salt damage it can be concluded that cyclic variation of the relative humidity across a range of about 44%–47% is critical because a large fraction of the salt mixture in the wall is subject to crystallization cycles and severe damage has to be expected. Fluctuations of the relative humidity between 47% and 77% also causes crystallization cycles, involving only potassium ni-

trate, however. Since the amount of niter precipitated is rather small compared to the total concentration of hygroscopic salts (about 0.3 weight percent KNO_3 at 47% relative humidity) salt damage caused by humidity fluctuations above 47% is expected to be less severe. Finally, no salt crystallization occurs at relative humidities above 77%.

Additional calculations have been carried out to determine the influence of the salt mixtures on the moisture content of the stones. The results are shown in Fig. 3. Above 44% relative humidity the salt mixture picks up a significant amount of water. The moisture content strongly increases at humidities above 70%–75% and, finally, at a relative humidity of 89% the saturation value of the sandstone is reached (6.4 w.% of water) which means that the available pore space is completely filled with a salt solution. Due to the swelling and shrinking of the clay minerals the sandstone used at Birkenfeld Convent is very sensitive to large moisture variations. It can be seen from Fig. 3 that the hygroscopic salt mixture might therefore be also responsible for additional mechanical stress at rather high relative humidities where the salts are completely dissolved and no crystallization occurs.
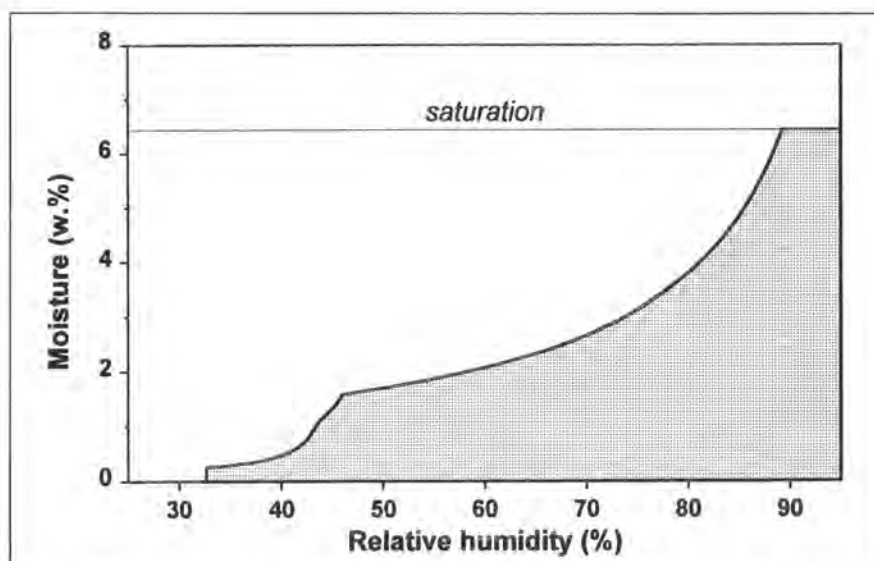
Fig. 3 Hygroscopic moisture at 25°C (height: 3 m, depth: 0 – 0.3 cm)

4. Conclusions

The analytical results of the ion concentrations in the northern wall of Birkenfeld Convent confirmed that the base of the wall is strongly contaminated with salts. The analysis of vertical and depth profiles of the salt concentrations has shown that input with rising damp is the main source of nitrate, chloride, magnesium, potassium and nitrate. Dry deposition of SO_2 is the dominant source of sulfate in the wall. Most of the sulfate found is balanced by calcium as the counter–ion indicating the presence of sparingly soluble gypsum. Therefore, the salt system in the wall can be characterized as a mixture of two fractions, a hygroscopic salt fraction which is subjected to cyclic dissolution and crystallization and gypsum most of which remains in solid form at all times.

It follows from the analysis of the crystallization properties of the hygroscopic salt mixture in the zone of maximum salt enrichment at a height of 3 m that, under normal outdoor climatic conditions, only a rather small amount of niter (KNO_3) would be subject to crystallization/dissolution cycles. Other salts would probably remain in solution at all times (see Fig. 2). The rate of damage due to salt crystallization alone is therefore expected to be moderate. The situation becomes different, however, for the indoor environment where the climatic conditions are largely determined by the kind of usage of a building. At present there are no heating facilities installed and the low relative humidities required to cause the crystallization of the main fraction of the hygroscopic salts are hardly ever occurring. It follows that the walls are moist at all times which might promote other undesirable processes (e.g. growth of microorganisms and swelling and shrinking effects). Another usage of the basement, however, as it has been taken into consideration by the owners of the building, would certainly strongly affect the climatic conditions. Heating would probably cause very low relative humidities during winter resulting in the crystallization of a large fraction of the salts present and therefore severe damage has to be expected.

Under normal outdoor climatic conditions the hygroscopic salt fraction is also responsible for large variations in the moisture contents of the wall (see Fig. 3) leading to additional mechanical stress due to swelling and shrinking which is often seen as a major damage process for stones rich in clay minerals as the one used at Birkenfeld Convent[9]. Thus it is expected that both processes, crystallization of

niter and swelling and shrinking of the clay minerals, are responsible for the strong damage observed at the base of the building.

Finally, gypsum, due to its low solubility, does not significantly influence the moisture content of the stone and only a small fraction of the gypsum present will ever be subject to dissolution–crystallization cycles. However, large concentrations of gypsum strongly influence the damage processes discussed so far. Gypsum deposits in the pore space affect the pore size distributions. For example, from the maximum sulfate and calcium concentrations found a gypsum concentration of 2.85 w.% (as $CaSO_4 \cdot 2H_2O$) can be calculated. Neglecting the differences in the densities of gypsum and the sandstone this amount corresponds to about 20% by volume of the water accessible pore space. It has been recently shown[9] that gypsum deposits in the pore space enhance the effect of swelling and shrinking processes and therefore accelerate the damage process. Similar effects of gypsum might also be expected with respect to the crystallization of hygroscopic salts.

It can be concluded that the salt contamination of the wall is largely responsible for the strong damage of the sandstone. The deleterious effects of the salts, however, are to be seen as the combined influence of different processes controlled by both, the crystallization and hygroscopic properties of the salt mixture and the properties of the stone material. Chemical equilibrium models allowing for the prediction of phase behaviour of salt mixtures are very helpful in this respect.

References

1. Arnold A. and K. Zehnder: Salt weathering on monuments. In: Zezza F. (ed): *The conservation of monuments in the Mediterranean Basin. Proceedings of the 1st international symposium.* Bari 1989, 31–58.

2. Steiger M., H.-H. Neumann, A. Ulrich and W. Dannecker: Chemische Zusammensetzung und Verteilung löslicher Salze in Natursteinmauerwerk. In: Snethlage R. (ed.): *Jahresberichte aus dem Forschungsprogramm Steinzerfall – Steinkonservierung, Band 3 – 1991.* Verlag Ernst & Sohn, Berlin 1993, 21–33

3. Price C.A. and P. Brimblecombe: Preventing salt damage in porous materials. In: *Preventive conservation: practice, theory and research.* International Institute for Conservation, London 1994, 90–93.

4. Steiger M.: Crystallization properties of mixed salt systems containing chloride and nitrate. Paper presented at: *EC Workshop Research on the Conservation of Brick Masonry Monuments, 24–26 October 1994, Leuven Belgium (in press).*

5. Steiger M. and W. Dannecker: Hygroskopische Eigenschaften und Kristallisationsverhalten von Salzgemischen. In: Snethlage R. (ed.): *Jahresberichte aus dem Forschungsprogramm Steinzerfall – Steinkonservierung, Band 5 – 1993.* Verlag Ernst & Sohn, Berlin 1995, 115–128.

6. Pitzer K. S. Ion interaction approach: theory and data correlation. In: Pitzer K. S. (ed.): *Activity Coefficients in Electrolyte Solutions.* CRC Press, Boca Raton, Florida 1991, 75–154.

7. Leisen H. and R. Snethlage: Beispiel einer Musterkonservierung am Kloster Birkenfeld. In: Snethlage R. (ed.): *Jahresberichte aus dem Forschungsprogramm Steinzerfall – Steinkonservierung, Band 1 – 1989.* Verlag Ernst & Sohn, Berlin 1991, 291–299.

8. Fitzner B. and R. Kownatzki: Klassifizierung der Verwitterungsformen und Kartierung von Natursteinbauwerken. In: Snethlage R. (Hrsg.): *Jahresberichte aus dem Forschungsprogramm Steinzerfall – Steinkonservierung, Band 1 – 1989.* Verlag Ernst & Sohn, Berlin 1991, 1–13.

9. Wendler E. and R. Rückert–Thümling (1992): Gefügezerstörendes Verformungsverhalten bei salzbefrachteten Sandsteinen unter hygrischer Wechselbelastung. In: *3. Int. Koll. Werkstoffwissenschaften und Bausanierung.* S. 1818 – 1830. Technische Akademie Esslingen.

Joao Bordado

Impregnation with reactive polymers as preservation technique for stones

Impregnation with reactive polymers as preservation technique for stones

J. Bordado
Hoechst Portuguesa SA Research and
Development Division
2726 MEM MARTINS – PORTUGAL

1. Introduction

Consolidation of stones from historical buildings as well as old ceramic tiles is nowadays performed with low concentration polymer solutions and a number of different polymer structures are used for this purpose.

Two different objectives can be considered when performing the treatment by impregnation: consolidation and/or hydrofobization.

A general agreement exists that the treatment procedure should conduct to an internal coating of the existing pores without obstruction or major reduction of the macroporosity.

2. Impregnation technology

Polymer solutions with a low solids contents, in general lower than 10%, are sprayed over the exposed surfaces and allow to impregnate. A new spraying should be performed within a few minutes without allowing the first to dry. This procedure is continued until there is a clear indication that the saturation occured (no further absorption).

The polymer solution should have a low viscosity and adjusted surface tension in order to facilitate the impregnation process. Vynil acetate copolymers, polymethacrylates and aliphatic polyrethanes are amongst the more common polymers used but in all cases an intrinsic flexibility has to be provided in the polymer chain since it is essential not to use external plasticizers.

The more modern treatments include a crosslinker and binder to the stone surface (chemical binding) and the results and durability is outstanding when compared with the conventional monocomponent systems.

3. Performance and durability

A number of methods can be used to estimate the performance of the treatment, and the accelerated weathering tests allow for a comparative prediction of durability.

Unfortunately most of this tests are destructive and therefore of limited use. The Karsten tube and the Ultrasound propagation method are therefore the more useful non–destructive tests.

4. Reactive polymers

Two component systems, including a chemical binder to the stone surface have been proved to be the more reliable and the impregnating polymer solutions with the best forecasted durability (based on comparative results of the accelerated weathering test).

Since the acurate dosing of the binder and crosslinker is not easy to perform during field application, tests are being conducted to try to include the binder group as a side group in the polymer chain.

The obtained reactive prepolymer solutions have however a limited shelf life of 6 month at 25°C and this might in some cases be a limitation in the market. Results on the performance of this new reactive prepolymers will be presented in comparison with the conventional systems.

5. Acknowledgements

Basile Christaras
Anna Kassoli–Fournaraki
Emilio Galán
Luis Aires-Barros

Origin and stone material characteristics in the protection of monuments. The case of the archaeological site of Eleusis, in Athens

Origin and stone material characteristics in the protection of monuments.
The case of the archaeological site of Eleusis, in Athens

B. Christaras   —   *School of Geology, Aristotle University of Thessaloniki, 54006 Thessaloniki, Greece*

A. Kassoli-Fournaraki   —   *School of Geology, Aristotle University of Thessaloniki, 54006 Thessaloniki, Greece*

E. Galan   —   *Dept. de Cristalografia y Mineralogia, Faculty of Chemistry, University of Seville, Sevilla, Spain*

L. Aires-Barros   —   *Lab. de Mineralogia e Petrologia, Instituto Superior Tecnico, Lisboa, Portugal*

Abstract

In the present paper the Temple of Eleusis was used as an example in order to show the necessity of the materials description and origin as a first step in the investigation of the deterioration of stones and the protection of monuments, in addition to the study of their physical and mechanical properties. Having this as a guide, different techniques and methodologies were used for the investigation of the building stones. Furthermore, there was an attempt to localise quarries in the broader area of Attica and correlate the monument's rock material with the geological formations of the area. For obtaining a complete picture of the existing situation of the Eleusis rock materials the following investigation methods were used. a) Detailed mineral identification and petrographical observations of the natural stones, b) mineralogical and chemical study of the black crusts, dusts, efflorecences and pittings and c) physical and mechanical properties of the rock materials.

1. Introduction

The greatest dangers for the historical monuments are weathering and air pollution. Building stones are susceptible to various atmospheric factors causing their destruction, especially in Mediterranean basin, where the marine spray is a permanent cause of natural pollution, not only on the coast but also further inland. Ground stability investigation, at the foundation area of a monument, contributes also to the definition of the protection measures. Mediterranean countries present very complicate geotectonic related to important natural hazards.

In this framework no protection measures can be taken without previous petrographical characterization of the stone material. These data will not only be used in the decision of the more proper conservation technique but also in exploration of the quarry which could offer material for restoration. Furthermore the use of testing material from the quarry is very useful, given that only a minimum quantity of original material is possible to be used. The study of the physical and mechanical properties is also important. These properties are related not only to the weathering but also to the stability of the building.

In the present paper the Temple of Eleusis was investigated regarding the above characteristics in the framework of the EU project "Marine spray and polluted atmosphere as factor of damage to monuments in the Mediterranean coastal environment (EV5V–CT92–0102)".

The Temple of Eleusis is situated in one of the most historical and significant ancient cultural centres of Attica, the city of Eleusis, the mother country of the philosopher Aeschylus. In the Temple, the Athenians used to worship the goddess of agriculture, Ceres, and her daughter Persephone, by extraordinary ceremonies which constituted the "Eleusis Mysteries". Recent excavations proved that this sacred centre existed during the prehistoric period and was active till the 4th AD century. In the existing ruins of the Temple, one can distinguish the traces of successive constructions, representing all the periods of antiquity, from pre–Mycenae to Roman period. The site corresponds to a typical urban–centre profile of in-

tense and diversified industrial activity as well as that of climatic conditions favouring photo–chemical pollution in the presence of an atmosphere highly charged by suspended particles

2. Geological setting of Attica and origin of the stones used in Eleusis Temple

Attica is characterised by a complicated geological structure consisted of several alpine rock units which form different tectonic napes (Katsikatsos et al. 1986). Figure 1 illustrates a geological map of this area. Different views of the Eleusis Temple ruins, as well as the identified rock types on the building stones and sampling sites are shown in Figures 2 and 3.

From base to top we distinguish the au-tochthonous Attico–Cycladic crystalline complex, the Neohellenic tectonic nape and the Subpelagonian unit.

The autochthonous system of metamorphic formations is represented by schists and gneisses with horizons and intercalation of marbles (SAMPLES B and C, in Table 1) and crystalline dolomites, with a total thickness up to 2500 m. The age of these metamorphic formations is Triassic to Upper Cretaceous (Marinos & Petrascheck 1956, Papadeas 1970, Katsikatsos 1976, 1977).

The Neohellenic nape consists of phyllites, schists and quartzites with intercalation of crystalline limestone and metabasic igneous rocks as well as serpentinite bodies. The upper formations are including Upper Cretaceous
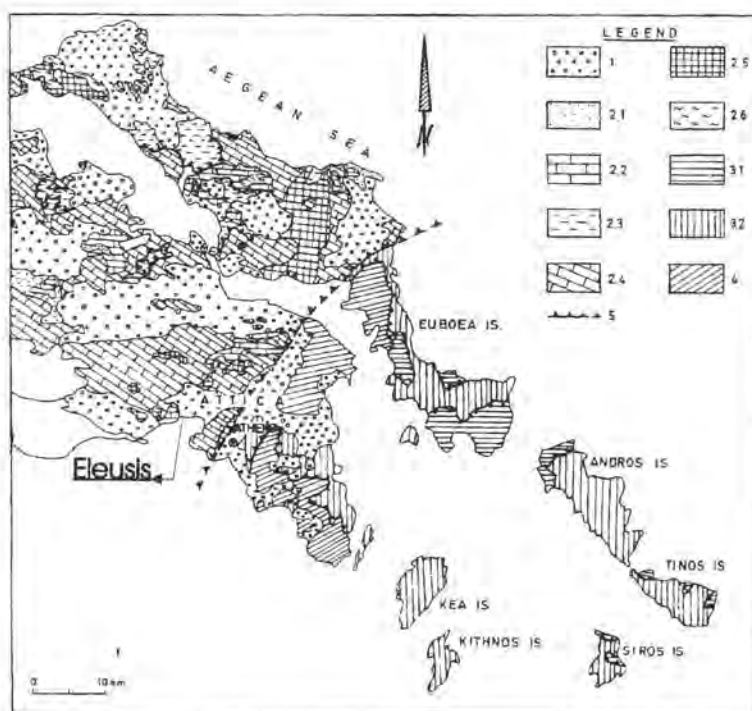
Fig. 1 Geotectonic map of Euboea–Attica and N. Cyclades. (after Katsikatsos, 1977). 1. Neogene and Quaternary formations; 2. Pelagonian zone; 2.1. Flysch; 2.2. Upper Cretaceous limestones; 2.3. Eohellenic nape formations; 2.4. Middle Upper Triassic–Upper Jurassic limestones and dolomites; 2.5. Neopalaeozoic–Middle Triassic formations; 2.6. Crystalline basement; 3. Neohellenic nape; 3.1. Ochi unit; 3.2. Styra unit; 4. Autochthonous system; 5. Overthrust.
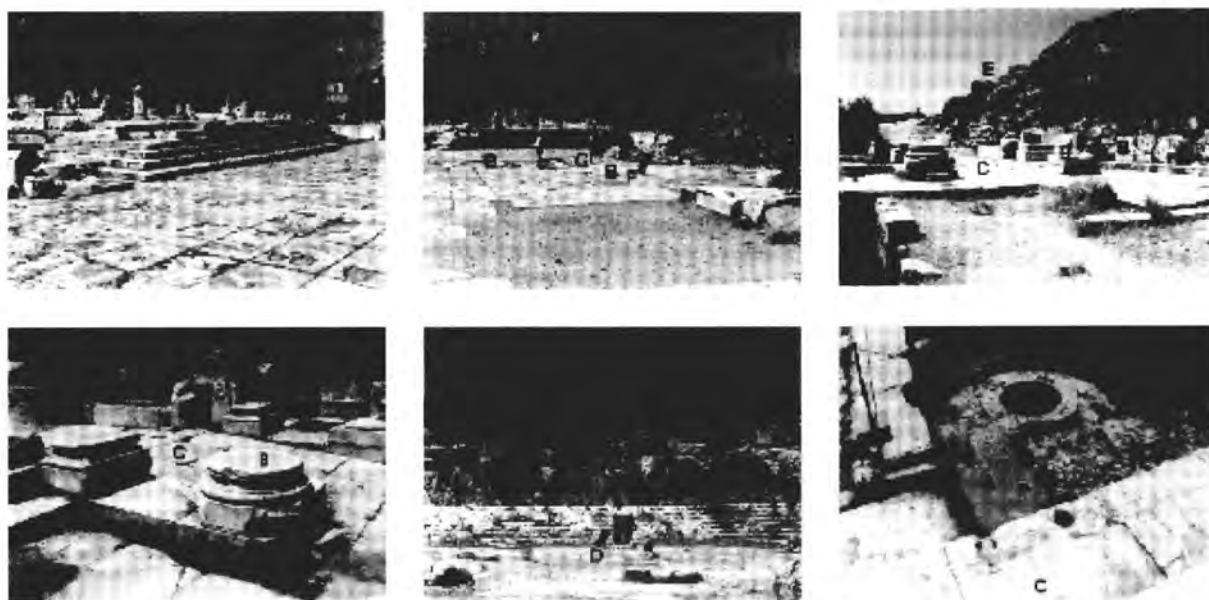
Fig. 2   Views from the archaeological site of Eleusis. The sites of the different rock types are also figured.
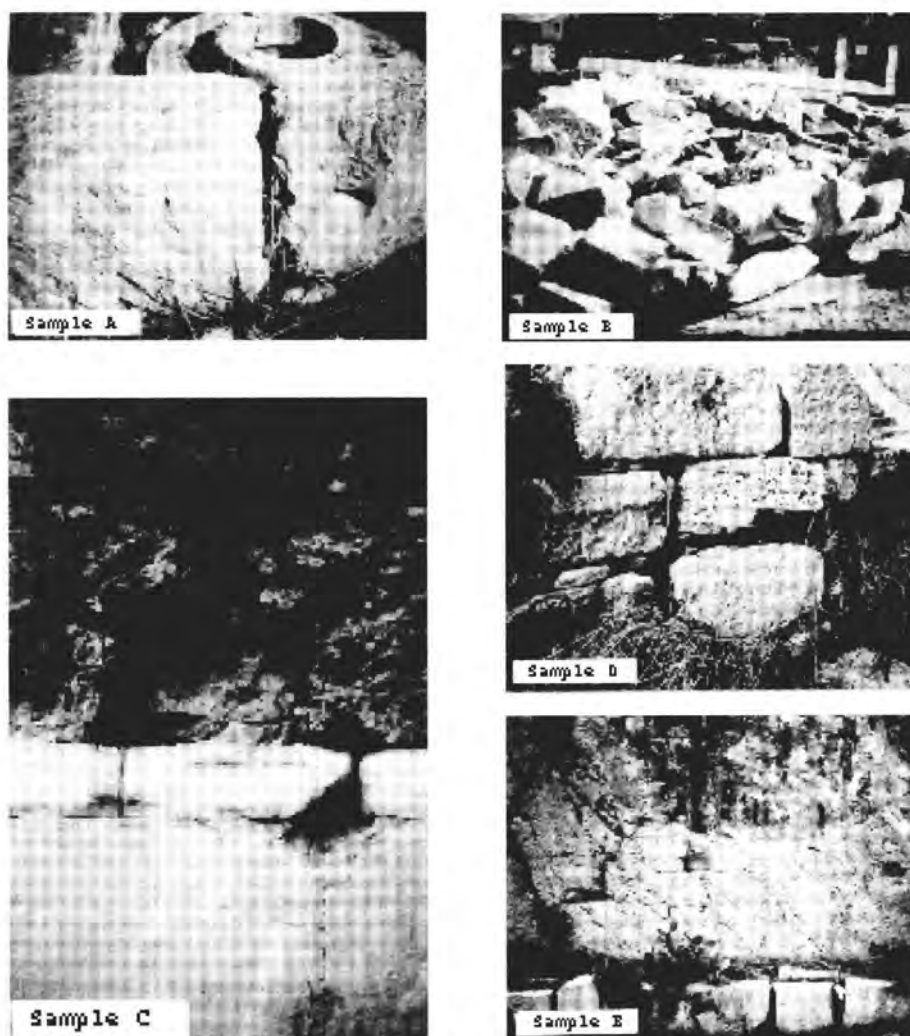
Fig. 3   Sampling sites of the rock types determined in Eleusis Temple.

crystalline limestones (Lepsius 1893, Kober 1929, Marinos & Petrascheck 1956, Leleu & Newmann 1969, Katsikatsos 1977). The total thickness exceeds 400 m and overthrusts the autochthonous units.

The Subpelagonian unit, which is the main tectonic unit of Eleusis area, overthrusts the Neohellenic nape and the autochthonous units. According to Dounas (1971), Katsikatsos (1977) and Katsikatsos et al. (1986) it consists of the following formations (Figure 1):

a) The Palaeozoic crystalline basement (two-mica gneisses, migmatites and amphibolites) overlain by clastic sediments of Permian and Carboniferous age with visible thickness of 800 m.

b) The lower–Middle Triassic group of a thickness exceeding 500 m, consisted of argillaceous shales and metasandstones, basic igneous rocks and limestone intercalation.

c) The upper Triassic – Upper Jurassic neritic limestones and dolomites with a thickness of more than 1000 m. They consist of a lower unit of white to white grey, massive to thick bedded, crystalline karstic limestone (SAMPLE E, in Table 1) and dolomite, strongly connected, and fractured. The upper unit consists of greyish to dark–grey limestone (SAMPLE A, in Table 1) and dolomite containing calcareous chert layers and nodules.

d) The Eohellenic tectonic nape comprising deep sea sediments, volcanic and ultrabasic rocks.

e) The Upper Cretaceous limestones of Cenomanian – Maestrichtian age, with a thickness ranging from 150 m to 800 m, transgressivelly lying over the older formations. Red–brown bauxite deposits occur under the limestones. Red clays (terra rossa) are intercalated between the bauxite and the overlying limestones. In the lower horizons the limestone is white–yellow (SAMPLE D, in Table 1) to green–brown, thin–bed-

ded, often nodulous, alternating with marly limestones and marls. In the upper horizons the limestone is greyish brown, medium to thick–plated, locally dolomitised (SAMPLE G, in Table 1), with chert nodules and microfossils. In the upper–most horizons, the limestone is thin bedded brown (SAMPLE F, in Table 1) to greenish–brown alternating upwards with conglomerates and sandstones.

f) The Maestrichtian flysh with sandstones, siltstones and limestone intercalation.

g) These alpine rocks are overlain by Neogene and Quaternary deposits (Dounas 1971). The Neogene sediments are divided into two systems. The lower system of marine blackish and lacustrine deposits which consists of marls, clays, sandstones, marly limestones and conglomerates, containing thin layers of lignite. The upper system of continental facies, consists of a) red–brown clays, sandy clays and mud alternating with sandstones and conglomerates, b) thick–bedded conglomerates with pebbles of Mesozoic limestones connected by reddish to reddish – brown sandy marl. The Quaternary deposits consist of torrential deposits and alluvial fans containing compact conglomerates and cemented screes, very cohessive, mainly of limestone debris.

3. Mineralogy – Petrography of stones

3.a. Analytical techniques

The petrographical investigation of the Eleusis Temple rock material, included a) observation of thin sections under the polarizing microscope and b) X–ray diffraction analysis.

The X–ray diffractograms were obtained on randomly oriented samples, using a Philips diffractometer, Ni–filtered Cu$_{K\alpha}$ radiation. The scanning speed was 1° per minute over the interval 3–60° of 2θ.

Table 1 Rock types used in Eleusis Temple and samples studied

ROCK TYPE	MONUMENT
Grey micritic limestone, SAMPLE A	Kallichoron Well, Telestirion
White "Pentelic" marble, SAMPLE B	Temple of Artemis (Columns), Greater Propylaea, (Columns), Smaller Propylaea (Columns)
White grey marble, SAMPLE C	Kallichoron Well, Smaller Propylaea (Floor)
Yellow microsparitic limestone, SAMPLE D	Plutoneion, Telestirion
Grey biosparitic limestone, SAMPLE E	Smaller Propylaea
Yellow–brown oosparitic limestone, SAMPLE F	Artemides temple (Basement), Kallichoron Well, Smaller Propylaea (Walls)
Yellow–brown biomicritic dolomite, SAMPLE G	Greater Propylaea (Basement), Smaller Propylaea (Walls), Artemides temple (Basement).

3.b. Microscopic observations

The microscopic observation of the samples from Eleusis Temple gave the following results:

SAMPLE A: Grey micritic limestone. Very fine–grained limestone, including few fossils (sponge spicules, radiolaria, ostracods, crinoid ossicles, echinodermal stem plates and bivalve filaments), which though often deformed, are still recognisable. Medium–grained recrystallized calcite in forms of veins and nests, is observed in places. The calcite veins crosscut the fine–grained matrix. Some vugs and stylolites are cemented by sparry calcite. Thin veins of iron oxides ramify in several places of the rock.

Constituents: Calcite, traces of quartz.

SAMPLE B: White marble. Medium–grained well recrystallized marble with granoblastic polygonal texture. The grain size indicates increasing intensity of metamorphism, that is, possible high temperature and low deformation rates. Tangential to structural contacts between grains are observed. The porosity is very low (< 5%) of intercrystalline type according to rhomboedral cleavage planes. Porosity occurs inside the calcite crystals and between the grains there is no visible anisotropy.

Constituents: Calcite mainly in polygonal isometric grains, frequently multitwinned. Dolomite is a minor phase. Few prismatic needles of muscovite participate also as accessories as well as some quartz grains, zircon and opaques, indicating impurities in the primary rock.

SAMPLE C: White–grey marble. Fine– to medium– grained marble with a banded, granolepidoblastic texture. Calcite appears sometimes recrystallized. Multitwinning of calcite crystals is frequently observed. Structural or slightly tangential contacts between grains are observed. Porosity is very low (5–10%). Parallel fractures developed following the most fine–grain bands, which produce a very important channel porosity. There is also intercrystalline porosity according to the rhomboedral

cleavage. Alteration borders in fractures are observed.

Constituents: Calcite, traces of quartz, retaining their detrital character and indicating siliceous impurities in the primary limestone. Traces of thenardite and white mica are also present.

SAMPLE D: Yellow limestone. Very fine-grained, patchily recrystallized microsparitic limestone with many pellets, pseudopelloids, very small calcareous intraclast, and bioclast (echinodermal "ghost" fragments, sponge spicules, radiolaria, mollusc filaments–possible gastrops). Cryptocrystalline lenses are observed to develop. Porosity is medium (25%), and intercrystalline, moldic and geode type. Bioclasts and original matrix have undergone a dissolution–recrystallization process.

Constituents: Calcite and dolomite in equal quantities and minor quartz.

SAMPLE E: Micritic limestone. Strongly tectonized, deformed and recrystallized single-phase limestone. Fine– to medium–grained. The calcite crystals have bent cleavages, deformation twins and deformation lamellae. Veins of tectonized, recrystallized calcite grains crosscut the matrix. Big bioclasts composed of fragments of mollusk shells (bivalves, possible oysters) with prismatic, radial and interbreed texture. Cement is granular sparitic. No porosity was observed.

Constituents: Calcite.

SAMPLE F: Oosparitic yellow–brown limestone. Microcrystalline, oolitic single phase limestone. Recrystallization of calcite in form of nests is locally observed. Dissolved fossil remains corresponding to bivalves, ostracodes, gastropods and bryozoos are observed. In addition, ooids and pelloids are found. Intraclasts occur. Micritic mud is absent. Porosity (interparticle, intraparticle and moldic type) is high.

Constituents: Calcite. Quartz, zircon, rutile as terrigenous.

SAMPLE G: Biomicritic yellow–brown dolomite. Micro– to crypto–crystalline dolomite. Few spherical to ellipsoidal quartz crystals are observed. Dissolved fossil remnants corresponding to bivalves, ostracodes, echinodermal stem plates, are found. Detrital grains and bioclasts are less than 10% of the rock. Porosity is moldic.

Constituents: Dolomite, quartz as minor phase, traces of feldspars and white mica.

3.c. Results of X–Ray diffraction analysis

X–ray diffraction analysis was applied on all samples derived from the Eleusis Temple (Greece). The X–ray method was used in order to verify the microscopic observations and determine the mineralogical composition of the very fine grains. The XRD results are presented in Table 2.

4. X–Ray diffraction and infra–red spetroscopy and X–ray fluorescence study of black crusts, yellow and gray dusts, white efflorescences and pink pittings

During the field work at Eleusis archaeological site, besides the characterization of the main seven rock–types used in the Temple, a lot of samples such as black crusts, white efflorescence, pink pittings and several type of coloured dusts, taken from Prostilio in Roman Court as well as from the Greater Propylea and Telesterion have been studied by XRD and IRS and XRF. In Tables 3 and 4 the main conclusions obtained from this study are presented.

5. Physical and mechanical properties

The rock samples from the Eleusis Temple were measured for their dry density (d), water absorption (Ab), dry compressional wave velocity (v_p), compressive strength (σ_c), tensile strength (σ_t), modulus of elasticity (E), cohesion (c), angle of internal friction (φ) and abrasion resistance (AR) (Table 5). Tests were applied on minicores of 1 in. diameter and 30 mm height, prepared using a core drilling ma-

Table 2   Eleusis Temple – XRD analysis of the samples studied.

Samples/Minerals	A	B	C	D	E	F	G
Calcite	M	M	M	M	M	M	–
Dolomite	–	m	–	M	–	–	M
Quartz	tr	m	tr	m	–	–	m
Muscovite	–	m	–	–	–	–	–
Thenardite	–	–	tr	–	–	–	–
Feldspars	–	–	–	–	–	–	tr

M : Major phase, m : minor phase, tr : traces, – : absent

chine. Abrasion resistance was measured on specimens of 1 in diameter and 10 mm height. Minicores without visible fractures were collected carefully to be representative of the lithology. The surfaces of the minicores were shaped to ensure flat ends. The height to diameter ratio of specimens generally required for mechanical tests is 2:1 to 2.2:1 (Jaeger and Cook, 1979) but the specific conditions (material derived from the monument) obliged us to use specimens with the above dimensions. All tests were performed acording to ASTM specifications (Christaras, 1996); the abrasion resistance was measured according our previous technique (Christaras, 1995).

6. Conclusions

This research was performed in the framework of the EU project "Marine spray and polluted atmosphere as factor of damage to monuments in the Mediterranean coastal environment (EV5V–CT92–0102)". The aim of the project was to establish a common methodology in investigating the deterioration of stones. In the frame of this investigation, it was verified that without the detailed description of the existing situation of a monument's construction material, it is not easy to proceed to protection measures. Having this as a guide, different techniques and methodologies were

used for the investigation of the Eleusis building stones. All these methods were used in order to determine the degree of deterioration of the Eleusis monument, which is situated in an area of high industrial pollution impact.

Furthermore, there was an attempt to localise quarries in the broader area of Attica and correlate the monument's rock material with the geological formations of the area. For obtaining a complete picture of the existing situation of the Eleusis rock materials the following investigation methods were used. a) Detailed mineralogical and petrographical observations of the natural stones, b) mineralogical and chemical study of the black crusts, dusts, efflorecences and pittings and c) physical and mechanical properties of the rock materials.

The detailed mineralogical and petrographical investigation of the studied rock samples matches very well with the physico–mechanical values, measured for the same samples. This means that the resistance of the rock material is closely dependent on the mineralogical composition, corrosion, texture etc.

SAMPLE	MINEROPETROGRAPHY	XRD STUDY		IRS STUDY
N° 1–Floor of Greater Propylea. "Black ampoules"	Black crusts and ampoules on the floor. Limestone transformed by acid rains (?)	Outer black crust Black oolithes Yellowish crust Crystalline agregates	cc + qz (tr) cc + qz cc + qz + gt (tr) cc	cc + qz cc + qz cc + qz + altered silicates cc
N° 2–Floor of Greater Propylea. Samples from a fracture	Like sample No 1	Yellowish zone Black zone	cc + qz cc + qz	cc + qz cc + qz
N° 3–Pentelic marble	White marble formed by a mosaic of equant calcite. Small grains of quartz and a few mica flakes	Pinkish face Black face brown crust black crust White efflorescences	cc + qz cc + qz + gt cc + qz cc + qz cc	cc + qz + gy cc + qz + gy cc + gy + qz (tr) + oxl (tr)
N° 4–Yellow limestone 4th Column Telesterion	Yellowish micritic limestone decayed in yellow dust	Yellow dust Black crust	cc + qz gy + qz + cc (tr)	cc + qz + gy (tr) + nitrates cc + gy + qz (tr) + nitrates
N° 5–Prostilio	Like sample No 3	Brown crust Light pinkish dust Black crust White efflorescences	cc + qz cc + gt + qz cc + qz gy + cc	cc + qz cc + qz cc + qz gy + cc + oxl
N° 6–Rose pentelic marble. Column in Greater Propylea 1st column, 3rd row	Like sample No 3, rich in pink pitting	Light pinkish face Brown–yellowish zone	cc + gt +qz cc + gt	cc + altered silicates
N° 7–Yellow limestone Stepped Terrace	Yellow mitritic limestone	Whitish zone Romboedral crystals Yellow dust Borrioidal grey crusts	cc + dl cc + qz (tr) gy + cc (tr) gy + cc + qz (tr)	cc + dl + altered silicates cc + dl (tr) + qz (tr) + sulphates (tr) cc + qz (tr) + sulphates (tr)

cc: calcite, qz: quartz, gy: gypsum, gt: goethite, ox: oxalates, dl: dolomite, and tr: traces

B. Christaras, A. Kassoli-Fournaraki, E. Galan and L. Aires-Barros

Table 4 The temple of Eleusis (Greece). XRF results of crusts, dusts and efflorescences.

	ELEMENTS																		
SAMPLE	Na	Mg	Si	P	S	Cl	K	Ti	V	Cr	Mn	Fe	Zn	Br	Rb	Sr	Y	Pb	Cu
N° 1																			
White sample																			
Black crust			tr	tr	tr	tr	tr	tr		tr	o	o	o			tr	tr	tr	
N° 2																			
Yellow dust			o	tr	tr	tr	o	tr		tr		tr				tr		tr	
Black dust		tr	tr	tr	tr		o	tr		tr	tr	o	tr			o		o	
N° 3																			
Pinkish face			o	o	o	tr	o	o	tr	o	o	+	o			o			
Black crust		tr	tr	o	tr		o	o	tr	tr	tr	o	tr			o		tr	
N° 4																			
Pelletized sample	++	tr	o	o	o	++	+	o	tr	tr	o	o	tr	tr		++	o	o	tr?
N° 5																			
Brown crust			tr	o	o	o	o	o	tr	tr	tr	tr	tr			o		o	
Black crust		tr	tr	o	o	tr	o	o	tr	tr	tr	tr	tr			o		o	
Green (lichenic) crust		tr	tr	o	o	tr	+	o	o	tr	tr	tr	tr			o		tr	
N° 6																			
Rose Pentelic marble								Like sample N° 5											
N° 7																			
Brown dust			tr	o	o	tr	o	tr	tr	tr	o	o	tr	o		o	o	tr	
Pelletized sample	o	+	tr	o	o	o	+	tr	tr	o	o	+	tr	tr	tr?	+	o	++	

Present   o
Abundant   +
V. m. abundant   ++
Traces   tr

Note: All samples have been tested directly by XRF
Sample 4 and 7 have been previously powdered and pelletized

Table 5 Physical and mechanical properties of samples studied, from the Temple of Eleusis. d: density, Ab: water absorption, σ_c: compressive strength, σ_t: tensile strength, c: cohesion, φ: angle of internal friction, E: Young's modulus (c, φ and σ_t were measured using the "Brazilian method")

ROCK TYPE	Vp (m/s)	d (gr/cc)	Ab (%)	σ_c (MPa)	σ_t (MPa)	φ°	c (MPa)	E (MPa)	AR %
SAMPLE A Gray micritic limestone	6486	2.68	0.68	77.4	9.73	42	17.38	20650	3.56
SAMPLE B White "pentelic" marble	5833	2.71	0.22	99.5	11.50	44	20.90	38480	1.40
SAMPLE C White gray marble	5776	2.73	0.35	88.5	10.62	43	19.00	33200	3.07
SAMPLE D Yellow limestone	4237	2.48	5.19	48.7	6.20	41	10.96	15480	5.08
SAMPLE E Gray biomicritic limestone	5300	2.56	0.41	57.5	6.64	44	12.07	17600	4.00
SAMPLE F Yellow–brown limestone	5073	1.76	1.2	50.9	5.50	45	10.43	14500	5.72
SAMPLE G Yellow–brown fossilif. limestone	3893	2.42	3.51	48.7	5.50	45	10.05	14500	5.98

7. References

1. Christaras, B. (1995): Mechanical behaviour of basalts from Costa Rica rift, Hole 504B, Leg 137. *Proc. ODP, Sci.* Results, College Station, TX, 137/140, pp. 347–351.

2. Christaras, B. (1996): Non destructive methods for investigation of some mechanical properties of natural stones in the protection of monuments. Bull. IAEG (in press).

3. Dounas, A. (1971): Geology of the area between Megara and Erythrai. Ph.D. thesis, Univ. of Athens,

4. Jaeger, J.C. & Cook, N.G.W. (1979): Fundamental of Rock mechanics (3rd ed.), Chapman & Hall, New York, 593 p.

5. Katsikatsos, G. (1976): La structure tectonique de l' Attique et de l'ile d' Eubee. *Bull. Soc. Geol. France*, 19, 75–80, Paris

6. Katsikatsos, G. (1977): La structure tectonique d'Attique et de l'ile d'Eubee. *VI Colloquium on The Geology of the Aegean Region*, Athens, I, 211–228

7. Katsikatsos, G., Migiros, G., Triantaphyllis, M., Mettos, A. (1986): Geological structure of internal hellenides (E. Thessaly–Sw. Macedonia, Euboea–Attica–Northern Cyclades islands and Lesvos), *IGME, Geol. & Geoph. Res. Special Issue* pp. 191–212, Athens.

8. Kober, L. (1929): Beitrage zur Geologie von Attika. *Sitzungsb, Akad. Wiss. Mat–Nat.* Kl., 138, 299–327, Wien.

9. Leleu, M. & Neumann, M. (1969): L'age des formations d'Attique: du paleozoique au mesozoique. C. R. Ac. Sc. Paris, D, 268, 1361–1363.

10. Lepsius, R. (1893): Geologie von Attika, Berlin

11. Marinos, G. & Petrascheck, W.E. (1956): Laurium. *Geol. geophys. Research*, 4, 1–247, Inst. Geol. Subs. Res., Athens.

12. Papadeas, G. (1970): Zur Stratigraphie und Altersstellung der Metamorphen Serien NE von Athen (Marathon). *Praktika Akad. Athinon*, 1969, 44, 10–18 Athen.
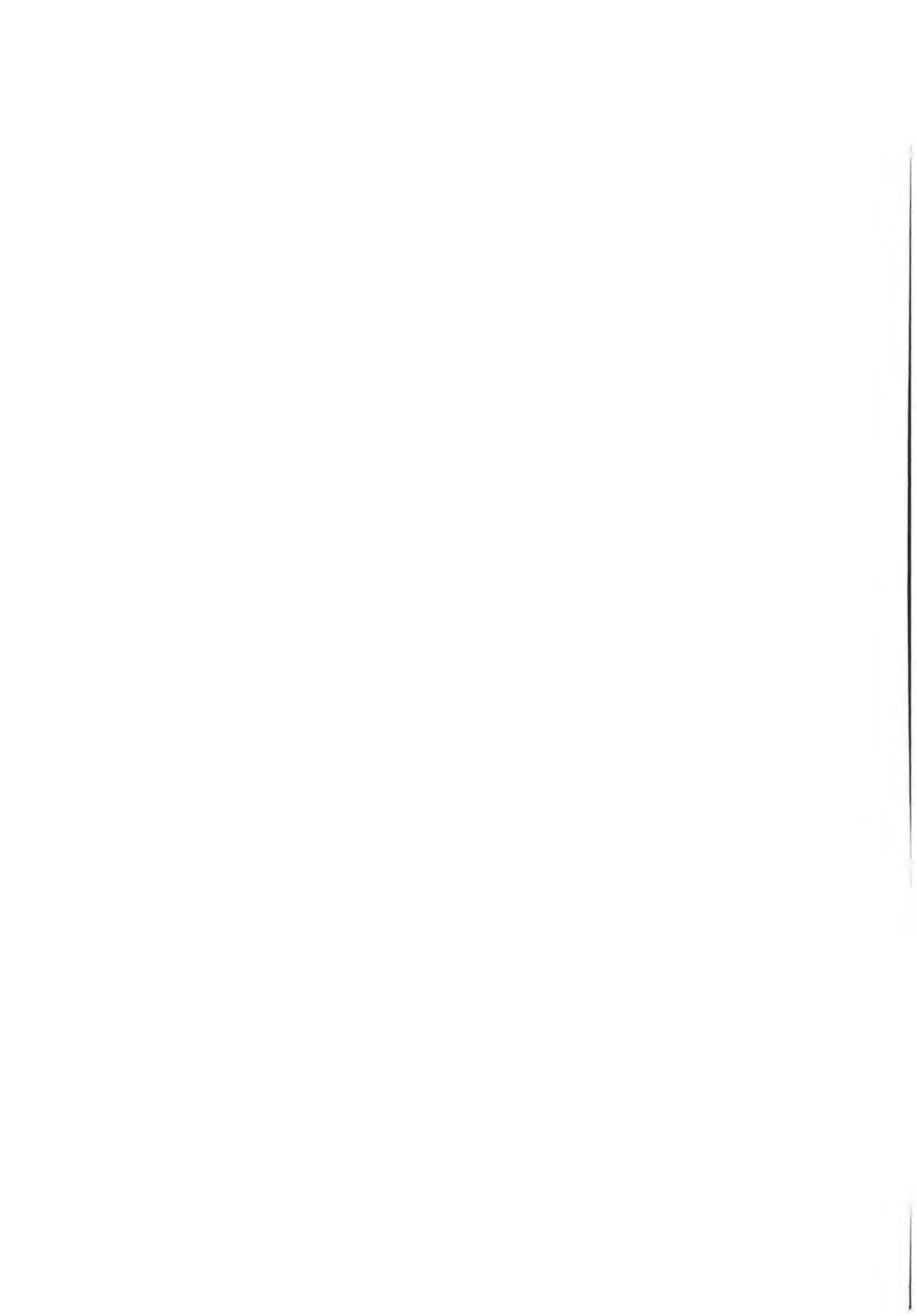
Basile Christaras

Particularities in studying the physical and mechanical properties of stones in monuments.
Examples from the Mediterranean basin
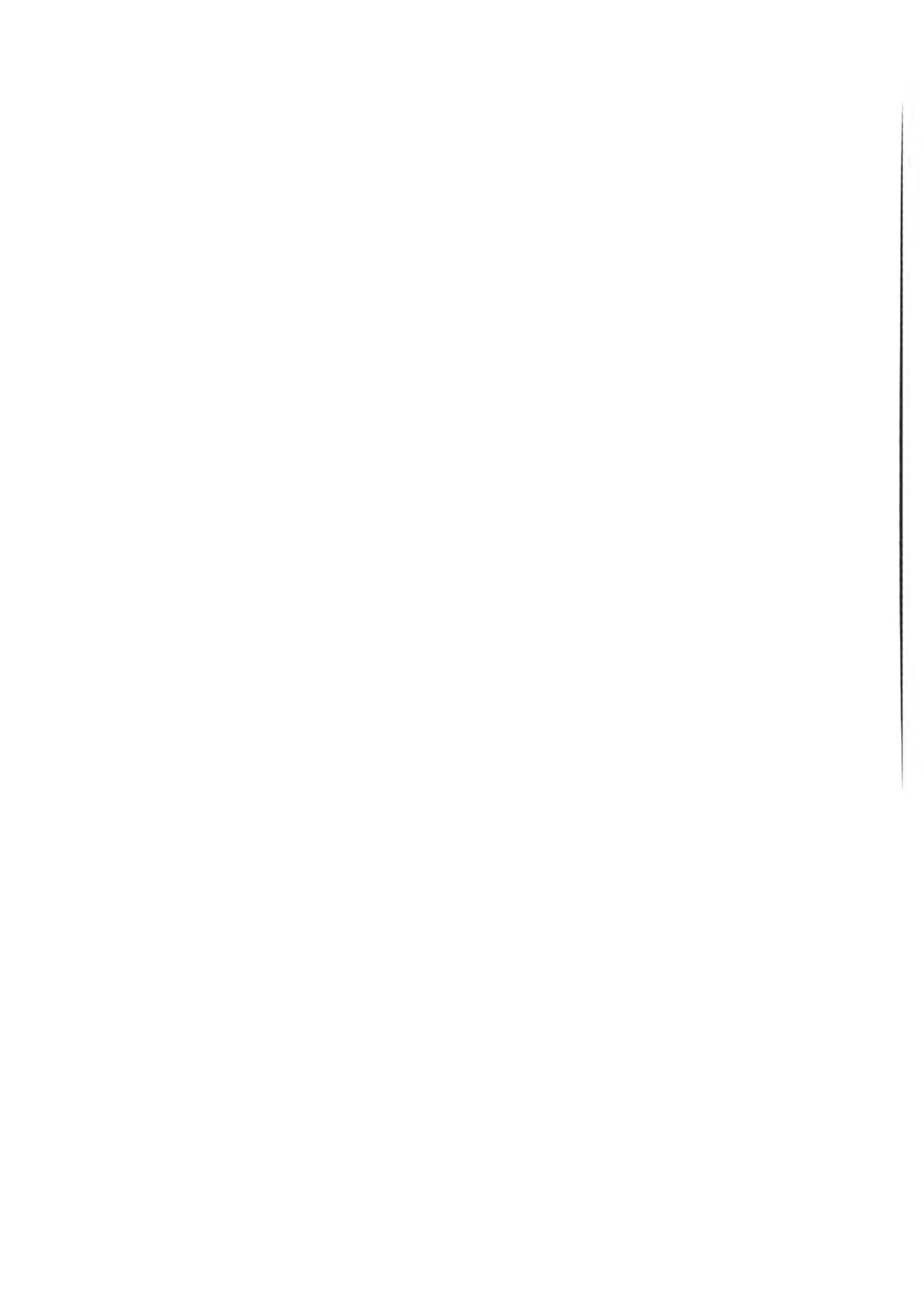
Particularities in studying the physical and mechanical properties of stones in monuments. Examples from the Mediterranean basin

B. Christaras
Lab. of Engineering Geology & Hydrogeology,
School of Geology, Aristotle University of Thessaloniki,
54006 Thessaloniki, Greece

Abstract

The investigation of the physical and mechanical properties of stones in monuments needs non destructive methods and small quantity of testing material. The non destructive methods can be divided in laboratory and *in situ* techniques. P & S wave ultrasonic velocities and Schmidt hammer can be used for both *in situ* and laboratory measurements, in contrast to the compressive strength and abrasion resistance that can be used only for investigation in the laboratory. In the present paper the above methods were used for the study of properties like the mechanical anisotropy, weathering degree, mechanical strength and deformation ability of stones, using data from The Cathedral of Bari, in Italy, the Temple of Eleusis, in Greece, the Cathedral of Cadiz, in Spain and the church of Sta Marija Ta' Cwerra, in Malta. This investigation was performed in the framework of the EU project "Marine spray and polluted atmosphere as factor of damage to monuments in the Mediterranean coastal environment (EV5V–CT92–0102)".

tion area of a monument, contributes also to the definition of the protection measures. Mediterranean countries present very complicate geotectonic related to important natural hazards.

Weathering effects on the physical and mechanical properties of natural stones of monuments causing stability problems. These properties cannot be easily studied using the common methods used for investigation in the modern construction, because these methods need a big quantity of testing material.

In this framework the use of non destructive techniques for determining the physical and mechanical properties of natural stones is very important because only a small quantity of testing material is needed. Methods using P & S wave velocities, Schmidt hammer resistance and abrasion resistance provide data related to the elasticity, uniaxial compressive strength, anisotropy and weathering resistance of the stones. Porosity, dry density and water absorption are physical characteristics that can also provide data related to weathering.

In the present paper the above methods were used for the study of properties like the mechanical anisotropy, weathering degree, mechanical strength and deformation ability of stones, using data from The Cathedral of Bari, in Italy, the Temple of Eleusis, in Greece, the Cathedral of Cadiz, in Spain and the church of Sta Marija Ta' Cwerra, in Malta. This investigation was performed in the framework of the EU project "Marine spray and polluted atmosphere as factor of damage to monuments in the Mediterranean coastal environment (EV5V–CT92–0102)".

1. Introduction

One of the greatest dangers for the historical monuments is weathering, caused by climatic changes and air pollution. Building stones are susceptible to various atmospheric factors causing their destruction, especially in Mediterranean basin, where the marine salts are a permanent cause of natural pollution, not only on the coast but also further inland. Ground stability investigation, at the founda-

2. Physical and mechanical properties used

The physico–mechanical properties of the collected samples were measured according to the following methodology.

i.   *DRY DENSITY (d, ASTM C 97–47):* It obtained by dividing the dry weight (after drying for 24h at 110°C) of the specimens by the total volume (solids and voids). Weights were determined using a FX–320, A&D automatic electronic balance (310 gr. x 0.01 gr. and 60 gr. x 0.001 gr.). The total volumes were measured using an EIJKELKAMP Vacuum Air Pycnometer. For total volumes, saturated samples were used.

ii. *WATER ABSORPTION (Ab, ASTM C 97–47):* It was calculated by dividing the absorbed water weight (after a bath of 24h, in vacuum) by the dry weight of specimens.

iii. *(ULTRASONIC VELOCITY (v_p, ASTM 597, ASTM D 2845– 83):* It is a good index characteristic of the physico–mechanical behaviour of the rocks. For this purpose a PUNDIT ultrasonic non destructive digital tester was used. Measurements were applied along the axis of the core samples and the travel time of the 54–KHz source pulse was measured. Water pump grease, covered with a specific membrane, was used as coupling media, to improve the acoustic contact between the sample and the transducers. The instrument was calibrated with aluminium standards. Thickness and travel time corrections were calculated by performing a linear regression between the actual and the measured times. Ultrasonic velocity is related to the elastic moduli of rocks, such as Young's modulus and Poisson's ratio (Christaras et al, 1993, Topal, 1995). Furthermore, it is a very good index for rock quality classification and weathering determination. Tests were made using the direct or the indirect method, depending on the case. The direct method is referred to the arrangement of the transducers of the apparatus on the opposite surfaces of the specimen tested. The indirect method, used especially on in–situ measurements, is referred on arrangement of the transducers on the same surface of the stone. The direct transmission arrangement is the most satisfactory one since the longitudinal pulse leaving the transmitter are propagated mainly in the direction normal to the transducer face. In general, the pulse velocity determined by the indirect method of testing will be lower than that using the direct method. If it is possible to employ both methods of measurement then a relationship may be established between them and a correction factor derived. According to the manual of the apparatus used, when it is not possible to use the direct method an approximate factor of 1.05 could be used for the determination of the pulse velocity obtained using the direct method.

iv. *ABRASION RESISTANCE (AR):* It is an expression of hardness measured as "abrasion loss of weight (AR, %)". The method used is based on the calculation of the loss of weight of a pre–weighted sample after abrasion for a constant time under constant conditions. For this purpose a "LOGITECH – LP 30" thin–section lapping machine with constant rotation of 40 rpm is used. Tests are applied on mini–cores of 1 in diameter and 10–mm high, rather than 30 mm, which was the ordinary height used for the other tests, ensuring no damage of the edges. The polishing material (sand) is emery of grain size No. 400 and the specimens are loaded with 2 kg. The abrasion time is 1/2 hr. Test results are accurate and repeatable not only for fine –grained rocks, like the pentelic marble, but also for medium– and cross-grained rocks without very big phaenocrystals (e.g. trachyte etc.). Our previous studies on specimens of different

rock types (Christaras, 1995) provided significant correlation between abrasion loss of weight and the other common physico–mechanical properties.

v. *UNIAXIAL COMPRESSIVE STRENGTH (σ_c or UCS):* Uniaxial compressive strength (UCS, in MPa) was measured according to ASTM C 97–47 specifications by dividing the compressive force by the surface of the base of the cylindrical specimen. For this purpose a 100/450–KN Weber PW 40E compression machine was used, calibrated according to the instructions of the factory. The machine was equipped with an electro–hydraulic directly connected motor–driven pump, a solenoid valve, and a pressure valve. A low–pressure contact pressure gauge, inductively operated as desired (indication range 25% of main contact pressure gauge: 100 KN), with automatic closing and shut–off valve.

vi. *YOUNG'S MODULUS OF ELASTICITY (E):* Deformation data for specimens undergoing strength tests may be obtained and used to calculate the static elastic moduli of intact rock. The modulus of elasticity, or Young's modulus is one of the most common used. The static modulus of elasticity, which is a form of Hook's law, is derived from applied axial compressive stresses and resulting axial strains ($E_s = \sigma_n/e$, where *E*: Young's modulus, in GPa, σ_n: normal stress and e: axial strain). Rate of stress application will result in different E–values, for the same material. The values for E–modulus may be obtained from stress–strain diagrams. Of the average modulus, tangent modulus and secant modulus referred to in the literature, the last one is more commonly used, as it predicts the maximum elastic deformation that would occur at 50% of the ultimate strength (Johnson and De Graff, 1988). In the present investigation Young's modulus was measured using the

secant modulus method. Unfortunately the small size of the specimens did not permit us the use of high–precision deformation gauges. Thus, deformation was measured using a "KYOWA" micrometer connected to an amplifier. The precision of the instrument was 0.01 mm; a third digit precision is given by an amplifier.

vii. *TENSILE STRENGTH (σ_t), COHESION (c), ANGLE OF INTERNAL FRICTION (φ):* It was measured according to the indirect "Brazilian method" (Duriez et Arrambide, 1962) consisted in breaking the dry minicores placed horizontally between the plates of a press. The tensile strength is obtained by dividing the applied compressive force by the half lateral surface of the cylindrical specimens. Besides a compressive stress, equal to 3 σ_t is obtained in the same time. For each sample, two Mohr circles are traced, the first with $\sigma_c>0$ and $\sigma_r=0$ and the second with $\sigma_c<$) and $\sigma_c=3|\sigma_t|$. The angle of internal friction and the cohesion are also calculated according to the relationships $\tan^2(45°-\varphi/2) = \sigma_t/(\sigma_c-3\sigma_t)$ and $c=(\sigma_c/2) \tan (45°-\varphi/2)$.

viii. *SCHMIDT HAMMER VALUE (SHV):* The Schmidt hammer is designed to carry out instant non destructive tests on in–situ concrete or stone without damage, to give an immediate indication of their compressive strength, using the calibration curve supplied with each instruction (linear regression). Test values is better to be used in relation to fresh values. The method can easily be used for hardness scanning and weathering mapping of a stone surface (Christaras, 1996).

ix. *MECHANICAL ANISOTROPY:* Stones do not behave mechanically in the same way along different directions. Orientation of minerals in rocks cause anisotropy phenomena, referred to the physical and mechanical properties. Deformation is one of the more important properties re-

lated to the rock fabric. This property is expressed by the Young's modulus (E), obtained either statically using loading techniques, or dynamically using ultrasonic and resonance frequency techniques. Weathering is also related to the rock fabric, causing different results in different directions (Zezza, 1991, Christaras, 1996).

3. The Temple of Eleusis in Greece

The Temple of Eleusis is situated in one of the most historical and significant ancient cultural centres of Attica, the city of Eleusis, the mother country of the philosopher Aeschylus. In the Temple, the Athenians used to worship the goddess of agriculture, Ceres, and her daughter Persephone, by extraordinary ceremonies which constituted the "Eleusis Mysteries".

Recent excavations proved that this sacred centre existed during the prehistoric period and was active till the 4th AD century. In the existing ruins of the Temple, one can distinguish the traces of successive constructions, representing all the periods of antiquity, from pre–Mycenae to Roman period. The site corresponds to a typical urban–centre profile of intense and diversified industrial activity as well as that of climatic conditions favouring photo–chemical pollution in the presence of an atmosphere highly charged by suspended particles.

The rock samples from the Eleusis Temple were measured for their dry density (d), water absorption (Ab), dry compressional wave velocity (v_p), compressive strength (σ_c), tensile strength (σ_t), modulus of elasticity (E), cohesion (c) and angle of internal friction (φ) . Tests were applied on minicores of 1 in. diameter and 30 mm height, prepared using a core drilling machine. Abrasion resistance was measured on specimens of 1 in diameter and 10 mm height. Minicores without visible fractures were collected carefully to be representative of the lithology. The surfaces of the minicores were shaped to ensure flat ends. The height to diameter ratio of specimens generally required for mechanical tests is 2:1 to 2.2:1 (Jaeger and Cook, 1979) but the specific conditions (material derived from the monument) obliged us to use specimens with the above dimensions. All the samples used were collected from the ruins of the Temple (walls, basement, columns, etc,). The test results are given in Table 1.

Fig. 1   Columns of pentelic marble in the Temple of Eleusis

Table 1 Physical and mechanical properties studied samples from the Temple of Eleusis. d: density, Ab: water absorption, σc: compressive strength, σt: tensile strength, c: cohesion, φ: angle of internal friction, E: Young's modulus (c, φ and σt were measured using the "Brazilian method")

ROCK TYPE		V_p (m/s)	d (gr/cm³)	Ab (%)	σ_c (MPa)	σ_t (MPa)	φ°	c (MPa)	E (MPa)	AR %
SAMPLE A	Gray micritic limestone	6486	2.68	0.68	77.4	9.73	42	17.38	20650	3.56
SAMPLE B	White "pentelic" marble	5833	2.71	0.22	99.5	11.50	44	20.90	38480	1.40
SAMPLE C	White gray marble	5776	2.73	0.35	88.5	10.62	43	19.00	33200	3.07
SAMPLE D	Yellow limestone	4237	2.48	5.19	48.7	6.20	41	10.96	15480	5.08
SAMPLE E	Gray biomicritic limestone	5300	2.56	0.41	57.5	6.64	44	12.07	17600	4.00
SAMPLE F	Yellow-brown limestone	5073	1.76	1.2	50.9	5.50	45	10.43	14500	5.72
SAMPLE G	Yellow-brown fossilif. limestone	3893	2.42	3.51	48.7	5.50	45	10.05	14500	5.98

Table 2 Density (d), Water absorption (Ab), Uniaxial compressive strength, (UCS, MPa), Young's modulus (E, GPa) and Ultrasonic velocities of limestones from Cadiz (quarry), along the x,y,z direction as well as Ratio z/x of the ultrasonic velocity (V, Km/s), uniaxial compressive strenght (UCS, MPa) and Young's modulus (E, GPa).

No	d (gr/cm³)	Ab (%)	UCSz (MPa)	UCSx (MPa)	Ez (GPa)	Ex (GPa)	Vx (Km/sec)	Vy (Km/sec)	Vz (km/sec)	Vz/Vx	UCSz/UCSx	Ez/Ex
I	2.66	5.45	76.10	76.03	16.30	17.44	4.54	4.54	4.36	0.96	1.00	0.93
II	2.60	4.42	82.60	79.20	20.00	18.03	4.8	4.49	4.84	1.01	1.04	1.11
III	2.54	4.74	85.86	86.44	20.51	21.25	4.95	4.91	4.88	0.99	0.99	0.96
IV	2.53	4.41	76.98	83.53	17.12	19.92	4.89	4.9	4.34	0.89	0.92	0.86
V	2.63	3.6	90.69	89.52	25.06	24.03	4.97	5.1	5.11	1.03	1.01	1.04
VI	2.54	3.38	91.92	93.67	26.48	27.65	5.15	5.1	5.09	0.99	0.98	0.96
VII	2.48	3.63	78.58	89.32	21.34	24.95	5	4.89	4.46	0.89	0.98	0.86
VIII	2.65	3.70	96.58	97.97	27.80	29.90	5.2	5.07	5.17	0.99	0.99	0.93
IX	2.56	3.63	89.46	90.35	27.90	26.38	5.1	5.1	5.11	1.00	0.99	1.06
X	2.60	3.95	93.11	89.23	28.26	25.79	5.1	5.15	5.17	1.01	1.04	1.10
XI	2.80	2.68	82.03	84.40	22.75	22.50	4.9	4.9	4.68	0.96	0.97	1.01

4. The Cathedral of Bari in Italy

The Cathedral of Bari, Italy, is of the XII century and is located in the central Mediterranean where it is exposed to marine environment influenced by air currents both from the north and from the south–east. It is constructed with Cretaceous limestone and has four portals in marble, including the central one, and fifth portal in limestone.

The monument shows notable phenomena of sulphurization of the marble and weathering of the limestone on both the external facade and inside the church The rock samples form Bari, were tested for their dry density (d), water absorption (Ab) and dry compressional wave velocity (Vp). The samples were very small, so the above physical properties were measured on specimens without specific dimensions. Test results are given in Table 3.

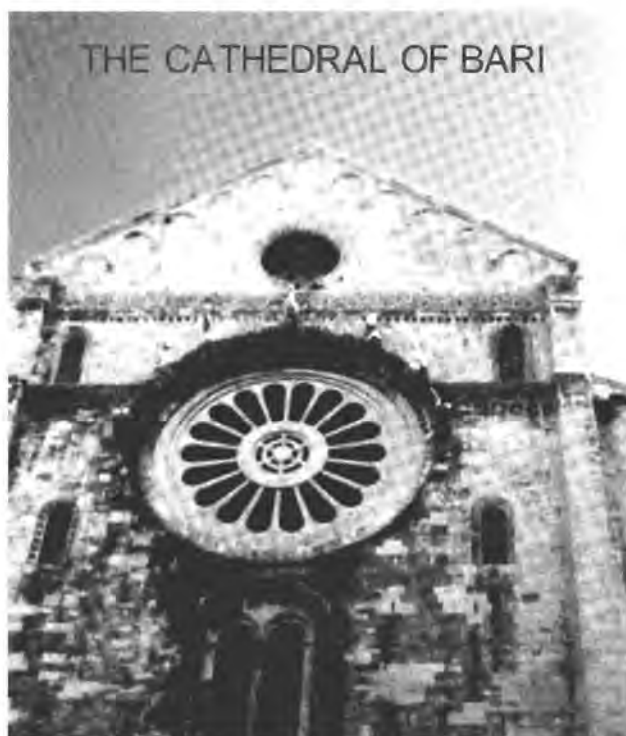*Fig. 2 The Cathedral of Bari (Italy).*

Table 3   Physical properties of limestone samples from Cathedral of Bari. d: dry density, Ab: water absorption, Vp: ultrasonic velocity

Samples	d (gr/cm^3)	Ab%	Vp (m/s)
30	1.85	4.10	4100
31a	2.30	2.10	4400
31b	2.31	2.48	4500
32	2.31	2.50	4500
41	2.29	2.58	4500

5. The Cathedral of Cadiz in Spain

The Cathedral of Cadiz (18th and 19th centuries) may be considered the masterwork of Vicente Acero y Arebo. The building's style is "post–dated". He planned the interior with three naves, an ambulatory surrounds the chancel, which is of circular plan and covered by a dome (upon tambour). The styles adopted during the Cathedral's construction can be summarised as follows: Baroque period for the ground–plan and interior elevations up to the capitals, Rococo in its ornamentation and of Neo–classical style in the shell of the principal facade, dome and towers.

Eleven representative specimens of limestone, collected from the quarry, probably used for the construction, were tested regarding their density (d), water absorption (Ab), ultrasonic velocity (V), uniaxial compressive strength (UCS) and elastic modulus (E). The specimens used were cubic, of dimensions 5x5x5 cm. The ultrasonic velocity was measured along the three axes x, y, z of the specimens, in order to determine the probable

Cathedral of Cadiz

anisotropy existed. For the same reason the uniaxial compressive strength and the Young's modulus were measured along the axes x & z.

The test results, given in Table 2, were interpreted statistically in order to determine significant correlation between the properties examined. Furthermore correlation diagrams of the anisotropy of ultrasonic velocities, compressive strength and elastic modulus, measured along the different axes were made in order to determine a significant relationship between the results of these methods.

The changes of the magnitude of the properties studied as well as the correlation observed between these properties are given in the diagrams of the Figures 4 and 5. The diagram of Figure 4 provides a relationship between the properties tested.

This relationship is more significant between the properties detected along the same direction.

This relationship becomes more significant in the diagram of Figure 5 where the changes of the ratios Vz/Vx, UCSz/UCSx and Ez/Ex, along the z and x axes improve the dependence of these properties on the anisotropy of the rock material. Furthermore no significant relationships are observed, in Figure 4, between the "linear" properties, such as the ultrasonic velocity, the uniaxial compressive strength and the Young's modulus, and the "volume" properties, such as the dry density and the water absorption.

The relationships of the ultrasonic velocity with the uniaxial compressive strength and the elasticity (Young's modulus), along the same axis, is presented in Figure 5. These diagrams provide a very significant correlation between the above properties, separately for the axes z and x. The influence of the anisotropy on the physico–mechanical behaviour of a stone is more clear in the diagrams of Figure 5. In these diagrams a very significant correlation is observed between the ratios Vz/Vx, UCSz/UCSx and Ez/E. According to these diagrams, the use of the non destructive method of the ultrasonic velocity is possible for measuring the anisotropy of the material as well as the change of its compressive strength and elasticity.

CADIZ. Biocalcarenite from the quarry. Physical and mechanical properties.
Cubic specimens (5x5x5 cm) tested along the x,y,z directions.
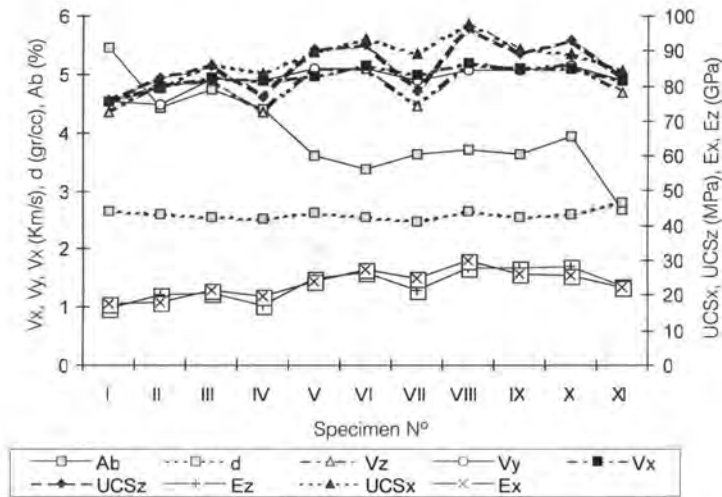
Fig. 4   Changes of physical and mechanical properties of the biocalcarenite used in the construction of
the Cathedral of Cadiz. The specimens were collected from the quarry.
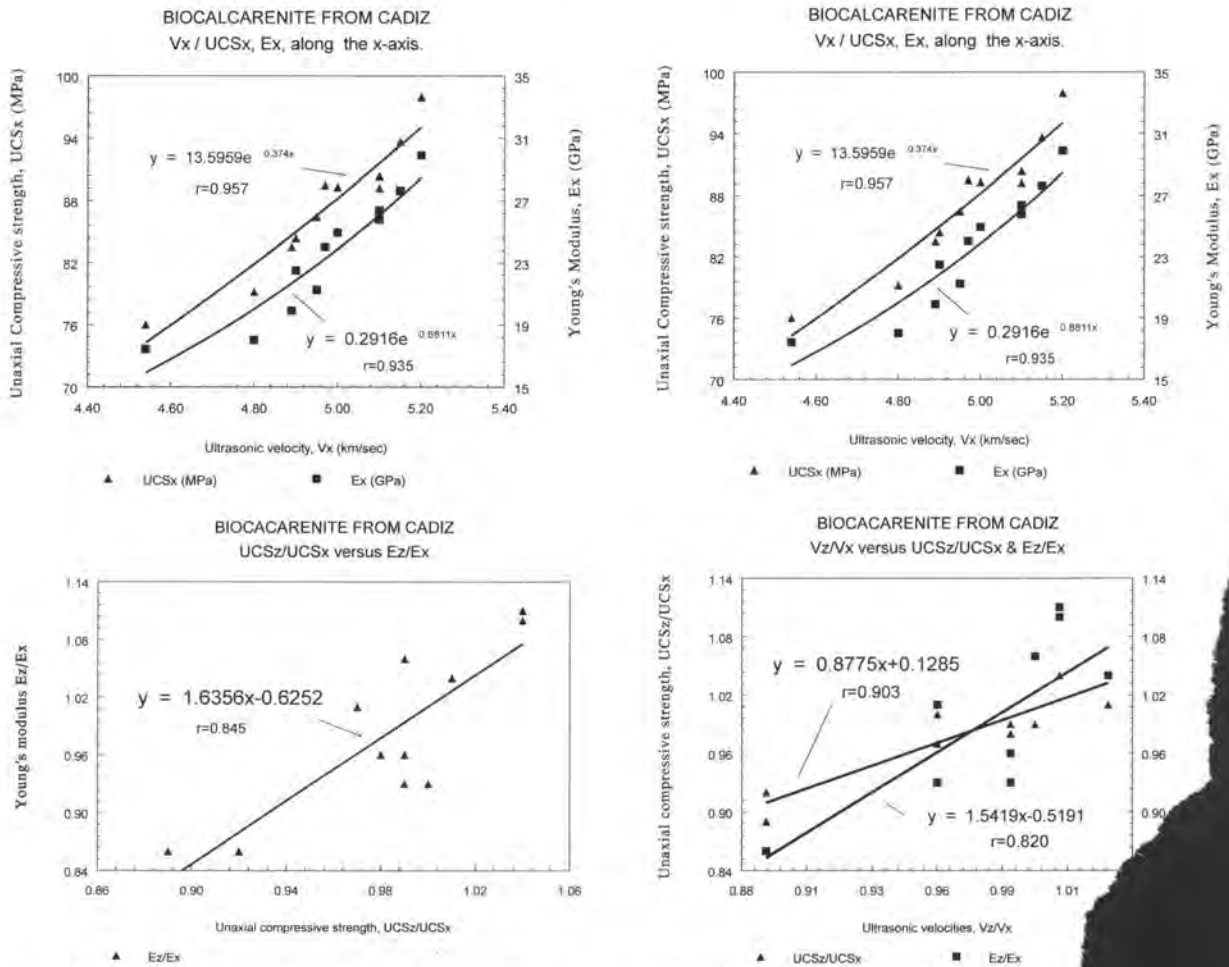
Fig. 5   Biocalcarenite used in the Cathedral of Cadiz. Samples collected from the quarry. Co
diagrams of the mechanical properties along the x and z axis.

6. The church of Sta Marija Ta' Cwerra in Malta

The Church of Sta Marija Ta' Cwerra at Siggiewi, in Malta, is located on an island, in the centre of the Mediterranean, having a typical marine environment. The church is constructed with Globigerina limestone, which is the main rock type in the island. It is mentioned that this rock is the only raw material used in the construction of all the old and new buildings in the island.

Twenty representative specimens of limestone, collected from the Mqabba quarry in Malta, were tested regarding their density (d), water absorption (Ab), ultrasonic velocity (V), uniaxial compressive strength (UCS) and elastic modulus (Young's modulus, E). The specimens used were cubic, of dimensions 5x5x5 cm. The specimens were collected from two different geological layers, which are exploited for construction materials, in the same quarry.

It is very probable that stones from both layers were used in the construction of the church in study. The specimens 1 to 10 correspond to the lower layer while the specimens 11 to 20 correspond to the upper layer. The ultrasonic velocity was measured along the three perpendicular axes, x, y & z while the uniaxial compressive strength and the elasticity were measured along the axis z, which corresponds to the z–axis of the rock formation in the field. This axis is perpendicular to the stratification of the limestone.

Test results are given in Table 4. These results were interpreted statistically in order to determine relationships that express the interaction of the physico–mechanical properties of the stones. Tests on specimens, well prepared, taken from the south wall of the church, gave the following mean values: d= 1.77 gr/cc, Ab=15.6%, V= 2.986 Km/s, UCS= 40.93 Mpa, E= 10.20 Gpa.

According to Figure 8, the test results differ in the two layers. The uniaxial compressive strength, the elastic modulus, the ultrasonic velocity and the dry density are always higher

Fig. 6   A part of the external southern wall of the church. Numbers correspond the points of measurements.

in the upper layer while the water absorption is higher in the bottom. Consequently, the above properties provide significant correlation, separately in each layers (Figure 9). These diagrams show that the water absorption correlates significantly with the dry density while the ultrasonic velocity correlates with the uniaxial compressive strength and the Young's modulus, providing a possible use for the determination of the changes of the mechanical behaviour.

In–situ measurements were also made, on the external part of the south wall, in addition to the above laboratory tests. This wall is strongly weathered and presents very important changes of weathering from place to place corresponding to probable changes of the mechanical behaviour. A part of the wall was investigated regarding the indirect ultra-

sonic velocity (V) (arranging the transducers on the same surface) in relation to the Schmidt hammer values (SHV). Test results are given in Table 5. The compressive strength (CS) corresponding to the Schmidt hammer values measured, are also given in the same Table. The significant correlation that presents the ultrasonic velocity with the Schmidt hammer values in Figure 7 provide a possible used of both of them in determining the weathering and the mechanical behaviour of a weathered surface. The points where the tests were applied on the wall are given in Figure 6. In order to measure the indirect ultrasonic velocity, a mean value of three measurements in different distance were used, and the results were verified to be similar, so as to avoid errors from cracks.

STA MARIJA TA' CWERRA, MALTA
Limestone from the wall

$y = 12.3464e^{0.5589x}$
$r=0.969$

$y = 22.5176e^{0.2432x}$
$r=0.967$

Schmidt hammer value, SHV

Correspond. compress. strength, CS (MPa)

Indirect ultrasonic velocities V (Km/s)

▲ SHV   ■ CS (MPa)
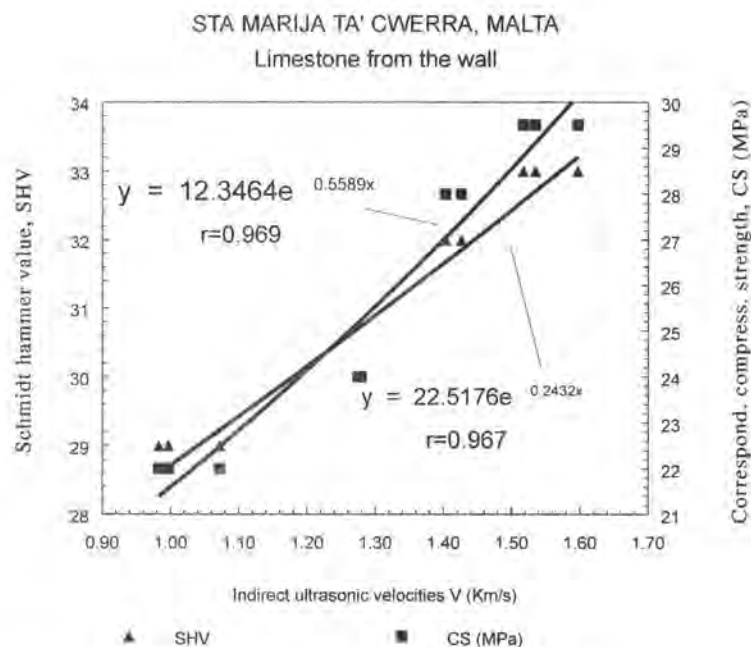
*Fig. 7   Correlation between the surface compressive strength and
the indirect P–wave velocity measured on the external
south wall of the church of Sta. Marija Ta' Cwerra.*

MALTA. Limestone from the Mqabba quarry. Physical
and mechanical properties. Samples 1-10: Lower layer.
Samples 11-20: Upper layer
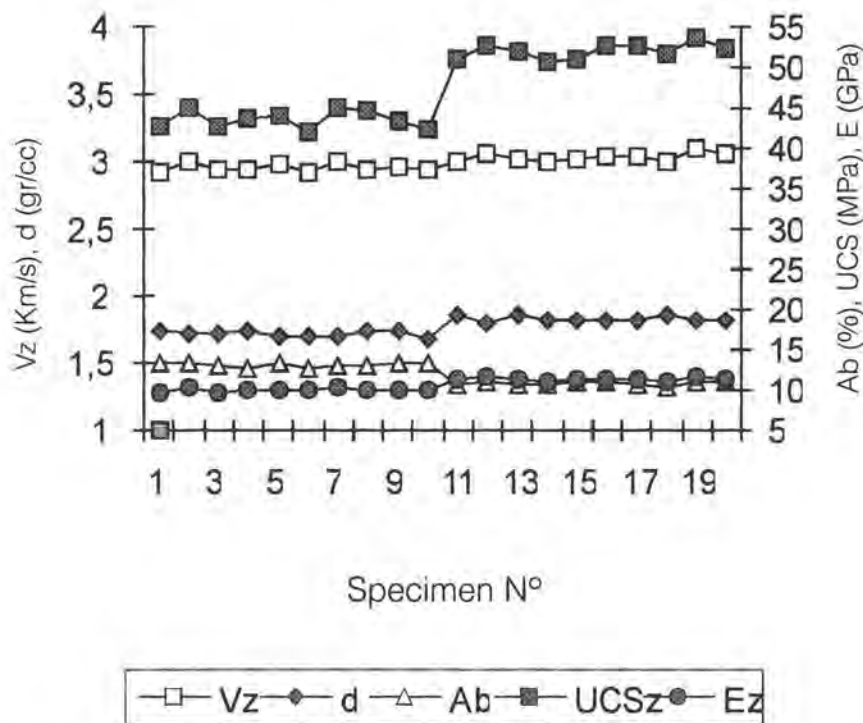
Specimen N°

*Fig. 8 Limestone used in the construction of the church of Sta. Marija Ta' Cwerra. Physical and me-
chanical properties of specimens from the Mqabba quarry. The tests were applied perpendicularly
to the stratification. Samples 1–10: Lower Layer. Samples 11–20: Upper layer*
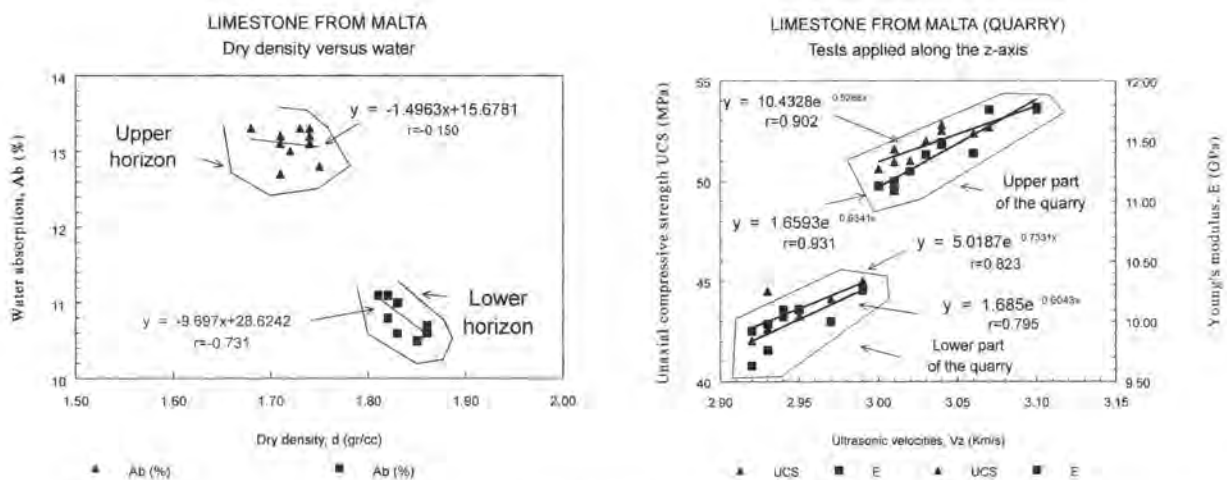
*Fig. 9 Limestone used in the construction of the church of Sta. Marija Ta' Cwerra. Samples collected
form the Mqabba quarry. Correlation diagrams of the mechanical properties, separately for
each layer*

Table 4   Density (d), Water Absorption (Ab), Uniaxial compressive strength along z–axe (UCSz), Young's modulus along z–axe (Ez) and Ultrasonic velocities (Vx,y,z), along x,y,z directions, of the limestones from Malta (quarry). Samples 1–10: Lower layer, Samples 11–20: Upper layer.

No	d (gr/cm³)	Ab (%)	UCSz (MPa)	Ez (GPa)	Vx (Km/sec)	Vy (Km/sec)	Vz (Km/sec)
1	1.74	13.3	42.55	9.63	2.85	2.86	2.92
2	1.73	13.3	45.03	10.27	2.98	2.99	2.99
3	1.72	13.0	42.64	9.76	2.89	2.99	2.93
4	1.75	12.8	43.54	10.10	2.98	2.94	2.94
5	1.71	13.2	44.12	10.00	2.75	2.78	2.97
6	1.71	12.7	42.04	9.92	2.85	2.70	2.92
7	1.71	13.1	44.92	10.26	2.97	2.95	2.99
8	1.74	13.1	44.51	9.98	2.90	2.80	2.93
9	1.74	13.2	43.27	10.10	2.86	2.77	2.95
10	1.68	13.3	42.24	10.06	2.86	2.84	2.94
11	1.86	10.7	50.97	11.17	3.05	2.99	3.01
12	1.81	11.1	52.69	11.76	3.07	3.12	3.07
13	1.86	10.6	52.01	11.39	3.07	3.03	3.03
14	1.83	10.6	50.61	11.13	3.11	3.07	3.00
15	1.83	11.0	51.02	11.25	3.03	3.03	3.02
16	1.83	11.0	52.81	11.49	3.07	3.08	3.04
17	1.82	10.8	52.52	11.47	3.02	3.06	3.04
18	1.85	10.5	51.60	11.09	3.04	3.00	3.01
19	1.83	11.0	53.57	11.78	3.13	3.08	3.10
20	1.82	11.1	52.40	11.40	3.04	3.11	3.06

Table 5   Indirect ultrasonic velocities (V), Schmidt hammer values (SHV) and the derived compressive strengths (CS) of the limestone external south wall of Sta. Marija Ta' Cwerra (Malta)

No	Lenght/Time (cm/s)	Mean V (Km/s)	SHV	CS (MPa)
1	3/29.4 5/51.2 6/62.5	0.983	29	22.0
2	3/24.2 5/38.7 6/46.4	1.275	30	24.0
3	3/27.5 5/48.1 6/55.2	1.072	29	22.0
4	3/29.9 5/49.6 6/62.1	0.997	29	22.0
5	3/21.5 5/34.1 6/42.2	1.426	32	28.0
6	3/19.5 5/32.0 6/39.1	1.535	33	29.5
7	3/20.0 5/32.9 6/39.2	1.517	33	29.5
8	3/18.8 5/31.4 6/37.4	1.597	33	29.5
9	3/21.4 5/35.2 6/43.2	1.403	32	28.0
10	3/23.3 5/39.2 6/47.1	1.279	30	24.0

7. Conclusions

In the present paper four Mediterranean monuments were studied regarding the physical and mechanical properties of the building stones used. This research was performed in the framework of the EU project "Marine spray and polluted atmosphere as factor of damage to monuments in the Mediterranean coastal environment (EV5V–CT92–0102)".

During this study several non–destructive experimental methods were used in order to determine their ability in investigating the changes of the physico–mechanical behaviour of the stones regarding to their anisotropy and weathering conditions. The purpose was to establish a common methodology of research, in which the minimum testing material from the monument is necessary to be used.

The abrasion resistance proposed technique can provide data concerning the surface hardness of a rock sample. The knowledge of this property is very useful, especially after accelerated experimental weathering and consolidation.

The P & S waves velocities, using the direct and indirect methods, provide data not only for the mechanical behaviour and the deformation ability of a stone but also for its anisotropy, the weathering conditions and the depth of weathering at a stone surface. It can also be used to distinguish very similar geological layers, like in the limestone of Malta. It can be used for laboratory and *in situ* measurements.

The Schmidt hammer can be used in the weathering mapping of a stone wall surface, providing data which are related to the surface weathering conditions as well as to the surface compressive strength of the stones. The test results collected using this method are related significantly to that collected using the indirect ultrasonic technique, confirming so the accuracy of the method used.

The uniaxial compressive and tensile strengths were performed using only small specimens and the results were correlated with other acceptable properties.

The dry density and the water absorption were also used to provide data concerning the behaviour of the stones of study.

8. References

1. Christaras, B., Auger, F. & Mosse, E. (1993): Determination of the elastic moduli of rocks. Comparison of the ultrasonic velocity and mechanical resonance frequency methods to the direct static one. *Materials & structures*, 27, pp. 222–228.

2. Christaras, B. (1995): Mechanical behaviour of basalts from Costa Rica rift, Hole 504B, Leg 137. *Proc. ODP, Sci. Results*, College Station, TX, 137/140, pp. 347–351.

3. Christaras, B. (1996): Non destructive methods for investigation of some mechanical properties of natural stones in the protection of monuments. Bull. IAEG (in press).

4. Duriez, M. ET Arrambide, J. (1962): Nouveau tratté (des matériaux de construction. Dunod, Paris.

5. Jaeger, J.C. & Cook, N.G.W. (1979): Fundamental of Rock mechanics (3rd ed.) Chapman & Hall. New York, 543 p.

6. Johnson, R.B. & De Graff, J.V. (1988): Principles of Engineering Geology. John Wiley & Sons Publ., New York, 497 p.

7. Topal, T. (1995): Ultrasonic testing of artificially weathered cappadocian tuff. Proceed. of Congr. LCP '95: Preserv. and Restor. of Cultur. Heritage, Montreux (in press).

8. Zezza, U. (1991). Decay evolution depending on the textural anisotropy of marbles in monuments. Proceed. 2nd Intern. Sypm. Conserv. Monum. Medit. Bassin, Geneve, pp. 289–302.

Rossella Corrao
Giovanni Rizzo
Carmelo Sunseri

Weathering of building stones in the mediterranean coastal environment. Analysis of samples from Hopps Palace in Mazara del Vallo (Sicily)

Weathering of building stones in the mediterranean coastal environment. Analysis of samples from Hopps Palace in Mazara del Vallo (Sicily)

R. Corrao — *Dipartimento di Progetto e Costruzione Edilizia, Università di Palermo, Italy*
G. Rizzo — *Dipartimento di Ingegneria Chimica dei Processi e dei Materiali, Università di Palermo, Italy*
C. Sunseri — *Dipartimento di Ingegneria Chimica dei Processi e dei Materiali, Università di Palermo, Italy*

Abstract

In this work a case of stone decay process in the Mediterranean area is presented. Hopps Palace is the residential part of a wine factory, built at the beginning of XIX century in Mazara del Vallo, a town located on the south-west coast of Sicily.

A calcarenite with poor mechanical properties and high porosity was used for walls, whereas a material with higher properties was used for pilaster strips and skirting board. Significant effects of stone alteration are evident in different parts of the building.

As a preliminary approach to the understanding of the origin of such destructive phenomena, samples were taken from different points of the building. For comparison samples were also taken from two other buildings, where similar stones were used (probably from the same quarries): one in a rural area (no direct marine spray and no air pollution), the other one in the center of the town (moderate effect of marine spray, high concentration of air pollutants).

All samples of weathered stone were observed by Scanning Electron Microscope (SEM), equipped with Energy Dispersive X-ray microprobe. Taking into account the different weathering conditions due to the original location and orientation of samples, data can be partially related to the morphology of the degraded parts of the buildings.

Moreover some comments are reported on a recent restoration of the left wing of the palace, carried out without a proper knowledge of the origin of the stone decay processes.

1. Introduction

The Countries of the Mediterranean Basin have the huge responsibility of the maintenance of the most important and valuable heritage of monuments in the world, which the great civilizations of the past used to build there for thousands of years. In spite of the idea of eternity still suggested by some magnificent constructions, all building materials, both natural and artificial, undergo degradation processes, which could distort or even interrupt the cultural message from our forefathers.

Limestone is a building material used in a great variety of valuable monuments, as it is abundant all over that geographic area. For this reason the decay processes of limestone have been widely investigated by many researchers (1–14) taking into account two main factors: on one hand both composition and structure of the stone, on the other hand the environmental conditions of the site.

A multi-disciplinary approach to the understanding of degradation mechanisms is the only correct procedure for a successful conservation intervention. In view of this important goal, it is helpful to consider many examples of degraded materials in different environmental conditions. The coastal belt of the Mediterranean Basin is an interesting laboratory, rich of such examples.

2. Environmental conditions

Mazara del Vallo, located on the south-west coast of Sicily, has a central position in the Mediterranean Basin (Fig. 1).

Fig. 1 Location of Mazara del Vallo

It rises on the left side of Mazaro river. Since 827, arabians called this river «Wadi al Wagnum»[1] with reference to the "Marrobbio"[2] phenomenon. The flat land surrounding the town is chacterized by emerging rocks, called "sciare", and by the presence of a lot of quarries, still producing ashlars of calcarenite used for building in that area. Its climate is mild during all the year (15). In winter, due to the effect of warm mediterranean waters, the average temperature never drops beneath 10°C. Therefore there is no problem related to freezing of water in the pores of the stone, while it cannot be neglected that abundant rains produce washing of the surface of the buildings.

In summer strong solar radiation with a long dry spell sometimes produces peaks in the maximum temperature up to 30–35°C. This often occurs when "Scirocco" blows, a violent wind from south–east. These concurrent factors favour the formation of marine spray, its deposition on the surface of monuments and the rapid evaporation of water from the surface.

As for the air quality, the situation is quite favourable, because of the absence of polluting industrial activities. The main source of aggressive components in the air is the circulation of vehicles. As a minor contribution, also the decomposition of organic matter, deposited on the shore by both seastorms and "Marrobio", can be mentioned.

3. Hopps Palace

It was built outside the walls of the old city, during the first thirthy years of XIX century. It is part of the Hopps wine factory, considered by Puglisi «...the second wine factory built in Sicily...» (16). It was completed in 1832 and was the residence of Hopps family, one of the english families given to production of Marsala wine, living in that region from the end of XVIII century to the first years of XX century (17).

---

[1] «Wadi al Wagnum», «fiume dello spiritato», so called by the arabian geographer Edrisi.

[2] The "Marrobbio" phenomenon consists of a sudden and violent sea agitation and rising of water level, occurring just after a calm period following the breathing of strong winds from second to fourth quadrant. According to the Hydrographical Institute of Genoa, this is due to the contemporary rage of strong winds from west and from south–east: as effect of the waves produced by these two opposite streams, sea water level rises. This phenomenon occurs with particular intensity on the shore of Mazara del Vallo. As a consequence also the level of Mazaro river rises and mud, algas and ground materials are trasported ashore, where they decay in the following days, thus producing some aggressive gases, such as H_2S, and smelling rotten.
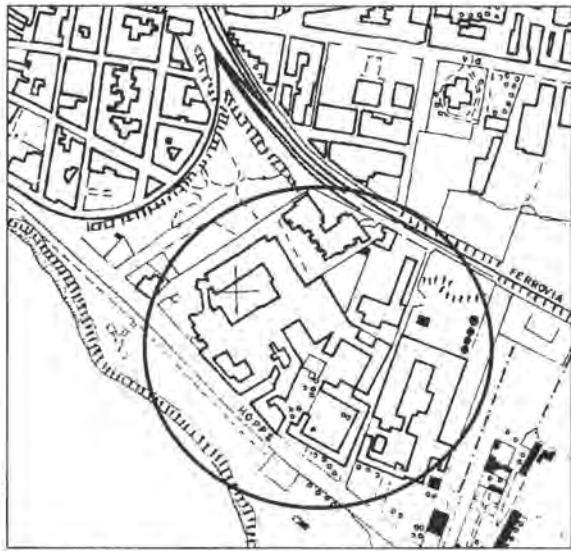
Fig. 2 Hopps Palace with wine factory

The palace, with multiple courtyards surrounded by sheds and stores of the wine factory, was a symbol of the economic power of the borning ninteenth century middle class (Fig. 2).

Nowaday its ruinous state testifies the default of the social and economic conditions that favoured the success of such entrepreneurial activities. It was built in front of the sea in a classical style, pseudo–reinassance, with the use of decorative elements as partitions of the façade, made of a stone of good quality that did not need plastering.

The façade is composed with six pilaster strips, including two angular elements. These intersect other decorative horizontal bands at the first floor, the basament and the cornice, all made of the same large ashlars as the pilasters. The same material was used to square the windows of both the ground floor and the first floor.

The walls included in the squares of the façade were built with ashlars of calcarenite of poorer quality, which most probably was cheaper than that used for the decorative elements. For this reason their surfaces were originally covered by plaster.

4. Materials

The significant differences pointed out in the decay level of different architectonic elements of the façade (pilaster strips, cornice, basament, walls), in spite of the fact that they had been exposed to the same ageing conditions, suggest the opportunity of investigating the properties of the original materials as quarried. Unfortunately the documents available about the building of the palace are not enough for locating for a certainty the sites where the ashlars were quarried from. However, historical data about many monuments built in the same period (17, 18), indicate two areas as probable origin of the materials: the quarries of "Terrenove", west of Mazara, for ashlars of decorative elements, the quarries of "San Nicola", south–east of Mazara, for ashlars of the walls. In the second part of this study, samples taken both from the quarries and from unweathered parts of the building will be analysed with the cooperation of geologists, in order to investigate their chemical and mineralogical characteristics and their porosity. The results will possibly confirm the assumption about the origin of the ashlars and in any case they will supply the basic knowledge for thoroughly understanding the mechanisms of degradation processes occurred in the building during more than one century.

For the time being an exhaustive study of the materials from both quarries is available in the literature (19). According to the assumption that they were used originally in Hopps Palace, in the following the main properties of such stones are reported from this study.

As for the area of Terrenove, the quarries are still active and «...present a red and thin outcrop (about 50 cm). The ashlars quarried are yellow–reddish, medium–grained with the presence of big fragments of lamellibranchia's valves and small calcareous pebbles. Good cementation allow to quarry well squared ashlars...» (19).

On the contrary the San Nicola quarries
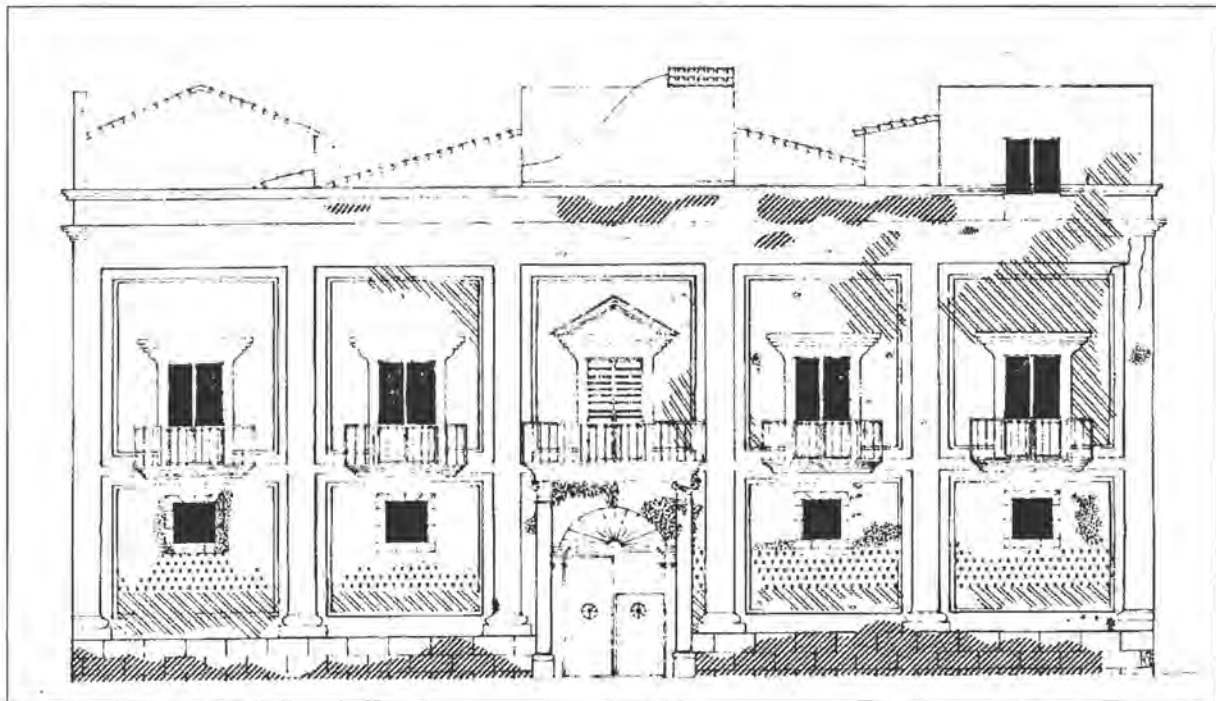
Fig. 3   Hopps façade before the last "restoration" of the left wing. The degraded areas are pointed out according to NorMaL 1/88
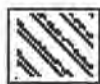
Erosion	*Staining*	*Efflorescence*	*Sanding*

produce a yellow calcarenite, medium–grained, showing high porosity and poor cementation, with many fragments of lamellibranchia's valves and macrofossils. It is difficult to obtain well squared ashlars from these material because of its low mechanical properties.

It can be pointed out that, due to its high porosity, the stone from San Nicola has poorer quality than Terrenove stone with reference to both mechanical properties and durability.

5. Decay processes

De visu observation of the façade reveals the presence of many different forms of decay, as pointed out in Fig. 3 according to NorMaL 1/88 standard (20). The morphology of both alteration and macroscopic degradation of the stone in some areas suggests the action of concurrent processes (21), such as erosion, efflorescence, staining, sanding. The location of de-

graded areas on the façade indicates the major role of water migration in the porous materials. It is caused by many different factors such as defects in the system of drain pipes and gutters, rain washing of the walls, rising of damp from the ground in to the walls, marine spray from the nearby shore. Furthermore the deep erosion of the ashlars under the windows of the ground floor could be increased also by the action of winds, carrying sand from the surroundings.

Because of the location of the palace, with its principal façade in north–west south–east direction, on the sea shore drive, exposed to strong winds of Scirocco and Maestrale and to the direct action of marine spray, as a first rough approach to diagnosis of present ruinous conditions of the building, we embraced the reasonable assumption that the most relevant contribution to stone deterioration can be related to salt decay (22).

Fig. 4a Level of decay under the windows of the ground floor as compared with the good conditions of the pilaster strip
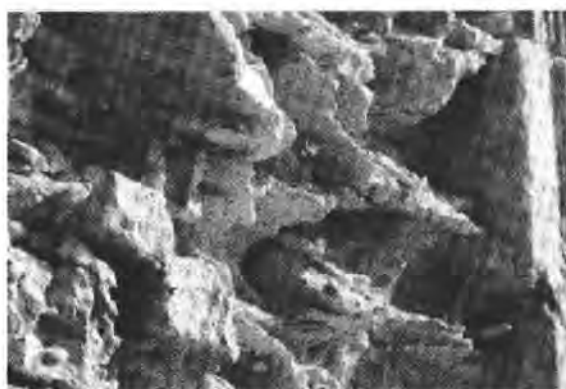
Fig. 4b Detail of the ashlars under the windows
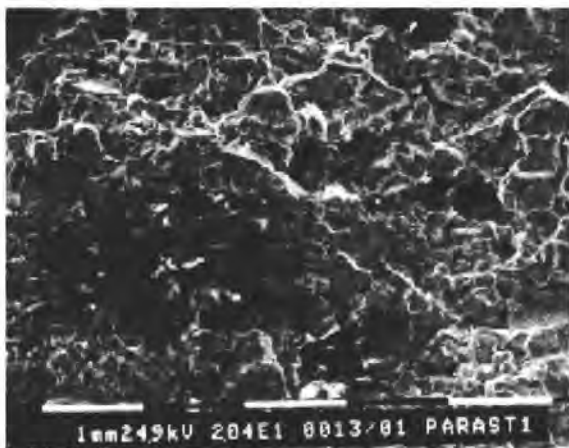
Fig. 4c Micrograph of a sample from the pilaster strip
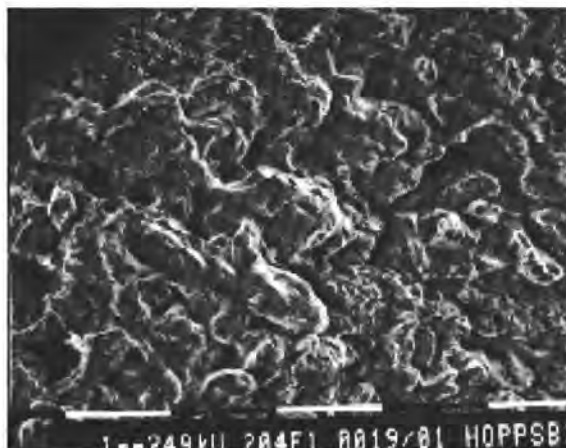
Fig.4 d Micrograph of a sample from degraded ashlars under the window

Surface samples were taken from ashlars of both materials, i.e. from walls and from pilaster strips and skirting board, in different parts of the building exposed to weathering agents. The morphology of alteration produced by salt was observed at SEM equipped with EDX microprobe and some indicative micrographs are shown in Figs. 4a to 4d. Microanalysis confirmed the presence of marine salt in all samples. It is worth pointing out the absence of black crusts, due to the low level of pollutants in that area.

Samples were also taken from other buildings, where ashlars very similar to San Nicola stone were used. The first, a palace coeval of Hopps Palace, is in the center of the town and

the second is a farm house north of Mazara, far from the seacoast. Aim of this further investigation was to compare the effect of different environmental conditions, i.e. on one hand moderate effect of marine spray and wind and high concentration of air pollutants in the center of the town, on the other hand no direct marine spray and absence of air pollution in the rural area. Some results are shown in Figs. 5a to 6b. Microanalysis indicates the presence of salt in samples from the palace in the center of the town, where forms of degradation similar to Hopps Palace can be observed. As for the farm house, in spite of the absence of salt, alveolization and deep erosion are present, probably due to the concurrent action of wind and other causes that are not taken into account in this study.

Fig. 5a   Evidence of sanding process on ashlars in a
          building in the center of Mazara del Vallo

Fig. 6a Building in the country side north of
         Mazara del Vallo, far from the shore

6. Conclusions

Hopps Palace, built on the seashore drive more than one century ago, has been significantly damaged by many weathering agents, first of all marine salt supplied by both winds and rising damp (Fig. 7). A major mechanism of degradation is migration of salt in the
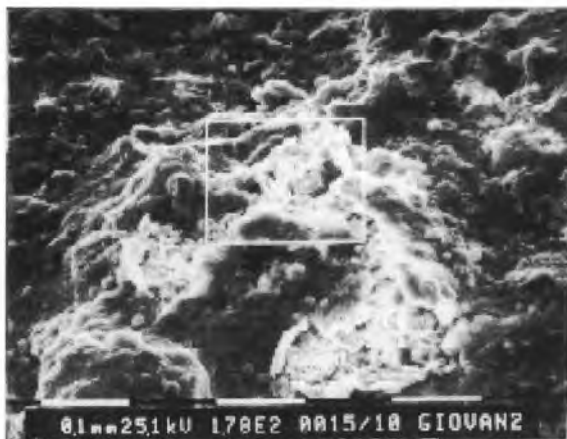
Fig. 5b   Micrograph of sample from degraded ash-
          lars. EDX analysis on the squared area in-
          dicates a significant presence of salt

Fig. 6b   Micrograph of the sample taken from de-
          graded ashlars of the corner

Fig. 7   Hopps Palace before the last restoration

Weathering of building stones in the mediterranean coastal environment.
Analysis of samples from Hopps Palace in Mazara del Vallo (Sicily)

289

porous material, favoured by water presence in the stone as a result of poor maintenance condition of the building and by subsequent crystallization at the surface. The effect on calcarenite is related to its porosity, i.e. to permeability and mechanical properties. Data in Tab. 1 account for the different response to this weathering mechanism shown by pilaster strips and skirting board on one side and walls on the other side.

Tab. 1   *Properties of calcarenite from Terrenove and San Nicola quarries.*

	Terrenove	San Nicola
Density (Kg/m^3)	2624	2614
Apparent density (Kg/m^3)	1743	1566
Water absorption, immersion (weight %)	14.82	20.04
Water absorption, capillarity (weight %)	15.16	20.70
Compressive strength, dry (MPa)	4.90	2.57
Compressive strength, saturated (MPa)	2.89	1.47

A thorough understanding of all degradation processes affecting the building needs further investigation. This preliminary study gives a description of the present condition of the stone and suggests the opportunity of using desalination procedure before any other improving operation. This is confirmed by the failure of a recent "restoration" intervention, not taking into account this suggestion. As shown in Figs. 8a and 8b efflorescences have alredy appeared on the surface of the plaster, so that a short lifetime of this protective layer can be predicted.

Fig. 8b   Detail of the left corner of the façade with evidence of efflorescences on both the skirting board and the plaster

Fig. 8a   Hopps Palace after the last "restoration"

7. References

1. Rossi Manaresi R., Ghezzo C., "The biocalcarenite of the Agrigento greek temples: causes of alteration and effectiveness of conservation treatments", *Rilem International Symposium on Deterioration and Protection of Stone Monumentes*, Paris, June 5th–9th 1978

2. Efes Y., "Investigations on correlations between the porosity and the corrosion of natural stones", *3rd International Congress on the Deterioration and Preservation of Stones*, Venezia, October 24th–27th 1979, Proceedings p. 231–243

3. Fiumara A., Riganti V., Veniale F., Zezza U., "Sui trattamenti conservativi della pietra d'Angera", *ibidem*, p. 339–355

4. Martin C., "Dessalage d'elements sculpturaux: un étape importante dans la restauration de pierres alvéolisées", *ibidem*, p. 377–387

5. Alaimo R., Deganello S., Montana G. "I marmi del Chiostro del Duomo di Monreale e della Cattedrale di Palermo. Aspetti genetici delle fasi presenti nelle superfici di alterazione. Nota I: problematica geochimica e descrizione delle superfici di alterazione", *Miner. Petrogr. Acta*, Vol.XXX, p.271–286 (1986–87)

6. Zezza F., Introductory lecture of *1st International Symposium on The Conservation of Monuments in the Mediterranean Basin*, Bari, June 7th–10th, 1989, Proceedings p. 7–28

7. Cereceda M.L., Alonso Matilla L.A., Alonso Pascual J., Galvan Llopis V., "Characteristics, forms and mechanism of weathering of stone caused by the salt spray in the stone used in the main monuments of the city of Alicante (Spain)", *ibidem*, p. 91–96

8. Rossi Manaresi R., Tucci A., "Pore structure and salt crystallization: *salt decay* of Agrigento biocalcarenite and *case hardening* in sandstone", *ibidem*, p. 97–100

9. Alarcòn–Parra S., Garcìa–Vallès M., Vendrell–Saz M., "The decay of monumental limestones on a rural mediterranean environment", *3rd International Symposium on the Conservation of Monuments in the Mediterranean Basin*, Venezia, June 22nd–25th, 1994, Proceedings p. 523–531

10. Garcìa de Miguel J.M., Sànchez Castillo L., Gonzàles Aguado M.T., "Characterization and deterioration causes of the Novelda stone", *ibidem*, p. 547–554

11. De Grado A., Puche O., Calvo B., "Hontoria's stone (Burgos, Spain). Characteristics and weathering", *ibidem*, p.589–603

12. Gomez F. "Quelques tecniques pour caractérisier l'alteration de la pierre sur un monument de la Région Mediterranéenne", *ibidem*, p. 605–609

13. Tucci P., Armiento G., Menichini P., Esposito R., "I materiali lapidei della facciata de *Le Monacelle* di Ostuni e le loro antiche cave di provenienza", *ibidem*, p. 611–617

14. Johnson J.B., Montgomery M., Thompson G.E., Wood G.C., Sage P.W., Cooke M.J., "The influence of combustion–derived pollutants on limestone deterioration: 1. The dry deposition of pollutant gases", *Corrosion Science*, Vol.38, 1996, p.105–135

15. Regione Siciliana. Ass. dei LL. PP. Servizio Idrografico Sez. Aut. del Genio Civile, *Annali Idrologici*, Palermo, Arti Grafiche Siciliane

16. Puglisi G., *La Sicilia e i suoi vini: ragguagli sugli stabilimenti enologici siciliani*, tip. F.lli Puglisi, Palermo, 1884

17. Corrao R., *Gli inglesi e le fattorie vinicole dell'Ottocento*, Report DPCE, University of Palermo, 1995

18. Corrao R., *Gli Hopps a Mazara del Vallo. Vicende di una famiglia inglese e della sua fattoria vinicola*, Report DPCE, University of Palermo, 1995

19. Cusimano G., Di Mino A., Gioè S. *Su alcune proprietà tecnologiche delle calcareniti plio–quaternarie della Sicilia occidentale*, Quaderni dell'Istituto di Costruzioni Stradali dell'Università di Palermo, 1975

20. NorMaL 1/88 *Alterazioni macroscopiche dei materiali lapidei: lessico*, C.N.R. Centri di Studio di Milano e Roma sulle Cause di Deperimento e sui Metodi di Conservazione delle Opere d'Arte – I.C.R. Istituto Centrale per il Restauro, 1990

21. Corrao R., De Vecchi A., "L'influenza dei fattori ambientali sul fenomeno dell'erosione nei paramenti in pietra", in Fumo M., Ausiello, G., *Il progetto nello spazio della memoria: segni, idee e potenzialité*, Proceedings, vol. I, Napoli, CLEAN Edizioni, 1995 p.187–196

22. Amadori M. L., Lazzarini L., Massa S., "Il deterioramento da sodio cloruro di rocce compatte e porose a Venezia", *1st International Symposium on The Conservation of Monuments in the Mediterranean Basin*, Bari, June 7th – 10th, 1989, Proceedings p. 83–89

Vasco Fassina
Anna Mignucci
Andrea Naccari
Antonio Stevan
JoAnn Cassar
Alex Torpiano

Investigation on the moisture and salt migration in the wall masonry and on the presence of salt efflorescences on stone surface in the Church of Sta. Marija Ta' Cwerra at Siggiewi, Malta

Investigation on the moisture and salt migration in the wall masonry and on the presence of salt efflorescences on stone surface in the Church of Sta. Marija Ta' Cwerra at Siggiewi, Malta

V. Fassina — *Laboratorio Scientifico–Soprintendenza ai Beni Artistici e Storici di Venezia*
A. Mignucci — *Laboratorio Scientifico–Soprintendenza ai Beni Artistici e Storici di Venezia*
A. Naccari — *Laboratorio Scientifico–Soprintendenza ai Beni Artistici e Storici di Venezia*
A. Stevan — *Syncro, AEC*
J. Cassar — *University of Malta*
A. Torpiano — *University of Malta*

1. Introduction

The aim of the present paper is to present the results obtained on the survey of the process of weathering of globigerina limestone on the Church of Sta. Marija Ta' Cwerra at Siggiewi, in the South West of Malta, which is one of the four pilot monuments studied in the E. C. Project "Marine Spray and Polluted Atmosphere as Factor of Damage to Monuments in the Mediterranean Coastal Environment".

The external walls of the church were not plastered, which is quite a usual situation for Malta. However, at some point in the past the lower course were coated with a cement–based mix, probably in an attempt to stop deterioration in this area. All four walls of the church show severe deterioration on the external faces, for about two–thirds of the height (between four to six meters from the ground). The lower courses, as already stated, are cemented over and therefore could not be examined. The middle courses are, however, badly deteriorated, mostly in the form of pronounced alveolar weathering of many of the stones, as well as the powdering of several areas; many of the blocks have also lost from the joints area. The uppermost courses, on the other hand, are much better preserved, the stone appearing quite sound, and having developed a red–brown patina quite typical of local building stone. There are, however, areas, particularly in sheltered locations, of black crust formation.

The walls are also severely deteriorated on the interior, up to the height of the cornice. The walls here are plastered, but in several areas the plaster has fallen away revealing powdering and flaking stone underneath. Some of the decorative elements in stone are also badly deteriorated, to the extent that the carvings in some places have almost completely disappeared. In general, the inside of the church appears to be more severely deteriorated than outside, occurring also to a greater height.

On the external surface alveolar erosion is present, with missing of large pieces of stone, while indoor salt efflorescences are visible, mainly near mortars.

2. Experimental part

In order to ascertain moisture and salt contents in the wall masonry and salt efflorescences on stone surface of the church, four sampling campaigns were carried out at different times.

First campaign–March 1993: samples of efflorescences were taken. In order to identify the crystalline phases x–ray diffraction was carried out. On the same samples the amount of soluble salts present was determined quantitatively by ion chromatography .

Second campaign–July 1993: samples of efflorescences were taken. Crystalline phases were identified by x–ray diffraction, while the amount of soluble salts was quantitatively determined by ion chromatography.

Third campaign–September 1993: samples of drilling core from different walls and at different heights were taken. The core samples were taken at four levels: 50, 150, 250 and 350 cm from the ground, and at two depths, 0–5

and 5–15 cm. The amount of soluble salts and the moisture content were quantitatively determined by ion chromatography and weighting measurements.

Fourth campaign–March 1995: samples of different kind have been taken. A first set consists of drilling core samples were collected at two levels (0.5 and 2.5 m) and analysed as in the third campaign, in order to identify the moisture and salt contents.

A second set of samples includes: limestone fragments; mortar fragments; saline efflorescences.

In order to assess the salt efflorescence composition and the stone behaviour in respect to the moisture adsorption, the following analyses have been carried out:

1) *X–ray diffraction to identify mineralogical phases present in the efflorescence and in the mortar;*

2) *Ion chromatography analysis to determine the quantity of soluble salts present in the efflorescence, in the mortar and in the stone;*

3) *Polished cross sections to observe the presence of external layers;*

4) *Semi–quantitative analysis of chemical elements by EDAX carried out on polished cross sections to recognise the saline distribution in respect to depth into the stone;*

3. Discussion of results

3. 1. Analyses of drilling core samples

In samples taken in the third campaign, moisture content shows a decreasing trend according to the increase of height from ground floor. Comparison of moisture content at each level generally shows higher values for samples taken at 5–15 cm of depth with respect the superficial ones. The highest moisture value measured was 12% at 50 cm of height and

5–15 cm of depth, in the north wall. At 350 cm, the maximum level measured, moisture values were between 1 and 2% indicating that rising damp is practically ceased.

As regards anions in wall masonry, a typical distribution is observed: sulphates, with a relatively low solubility are mainly concentrated in lower parts of the walls, while chlorides and nitrates in upper levels (figs. 1, 2, 3). Salts, dissolved in the water inside the walls, are transported vertically by capillary rising damp. When water evaporates there is a fractionate precipitation of different salt phases, according to their solubilities. A similar example of this salt distribution was found in the wall masonry of main façade of the Church of Sta. Maria dei Miracoli, in Venice.

The highest values of anions were found in the south wall (Tab. 1):

– chlorides have their maximum value of 3.57%, at 2.5 m of height and 0–5 cm of depth,

– nitrates reach the maximum of 1.49% at same level and depth,

– sulphates show the maximum value of 1.65%, at 0.5 m of height and 0–5 cm of depth.

As regards fourth campaign, only two levels: 0.5 and 2.5 cm from the ground were considered (fig. 4); the highest moisture value was 12,8%, in the north wall, at 0.5 m of height and from 5 and 15 cm of depth. In both campaigns, for the other walls, the moisture reached maximum values between 8 and 9% at 50 cm of height. As regards anions, in this campaign their values were generally lower than in the third campaign. This very probably could be ascribed to different meteorological conditions, occurred before sampling campaigns. Chlorides have their maximum concentration of 1,35% at 250 cm of height and 0–5 cm of depth in the west wall, nitrates reach 0,88% at the same height and depth of the north wall, sulphates reach 0,24% at 0.5 m of height and 0–5 cm of depth in the east wall (Tab. 2).

Fig. 1   *Amount of chlorides in each wall (third campaign).*
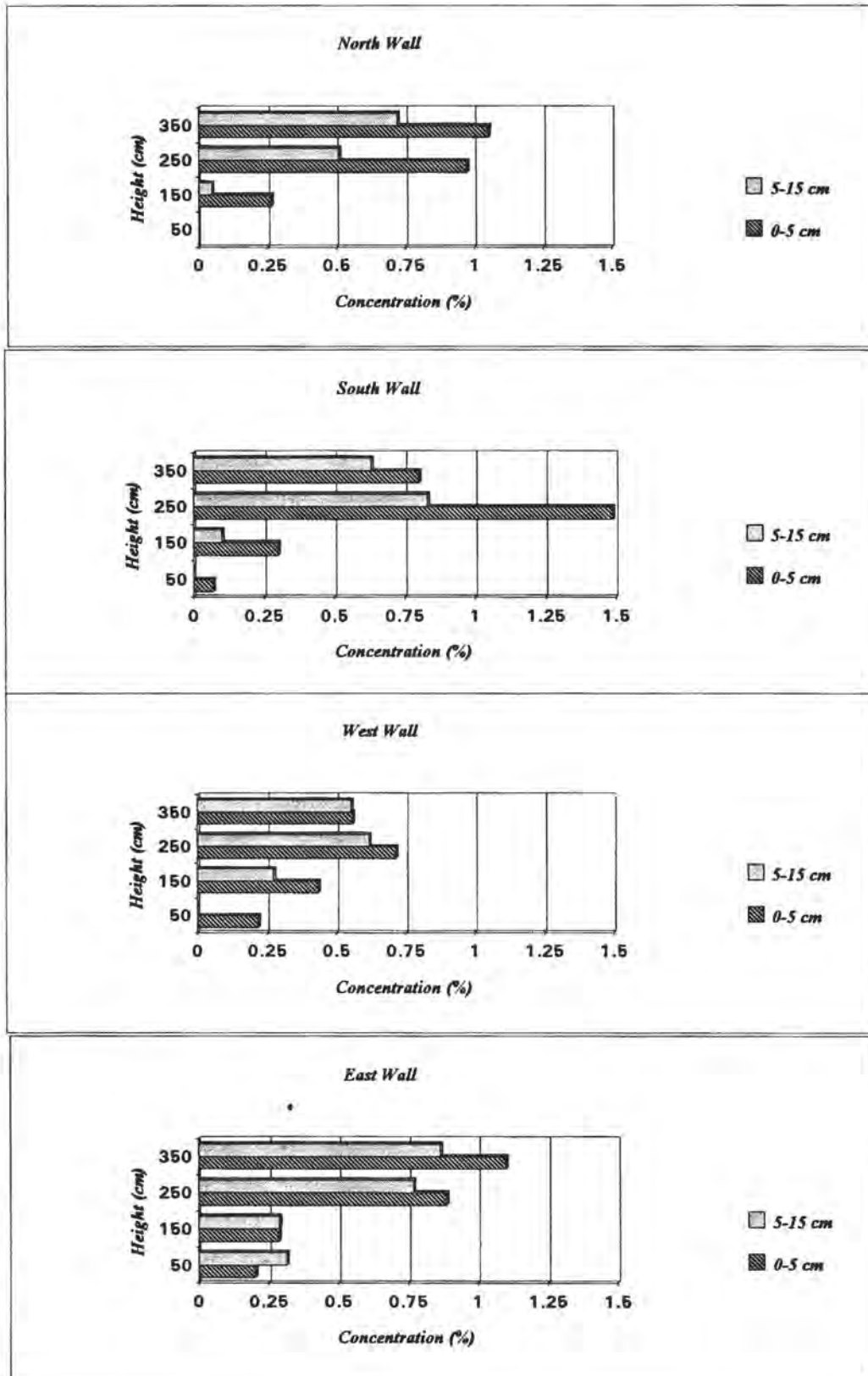
Fig. 2   Amount of nitrates in each wall (third campaign).
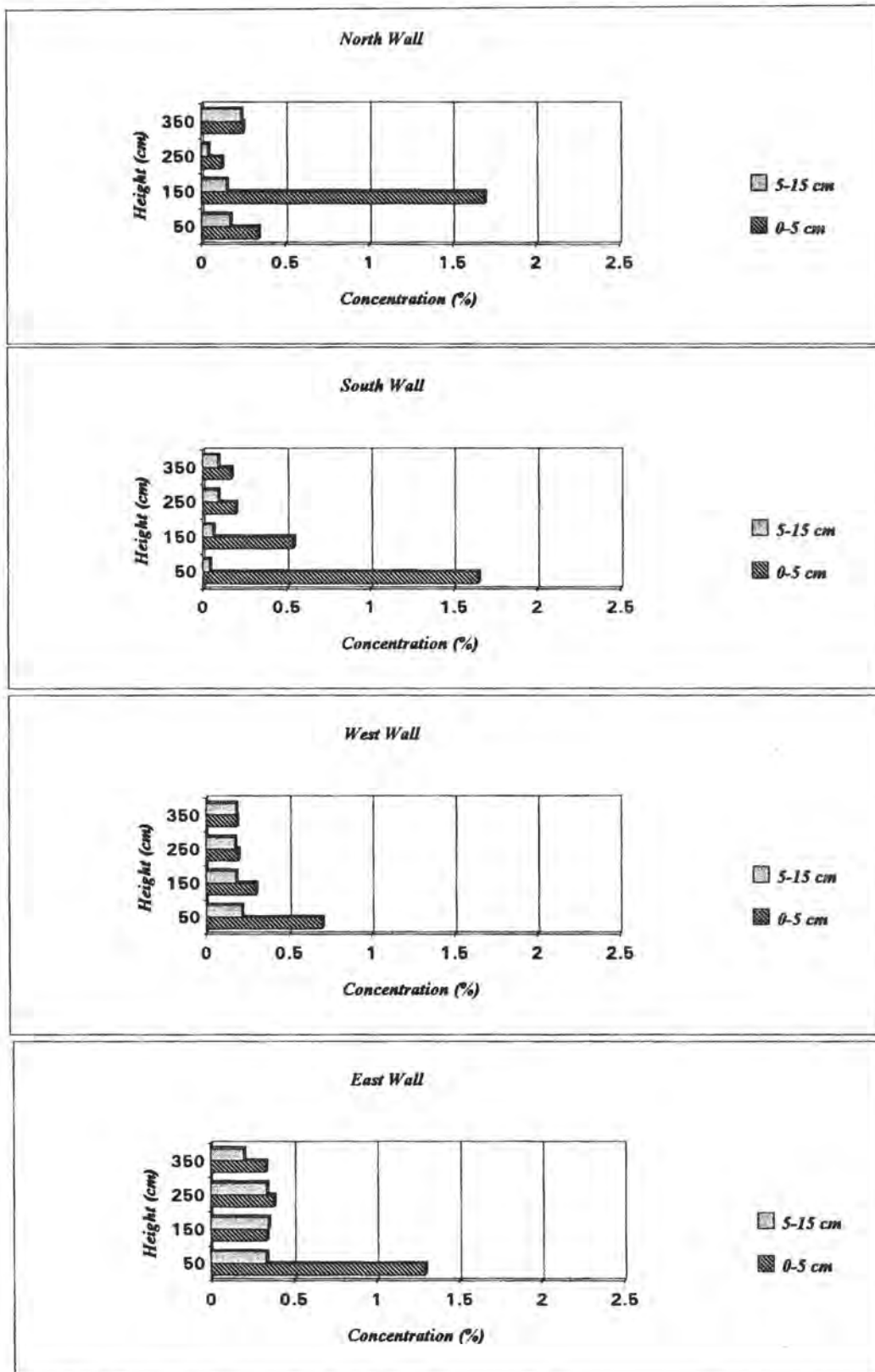
Fig. 3   Amount of sulphates in each wall (third campaign).

Tab. 1 Drilling core samples: moisture and water soluble anions content (third campaign).

Sample no.	Location (wall)	Height (m)	Depth (cm)	Moisture %	Cl^- %	NO_3^- %	$SO_4^=$ %
1	north	0.5	0 – 5	11.5	0.02	–	0.34
2	north	0.5	5 –15	12.0	0.01	–	0.17
3	north	1.5	0 – 5	4.6	0.17	0.27	1.69
4	north	1.5	5 –15	9.3	0.06	0.05	0.15
5	north	2.5	0 – 5	3.8	0.66	0.97	0.12
6	north	2.5	5 –15	4.6	0.60	0.51	0.04
7	north	3.5	0 – 5	2.9	1.46	1.05	0.25
8	north	3.5	5 –15	4.6	0.86	0.72	0.24
9	south	0.5	0 – 5	7.3	0.06	0.07	1.65
10	south	0.5	5 –15	8.5	0.02	–	0.04
11(+)	south	1.5	0 – 5	3.8	0.50	0.30	0.54
12	south	1.5	5 –15	8.2	0.24	0.10	0.06
13	south	2.5	0 – 5	4.2	3.57	1.49	0.03
14	south	2.5	5 –15	3.1	0.92	0.83	0.20
15	south	3.5	0 – 5	2.1	0.92	0.80	0.02
16	south	3.5	5 –15	1.7	0.58	0.63	0.09
17 (*)	west	0.5	0 – 5	8.0	0.12	0.22	0.70
18 (*)	west	0.5	5 –15	8.5	0.10	–	0.22
19 (*)	west	1.5	0 – 5	3.1	0.67	0.44	0.30
20 (*)	west	1.5	5 –15	3.7	0.76	0.27	0.18
21 (*)	west	2.5	0 – 5	2.0	2.27	0.72	0.20
22 (*)	west	2.5	5 –15	2.2	1.12	0.62	0.18
23 (*)	west	3.5	0 – 5	1.1	0.49	0.56	0.19
24 (*)	west	3.5	5 –15	1.0	0.47	0.55	0.18
25	east	0.5	0 – 5	6.9	0.10	0.20	1.29
26	east	0.5	5 –15	8.5	0.02	0.32	0.34
27	east	1.5	0 – 5	4.4	0.17	0.29	0.34
28	east	1.5	5 –15	5.4	1.68	0.29	0.35
29	east	2.5	0 – 5	3.1	0.67	0.89	0.38
30	east	2.5	5 –15	3.3	2.34	0.77	0.34
31	east	3.5	0 – 5	2.7	2.57	1.10	0.33
32	east	3.5	5 –15	3.4	1.00	0.87	0.20

(*) All samples taken at height calculated from platform (i.e. 22 cm above floor).

(+) Some sample lost.

Tab. 2 Drilling core samples: moisture and water soluble anions content (fourth campaign)

Sample no.	Location (wall)	Height (m)	Depth (cm)	Moisture %	Cl⁻ %	NO₃⁻ %	SO₄⁻ %
1a	north	0.5	0–5	12.5	0.04	0.00	0.01
1b	north	0.5	5–15	12.8	0.04	0.00	0.00
2a	south	0.5	0–5	8.0	0.08	0.02	0.06
2b	south	0.5	5–15	8.7	0.05	0.00	0.02
3a	west	0.5	0–5	8.5	0.07	0.03	0.05
3b	west	0.5	5–15	9.2	0.04	0.01	0.00
4a	east	0.5	0–5	8.5	0.06	0.02	0.24
4b	east	0.5	5–15	9.0	0.04	0.02	0.13
5a	north	2.5	0–5	3.9	0.57	0.81	0.04
5b	north	2.5	5–15	4.4	0.54	0.58	0.06
6a	south	2.5	0–5	3.7	0.71	0.61	0.00
6b	south	2.5	5–15	3.8	0.69	0.66	0.00
7a	west	2.5	0–5	3.1	1.35	0.43	0.00
7b	west	2.5	5–15	3.3	0.65	0.51	0.00
8a	east	2.5	0–5	4.2	0.70	0.75	0.01
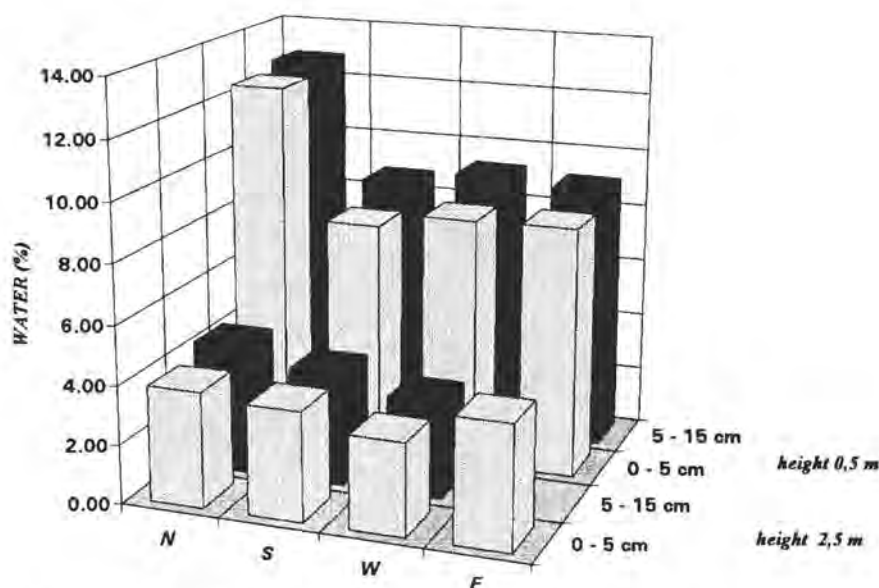
Fig. 4   Moisture content in the wall–masonry (fourth campaign).

3. 2. Analyses of salt efflorescences

3. 2. 1. Ion chromatography analyses

The first two campaigns were focused on the identification of the main causes of the stone decay and of their alteration products. On all the walls salt efflorescences, due to the rising damp and marine aerosol, were found. Ion chromatography analyses show a certain amount of chlorides and nitrates. In the fourth campaign samples from wall surface are not pure efflorescences, but they include Globigerina limestone and mortar fragments. As regards sample location we tried to make a homogeneous sampling at different heights, but

unfortunately on the East and West wall it was possible to take only a few samples. For this reason the results of analyses can not be fully compared and only qualitative consideration can be made.

Ion chromatography analyses have been carried out on all the samples (Tab. 3, 4, 5, 6). The results show the presence of chlorides (Cl⁻), nitrates (NO$_3^-$) and sulphates(SO$_4^-$).

An evaluation of salt distribution (average and maximum–minimum values) per wall and per height has been carried out. Chlorides and nitrates are generally more concentrated on south wall, while sulphates on north wall. The distribution per height shows a general highest concentration of chlorides and nitrates around 2.5–3.0m (Cl⁻max.=4.17%, NO$_3^-$ max. =4.38%), and a concentration of sulphates around 0.5–1.0 m (SO$_4^-$ max. = 46.21%).

Tab. 3   Quantitative analysis of soluble salts of the second set of samples by ion chromatography, north wall (fourth campaign).

North wall	height (m)	Cl %	NO$_3$ %	SO$_4$ %
	between 0.0 and 0.5 m			
sample 31A/95	0.50	0.61	0.51	46.21
sample 31B/95	0.50	2.27	3.00	7.73
average		**1.44**	**1.76**	**26.97**
	between 0.5 and 1.5 m			
sample 1B/95	0.60	0.16	0.11	17.47
	between 1.5 and 2.5 m			
sample 34B/95	1.60	0.29	0.45	17.57
	between 2.5 and 3.5 m			
sample 2/95	3.28	1.43	1.07	0.10
sample 3/95	2.85	2.27	2.08	0.42
sample 4/95	3.30	0.79	0.79	0.19
sample 20/95	2.65	3.41	4.38	0.39
average		**1.97**	**2.08**	**0.27**
	over 3.5 m			
sample R/95	>5	0.47	0.36	0.02
sample 17A/95	3.70	0.42	0.40	0.02
sample 17B/95	3.70	0.66	0.39	0.04
sample 17C/95	3.70	1.29	0.55	0.07
sample 18/95	3.70	2.80	0.86	0.28
sample 19/95	5.60	0.63	0.21	0.03
average		**1.04**	**0.46**	**0.08**

Fig. 5   Anions average concentration (%), north wall, (fourth campaign).

Tab. 4   Quantitative analysis of soluble salts of the second set of samples by ion chromatography, south wall (fourth campaign).

South wall	height (m)	Cl %	NO₃ %	SO₄ %
	between 0.5 and 1.5 m			
sample 32/95	1.20	0.46	0.54	12.35
33/95	1.20	0.45	0.55	12.25
average		0.46	0.54	12.30
	between 1.5 and 2.5 m			
sample 16/95	1.92	0.82	0.83	0.02
	between 2.5 and 3.5 m			
sample 5/95	2.80	3.69	3.30	0.65
sample 6/95	2.80	3.52	3.04	0.39
sample 7/93	2.95	1.99	1.76	0.16
sample 10/95	2.70	4.19	1.70	0.19
sample 11A/95	2.70	1.17	0.89	0.06
sample 11B/95	2.70	1.03	0.91	0.15
sample 12/95	2.80	4.17	2.57	0.35
sample 13/95	2.70	0.79	0.50	0.02
average		**2.41**	**1.62**	**0.19**
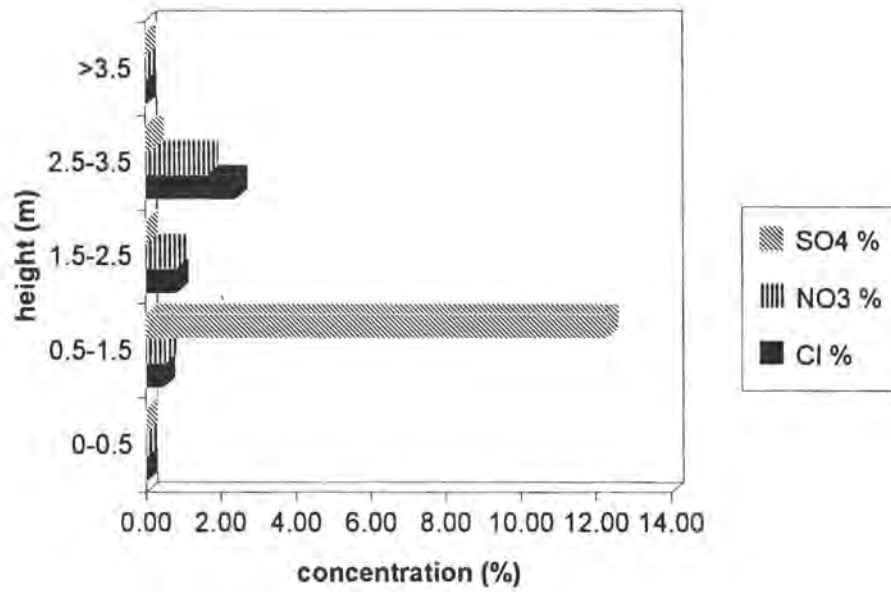
Fig. 6   Anions average concentration (%), south wall, (fourth campaign).

*Tab. 5   Quantitative analysis of soluble salts of the second set of samples by ion chro-
matography, east wall (fourth campaign).*

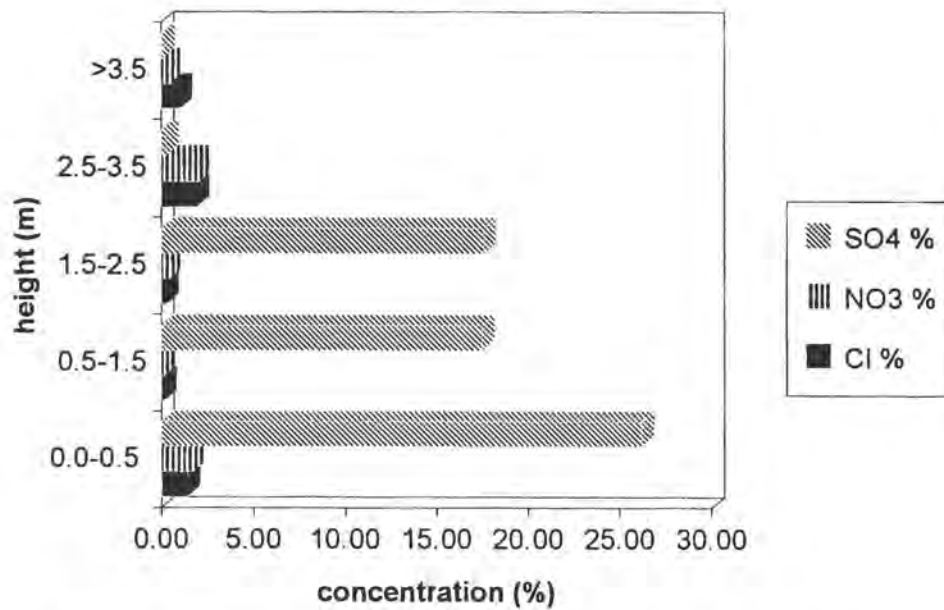| East wall	height (m)	Cl %	NO₃ %	SO₄ %
	between 2.5 and 3.5 m			
sample 21/95	3.00	0.84	1.01	0.07
sample 22A/95	3.30	0.94	0.89	0.02
sample 22B/95	3.30	1.28	1.63	4.93
sample 23/95	3.30	0.47	0.55	0.03
average		0.88	1.02	1.26
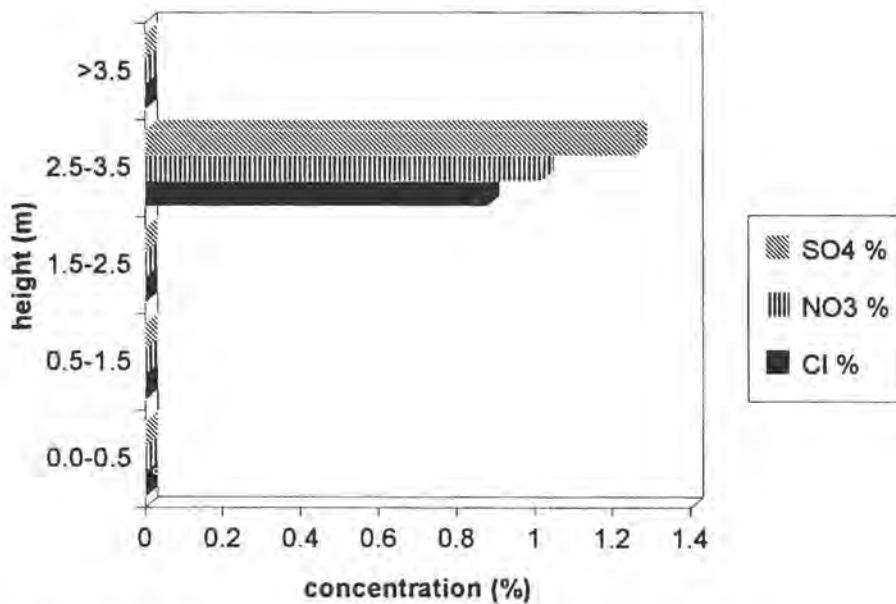
Fig. 7   Anions average concentration (%), east wall, (fourth campaign).

Tab. 6   Quantitative analysis of soluble salts of the second set of samples by ion chromatography, west wall, (fourth campaign)

West wall	height (m)	Cl %	NO$_3$ %	SO$_4$ %
	between 1.5 and 2.5 m			
sample 9/95	2.50	2.21	2.20	0.22
sample 14/95	1.90	0.47	0.29	0.07
sample 15/95	>2.50	0.59	0.18	0.18
sample 28/95	2.20	2.84	2.39	0.57
sample 29/95	2.30	3.78	0.35	0.12
sample 30/95	2.15	1.64	1.20	0.18
average		**1.92**	**1.10**	**0.22**
	over 3.5 m			
sample 24/95	>3.50	0.57	0.48	0.01
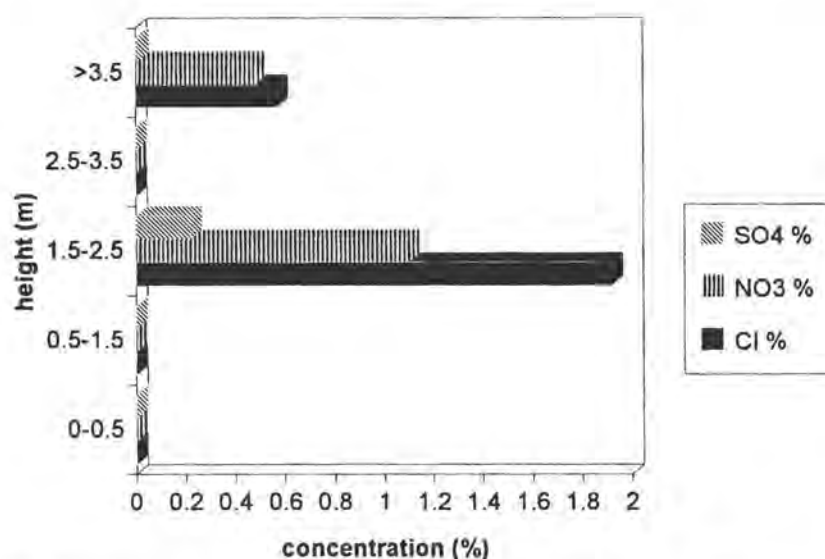
Fig. 8   Anions average concentration (%), west wall, (fourth campaign).

Series of samples on the same vertical line have been considered. Their chromatographic analyses results have been compared to identify an anion concentration trend depending on height.

North wall

On the north wall three series have been recognised, represented by samples

31(AB)/95–34(AB)/95, 3/95–2/95 and
17(ABC)/95–19/95–R/95

(height varying from 0.5 m to > 5 m).

Chlorides and nitrates show a maximum value at h = 2.85 m (Cl⁻ = 2.27%, NO$_3$⁻ = 2.08%), while sulphates at h = 0.5 m (SO$_4$⁻ = 46.21%). This trend is similar to the one observed on drilling core samples taken on wall masonry.

Samples marked A, B, C have been collected from the same point on the wall, but at different depths into the stone. As a merely qualitative consideration, we can say that sulphates show a general higher concentration on the surface of the wall, while chlorides and nitrates are more concentrated a little deeper in the stone.

South wall

On the south wall three series have been recognised, represented by samples 33/95 – 12/95, 11 (AB)/95 – 5/95 – 6/95 and 10/95/ 7/95 (height varying from 1.20 m to 2.95 m). Chlorides and nitrates present a maximum of concentration at h = 2.80 m (Cl⁻ = 4.17%, NO_3^- = 3.30%), while sulphates at h= 1.20 m $(SO_4^-$ = 12.25%), but in this case we did not take any sample from the lower part of wall masonry. In samples marked by A, B sulphates are concentrated on the sample surface, while chlorides and nitrates deeper in the stone as on the north wall.

West wall

On the west wall only one series has been recognised, represented by samples 30/95 – 28/95 – 29/95 – 15/95 (height varying from 2.15 m to < 2.5 m). In this case it is not possible to single out a trend due to the lack of sampling at different heights. We can only observe that chlorides and nitrates present a different behaviour in respect to the other walls. In fact they present a maximum concentration at h = 2.20 m (Cl⁻ = 3.78%) and a decrease at h > 2.5 m (Cl⁻ = 0.59%), instead of a further increase. This could be probably ascribed to the sampling procedure.

East wall

On the east wall only one series, consisting of three samples: 22(AB)/95 and 21/95, has been recognised. As all samples are taken almost at the same height (h = 3.0–3.30 m), it is impossible to recognise a trend. The apparently anomalous high sulphate concentration at h = 3.30 m $(SO_4^-$ = 4.97%) is probably be due to the presence of a barium sulphate layer identified by EDAX analyses.

All chromatographic analyses results have been divided up into classes, representing concentration range, and concentration frequency has been observed. We considered the all samples together.

Chlorides: all classes of chlorides concentration, from 0.0–0.5% to 4.0–4.5%, are represented

and 54% of events falls equally into the first two classes (0.0–0.5% and 0.5–1.0%).

Nitrates: concentration varies between the classes 0.0–0.5% and 4.0–4.5%. All classes are represented except the 3.5–4.0%. 63% of events falls into the first two classes, with a maximum (34%) in the range 0.5–1.0% of concentration.

Sulphates: these present a wide value distribution from class 0.0–0.5 to class 46.0–47.0% but with many ranges in between not represented. The maximum frequency (73%) is in the 0.0–0.5% range of concentration. This is due to the different origin: Cl and NO₃ are ascribed to rising damp, on the contrary sulphates are coming from mortars.

3. 2. 2. X–ray diffraction analyses

In the first campaign, a large amount of halite (NaCl) and small amount of Sylvite (KCl) were found by x–ray diffraction. In the second one, samples from south, east and west walls show mainly the presence of halite (NaCl), while from north wall a decreasing amount of thenardite (Na_2SO_4) with the height was detected. The latter can take place from dissolution of soluble salts of cement mortars.

In the fourth campaign, diffractometric analyses have been carried out on 16 samples: calcite has been found in all samples and it is due to the stone or mortar presence in the powder analysed. The same origin is ascribed to the quartz, which is present in low amount almost in all samples.

Saline efflorescences mainly consist of *halite* crystals which are of marine origin. Halite is present in 12 samples: 3/95, 9/95, 10/95, 11B/95, 12/95, 18/95, 19/95, 20/95, 22A/95, 22B/95, 31A/95 and 31B/95 in traces or medium amount.

The other mineralogical phases found are:

1) *gypsum* which is present in four samples (1B/95, 22B/95, 31B/95 and 34A/95), probably due to gypsum plastering;

Investigation on the moisture and salt migration in the wall masonry and on the presence of
salt efflorescences on stone surface in the church of Sta. Marija Ta' Cwerra at Siggiewi, Malta
305

2) *thenardite* which is present in two samples (31A/95 and 34B/95), is probably from cement;

3) *mirabilite* and *trona* which are present in the same sample (31A/95), are also probably from cement as thenardite.

Diffractometric results closely correspond to chromatographic one. Nitrates represent the only problem. In fact nitrates are found even in high percentage (around 4%) with chromatographic analyses, while they are not detected with diffractometric analyses. This is probably due to the equilibrium relative humidity low values characteristic of nitrocalcite (RH=50.0% at T=25°C) and nitromagnesite (RH=52.9% at T=25°C. Amoroso and Fassina, 1983), which determine the dissolution of these salts in a higher relative humidity ambient.

With regard to crystallisation pressures, halite is the most dangerous salt. According to Winkler (1975) data, with an hypothetical C/Cs=2, where C is the actual concentration of the solute during crystallisation and C_s is the concentration of solute at saturation, and T=0°C, the halite crystallisation pressure is 554 atm, while the gypsum one is 282 atm, the thenardite one is 292 atm and the mirabilite one is 72 atm. On the other hand if we consider the molar volume, mirabilite with a $Vm = 220$ cm^3/mole is the most dangerous salt. Halite has a $Vm = 28$ cm^3/mole, gypsum a $Vm = 55$ cm^3/mole and thenardite a $Vm = 53$ cm^3/mole. In this specific case, moreover, we found mirabilite and thenardite together in the same sample. That would seem to show that phase transitions between the anhydrous and the hydrate forms easily occurs in the stone, producing hydration pressure in the pores that is particularly effective because of the rapidity of the change. The transition of sodium sulphates thenardite to mirabilite is more rapid than hydration of other salts: it takes about 20 minutes at 39°C.

Tab. 7   X–ray diffraction results (fourth campaign).

Samples	Gypsum	Calcite	Halite	Mirabilite	Thenardite	Trona	Quartz
1B/95	***	***	-	-	-	-	*
3/95	-	***	*	-	-	-	-
7/95	-	***	-	-	-	-	-
9/95	-	***	*	-	-	-	-
10/95	-	***	**	-	-	-	*
11B/95	-	***	*	-	-	-	*
12/95	-	***	*	-	-	-	-
18/95	-	***	*	-	-	-	-
19/95	-	***	**	-	-	-	*
20/95	-	***	*	-	-	-	-
22A/95	-	***	*	-	-	-	*
22B/95	**	***	*	-	-	-	**
31A/95	-	*	*	***	**	*	-
31B/95	*	***	*	-	-	-	-
34A/95	**	***	-	-	-	-	*
34B/95	-	***	-	-	**	-	-

*** *abundant*
** *middle amount*
* *small amount*
− *absent*

3. 3. SEM and EDAX analyses of polished cross section

Polished cross section of 12 samples have been done in order to observe the presence of salts on the stone surface and their penetration into the rock. Edax analyses, carried out on the same vertical across the samples, show the saline distribution in respect to depth.

In sample 9/95 it is possible to recognise a chlorine concentration trend, moving from the sample surface into the stone. The sample is about 2500 m thick and consists of two layers: mortar for the first about 900 m, and Globigerina limestone for about 1600 m. Chlorine presents a peak of concentration in the transition zone between mortar and limestone (Cl = 79.11%). Moving through the mortar from the transition zone to the external surface, chlorine concentration shows a rapid decrease and then a progressive increase reaching value Cl = 24.34% on the surface.

Inside the limestone, chlorine presents a low concentration, except for lower margin of the stone, where its presence is probably due to a contamination, during sampling, between the stone fragment and the external salts.

Sulphur trend is shown by sample 34A/95 which is a Globigerina limestone fragment about 1200 m thick. In this case the salts are concentrated on the stone surface (S = 37.82%) and progressively decrease moving inside the

stone. Because the samples present a different structure we can not properly compare the two different trends shown by chlorine and sulphur and say that chlorides and sulphates present a different behaviour. In fact sample 9/95 consists of two layers (mortar and limestone) with different characteristics which may condition the salts migration, while sample 34A/95 is a limestone fragment with the same characteristics through all its thickness.

4. Conclusions

Moisture content in the wall masonry shows a decreasing trend according to the increase of height and is practically ceasing at 3–4 meters. Comparison of moisture content at each level generally shows higher values for samples taken at 5–15 cm of depth with respect the superficial ones.

As regards anions in wall masonry sulphate are mainly concentrated in lower parts of the walls, while chlorides and nitrates in upper levels. This is a typical distribution previously observed by other authors. Salts, dissolved in the water inside the walls, are transported vertically by capillary rising damp.

When water evaporates there is a fractionate precipitation of different salt phases, according to their solubilities. Sulphates remain at lower levels because they have a low solubility.

Tab. 8a Chlorine depth profile in cross sections (fourth campaign).

Sample 9/95							
Depth	0 μ	450 μ	850 μ	900 μ	975 μ	1550 μ	2500 μ
Cl %	24.34	17.46	5.14	79.11	0.00	3.94	22.62

Tab. 8b Sulphur depth profile in cross sections (fourth campaign).

Sample 34A/95				
Depth	0 μ	40 μ	520 μ	1200 μ
S %	37.82	35.03	13.28	0.00
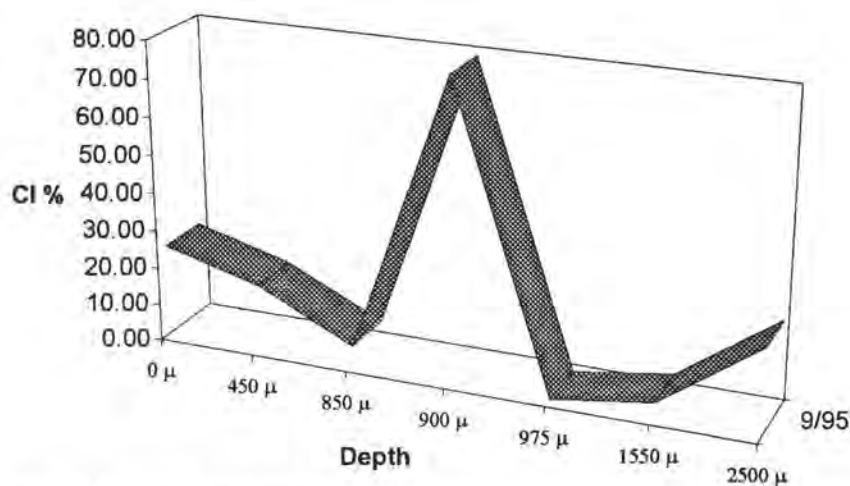
Fig. 9   Sample 9/95. Chlorine depth profile.
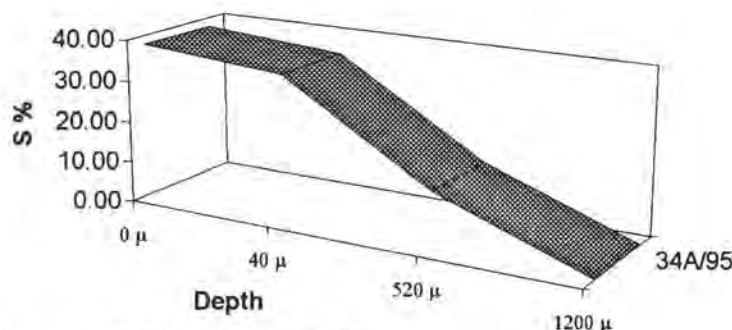
Fig. 9   Sample 34A/95. Sulphur depth profile.

As regards nature and origin of efflorescences XRD analyses show the presence of halite (NaCl) on the south, east and west wall, while on north wall thenardite (Na_2SO_4) was found.

The other mineralogical phases found are:

– *gypsum which is present in four samples probably due to gypsum plastering;*

– *thenardite which is present in two samples probably from cement;*

– *mirabilite and trona which are present in the same sample (31A/95), are also probably from cement as thenardite. Diffractometric results closely correspond to the chromatographic ones.*

As regards crystallisation pressures, halite is the most dangerous salt. In this specific case, moreover, we found mirabilite and thenardite together in the same sample. That would seem to show that phase transitions between the anhydrous and the hydrate forms easily occurs in the stone, producing hydration pressure in the pores that is particularly effective because of the rapidity of the change. The transition of sodium sulphates thenardite to mirabilite is more rapid than hydration of other salts: it takes about 20 minutes at 39°C.

Comparison among superficial samples and drilling core from wall masonry was also carried out. All comparison between this two series of samples can only be qualitative be-

cause of the different methods of sampling and because of the heterogeneity of the surface samples compared to the drilling core ones. Absolute value differences can be due to the different way of sampling, so it is possible to compare only a trend of variation. Moreover some walls and heights are not completely represented and, in this case, such kind of comparison is impossible too.

The height at which the maximum concentration occurred is almost the same in the two series for all the three anions (Cl^- and NO_3^- around 2.5–2.7 m and SO_4^- around 0.5 m). But in this series of samples chlorides are more concentrated on the south wall, while for drilling core samples the maximum is on the west wall; the nitrates maximum is on the north wall for both series; and sulphates maximum is on the north wall instead of the east. On the east wall however there are no samples from h = 0.5 m where sulphate concentration maximum is expected to be.

In conclusion the presence of sodium chlorides efflorescences is ascribed to rising damp phenomenon. Generally gypsum and thenardite detected inside the church are formed by leaching of mortars or plasters. The strong decay visible on the external side at 4–6 meters is in the correspondence to the maximum rising damp height reached by salts which deposited on subsurface the salt efflorescences coming from sub–soil. The pressure of crystallization causes detachment of scales and consequently a progressive missing of large fragments of surface stone.

5. Acknowledgements

6. References

1. Amoroso, G., Fassina, V. *Stone decay and conservation: atmospheric pollution, cleaning, consolidation and protection.* Elsevier Science Publishers, Amsterdam, 1983, 42–48.

2. Arnold, A. *Determination of mineral salts from monuments.* Studies in Conservation, 29, 1984, 124–128.

3. Arnold, A., Zendher, K. *Decay of stony materials by salts on humid atmosphere.* Proceedings of VIth International Congress on Deterioration and Conservation of Stone. Torun, 1988, 139–149.

4. Baggio, P., Bonacina, C., Stevan, A. G., Fassina, V. *Influence of Interior Micro climate and Moisture Migration on the Marble Decay in the S. Maria dei Miracoli Church in Venice.* ICOM Committee for Conservation, 10th Triennial Meeting, 1, Washington, 1993, 339–344.

5. Winkler, E. M. *Stone: properties, durability in man's environment.* Springer–Verlag, New York, 1973, 110–125.

Vasco Fassina
Antonia Moropoulou
Andrea Rattazzi

Principal decay patterns on the archaeological site of Demeter Sanctuary in Eleusis: weathering mechanism
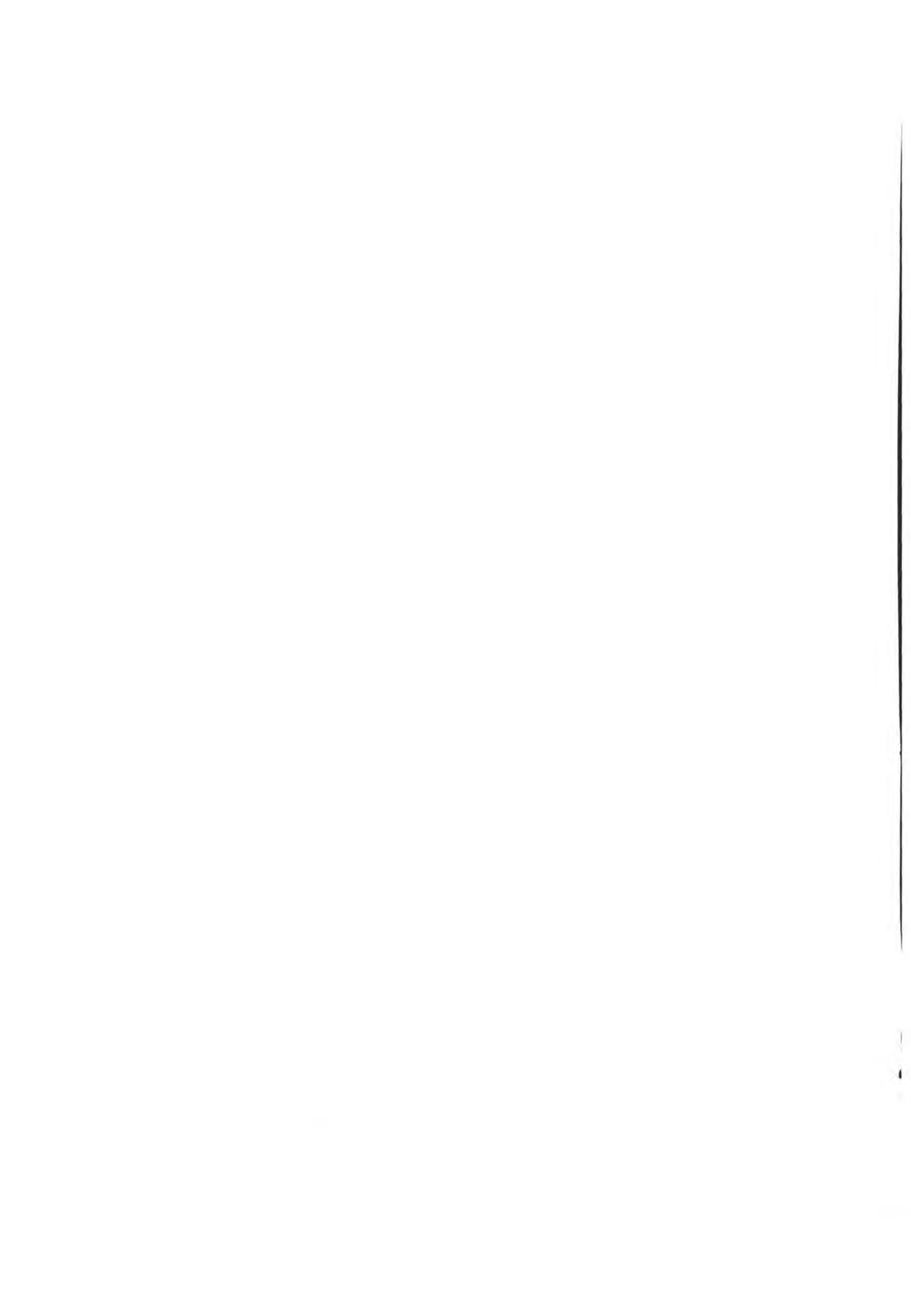
Principal decay patterns on the archaeological site of Demeter Sanctuary in Eleusis: weathering mechanism

V. Fassina   – *Laboratorio Scientifico–Soprintendenza ai Beni Artistici e Storici di Venezia – Italy*
A. Moropoulou – *National Technical University of Athens, – Greece*
A. Rattazzi   – *Fondazione Cesare Gnudi, Bologna – Italy*

1. Introduction

According to preliminary observations carried out by Greek group involved in this project the Eleusis area corresponds to a typical urban–centre profile of intense and diversified industrial activity characterised by a highly polluted atmosphere, heavily charged by suspended particles. Hence, observations and measurements on the surface of marble monuments in the archaeological site of Eleusis would be indicative of the stone decay phenomena caused by air pollution and specifically by suspended particle attack.

The main decay phenomena in relevance to the environmental factors and in the sequence of the frequency that they are observed, are as follows:

– *granular disintegration and detachment, the most general and important weathering, concerning yellowish limestone and biocalcarenites as well as marble, presented at washed out surface areas, or on surface areas facing the sea;*

– *biological attack to the stone;*

– *chromatic alteration from the white of the Pentelic marble to the rusty–yellow colour at the washed out surfaces and mainly where water rebound phenomena occur;*

– *soiling (loose dirt deposits) are frequently present at horizontal top sides of numerous building stones relief in form of micro–karst. The micro–karst are formed by solution processes resulting from accumulation of rain water reacting with suspended particles deposited during long period of dry deposition;*

– *black grey crust formations formed on hollows;*

– *black crust strongly attached at the surfaces often present in unwashed areas;*

– *loose deposition inside hollow;*

– *orange–coloured crust very thin and firmly attached to the stone surface.*

2. Sampling concerning decay patterns

Samples were taken from different parts of the archaelogical site according to the following criteria:

– *the degree of decay through macroscopic observation;*

– *the orientation of the individual architectural elements;*

– *the degree of sheltering from rainwater (black areas);*

– *the exposure to direct rainfall (washed out areas);*

– *black ampoules in the groundfloor.*

According to the macroscopic observation and classification of decay patterns the following sampling was performed at the Eastern Triumphal Arch concerning crusts, deposits at washed out and sheltered areas.

In order to compare the weathering processes of similar materials well studied in Venetian environment it was decided to take samples only from marble. In this way it has been avoided the comparison with other types of limestone present in Eleusis that being characterised by different structure and texture properties could suggest not comparable behaviour.

E1 Black–grey deposit from sheltered area (front side–Northern winds).   E14 Black deposit, from a sheltered area with marked marble decohesion.

E4 Black crust from sheltered area (right back side).   E7 Dendritic crust and brown powder of the dentils from a sheltered area, (front side–Northern winds).

E11 Black powder from a horizontal area.   E15 Black crust from a sheltered area.

E2 Yellow–grey layer from washed out area (left front side–Eastern winds).   E3 Yellow–brown layer from washed out area (back side–Southern winds).

E10 Red–brown crust from sheltered area (back side).   E12 Red patina on the marble.

E16 Red patina from the basis of the middle column.   A2 Brown patina on the marble from the column ground.

E5 Grey–black crust, from ampoules on the groundfloor of the basement column on the right of the Triumphal Arch.   E6 Yellow–pink layer near grey–black crust (sample E5) in washed out area.

3. Experimental procedure

To assess the different alteration products the following analytical methods were used:

– *Cross sectioning* to separate the different layers on the surface;

– *SEM* (scanning electron microscopy) analysis to provide morphological information on crystals;

– *EDS* depth profile microanalysis on cross–sections;

– *X–ray diffraction* used in order to check whether an interrelation exists on crystalline phases and possible transformations between dust and suspended particles depositions and surface encrustations (cementitious crusts)

– *Ion Chromatography*, to evaluate the salts that are present in the crust;

– *Chemical analysis* such as atomic absorption and emission spectrometry (AAS/AES) and energy dispersive X–ray fluorescence (EDXRF).

4. Results and discussion

Optical microscope observations in reflected light and SEM–EDAX analysis of cross–sections

In addition of optical microscopic observations on some samples a depth profile analysis was carried out, in order to obtain information about the chemical composition of the decay products, especially on the thickness of gypsum layer and black carbonaceous particles which are commonly present on monuments in an urban and or industrial area.

Generally this analysis is carried out by using the line–scan analysis which correspond to the microprobe analysis along the line of the electron beam. This is a very useful tool but if the sample is not homogeneous like stone samples coming from black crust it cannot be representative of different layer deposited on marble surface.

For this reason the depth profile analysis was carried out by analysing a rectangular area 35x50 μm moving from the external surface

towards the internal part of the sample until to reach the sound marble.

Black–grey soiling from sheltered area (sample E1)

On the substratum single calcite crystals are clearly visible. In contact with the marble there is a layer which is yellow–brown–black coloured moving from inner to outer part. Red iron oxides and black carbonaceous particles are visible.

The SEM–EDAX show mainly the presence of a gypsum layer. Silicon is present in the range from 5 to 9%, typical of urban environment. Iron is about 2%.

Depth profile analyses show the presence of a constant composition of gypsum (Ca=52–62%, S=30–35%) until 140 µm, from this point gypsum is decreasing (table 1; figure 1).

Table 1 EDAX analyses on sample E1b

Depth Elem.	35	70	105	140	175
Si	7.1	5.0	9.3	9.2	5.5
S	34.9	30.6	30.2	31.1	22.1
Ca	53.9	61.8	56.4	52.0	67.5
Fe	2.7	0.3	0.4	2.8	2.0
K	0.6	1.3	1.7	1.7	1.5
Mg	-	-	-	0.3	0.2
Ti	-	-	-	0.8	-
Al	0.7	1.0	2.0	2.0	1.2
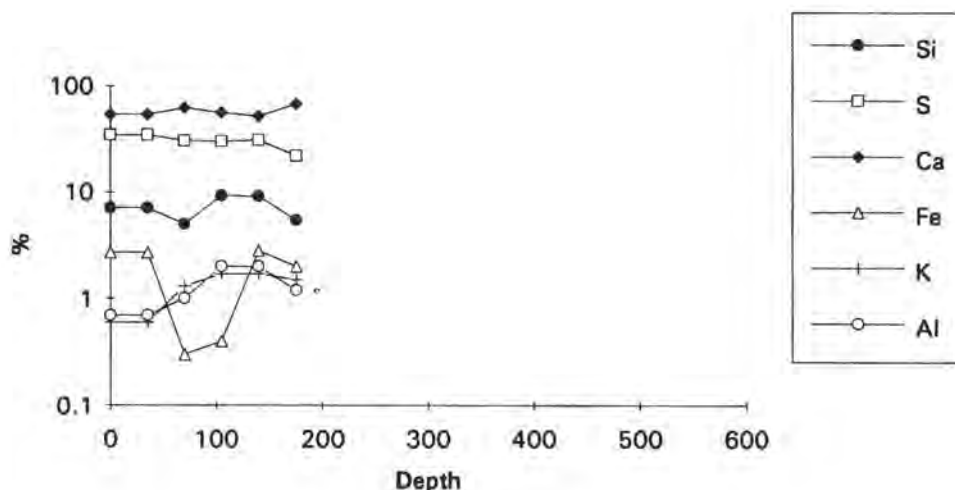
Fig. 1 sample 1 Eb

Black deposit from a sheltered area with marked marble decohesion (sample E14)

A yellow–brown–black coloured layer contains red iron oxides and carbonaceous parti-

cles. The white particles were identified by EDAX as zinc oxide and barium sulphate. The composition of superficial layer is constant (Ca=52–55%, S=33–35%) until 140 μm, and then start to decrease sharply (table 2, figure 2).

Table 2 EDAX analyses on sample E14

Depth Elem	35	70	105	140	175
Si	7.8	6.8	8.3	6.3	5.0
S	33.6	35.2	35.2	35.5	25.2
Ca	53.3	53.5	52.4	54.6	66.9
K	1.4	0.5	1.2	1.1	0.5
Al	1.0	1.1	1.1	1.0	0.6
Fe	3.0	3.5	1.7	1.2	1.6
Mg	-	-	-	0.2	0.7
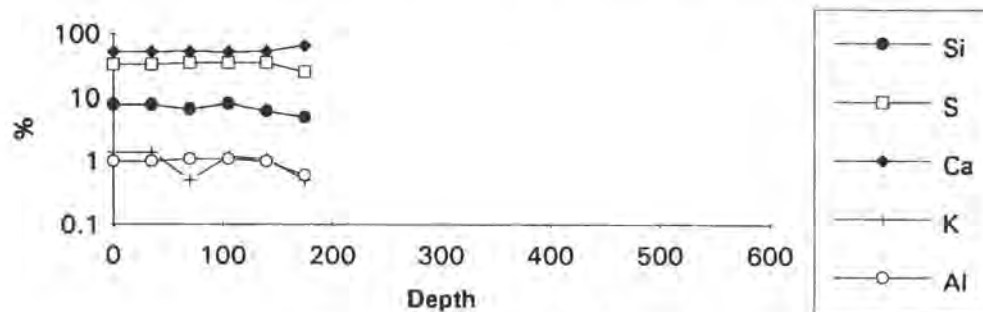
Fig. 2 sample E14

Black crust from sheltered area (sample E4)

The feature of the crust is similar to the previous sample, in fact the interior part of the crust is yellow–brown. The thickness is a little bit higher, 700–800 μm. On the exterior part carbonaceous particles are most abundant. Also

iron oxides particles are visible. EDAX shows the same composition: the main component is gypsum while Si and Fe are minor components. Depth profile analyses show a constant composition of gypsum (Ca=55–59%, S=29–35%) until 245 μm. For deeper strata the gypsum concentration is sharply decreasing (table 3, figure 3).

Table 3 EDAX analyses on sample E4

Depth Elem.	35	70	105	140	175	210	245	280
Si	4.5	4.5	5.6	5.6	6.3	4.9	5.0	2.6
S	35.1	34.6	35.0	33.9	28.8	32.3	29.7	10.7
Ca	50.0	56.7	53.8	55.9	59.3	58.9	60.8	86.0
K	0.9	0.9	1.0	1.1	1.1	1.1	1.2	0.8
Al	1.0	0.9	0.9	1.0	1.0	0.9	1.0	0.7
Mg	-	-	-	-	0.4	-	0.3	-
Fe	1.5	2.3	3.8	2.6	3.0	1.8	2.0	-
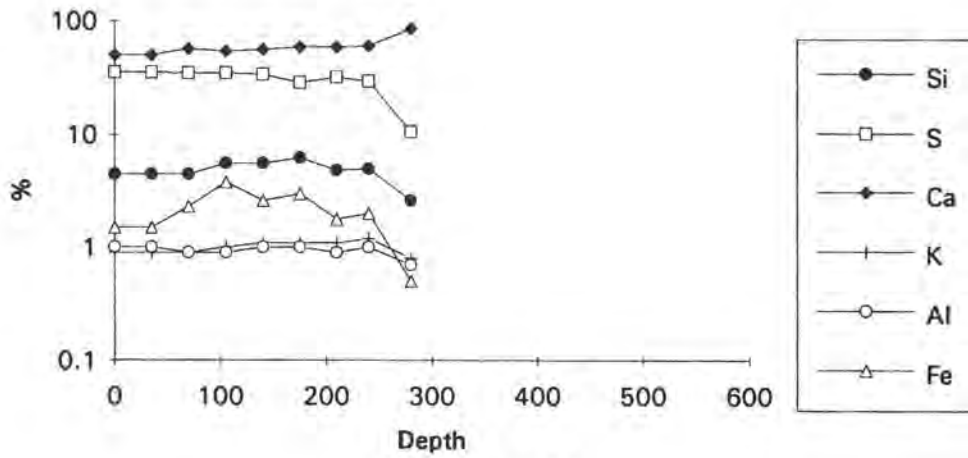
Fig. 3 sample E4

Black dendritic crust from a sheltered area (sample E7)

The inner zone of the dendritic crust is brown–yellow, and grey in the outside one. In particular on the external part, carbonaceous particles and iron oxides are very abundant. The depth profile analysis shows a notable uni-formity in the elemental composition (Ca=52–59%, S=30–35%) until a depth of 385 μm. For deeper strata an increase of Si, K, Al and Fe contents was observed. The latter probably is ascribed to suspended particles emitted by cement industry (table 4, figure 4).

Table 4 EDAX analyses on sample E7

Depth Elem.	35	70	105	140	175	210	245	280	315	350	385	420	455	490	525	560
Si	9.1	4.4	6.5	6.9	8.4	7.6	7.4	4.9	6.3	7.0	8.7	10.6	10.2	19.6	14.6	16.8
S	32.9	32.4	35.0	32.8	33.7	34.0	30.2	32.9	30.6	30.9	30.2	23.0	26.4	29.7	29.6	28.5
Ca	52.0	58.4	53.1	54.0	52.0	54.9	57.3	59.1	58.2	56.7	54.4	59.1	56.1	49.1	45.6	44.5
K	0.9	0.8	1.1	1.1	1.3	1.0	1.0	1.0	1.1	1.0	1.3	1.6	1.7	2.0	2.2	2.2
Al	1.8	0.6	1.8	1.8	2.1	1.6	1.8	0.6	1.5	1.7	2.4	2.4	2.4	3.2	3.6	3.8
Fe	3.3	3.2	2.0	2.1	1.9	0.5	1.7	1.4	1.9	2.2	2.4	2.6	2.6	3.0	3.5	3.5
Mg	-	0.2	0.5	0.6	0.6	0.5	0.7	-	0.4	0.5	0.6	0.6	0.5	0.3	0.9	0.9
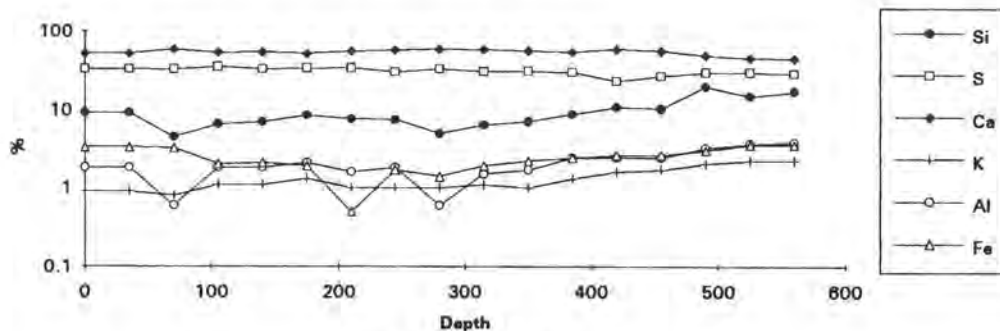
Fig. 4 sample E7

Black soiling from a horizontal area (sample E11)

A grey–brown layer contains particles of various colour: white spherical particles of TiO$_2$ together with yellow–red particles of iron oxide. Depth profile analyses show a uniform and constant composition of gypsum (Ca=53–60%, S=25–33%) until 350 µm. The brown layer observed is due to iron oxide particles which were confirmed at EDAX showing the maximum percentage of Fe. On the surface until 35 µm there is a layer rich in Si and Al (table 5, figure 5).

Table 5 EDAX analyses on sample E11

| Depth / Elem	35	70	105	140	175	210	245	280	315	350
Si	10.4	7.0	6.9	7.4	10.4	7.0	9.1	6.8	9.7	9.7
S	24.9	29.4	32.8	30.4	29.1	27.3	25.6	29.3	27.7	27.6
Ca	57.1	58.0	55.7	56.4	55.0	53.5	59.7	58.2	57.2	57.8
K	1.1	0.8	1.1	0.9	1.3	0.7	1.4	0.9	0.9	0.9
Al	5.1	1.4	1.4	1.5	1.7	1.4	1.6	1.1	1.3	1.4
Ti	-	-	-	1.3	-	1.0	-	-	-	-
Fe	1.4	3.4	1.6	1.6	2.5	9.1	2.2	3.3	2.6	2.0
Mg	-	-	0.6	0.4	-	-	0.4	0.4	0.5	0.6
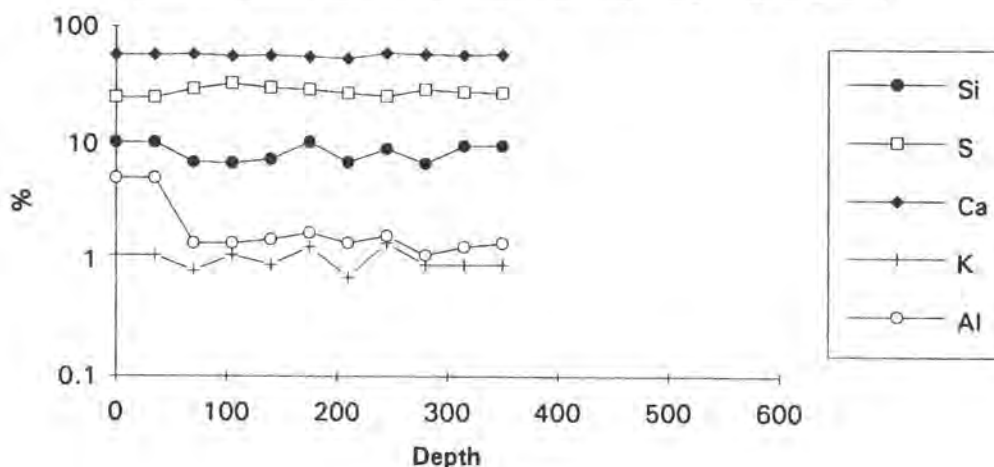
Fig. 5 sample E11

Black soiling from a sheltered area (sample E15)

The external part is grey, while the internal one is brown. The section is similar to the previous one. The composition of gypsum is almost constant.

Depth profile analyses show that in correspondence of brown layer in the range between 250 and 450 µm an increase in the concentration of Si and Fe was measured (table 6, figure 6).

Table 6: EDAX analyses on sample E15

Depth / Elem	35	70	105	140	175	210	245	280	315	350	385	420	455
Si	4.0	3.5	6.8	6.1	5.1	5.3	6.6	12.4	14.2	12.5	8.6	6.1	12.6
S	35.9	37.5	32.1	34.7	33.8	30.6	28.7	22.8	23.2	23.3	27.8	31.1	28.9
Ca	57.7	58.5	57.0	56.8	58.8	60.2	59.6	58.3	55.0	55.9	56.9	56.8	50.5
Al	0.7	0.5	0.8	0.8	0.7	0.9	1.1	1.8	1.8	2.0	1.6	1.4	1.9
K	0.5	0.5	1.0	0.5	0.5	1.1	1.5	1.7	2.1	2.1	2.0	1.6	2.3
Fe	1.8	-	2.3	1.5	1.5	2.0	2.2	2.6	3.3	3.8	2.8	2.7	3.5
Mg	-	-	-	-	-	-	0.2	0.4	0.3	0.4	0.4	0.3	0.3
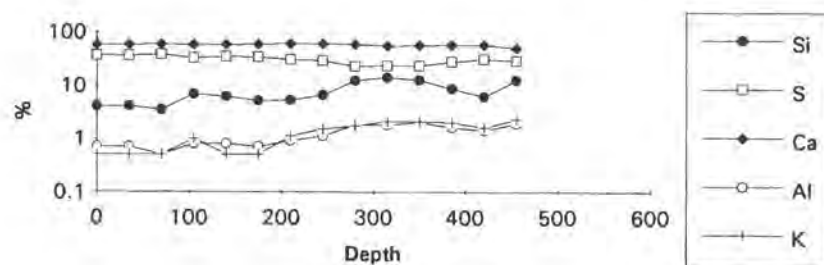
Fig. 6 sample E15

Yellow–grey layer from washed out areas (sample E2)

A thin yellow layer is visible above the typical texture of the marble. Small quantities of gypsum are present in the cracks. Micro–organisms (fungi and algae) have been identified and the biological attack is clearly visible. The fragments shows an abundant yellow deposit, together with inclusions of carbonaceous particles. The yellow deposit grows into the empty spaces of the decohesionated marble.

Yellow-brown layer from washed out areas (sample E3)

A thin brown–yellow discontinuous deposit is visible on the surface. The sample contains a brown powder probably formed by particulate from soil carried by the winds. In some parts the deposit is included in granular spaces, in other areas an enrichment of silicon was detected by EDAX (Si=21%). Small particles of iron oxides have also been detected.

Red–brown crust from sheltered area (sample E10)

An orange yellow layer mainly formed by iron oxides and a few carbonaceous particles is visible on the external surface. Gypsum has a constant composition (Ca=52–56%, S=30–32%) until 140 μm. From this point the gypsum shows a decreasing trend and correspondingly silicon is increasing from 7 to 20% in the range 140–280 μm (table 7, figure 7). Iron is present in discrete amounts, 2–5%, in the range 0–350 μm. In the range 350–490 μm iron increases as is clearly visible in optical microscopic observation of cross–section. The abundant presence of iron and silicon is ascribed to cement industry.

Table7 EDAX analyses on sample E10

| Depth Elem.	35	70	105	140	175	210	245	280	315	350	385	420	455
Si	7.8	7.2	7.9	11.8	19.6	19.6	20.0	14.1	10.2	13.4	14.2	11.2	17.6
S	32.5	35.4	30.5	25.0	15.5	15.5	7.6	8.6	5.1	3.0	3.2	2.0	2.5
Ca	52.0	52.2	55.9	56.3	55.3	55.3	60.2	61.4	75.0	70.8	60.4	64.9	54.3
K	1.6	1.2	1.6	1.8	2.9	2.9	3.1	3.4	2.0	2.8	4.4	4.3	3.8
Fe	4.0	2.0	2.3	3.0	3.4	3.4	5.2	4.6	3.2	4.7	11.0	10.5	12.1
Al	1.8	1.7	1.5	1.8	2.8	2.8	2.6	3.5	1.9	2.2	2.7	2.5	3.5
Mg	0.2	0.3	0.3	0.2	0.4	0.4	0.4	0.5	0.4	0.3	0.5	0.4	1.1
P	-	-	-	-	-	-	-	3.4	1.7	2.0	2.7	2.7	3.2
Cl	-	-	-	-	-	-	0.7	0.6	0.5	0.8	0.8	1.6	1.9
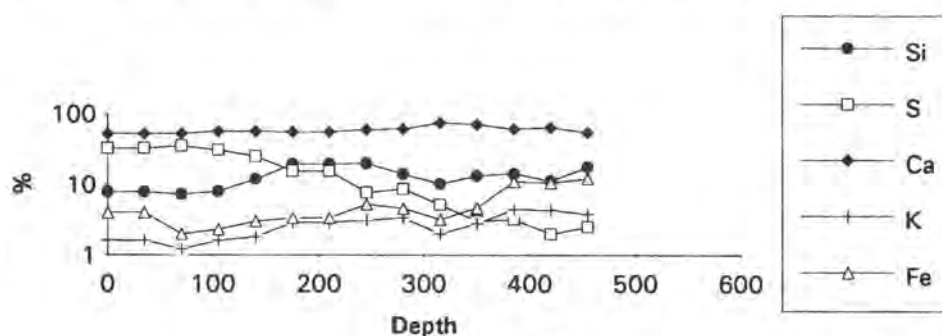
Fig. 7 sample E10

Rusty patina on washed out areas (sample E12)

In this section three layers are visible: on the top a brown superficial deposit, 50 μm thick, is characterised by gypsum and carbonaceous particles; in the intermediate layer the white feature visible is characterised by a decreasing amount of gypsum, absence of carbonaceous particles and presence of high concentration of silicon (Si=36%); the internal layer is yellow coloured (table 8, figure 8).

Table 8 EDAX analyses on sample E12

Elem.	Depth 35	70	105	140	175
Si	6.6	6.8	36.9	31.8	29.7
S	27.4	31.6	10.9	7.7	7.8
Ca	58.4	58.3	46.0	50.4	52.9
Al	1.7	0.9	0.9	1.5	1.6
K	1.6	0.9	1.5	1.9	2.0
Ti	-	-	-	0.8	-
Fe	2.1	0.3	-	2.7	2.6
Mg	0.6	0.7	0.9	1.0	1.2
Cl	1.6	0.4	3.0	2.1	2.1

Fig. 8 sample E12

Red patina from the basis of a column (sample E16)

Under the optical microscope the superficial yellow–orange layer visible is composed by iron oxide. X–ray map distribution analysis show a very thin deposit of silicon on the surface until 100 μm. Unexpected large amount of phosphorous is present in the range between 50 and 200 μm (table 9, figure 9)

Table 9 EDAX analyses on sample E16

Elem.	Depth 35	70	105	140	175	210
Si	7.8	2.9	3.8	8.1	1.0	0.5
S	2.5	2.8	3.2	3.2	2.5	0.5
Ca	5.0	73.1	66.4	65.5	82.8	96.7
Al	0.9	0.6	1.0	1.6	0.5	0.5
Fe	83.9	1.7	4.5	4.0	0.5	0.5
P	-	18.8	20.6	17.6	13.6	3.3
Cl	-	-	0.5	-	-	-

Fig. 9 sample E16

Brown patina at the basis of the column where water rebound phenomena occur (sample A2).

On the surface there is a thin (15 m of thickness) brown layer containing fine iron ox- ides and carbonaceous particles. EDAX (table 10) shows the presence of a large amount of silicon (about 80–83%), (analyses 1–2). Below the yellow layer, thick about 30 m, contains a lower amount of silicon (45–54%) and a discrete amount of iron which is responsible of the yellow colour. In the inner part, algae and fungus hypae are visible, together with yellow stains due to limonite products.

Grey–black–crust from ampoules on the ground-floor (sample E5)

Under the optical microscope a very thin black layer, thick 35 μm, is visible. EDAX shows that this layer is composed mainly by gypsum (Ca=56%, S=37%) and a very few amount of silicon (Si=5%) is present. Iron is completely absent.

Table 10 EDAX analyses on sample A2

Analysis Elem.	1	2	3	4
Si	83.0	80.0	53.6	44.6
Mg	-	-	0.8	1.1
Al	1.9	2.5	4.8	2.4
Cl	1.0	-	-	0.6
K	1.4	-	2.8	1.0
Ca	12.6	17.4	31.9	42.6
Fe	-	-	6.0	7.7

Below a very thick white layer is visible. The depth profile microanalysis shows a very large, but not uniform, amount of silicon which increases in the depth 70 to 210 μm and successively decreases until 385 μm. In the same layer of Si also iron is present (table 11, figure 10). In the inner part a thin black layer is visible in contact with the original marble. This grey–black layer is similar to the external one. The silicon rich layer is in between two thin gypsum layer containing carbonaceous particles. SEM backscattered analysis show a very thin white layer of barium sulphate. In

Table11 EDAX analyses on sample E5

| Depth Elem.	35	70	105	140	175	210	245	280	315	350	385	420	455	490
Si	5.2	38.2	46.0	45.7	60.3	29.6	14.5	22.7	22.4	30.7	19.5	6.1	5.3	7.8
S	37.5	4.0	1.6	1.7	1.5	1.3	1.3	1.4	1.4	1.6	1.8	0.9	0.9	1.0
Ca	55.7	55.9	48.5	48.6	29.7	65.8	81.6	72.0	71.0	63.6	71.4	89.3	90.5	87.5
K	0.1	0.1	0.1	0.1	0.1	0.1	0.1	0.2	0.3	0.9	1.8	1.1	0.9	1.0
Al	0.9	1.2	1.0	1.1	1.1	1.1	0.8	0.9	1.1	1.2	2.0	0.8	0.6	0.8
Fe	-	-	2.0	1.8	6.0	1.4	1.2	1.3	3.2	1.3	2.7	1.4	1.1	1.3
Mg	-	-	-	0.4	0.3	0.3	0.3	0.3	0.5	0.4	0.4	0.3	0.3	0.4
Cl	0.6	0.7	0.8	0.8	1.0	0.4	0.3	0.3	0.3	0.3	0.2	0.1	0.2	0.2
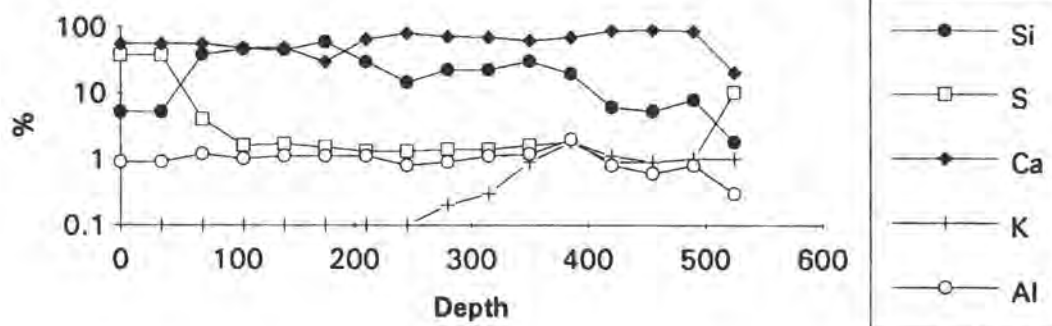
Fig. 10 sample E5

the left fragment the layer is thick, sometimes larger than 1 mm. It includes yellow, white and colourless granules, black and red particles of different size and yellow stains. The carbonaceous particles are not very abundant but often are of considerable size. The white granules are of calcite nature and, the yellow ones, of quartz origin. Iron oxides of large size are present in the upper part. Fungi and algae are visible, even if not frequently. The upper part shows a transition in the colour, from yellow–pink to white–grey. The main constituent is gypsum. The fragment II from left is similar to the previous section even if the biological attack is more evident in the upper part of the crust. Close to the surface the intensity of yellow colour decreases. The SEM observations show a thin but well crystallised gypsum layer. It points to the external part, on the surface and on the curved zone. In contact with gypsum there is a layer with a large Si content (about 63%), that in the lower part increases to 74%. In some points of the border there is, in addition, gypsum. In the upper part of the thick layer, which seems a plaster, only Ca and Si are present and the Si content varies following the analysed points. The Si content de-

creases from outside to inside (11%) in the marble contact zone. The composition of the layer is probably connected to the chimney emission of the surrounding industrial zone. Iron oxides are also present.

Yellow–pink layer near grey–black crust (sample E6)

The stereoscopic observations show three layers. The external layer is very thin and red–brown coloured. Carbonaceous particles and iron oxides are present. Silicon is present in large amount together with significant amount of Fe and Al. Below the brown layer a pink–yellow layer which includes white or colourless clasts are well visible. It seems a plaster, which becomes light in the upper part.

The marble is present at the basis together with iron oxides stains. In the upper part, in contact with the surface. In the upper part of the lower layer the Si content ranging from 26 to 42% could be connected with the quartz present in the analysed area.

Table 12 EDAX analyses on sample E6

Analysis Elem.	1	2	3	4	5	6	7	8	9
Mg	-	-	-	-	0.3	-	2.7	7.2	15.4
Al	2.7	3.2	2.5	-	1.1	1.4	20.9	-	-
Si	86.6	87.0	66.4	18.8	32.9	32.5	38.4	-	-
Cl	1.2	-	1.4	-	0.2	-	-	-	-
K	0.8	-	0.8	-	0.6	1.2	19.1	-	-
Ca	5.6	5.0	18.4	81.1	63.6	62.9	18.9	92.7	84.5
Fe	2.9	4.5	10.3	-	1.2	1.9	-	-	-

5. Conclusions

The main decay phenomena macroscopically described in the introduction has been investigated by analytical methods which allowed us to make the following classification:

a) *From sheltered areas crusts formation from grey to black were detected. It is possible to distinguish two types of black crust.*

Samples E1 and E14 are very similar they contain a gypsum layer with a constant composition until 140–150 μm together with a few amount of iron oxides. Carbonaceous particles are mainly located on the surface and show a decreasing amount moving towards the inner part of the marble. Samples E4 and E7 are very similar and the gypsum layer is more thick than previous samples thus indicating that the sulphation processes have reached a higher rate of formation.

b) *From sheltered areas grey soiling formation were detected. In this case carbonaceous particles and silicon cementitious particles and gypsum layer are deposited above a brown iron oxide rich layer.*

Sample E11 and E15 has the same feature.

c) *From washed out areas yellow–brown layer were observed.*

Samples E2 and E3 show a thin yellow layer visible above the typical texture of the marble. Small quantities of gypsum are present in the cracks. The yellow–brown feature is due to particulate from soil carried by the winds. Small particles of iron oxides have also been detected by EDAX.

d) *Brown layer with soiling dust from sheltered and washed out areas were observed.*

Samples E10 and E12 were taken respectively from sheltered and washed out areas. They show the same brown superficial deposition of iron oxide and also a silicon increasing amount in the layer underneath the superficial gypsum layer. Sample E10 show an increasing amount of iron oxide moving towards the inner part of the marble. The abundant presence of iron and silicon is ascribed to cement industry.

e) *Red patina composed by iron oxide and silicon like in the E16 sample at the basis of a column.*

f) *Grey–black–crust from hollow on the ground-floor (sample E5) This crust is formed by a very thin gypsum layer which is deposited on a very thick silicon rich layer.*

Carbonaceous particles and iron oxides are present. Silicon is present in large amount together with significant amount of Fe and Al.

For the white marble the influence of the heavily polluted atmosphere in a marine environment is varying, resulting in several weathering patterns, mainly in the form of crusts.

Rusty, yellow patinas on washed out areas, firmly attached black grey crusts in contact with water and cementitious crusts in hollow groundfloor characterise the various material – environment interactions taking place.

Dust and deposition analysis give indications for the causes of the various crust formations. In particular, cement industry depositions could be related to the cementitious surface encrustations.

Salt crystals embedded give evidence to the characteristic synergy of air pollution, suspended particles deposition and marine spray producing damage to the stone surface.

Black crust formed on the hollow are mainly composed by cementitious particles. This type of decay was not generally found and it was ascribed to the deposition of suspended particles emitted from cement industry neighbourhood the archaelogical site. The howoll are formed by solution processes resulting from accumulation of rainwater reacting with suspended particles deposited during long period of dry deposition.

6. Acknowledgements

R. Fimmel
P.W. Mirwald
St. Brüggerhoff

Baumberg calcareous sandstone –a sensor material for various environmental influences– comparative results of a field exposure study

Baumberg calcareous sandstone
– a sensor material for various environmental influences –
comparative results of a field exposure study

R. Fimmel — *Institut f. Mineralogie, Univ. Innsbruck*

P.W. Mirwald — *Institut f. Mineralogie, Univ. Innsbruck*

St. Brüggerhoff — *Zollern Institut beim Deutschen Bergbau – Museum, Bochum*

1. Introduction

In the frame of an extended field exposure study Baumberg calcareous sandstone (BCS) which is well known for its weathering sensitivity and susceptibility for air poluttion components, in particular of SO_2, was exposed in West– and South–Germany at six sites and in the Tyrolian Alps at three sites of very different climate and anthropogene environment conditions. The duration of the exposures was five years in Germany and two years in Tyrol. Despite the difference in exposure duration the results allow to draw first principal conclusions.

2. Experimental

On most of the sites data of contineously monitored metereological parameters and a selection of important pollution data are available.

Stone slabs (50x50x5 mm) of this biomicritic material served as samples. Mounted on Mank–carrousels, they were exposed under "dry" and "wet" conditions. The starting material has been carefully characterized with respect to its basic properties such as mineral composition, inherent salt contents (SO_4^{2-}, NO_3^-, Cl^-, F^-), pore properties and hygric behavior.

In the following figures, only a representative number of five sites is shown.

We used "SO_2 presentation" (gm^{-2}) as the variable parameter which represents the product of the average of the pollution component, the average wind speed and the duration of exposure (in seconds).

3. Results and Discussion

In fig. 1 data of mass changes of BCS due to wet exposure are plotted versus the presentation amounts of SO_2 obtained from five representative sites (Eifel (Ei), München (Mü), Kempten (Ke), Innsbruck (Ibk) and Obergurgl (Og).

The data of all exposure sites uniformly show decrease in sample mass, a behavior which is only slightly modified by the specific environmental parameters conditions of the sites. Fig. 2 and 3 give the data of sample mass changes from the selected sites under dry weathering conditions and corresponding sulfate content analyse each plotted versus the SO_2 presentation.

The samples exposed in Germany exhibit all a typical tendency: the mostly positive mass changes of the samples are smaller than the mass of sulfate contents.

The samples exposed in Tyrol differ significantely. In Innsbruck both parameters, sample mass and mass of sulfate, show also increasing behavior. However, there is a slight tendency to be observed: the gain in sample mass exceeds that of the sulfate content. A completely different behavior is observed in Obergurgl: very small sulfate contents contrast with dramatic mass losses.

The samples which had been exposed with beginning of summer under wet conditions exhibit no mass losses (Ei, Ibk) or show even small mass increases (Mü, Ke). Sample mass increases have been documented, in addition,

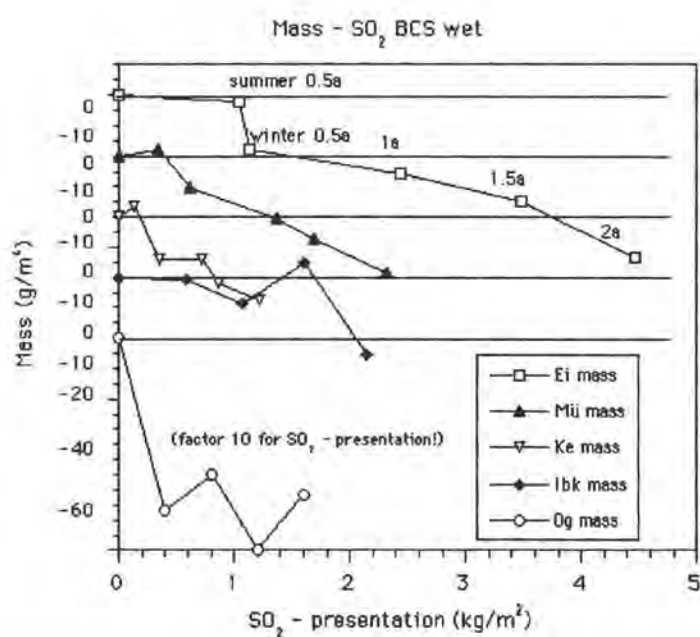*Fig. 1   Mass changes of wet exposed BCS–slabs in a period of two years. Abbreviation of sites: Ei=Eifel,*
Mü=München, Ke=Kempten, Ibk=Innsbruck, Og=Obergurgl.
(Notice that SO₂ presentation of Og–data has been enlarged by the factor of ten.)

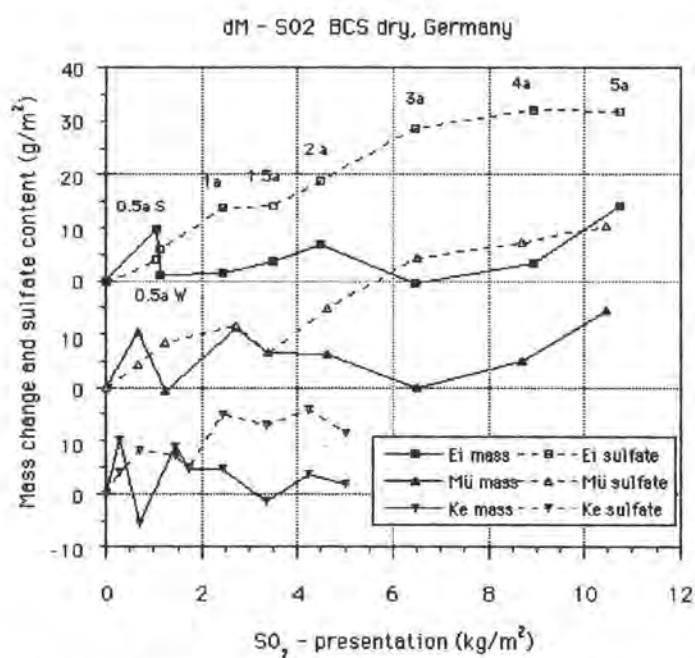*Fig. 2   Mass change and sulfate content of dry exposed BCS–slabs in a period of five years in Germany.*
Abbreviations see fig. 1.

dM - SO₂ BCS dry Tyrd
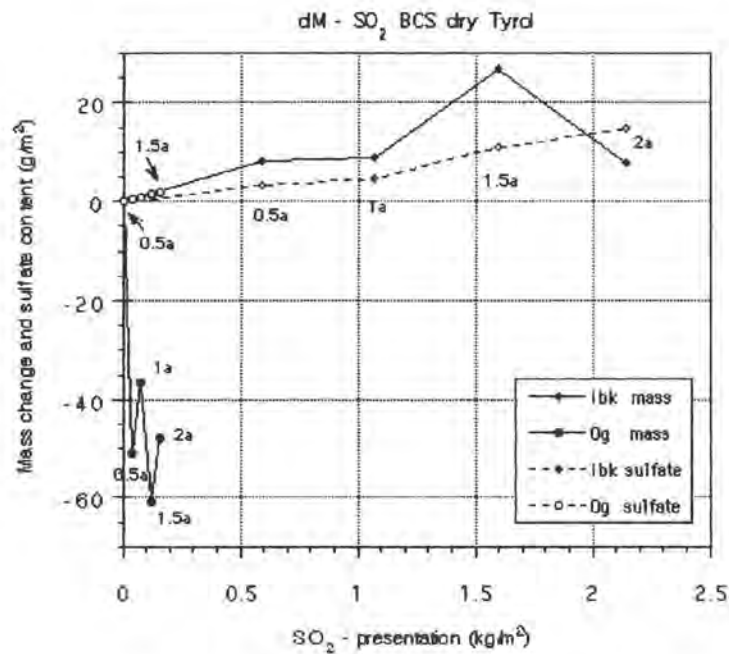
Fig. 3 *Mass change and sulfate content of dry exposed BCS–slabs in a period of two years on two sites in Tyrol. Abbreviations see fig. 1.*

for Ibk and Og when sampling was taking place at the end of summer season. This finding may be related with mass gain, mostly due to biogen activities inside or on the surface of the samples.

The severe impact of winterly frost and thaw cycles is well documented in the data. For the alpine sites Ibk and Og, in particular for the Og–site, a distinct mass decrease is observed. The significant mass losses in the winter season in Og enable apparantely the biogen reactivation in the following summer season. A specific influence of rain solubility on the samples materials has to be assumed but can not be quantified explicitly. But, possibly, the range of amounts in yearly precipitation (Mü ca. 1050 mm/a and Ibk ca. 750 mm/a) is not wide enough for producing significant differences.

The "dry" exposed slabs indicate that the

observed weathering effects represent the integral sum of a number of partial processes which lastly represent a complex decay system. On the basis of the available data it is possible to distinguish a number of various partial processes:

– *formation of autigenic gypsum,*

– *deposition of exogenic gypsum,*

– *mechanically induced grain loss and*

– *dust deposition (including biogen material).*

These processes for which a rough quantitative estimate will be derived in the following may be considered the major components of the bulk weathering process.

The analysed amount of sulfate is usually assumed to represent the reaction of SO_2– immision with the carbonate material. However, the analyses of Obernkirchner sandstone (OKS), a carbonate free quarzitic sandstone

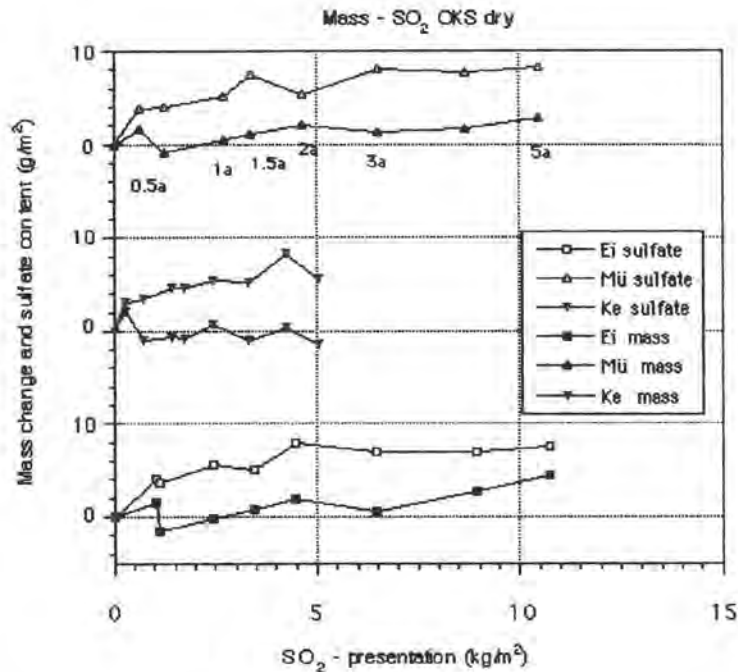Fig. 4   Mass change and sulfate content of dry exposed Obernkrichner sandstone (OKS) an German sites.
          These data are the basis for determining the mass of exogenic sulfate deposition. Abbreviations see fig. 1.

which was simultaneously exposed on the German sites revealed considerable amounts of sulfate (fig. 4). We conclude, that considerable amounts of "exogenic sulfate" are deposited on the exposed materials. This means for the carbonate materials that the bulk amount of analyticaly determined sulfate is partially of exogenic and partially of autigenic provenience.

3.1 Estimation of partial weathering processes

In a first step the bulk sulfate was analysed for the BCS samples. In a second step the autigenic gypsum of the BCS-samples of the German sites has been determined by subtracting the amount of sulfate determined on the OKS–samples from the bulk mass of sulfate analysed on the BCS–samples. Porosity and grain sizes of both materials does not essentially differ in adsorption behavior and therefore does not impair this estimate in a significant way.

Since no simultaneous exposure of BCS and OKS has been performed on the Tyrolian sites, we used linear regression of the data for estimating the exogenic and autigenic portions of the analysed bulk amount of sulfate.

Thirdly, the difference in mass changes as determined on the samples and calculated from the sulfate analyses has been determined to give an estimate for the net losses of substance (stone materials plus sulfate plus small amounts of "dust").

Fig. 5 displays a quantitative estimate for the different partial processes of BCS (dry exposition) for eight exposure sites. The amount of "dust", which is in terms of mass a relatively unimportant quantity, has been estimated.

– A striking result of this estimation is the considerable amount of exogenic sulfate for the highly industrialised areas around Duisburg, Dortmund and Nürnberg, which are already
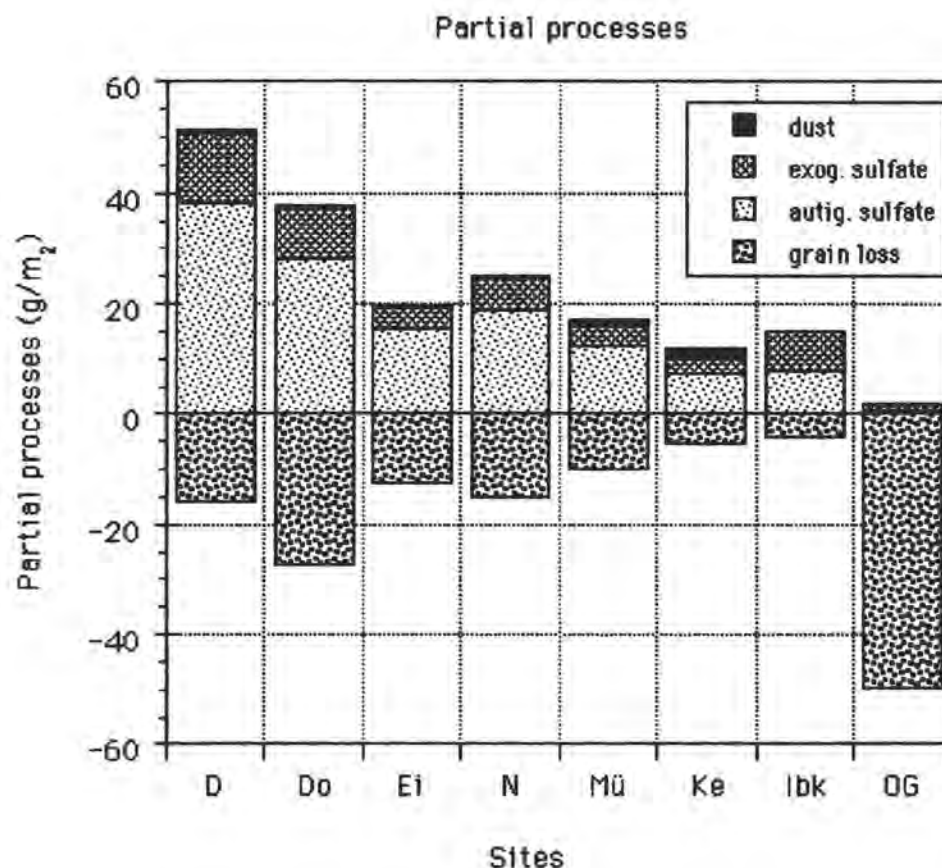
Partial processes

Fig. 5   *The major partial processes at "dry weathering" of BCS determined for eight sites in Germany and Tyrol. N=Nürnberg, D=Duisburg, Do=Dortmund. For other abbreviations see fig.1.*

characterized by a considerable SO_2-pollution level.

– The only site with a really low pollution situation is Obergurgl; the other socalled "pure air areas" of Kempten and Eifel has to be classified as medium polluted areas.

– It is interesting that the alpine town of Innsbruck is also characterized by a medium pollution situation and does not distinguish from the other middle European areas studied.

Furthermore, there seems to be a direct correlation between material loss and sulfate content (except Duisburg). The only exception in this respect is represented by the data from

Obergurgl where the maximum materials losses observed have to be correlated with the impact of the severe alpine climate.

This very specific reactivity of BCS on various environmental loads and specific climate impacts indicated by the presented data suggests that this stone can be used as a sensor material.

4. Acknowledgements

B. Fitzner
K. Heinrichs
M. Volker

Model for salt weathering at maltese globigerina limestones

Model for salt weathering at maltese globigerina limestones

B. Fitzner, K. Heinrichs, M. Volker
Geologisches Institut, Rheinisch – Westfälische
Technische Hochschule Aachen (RWTH)
Arbeitsgruppe "Natursteine und Verwitterung" Wullnerstraße. 2, 52062 Aachen, Germany

Abstract

Tertiary Globigerina limestones were used predominantely for the construction of Maltese monuments. This concerns the famous Megalithic temples and monuments of later construction periods. Today the monuments show weathering damages of different type, intensity and distribution. As a consequence of the marine environment of Malta, salt weathering has been recognized as main weathering process responsible for the degradation of monuments.

Globigerina limestones were characterized according to petrographical properties. The phenomenologic weathering damages were registered, documented and evaluated at representative monuments by means of the monument mapping method.

According to the investigation results, varieties of Globigerina limestones can be differentiated with respect to petrographical properties and susceptibility to salt weathering. A model for salt weathering of different Globigerina limestone varieties used at Maltese monuments has been worked out.

1. Introduction

The majority of Maltese monuments were constructed from natural stones of the island. Malta is mainly composed of Oligocene–Miocene sediments. Stratigraphically, this mid–Tertiary sequence of sediments is subdivided into formations of Lower Coralline Limestone, Lower Globigerina Limestone, Lower main conglomerate, Middle Globigeri-na Limestone, Upper main conglomerate, Upper Globigerina Limestone, Blue clay, Greensand and Upper Coralline Limestone (ALEXANDER, 1988). Since antiquity until today mostly the Globigerina limestones – and here predominantly those of the Lower Globigerina Limestone formation – were used for monument construction. These limestones – representing a soft stone material which can be worked easily – cover large parts of Malta. The main quarries are located in the Siggiewi – Mqabba – Qrendi area. According to information given by quarry owners, different qualities of Globigerina limestones can be distinguished.

Very important periods for the construction of the Maltese stone monuments were Neolithic, Renaissance and Baroque. Today the monuments show weathering damages of different type, intensity and distribution. Within the framework of the international research project "Marine spray and polluted atmosphere as factors of damage to monuments in the Mediterranean coastal environment" – supported by the European Commission – different research groups in interdisciplinary cooperation have executed investigations on the degradation of the Globigerina limestones. The Church of Sta. Marija Ta' Cwerra, which is located in the village of Siggiewi in the southwest of Malta, was chosen as reference monument. According to the results concerning the church, salt weathering due to marine environment is the essential weathering process for the degradation of Globigerina limestones. This scientific finding also applies to most of

Maltese monuments made from Globigerina limestones.

Besides investigations in the framework of the EC–project, the authors have carried out additional investigations including petrographical studies on Globigerina limestone samples from various quarries, as well as registration, documentation and evaluation of weathering damages at different monuments. Based on the whole of results, a model has been derived for the salt weathering of Glogigerina limestones at monuments.

2. Petrographical properties

For the petrographical characterization of unweathered Globigerina limestones of the Lower Globigerina limestone formation, samples were taken from different layers of the quarries no. 1 near Siggiewi (2 layers), no. 10 near Tal–Balal (1 layer) and no. 27 near Mqabba (11 layers). The quality grades assigned to the individual layers by the quarry owners were noted correspondingly. These quality grades refer to the weathering susceptibility of the limestones. Mineral composition, microstructural properties as well as water and humidity transport properties were studied. X–ray diffraction, thin section microscopy with image analysis, scanning electron microscopy, mercury porosimetry, nitrogen sorption and different water absorption/desorption tests were the applied procedures.

Samples taken from the Church of Sta. Marija Ta' Cwerra in Siggiewi were also studied and compared to those of the quarries. Sampling was not possible of further monuments under investigation.

Based on results obtained for the quarry samples, the Globigerina limestones can be classified as almost pure limestones. The carbonate components are micrite, sparite and bioclasts with variation of contents. Micrite – microcrystalline calcite – is the main constituent of the limestones. The samples from the eleven layers of the quarry near Mqabba have

shown contents of micrite mostly in the range between 60 vol.–% and 74 vol.–% referring to pore–free stone volume. The content of sparite on these samples ranges between 10 vol.–% and 30 vol.–%. Most frequently it amounts to about 20 vol.–%. The content of bioclasts ranges between 4 vol.–% and 16 vol.–%. Samples taken from the quarries near Siggiewi and near Tal–Balal show higher contents of micrite (Siggiewi: 80 vol.–%, Tal–Balal: 88 vol.–%). The contents of sparite and bioclasts are correspondingly lower. Quartz (< 2 vol.–%), Fe–oxides/hydroxides (mostly < 1 vol.–%), glauconite, feldspar and kaolinite (extreme low contents) are secondary components of the Globigerina limestones. Following the classification for limestones according to FOLK (1962), the Globigerina limestones are to be classified as biomicrites.

The Globigerina limestones are characterized by high total porosities ranging from about 32 vol.–% up to 40 vol.–%. The pore size distributions vary significantly. The maximum size of pore radii amounts to 100 m. The pore surface of analyzed samples ranges between 2 $m^2 \cdot g^{-1}$ and 13 $m^2 \cdot g^{-1}$. In correlation to the variation of porosity properties, water and humidity transport properties vary, too. The water uptake rate of samples ranges between 14 weight–% and 23 weight–% under atmospheric pressure, between 17 weight–% and 23 weight–% under pressure of 150 bar. The saturation coefficient ranges between 0.8 and 1.0. The capillary water uptake rate of the analyzed samples ranges between 3 $kg \cdot m^{-2} \cdot h^{-1/2}$ and 18 $kg \cdot m^{-2} \cdot h^{-1/2}$. The water vapor diffusion resistance ranges between 10 and 20.

Based on petrographical results, differences concerning "stone quality" could be deduced and explained. For all the following considerations regarding salt weathering at the Globigerina limestones, "good quality" limestones and "bad quality" limestones will be distiguinshed in principle.

In Table 1 the stone properties of representative samples with "good quality" and, re-

Table 1 *Stone characteristics of good quality and bad quality Globigerina limestones shown by means of representative samples.*

Globigerina Limestones			
Stone characteristics		**Good quality** sample Q02700009	**Bad quality** sample Q02700003
Mineral composition	Carbonate components [Vol.-%]	Sparite 18.3 Micrite 74.8 Bioclasts 6.3	Sparite 22.2 Micrite 71.0 Bioclasts 4.3
	Accessory components	Quartz, Feldspar, Glauconite, Fe-oxides/-hydroxides	Quartz, Feldspar, Glauconite, Fe-oxides/-hydroxides
	Clay minerals	--	Kaolinite
	Petrographical classification (Folk, 1962)	Biomicrite	Biomicrite
Microstructural properties	Total porosity [Vol.-%]	34.8	33.0
	Portions of pores with radii < 0.0019 µm 0.0019 - 0.1 µm 0.1 - 3 µm > 3 µm	[Vol.-%] 0.1 1.2 21.3 12.2	[Vol.-%] 0.4 3.5 23.4 5.7
	Maximum pore radius [µm]	100	75
	Pore surface [$m^2 \cdot g^{-1}$]	3.4	12.8
Water and humidity transport properties	Water uptake rate (atmosph. pressure) [weight-%]	20.8	14.1
	Velocity of water uptake	+	±
	Capillary water uptake w-value [$kg \cdot m^{-2} \cdot h^{-1/2}$]	9.6	3.1
	Velocity of water desorption	+	±
	Water vapor diffusion resistance µ [-]	15.8	19.9
Weathering behaviour in salt crystallization simulation test		**slight** damages esp. granular disintegration	**severe** damages esp. crumbling and contour scaling

spectively, "bad quality" Globigerina limestones are shown. Comparing good and bad quality limestones, the following statements can be made. Referring to the mineral composition, good and bad quality limestones are very similar apart from a very low content of clay mineral kaolinite in bad quality limestones. Thus, a correlation between mineral composition and different stone qualities can not be recognized.

Referring to microstructural properties, good and bad quality limestones show significant differences. The bad quality limestone differs from the good quality limestone, especially for a lower portion of large pores and higher portion of small and very small pores resulting in a significantly higher pore surface. The variations of porosity properties correlate with variations of water and humidity transport properties. Good quality limestones show higher water uptake rates, a higher velocity of water absorption and desorption and a lower vapour diffusion resistance compared to bad quality limestones.

According to current theories, the susceptibility of stone material to salt weathering is conditioned by the porosity characteristics and here especially by the proportion of large pores to small pores assuming a sufficient total porosity (FITZNER 1994). Due to thermodynamic reasons, salt crystallization starts in the large pores. Small–dimensioned pores serve as supply reservoir for salt solutions, thus allowing the growth of salt crystals. After the filling of large pores, the crystallization process continues in direction of smaller pores. Here critical crystallization pressures resulting in stone deterioration can occur. With respect to Globigerina limestones, this means that at comparable salt concentrations critical crystallization pressures are less likely to occur in good quality limestones than in bad quality limestones. This way, a higher resistance of good quality limestones to salt weathering can be explained.

This was proved by salt crystallization simulation tests on representative samples of good and bad quality Globigerina limestones (Table 1). At good quality limestones slight granular disintegration was generally noticed. At bad quality limestones severe damages occurred.

Characteristic weathering forms were contour scaling and crumbling resulting in significant loss of stone material.

The petrographical properties of unweathered parts of the samples taken from the Church of Sta. Marija Ta' Cwerra in Siggiewi are in good relation with those of good quality Globigerina limestones found in the quarries. Halite was identified as newly–formed mineral due to weathering in numerous weathered samples of the church.

3. Weathering forms

For the registration, documentation and evaluation of weathering damages, the monument mapping method was applied as an experienced non–destructive procedure. The monument mapping method is based on an internationally recognized classification scheme which defines weathering forms at natural stones clearly and completely according to phenomenologic/geometric criteria (FITZNER & KOWNATZKI, 1990; FITZNER, HEINRICHS & KOWNATZKI, 1992; FITZNER, HEINRICHS & KOWNATZKI, 1995). By means of this classification scheme all weathering forms at the monument are mapped in detail stone by stone. Thus, the complete stone surface is described and documented precisely and objectively according to type, intensity and distribution of weathering forms. All information gained with the monument mapping method are processed in special computer programmes. The information can be organized systematically, graphically illustrated and quantitatively evaluated.

Different ages, architectural styles and locations were considered for the selection of Maltese monuments to be studied. This was important in order to guarantee that conclusions concerning the model for salt weathering

are meaningful for the majority of the Maltese monuments made from Globigerina limestones. In addition to the Church of Sta. Marija Ta' Cwerra in Siggiewi (18th century), the following monuments were selected for investigations: Megalithic temples of Hagar Qim and Mnajdra (Neolithic) at the southern coast of Malta, fortification (16th century) and Church of St. Catherine (16th – 18th century) in Valetta located in the northeast of Malta and Couvre Porte (18th century) in Vittoriosa located at the northeastern coast of Malta.

The mapping results obtained for the Church of Sta. Marija Ta' Cwerra, Couvre Porte and the Megalithic temples of Hagar Qim have been described in detail in FITZNER, HEINRICHS & VOLKER (in press). The mapping results gained for the Church of Sta. Marija Ta' Cwerra in Siggiewi and Couvre Porte in Vittoriosa are summarized in the following, because these two monuments will be refered afterwards to when explaining the model for salt weathering.

The Church of Sta. Marija Ta' Cwerra in Siggiewi was built probably in the 16th century. The monument of today dates back to a rebuilding in the 18th century. Investigations were carried out at the four outer walls of this free–standing small church. Three zones in vertical order at the church can be distinguished. The lower part of the façades had been covered with mortar. Thus a mapping of stone damages was not possible. Upwards a zone follows with at least moderate up to severe damages. The third comprises the upper part of the façades. With the exception of few building stones this third zone has remained in rather good condition.

Granular disintegration and relief – a morphological change of the stone surface – by rounding/notching are the prevailing weathering forms, both occuring with mainly slight intensities. Detachment and loss of stone material are characteristic for the middle zone. At most of the building stones in this zone relief by rounding/ notching occurs. Re-

lief in the form of alveolae affects numerous building stones, too. Uniform back wathering parallel to the stone surface is another frequent weathering form, most significant at the south façade.

Referring to detachment of stone material, the granular disintegration is the most frequent weathering form, occuring mainly with moderate or even high intensity. Further frequent weathering forms which describe the detachment of stone material are granular disintegration to flaking, flaking (detachment of small thin stone elements following the profile of the stone surface), flaking to contour scaling and contour scaling (detachment of larger stone elements following the profile of the stone surface). The south façade shows the highest percentage of building stones affected by contour scaling. In most cases back–weathered building stones are concerned. The scales mostly are rather thin.

In the mapping period, efflorescences could be seen on the surface of numerous building stones, especially at those of the south façade.

The Couvre Porte is part of the southern landward fortification of Vittoriosa. According to the inscription on its front, the gate was built in 1722. The front façade was mapped completely. The majority of building stones show extensive damages. Relief by rounding/notching affects numerous building stones. Relief in form of alveolae mainly occurs at the lower parts of the gate. At the pillasters intense back weathering occurs. Most of the building stones at Couvre Porte show recent detachment of stone material. Manifold weathering forms occur, frequently in combination. The high percentage of building stones affected by contour scaling is very impressive. Compared to the Church of Sta. Marija Ta' Cwerra, at Couvre Porte thicker and also multiple scales occur very frequently. Besides this difference, the building stones affected by contour scaling are distributed all over the façade at Couvre Porte, in contrast to the zonation at the Church of Sta. Marija Ta' Cwerra.

4. Model for salt weathering

The results obtained by the different EC–research groups have shown that salt weathering as a consequence of marine influence must be considered as the essential weathering process which determines the degradation of the Globigerina limestones used at the Maltese monuments. High concentration of halite can be found in the building stones of the monuments. Frequent seasonal and daily variations of relative air humidity with respect to the equilibrium relative humidity of halite (about 75%) are likely to result in high frequencies of salt solution–salt mobilization–salt crystallization cycles.

According to the petrographical studies, different qualities of Globigerina limestones with respect to salt weathering can be distinguished. Besides good and bad quality limestones, also transition qualities occur. However, the term "good quality" is justified only in a restricted way, as it can be seen from the example of the Church of Sta. Marija Ta' Cwerra. Slight up to severe weathering damages occur at this monument which was built with good quality Globigerina limestones. The significant zonation at this monument according to types and intensities of weathering forms leads to the following statements. The zonation of weathering damages obviously indicate different salt concentrations. The zone with severe weathering damages is characterized by high concentrations of halite. Obviously, this zone is affected intensively by rising damp resulting in intense salt accumulation. Thus, the uppermost boundary of the zone with severe damages correlates to the highest level of rising damp. The predominantely slight weathering damages in the upper zone of the church indicate comparatively lower salt concentrations. Therefore, the term "good quality limestone" is not always appropriate. With increasing salt load the susceptibility of these limestones to salt weathering increases, too. Nevertheless, the good quality limestones confirmed to be the better stone material, compared to bad quality limestones, as the bad quality limestones show severe damages even at low salt loads. This can be seen at the Couvre Porte in Vittoriosa. The occurrence of intense weathering damages all over the façade indicates that this monument was built with bad quality limestones. Obviously, severe stone degradation is characteristic for bad quality limestones independent of salt load variations, since even building stones in the higher parts of the façade – for which again lower salt concentrations can be assumed – have suffered severe damages.

Based on the results obtained for the Church of Sta. Marija Ta' Cwerra, Couvre Porte and for further monuments, characteristic chronological sequences of weathering forms could be deduced in dependence on stone qualities and salt load variation (Figure 1). At low salt loads, good quality Globigerina limestones show granular disintegration, flaking and the transitional form granular disintegration to flaking as characteristical weathering forms relevant to detachment of stone material (line 1). Relief – the morphological change of the stone surface – predominantely by rounding/notching is the consequent weathering form as regards loss of stone material. In general, all these weathering forms are of slight intensity only. Correspondingly, the damages are to be rated as slight.

At medium salt load the good quality limestones again follow either line 2a or line 2b – predominantely line 2a – whereas line 3 is not reached. This concerns, for example, the transitional zone between parts of monuments affected by high salt load as a consequence of rising damp and parts of the monuments with low salt load. This can be seen, for example, at the façades of the Church of Sta. Marija Ta' Cwerra. The damages can be rated mostly as moderate in this case.

At high salt load the good quality limestones may follow two different chronological sequences (lines 2a and 2b). Granular disintegration, but also granular disintegration to flaking and flaking are typical primary weathering
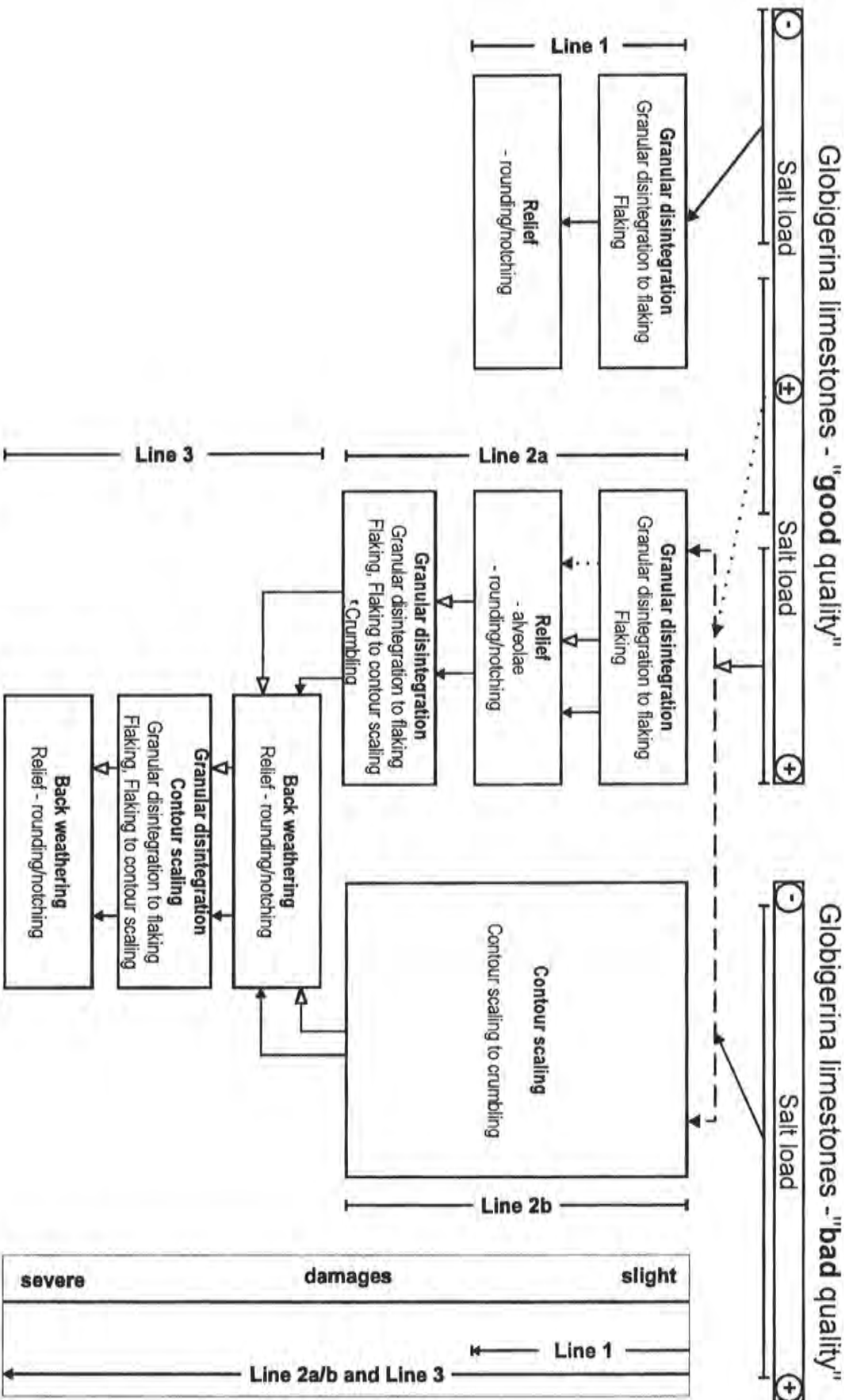
Fig. 1 Characteristic chronological sequences of weathering forms at Globigerina limestones in dependence on stone quality and degree of salt load.

forms of the first sequence (line 2a), which is followed predominantely. They result very frequently in the formation of relief in form of alveolae or in form of rounding/ notching. Further granular disintegration, but also granular disintegration to flaking, flaking and additionally flaking to contour scaling and crumbling lead to receding of the stone surface. Back weathering – the uniform loss of stone material parallel to the original stone surface – is the prevailing weathering form. Herewith the chronology of weathering forms enters line 3. This stage of back weathering is also reached as a consequence of contour scaling and contour scaling to crumbling. These weathering forms represent the second possibility of primary weathering forms of good quality limestones at high salt load (line 2b). At the back–weathered stone surfaces the detachment of stone material continues, especially in the form of granular disintegration and contour scaling, but also in the form of granular disintegration to flaking, flaking or flaking to contour scaling (line 3). Particularly further back weathering is the consequence of this. The degree of damages resulting form the complete sequence of lines 2a/2b and 3 must be rated as severe.

The bad quality limestones first follow line 2a or 2b independent of the degree of salt load. In comparison to good quality limestones, bad quality limestones much more often follow line 2b. In contrast to good quality limestones, they frequently pass through line 3 already at lower salt load. Thus they may suffer severe damages almost independent of the degree of salt load.

Referring to lines 2a and 2b it is worth noting that both lines may be followed at the same building stone. This concerns both good and bad quality limestones and might be due to inhomogeneities in the limestones.

In Figure 2 the state of weathering at the south façade of the Church of Sta. Ta' Cwerra (good quality Globigerina limestone) and at the Couvre Porte (bad quality Globigerina

limestone) is illustrated according lines 1, 2a/2b and 3, which refer to the chronology of weathering forms described in this chapter and presented in Figure 1. The figure confirms the interrelations between stone quality, salt load and sequences of weathering forms.

Comparing again good and bad quality Globigerina limestones with respect to lines 2a and 2b, the following trends were observed. Good quality limestones follow rather line 2a than 2b. This means, that in the primary phase of weathering the detachment of grainy, respectively, small–dimension stone elements is very characteristic. Bad quality limestones follow line 2b very frequently. This means, that especially the detachment of larger–dimension stone elements (scales, crumbs) is very characteristic at the beginning of weathering. The results of salt crystallization simulation tests have confirmed these trends, which can be explained by the different water and humidity transport properties of the different Globigerina limestone varieties. Good quality limestones show higher water uptake rates, a higher velocity of water absorption and desorption and a lower vapour diffusion resistance, compared to bad quality limestones. Referring to the situation at monuments this means, that in the phase of rain fall good quality limestone can take up a high amount of water within short time. Bad quality limestones will take up a lower amount of water and this more slowly. In this phase the maximum of the humidity distribution will be close to the stone surface in both cases. After a longer phase of rainfall the water is penetrated into the stone material deeply.

In the phase of drying, the humidity distribution in the limestones will be conditioned essentially by the capillary transport properties. Good quality limestone is characterized by very good capillary transport of water. Thus the water tranport can keep abreast with evaporation for a long time. The capillary stream to the stone surface will be interrupted rather late. This means that the front of evaporation in the limestone will be close to the stone surface. Referring to bad quality lime-

Couvre Porte/Vittoriosa

Church of Sta. Marija Ta'Cwerra/Siggiewi
South façade

Line 1

Line 2a and/or 2b

Line 3

1m

1m
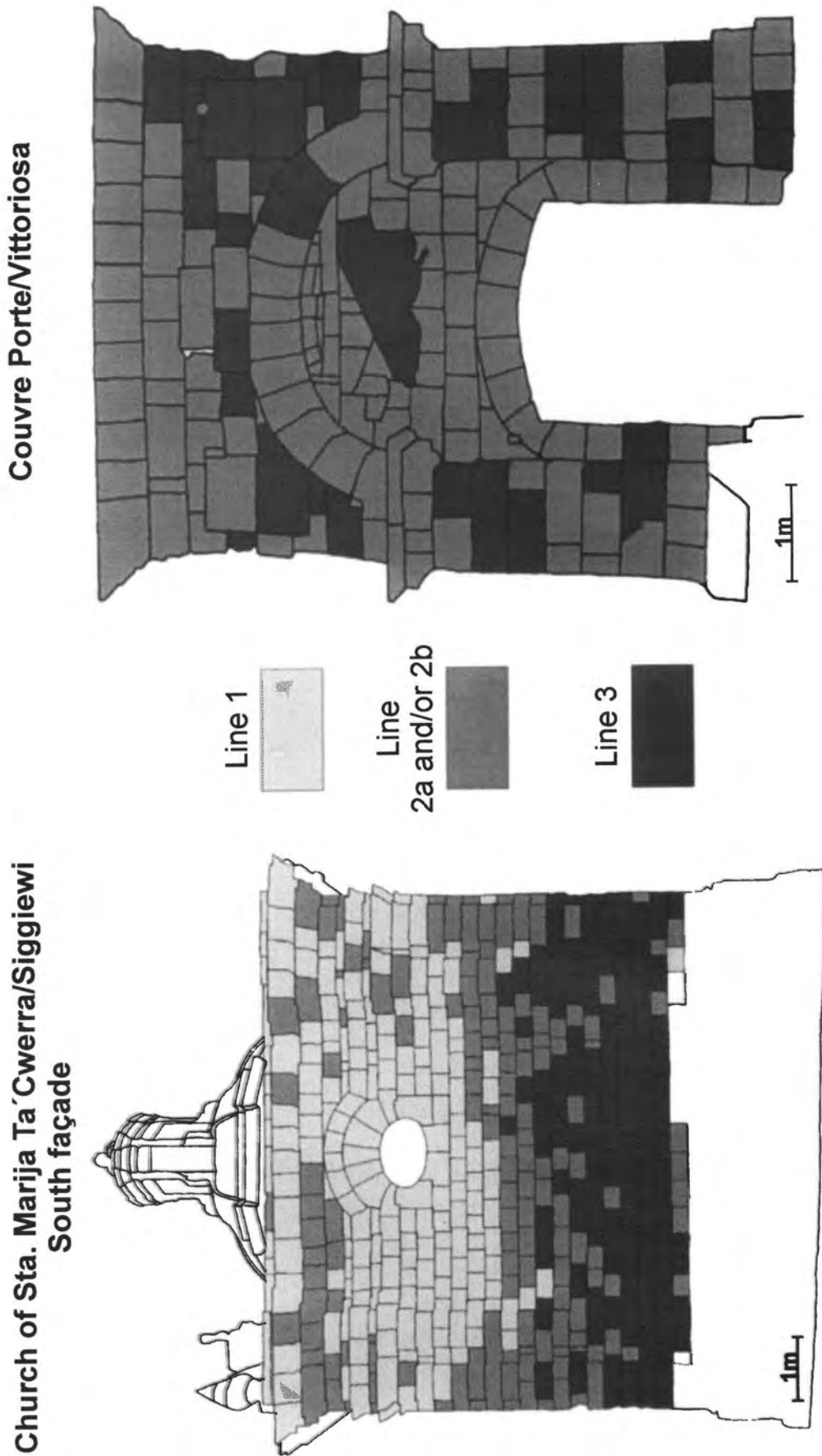
Fig. 2 State of weathering at the Church of Sta. Marija Ta' Cwerra / south façade and at Couvre Porte expressed by lines 1, 2a/2b and 3 refering to the chronology of weathering forms presented in figure 1.
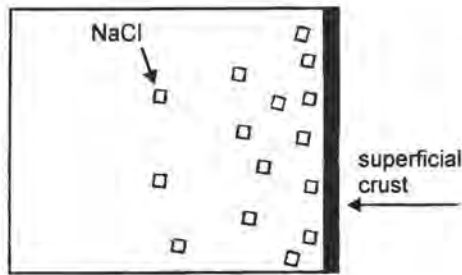
a) Phase 1: Formation of a superficial crust by recrystallization of dissolved calcite. At the same time accumulation of salt.
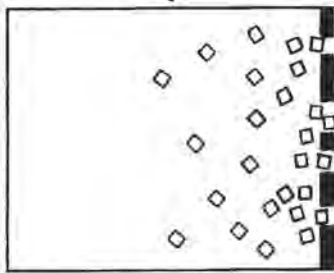
b) Phase 2: Cracking and/or partial loss of the crust due to mechanical stress, eg. evoked by salt crystallization. Further accumulation of salt.
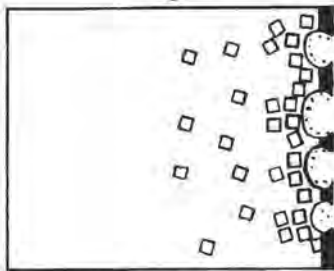
c) Phase 3: Increase of evaporation at parts where the crust is lost. Salt crystallization near to the stone surface evokes detachment of stone material such as "granular disintegration" and "flaking" and by this the formation of alveolae.
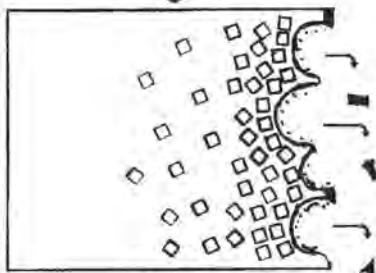
d) Phase 4: Further salt crystallization results in further detachment of stone material. Increasing depths of the alveolae. Rests of the crusts get hollowed out from below and then fall of with adherent stone material. Intersection of the alveolae. Salt accumulation and detachment of stone material continue.
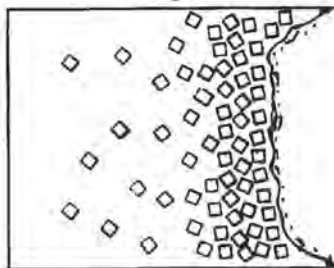
e) Phase 5: Final phase of the alveolar weathering. Receded stone surface - "back weathering". Further detachment of stone material may increase the depth of back weathering.

Figs. 3a-e Phases of alveolar weathering at Globigerina limestones.

stones – characterized by minor capillary transport of water – the capillary stream towards the stone surface will be interrupted earlier. Thus the front of evaporation in the limestone will be deeper in these limestones. Correspondingly, at good quality limestones, salts will crystallize closer to the stone surface in comparison to bad quality limestones. This explains the detachment of mainly small–dimension stone elements at good quality limestones and the detachment of mainly larger–dimension stone elements at bad quality limestones in early phases of salt weathering. In case of rising damp the situations will be more or less comparable to those described just before. In this case, however, at bad quality limestones in lower parts of monuments the front of evaporation and salt crystallization may be located exceptionally close to the stone surface.

This explains, that the formation of alveolae as a consequence of the detachment of grainy, respectively, small–dimension stone elements frequently is limited to lower parts of monuments built with bad quality limestones, as it has been described for Couvre Porte.

It has to be remarked, that water and humidity transport, zones of salt crystallization and weathering forms probably depend on certain variations due to different location, exposition and architectural structure of monuments. The south façade of the Church of Sta. Marija Ta' Cwerra shows the highest percentage of severely damaged building stones, although comparable salt load occur in all the four façades of the church in the zone concerned. The same trend was observed at other monuments, too. It can be assumed, that high solar irradiation influences humidity transport, evaporation and salt crytallization, determining an increase in the frequency of salt crystallization cycles. This again provokes the quicker development of severe damages.

As last contribution to the model of salt weathering at Globigerina limestones the different phases of alveolar weathering related to salt influence are described. Results presented in this

context by VANNUCI et al. (1994) were considered. As it has already been mentioned, the formation of alveolae is especially characteristic for good quality limestones at medium to high salt load. Five different phases of aleveolar weathering can be distinguished (Figure 3a–e).

In phase 1 a superficial crust develops by recrystallization of dissolved calcite (Figure 3a). At the same time salt accumulates. Due to different porosity properties and different water transport properties, the formation of such hardened zones is more probable at good quality limestones than at bad quality ones.

In phase 2 (Figure 3b) the crust gets cracked and partially lost due to salt crystallization and/or mechanical stress at the interface of crust and stone interior. Salt further accumulates in the pore space.

At parts of the building stones where the crust has been lost the rate of evaporation increases. Salts crystallize close to the stone surface resulting in granular disintegration and flaking, with the formation of alveolae, the depth of which increases more and more (phase 3, Figure 3c, see also early stage of line 2a in Figure 1).

In phase 4 (Figure 3d) the dimension of the alveolae has increased so that rests of the crust get hollowed out from below. The rests of the crust with adherent stone material fall from the stone surface. The alveolae intersect. The accumulation of salt may further increase up to the further detachment of stone material in the form of granular disintegration, granular disintegration to flaking, flaking, flaking to contour scaling or crumbling (see late stage of line 2a in Figure 1).

This detachment of stone material leads to a rather uniformly receded stone surface (phase 5, Figure 3e), which represents the final stage of the alveolar weathering. This situation corresponds to "back weathering" as regards the mapping of weathering forms (see first stage of line 3 in Figure 1). Further detachment of stone material as consequence of salt load can lead to further back weathering.

5. Conclusions

Different states of degradation occur at the Maltese monuments built with Globigerina limestones. These differences refer to the intensity of salt weathering, which has been recognized as decisive weathering process leading to stone degradation. The intensity of salt weathering again is basically controlled by stone characteristics – especially porosity properties – and degree of salt accumulation. The model of salt weathering presented provides essential information on the interrelations between Globigerina limestone qualities, salt load and development of phenomenological weathering damages. Certainly, this model is representative for the majority of the Maltese monuments built with Globigerina limestones. The model allows the explanation of recent degradation states at the monuments, as well as prognoses on progress of degradation. Furthermore, it provides an important basis for the deduction of requirements in terms of appropriate preservation measures for the monuments.

6. Acknowledgements

7. References

1. Alexander, D.: A review of the physical geography of Malta and its significance for tectonic geomorphology.– Quaternary Science Reviews, Vol. 7, pp. 41–53, Oxford – Great Britain, 1988.

2. Fitzner, B.: Porosity properties and weathering behaviour of natural stones – methodology and examples.– Proceedings of the C.U.M. 2nd Course "Stone materials in monuments: diagnosis and conservation", Heraklion – Crete, 24.–30.05.1993, pp. 43–54, C.U.M. University School of Monument Conservation, 1994.

3. Fitzner, B., Heinrichs, K. & Kownatzki, R.: Classification and mapping of weathering forms.– Proceedings of the 7th International Congress on Deterioration and Conservation of Stone, Lisbon, 15.–18.06.1992, pp. 957–968, Laboratorio Nacional de Engenharia Civil – Lisbon, 1992.

4. Fitzner, B., Heinrichs, K. & Kownatzki, R.: Weathering forms – classification and mapping. Verwitterungsformen – Klassifizierung und Kartierung.– In: SNETHLAGE, R. (ed.): Naturwissenschaft und Denkmalpflege, Natursteinkonservierung I, pp. 1–48, Förderprojekt des Bundesministers für Bildung, Wissenschaft, Forschung und Technologie, Verlag Ernst & Sohn, Berlin, 1995.

5. Fitzner, B., Heinrichs, K. & Volker, M.: Stone deterioration of monuments in Malta.– LCP Congress, Montreux – Switzerland, 25.–29.09.1995, in press.

6. Fitzner, B. & Kownatzki, R.: Bauwerkskartierung–Schadensaufnahme an Naturwerksteinen.– Der Freiberu fliche Restaurator, 4, pp. 25–40, Kiel, 1990.

7. Folk, R.L.: Spectral subdivision of limestone types.– Amer. Ass. Petrol. Geol., Mem., 1, pp. 62–84, Tulsa, Okl., 1962.

8. Vannuci, S., Alessandrini, G., Cassar, J. Tampone, G. & Vannuci, M.L.: Templi megalitici preistorici delle isole maltesi: cause e processi di degradazione del Globigerina Limestone.– In: Fassina, V, Ott, H. & Zezza, F. (Eds.): 3rd Int. Symposium on the Conservation of Monuments in the Mediterranean Basin, Venice, 22.–25.06.1994, pp. 555–565, Soprintendenza ai Beni Artistici e Storici di Venezia, 1994.

B. Fitzner
K. Heinrichs
M. Volker

Monument mapping – a contribution to monument preservation
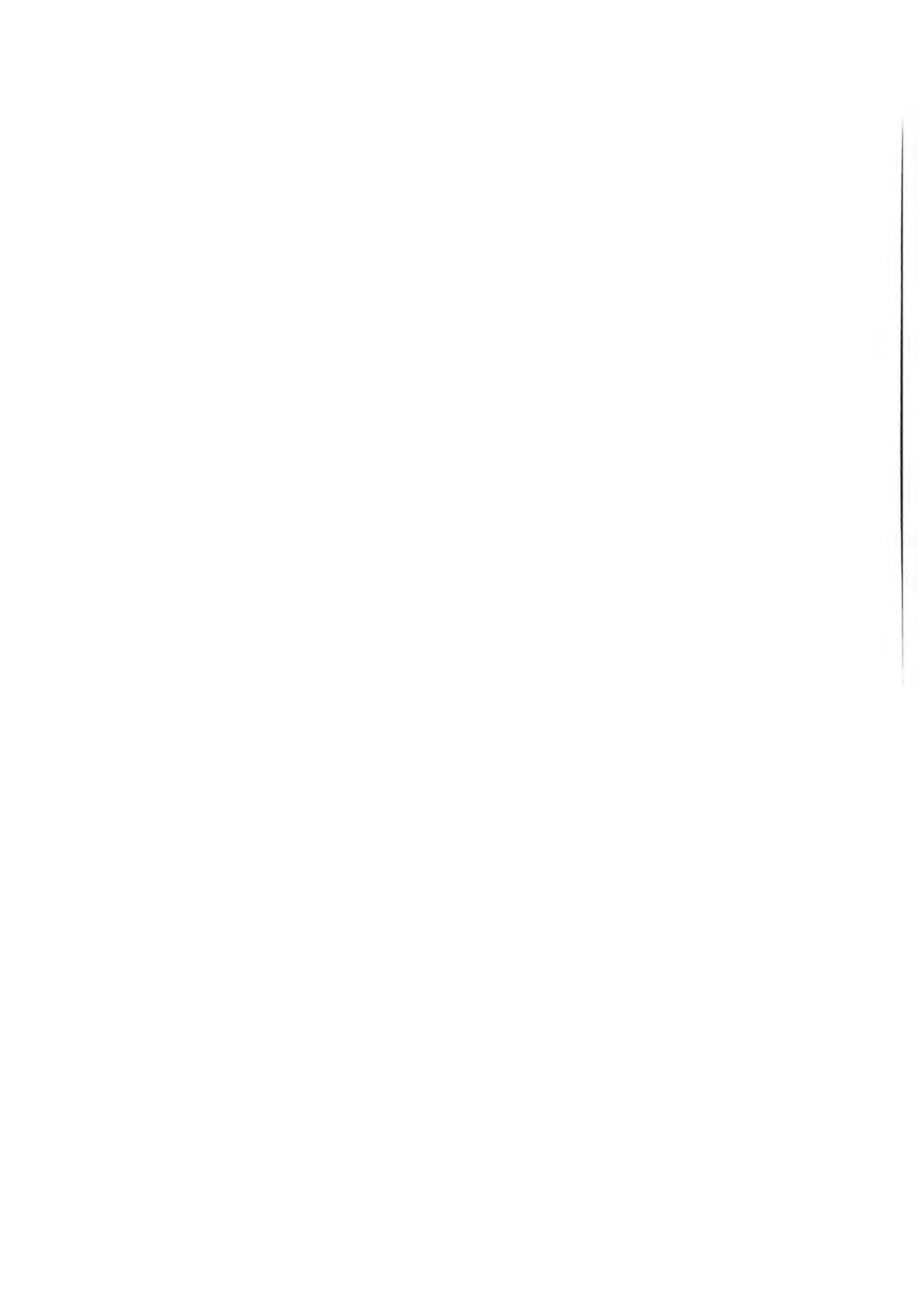
Monument mapping – a contribution to monument preservation

B. Fitzner, K. Heinrichs and M. Volker
Geologisches Institut, Rheinisch – Westfalische
Technische Hochschule Aachen (RWTH)
Arbeitsgruppe "Natursteine und Verwitterung" Wullnerstrabe 2. 52062
Aachen, Germany

Abstract

Increasing degradation of natural stone monuments requires preservation concepts based on reliable scientific results. It is essential to know the stone materials used and the state of deterioration. Type, extent and distribution of stone types and apparent weathering damages can be registered, documented and evaluated precisely by means of the monument mapping method. For the registration of weathering damages a precise classification scheme was developed. Based on the results gained with the monument mapping method, preservation measures can be decided in terms of type, extent and urgency.

1. Introduction

Natural stones often were used as building material for monuments. Many of these monuments have suffered severe damages as a consequence of weathering. The use of stone materials susceptible to weathering, as well as insufficient monument maintenance or inappropriate past preservation measures have often intensified velocity and extent of stone degradation. Nowadays, all experts agree that a reliable damage diagnosis is the fundamental prerequisite to preserve monuments perfectly and economically. This approach requires the cooperation between scientists, monument owners, restorators, curators, architects and engineers. Important apects of a damage diagnosis are registration, documentation and evaluation of apparent weathering damages in relation to the stone types used. The state of damage can be characterized by various methods.

In principle, phenomenological methods and measuring procedures can be distinguished. The monument mapping method has been developed as a non–destructive, time– and cost–efficient phenomenological procedure. An internationally recognized classification which defines weathering forms clearly and completely was developed as the basis for the mapping method. This classification ensures an objective and reproducible recording of the weathering forms at site. Thus the mapping method guarantees highly precise information on weathering forms and stone types at surfaces of sculptures, facades or even entire monuments. All information gained with the monument mapping are processed by special computer programmes, and thus can be organized systematically, illustrated graphically and evaluated quantitatively for any scientific problem and for any practical question. Information on causes and mechanisms of deterioration can be deduced as well as prognoses regarding progress of decay. Damage categories have been established for a conclusive evaluation of the weathering state and as a practical basis for the deduction of preservation measures.

2. Classification of weathering forms

Weathering forms are the result of weathering process occurring at the surface of natural stones and provide information on weathering factors which initiate and condition the process itself. As natural stones are subject to a very complex open system of na-

ture, a clear, genetically oriented classification scheme of weathering forms is impossible. A practicable classification of all weathering forms can only be made according to geometric and phenomenologic criteria. Such a classification scheme was established and developed systematically (FITZNER, 1990; FITZNER & KOWNATZKI, 1990; FITZNER & KOWNATZKI, 1991; FITZNER, HEINRICHS & KOWNATZKI, 1992). The optimized version is described and illustrated in detail in FITZNER, HEINRICHS & KOWNATZKI (1995). Figure 1 shows the general structure of the classification scheme.

The hierarchical scheme comprises four groups of weathering forms in the uppermost level: loss of stone material, deposits, detach-ment of stone material, fissures/ deformation.

In the second level there is a subdivision into 29 main weathering forms like back weathering, relief, break out, discoloration, soiling, loose salt deposits, crust, biological colonization, granular disintegration, crumbling, splintering, flaking, contour scaling, fissures etc. In the third level of the classification scheme the main weathering forms are further differentiated into 60 individual weathering forms in total. With the additional use of intensity parameters the classification scheme reaches its highest degree of differentiation. Table 1 presents as an example the corresponding individual weathering forms of the main weathering form "relief".
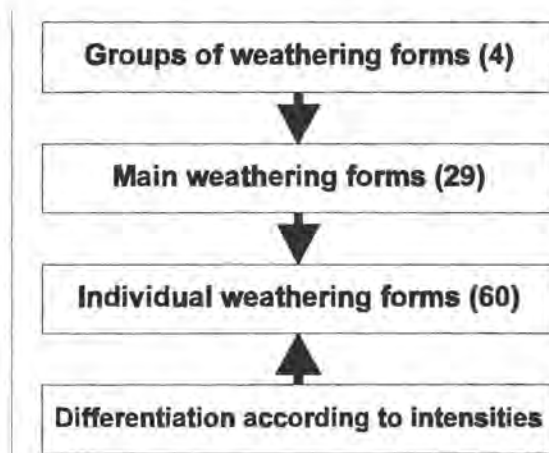
Fig. 1 Classification scheme of weathering forms – levels of differentiation.

3. Mapping and evaluation of stone types and weathering forms.

The monument mapping comprises the complete description, recording and documentation of stone types used at a monument (lithological mapping) and of the apparent weathering forms (mapping of weathering forms). In the majority of monuments different stone materials were used. This diversity may have been due to considerations concerning architecture, workability or art. The proximity and output of quarries also may have

been important in this regard. Stone replacement during rebuilding or restoration phases in the course of time may have contributed to this diversity of stone materials. The need for an exact documentation of stone types becomes more important as the number of stone types used at monuments increases. The first step of the lithological mapping includes an inventory of apparent stone types. Thus an overview of the stone types is produced which can be tailored to the objectives of the investigations. The monument areas to be surveyed are mapped progressively stone by stone so

Table 1 Detail of the classification scheme of weathering forms.

Main weathering form	Individual weathering forms
Relief *Morphological change of the stone surface due to partial resp. selective weathering*	**Rounding/notching** Relief by rounding of edges or notching / hollowing out. Concave resp. convex, soft forms.
	Alveolar weathering Relief in the form of closely spaced cavities (alveolae). Form comparable to honeycombs.
	Weathering out dependent on stone structure Relief dependent on structural features such as bedding, foliation, banding etc. Frequently striped pattern.
	Weathering out of stone components Relief due to selective weathering of stone components being sensitive to weathering (clay lenticles, nodes of limonite etc.) or due to break out of compact stone components (pebbles, fossil fragments etc.). Hole-shaped forms.
	Clearing out of stone components Relief in the form of protruding compact stone components (pebbles, fossil fragments, concretions of iron etc.) due to weathering of the stone material around being more sensitive to weathering.
	Roughening Finest relief resp. alteration of gloss due to the loss of smallest stone particles or corrosion at stone surfaces smoothed by sawing, grinding or polishing.
	Micro-karst Relief due to corrosion at soluble rocks, especially at carbonate rocks. Manifold shapes.
	Pitting Relief in the form of small pits at soluble rocks, especially at carbonate rocks, due to corrosion processes induced biogenically.

that the distribution of the different stone types gets documented and the amount of each stone type can be determined. This is important for later correlations between stone types and weathering forms.

By means of the mapping of weathering forms, all weathering forms and its combinations at the building stones concerned are registered systematically on the basis of the classification of weathering forms. A prerequisite for a very detailed mapping of weathering forms is the accessibility of the investigation area.

A special computer software – VIA / Virtual

Image Analizer – has been developed for the processing of all information gained with the monument mapping method. In a first step monument plans are digitalized and stored as raster images. The computer programme identifies all building stones, numbers them automatically and calculates their surface areas (Figure 2). Thus a basic list of reference is created. In the next step the information gained with the monument mapping are integrated for all the building stones by means of clearly defined codes (Figure 3). In this way a complete information list is set up. The information can be organized or selected systematically, can be illus-


```
No    Area  Info

 .
 .
 .
18    11128  Ro1  Bi3
19    12175  Ro1
20    19741  Ro1  Bi3
21     4794  Ro1
22     4811  Ro1
23    15216  Ro1  Bi3
24    12960  Ro1
25    11628  Ro1  Bi3
26    12429  Ro1  Bi3
27     1824  Ro1
28    11578  Ro1
29     1513  Ro1
30    26139  Ro1  Bi2
31    23918  Ro1  eF3
32    16302  Ro2  eF3  eS2
33    14815  Ro1  eF3
34    15248  Ro1  eS2
35    15892  eF3
36    19159  Bi5
37     9722  eS2  Pu-eS5
38     9007  uW3  sW3  eF3  eS2
39    15094  uW4  sW3  Bi4  eF4  eS2  eS3
40     9475  uW4  sW3  Bi4  eF4  eS2
41    21096  Ro1  Ro3  Ro5  eF1  eF3
42    24644  sW3  Ro1  Bf3  eF1  eF4  eS2
                  Gs-eF2
43    16450  zW5  Ro1  eF4
44     9719  Ro1  eF3
45    11581  Ro5  Ra4  eF1
46    24655  Ro5  eF3
47    16887  Ro5  Ra4  eF3  qS2
48    10574  Ro5  eF2
49    13469  Ro5
50     5660  Ro4  eF2
51     2187  Ro4  eF2
```

Fig. 3 List of information. Data file with number and surface area of building stones. The abbreviations represent weathering forms and its intensities.

Fig. 2 Plan with numbering of building stones.

Legend:
- Drachenfels-Trachyte
- Selters-Trachyte
- Trachyandesite
- Basalt
- Roman-Tuff
- Weibern-Tuff
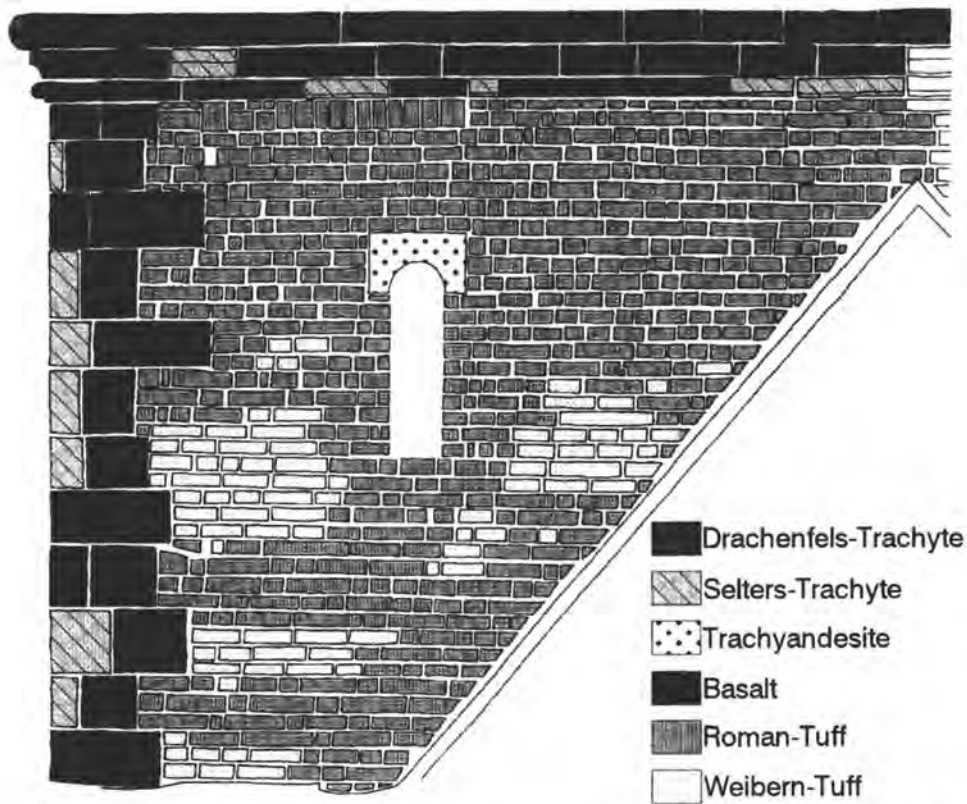
Fig. 4 St. Quirin Minster/Neuss – Germany. Tower – part of the west façade. Lithological mapping.

Legend:
- Dark crust, slight
- Dark crust, moderate
- Dark crust, severe
- Soiling
- Efflorescences, slight
- Biological colonization
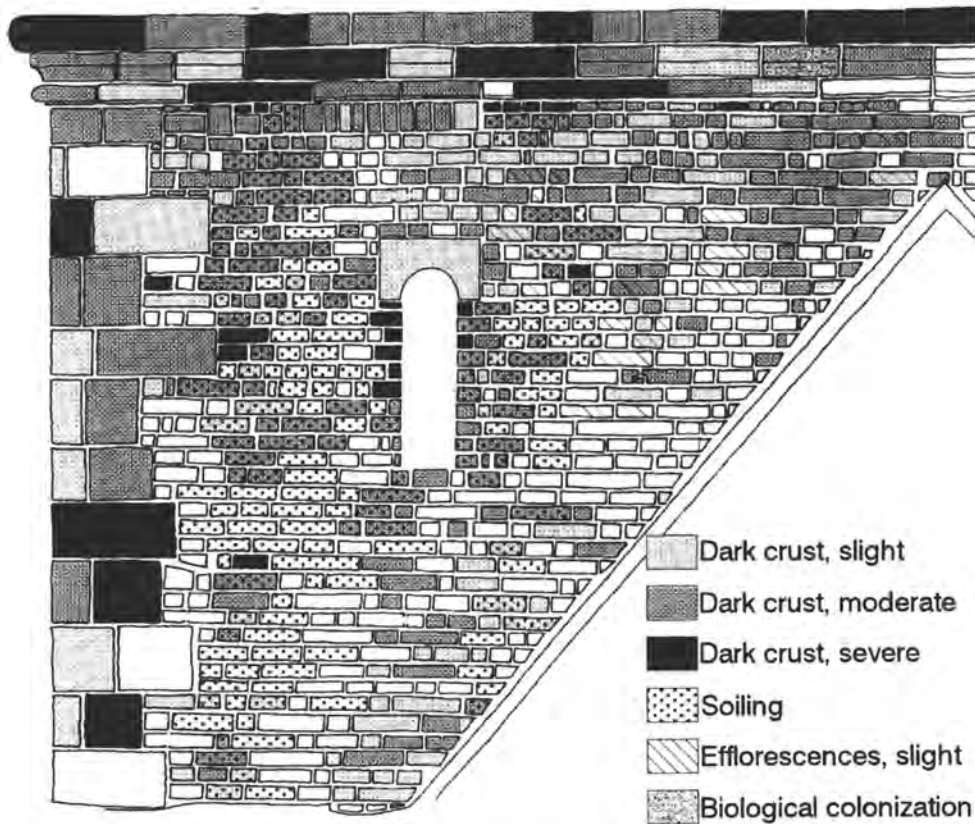
Fig. 5 St. Quirin Minster/Neuss – Germany. Tower – part of the west façade. Mapping of weathering forms referring to "deposits".

Fig. 6 St. Quirin Minster/Neuss – Germany. Tower – part of the west façade. Damage categories referring to "loss of stone material", "fessure" and "detachment of stone material".

* - Removal, fixation or consolidation of loosened stone material; stone repair
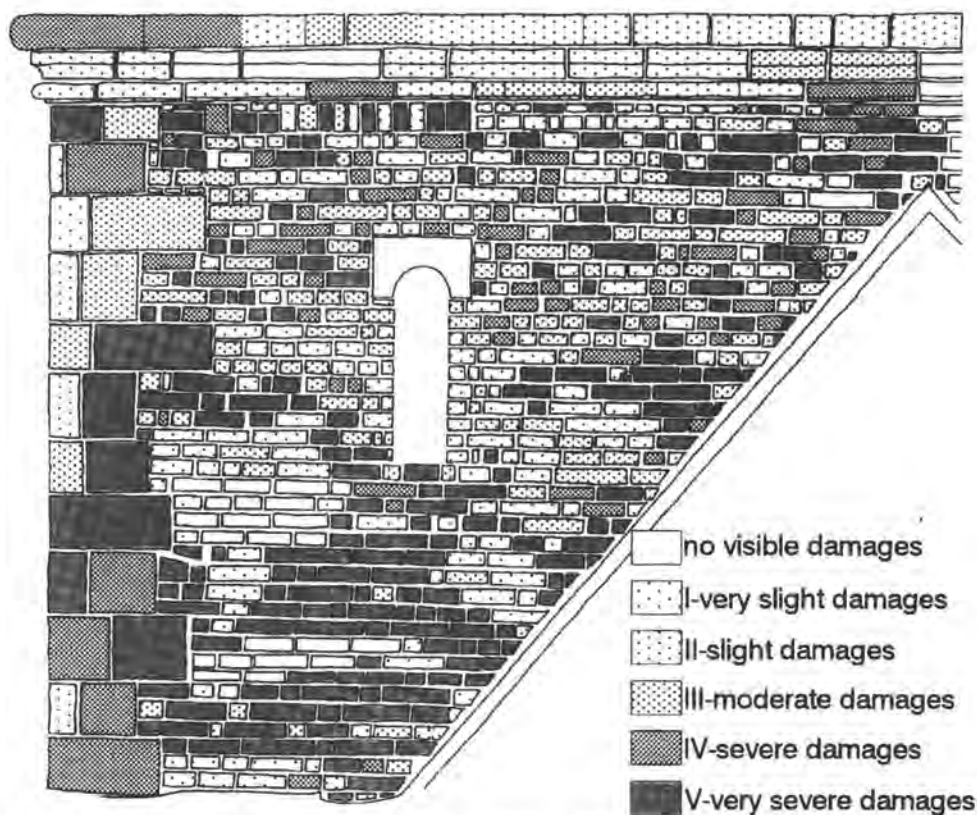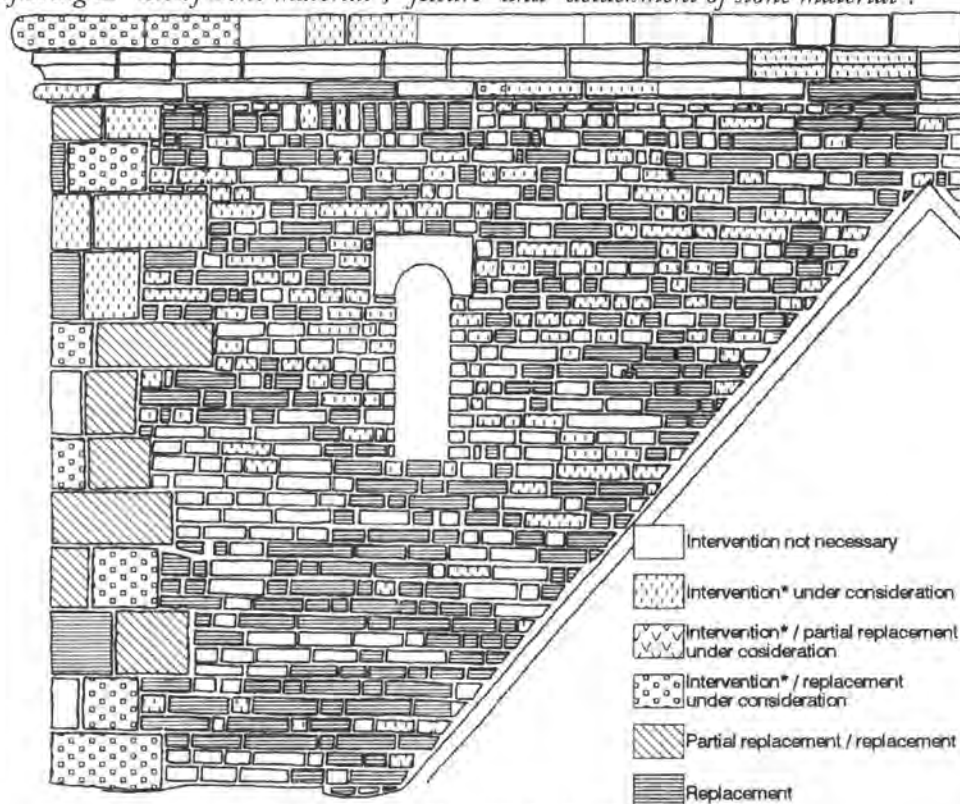
Fig. 7 St. Quirin Minster/Neuss – Germany. Tower – part of the west façade. Preservation plan.

trated graphically – with colors and/or symbols – and can be evaluated quantitatively – either refering to stone surface or to number of building stones concerned – for any scientific problem and for any practical question.

Interelations can be shown, for example, between weathering forms on the one hand and the factors stone type, stone tooling, exposition of the stone surface, exposition period of the stone surface or environmental influences on the other hand. By correlation of stone types and corresponding weathering forms the susceptibility of the individual stone types to weathering can be compared and judged. Zonation of weathering forms can indicate local special importance of certain factors such as humidity or salt load, high depositions of pollutants or mechanical stress. In numerous cases the mapping results allow to deduce chronological sequences of weathering forms and thus to characterize the development and progress of damages.

The weathering forms can be presented in the raster image on the monitor as well as in printed plans according to different modes. For example, all weathering forms can be shown in the same plan, thus providing an overall–view. Furthermore, they may be presented in seperate plans according to groups of weathering forms. Here the plan "loss of stone material" permits a precise estimation regarding the extent of stone material already lost, which is particularly important for original stone material. The plan "deposits" would allow indications with respect to measures such as cleaning. The plan "detachment of stone material" would characterize building stones clearly which are in danger of losing stone material. Besides these modes of illustration also plans with only one selected weathering form may be relevant for certain questions, such as the illustration of loose salt deposits with respect to desalting measures. Furthermore, there is the possibility to choose between illustrations of weathering forms either for all stone types or for each stone type separately. This concerns all three modes of illustration described just before in the same way.

4. Damage categories and preservation measures

The mapping of weathering forms provides very detailed information, which is absolutely necessary for scientific and practical questions. Architects, restorators, engineers etc. very often expect a conclusive evaluation of the weathering state with regard to type, urgency and extent of preservation measures. For this purpose damage categories have been established. All main weathering forms and the corresponding individual weathering forms have been correlated to damage categories considering different intensities of weathering forms (FITZNER, HEINRICHS & KOWNATZKI, 1992; FITZNER, HEINRICHS & KOWNATZKI, 1995). Five damage categories were defined: I – very slight damages, II – slight damages, III – moderate damages, IV – severe damages, V – very severe damages. With respect to preservation measures this means from damage category I to damage category V an increasing necessity and urgency. For the correlation of weathering to damage categories it has been considered whether the weathering forms occur at parts of the ashlar or at architectonic decoration parts. As the value of architectonic decoration parts generally is rated higher in comparison to ashlar, the weathering forms at such decoration elements have been correlated to relatively higher damage categories. The correlation made between weathering forms and damage categories must be considered as proposal owing to long–term experience as regards damage diagnosis at natural stone monuments. It may be modified according to the importance of a monument or according to certain aspects of monument preservation. A direct recording of damage categories at a monument is not reasonable, because damage categories – in contrast to weathering forms – to a certain extent are not objective. This means that the mapping of weathering has to be the basis for the later application of damage categories. The correlation system made for weathering forms and damage categories is stored in the computer programme VIA, too. Thus the transformation of the real weathering forms registered at a monument into damage categories can be made auto-

matically by this programme. Following the damage categories – considering the weathering forms they result from and considering the stone types they refer to – appropriate preservation measures can be decided in terms of type, urgency and extent. This final information again can be illustrated in monument plans. For architects, engineers etc. this means an important basis for planning preservation concepts and for evaluation of corresponding costs.

5. Example

As an example for the application of the monument mapping method the St. Quirin Minster in Neuss/Germany is presented. The late Romanic vaulted basilica dating back to the 13th century has been subject to various changes in the course of time as regards stone materials and architectonic structure. More than ten different stone types were used for the outer facades, predominantely different tuffs, trachytes and basalts, subordinately sandstones, limestones and slates. Figure 4 shows the lithological mapping for a part of the west facade of the tower. Tuffs were used for the main ashlar only. Roman Tuff mainly represents original stone material whereas Weibern Tuff represents stone material of a younger restoration phase. Trachytes occur at mouldings and lisenes. Drachenfels–Trachyte represents original stone material, Selters–Trachyte stone material of a younger restoration phase. Basalt in this area was used exclusively in the moulding.

The weathering forms at the facade were mapped in detail. Figure 5 shows the plan with all weathering forms registered as concerns the group of weathering forms "deposits" such as crust, soiling, efflorescences and biological colonization. It was no need to correlate these weathering forms describing deposits to damage categories and finally into prervation measures as a careful cleaning of the facade had been decided in any case. However, this plan will be taken as reference for judging the success of the cleaning procedure. Thus, with respect to all further types of preservation meas-

ures only the weathering forms of the three other groups "loss of stone material", "detachment of stone material" and "fissures/deformation" were considered in the following. All corresponding weathering forms of these three groups were correlated to damage categories (Figure 6). Comparing this plan and the lithological plan (Figure 4) it can be seen, for example, that a high number of building stones of Roman Tuff – mainly original stone material – shows already moderate, severe or even very severe damages, whereas the building stones of Weibern Tuff – stone material of a younger restoration phase – so far mostly have remained in rather good condition. This is probably due to the much shorter period of exposure of the Weibern Tuffs.

Based on own experience and considering the historical importance of the different stone types rated by the monument preservation authorities, preservation measures were attributed to the building stones in dependence on the damage categories determined before (Figure 7). In a further step this preservation plan has been evaluated quantitatively as shown in Table 2. For each individual stone type the percentage of building stones concerned by the different preservation measures is presented. As can be seen, for example, a high percentage of building stones regarding Selters–Trachyte and Roman Tuff in this part of the St. Quirin Minster has to be replaced, whereas interventions at the building stones of basalt in most cases are not necessary at all.

6. Conclusions

The monument mapping method has proved to be a reliable non–destructive procedure, by which the weathering state of all natural stone monuments and all stone types can be characterized objectively and precisely. The method provides sufficient qualitative and quantitative information on type, extent and distribution of stone materials and weathering damages. The special computer software devel-

Preservation measures	Percentage of building stones						
	All stone types	Drachen-fels-Trachyte	Selters-Trachyte	Trachy-andesite	Basalt	Roman-Tuff	Weibern-Tuff
intervention not necessary	36.6	46.3	33.3	100.0	66.7	30.2	71.7
intervention* under consideration	20.3	22.0	—	—	33.3	21.9	11.8
intervention* / partial replacement under consideration	—	—	—	—	—	—	—
intervention* / replacement under consideration	1.3	14.6	25.0	—	—	—	—
partial replacement / replacement	1.0	17.1	—	—	—	—	—
replacement	40.8	—	41.7	—	—	47.9	16.5
	100.0	100.0	100.0	100.0	100.0	100.0	100.0

Table 2   St. Quirin Minster / Neuss – Germany. Tower – part of the west façade. Percentage of building stones concerned by the different preservation measures – referring to the different stone types in total and individually.

*– Removal, fixation or consolidation of loosened stone material; stone repair

oped allows manyfold possibilities of illustration and evaluation tailored to the objectives of diagnosis. Based on the detailed results gained with the monument mapping appropriate preservation measures can be decided. Thus, the monument mapping method can be recommended as standard procedure for damage diagnoses in the field of monument preservation and, furthermore, also for the control of preservation measures as well as for the long–term observation of monuments.

7. Acknowledgements

8. References

1. Fitzner, B.: *Mapping of natural stone monuments – documentation of lithotypes and weathering forms.–* Proceedings of the Advanced Workshop "Analytical methodologies for the investigation of damaged stones", Organizers: F. Veniale & U. Zezza, Pavia, 14.–21.09.1990, 24 pp., La Goliardica Pavese, 1990.

2. Fitzner, B., Heinrichs, K. & Kownatzki, R.: *Classification and mapping of weathering forms.–* Proceedings of the 7th International Congress on Deterioration and Conservation of Stone, Lisbon, 15.–18.06.1992, pp. 957–968, Laboratorio Nacional de Engenharia Civil – Lisbon, 1992.

3. Fitzner, B., Heinrichs, K. & Kownatzki, R.: *Weathering forms – classification and mapping. Verwitterungsformen – Klassifizierung und Kartierung.–* In: SNETHLAGE, R. (ed.): Naturwissenschaft und Denkmalpflege, Natursteinkonservierung I, pp. 1–48, Förderprojekt des Bundesministeriums für Bildung, Wissenschaft, Forschung und Technologie, Verlag Ernst & Sohn, Berlin, 1995.

4. Fitzner, B. & Kownatzki, R.: *Bauwerkskartierung – Schadensaufnahme an Naturwerksteinen.–* Der Freiberufliche Restaurator, 4, pp. 25–40, Kiel, 1990.

5. Fitzner, B. & Kownatzki, R.: *Klassifizierung der Verwitterungsformen und Kartierung von Natursteinbauwerken.–* In: Snethlage, R. (ed.): Jahresberichte aus dem Forschungsprogramm "Steinzerfall – Steinkonservierung" 1989, pp. 1–13, Förderprojekt des Bundesministers für Forschung und Technologie, Verlag Ernst & Sohn, Berlin, 1991.
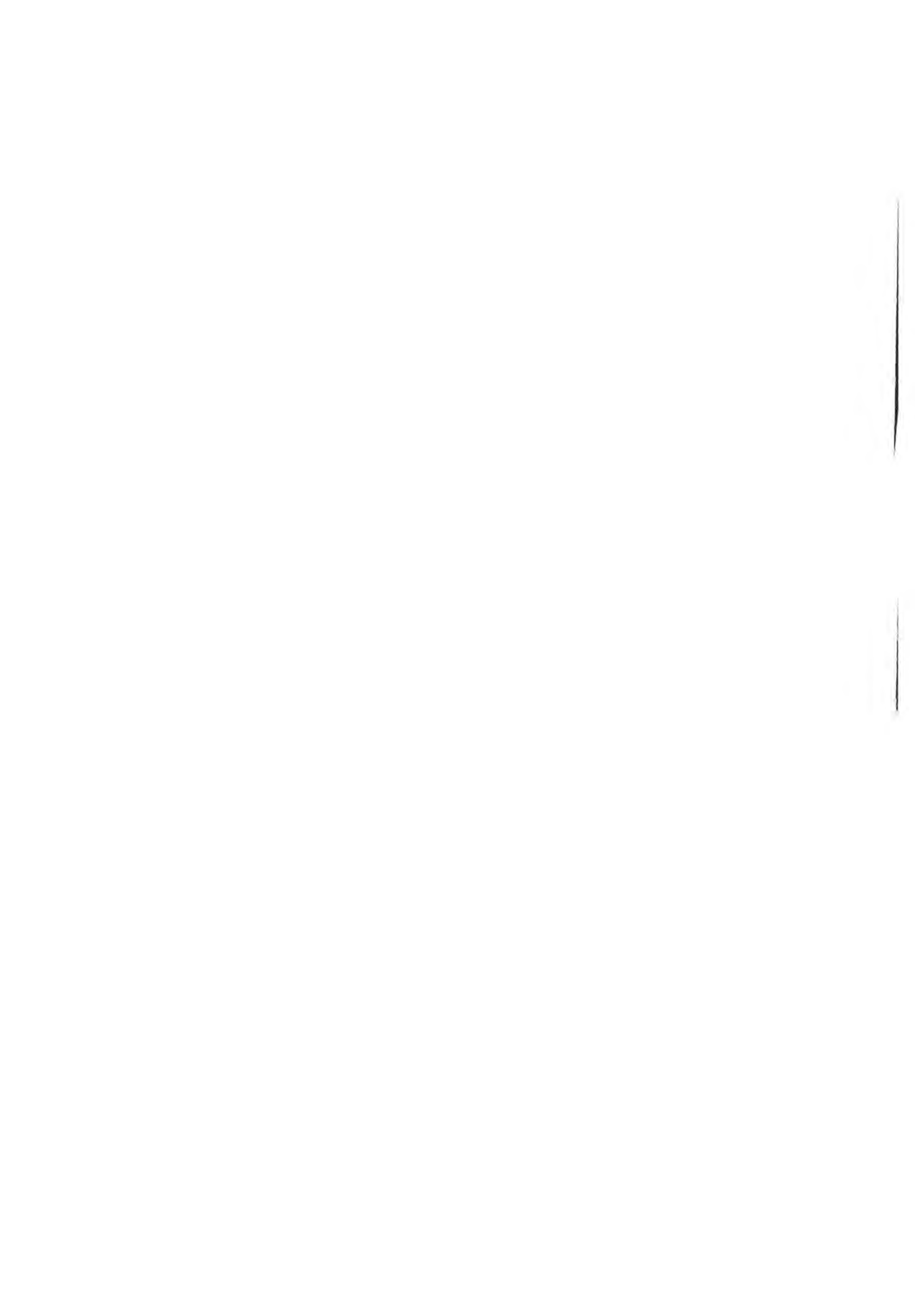
B. Fitzner
R. Kownatzki
D. Basten

Porosity properties and weathering
behaviour of natural stones
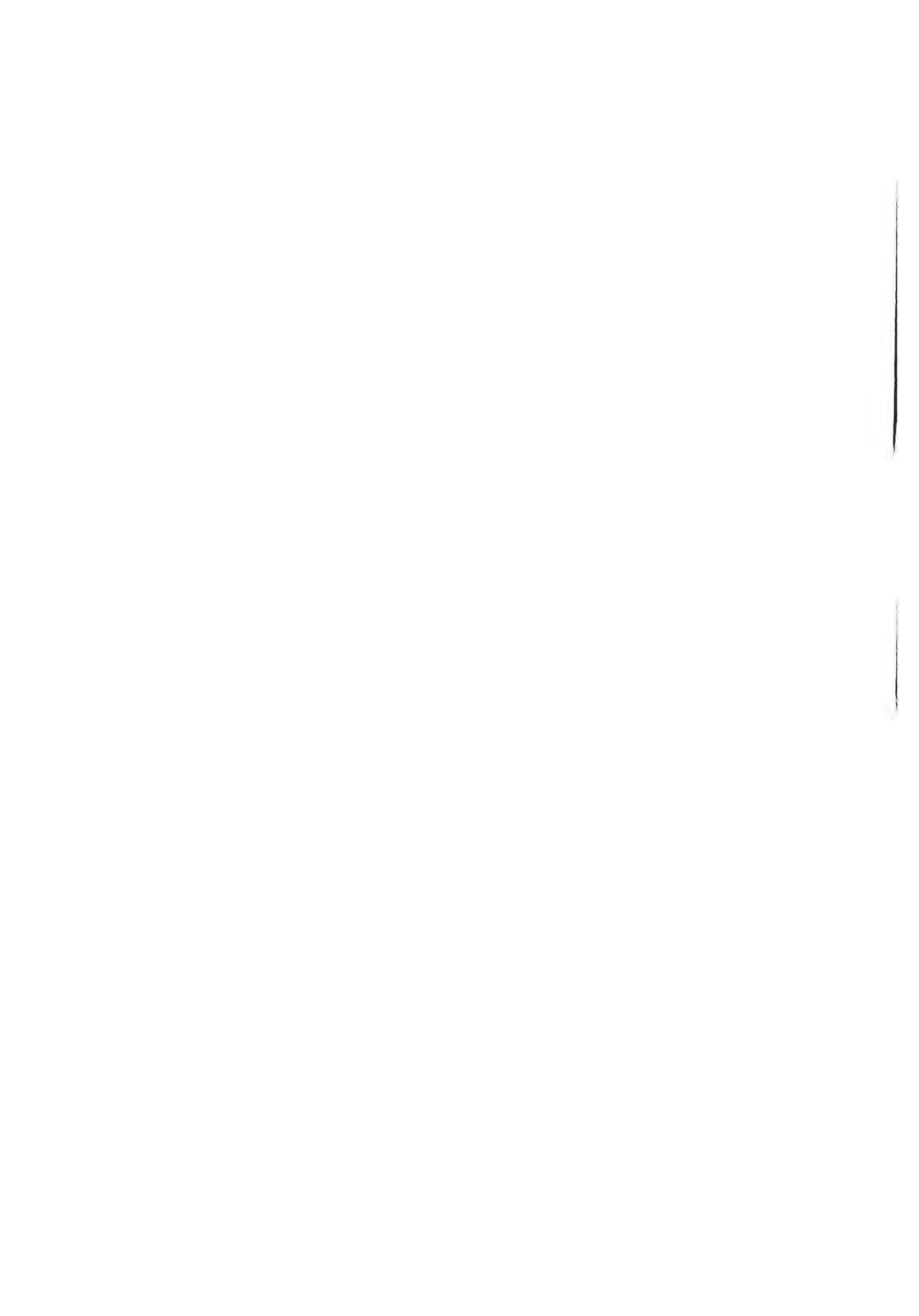
Porosity properties and weathering behaviour of natural stones

B. Fitzner, R. Kownatzki, D. Basten
Rheinisch – Westfalische Technische Hochschule Aachen
Geologisches Institut / Arbeltsgruppe "Natursteine und Verwitterung"
WullnerstraBe 2, 52062 Aachen, Germany

The pore space of natural stones influences the stone properties and controls the weathering behaviour decisively. Characteristics such as total porosity, pore size, pore form, pore distribution and pore surface can be taken for describing stone pore space. The reliable characterization and measurement of pore space requires different combined measuring procedures such as thin section microscopy, scanning electron microscopy mercury porosimetry and nitrogen sorption method.

The pore space controls especially the physical weatherability of natural stones. Investigations on porosity properties were executed at various sandstones. Owing to different genesis the sandstones show a wide range of porosity properties. The weathering behaviour of these sandstones was studied at monuments and additionally in weathering simulation tests. The results provide clear correlations between total porosity and pore size distribution on the one hand and the sensibility respectively resistancy against physical weathering, in particular freeze–thaw cycle weathering and salt weathering, on the other hand.

The pore space of the natural stones is modified by the weathering processes. Differences regarding porosity in the weathering profile can be taken as indicator for the weathering state. Thin section microscopy in combination with image analysis allows the visualization and quantitative evaluation of complete porosity profiles and thus the determination of characteristical weathering zones.
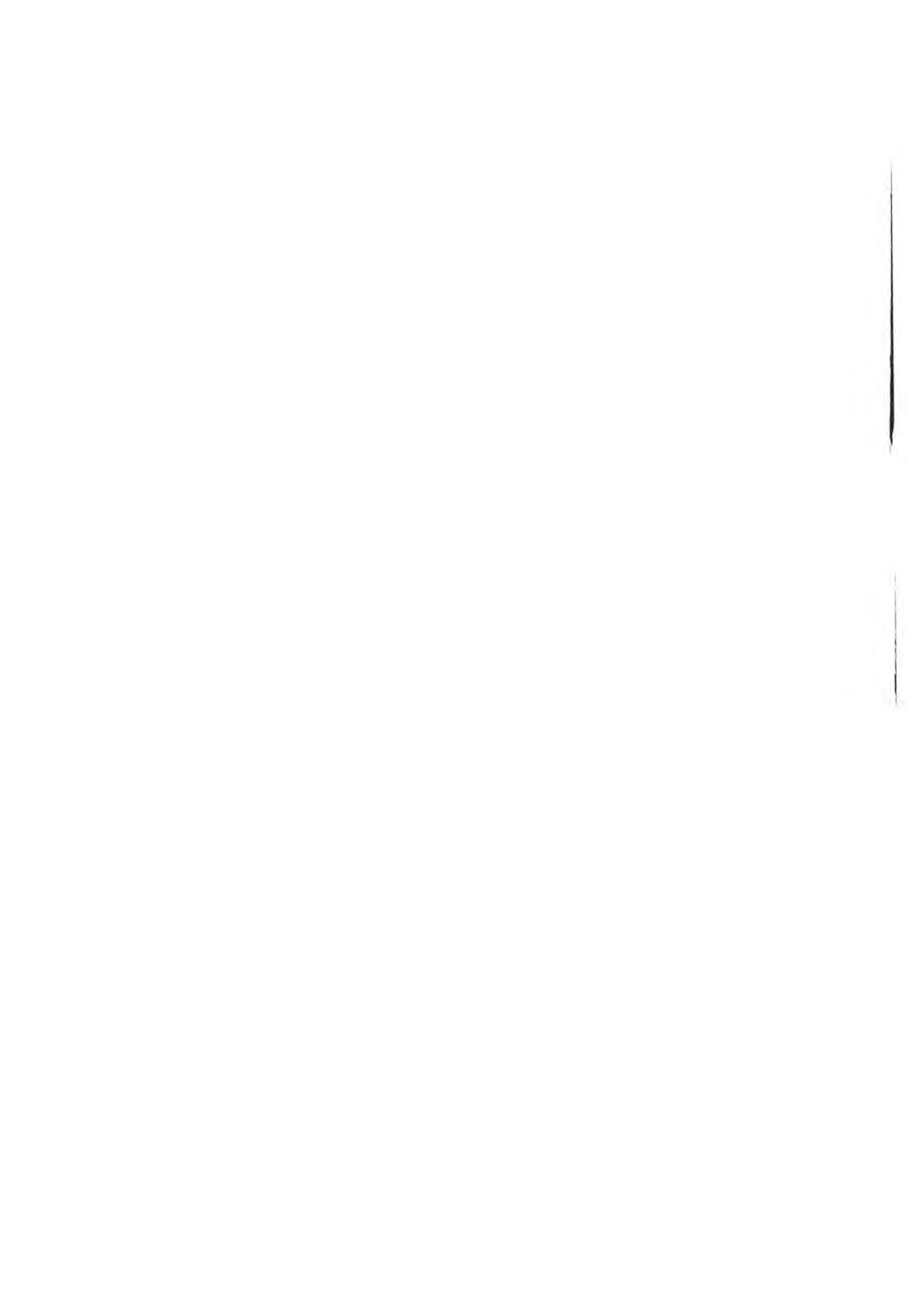
E. Galán
M.A. Guerrero
M.A. Vázquez
M.I. Carretero
P. Ortiz

The Cathedral of Cadiz (Spain).
Environmental study
and stone damage evaluation
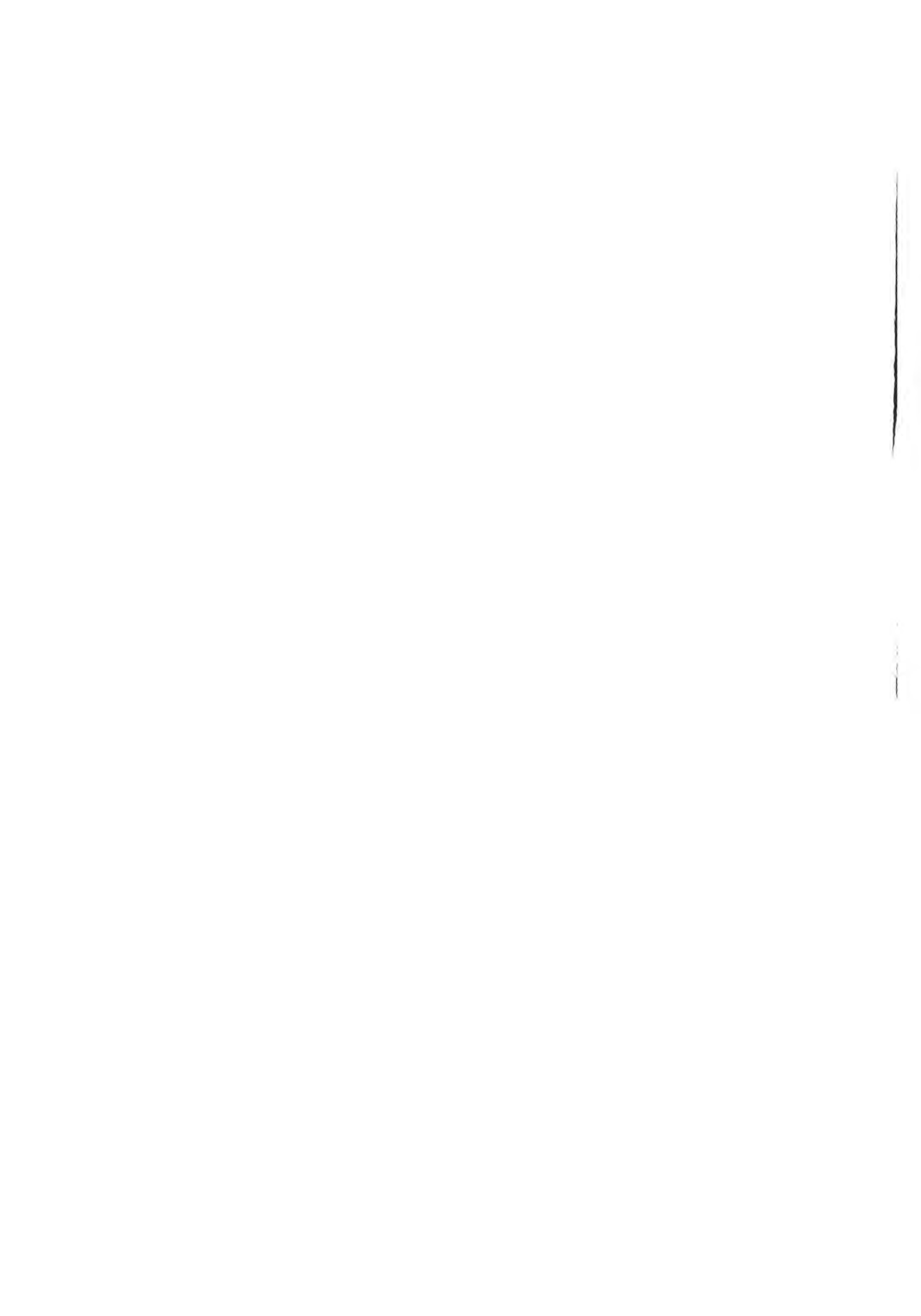
The Cathedral of Cadiz (Spain). Environmental study and stone damage evaluation

E. Galán, M.A. Guerrero, M.A. Vázquez, M.I. Carretero, P. Ortiz
Departamento de Cristalografía, Mineralogía y
Química Agrícola. Facultad de Química.
Universidad de Sevilla. Apdo 553, 41071 Sevilla, SPAIN

Abstract

To understand the relationship between environmental factors and stone damage of cultural heritage in the Mediterranean coast, the Cathedral of Cadiz was choiced as pilot monument for the Spanish Sub–project, whitin the CE General Project "Marine Spray and Polluted Atmosphere as Factors of Damage to Monuments in the Mediterranean Coastal Environment". The Cathedral of Cadiz, located very closed to the sea, is severely damaged by the corrosiveness of marine environment.

The Cathedral of Cadiz (18th and 19th centuries) in baroque–rococo and neoclassical styles was mainly built with Jurassic oolitic limestones, Triassic dolomite marbles and Upper Neogene calcarenites. Nowadays, these construction materials, particularly marbles and limestones, are in advanced state of deterioration essentially due to salts precipitation and dissolution phenomena. The weathering forms produced by crystallization cycles (efflorescences, swelling, fissures, fractures and spalling with loss of material) began to be dangerous inside the Church since early 19th century.

For the evaluation of the environmental effects on stones, it was necessary the coordination between an interdisciplinary net. According to the programme of the project the following investigations were carried out: a yearly monitoring of environmental parameters inside and outside the building, analysis of weathering sea factors, petrophysical, mineralogical and chemical studies of building stones and their alteration products (efflorescences and crusts), description of alteration forms at different levels and quantification of damage by non destructive techniques. The cronograms of environmental parameters show a coastal mediterranean clima modified by atlantic influence. The "boundary conditions", based on equilibrium relative humidity vs temperature, allow to forecast locally (in time and space) the salts crystallization–dissolution processes on stones. The theoretical estimation of crystallization phenomena, along with the other data available from the investigations before cited, would explain reasonably salts occurrence and stone damages. These investigations could be a methodological model for the evaluation of stone decay.

Until now, numerous studies have been made on this Cathedral, though no single plan of action of general character has been successful. For this reason, these investigations are an important advance in the building knowledge, that will allow to design experiences very soon in order to reduce the effects of salts crystallization.

Keywords: Environmental study, stone damage, Cathedral, Cadiz (Spain)

1. Introduction

Whitin the frame of the EC–Project EV 5V–CT92–0102 coordinated by Prof. Fulvio Zezza, the Cathedral of Cadiz was selected as the emblematic monument for the Spanish sub–project.

The Cathedral of Cadiz (18th and 19th

centuries) may be considered the masterwork of Vicente Acero y Acebo. The styles adopted during the construction are: Barroque, Rococo and Neoclassical. The ground plant has a latin cross arrangement formed by the central and transcept naves. The Cathedral of Cadiz finds itself situated to the south of the city, separated from the sea by an avenue.

As a first approach to damage evaluation, the vaults stones damage is the main problem of the Cathedral, i.e. more than 150.000 m³ of stone from Estepa used to build the second interior body are severely damaged. Fissures, fractures, spalling, detachment cause the loss of material, which may become dangerous to public worship in spite of the two protective nets that catch the pieces of large size.

2. Methodology

The evaluation of the influence of marine environment in the Cathedral has been based on three different and complementary investigations (Table I):

a) *Environmental characteristics determination: Control of climatic variations and environmental parameters inside and outside the Cathedral.*

The control of climatic variations and the distribution of thermohigrometric levels on the walls during a year (April/94–March95) have been carried out by a delta–logger equipment provide with adequate sensors.

In order to evaluate the influence of environmental and microenvironmental conditions on the decay of stone, the following parameters have been studied:

- *Macroclimate around the building: Rainwater, wind velocity and direction, temperature and relative humidity of air and sun radiation.*

- *Microclimate close to the surface of the stone inside the Cathedral: relative humidity and temperature of the interphase, and stone surface temperature.*

- *Salts paths way: Rainfall water, total suspended particles, aerosols and condensation water. The sampling was carried out seasonable and ionic contents were analysed by IC, FRX and conventional chemical techniques.*

b) *Stone characterization: Petrography (OM, SEM), mineralogy (XRD), chemistry (AAS, IR, FRX) and physical properties (total porosity and pore radius distribution by Hg–porosimetry combined with BET and image analysis of thin section microscopy, density, UCS, elastic modulus, point–load index and water absoption).*

c) *Damage evaluation: Identification of forms of stone decay (SEM, XRD, IC, FRX, and conventional chemical analysis), and damage evaluation by non destructive techniques (mapping of weathered monuments by computerized analysis in combination with ultrasonic pulse measurements and detailed mapping of weathering forms).*

3. Results

Stone characterization

The main stones used in the construction of the Cathedral of Cadiz are the followings:

- *White limestones (Middle–Upper Jurassic oolitic limestones) from Estepa (Sevilla) used in the second section (pilars and vaults).*

- *White marbles (Triassic dolomite marbles) from Mijas (Málaga) used in plate covering, columns and capitels for the first section.*

- *"Black marbles" (sparitic limestones) from Cueva de Geli (Málaga) used in column bases and pedestals*

- *"Red marbles" (oolitic limestones) from Mijas (Málaga) used in ornaments.*

- *Upper Neogene Biocalcarenite (Ostionera) from Sancti Petri (Cadiz) used as structural stone (walls and foundations).*

A systematic sampling of stone materials was carried out in the Cathedral for the characterization of lithothypes with a research of

the main quarries. A more detailed study is presented in this volume (Galán et al.)

Because of the second interior body of the Cathedral was built mainly of Estepa stones and it shows the main trouble of stone conservation, an exhaustive research of physical and mechanical properties of oolitic limestones was carried out.

Limestone from "Sierra de Estepa" are homogeneous, very pure, compact, with low water–soption and medium high strength. From these quarry samples, the most similar variety to those of building stone was choiced. This limestone from "Sierra de Estepa" has a total porosity of 10–15% due to interparticle pores with rarely intraparticle ones, and a high mechanical strength (*uniaxial compressive strength: 75–100 Mpa, elastic modulus: 15–30 Gpa, point load index I(50): 2.5–5.0 Mpa*). These stones are very compact (*density: 2.70 g/cm³*) due to a porosity with mainly small pores and very small and large pores subordinate (*medium pore radius: 0.09–0.17 μm*) this type of porosity means low water absorption (*absorption: 3.25–5.50%*) with two phases in kinetics absorption slopes (the first is fast and the second one is slow and larger until reaching the equilibrium).

Damage evaluation

The degradation of Temple's vaults, which was already described in the Chapter–council register as "crumblings and hailstones" in 21th February 1839, is still the main conservation problem. This situation is due to fissures, fractures, detachment and loss of material (see figure 1), that are affecting a large surface stone with very severe damage. Limestones suffer much spalling specially near joints in which the mortar acts as solution paths ways and salts reserver. Near corner and sculptural reliefs, outburst and back weathering are the most striking weathering forms. Ornamental motives favour the weathering of stones, as it can been deduced from the width of grey level hystogram showed in figure 2.

The surfaces with granular disaggregation and detachment are in correspondence with two strata (figure 3), the upper layer (till 1.15–1.50 cm) is the most damaged with ultrasonic pulse velocities of 3.3Km/s, the second layer, less decayed, is characterized by slightly higher velocities (3.6–3.7Km/s).

The severe stone damage inside the cathedral described before is due to crystallization of salts from aerosols, mortars, groundwater and percolation water. The main stone mechanisms quite well development inside the Church are produced by increase in capillary and interstical volume caused by salts crystallization and hydration. Spalling, scalling, chipping and granular desintegration are caused by salt cycles. The main salts found in oolitic limestones are trona, natron and occasional halite. The sodium chloride have two actions: a)"crystallization pressure" which can break the pores and b)when it is in dissolution influences calcite solubility increases. Anion CO_3^{2-} and HCO_3^- can precipitate with sodium as efflorescences or can reprecipitate with calcium forming crust and even stalactites.

Environmental characteristics

With regard to the period April/94–March95, the warmer months were June, July August and September, reaching maxima of 31.0–32.5°C; these high temperatures correspond to the maximun of sun radiation (1 Kw/m2). The colder period was January–February with minimun of 5°C. The highest oscilations were in September and in June. About relative humidity, the average of this year is 77.7%, oscilations range between 18–100%. The yearly maxima average of rainfall water was 34.30 mm, the dryness in Andalusia reached centuries records in this period. In Cadiz bay the wind blows striking from WNW with a velocity that reached up a maximun of 24.53 m/s. In the Cathedral, due to its location, these winds mean an important physical erosion in exterior walls.

Table 1 Work programme

STEPS		RESEARCH	TEAMS	TIME FLOW CHART (years)
Environmental Characteristics	MEP	Monitoring of Environmental and microenvironmental parameters	DECMAS	
	MMC	-Study of macroclimate around the building: action of rain-water and influence of marine spray -Study of internal microclimate: distribution of thermohigrometric levels on walls and reactivity of condensation waters	{ DECMAS UIA	
	SPM	Air sampling of suspended particles and chemical analysis	{ DECMAS UIA	
	TMP	Data treatment of monitoring parameters	{ LAMPIST DECMAS	
Stones Characterization	MPS	Minero-petrographic studies of stones materials	DECMAS LAMPIST EGGEO-AUTH	
	PML	Physical and mechanical analysis of building and quarries stones	{ EGGEO-AUTH GI-RTA DECMAS	
Damage Evaluation	MPC	Systematic mineralogical, petrographical and chemical examination of weathered stones and crusts	{ LAMPIST UIA DECMAS	
	CWA	Chemical analysis of soluble salts	{ UIA DECMAS	
	DPC	Applications of trace and microanalysis techniques to investigate the composition and elemental depth profiles in weathered stones	UIA	
	MAP	Mapping of selected weathered zones and in situ evaluation damage by non destructives techniques	{ GI-RTA IGAG-BA	

TEAMS:
DECMAS. Departamento de Cristalografía, Mineralogía y Química Agrícola. Facultad de Química. Universidad de Sevilla. Spain.
UIA. Departament of Chemistry. University of Antwerp. Belgium.
LAMPIST. Laboratorio de Mineralogia e Petrologia. Instituto Superior Tecnico. Lisbon. Portugal.
EGGEO-AUTH. Lab. Engineering Geology-Hydrogeology. Dept. of Geology and Physical Geography. School of Geology. Aristotle University of Thessaloniki. Greece.
GI-RTA. Geologisches Institut. Rheinisch-Westfalische Technische Hochschule-Aachen-Germany.
IGAG-BA. Istituto di Geologia Applicata e Geotecnica. Facoltà di Ingegneria-Politecnico di Bari.I. Italy.

Fig. 1.a.
Severe damage inside the Cathedral.
(Pillars: oolitic limestones).
Main weathering forms: outburst, back weathering,
relief, scales and scales to spalling.
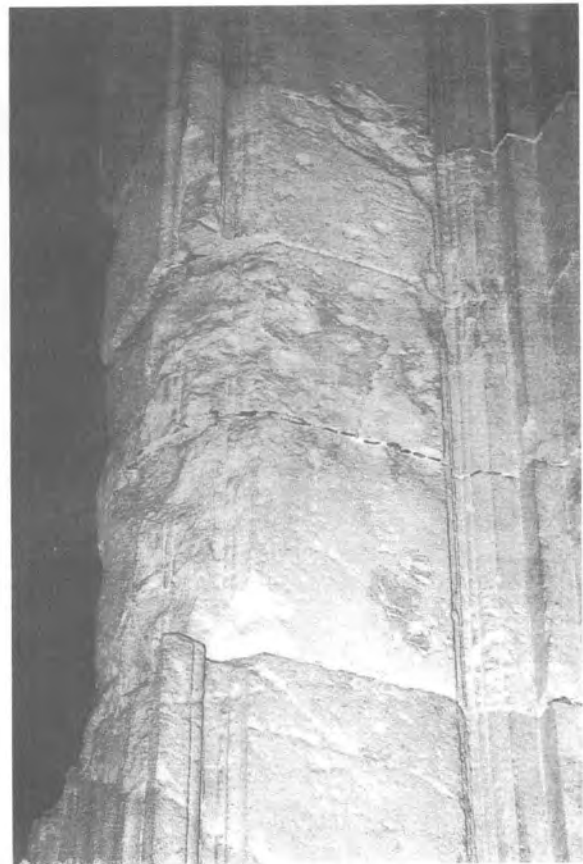
Fig. 1.b. Mapping of weathered forms. Pillar inside the Cathedral.
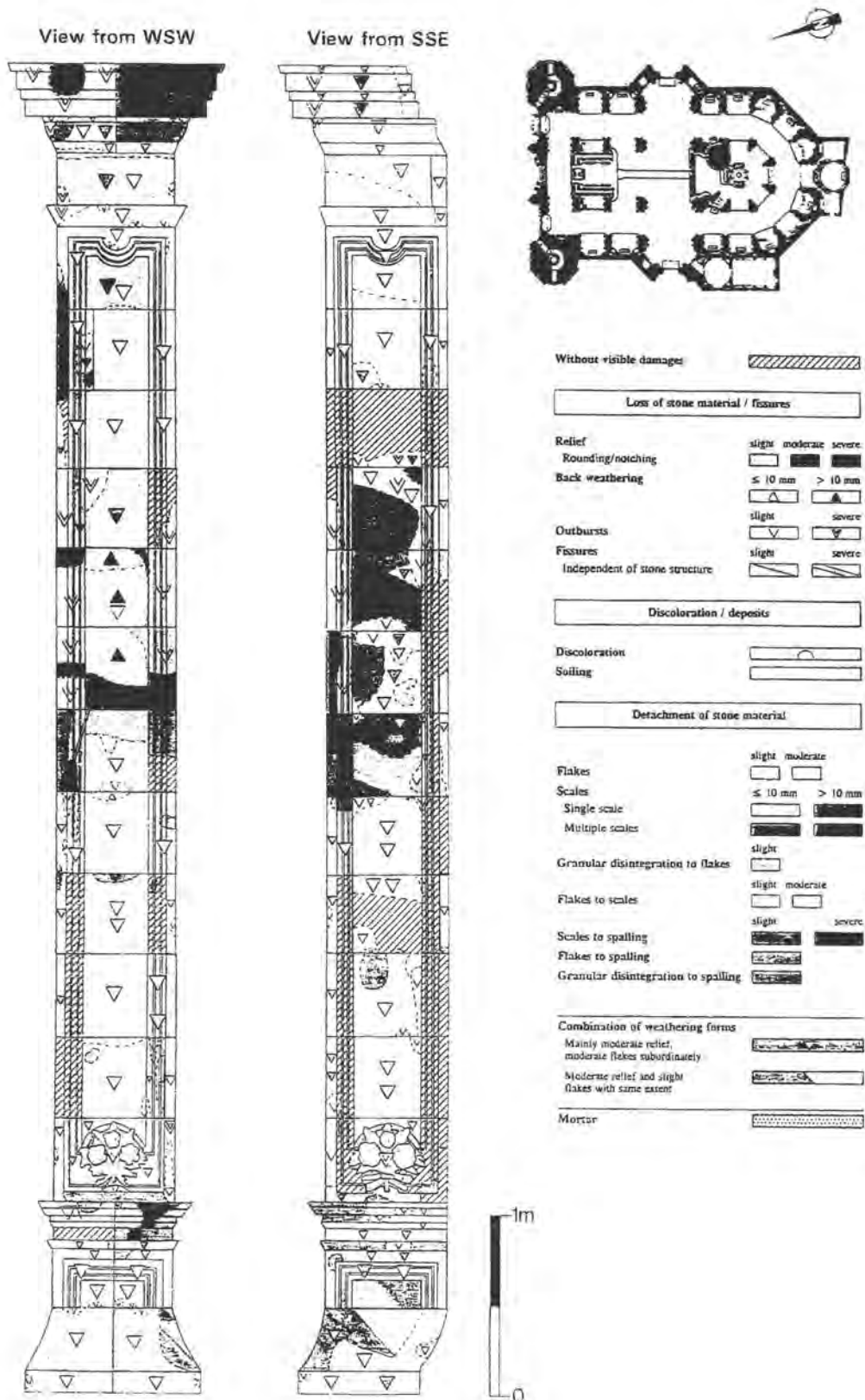
Fig. 1.c. Damage categories. Pillar inside the Cathedral.

View from WSW   View from SSE

No visible damage

Damage category II - slight damage

Damage category III - moderate damage

Damage category IV - severe damage

Damage category V - very severe damage

Mortar

1m

0
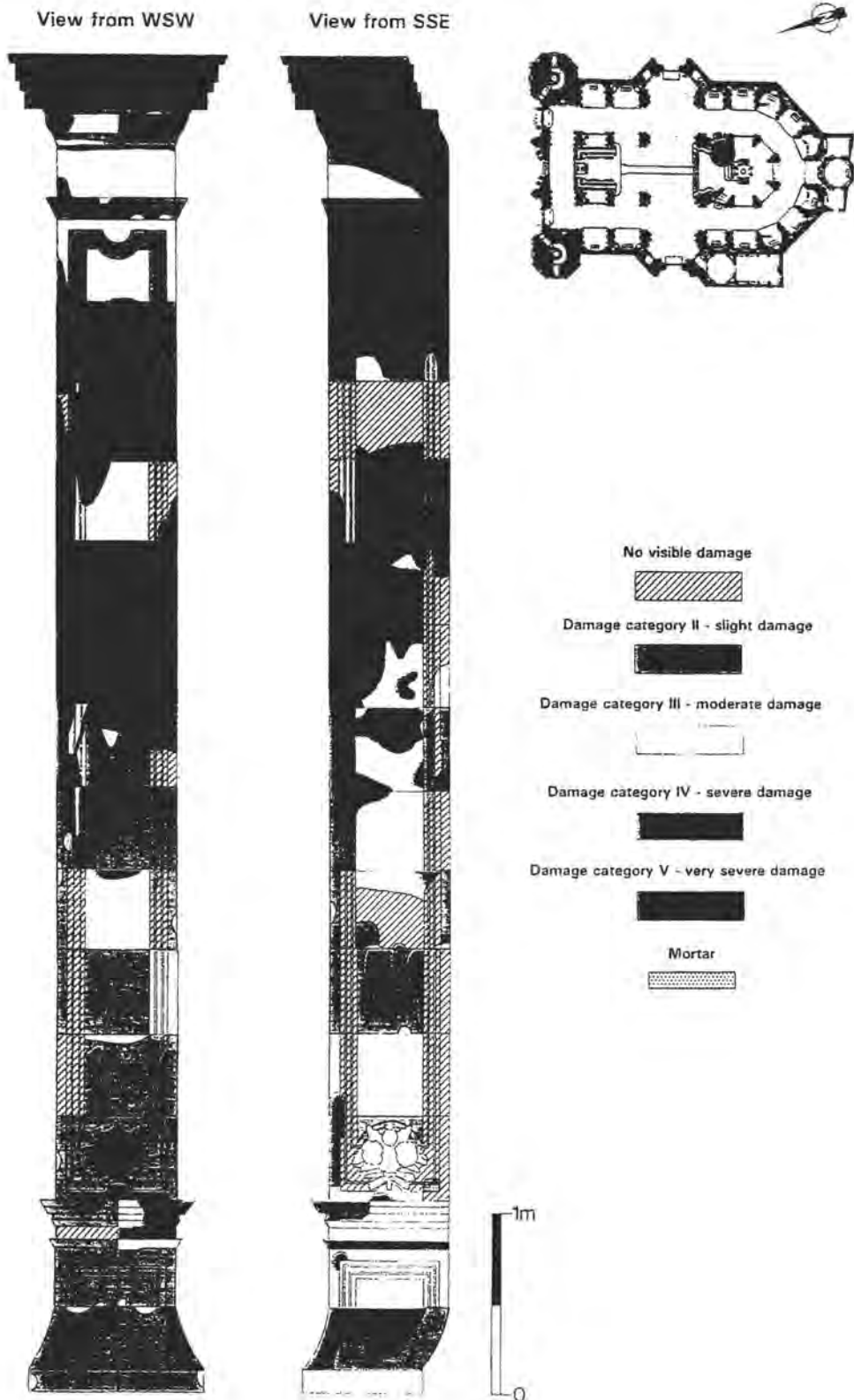
Fig. 2   Application of digital image processing (grey level hystograms)

SECTION 1. Block oolitic limestone affected by detachments and granular disaggregation.

SECTION 2. Scultural reliefs on a block of white oolitic limestone affected by detachments
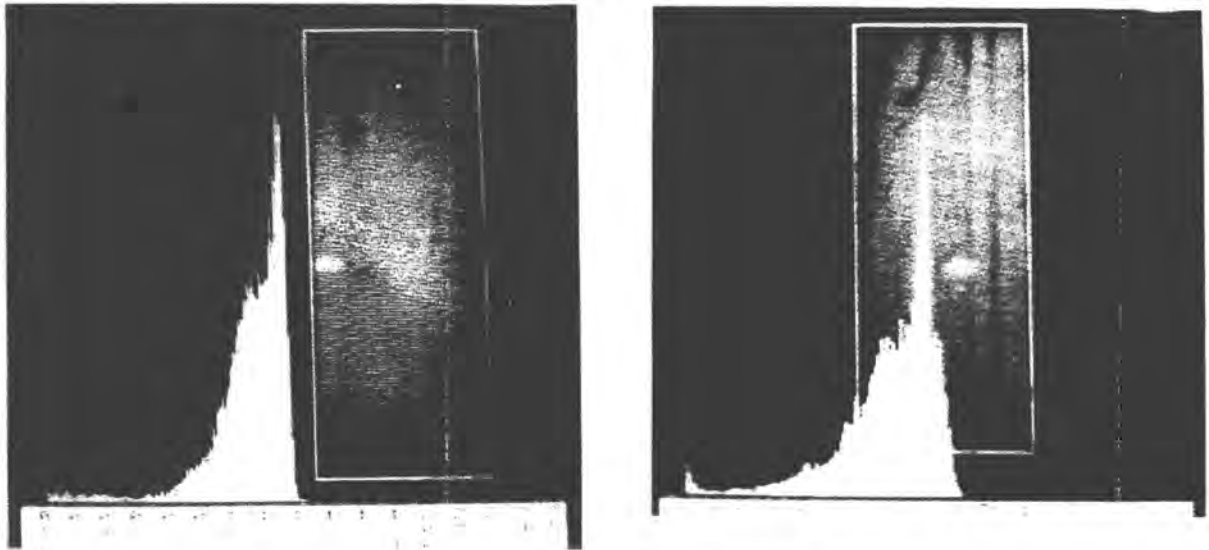
Fig. 3   Application of ultrasonic pulse velocities on weathered stones.
SECTION 1. Block oolitic limestone affected by detachments and granular disaggregation.

Ultrasonic Velocities

3.3 km/s

3.6 - 3.7 km/s

Depth scale

0   2   4

cm
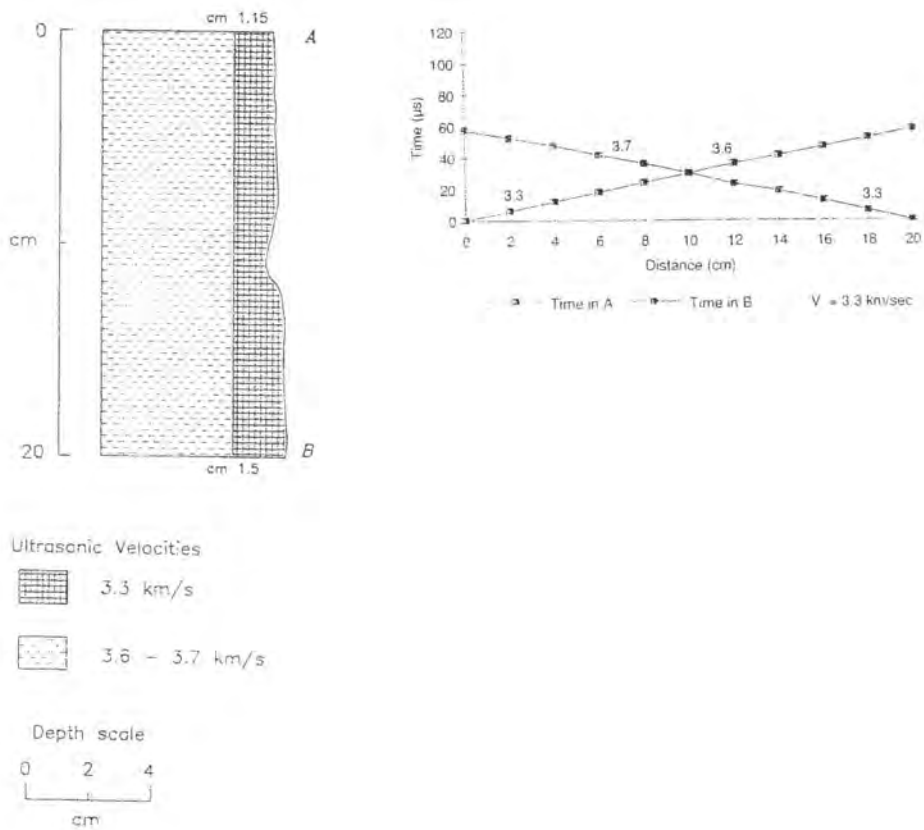
Thermohygrometric conditions, inside the Temple concerned to a pillar, are summarized in figure 4.

The boundary conditions, based on equilibrium relative humidity vs temperature, forecast locally the occurrence of natron,

trona, thenardite and halite. The salts found in the Cathedral are not only influenced by thermohygrometrics conditions but also by other environmental parameters, so we have found trona, natron and occasionally halite.

Aerosol, suspended particles, condensation waters and rainwaters have a high ionic contents. Chlorides, bicarbonates, sulphates, calci-

um and sodium are more aboundant than magnesium or nitrates, so these last ions are displaced in efflorescences crystallization.

Urban and industrial characteristics of Cadiz, combined with climatological environment means low levels of antropogenic pollution. Marine spray composition shows that the problem by pollution in this open–space is negligible in comparison with those produced by marine winds saturated with aerosols and water droplets.

In summary, the main environmental degradation factors for the Cathedral of Cadiz, are the marine spray, stongly moved by WNW dominats winds, and thermohygrometrics conditions.
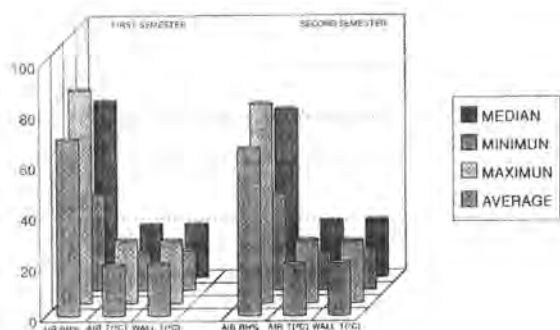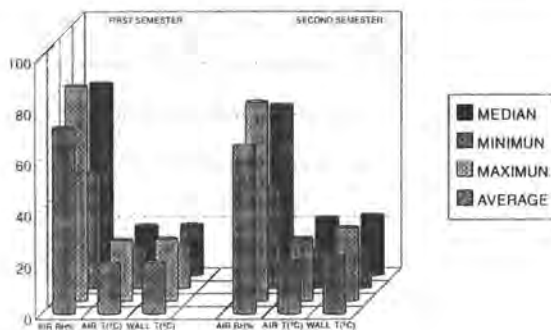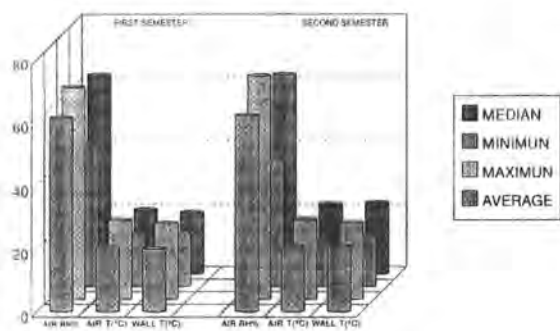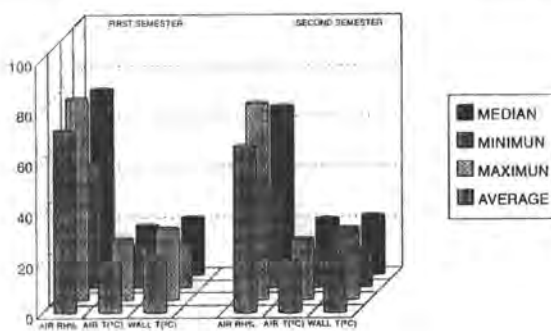
Fig. 4 *Yearly distribution of thermohygrometrics leves on walls.*

Conclusions

For the evaluation of environmental effects on stones, it is necessary an interdisciplinary scientific net. In particular, this project has been an important advance in the knowledge of the Cathedral of Cadiz and in the mechanism of stone decay.

The investigation, that is going on, provides of suitable data for a future control and a reduction of the effects of salts crystallization in Cadiz Cathedral.

Aknowledgements

References

1.   Zezza, F. *Marine spray and polluted atmosphere as factors of damage to monuments in the Mediterranean coastal environment.* 1–5 Reports to the Comission of the European DG XII June 93–June 95.

Herbert Juling
Frank Schlütter
Martin Langenfeld
Rockus Blaschke

Cryo–preparation during scanning electron microscope investigations to visualize salt–solutions inside the pores of historical building materials
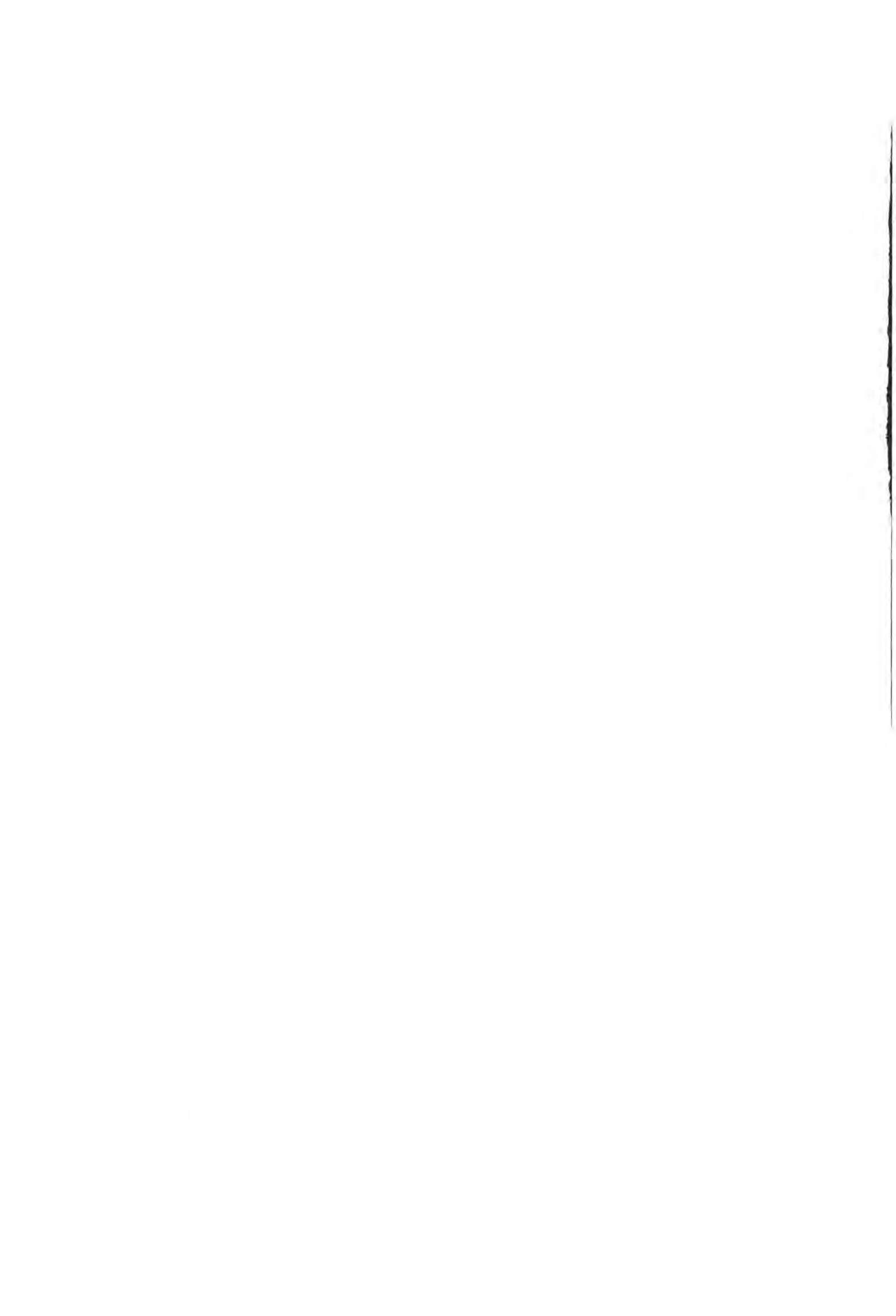
Cryo–preparation during scanning electron microscope investigations to visualize salt–solutions inside the pores of historical building materials

H. Juling, F. Schlütter, M. Langenfeld, R. Blaschke
Amtliche Materialprüfungsanstalt (MPA)
Bremen, Germany 'Analytische Baustoffmikroskopie'
Paul–Feller–Str. 1, D–28199 Bremen

1. Abstract

The damage effects of salt hydratization and crystallization inside the pores of buildings materials is undoubted one of the greatest problems in conservation and restoration of monuments. Theoretical studies supported by simple laboratory experiments give basic imaginations of isolated damage mechanisms. But the real environmental conditions on a building are quite different and very complex because of capillary forces, gradients during salt migration, marginal surface effects, and unknown salt mixtures.

Using conventional microscopical preparation methods with drying the specimen and using vacuum during investigations by scanning electron microscopy the real behaviour of the salt solutions is falsified and many artefacts take place. An alternative way is to use cryo–preparation methods. Using this methods it is able to study the real behaviour of the pore solutions under several points of view.

To give an example in this contribution the results of microscopical investigations are presented, which were made in the interface between an applied conservation mortar and NaCl infected brick surface. The migration of the salt solutions from the brick into the morter are visualized and interpreted.

2. The Cryo–preparation technique

During cryo–preparation the sample material is freezed in melting nitogen. Liquid nitrogen is cooled down by extracting evaporation heat down to temperatures about –210°C and the socalled slush nitrogen looking like snow is formed. Because of the low temperature the Leidenfrost phenomena of an heat insulating gas–cushion is avoided.

During this procedure the sample material is cooled with such a high cooling velocity that the liquid phases inside of the pores are not able to dehydrate or crystallize but freeze in a quasi–amorphous state.

After this preparation the samples are investigated in a field emission scanning electron microscope (FEM) meanwhile cooled continuously on a constant temperature of –130°C.

By using this investigation method it is possible to visualize and study the real mechanisms of salt migration and damage inside the pores of building materials under real environmental conditions.

3. The Problem

During past projects concerning the restoring possibilities of high salted brick walls the coating with consolidation mortars were discussed. Sponsored by the German department of Science (BMBF) a new mortar system on the basis of Hüttensand, gipsum and cement was developed.

A real brick wall of the Kampischer Hof in Stralsund (Germany) was coated with this mortar and the same was done in laboratory with a removed original brickstone of the same wall. Before coated this stone it was devided in several pieces of 1.5 x 1.5 x 6 cm sizes and after

that put together again.

This fresh coated pieces were sampled and fixed by cryo–preparation on different times:

1. five minutes after coating

2. 60 min after

3. on the beginning of setting (after 14 h)

4. after the end of setting (23 h)

4. Results

Already five minutes after applying the mortar it could be seen that the salt in the brick is mobilized and migrates into the mortar because of the input of moisture. In the brick itself salt crystals are present which show first effects of solution. In the first millimeters of the mortar at this time already salt solutions are detectable.

The mortar itself at this time looks like a rubbish heap of the several components.

One hour after applying the mortar the migration of salt solution from the brick into the mortar has continued. Indications for the beginning of hydratization of the cementary binder are not yet visible.

At the beginning of setting after 14 hours first hydrate phases can clearly been seen as seperate small fibres. At the end of setting these phases look like clouds with very fine structures resulting in a high strength of the mortar.

During freezing the samples an artefact took place at which the causality is not yet clear but it is an advantage for the visualization of the salt migration. In many freezing procedures before on several samples with salt solution with the same intention we observed in spite of the very high cooling velocity structures in the amorphous freezed liquid. Till now we explain these effects as the beginning of the building of ice crystals during the cooling procedure in the solution liquid. Because of sublimation processes during the investigation in vacuum the water evaporates and leaves nega-

tive structures in the frozen saturated salt solution. If the salt solution is at the momernt of cryo preparation already saturated as in our example in the

brick after solution of the bulk salt crystals no ice structures can be observed. On the other hand we can be sure that in the mortar exists a decreasing gradient in salt concentration of the pore liquid up to the surface.

In microscopical images we see therefore an increasing number respectively volume of ice structures in the solution liquid.

For this reprint we unfortunately have to relinquish scanning electron micoscopical fotographs and want to direct your attention on the poster at the workshop.

5. Acknowledgements

M. Koui

K. Bisbikou

Use of liquid crystals as deterioration indicators on marble surfaces at the Archaeological Site of Eleusis
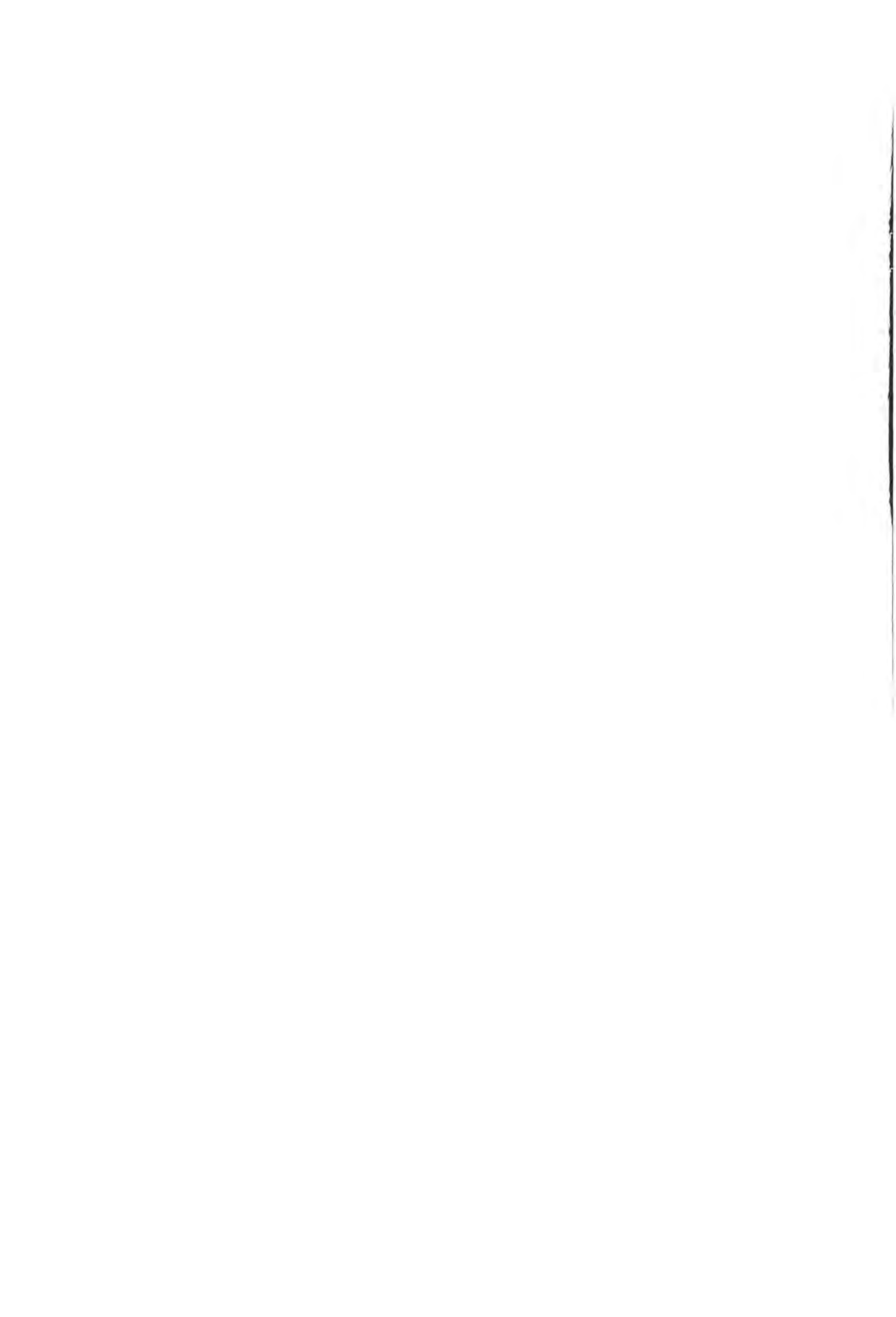
Use of liquid crystals as deterioration indicators on marble surfaces at the Archaeological Site of Eleusis

M. Koui and K. Bisbikou

*Department of Chemical Engineering, Material Science and Technology Sector,
National Technical University of Athens, Zografou Campus, 9 Iroon Polytechniou street,
Zografou 15780, Athens, Greece.*

Key words: marble, crust, differentiation, liquid crystals, preservation.

Abstract

Based on our previous work, with which it was proved that the selectively reflected light from cholesteric liquid crystals also depends on the adsorption properties of the surface of their supports, we use them to distinct different types of deteriorating crusts on the ancient marbles.

We have differentiated three different types of crusts: the washed out areas, the loose depositions and the cementitious encrustations, successfully.

This is interesting for the study of the preservation and restoration of ancient monuments, or new buildings. Thus, the liquid crystals can be used as deterioration indicators, in situ, for the differentiation of marble crusts.

1. Introduction

Liquid crystals are mysterious and extremely useful, thus providing scientist and engineers with one of the most active and stimulating fields of scientific and industrial research. They constitute a fascinating state of condensed matter between crytalline solids and isotropic liquids, exhibiting rheological behaviour similar to those of liquids and anisotropic physical properties similar to those of crystalline solids in the same thermodynamically stable phase. Their dual nature and easy response to electric, magnetic and surface forces have generated in innumerable applications.

Besides the familiar numeric displays and temperature sensors, one now finds liquid crystals in high resolution TV displays, projection systems, optical computing, fibres with tensile strength greater than steel and even in paintings.

In our previous studies[1-4] it has been shown that when solid sorbents, with high physical absorption properties, are used as supports for cholesteric liquid crystals, the selectivily reflected light of the latter is influenced[1-4]. This may be attributed to the fact that the sorbents act on the sorbates with strong mechanical and/or electrical forces due to applied pressure[5-6] or electric field[7-10] respectively, resulting from the sorbents. This working hypothesis was further studied. Aiming at that, we differentiated between the electrolytically prepare[1-3] $\gamma_1-Al_2O_3-\gamma_2Al_2O_3$ prepared with several current densities[1-3], as well as the chemically and electolytically prepared ZnO and Fe_3O_4[1-3], the copper mechanically cleaned and electroplated[1-3], the nickel electrodeposited with different orientation11 (secondary structure) and also we differentiated in situ marble from gypsum and $CaCO_3$ from inversion of gypsum[4]. In all cases the $\lambda-\lambda'$ (where λ and λ' the wave length at the pick of the spectrum for the cholesteric mixture on each support and on blackened glass correspondingly) against temperature of the support was plotted and quantitatively compared with the measured and/or deduced sorptive properties of each support[1-4].

In the present work, following the same experimental procedure and using the same

mixture of cholesteric liquid crystals, we tried to differentiate three different types of crusts: the washed out areas, the loose depositions and the cementitious encrustations, which have been formed on the marble surfaces of the ancient monuments.

We have chosen these three types of crust because these are some of the types, that are often met in the marble surfaces.

2. Experimental

2.1 Origin

The samples were Pentelic marble specimens from the archaeological site of Eleusis on which the three types of crusts are observed[12, 13]:

– **Washed out surfaces as** chromatic alteration from the white of the Pentelic marble to the rusty–yellow color, mainly where water rebound phenomena are present. They occur recrystallized calcite covered by quartz and various particles containing major Si, Al and Fe concentrations. The major Fe, Si and Al concentrations are observed at the interface between the recrystallized calcite

and the original surface. Chlorite salts of K and Na are also evidenced even down to 500 μm (fig. 1).

– **Black crust formations** in the form of **loose depositions,** formed at the surfaces from rain water and presenting an anomalous relief with high friability. They consist of gypsum and of secondary calcite. Wherever water contacts the marble surfaces, recrystallized calcite is formed. On the contrary, where no such contacts are observed, loose depositions are met along with gypsum, mainly comprising the black crust of 500μm depth. At the surface are also observed quartz, feldspars and spherical Fe-rich particles (fig. 2).

– **Cementitious encrustations** as pitting on the marble and limestone surfaces especially on the horizontal surfaces like pavements. They are amorphous formations, 250–300 μm thickness, rich in Ca, Si, Al, Ti and Fe coating the secondary calcite. The XRD results give evidence to the high calcitic content, while lower percentages of gypsum, quartz, alkali–feldspars, mica, chlorite and cementitious compounds are also present (fig. 3).
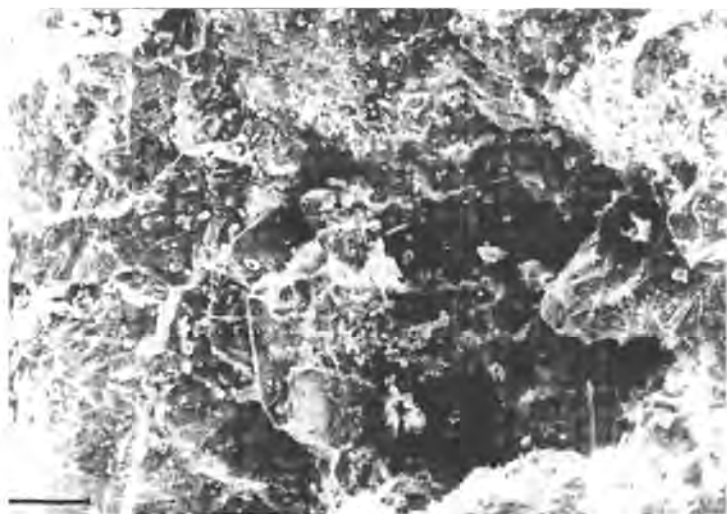
Fig. 1 Washed out surfaces (326x)
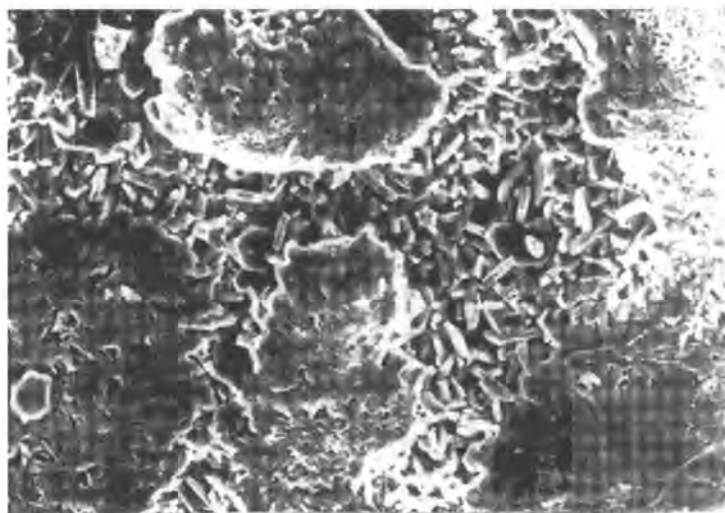
Fig. 2   Black crust formations in the form of loose depositions (326x)
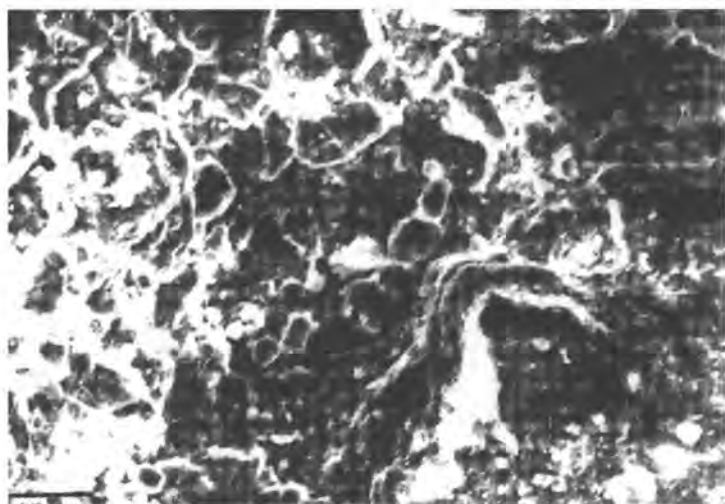
Fig. 3 Cementitious encrustations (750x)

2.2 Shape and dimension of specimens

The dimensions of all specimens were 2cm x 1cm x 0.3cm, suitable to fit in the Spectrophotometer holder. This procedure took place after smoothing the back side of the surface in examination.

2.3 Procedure

On the surface of the specimens a diethylether solution 10% mixture of cholesteric liquid crystals (1:4 per weight) was spread[3]

- cholestery[1-4]–corbomethoxyoxybenzoate $(C_{36}H_{52}O_5)$

- cholesteryl oleyl carbonate $(C_{46}H_{80}O_3)$

On all types of specimens visible diffuse reflectance spectra[3-4] at several temperatures (25°C, 26°C, 27°C, 28°C) were taken after covering the surface with the above mentioned cholesteric mixture as well as on inactive surface of blackened glass as reference.

For the measurements, a Perkin Elmer double beam spectophotometer (mod. Lamda 3) for visible light with an integrating sphere attachment was used. Each of the specimens with the cholesteric mixture was placed on a special thermostated block–heater in the apparatus (in the place designated for back reflection measurements) and

was normal to the light beam. In this way the spectra were taken at a desirable constant temperature ±0.1°C. The accuracy of the measurements was ±0.5 nm.

For accuracy and reproducibility reasons spectra were taken for six specimens of the same type of crust and at the same temperatures.

For all cases the wavelength at the peak of the spectra was determined. The difference $(\lambda-\lambda')$ of wavelengths at the peaks for the specimens (λ nm) and blackened glass (λ' nm) was found to be the most sensitive measure of the shift of the peaks (see detail in References 3,4,11).

3. Results and Discussion

The results of the laboratory measurements for the three different types of crusts are shown in detail in Tables 1, 2 and 3. These Tables present the selective reflected light (color) (λ nm) at the peaks of the spectra.

Table 4 presents the mean values (λ nm) of the results, which are shown in Tables 1, 2 and 3

in detail. From the values of Table 4 can be obtain the fig. 4. In this Figure the differentiation of the three types of crusts is observed.

The washed out crust presents the lowest selectively reflected light values while the cementitious encrustations shows the greatest. The loose deposition formations show an intermediate ones.

We can suppose, according to our recent measurements (SEM, EDX), that this differentiation in the wavelength values is due to the different pore size distribution and to the different texture of the three type of crusts as well as to their totaly different chemical composition.

It is important to be mentioned that we can visually observe the shift of the selective reflected light to larger wave length as the sorptive abilities of the solid support (crusts) increase.

Thus, through this non destructive method in situ, different colors can be observed on the surfaces of different crusts, the dinstiction among them is feasable.

Table 1

Washed out surfaces	Temperature °C			
	25	26	27	28
Wavelength λ (nm)	635	494	446	430
	611	488	443	424
	604	505	448	425
	617	496	444	423
	645	510	453	427
	667	497	458	434
Mean values	630	498	449	427

Table 2

Loose depositions	Temperature °C			
	25	26	27	28
Wavelength λ (nm)	679	523	462	434
	750	557	480	440
	700	531	472	434
	665	528	461	432
	618	517	470	430
	665	524	463	432
Mean values	680	530	468	434

Table 3

Cementitious encrustations	Temperature °C			
	25	26	27	28
Wavelength λ (nm)	730	570	480	452
	676	510	460	428
	750	580	599	464
	718	545	473	430
	674	507	454	423
	725	559	485	440
Mean values	712	545	477	440

Table 4

Temperature (°C)	25	26	27	28
Type of specimens	λ (nm) mean values of 6 measurements			
Washed out surfaces	630	498	449	427
Loose depositions	680	498	468	434
Cementitious encrustation	712	545	477	440
Blackened glass	515	451	423	411
Type of specimens	λ – λ' (nm)			
Washed out surfaces	115	47	26	16
Loose depositions	165	79	45	45 23
Cementitious encrustation	197	94	54	29
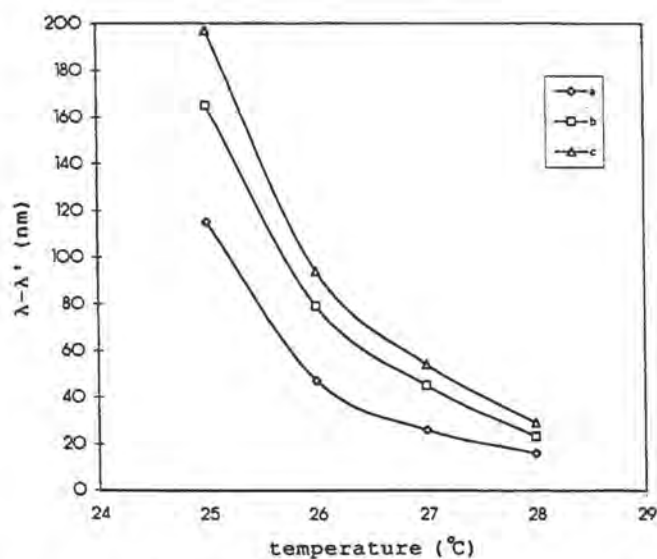
Fig. 4 λ–λ' vs temperature. Surface: a) washed out, b) loose depositions, c) cementitious encrustations

References

1. Th. Skoulikidis and M.Koui, Mol. Cryst. Liq. Cryst. 61, 31 (1980).

2. Th. Skoulikidis and M.Koui, Scuola sui Crystalli Liquidi, UNICAL–81, University of Calabria, Italy (1981).

3. Th. Skoulikidis and M. Koui, Mol. Cryst. Liq. Cryst., 95, 323 (1983).

4. Th. Skoulikidis, M. Koui, and A. Kostoudi, Mol. Cryst. Liq. Cryst. 206,117 (1991).

5. P. Polmann, Ber. Busenges Phys. Chwm., 78, 374 (1974).

6. P. Polmann, J. Phys E. Scien. Instrum., 7, 490 (1974).

7. P.G. de Gennes, The Physics of Liquid Crystals Clarendon Press, Oxford (1974).

8. G.H.Brown Advances in Liquid Crystals Vol.2, Academic Press, New York (1976).

9. G. H. Brown, J. Colloid interface Sci., 58, 534 (1977).

10. G. Meier, E. Sackmann and J.G. Gradmaier Applications of Liquid Crystals Springer–Verlag, Berlin (1975).

11. Th. Skoulikidis, S. Polymenis and A.Kostoudi, Mol. Cryst. Liq. Cryst, 158, 197 (1988)

12. A. Moropoulou, K. Bisbikou, Mat. Res. Soc. Symp. 352, 745, (1995).

13. A. Moropoulou, K. Bisbikou, R. Van Grieken, K. Torfs, F. Zezza, F. Macrì, *"Origin and growth of deteriorating crusts on ancient marbles in industrial atmosphere"* Atmospheric Environ. in press (1996).

V. Massa
G. Pizzigoni
M. Chiavarini

The study of the salts distribution on frescoes.
A non–destructive assessment method
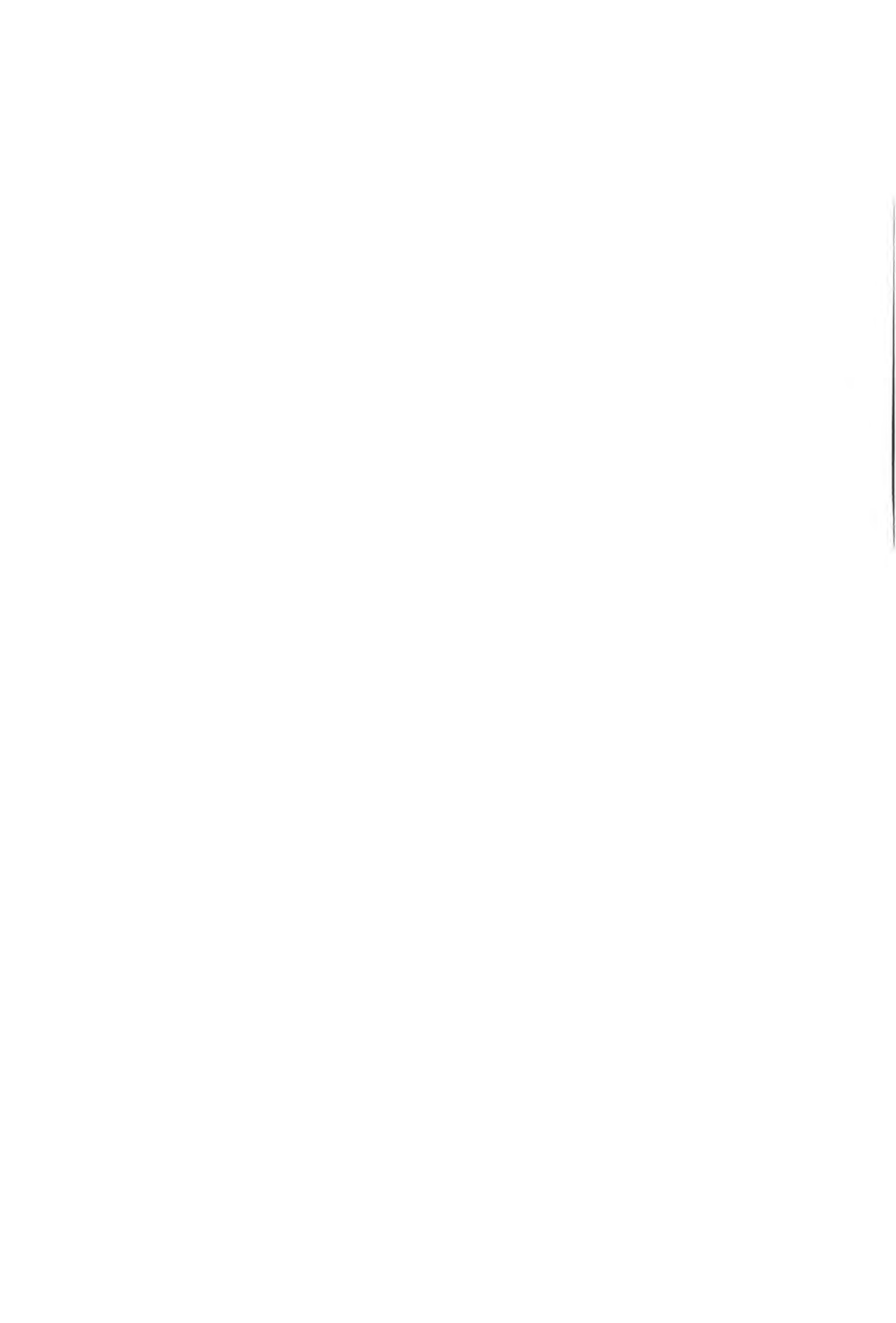
The study of the salts distribution on frescoes.
A non–destructive assessment method

V. Massa, G. Pizzigoni, M. Chiavarini
Syremont, Via Fauser 4, 28100 Novara

Abstract

The well–known wall painting called "Maestà", painted in 1315 by Simone Martini in the Palazzo Pubblico of Siena, was severely affected by salts like sulphates, chlorides, nitrates. Their distribution study was needed to understand their origin and to perform a correct restoration and conservation plan.

The problem appeared very complex, due to the nature of the painting (a fresco largely gilded and distempered); and due to the many factors to be considered as a possible cause of the salts. In fact, the supporting wall was originarily perimetric (i.e., exposed to rains) and contains a waste–pipe, a chimney, etc. formerly used; furthermore, the lower floors of the building had been used as a ware–house of salt and the upper floor, the attic, is frequented by pigeons.

The salts distribution was assessed through classical analytical determinations on samples collected according to a newly developed, non–destructive and non–invasive, sampling method. Sulphates were sampled by means of pads based on ion–exchange resins, acting through contact reactions; nitrates and chlorides (very soluble salts) were sampled by means of cellulosic pads, acting by absorption. Over 70 samples have been collected for each anionic species, covering the whole surface of the painting and without affecting its integrity.

The achieved results allowed the construction of maps showing, for each position of the artworks, the amount of each investigated anion. Their entity varies considerably from point to point, approx. 30, 100 and 600 times

respectively for sulphates, chloride and nitrates; the maximum local amount of sulphates, f.e., corresponds to $10 g/m^2$, a really risky value.

The maps helped very much the cleaning intervention and contributed to better understand the decay phenomena.

1. Introduction

The well–known wall–painting called "Maestà" was painted by Simone Martini in 1315, on the back wall of the room Mappamondo in the Palazzo Pubblico of Siena. The painting is a fresco, largely gilded and distempered; the supporting wall was originarily perimetric, i.e. exposed to outdoor weather; inside it, a formerly used chimney, and some pipes collecting waste water and rain water from the upper Loggia, are present. Furthermore the lower floors of the building had been used for a long time as a ware–house of salt, and the upper floor, the attic, is very frequented by pigeons still now. The first decay problems appeared at the end of the 15th century, when "humidity and water infiltrations" were noted.

Starting from 1871, conservative interventions are documented. Initially gypsum was injected to consolidate the supporting plaster, and the lower decorative part of the fresco was largely restored. Llater on (appr. in 1920) a protective layer of wax was applied in order to limit the decay due to humidity; after 15 year the fresco was cleaned and the wax removed and substituted with paraffin, in order to con-

solidate the painted surface and protect it against humidity. In 1952, as a whitish dimming appeared, a new cleaning intervention was performed to remove paraffin. A further cleaning test was performed in 1983, followed by a consolidating treatment with barium hydroxide, on a zone situated down left.

In more recent years a global conservative project has been planned, based on a scientifically rigorous approach; to the purpose all available, both historic and technical information was collected and critically evaluated; and extended investigations were performed to assess the macro and micro climate, the decay conditions, the chemical–physical and microbiological risk factors, etc. and to define the most suitable restorative and conservative interventions. In this frame, the assessment of salts distribution was a very crucial point; in fact, previous analytical determinations showed an extended presence of nitrates, chlorides and sulphates, with calcium as main cation.

The present paper reports on this topic.

2. Experimental

The methodology used to assess the salts distribution consists on the following main steps:

a) *sampling on the surface of the fresco by means of a non–destructive innovative method;*

b) *analytical determinations of the anions;*

c) *construction of maps reporting the amount of each investigated anionic species, referred to the sampling position.*

Referring to the point a), the chlorides and nitrates, very soluble salts, were sampled by means of wet cellulosic discs with a diameter of 40 mm, acting by absorption. The sulphates, less soluble salts, were sampled by means of pads based on anionic–exchange resins, acting through contact reactions; formulations were been prepared, mixing the resin powder with ammonium carbonate; they

were been applied using a syringe, in form of discs with 20 mm diameter and about 5 mm thickness. Both series of discs were regularly spaced on the fresco and kept wet for one hour. Over 70 samples have been collected for each studied anionic species, examining the whole surface of the painting and without affecting its integrity; each sampling position was recorded.

Referring to the point b), we used the ionic chromatograpy to determine nitrates and chloride, and XRF to determine the sulphur content; the values were expressed in g/m^2 of anions, considering the known dimensions of the sampling discs.

Referring to the point c), the achieved salts data were processed referring to the photogrammetric coordinates, allowing several types of mapping, like isolevel curves, false colours and interpolating threedimensional surfaces.

3. Results

The obtained data cannot be considered as an accurate assessment of the value of the salts amount in each position; they are very probably underestimated because the sampling time was purposely limited in order to avoid any possible damage to the artwork. In fact, the study aimed to describe the salts distribution, whereas their precise amount was less interesting.

The results are available in numerical tables and in several graphical elaborations; the figg. 1–3 show the isolevel curves referred to photogrammetric restitutions.

The entity of nitrates (fig. 1) varies considerably from point to point, that is appr. 600 times, with a maximum of 6 g/m^2. The map shows some major singularities:

– *a maximum zone at the up right corner;*

– *a vertical line of maxima crossing the right group of figures;*

– *a maximum close to the test area treated with barium hydroxide.*

The variation range of chlorides (fig. 2) is smaller, appr. 100 times, and their entity is up to 1 g/m^2; these values are smaller than the nitrates ones, but their distibution is similar, showing analogous singularities.

The sulphates entity (fig. 3), varying appr. 30 times from point to point, is high up to 10 g/m^2, and appears very risky. The major singularities are:

— *a maximum zone at the up right corner;*

— *some low values zones in the canopy area, in the down left treated area, approximately in the middle of the right edge.*

Comparing the results with other information, and particularly with the structure of the wall (fig. 4), we can state some conclusions.

The up right corner, maximally affected by all investigated anions, is particularly exposed to the outdoor aggression; water and pollutants penetrate from the upper Loggia and from the very close window on the right wall, and their migration is emphasized by the local thermic gradient due to the sun and the ventilation, expecially when the windows are open.

The vertical line of maxima regarding nitrates and chlorides corresponds to the waste water pipe existing in the wall; we can presume that small leaks penetrate the wall during the time and are responsible of the salts amount. On the other side, the small amount of chlorides and their distribution very similar to the nitrates one, let us exclude that they came from the ancient salt ware–house of the lower floors.

The low values of sulphates in the canopy area and on the right edge correspond to zones with remarkable lacks of the original painting layers, submitted to various restorative interventions.

Finally the down left area, previously treated, present very low values of sulphates which were been transformed in barium sulphate, pratically insoluble in the used sampling conditions; moreover its consolidating action limited the water penetration from the sur-
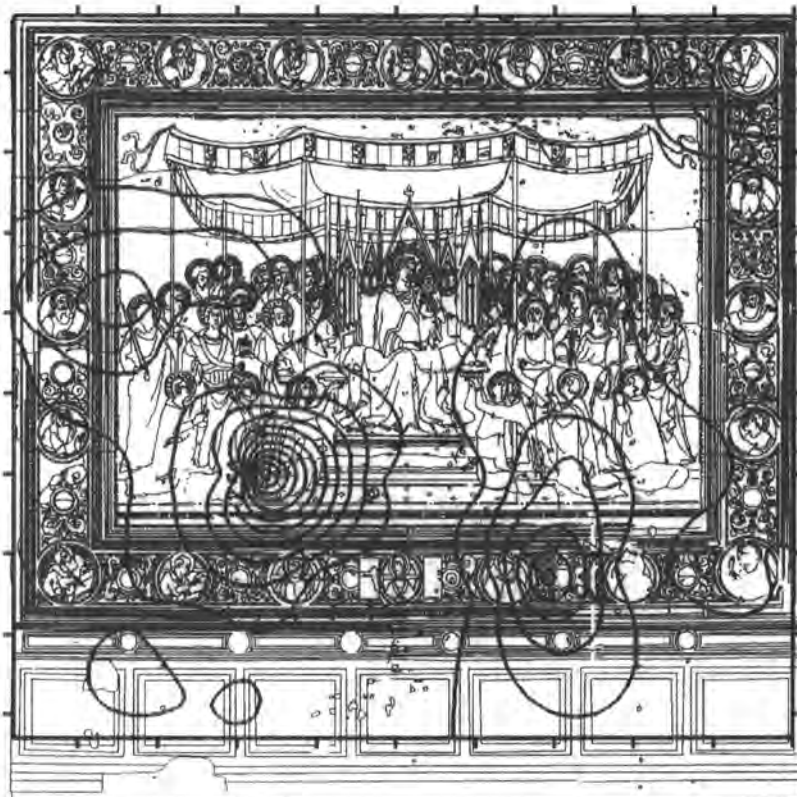
Fig. 1 Nitrates distribution on the fresco Maestà (Isolevel curves).
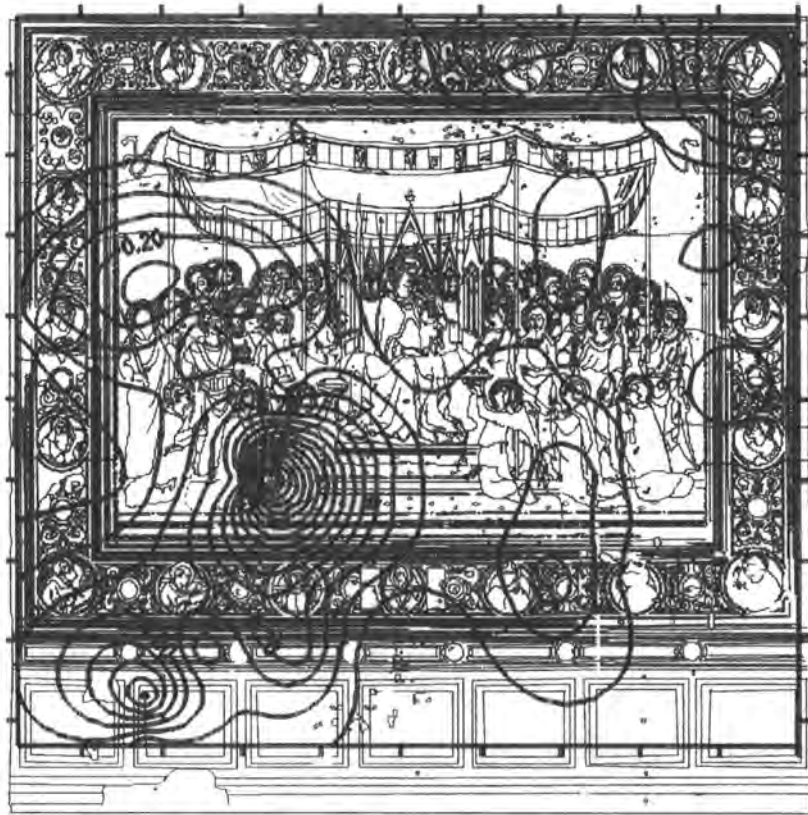
Fig. 2 Chlorides distribution on the fresco Maestà (Isolevel curves).
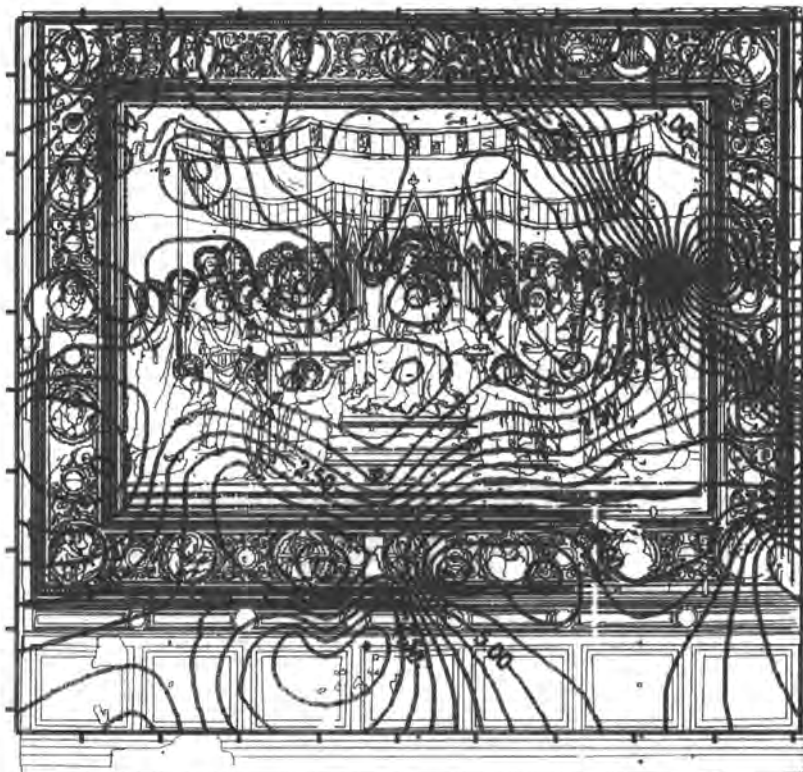
Fig. 3 Sulphates distribution on the fresco Maestà (Isolevel curves).
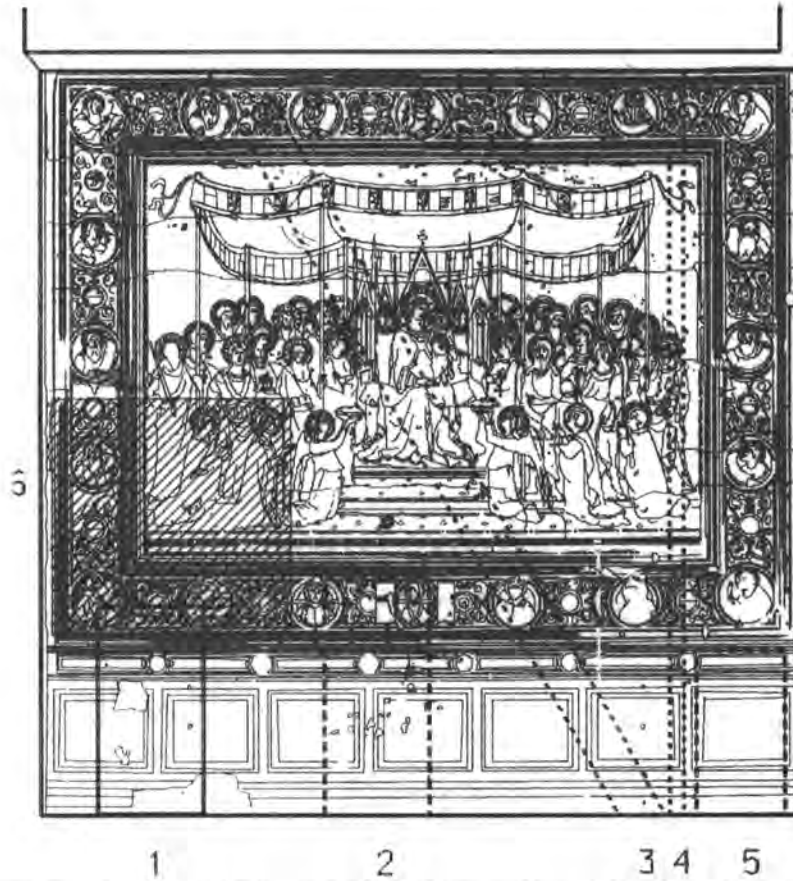
Fig. 4 Main structural details of the fresco wall. 1.Present door 2.Previous door 3.Chimney 4.Waste water pipe 5.Previous door 6.Cleaning and consolidating test area (1983)

rouding zones, so that nitrates and chlorides increased close to the treated area.

We can also note that there are some higher values of sulphates, roughly corresponding to the chimney existing into the wall; such a trend is likely but it cannot be stated basing on the available information.

4. Final remarks

A newly developed, non–destructive sampling methodology allowed to map the salts distribution on the fresco "Maestà" without affecting its integrity.

The obtained data contributed to assess the decay condition of the artwork, to identify the decay causes and mechanisms, to perform suitable restorative and conservative interventions. Some tests have been repeated during and after restoration, confirming the achieved results.

5. Aknowledgment

6. References

1. I. Massari – *Relazione Sanamuro*, 12/12/1977

2. M. Fondelli et al. *"Maestà di Simone Martini a Siena – Rilievo fotogrammetrico"*– Relazione Università di Firenze, 1989.

3. V. Massa, E. Mello, G. Perucca, G. Pizzigoni *"La Maestà di Simone Martini – Attività di supporto alla conservazione"* – Relazione Syremont, settembre 1991.

4. G. Pizzigoni, G. Perucca, V. Massa – *"Diagnostica ambientale e materica per la Maestà di Simone Martini"* – III Int. Conference on non–destructive testing, Viterbo, 4–8/10/1992.
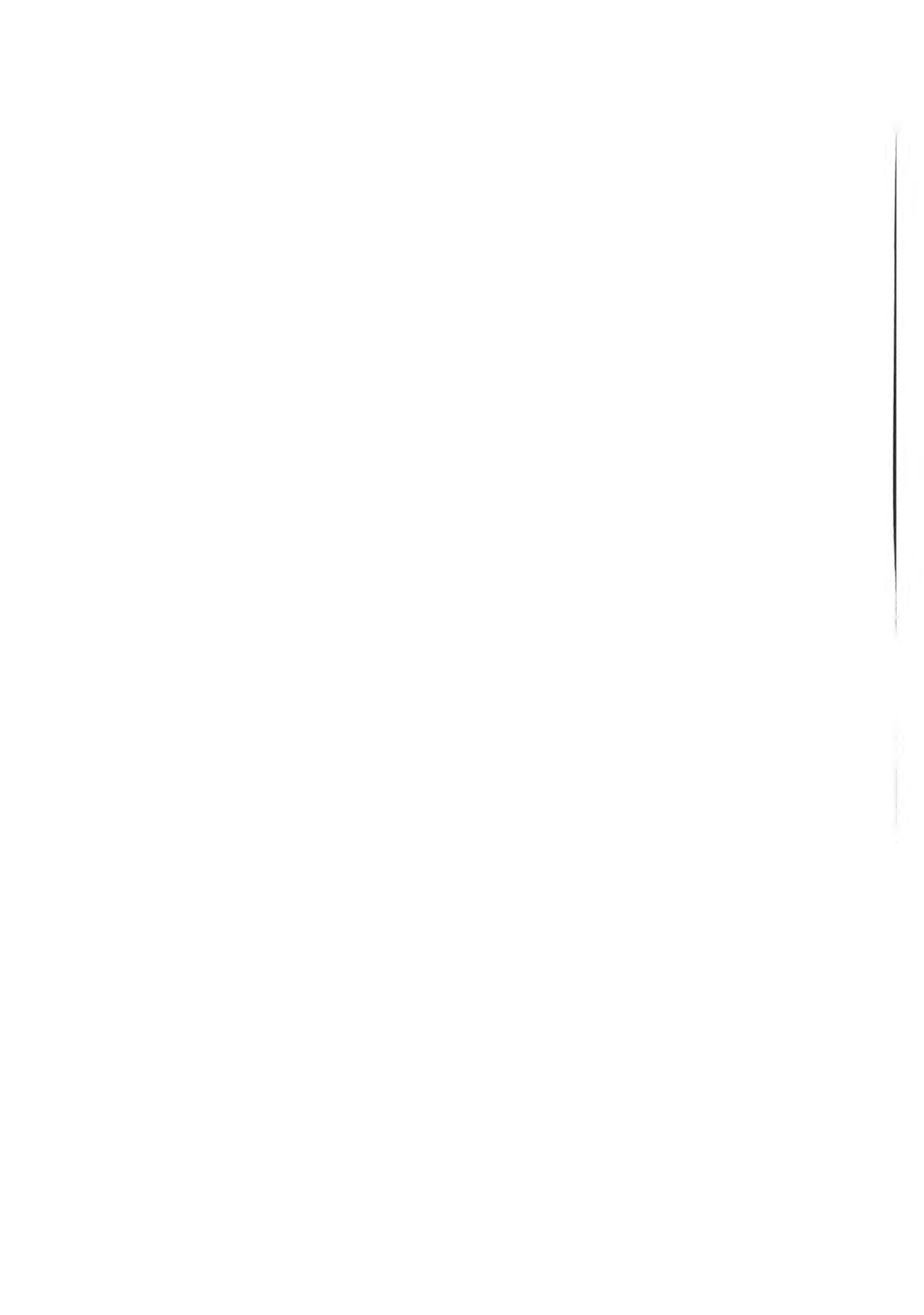
A. Maurício
L. Aires–Barros
V. Fassina
J. Cassar
A. Torpiano

Multivariate data analysis applied to salt efflorescences occurring at Sta. Marija Ta' Cwerra Church (Malta)
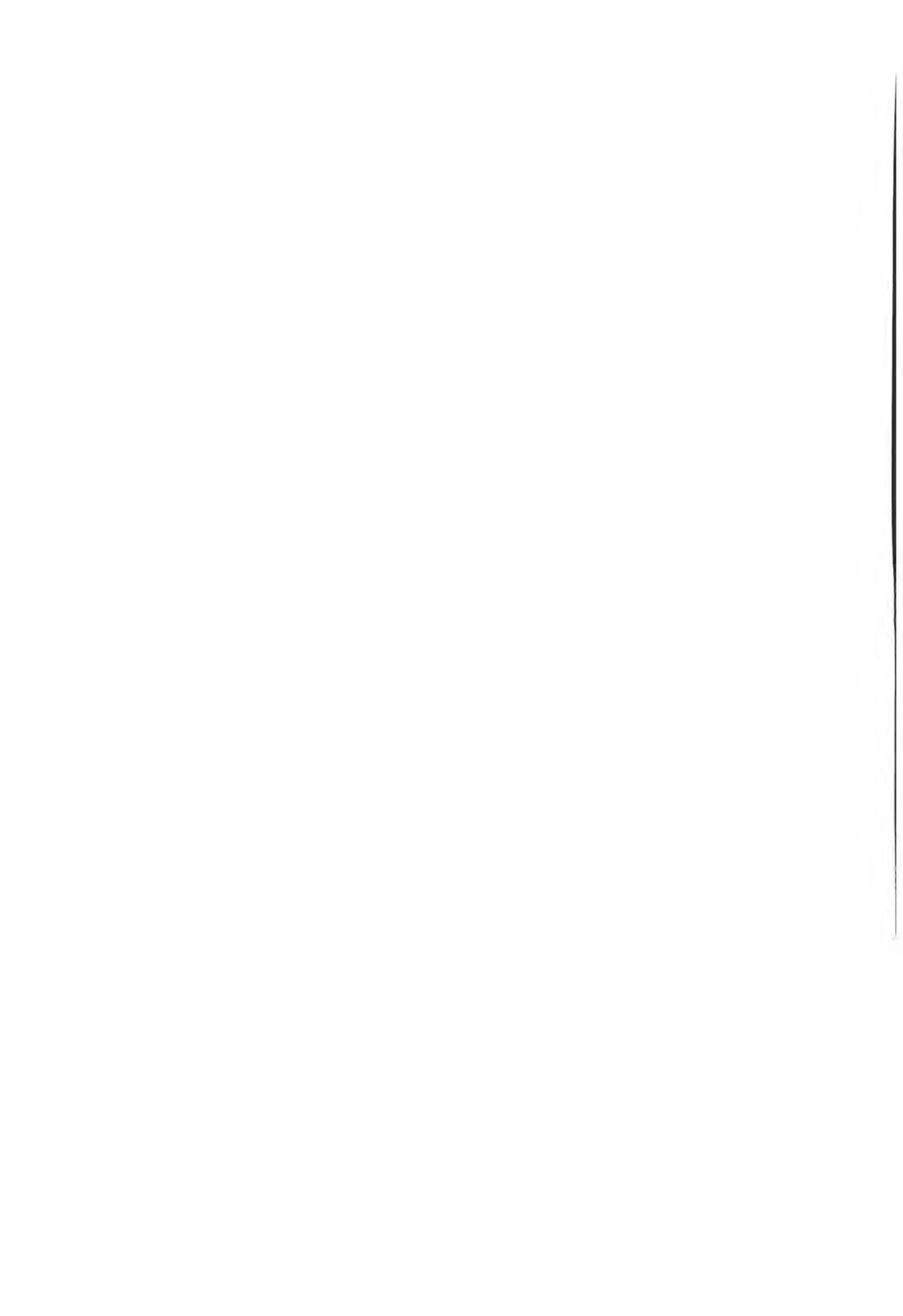
Multivariate data analysis applied to salt efflorescences occurring at Sta. Marija Tà Cwerra Church (Malta)

A. Maurício — *Laboratory of Mineralogy I.S.T. Technical University of Lisbon, Portugal*
L. Aires–Barros — *Laboratory of Mineralogy I.S.T. Technical University of Lisbon, Portugal*
V. Fassina — *Lab. Scientifico Soprintendenza ai Beni Artistici e Storici di Venezia, Italy*
J. Cassar and A. Torpiano — *Institute for Mansonry, University of Malta*

Abstract

Benzécri Multiple Correspondence Factor Analysis (MCFA) is applied to data obtained by chemical analytical techniques of salt efflorescences collected at Sta. Marija Ta' Cwerra Church, in Malta.

The information gathered is multivariate and simultaneously qualitative and quantitative.

This study shows the power as well as the limitations of MCFA in the search for relationships among groups of variables of quite different origin. It allows also to get information, insight and knowledge from sets of qualitative and quantitative variables with an economy of starting hipothesis.

MCFA seems an important and powerful mathematical tool to be adopted in data processing supporting a new methodology for studies based in interdisciplinary analytical techniques applied to the understanding of the monuments stone decay phnomena .

1. Introduction

The project "**Marine spray and polluted atmosphere as factors of damage to monuments in the Mediterranean coastal environment**" aims to make a scientific study of the process of weathering on monuments with particular reference to the Mediterranean coastal areas of Southern Europe where two factors act together to cause stone decay: the marine aerosol and atmospheric pollution (Zezza, 1994). The complexity of the phenomenon of weathering and environmental pollution of stones (characterized by different chemical, physical and textural properties) requires a selection of analytical techniques and the application of appropriate methods of investigations.

Within the framework of the project step "Data processing", this paper attempts to contribute to the improvement of a methodology for studies which can assist the understanding the phenomena of stone decay. This methodology will allow to control the decay process in a better way and also to setup and adopt the most appropriate conservative and restoration policies whenever necessary.

In this methodological context, analysis of data obtained by chemical analytical techniques applied to salt efflorescences, on samples collected at Sta. Marija Ta' Cwerra (Malta) is made.

These data were collected and chemically analysed as part of the project steps of the work program indicated by the time flowchart.

The information gathered is multivariate and simultaneously qualitative (location and height where the samples were collected) and quantitative (ion cromatography of some salt percursors). To study this kind of information, Benzécri Multiple Correspondence Factor Analysis (MCFA) was used. This is a tool suited to analyse and synthesize multivariate qualitative and quantitative observations and variables simultaneously (Lebart et al., 1984)

2. MCFA study of salt efflorescences chemical analysis by ion cromatography

In the context of mineralogic, petrographic and chemical analysis the result of preliminary observations of salt efflorescences show that the church presents an alteration which is preferentially located between 4 and 6 m both inside and outside.

On the external surfaces the alveolar erosion is very advanced, specially on south wall, and results in the loss of large pieces of stone. In the internal side the alteration is located at the same height where also salt efflorescences are visible and are located not only near mortars. Soluble salts were detected by means of ion cromatography. The anions present are: chlorides, sulphates and nitrates (Table l).

Table 1– Sampling July 93: Salt efflorescences inside the church.

Sample	Location	Height (m)	F⁻ (%)	NO_3^- (%)	Cl⁻ (%)	SO_4^- (%)
1	N	0.9	0.046	0.124	0.141	52.50
2	N	1.6	0.000	0.766	3.120	22.70
3	N	1.7	0.000	1.160	0.373	32.90
4	N	2.0	0.000	1.500	1.460	13.50
5	SE	1.7	0.082	0.308	23.50	0.345
6	SE	1.6	0.082	0.262	12.50	0.420
7	S	1.9	0.088	0.000	57.70	0.577
8	S	1.9	0.089	0.049	45.80	0.183
9	S	1.7	0.102	0.063	44.50	0.223
10	S	1.9	0.088	0.295	18.60	0.123
11	SW	1.8	0.032	2.190	1.420	31.40
12	W	1.8	0.100	0.814	26.80	0.399
13	NW	1.7	0.120	0.257	27.40	0.433

The data model consists of a matrix (13x6) (Table 1) containing the ion cromatography quantitative results for F⁻, Cl⁻, NO_3^-, SO_4^-. Two columns contains the location and height of the collected samples. In order to homogenize all variables (qualitative and quantitative) data was codified into classes:

Height (m)

A1 → 0.90 –1.60
A2 → 1.60 –1.70
A3 → 1.70 –1.80
A4 → 1.80 –1.90
A5 → 1.90 –2.00

Location

L1 → North
L2 → SE
L3 → South
L4 → SW
L5 → W
L6 → NW

F⁻ (%)

FO → 0.000
FB → 0.000 – 0.082
FM → 0.082 – 0.089
FA → 0.089 – 0.12

C⁻ (%)

CB → 0.141 – 3.12
CM → 3.12 – 26.8
CA → 26.8 – 57.7

NO3⁻ (%)

NO → 0
NB → 0 – 0.257
NM → 0.257 – 0.766
NA → 0.766 – 2.19

SO4⁼ (%)

SB → 0.123 – 0.399
SM → 0.399 – 13.5
SA → 13.5 – 52.5

A Burt matrix (25x25) crossing all classes was built for the data model. Each element of Burt matrix represents the absolute simultaneous occurrence frequency of the classes defined by the corresponding rows and columns; Burt matrix was submited to MCFA.

3. Results

The study considers the following aspects of MCFA:

1)- Contribution of the principal axis to total inertia;

With 5 principal axes it is possible to explain 76% of the information contained in Table 1 (E 1–24%, E2–16%, E3–15%, E4– 13%, E5–10%).

2)– Variables study

a)

Table 2 – Relative contribution of each variable to inertia explained by the axis (%)

Axis / Variab.	E1		E2		E3		E4		E5	
Location	21.7	H	28.4	H	27.5	H	32.2	H	25.4	H
Height	15.2	M	12.6	M	24.4	H	31.6	H	23.3	H
F^-	19.3	H	15.0	M	21.6	H	14.6	M	16.5	H
Cl^-	19.9	H	24.9	H	2.7	L	1.9	L	7.5	L
NO_3^-	10.9	M	11.2	M	22.9	H	16.8	M	10.7	M
$SO_4^=$	12.9	M	7.9	L	0.9	L	3.0	L	16.7	

H= High contribution to the setup of the axis; M = Mean contrib.; L = Low contribution.

Table 3–Coordinates of variable modalities relatively well represented on each principal axis.

Coord. / Modal	E1	E2	E3	E4	E5	Modality represented on axis (es)
L1	1.088	−0.788				E1/E2
L2		1.500	1.217			E2/E3
L3	−1.219					E1
L4					−1.969	E5
L5			−1.980			E3
L6				2.235		E4
A1			0.980			E3
A2				0.982		E4
A3			−1.485			E3
A4	−1.301			−0.962		E1/E4
A5					2.190	E5
F0	1.15	−0.914				E1/E2
FB		0.797			−0.616	E2/E5
FM	−1.301			−0.962		E1/E4
FA			−1.398			E3
CB	1.111					E1
CM		1.287				E2
CA	−1.139					E1
N0						
NB				0.724		E4
NM			1.063			E3
NA	0.864		−0.831			E1/E3
SB	0.705					E1
SM						
SA	1.104				−0.798	E1/E5

So, each axis represents well, observations with the following characteristics

E1-
L1 - North
L3 - South
A4 - (1.8-1.9m high)
F0 - absence of Fluor
FM - mean.values of Fluor
CB - low val of Cl⁻
CA - high val of Cl⁻
NA - high val.of NO₃⁻
SB - low val of SO₄⁻
SA - high val. of SO₄

E2
L1 -North
L2 -SE
F0 -absence of F⁻
FB -low val. of F⁻
CM -mean. val. of Cl⁻
NM -mean.val. of NO₃⁻

E3 -
L2 - SE
L5 - W
A1 - 0.9-1.6m high
A3 - 1.7-1.8m high
FA - high val. of F⁻
NM - mean. val. of NO₃⁻
NA - high val. of NO₃⁻

E4
L6 - SE
A2 - (1.6 - 1.7m high)
A4 - (1.8 - 1.9m high)
FM - mean. val. of F⁻
NB - low val. of NO₃⁻

E5
L4 - SW
A5 - (1.9-2.0m high)
FB - low val. of F⁻
SA - high val. of SO₄⁻

The interpretation of results contained in Table 2 suggests:

E1 - is mainly the result of the contribution of Location > Cl⁻ > F⁻;

E2 - practically doesn't consider the influence of SO₄⁻ but stresses the importance of Location and Cl⁻;

E3 - practically doesn't consider the influence of SO₄⁻ and Cl⁻ but stresses almost equally the importance of the others;

E4 - practically doesn't consider the influence of SO₄⁻ and Cl⁻ but stresses mainly Location and Height of the samples;

E5 - practically doesn't consider the influence of Cl⁻ and NO₃⁻ .It is maiuly the result of Location > Height > SO₄⁻ > F⁻ .

Each axis allows us to distinguish and/or to associate variable modalities amongst themselves and also observations if necessary. When used in conjunction with other axes it is possible to increase their resolution power in the study of modalities and/or observations.

b)- In what concerns the association between variable modalities on each principal axis we shall consider only those modalities whose representation quality on each axis is

considered relatively good (Q>0.25).The coordinates of those variable modalities are described on Table 3.

4. Interpretation of MCFA results

The study of MCFA results assumes the sampled values contained in Table 1 are representative of salt efflorescences chemical content distributed inside Sta. Marija Ta' Cwerra church in Malta.

Plotting the coordinates of well represented modalities on each axis (Figs. 1 to 5), helps the interpretation of previous Table 3.

1)- From Fig.1 it can be seen that E1 allows:

a) To classify variable modalities in two main groups. The first group (E1G1) associates, in the positive side of the axis, (SA, SB, NA, CB, FO, L1). This means that North observations inside the church are characterized probably by high and low values of sulphate, high values of nitrate, low values of clorine and absence of fluorine. The second group (E1G2) associates, on the negative side of the axis, (CA, FM, A4, L3). This means that sam-

ples collected on south wall at 1.8–1.9 m high are characterized probably by high values of clorine and mean values of fluorine.

b) To oppose E1G1 to E1G2. This means that this axis allows, from the point of view of location and height, to oppose samples from north wall to those of south

wall collected at 1.8–1.9m high. From the point of view of potential salt percursors it opposes, on the positive side of the axis, high values of sulphate, high values of nitrate, low values of clorine and absence of fluorine; to high values of clorine and mean values of fluorine, on the negative side of the axis.

Coordinates of modalities on E1
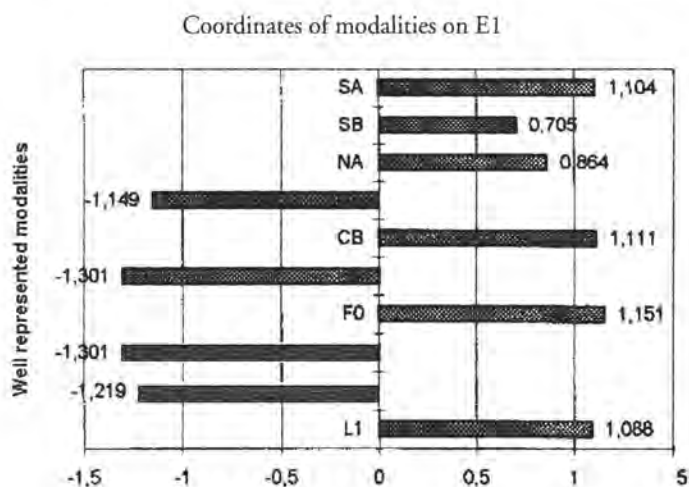
Fig1

2) From Fig. 2 it can be said that E2 allows:

Coordinates of modalities on E2
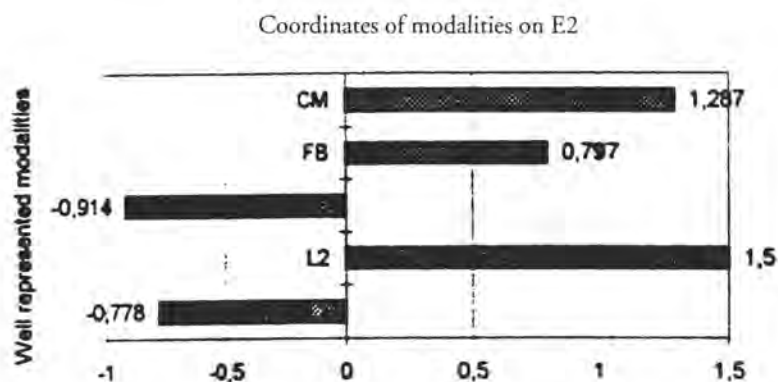
Fig. 2

a) To classify variables modalities in two main groups. The first group E2G1, in the positive side of the axis, (CM, FB, L2). This means that SE observations inside the church are characterized mainly by mean values of clorine and low values of fluorine. The second group E2G2 associates, in the negative side of the axis (L1,FO). This group represents samples

without fluorine on north wall.

b) To oppose E2G1 to E2G2. From the point of view of location variable this means that this axis opposes north and SE samples. From the point of view of salt percursors it opposes mean values of clorine and low values of fluorine on SE samples, to absence of fluorine in samples collected on north wall.

3) From Fig.3 it can be said that E3 allows:

Coordinates of modalities on E3
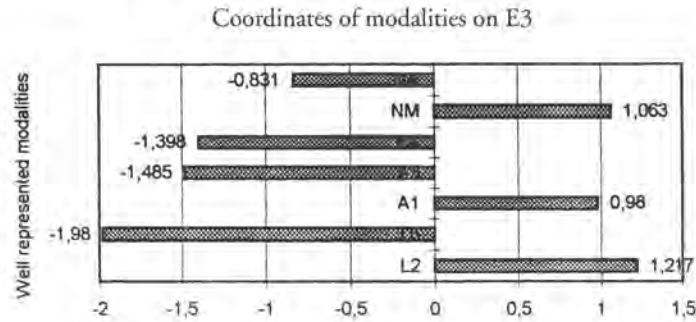
Fig.3

a) To associate on the first group (E3G1), located on the positive side of the axis, samples collected at 1.6m high on SE side of the wall to mean values of nitrate (L2, A1, NM). Located on the negative side of the axis, and connecting samples collected at 1.7–1.8 m high (L3, A3, FA, NA) with high values of fluorine and ni-

trate on west wall, is the second group (E3G1);

b) To oppose, from the point of view of location and height, (A3, L5) to (L2, A1). From the point of view of potential salt percursors this axis opposes mean values of nitrate to high values of nitrate and fluorine.

4) From Fig.4 it can be said that E4 allows:

Coordinates of modalities on E4
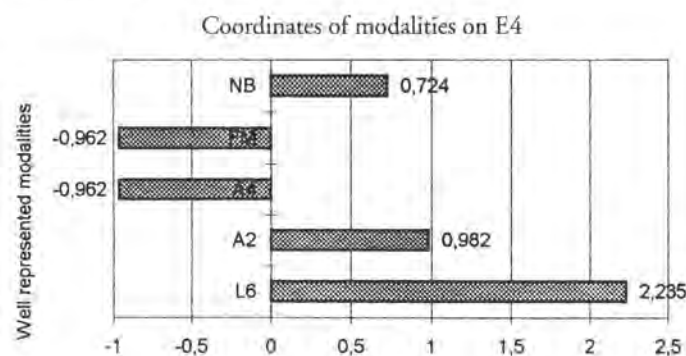
Fig.4

a) to classify SE samples collected at 1.6 m high on the group E4G1 (L6, A2, NB), located on the positive side of the axis. The second group E4G2 (A4, FM) classifies samples collected at 1.8–1.9m high with mean values of fluorine regardless the orientation of the wall.

b) To oppose E4G1 to E4G2. From the point of view of potential salt percursors, this axis opposes low values of nitrate, on samples collected at 1.6m high on SE side of the wall, to samples collected at 1.8–1.9 m high independently of wall orientation.

5) From Fig.5 it can be seen that it is not easy to give a consistent interpretation of the meaning of this axis because it seems to oppose samples collected at 1.9–2.0 height regardless of location and potential salt precursors contents to samples having high content of sulphate and low content of fluorine. However considering lower values of the quality of representation of variables modalities on this axis it is possible to suggest that it is possible to associate, in a weaker way, samples collected at 1.9–2.0 m high with mean values of clorine.

Coordinates of modalities on E5
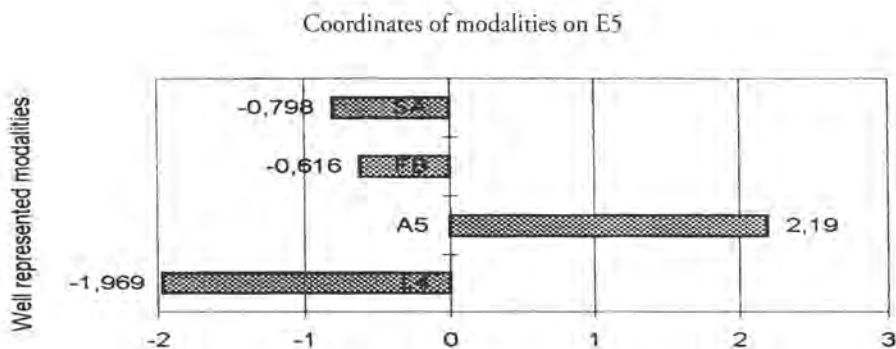
Fig.5

MCFA analysis performed shows that it is not easy to reduce the dimensionality of this data set. Besides, maybe owing to reduced dimension of data matrix and the apparent structure of the data, it is not possible to plot variables modalities on planar graphics that, could be more suggestive. This can be interpreted in the following way:

1) Previous analysis is one of several ways MCFA enables us to analyse Table 1 data set;

2) The assumption made about representativeness of the data set is not valid;

3) The assumption is valid but the phenomena is so complex that other MCFA must be tried on the same data set;

4) The sampling program must be modified in order to include other kinds of variables and much more observations in order to get more consistent results and insight into this kind of phenomena;

5) It will be important to separate intrinsic stone composition and underground contribution to overall salt percursors composition from that one resulting from the interaction with marine spray. This implies the need to setup some control studies along time in each studied monument regarding this kind of problems.

5. Conclusions

Evaporite minerals contribute significantly to mechanical weathering of monuments stones due to their response to "cycles" of air relative humidity and temperature and to the fact that they can affect the behaviour of gypsum crusts. So, it is important to know the way chemical substances, which are their precursors are distributed and related among them and are related with different locations of a monument, in order to access their potential damaging impact on building stones (Aires–Barros & A. Mauricio, 1995). MCFA is an important tool to help to account for some of such relationships.

This study illustrates the power and limitations of multivariate data analysis methods in the search for relationships among groups of variables. These relationships will be much more difficult or even almost impossible to describe when those variables are studied sepa-

rately by classical statistical methods. These methods are much more restrictive, among other things, owing to the difficulty of testing the hypothesis on which they are based.

Multivariate methods allows to consider the possibility to get some information, insight and knowledge from sets of qualitative and quantitative variables with an economy of starting hypohesis, because they are concerned mainly with possible mathematical structures of a given data set. This assumes that not only in the sampling and chemical–physical analytical phase of data acquisition but also in the interpretation of results of these data analysis process it is important the opinion of the monument conservator or of the experts in order to validate the results of a data analysis.

In this paper, the fact that data matrix is a relatively small one (13x6) illustrates one important characteristic of the study of these complex phenomena of interaction between monuments stones and the environment they are located in, namely, the great difficulty to obtain large sets of homogeneous data bases which could be used for several purposes. For instance, to compare results of data gathered from monitoring campaigns in different monuments (data from the environment but also and specially from the stone) and data gathered as a result of dynamic simulations of the critical environmental factors interactions with a given stone in a given monument (Maurício, A., 1994).

It would be interesting, in the context of this paper, concerned with a methodology for preliminary and deeper studies of the interaction monuments/environment, to have several sets of data matrixes with the same homogeneous structure collected in the other monuments. These homogeneous and enhanced salt efflorescences data matrixes allow us to compare the different monitored monuments and also to get insight to some kinds of relationships that could be revealed with the help of these data analysis methods, preparing a better way to more deeper studies.

7. Bibliography

1. Aires–Barros,L. & Mauricio A, Forecast of spatio–temporal probability of salt efflorescence occurrences on monuments stones, *Memórias n°4.pp. 161–167. Univ.Porto.Porto.* 1995.

2. Mauricio,A., Descricao, Análise e Modelagem de Alguns Factores de Alteraçïo e Alterabilidade de Rochas Carbonatadas (o Caso do Mosteiro dos Jerónimos), Ph.D.Thesis, Lisboa, 1994.

3. Lebart,L., A Morineau, K. Warwick, Multivariate Descriptive Statistical Analysis and Related Techniques for Large Matrices, John Willey & Sons, Inc, New York, 231p., 1984.

4. Zezza,E., Marine spray and polluted atmosphere as factors of damage in monuments in the Mediterranean coastal environment. *Proceed.IIIrd Int. Symp. Cons. Monumentsin the Medit. Basin, pp. 269273.Venice,* 1994)

A. Moropoulou
K. Bisbikou
M. Stagakis
G. Stathis
R. Van Grieken
K. Torfs

Environmental outdoor impact assessment on ancient monuments; the case of the Sanctuary of Demeter in Eleusis

Environmental outdoor impact assessment on ancient monuments; the case of the Sanctuary of Demeter in Eleusis

A. Moropoulou — *National Technical University of Athens – Material Science and Engineering Sector – Chem. Eng. Dpt., Iroon Poytechniou 9, Zografou Campus – Athens, Greece*

K. Bisbikou — *National Technical University of Athens – Material Science and Engineering Sector – Chem. Eng. Dpt., Iroon Poytechniou 9, Zografou Campus – Athens, Greece*

M. Stagakis — *National Technical University of Athens – Material Science and Engineering Sector – Chem. Eng. Dpt., Iroon Poytechniou 9, Zografou Campus – Athens, Greece*

G. Stathis — *National Technical University of Athens – Material Science and Engineering Sector – Chem. Eng. Dpt., Iroon Poytechniou 9, Zografou Campus – Athens, Greece*

R. Van Grieken — *University of Antwerp - Department of Chemistry, Universiteitsplein 1, B - 2610 Antwerp, Belgium*

K. Torfs — *University of Antwerp - Department of Chemistry, Universiteitsplein 1, B - 2610 Antwerp, Belgium*

Abstract

In Thriasian plain industrial air pollution causes an aggressive atmosphere, "attacking" the cultural Heritage. In the present work the aerosols, the several dust depositions, crusts and encrustations, mainly concerning white marble are examined in order to investigate the various correlations between the heavy polluted atmosphere and the weathering patterns.

In order to achieve a methodology for an integrated correlation between environmental conditions and crust types, the results of the Energy Dispersive X–Ray Fluorescence, X–Ray Diffraction and Porosity analysis along with characteristic weathering products of the crusts, the orientation of the weathered surfaces and their exposure to the rainfall have been included in the data matrix describing the statistical problem, elaborated by multivariate analysis. Statistical analysis and especially multivariate methods are used in order to provide a technique for predicting what type of weathering would be expected according to the environmental conditions in heavy industrial and marine atmosphere.

1. Introduction

The Sanctuary of Demeter in Eleusis [1] is studied as a pilot monument within the "Marine spray and polluted atmosphere as factors of damage to monuments in the Mediterranean coastal environment" project (EV5V–CT92–0102 contract between EC and CUM– Community of Mediterranean Universities, coordinated by Prof. F. Zezza) [2].

The Greater Eleusis area had been a rural area for years, the post– war period shifting it to industrial, with key manufacturing sectors, basically metallurgical and chemical ones. The Thriasian plain, in particular, has been dramatically "attacked" by several large and small industries causing an intense environmental and living standard decline. Air pollution causes an aggressive atmosphere, "attacking" the cultural Heritage, the dust–fall emissions from industries being the most important factor [3].

Five different carbonate rocks, gray – micritic limestone, white marble, white – gray marble, yellow limestone and biomicritic gray limestone are identified as building materials, presenting in general, low porosity, mainly of interparticle type, and physical and mechanical properties matching their textural and structural characteristics [4]. Weathering patterns evolve according to the above intrinsic characteristics. For a given substrate, specifically for the white pentelic marble, the various crusts are formed according to the extrinsic factors [5]. Environmental monitoring takes place by a time series of measurements of aerosols, total depositions and rainwater samples.

In particular, the various material – environment interactions that are taking place, are characterized by: disintegrated washed out surfaces,

rusty yellow patinas, firmly attached black gray crusts in contact with percolating water, where recrystallized calcite shields amorphous depositions rich in S, Si, Fe and carbonaceous particles, black loose depositions in the water shelters, consisting mainly of gypsum and fly ash particles and cementitious crusts coating and pitting the horizontal surfaces [6].

In the present work the aerosols, the several dust depositions, crusts and encrustations, mainly concerning white marble are examined in order to investigate the various correlations between the heavy polluted atmosphere and the weathering patterns.

In order to achieve a methodology for an integrated correlation between environmental conditions and crust types, the results of the Energy Dispersive X–Ray Fluorescence, X–Ray Diffraction and Porosity analysis along with characteristic weathering products of the crusts, the orientation of the weathered surfaces and their exposure to the rainfall have been included in the data matrix describing the statistical problem.

2. Sampling and Physicochemical Analysis

Aerosol samples are taken every week by pumping air through Nuclepore filters. For the outside monitoring to Nuclepore filters with a different pore size (2 and 0.4 μm) are placed behind each other in a cascade geometry. During a whole week air is pumped through the filters at a flow rate of around 15 lt/min. Behind the pump a flow meter is installed, so that the total volume that has been pumped through the filters is known exactly. The samples were analyzed by Energy Dispersive X–Ray Fluorescence (EDXRF) using a X– ray spectrometer Tracor Northern Spectrace 5000, equipped with a Si(Li) detector an a low power X–ray tube with a Rh target, controlled by an IBM computer. The X–ray spectra were accumulated for 3000sec and analyzed using the AXIL software.

23 aerosol samples filtered with 2 and 0.4 μm pore size, i.e. a total of 46 samples, were collected during 1995 and analyzed.

Samples of crusts, dust deposits and encrustations were taken from different parts of the monument according to :

- *the decay pattern and the damage levels, assessed through macroscopic observation,*

- *the orientation of the individual architectural elements,*

- *the exposure direct rainfall*

- *the degree of sheltering from rainwater*

Table 1 *Sampling per crust type, sampling position and decay type*

Crust Sample N°	Sampling Position	Crust type	Decay type
1	E3	washed out	1
2	E6	washed out	1
3	A1	washed out – rusty yellow	1
4	E3'	washed out	1
5	E1'	black gray	2
6	E1	black gray	2
7	A2	black gray – rusty yellow	2
8	E1"	black gray	2
9	E4'	loose depositions	3
10	E4"	loose depositions	3
11	E4	loose depositions	3
12	E4"'	loose depositions	3
13	E5	cementitious	4
14	E9	cementitious	4
15	E5'	cementitious	4
16	E5"	cementitious	4

A total of 16 samples were collected according to the classification of crusts as shown in the Table 1.

Dust samples d1, d2 were collected from a column of the right side of the Lesser Propylaea and a wall on the left side of the Lesser Propylaea, respectively, as characteristic of the deposition and accumulation through the centuries on the weathered surfaces.

EDXRF analysis is performed as above, X–ray Diffraction (XRD) analysis, Optical Microscopy (OM) and Scanning Electron Microscopy (SEM) results are used as well [6].

The porosity of the crusts is determined by a specific procedure, where SEM photographs from the surface [7] were analyzed by a Digital Image Processing Software [8]; the results are used in the data matrix.

3. Statistical Analysis

Procedures used in the study

Primarily, the hypothesis to be assessed is the potential of "observations or individuals" from a multivariate data set which has to be further classified into two or more groups. To carry out this step the method of principal component analysis is used. It concerns a multivariate analysis allowing to create of new variables, called principal components as linear combinations of the initial ones. The superimposing of initial variables allows for evaluating the role of each one in the distinct groups [9, 10]. The objective is finally to provide a method for predicting which group is most likely to fall into a new case, or to obtain a small number of useful discriminating variables.

Statistical analysis and especially multivariate methods were used for first time by Moropoulou, Theoulakis et als. [11] in order to provide a technique for predicting what type of weathering would be expected according to the micro – environmental conditions at various locations in marine atmosphere.

Data matrix formation

Two statistical problems are dealt.

I. The data matrix describing the statistical problem of the correlation between aerosols 2 μm (23 Samples), 0.4 μm (23 Samples), dusts (2 Samples) and crusts (16 Samples), consists of 64 "observations" (raws), of all the samples and 14 independent variables (columns: Si, S, Cl, K, Ca, Cr, Mn, Fe, Ni, Cu, Zn, Br, Sr, Pb) concentrations obtained from the EDXRF results in ppm.

For the needs of discriminant analysis the same table includes a numeric variable D.C. (Discriminating Code) containing the codes used to group the "observations" (Table 2, 3).

II. The data matrix describing the statistical problem of discriminating the various crusts consists of 16 "observations" (rows) of all the crust samples analyzed and 12 independent variables. The variables Si, Mn, Cl, Y, Fe, Sr and Ca, present the results of the EDXRF analysis expressed in ppm. The porosity of the crusts (POR) is expressed in P%, as total porosity. Another group of variables concerns the critical environmental conditions [5,6] of the weathered surfaces and specifically the exposure to rainfall (REXP) and the surface orientation (SO). Numeric values are obtained as follows (Table 4, 5):

REXP: The value 1 is attributed to the washed out, rusty yellow surfaces and the cementitious crusts, directly exposed to rainfall. The value 0 is attributed to the sheltered areas, were only loose depositions are found. The value 0.5 to the surfaces percolated by water, where black gray crusts are firmly attached.

SO: The value 1 is attributed to the horizontal surfaces (cementitious and gray rusty yellow crusts), 0 to the perpendicular surfaces (washed out, rusty yellow surfaces and loose depositions) and 0.25 to the black gray due to some inclination from perpendicular allowing water percolation.

Table 2 Data Matrix 1.

AEROSOL 2 NO.	CRUST TYPE	AV-TYPE	Si	S	Cl	K	Ca	Cr	Mn	Fe	Ni	Cu	Zn	Ni	Sr	Pb
1		6	136	611	172	191	658	9	9	223	0	0	59	1	0	0
2		6	115	467	145	13	27	2	1	7	0	4	2	14	10	0
3		3	543	1534	298	352	4649	9	49	1667	16	0	92	23	0	78
4		3	427	529	1425	250	27	29	20	550	0	0	2	14	0	98
5		3	0	0	0	0	0	0	0	7	16	4	38	38	10	48
6		5	799	1298	629	526	5834	33	20	550	16	15	92	18	22	78
7		5	1600	1780	534	572	7473	0	44	971	4	8	52	14	20	76
8		5	1759	2034	638	775	14200	32	44	1146	16	29	138	38	56	68
9		6	1008	1082	433	434	5768	36	70	1582	9	15	61	20	17	202
10		7	1134	1822	433	443	6143	26	44	1650	11	18	81	26	27	0
11		7	853	1483	338	180	5768	23	70	1650	9	19	78	20	24	72
12		4	1210	1539	292	454	14010	41	33	3327	21	14	56	17	9	110
13		4	1483	1861	125	234	6515	788	37	1726	9	8	170	13	10	57
14		4	767	1771	476	418	5230	39	16	906	13	11	30	18	11	41
15		5	1194	1500	601	533	7970	24	37	1700	23	27	57	24	20	112
16		5	135	135	351	444	11546	17	76	2271	23	37	146	24	22	145
17		6	979	1210	112	343	6303	14	19	787	34	8	76	13	5.6	79
18		6	1350	1610	52	633	6600	11	10	663	6.4	11	72	19	9	76
19		7	583	194	133	180	4930	16	12	579	7.9	79	29	23	10	68
20		7	667	156	55	234	4740	18	10	868	3.4	12	63	19	9	96
21			840	408	66	227	5150	27	23	775	3.4	57	72	20	23	69
22			1110	1460	328	408	8640	21	20	659	6.8	68	78	16	11	158
23	AEROSOL 0.4 NO.		474	1930	140	757	9330	15	17	775	9.2	15	80	36	14	141
			553	1090	121	406	5390	12	27	727	9.2	21	169	38	12	182
24		2	25	145	53	363		23	6	21	2.3		5.8	6.9	6.9	45
25		2	0	138	32	0	0	13	8	14	0	1.2	4.7	7	5.9	35
26		1	0	255	51	0	0	29	24	16	14	21	5.8	8.1	4.6	34
27		1	0	54	21	0	65	9	5	38	3	3	7	5.7	4.5	38
28		1	32	84	84	46	58	11	11	11	0	3	12	5	4.5	51
29		2	0	408	55	0	0	22	0	180	0	3	9	7	4.4	66
30		2	35	203	66	0	135	21	18	33	10	3	5	7	7	7
31		2	0	352	72	0	59	9	0	34	0	0	5	7	7	9
32		2	0	372	62	0	58	18	5	29	8	2.2	2	7	5	8
33		2	0	411	51	0	0	27	7	39	8	3	5	7	5	6
34		2	0	495	38	43	0	21	18	43	7	3	12	7	13	47
35		2	28	245	48	46	31	30	0	24	4	2.3	4	7	8	22
36		2	32	691	57	31	43	28	0	55	4	2.3	6	7	9	23
37		2	0	282	54	38	57	14	7	34	9	2.3	9	5	9	0
38		2	0	282	23	41	30	16	37	33	6	11	12	7	6	0
39		2	47	418	11	38	42	11	0	16	8	7	5	7	4	30
40		2	0	285	54	0	62	16	19	180	5.6	2.2	14	5	8	66
41		2	0	388	38	43	53	22	24	34	5	3	8	5	9	47
42		2	0	330	10	43	43	18	18	16	7	0	4	7	7	68
43		2	23	403	12	17	20	17	10	18	4	7	9	5	7	84
44		2	20	238	36	37	65	14	12	24	4.2	11	63	5	23	72
45		2	29	152	19	29	52	14	9	16	4.4	16	29	4.8	19	108
46		2	20	108	14	0	74	12	0	27	2.3	15	169	6.9	6.9	45
CRUSTS																
E4	LOOSE DEPOSITION	3	26	19	0.51	6430	31	40.3	148	2540	15.9	39.4	77	12.6	203	85.5
A1	W.O. RASTY YELLOW	4	2.96	0.14	0.27	12200	373	35.9	166	934	0	0	48.1	0	220	101
A2	BG GRAY RUSTY YELLOW	5	5.2	0.42	0.43	7610	38.7	82.4	197	1170	18	17.4	59	5.5	230	104
A3	WASHED OUT	4	0.93	0.13	0.12	10600	33.7	235	625	625	5.8	8	19.8	4.2	177	110.4
E5	CEMENTITIOUS	5	3.8	0.25	0.35	7790	32.8	98	195	4070	20.2	23.5	136	4.71	204	270
E6	BLACK GRAY	6	1.9	0.14	0.14	7490	36.3	32.1	385	2370	5.48	9.66	56.7	4.8	194	119
E7	DUST	7	16.8	20.8	0.46	7510	14.6	96.7	229	13600	56.9	58.9	238	7.95	177	304
E8	DUST	7	4.2	16.6	0.42	6190	20.5	194	559	26300	108	111	599	9.53	346	354
E9	CEMENTITIOUS	6	3.5	0.6	0.38	10600	23.8	105	397	1870	47	226	226	5.93	250	322
E1	BLACK GRAY	4	3.7	0.31	0.33	6540	29.2	61.2	323	4000	11	35.3	94.6	5.5	216	89.6
E1	WASHED OUT	5	0.8	0.6	0.28	6540	31	58.2	280	4000	12	11	35.3	4.8	216	352
E3	BLACK GRAY	5	3.6	2.2	0.034	6660	293	52	325	4400	10	34.8	92.4	4	216	82.4
E4	BLACK GRAY	4	2.5	0.14	0.038	7610	38	38	330	1800	6.2	34.8	35.3	4.2	330	88.2
E4	CEMENTITIOUS	4	3.6	1.8	0.035	6840	31	34	330	4001	12	33.2	226	5.93	250	108
E5	CEMENTITIOUS	6	3.6	0.28	0.5	7110	24	92	380	14000	18	28	136	4.8	190	288
E5	CEMENTITIOUS	6	3.8	0.28	0.405	7240	28	94	390	11000	18	22.5	142	5.1	230	281
E4	LOOSE DEPOSITION	3	2.8	1.4	0.53	6620	31	32	150	2580	16	33.8	68	10	202	82
E4	LOOSE DEPOSITION	3	3	1.6	0.518	6580	31.1	34	153	2660	16	35.2	70	8	230	81
E4	LOOSE DEPOSITION	3	2.5	1.8	0.509	6680	38	38	147	2539	16	38.2	88.2	4.2	218	84

A. Moropoulou, K. Bisbikou, M. Siagkakis, R. Van Grieken, K. Torfs

Table 3   I   Statistical Analysis Results.

Principal Components Analysis		
Component Number	Percent of Variance	Cumulative Percentage
1	49.84422	49.84422
2	30.92492	80.76915
3	5.93784	86.70699
4	3.82125	90.52823
5	2.92220	93.45043
6	2.20904	95.65947
7	1.25577	96.91523
8	.82936	97.74460
9	.69209	98.43668
10	.64335	99.08003
11	.34000	99.42003
12	.28976	99.70980
13	.17025	99.88004
14	.11996	100.00000

Discriminant Analysis for C2.A			
Discriminant Function	Eigenvalue	Relative Percentage	Canonical Correlation
1	58.050920	69.72	.99150
2	12.768640	15.34	.96300
3	7.461544	8.96	.93905
4	3.721127	4.47	.88780
5	.916033	1.10	.69144
6	.345899	.42	.50695

Functions Derived	Wilks Lambda	Chi–Square	DF	Sig. Level
0	.0000119	595.12384	84	.00000
1	.0007050	381.00783	65	.00000
2	.0097071	243.33217	48	.00000
3	.0821370	131.21676	33	.00000
4	.3877792	49.73426	20	.00024
5	.7429977	15.59578	9	.07582

Discriminant Analysis for C2.A

Standardized Discriminant Function Coefficients						
	1	2	3	4	5	6
MB.Si	0.38268	0.19948	0.68756	−0.31751	−0.07583	0.47090
MB.S	−0.60264	−0.29528	−0.96095	−0.21195	0.24507	−0.41913
MB.Cl	−0.14251	−0.16433	−0.18408	−0.23010	0.04821	0.04050
MB.Ca	−0.23982	0.25066	−0.53711	0.01951	−0.25671	−0.20870
MS.K	0.68727	0.45397	−0.05309	−0.35015	0.40903	0.33011
MB.Cr	−0.31400	−0.93303	0.11459	0.36982	−1.01114	0.19245
MB.Mn	0.53078	−0.72787	−0.90262	0.08294	0.02526	0.80547
MB.Fe	−0.20149	−0.66413	−0.21310	−0.51980	0.02430	0.37408
MB.Ni	−0.58701	−0.18330	0.75877	−0.13486	1.50737	−0.46522
MB.Cu	0.73585	2.12042	1.36287	−0.16875	−1.32651	−0.01496
MB.Zn	−0.43826	−0.20516	−0.44399	−0.01106	−0.61315	−0.00336
MB.Br	−0.44492	0.13064	−0.58926	−0.52579	0.15345	0.02258
MB.Sr	0.47502	0.41050	−0.28551	0.15931	−0.02115	0.67477
MB.Pb	0.63901	−0.96166	0.41508	0.00401	−0.04909	0.62794

Unstandardized Discriminant Function Coefficients						
	1	2	3	4	5	6
Mb.Si	0.00134	0.00070	0.00242	−0.00112	−0.00027	0.00165
Mb.S	−0.00171	−0.00084	−0.00272	−0.00060	0.00069	−0.00119
Mb.Cl	−0.00076	−0.00088	−0.00098	−0.00123	0.00026	0.00022
Mb.Ca	−0.00011	0.00012	−0.00025	0.00001	−0.00012	−0.00010
MS.K	0.00078	0.00051	−0.00006	−0.00040	0.00046	−0.00037
Mb.Cr	−0.02095	−0.0555/8	0.00765	0.02468	−0.06747	−0.01284
Mb.Mn	0.01274	−0.001747	−0.02167	0.00199	0.00061	−0.01933
Mb.Fe	−0.00010	−0.00034	−0.00011	−0.00027	0.00001	0.00019
Mb.Ni	−0.07947	−0.02482	0.10273	−0.01826	0.20408	−0.06299
Mb.Cu	0.08608	0.24804	0.15942	−0.01974	−0.15517	−0.00175
Mb.Zn	−0.00698	−0.00327	−0.00707	−0.00018	0.00976	−0.00005
Mb.Br	−0.07415	0.02177	−0.09821	−0.08763	0.02557	0.00376
Mb.Sr	0.01964	0.01697	−0.01180	0.00659	−0.00087	0.02789
Mb.Pb	0.01707	−0.02569	0.01109	0.00011	−0.00131	0.01677
CONSTANT	−2.89408	0.56854	1.62137	2.47356	0.22510	0.42382

Table 4 Data Matrix II.

SAMPLING PER CRUST TYPE

CRUST SAMPLE N°	SAMPLING Position	CRUST TYPE	EXPOSURE TO RAINWATER	SURFACE ORIENTATION	RECRYSTALLIZED CALCITE	GYPSUM	Si	Mn	Cl	Y	Fe	Sr	Ca	POROSITY
1	E3	WASHED OUT	1	1	0	0,5	0,33	0,03	195	0,33	14,4	625	577	38,7	35,77
2	E6	WASHED OUT	1	1	0	0,5	0,31	1,9	360	0,18	13	2370	194	36,3	35,77
3	A1	WO RASTY YELLOW	1	1	0	0,5	0	2,96	186	0,27	13,7	934	220	37,3	33,5
4	E3'	WASHED OUT	1	1	0	0,5	0,33	1,1	280	0,28	13,8	1800	330	38	35,77
5	E1'	BLACK GRAY	2	0,5	0,25	1	0,25	3,7	325	0,35	14,8	40004	217	29,3	28,62
6	E1	BLACK GRAY	2	0,5	0,25	1	0,25	3,5	323	0,33	14,7	4000	216	29,2	28,59
7	A2	BG. GRAY RASTY YELLOW	2	0,5	1	0	0,5	5,2	197	0,43	16,3	1170	230	33,7	30,1
8	E1''	BLACK GRAY	2	0,5	0,25	1	0,25	3,6	330	0,34	14,5	4001	218	31	28,62
9	E4'	LOOSE DEPOSITIONS	3	0	0	0	1	2,5	147	0,509	7,69	2539	202	29,9	31,26
10	E4''	LOOSE DEPOSITIONS	3	0	0	0	1	3	153	0,518	8,88	2880	230	311	31,28
11	E4	LOOSE DEPOSITIONS	3	0	0	1	1	2,6	148	0,51	7,68	2540	203	35	33,28
12	E4'''	LOOSE DEPOSITIONS	3	0	0	0	1	2,8	150	0,53	8	2580	202	31	31,28
13	E5	CEMENTITIOUS	4	1	1	0	0	3,8	385	0,25	11,9	4070	204	32,8	25,51
14	E9	CEMENTITIOUS	4	1	1	0	0	4,2	397	0,38	10,6	18700	250	23,8	25,51
15	E5	CEMENTITIOUS	4	1	1	0	0	3,8	390	0,405	11,25	11000	230	28	25,51
16	E5''	CEMENTITIOUS	4	1	1	0	0	3,6	380	0,5	13	14000	190	24	25,51

Table 5   II   Statistical Analysis Results.

Principal Components Analysis		
Component Number	Percent of Variance	Cumulative Percentage
1	41.53458	41.53458
2	31.42692	72.96150
3	10.52320	83.48470
4	6.70075	90.18546
5	5.92284	96.10830
6	1.59912	97.70742
7	1.08635	98.79378
8	.83187	99.62565
9	.30610	99.93175
10	.04496	99.97671
11	.02157	99.99828
12	.00172	100.00000

Discriminant Analysis for C1.A			
Discriminant Function	Eigenvalue	Relative Percentage	Canonical Correlation
1	100324.50	81.27	1.00000
2	22535.44	18.25	.99998
3	591.92	.48	.99916

Functions Derived	Wilks Lambda	Chi–Square	DF	Sig. Level
0	.0000000	195.46892	36	.00000
1	.0000001	114.85570	22	.00000
2	.0016866	44.69547	10	.00000

Discriminant Analysis for C1.A

Standardized Discriminant Function Coefficients			
	1	2	3
M1.Si	−0.96503	0.05570	4.15487
M1.Mn	3.15202	0.88712	−9.75004
M1.Cl	−0.03747	0.04984	−0.76253
M1.Y	−0.34191	−1.15917	−0.29934
M1.Fe	−2.13777	−1.63713	−0.37316
M1.Sr	1.96737	1.28668	−4.93912
X1.Ca	−0.82794	−1.35032	−0.74193
M1.REXP	1.23730	−0.71164	0.22889
M1.SO	36.2687	66.1455	7.42770
M1.RCa	31.3993	64.2513	22.3012
M1.GYPSUM	−3.56428	−1.08065	10.3522
M1.POROSITY	0.00873	−0.07943	1.13229

Unstandardized Discriminant Function Coefficients			
	1	2	3
MI.Si	−1.51702	0.08757	6.53145
M1.Mn	0.06039	0.01700	−0.18679
M1.C1	−0.55946	0.74421	−11.3854
MG.Y	−0.44344	−1.50337	−0.38823
M1.Fe	−0.00067	−0.00052	−0.00012
M1.Sr	0.02217	0.01450	−0.05567
M1.Ca	−0.31078	−0.50686	−0.27849
M1.REXP	494.920	−284.555	91.5557
M1.SO	193.381	352.682	39.5039
M1.RCa	125.582	256.975	89.1943
M1.GYPSUM	−34.9998	−10.6116	101.655
M1.POROSITY	0.01035	−0.09410	1.34137
CONSTANT	−404.062	5.04012	−117.261

Another group of variables concerns the characteristic decay products, as analyzed (XRD and observed (OM and SEM) by mineralogical analysis [6, 12], and have specifically as follows:

RCa (Recrystallized calcite): The value 1 is attributed to the black gray surfaces, where an almost intact film of secondary calcite is observed to shield amorphous inclusions beneath. The value 0 is attributed to the loose depositions, cementitious and gray rusty yellow crusts, where no secondary calcite is recrystallized, while washed out and rusty yellow surfaces are covered partially by recrystallized calcite obviously fractured.

G (Gypsum): The value 1 is attributed to loose depositions, where gypsum is detected and well observed. Rusty yellow and cementitious crusts contain no gypsum at all (0). Black gray crusts (0.25), washed out surfaces (0.33) and gray rusty yellow crusts (0.5) contain several gypsum phases, as evaluated by SEM.
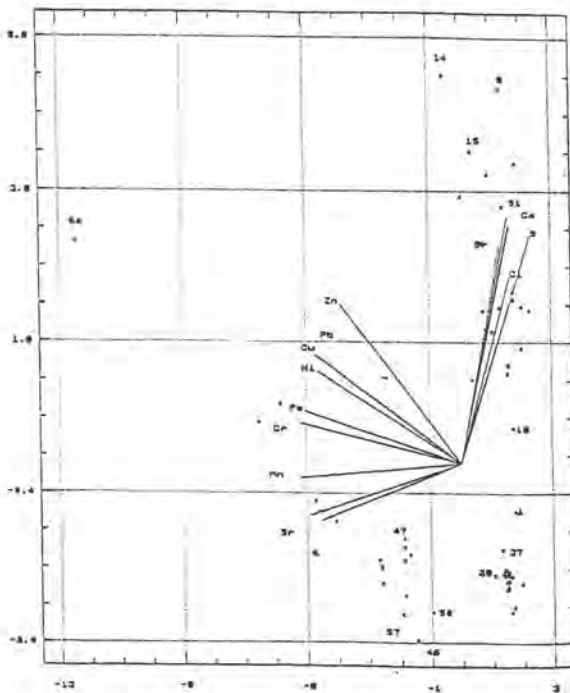
4. Results and Discussion

I. Principal components analysis is employed by using as data vectors the variables : Si, S, Cl, K, Ca, Cr, Mn, Fe, Ni, Cu, Zn, Br, Sr, Pb.

The first components accounts for 49,84% of the total variability, while the next two components account for an additional 30,92%. For the first two components, almost 81% of the total variability (Table 3) is accounted for. On the biplot (Fig.1) the 14 lines intersecting at (0,0) represent the original variables. The length of each vector is proportional to its contribution to the principal components, while the angle between any two of them is inversely proportional to the correlation between them. From this plot is concluded that "Si", "Ca", "S", "Cl", "Br" are strongly correlated and very important for the aerosols and especially for the large ones (>2 µm) appearing at the "observations" 1–23. These are deriving from TSP, industrial air pollutants and marine spray and are the main components of the large aerosols. Specific industrial contribution are under further investigation according to the isotopic ratio analysis of S [13].

Heavy metals like Zn, Cu, Pb, Ni, Fe, Cr, Mn, Sr, K present a weaker correlation and al of them seem to influence the crusts group (observations 47 – 64). However, apart from the correlation of Mn, Cr, Fe with the cementitious encrustations, it is not clear the specific correlation of the various crusts with the variables.

Discriminant Analysis

Discriminating code numbers 1, 2, 3, 4, 5, 6, 7 are given respectively to the points of the seven groups 1: (1,...,23), 2 : (24,...,46), 3: (47, 60, 61), 4: (48, 49, 50, 52, 57), 5: (48, 49, 58, 59), 6: (51, 55, 63, 64), 7: (53, 54). Discriminant analysis is employed using as data vector the 14 variables and entering as classification factor the variable Decay type. The plot of discriminant functions (Fig.2) shows a good discrimination by these variables.

Fig. 1 Scatterplot of principal analysis. Biplot of principal components analysis

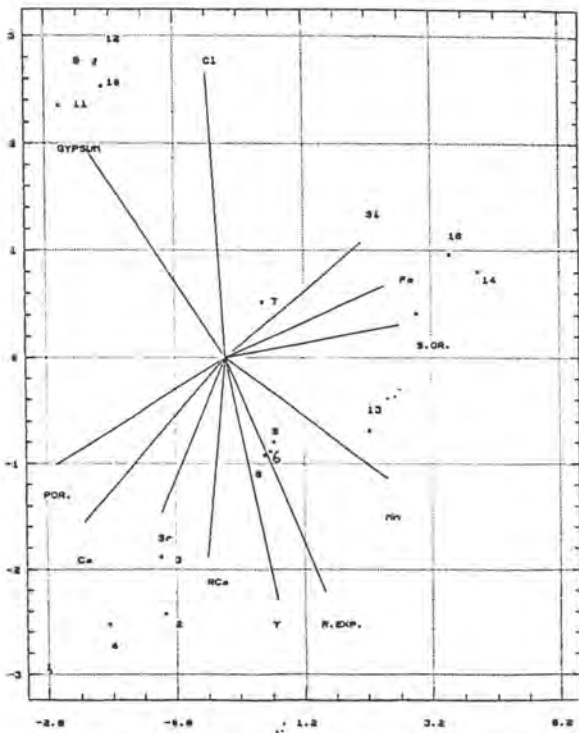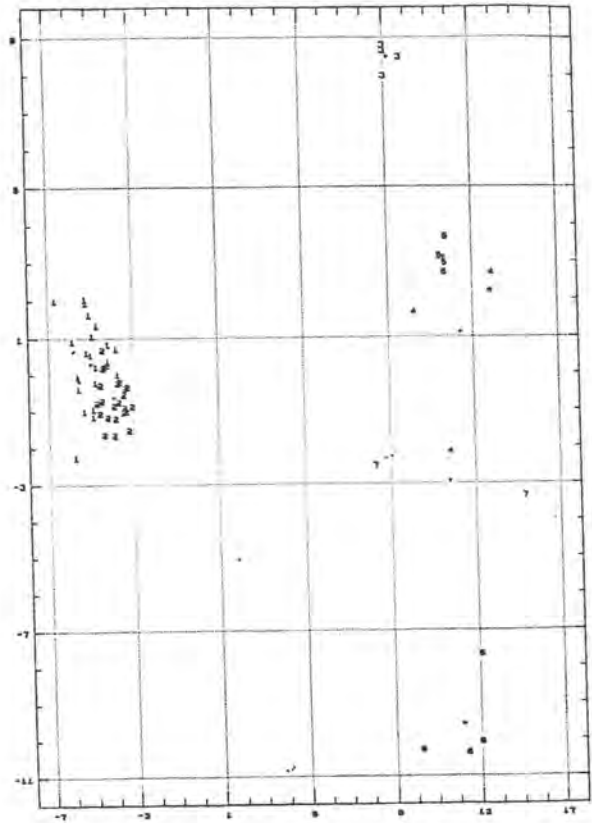*Fig. 2   Plot of discriminant function values*

Fig. 3   Scatterplot of principal analysis. Biplot of principal components analysis

Table 4 presents the generation of canonical functions. Two functions (number of groups – 1) have been obtained, allowing for discriminations among the seven groups. The ith discriminant function is of the form

$$D_i = d_{i1} Z_1 + d_{i2} Z_2 + ... d_{i6}Z_6 ,$$

where $Z_1, Z_2, ..., Z_6$ are standardized values of the original variables and the d_i are the standardized classification function coefficients. The unstandardized coefficients and the original variables can be used for the same purpose. The objective is to predict which group is most likely to fall into a new case or in other words to classify new observations. It is possible to classify a new case by evaluating each function, through the classification function coefficients, and assigning the case to the group corresponding to the highest function value.

Observations	1 – 23	Decay type 1
	24 – 46	Decay type 2
	47, 60–62	Decay type 3
	48, 50, 52, 57	Decay type 4
	49, 58, 59	Decay type 5
	51, 55, 63, 64	Decay type 6
	53, 54	Decay type 7

strongly correlated among them and with the "observations" 13, 14, 15, 16 related to cementitious crusts. This is explained by the C–S–A–F hydrated products detected by Laser Microprobe Mass Spectrometry (LMMS) [6], in the crusts characteristic of cement formations, therein called cementitious. This fact is in harmony with the strong correlation of the same variables and the large aerosols which due to the horizontal orientation of the exposed surfaces are preferential for large suspended particle depositions. To validate this observation fly ash was detected on the surfaces rich in Si, Fe etc.

"Y", "Mn" and "rain exposure" are strongly correlated among them and with the "observations" 5, 6, and 8 related to black gray crusts. This is explained by the nature of the crust [6] which is shielding amorphous depositions underneath a transparent layer of second-

II. Principal components analysis is employed by using as data vectors the variables : exposure to rain water, surface orientation, recrystallized calcite, gypsum, Si, Mn, Cl, Y, Fe, Sr, Ca, porosity (Table 4). The first components accounts for 41,53% of the total variability, while the next two components account for an additional 31,42%. For the first two components, almost 73% of the total variability (Table 5) is accounted for.

On the biplot (Fig.3) "gypsum" is strongly correlated with observations 9, 10, 11, 12 related to loose depositions. "Cl" is correlated through weaker. This is in agreement with other research results [6], where gypsum crystals are covering the black areas of loose depositions embedded by NaCl crystals from salt spray. "Si", "Fe" and "surface orientation" are

represent large aerosols
represent small aerosols
represent loose depositions
represent washed out – rusty yellow
represent black gray – gray yellow
represent cementitious crusts
represent dusts

ary recrystalliezed calcite, the rainwater percolation being the controlling factor. Observation 7 related to gray rusty yellow crust, very rich in Fe, is dispersed due to that correlation. High porosity "POR", concentrations of recrystallized calcite, presence of Sr and Ca, are strongly correlated among them and with the observations 1,2,3,4 related to washed out surfaces. The nature of this rather white, of yellowish crusts is that of a fractured recrystallized calcite embedded by suspended and penetrating particles [6]. It appears mainly on surfaces directly exposed to rainfall. Observations are characteristically classified according to the crust types : washed out – decay type 1, black gray – rusty yellow crust – decay type 2, loose deposition – decay type 3, cementitious – decay type 4. Discriminant analysis gives a good separation of the various crusts and permits to classify new data.

5. Conclusions

A general classification of environmental air–borne particles and marble neoformations discriminates for large and small aerosols, dusts and various crusts. Airborne particles are discriminated to the accumulated depositions in dusts and moreover the reacted ones in the surface encrustations. Variables like Si, S, Cl, K, Ca, Cr, Mn, Fe, Ni, Cu, Zn, Br, Sr, Pb play a significant role in that discrimination. Heavy metals discriminate for the accumulated depositions or neoformations but are not sufficiently to provide sub–classifications of the various crusts.

"Gypsum" is strongly related to loose depositions. "Cl" is correlated through weaker. "Si", "Fe" and "surface orientation" are strongly correlated among them and are related to cementitious crusts."Y", "Mn" and "rain exposure" are strongly correlated among them related to black gray crusts. Observation 7 related to gray rusty yellow crust, very rich in Fe, is dispersed due to that correlation. High porosity "POR", concentrations of recrystallized calcite, presence of Sr and Ca, are strongly correlated among them and related to washed out surfaces.

It is possible to classify a new case by evaluating each function, through the classification function coefficients and assigning the case to the group corresponding to the highest function value. This classification is validated by the chemical analysis and the in situ study as well.

Finally multivariate analysis may provide the basis for the management f environmental factors for the preservation of large archaeological sites.

Acknowledgments

References

1. Preka –Alexandri K. Eleusis. Ministry of Culture. Archaeological Receipts Fund. Athens, 1991.

2. Zezza, F., Marine spray and polluted atmosphere as factors of damage to monuments in the Mediterranean coastal environment, 3rd Int. Symp. on the Conservation of Minuments in the Mediterranean Basin, ed. by V. Fassina, H. Ott and F. Zezza, Publ. Soprintendenza ai Beni Artistici e Storici di Venezia, pp. 269 – 274, 1994.

3. Abazoglou, G., Christidis, A., Mourikis, D.: The dust fall at the Thriasian plain, Panhey of Chemical Engineers, 7/8, March/April, 1990.

4. A. Moropoulou, K. Bisbikou, B. Christaras, A. Kassoli-Fournaraki, N. Souros, Th.Makedon, B. Fitzner, K. Heinrichs : Examination of the weathering susceptibility of the building stones of Demeter Sanctuary in Eleusis, I: Origin, Petrography, and Physical, Mechanical and Microstructural Properties, Bollettino Geofisico, anno 18, N.1, pp. 37–48, 1995.

5. A. Moropoulou, K. Bisbikou, Environmental monitoring and damage assessment at the ancient Sanctuary of Eleusis, Greece, Materials Issues in Art and Archaeology IV, ed. By J.R. Druzik & P.B. Vandiver, Mat. Res. Soc. Symp. Proc., Vol.352, pp. 745 – 757, 1995.

6. A. Moropoulou, K. Bisbikou, R. Van Grieken, K. Torfs, F. Zezza, F. Macri : Origin and growth of deteriorating crusts on ancient marbles in industrial atmosphere, Atmospheric Environment, in press, 1996.

7. B. Fitzner, K. Heinrichs, Final CUM GI – RTA Report.

8. Unpublished results : PhD Cand. K. Bisbikou.

9. T. W. Anderson, An introduction to Multivariate Statistical nalysis, Wiley, New York, 1958.

10. B. W. Bolch and C. J. Huang, Multivariate Statistical Methods for Business and Economics, Prentice – Hall, Englewood Cliffs, New Jersey, 1974.

11. A. Moropoulou, P. Theoulakis, T. Chrysophakis, Correlation between stone weathering and environmental factors in marine atmosphere, Amospheric Environment, Vol.29, No.8, pp. 895–903, 1995.

12. V. Fassina, M. Rossetti, M. Oddone, S. Mazzochini & S. Calogero, Marine spray and polluted atmosphere as factors of damage to monuments in the Mediterranean coastal environment. An analytical study of some samples from the Sanctuary of Demeter in Eleusis (Athens), 3rd Int. Symp. on the Conservation of Minuments in the Mediterranean Basin, ed. by V. Fassina, H. Ott and F. Zezza, Publ. Soprintendenza ai Beni Artistici e Storici di Venezia, 287–294, 1994.

13. F. Buzek, J. Sramek, Sulfur isotopes in the study of stone monument conservation, Studies in Conservation, 30, pp. 171–176, 1985.

Ioana Neagoe
Cornelia Berindan

Types of chemical and biochemical degradation found as developed at Histria Fortress – Romania

Types of chemical and biochemical degradation found as developed at Histria Fortress – Romania

I. Neagoe, C. Berindan
Technical University Cluj–Napoca,
Str. C. Daicoviciu, Nr. 15, 3400
Cluj–Napoca, Romania

1. Introduction

Ancient Histria settlement is situated in the south–east of Romania, in a region nominated as Dobrogea. It is a very particular region concerning its deposits of limestones uniques in our country. It is an open territory which at the moment of the monument construction was lied by the Sea with the rest of the world. This is the reason which conducted to the building of a fortress by the romans made from the building material existent at the site.

From the chemical point of view, the evolution of these building materials among the years is very interesting presenting some specific damages we cannot find in another places. The atmospheric composition, winds all over the year, repeated frozen, marine salts and geographical orientation lead to the damages and degradation of the monument.

2. Material and methods

Eight samples were prelevated from the limestones found at the site of Histria which were analytical analyzed using the spectrophotometry of atomic absorbtion. These samples were taken in the first campaign – in spring 1995. These are chosen from the Great Wall, the exterior and interior part of the wall and also from the little gate. The results were confirmed by chemical analysis using the classic methods.

For the types and categories of degradation we take in consideration 148 pieces which were measured, verified and notated concerning their dimensions, chemical modification, salts, position in the wall and position of the wall. Also for the biofilm analysis we used the microscopic observation and biochemical characterization of it.

3. Results and discussions

At this monument we studied several damages appeared on the Great Roman Wall it's exterior side and the inside of the complex (interior wall) (Fig.1).

A part of the original building stones were replaced with stones from the same mineralogic category but new, and they were put on the original wall which conserved the whole modification due to marine salts, winds and repeated frozen during the centuries.

Because of the geographical orientation of the Great Wall which has an irregular highness between 2,5 – 4 m., the majority of aggressive damages appeared in the interior part of it, the exterior side is better conserved due to the protection offered.

The most usual categories of damage on the interior part of the wall are granular desintegration and loss of stone material (Fig.2, Fig.3).

All parts of the wall unprotected with new building stone, are characterized by the massive existence of the biological deposits and crusts (Fig.4, Fig.5). These deposits can be seen also on the new stones used at the restauration in 1954, fact the demonstrates the high level of humidity in the atmosphere and the salts concentration coming from the Sea Coast, easy to be found few km from Histria.

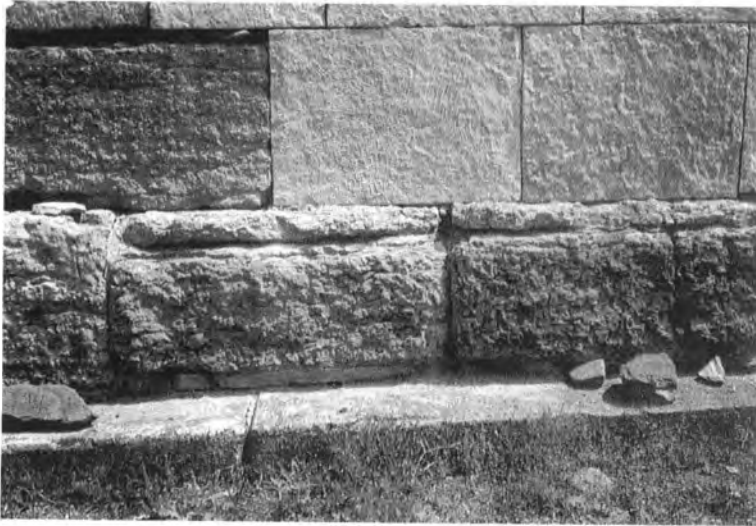Characteristic for this open zone which

Fig. 1   Damage and deterioration of the stone.

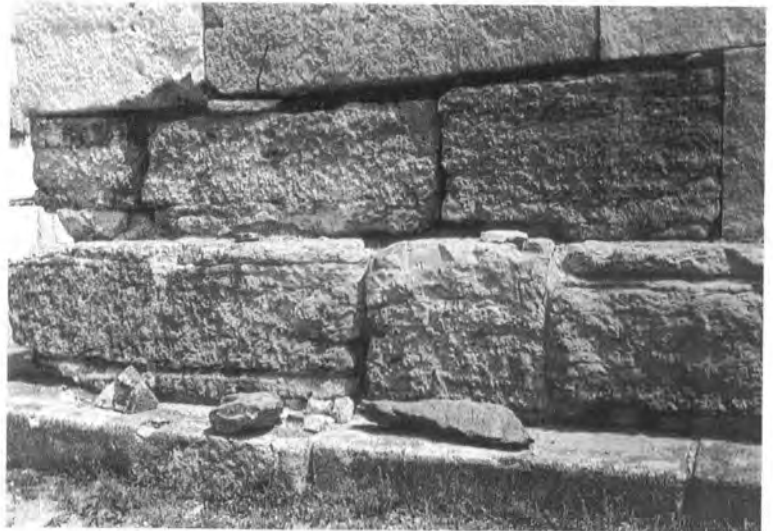Fig. 2   Damage and deterioration of the stone

Fig. 3   Damage and deterioration of the stone

Fig. 4 Damage and deterioration of the stone

Fig. 5 Damage and deterioration of the stone

present a rich vegetation at the level, are the degradations due to biological deposits, crusts on the majority of stones as well as loss of stone material, alveolar weathering, and crumbling.

At 80% from the building stones in the complex we find as modified their surface because of the atmosphere with a high level of marine salts and repeated winds and frozen a long part of the year. So we found the alveolar weathering up to 100–150 mm in the interior side of the wall with orientation to Sinoe Lake and Black Sea. The same aggressive degradation we can observe on the interior side of the wall, can be nominated in the whole complex (Fig.6, Fig.7).

Fig. 6 Damage and deterioration of the stone

Fig. 7 Damage and deterioration of the stone

The usual depth of alveoles is (50 mm up to 90 mm. We consider this category of degradation as the most violent, the percentage of it being about 20–21% (Table 1, Table 2).

From the totality of pieces taken in account which forms the architectural complex, 85% present visible modifications – specially granular desintegration, crumbling, loss of stone material, biological deposits and crusts. Also the stones counted from the exterior wall presents weathering alveolaes constantly at the level of 10–20 mm. In the interior wall we can find stones like those in Fig.7 where the loss of material is repeated and in big quantities.

Fig.8 presents a cumulum of damages observed like: biological deposits, outbursts, garnular desintegration, loss os stone material.

Tables 1 and 2 offer an image in procents of the stones affected in the interior wall, with

Table 1
Great Wall - lower part 60 stone (18 upper part)
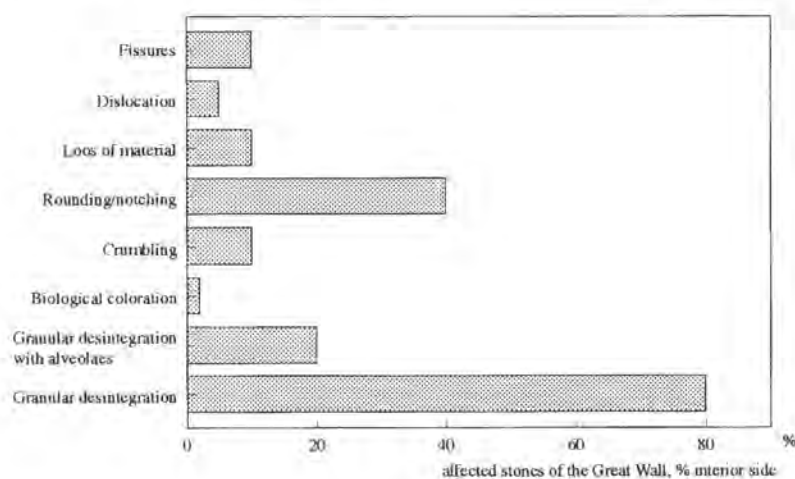*Quantitative evaluation of weathering forms*

affected stones of the Great Wall, % interior side

Table 2
Great Wall – middle part 70 (18 upper part)
Quantitative evaluation of weathering form

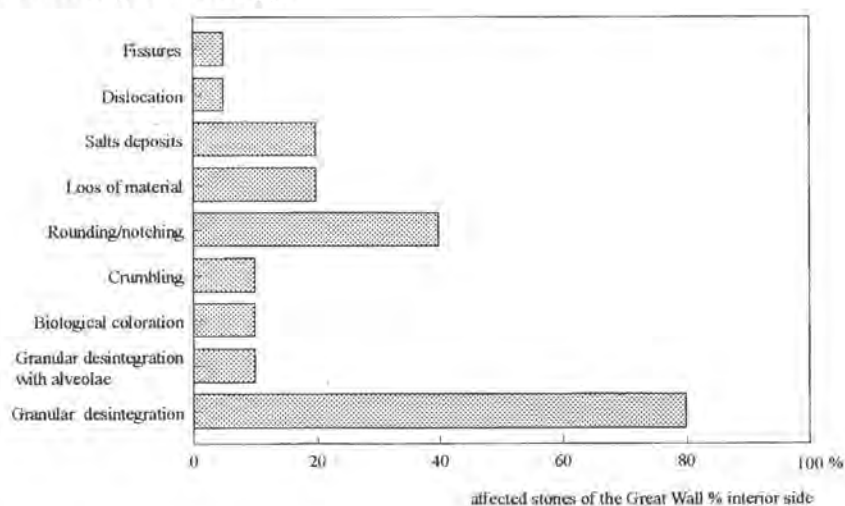affected stones of the Great Wall % interior side

Fig. 8 Damage and deterioration of the stone

respect to the high where they are found (level I – II).

Because of the existence between the Black Sea and Histria fortress of the Sinoe Lake which is made from an enclosure of the sea, we cannot atribute the totality of degradations and damages exclusively to the Black Sea. This situation is with respect to salts deposits we can found in the interior of the complex, specially in the region of the little gate of the great wall. The gate is situated at the same part of construction at the openning to Sinoe Lake. Here we founded more salts deposits than somewhere else in the ancient settlement. The quantitative evaluation we can take into account is dependent of the clear separation of the Black Sea effects and Sinoe Lake. At the moments of samples prelevation we could not do that separation. It remains a problem to be solved.

Even if the purpose of our study was the Great Roman Wall from chemical and biochemical point of vue, we used as a unit for general degradation a column found in the middle of the interior teritory (Fig.9). This one was all time (hundreds of years) under the atmospheric components action and suffered such important damages on it's stone structure, so any sample prelevation can due to it's final existence.

We put toghether the geographical position of the sea and the lake, of the stones which make the wall, and also their position on verticale – just to realise a general scale from very slight damages (1) up to very severe damages (Table 3). The main damage we can found is the granular disintegration which affect around 80% of the stones in the interior wall, biological deposits and crusts. In a less agressive measure we found marine salts deposits and loss of the stone material in the common points (20–40%).

Fissures and back weathering are noncharacteristic fenomenon, with a sporadic appearance.

The exterior part of the Great Wall which is protected by direct action of the sea and salt lake is less damage than the interior part (arround 25% from it). There we can found biological deposits in great procentage, granular desintegration (~ 10%), few alveolar weathering with salts deposits (> 10%). The biofilm has good conditions to develop as well as the crusts, because of the protection of the wall in front of winds, and marine salts.

From the chemical analysis we can see that the amount of NaCl, the water absorbtion and Fe_2O_3 contain is different from the national

Fig. 9 Damage and deterioration of the stone

Table 3
Histria monument
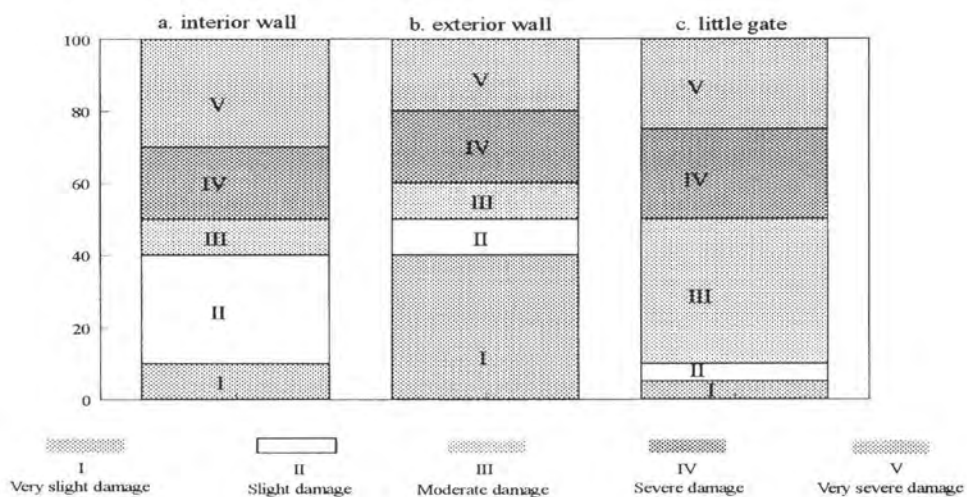*Evaluation of damage categories (148 stones)*

I	II	III	IV	V
Very slight damage	Slight damage	Moderate damage	Severe damage	Very severe damage

Table 4

Histria monument

Quantitative evaluation of chemical composition/standard (%)

	Sample 1 Stand	Sample 1 Found	Sample 2 Stand	Sample 2 Found	Sample 3 Stand	Sample 3 Found	Sample 4 Stand	Sample 4 Found	Sample 5 Stand	Sample 5 Found	Sample 6 Stand	Sample 6 Found	Sample 7 Stand	Sample 7 Found	Sample 8 Stand	Sample 8 Found
Moisture level	1,95	2,81	2,8	2,81	-	3		6,06	no	11,02	6	11	14	10,1		14,97
Loss by calcin.	3,20	3,28	10	12,6		3,37		35,11	standard	41,86	18,20	32,72	10	13,44		2,38
Scale MOH	3	3	4	4		3	2	2	found	3	2	2	2	2		3
Al$_2$O$_3$	18-20	18,34	3	2,41		15,75	>0,1	0,9	because of	0,97	1-1,5	1,37	3-3,5	3,45		2,38
TiO$_2$	0,4-0,5	0,79	0,9	0,14		0,9	>0,1	0,05	fossil	0,05	1,3	1,37	<0,1	0,22		0,15
Fe$_2$O$_3$	7-7,4	4,37	0,5	0,66		6,91	>0,1	0,16	comp.	0,21	<0,1	0,07	0,1-0,4	1,1		0,86
SiO$_2$	62-68	63,49	60-65	65,63		63,75	10-12	15,84		4,10	0,1-0,4	0,36	60-62	63,23		91,37
CaO	1,5	1,94	15	15,46		1,58	50	45,72		51,5	20-20,5	20,7	18-18,5	16,4		,49
MgO	1,1	1,76	0,5	0,89		2,74	>0,1	0,58		0,56	50	42,69	0,5-0,7	0,76		0,54
Na$_2$O	1-1,05	1,02	0,3	0,38		1,45	>0,1	0,24		0,21	>0,1	0,87	0,1-0,4	0,44		0,40
K$_2$O	2-3	4,73	1	1,30		3,38	>0,5	0,46		0,33	>0,1	0,48	1	0,95		0,73
Density (g/cm^3)										2,06	1-1,2	1,98	1,5	2,05		
Porosity (%)										22,7	20	21,77	15	20,7		

1. *Ferroginous schist – reddish – violet colour (intercalation between green schists)*

2. *Detritic limestone – calcarenite – turonian lower senonian*

3. *Unsufficient material*

4. *Microconglomerate – vacuolar aspect – cenomanian/samarian*

5. *Compact limestone with fossil components*

6. *Detritic limestone – calcarenite white – yellowish turonian*

7. *Calcarenite (weak statification – porosity) (braun–yellowish colour)*

8. *Lithic sandstone (very porous)*

Table 5

Histria monument. Analysis of different decay forms of weathering present on the eight samples chemical analyzed.

1. Ferroginous schist – reddish – violet colour (intercalation between green schists)

     – exfoliation, loss of stone material – 35%

2. Detritic limestone – calcarenite – turonian lower senonian

     – granular disintegration, alveolaes with marine salts – 85%

3. Unsufficient material

4. Microconglomerate – vacuolar aspect – cenomanian/sarmatian

     – alveolar aspect, granular disintegration, disscolour – 85%

5. Compact limestone with fossil components

     – biological deposits, black crusts – 45%

6. Detritic limestone – calcarenite white – yellowish turonian

     – black crusts, exfoliations, crumbling – 25%

7. Calcarenite (weak statification – porosity) (braun–yellowish colour)

     – granular disintegration – 80%

8. Lithic sandstone (very porous)

     – loss of stone material, crumbling – 50%

standard of these Dobrogea limestones (Table 4). The samples we prelevated are from the most founded limestone in complex construction, and from a level accesible which did not affect the wall.

As a general view of the damages and deteriorations caused by the effects of the sea, we concentrated the data we had in the Table 5.

As we already established the most affected areas are the lower and middle part of the wall and less the superior part where it is higher than 2 m. Also we most specify that a lot of ancient stones from this upper part were changed with new building stones. The most damaged part of the wall is the interior part specially the region found in the vicinity of the sea and salt lake.

4. Conclusions

1. *At ancient Histria settlement build by the romans, we can found limestones, marbles and siliceous stones used as building material. Each of these types of stones are characterized by a different average of deterioration and damage function of their localisation in the wall (vertical and horizontal) and of their chemical and mineralogical composition.*

2. *The order of procentage from high to low on the damage is:*

    a) *granular desintegration with alveolaes due to marine salts deposits;*

    b) *biological deposits made from: algae, fungi, marine parasits, bacteriae;*

c) *crusts from dust and soot;*

d) *outbursts – loss of compact stone fragments;*

e) *disscoloration – modification of the original colour of the stone.*

3. *The most affected stones in the Great Wall are those with a south orientation, in front of the Sinoe Lake and the whole interior side of the wall. The exterior side of the wall is less affected by chemical modifications.*

4. *Because of the sea coast winds which are very agressive eight months/year, the first and second levels (lower and middle) are the most damaged, those stones being used as a barrier in front of . The upper stones even when they were not replaced are less damaged.*

5. *In these regions of the wall unprotected by new building stone, and which are under a high of 2 m, we found the original stones covered, sometimes entierly by biological deposits.*

6. *We used as classification criteria for the intensity of degradations, the frequency and dimension.*

7. *A fenomenon which characterise other degradations on monuments: bach weathering, we found here quite rarely, only on a few types of limestones and in the most far point of the wall from the openning of the sea and salt lake.*

8. *We think that the high procentage of granular desintegration (> 80%), corelated with flakes appearance is a great part due to repeated frozen (– 20° C) which is more agressive on the interior side of the wall (direct action).*

9. *Iron and manganese crusts appers often in the vicinity of salts deposits and alveolaes. Those stones never presents black crusts or biological film or deposits due to the chemical surface composition which do not permit their adherence.*

10. *We used a general clessification of damage forms and deteriorations function of weathering form and place in the monument.*

5. Acknowledgements

6. References

1. Fitzner, B. and Kownatzki, R. – Bauwerkskartierung – Schadensaufnahme an Naturwerksteinen. Der Freiberufliche Restaurator, Vol. 4, Kiel, 1990, pp.25–40.

2. Fitzner, B. – Mapping of natural stone monuments – Documentation of lithotypes and weathering forms. Advanced Workshop "Analytical Methodologies for the Investigation of Damaged Stones", Pavia, Italy, 1990, 24 p.

3. Fitzner, B. and Kownatzki, R. – Studies on natural stone monuments – Methodology and examples. Science, technology and European cultural heritage: Proceedings of the European symposium, Bologna, Italy, 13–16 June 1989, Butterworth–Heinemann, Oxford, 1991, pp.930–934.

4. Fitzner, B. and Lehners, L. – Rhenish tuff – A widespread, weathering susceptible natural stone. Proceedings 6th International Congress IAEG, Amsterdam, Netherlands, 6–10 august 1990, A.A.Balkema, Rotterdam, 1990, pp.3181–3188.

5. Chemical analysis of stones, Bucuresti, E.D.P., 1981.

6. Cordos, E. – Spectrophotometry of atomic absorbtion, Cluj, 1984.

Simonetta Previtero

The replacement of the medieval blocks of limestone in the masonry of Bari Cathedral. A propaedeutic research for the study of the decay development in the time

The replacement of the medieval blocks of limestone in the masonry of Bari Cathedral. A propaedeutic research for the study of the decay development in the time

S. Previtero

Dipartimento di Scienze, Storia dell'Architettura e Restauro,
Facoltà di Architettura, Università di Pescara, Italy

The metrological study of the masonry of Bari Cathedral and the confrontation with the dimension of the plan, confirm dott. P. Belli D'Elia's thesis[1], according to that the present cathedral, built by the bishop Bisanzio and his successors from 1171 to 1267, includes the remains of a more ancient cathedral, whose mosaic flooring is still, in part, in a good state. The dimensions of the plan of the present cathedral, in fact, are multiple of the byzantine foot[2], while the masonry module is multiple of the longobard palm[3]. Probably the new cathedral was built by longobard skilled workers, overworking the existing foundations. We can also put forward the hypothesis that an architect *(magister latomus)* of byzantine culture and gem–cutters of longobard culture have contribute to its construction, and that the *"appareilleur"*, superintending the work, has been the mediator between the two cultures.

For a more detailed account about the history of the transformation of St. Sabino's church, I refer to the books mentioned in the bibliography.

It is important, however, to mention the opening, in the XVIth century, of the side chapels, obtained demolishing the masonry between the buttresses and rebuilding them in line with the outer side of the buttresses. We remind, then, that in the XVIII century these chapels were closed and the church was restored and adapted to the new taste, according to D.A. Vaccaro's project[4]. The masonry inside were ravaged by the strokes of the pick, to consent the adhesion of the stuccoes. The blocks that show the traces of the pick, laid upon the more ancient finishing touch of the gradine, are surely original.

The North bell tower of the cathedral collapsed in 1259 and it was ribuilt in 1315. It was struck by lightning in 1750, and then it was repaired. In 1773 it was struck by lightning another time and collapsing it damaged the organ. It was restored using blocks of *"tufo scorzo"* coming from a quarry called Madonna dell'Arena, and from S. Scolastica[5]. Damaged by lightnings in 1848 and in 1869, it was shored up. Now it has a reinforced concrete structure and the walling cores are in concrete, too.

The presumed restoration of the original "facies" of the cathedral started in 1902 and lasted about forty years, as you can see in the following plates. It has not been possible to ulteriorly detail the restoration phases, owing to the impossibility to examine the documents in the "Soprintendenza ai BB.AA.AA.AA di Puglia".

Many of the analyzed samples have been drawed from the dome (XIII century). So I'll describe the restoration of this part. The work began in 1902, according to arch. Bernich's project[6]. We learn from him that the blocks of

[1] P. Belli D'Elia: La Cattedrale di Bari, in "Alle sorgenti del Romanico. Puglia XI secolo", Bari, 1975.

[2] cm. 31,5

[3] cm. 21,5–21,8

[4] The works of marble was made by C. Tucci, the stuccoes by G. De Grecis.

[5] Archivio del Capitolo della Cattedrale di Bari, Serie Speciale: *"Esito portato dal canonico Don Vito Nicola Episcopo, d'Ordine di Sua Eccellenza Don Adelmo Pignatelli Arciv. di Bari, per il danno che cagionò un fulmine che cascò sopra del campanile dentro la notte del 18 aprile 1773 (...)"*. Cfr. payment in 1773 on May 1st and 3rd and in 1777.

[6] E. Bernich: *L'Arte in Puglia. La cupola del Duomo di Bari,* in "Napoli Nobilissima", vol.II, Napoli, 1903.

the dome appeared to the restorers "whiped" by the strokes of the pick, and that the windows had been enlarged.

However, the limestone material that formed the medieval blind arcades had been used as building material, and a lot of it to fill the empty of the eight niches.So the architect and the restorers started the identification of the single pieces of limestone and a kind of "anastilosi", as they can do, sticking the fragments with Mayer adhesive[7]. They reconstituted the drip–stone with blind arcades on corbels that turns around the dome, upon the niches, and they strenghtened the concave pendentives of connection.The reintegration of the incomplete parts was done by smooth surfaces. Then it was applied a thin layer of plaster all over the surface of the dome[8]. The restoration stopped in 1905. Other works were done in 1915[9].

As regards the outside masonry, we can see a lot of funeral inscriptions, whose date is the "terminus ante quem" these blocks of limestone were set running. The inscriptions followed the construction of this cathedral: we deduce this abserving that the epitaphs develop on more than one flanked blocks. A lot of inscriptions have a merely Gothic type, while one inscription on the west side of the South arm of the transept has characters attribuitable to the early Middle age. So we can say that the blocks on which this inscription is engraved were alredy there in that age.

This is a little contribute to the study of this precious monument, and I hope it will be useful for its preservation.

---

[7] P. Nencha: *Il restauro del cupolino nella cattedrale di Bari*, in "Rassegna tecnica pugliese", marzo 1905.

[8] Archivio del Capitolo della Cattedrale di Bari; serie Restauri Catt. fasc.0015 P, *"Progetto di lavori da eseguirsi sulla cupola della cattedrale di Bari. Napoli, addì 14 maggio 1902. Progetto Arch. E. Bernich, Direzione Arch. A. Avena;*

  1) *Spicconatura sull'estradosso della cupola riparandovi le lesioni, rifacendovi l'intonaco di coccio pesto della grossezza non minore di m.0,05 composto di frantumi di laterizi e malta fina con pozzolana, compreso il rivestimento di calce liquida unita a pozzolana vagliata e stucco finissimo (...)*

  2) *Scrostatura di lavori di stucco nell'intradosso della cupola e spicconatura di tutto l'intonaco. Parte cilindrica + parte sferica mq.398,69.(...)*

  3) *Rincocciatura saltuaria della superficie dell'intradosso e sulla parete cilindrica del tamburo per uguagliarsi tutte le parti mancanti sia prodotte da antichi buchi per anditi, sia per il paramento visto deturpato da perni ed appresature degli ornati di stucco e dalle abbrasature della cornice in pietra demolita (...)*

  4) *Arricciatura con malta vulcanica occorrente per potersi eseguire il rivestimento d'intonachi.*
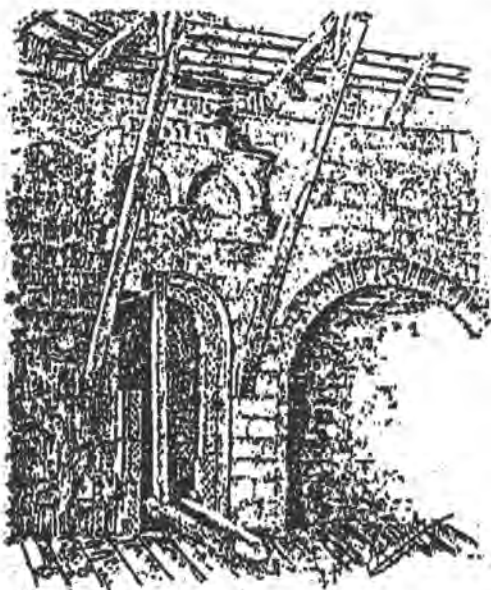
  5) *Intonaco sottile su tutta la superficie (mq.398,69).*

  6) *Dipintura a colla a tre passate sotto la cupola (...)*

[9] Archivio del Capitolo della Cattedrale di Bari, busta Restauri, fasc. 0024 P, anno 1915, (payment of £.8364,25 to the bidder Nacca and of 450 to his assistant Pantaleo).
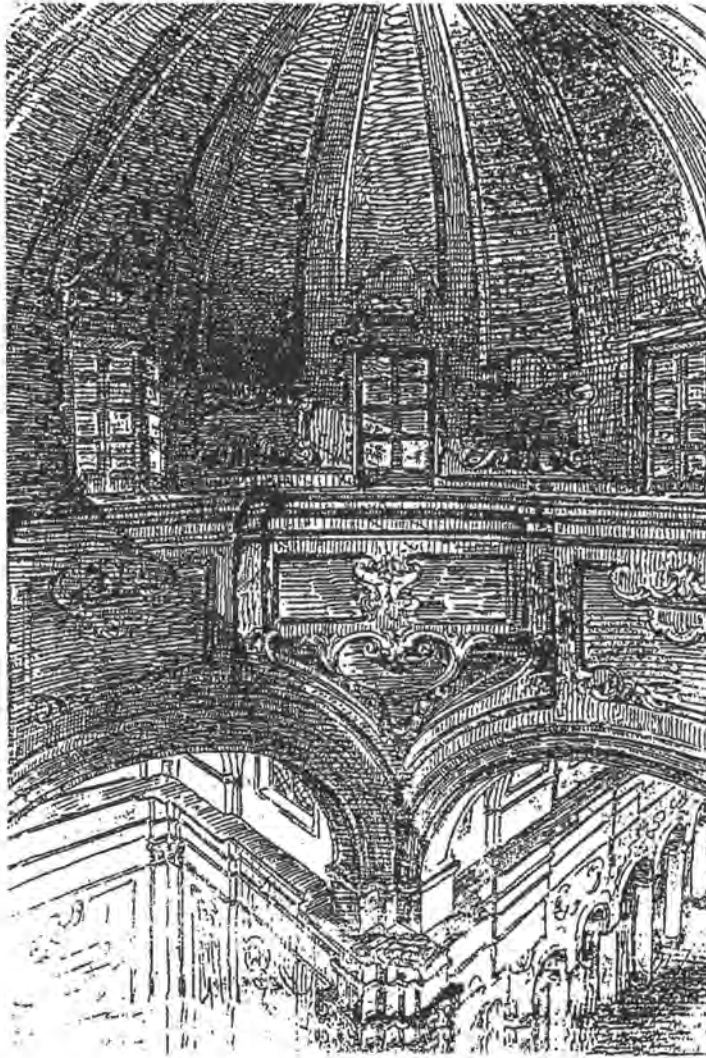
The dome in the XVIII century.

(from M. Pasculli Ferrara and E. Bernich)

In the XVIII century the intrados of the dome was decorated with stucco. Subsequently the surfaces of medievall ashlars were chiselled, the blind arcades were destroyed and the stone material was used to occlude the niches in the drum.
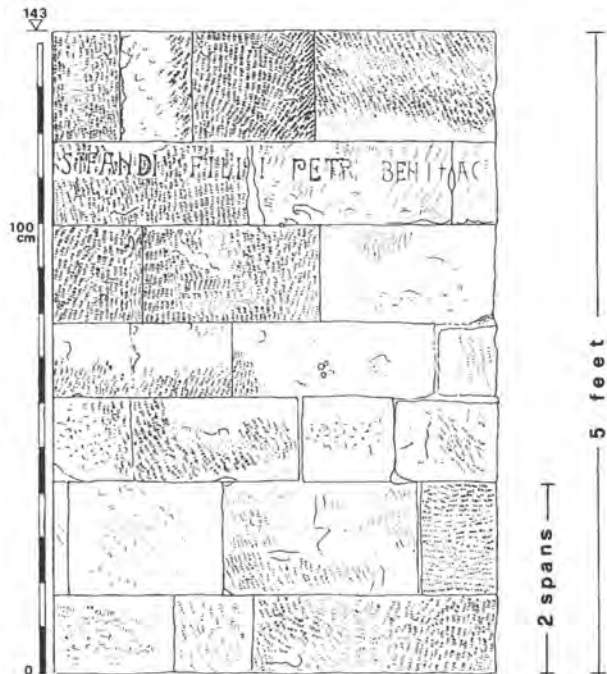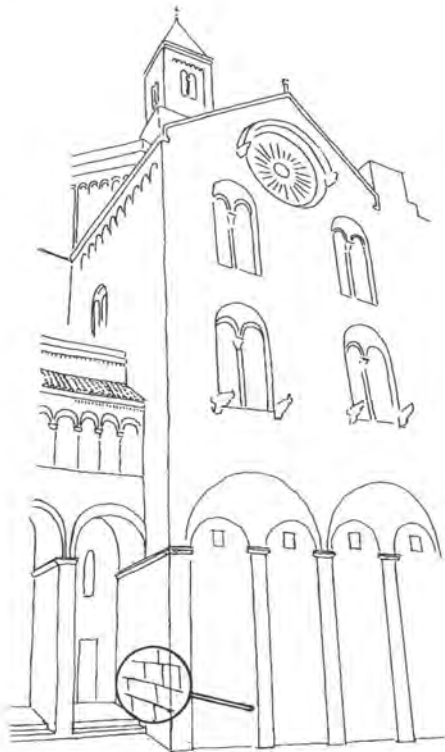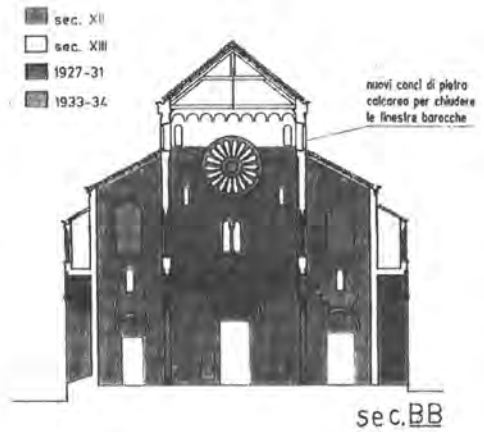
From the 1902 to the 1905 the architect Bernich restored the dome.

He removed the stucco thick cm.17, used the stone material that was in the niches to re-build the blind arcades and replaced some ruined blocks of limestone. Then they applied a thin layer of plaster all over the intrados of the dome.
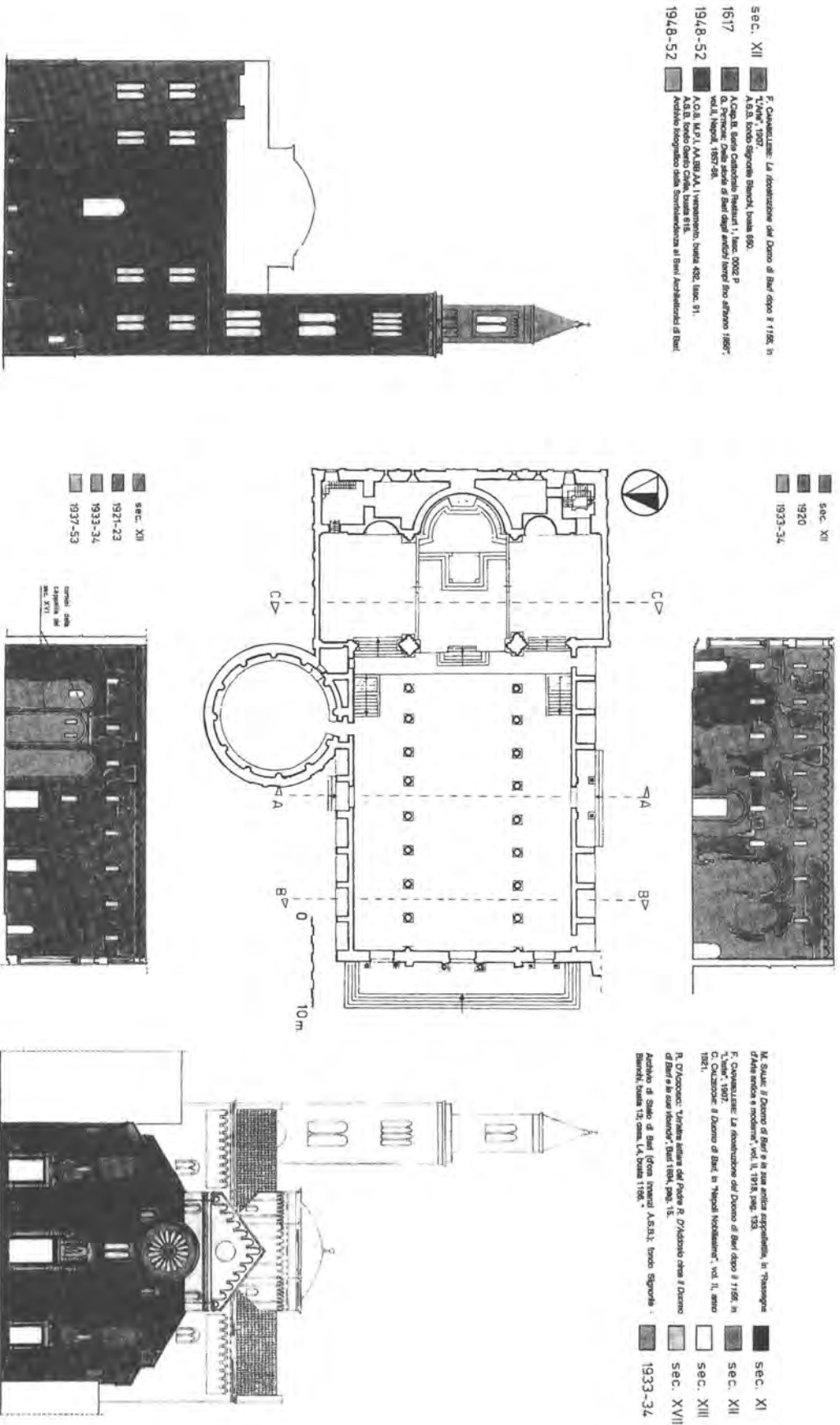
Now we can find traces of "scialbo" on the surface of some ashlars.
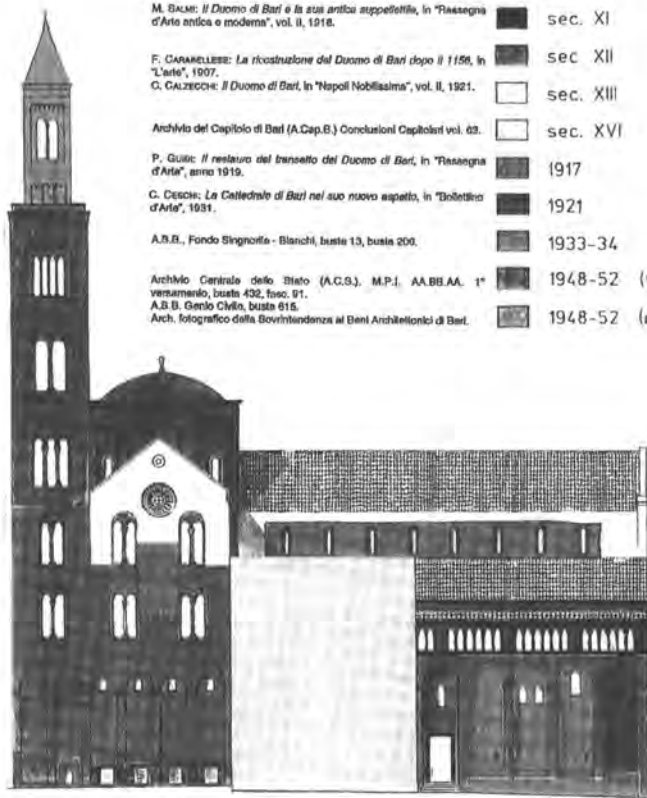
M. SALMI: *Il Duomo di Bari e la sua antica suppellettile*, in "Rassegna d'Arte antica e moderna", vol. II, 1918. — sec. XI

F. CARABELLESE: *La ricostruzione del Duomo di Bari dopo il 1156*, in "L'arte", 1907. — sec XII

C. CALZECCHI: *Il Duomo di Bari*, in "Napoli Nobilissima", vol. II, 1921. — sec. XIII

Archivio del Capitolo di Bari (A.Cap.B.) Conclusioni Capitolari vol. 62. — sec. XVI

P. GUIDI: *Il restauro del transetto del Duomo di Bari*, in "Rassegna d'Arte", anno 1919. — 1917

C. CECCHI: *La Cattedrale di Bari nel suo nuovo aspetto*, in "Bollettino d'Arte", 1931. — 1921

A.S.B., Fondo Signorile - Bianchi, buste 13, busta 200. — 1933-34

Archivio Centrale dello Stato (A.C.S.). M.P.I. AA.BB.AA. 1° versamento, busta 432, fasc. 91.
A.B.B. Genio Civile, busta 615.
Arch. fotografico della Soprintendenza ai Beni Architettonici di Bari. — 1948-52 (vecchi conci) — 1948-52 (nuovi conci)

sec. XII
sec. XIII
1927-31
1933-34

nuovi conci di pietra calcarea per chiudere le finestre barocche

sec. BB

143

100 cm

STEANDI FILII PETR BENIFAC

5 feet
2 spans

The module of the masonry is multilple of the Longobard foot.
In this region, called "Terra di Bari", Longobard traditions and laws were preserved for a long time, also during the Byzantine and the Norman rule.

The replacement of the medieval blocks of limestone in the masonry of Bari Cathedral. A propaedeutic research for the study of the decay development in the time

sec. XII
1920
1933-34

sec. XII — F. Cavallese: *La ricostruzione del Duomo di Bari dopo il 1156*, in "L'Arte", 1907.
1617 — A.S.B. fondo Signorile Bianchi, busta 560.
1948-52 — A.Cap.B. Salvo Collectotis Restauri 1, fasc. 0002 P
G. Petroni: *Della storia di Bari degli antichi tempi fino all'anno 1860*, vol.I, Napoli, 1857-58.
1948-52 — A.C.B. M.P.I.-A.A.BB.AA. I versamento, busta 492, fasc. 91.
A.S.B. fondo Gado Civile, busta 615.
Archivio fotografico della Soprintendenza ai Beni Architettonici di Bari.

sec. XII
1921-23
1933-34
1937-53

cornici della cappella del sec. XVI

sec. XI
sec. XII
sec. XIII
sec. XVII
1933-34

M. Sauar: *Il Duomo di Bari in sua antica suppellettile*, in "Rassegna d'Arte antica e moderna", vol. II, 1915, pag. 153
F. Cavallese: *La ricostruzione del Duomo di Bari dopo il 1156*, in "L'Arte", 1907.
C. Calzecchi: *Il Duomo di Bari*, in "Napoli Nocessione", vol. II, anno 1921.
R. D'Addosio: "L'infinita attività del Padre R. D'Addosio circa il Duomo di Bari e le sue relazioni", Bari 1664, pag. 15.
Archivio di Stato di Bari (fondo interno) A.S.B.I.: fondo Signorile Bianchi, busta 13; cass. I.4, busta 1166.

0 _____ 10m

Bibliography

1. LOMBARDI: *"Compendio cronologico delle vite degli Arcivescovi baresi"*, Napoli, 1697.

2. A. AVENA: *"Monumenti dell'Italia Meridionale"*, Roma, 1902.

3. F. CARABELLESE: *La ricostruzione del Duomo di Bari dopo il 1156*, in "L'Arte", 1907.

4. C. CALZECCHI: *Il Duomo di Bari*, in "Napoli Nobilissima", vol. II, 1921.

5. C. CESCHI: *La cattedrale di Bari nel suo nuovo aspetto*, in "Bollettino d'Arte", 1935.

6. N. LAVERMICOCCA: *Nuove osservazioni sulla Cattedrale di Bari*, in "Studi di Storia Pugliese", Galatina, 1971.

7. AA.VV.: *"Alle sorgenti del Romanico. Puglia XI secolo"*, Bari, 1975.

8. N. MILANO: *"Le chiese della Diocesi di Bari. Note storiche e artistiche"*, Bari, 1982.

9. P. BELLI D'ELIA: *"La Puglia"*, volume VIII di "Italia Romanica", Milano, 1986.

10. M. PASCULLI FERRARA: *"Domenico Antonio Vaccaro. Interventi Settecenteschi nella Cattedrale di Bari"*, Bari, 1986

R. Prickartz

Techniques and technologies for conservation measures at historic monuments

Techniques and technologies for conservation measures at historic monuments

R. Prickartz
Techische Hochschule Aachen Institut fur Baumaschinen und Baubetrieb Mies–van–der– Rohe–StraBe 1, 52074 Aachen – Germany

1. Introduction

Since 1986 the ibb deals with the development of technologies and techniques for the restoration and preservation of historic monuments in the course of a joint research project.

2. Survey

The aim of the mentioned project is to elaborate methods of treatment for cultural heritage monuments. The task is to develop materials and techniques which help to stop the decay of historic monuments, especially those made of natural stone. Natural scientists explore the decay mechanisms of natural stone, building material scientists develop new materials (such as mortars or stone preservation materials) and the ibb develops new techniques and devices for:

a) *eaning natural stone facades,*

b) *clearing of mortar joints and*

c) *application of stone preservatives.*

The ibb is charged to improve existing or to create new techniques so that their use does not cause further damage to the original substance and leads to a maximum quality result. The result of our research are the following devices:

3. Particle blasting technique for the cleaning of natural stone facades

The machine uses a dry compressed air technique to blast fine-grained glass beads on the stone surface. The operator can regulate the blasting energy without any time lag at the nozzle. The blasting particles are recycled by realizing a material flow system within the machine. The device is fabricated and sold by a company.

4. The Fugomat, a device for the removal of jointing mortar

The tool is a high speed water jet which is guided across the masonry by a xy–device hanging at the scaffolding. The water jet is controlled by joysticks. A clearing depth of about 10 cm can be achieved without damaging the stone even if the joints are very small. As an alternative or a completion to the water jet a small milling cutter can be installed. The fugomat is fabricated and sold by a company.

5. The fluid applicator

This is a device to apply stone preservatives on walls or figures. The fluid is sprayed by a nozzle and the spraying mechanism is moved by a device with electrical motors. The device is fixed at the scaffolding, The automatically controlled movement is necessary because it takes hours to apply a fluid quantity with a penetration depth of 10 or 20 centimeters. The applicator is available as a laboratory model.
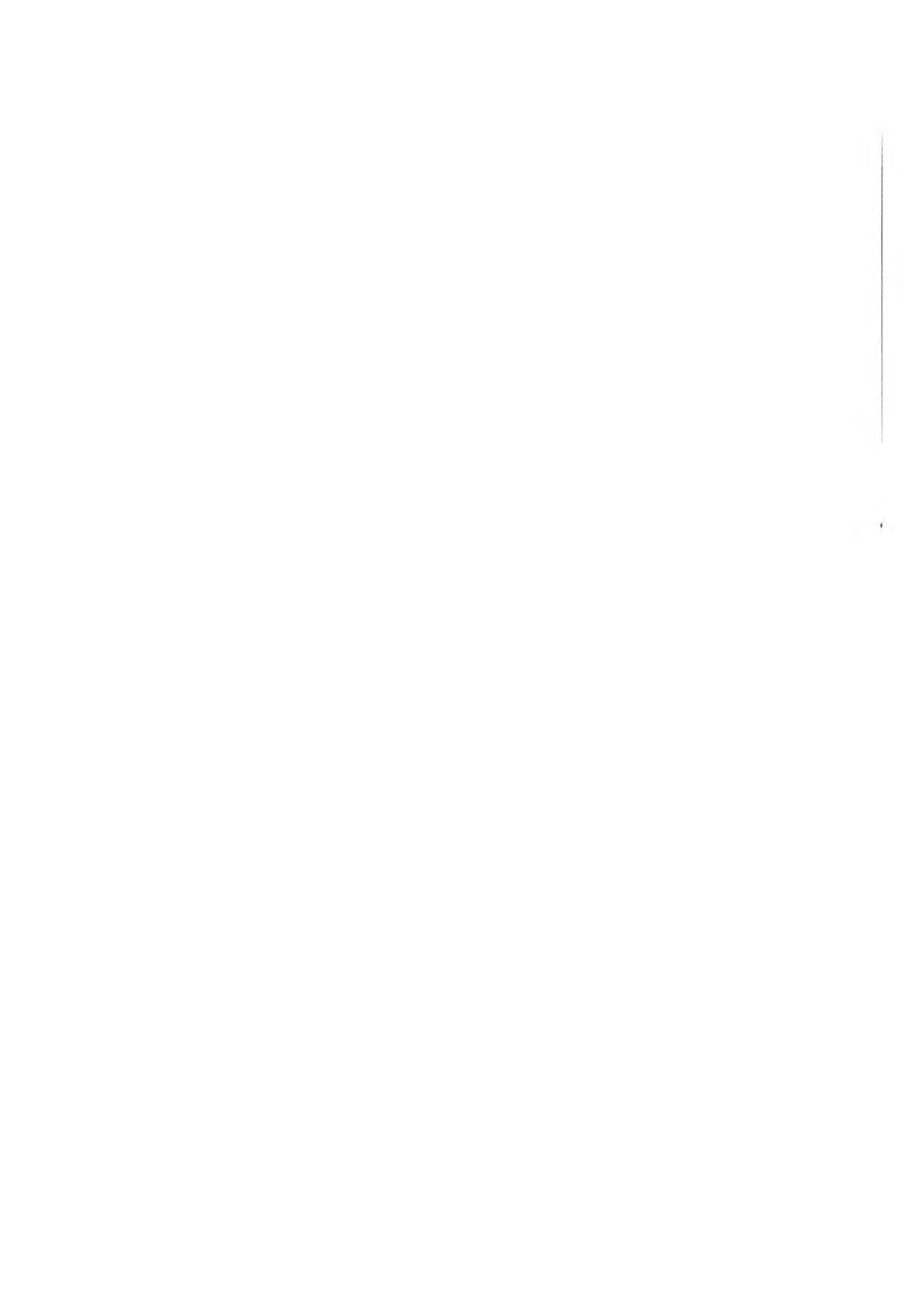
Karlien Torfs
René Van Grieken
JoAnn Cassar

Environmental effects on deterioration of monuments: case study of the Church of Sta. Marija Ta' Cwerra, Malta
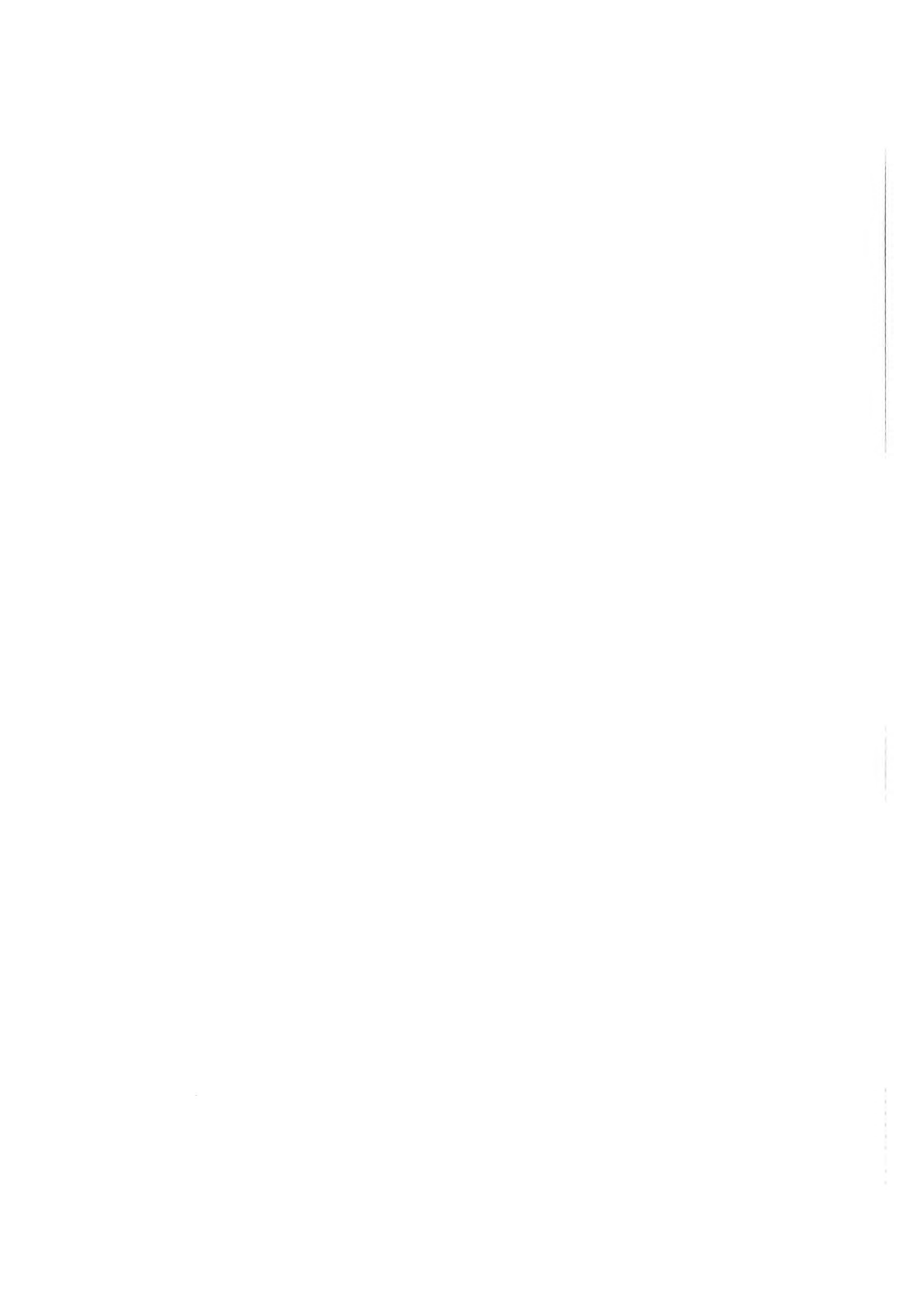
Environmental effects on deterioration of monuments: case study of the Church of Sta. Marija Ta' Cwerra, Malta

K. Torfs   — *Dept. of Chemistry, University of Antwerp (U.I.A.), B–2610 Antwerp, Belgium*
R. Van Grieken — *Dept. of Chemistry, University of Antwerp (U.I.A.), B–2610 Antwerp, Belgium*
J. Cassar   — *Institute for Masonry and Construction Research, University of Malta, Msida, Malta*

Abstract

To investigate the action of air pollution and the influence of marine aerosols on the weathering of historical monuments, the Church of Sta. Marija Ta'Cwerra in Malta has been selected for an extensive study. The research programme includes the chemical examination of the weathered stone at the outside and the inside of the building. Monitoring of environmental parameters (total deposition, aerosols and meteorological data) has been carried out for more than one year.

1. Introduction

The church of Sta. Marija Ta'Cwerra is located in the village Siggiewi, in the southwest of the island Malta, at a distance of 3 km from the sea. It is a free standing building from the 17th century, less than 10 by 10 metres. The church is built entirely of Globigerina limestone. This limestone has a high total porosity (35%) with mainly small pores ($2-5$ µm) [1]. The chemical composition of the stone is dominated by calcium carbonate (88 to 97%).

The four external walls of the church show severe deterioration, for about two–third of their height; the lower courses are cemented. The middle courses are deteriorated in the form of alveolar weathering as well as powdering of several areas. Most of the mortar has been lost from the joints in this area. The uppermost courses are better preserved. At the inside of the building, the plaster has fallen away in several areas revealing powdering and flaking stone underneath [2].

2. Sampling

On the inside of the church, efflorescence samples have been taken on the south wall, at a height of 1.7 m *(MA–1)* and at the north wall at a height of 0.3 m *(MA–2)*. On the outside, stone samples have been taken at the south wall only: *MA–3* is a sample from deep destruction of the stone, *MA–4* is an exfoliation sample, *MA–5* is a sample from the depth in the alveolar weathering.

The total deposition is sampled on the roof of the church by means of a funnel with an inner diameter of 20 cm, attached to a 1 L polyethylene bottle. The samples are collected every week. The funnel is rinsed with 50 mL of deionised water to collect also the dry deposition in the funnel. This rinsing water is added to the collecting bottle to ensure a new sample every week. The sampling has been carried out from March 1994 till December 1995; more than 80 samples have been collected. The meteorological data are gathered from the weather station 10 km away from the church.

To collect outdoor aerosols, a filter unit in cascade geometry provided with a top–hat inlet is used. Polycarbonate filters (Nuclepore) with a diameter of 47 mm and a pore–size of 2 µm and 0.4 µm are placed behind each other, in order to collect coarse and fine particles separately. The indoor aerosol sampling takes place using only one filter with a pore–size of 0.4 µm. A gas volume meter is placed behind the pump to measure the volume that is pumped through the filters. The sampling is

carried out during one week, exactly for the same period as the total deposition samples. The sampling at the inside of the building has been started in November 1994 and at the outside in March 1995, both lasted till December 1995. More than 30 inside aerosol samples have been collected, as well as 30 outside aerosol samples.

3. Sample preparation and analysis techniques

To determine the soluble salts in the stone, the samples are crushed. Around 100 mg of the resulting powder is dispersed in 100 mL of demineralised water. The aqueous suspension is filtered through a Millipore 0.2 μm pore size filter and the filtrate is analyzed for the ionic content using ion chromatography (IC), atomic absorption and atomic emission spectrometry (AAS/AES). Energy dispersive X–ray fluorescence (EDXRF) has been applied to the stone samples. For this purpose, about one gram of the crust samples is wet–ground in a McCrone Micronizing Mill. A few millilitres of the suspension is brought on a Mylar foil, which is glued on a Teflon ring, to obtain a sample thickness of around 1 mg/cm^2. The foil is dried in an oven at a temperature of 60°C. To analyze the stone composition in depth, the sample is imbedded in a resin, cut perpendicularly to the weathered crust, and polished without water. After carbon coating, electron probe micro–analysis (EPMA) has been applied.

The total volume of the total deposition sample is measured. The sample is filtered over a Whatman 41 filter. Weighing the filter before and after filtration gives the mass of the total suspended particles (TSP) in the total deposition. The pH of the filtrate is measured using a pH electrode, which is calibrated using buffer solution of pH 4 and 7. The HCO_3^- content is determined by titration. HCl is added to 10 mL of the sample till the colour of the methyl–orange indicator

changes from yellow to orange. The anion and cation analyses are carried out using IC/AAS/AES.

The aerosols are first analyzed by EDXRF. After EDXRF analysis the filters are leached in exactly 25 mL of deionised water. The suspension is filtered and the soluble ions are determined by IC/AAS/AES.

Ion chromatography (IC) is used for Cl^-, NO_3^- and SO_4^{2-} determinations; a Dionex 4000i instrument, equipped with a AS11 separator column is used; the eluent is 20 mN NaOH. Ca^{2+} and Mg^{2+} are determined by means of AAS, whereas Na^+ and K^+ are measured by AES, both by means of a Perkin Elmer 3030 spectrometer.

A Tracor Spectrace 5000 instrument is used for EDXRF. The instrument is equipped with a Si(Li) detector and a low power X–ray tube with a Rh target, controlled by an IBM computer. The X–ray spectra are accumulated for 3000 sec and analyzed using the AXIL software [3]. The calculation of the concentrations in the stone samples has been checked with soil standards: IAEA Soil 5 and BCR 142. For the aerosol samples the AXIL program calculates the concentration of the elements on the filters in μg/m^2. Since the surface of the filter and the volume that has been sampled are determined, the concentrations of the elements can be expressed in ng/m^3.

The instrument for EPMA is a JEOL JXA–733 Superprobe, equipped with the Tracor Northern TN 2000 energy dispersive X–ray detector system. The samples are excited with an electron beam of 1 nA and an electron energy of 25 keV. By recording energy dispersive X–ray spectra of subsequent small areas, perpendicular to the exposed surface, depth profiles are obtained, showing the elemental distribution through the sample, when proceeding from the outer surface layer towards the unaffected inner part. Concentrations of the elements are expressed in weight percent. They are calculated, using standards, after ZAF–correction.

4. Discussion of the results

4.1. Stone analysis

Table 1 presents the results of the leaching experiment. The concentrations of the ions in the stone are expressed in weight percent to the dissolved mass of the sample. Small enrich-

Table 1   Results of IC and AAS/AES on leachate samples (weight %).

	Cl^-	SO_4^{2-}	NO_3^-	Ca^{2+}	Mg^{2+}	Na^+	K^+
MA-1	58.2	0.49	0.00	1.55	0.01	21.9	0.05
MA-2	1.03	30.9	0.00	1.27	0.02	16.0	0.16
MA-3	8.30	3.06	5.40	9.45	0.27	4.26	0.69
MA-4	7.22	0.61	6.67	11.0	0.29	3.81	1.34
MA-5	13.2	0.00	4.39	13.3	0.23	42.5	0.53

ments of Cl^-, SO_4^{2-}, Ca^{2+} and Na^+ in sample MA–4 and of Cl^-, NO_3^-, Ca^{2+} and Na^+ are observed in samples MA–3 and MA–5. Aires–Barros [4] detected some halite using XRD in the samples from Malta on the inside and the outside; this is in agreement with our results. Most noticeable is the difference at the inside of the church between the salts at the north side and at the south side. The salt efflorescence from the south wall exists mostly of Na-Cl, while the efflorescence from the north side consists mainly of Na_2SO_4. Fassina [5] also found that the efflorescence at the inside of the church contains mainly chloride at the south wall and mainly sulphate at the north wall. The height of the sampling influences the distribution of the efflorescence: in the lower zone, the less soluble and less hygroscopic sulphates will be present, while in the upper zone, the chlorides accumulate [6]. This is in agreement with our results: the sample taken at 0.3 m contains mainly SO_4^{2-}, while the sample from 1.7 m height contains Cl^-.

Table 2 shows the EDXRF results of some samples from Malta. The samples from the outside contain quite high amounts of Si; S is almost not present in the outside samples from Malta. The inside sample contains a high amount of Cl,

Table 2   Results of EDXRF on the stone samples.

	MA-1	MA-3	MA-4
Si (%)	1.39	4.03	5.83
P (ppm)	N.D.	1.60	2.17
S (%)	2.27	0.94	0.92
Cl (%)	63.7	3.03	1.77
K (ppm)	4400	6240	5380
Ca (%)	13.6	39.2	40.8
Ti (ppm)	84.6	327	444
Cr (ppm)	N.D.	38.3	N.D.
Mn (ppm)	11.3	96.5	63.6
Fe (ppm)	352	1940	2160
Ni (ppm)	N.D.	14.4	17.7
Cu (ppm)	9.32	6.54	7.60
Zn (ppm)	17.1	21.8	23.0
Ge (ppm)	3.02	6.37	N.D.
As (ppm)	27.1	N.D.	N.D.
Br (ppm)	21.8	9.18	2.98
Rb (ppm)	0.77	9.62	8.48
Sr (ppm)	52.3	442	426
Y (ppm)	11.8	12.6	14.3
Zr (ppm)	4.11	17.5	19.7
Ba (ppm)	N.D.	N.D.	320
Pb (ppm)	N.D.	11.7	19.9

as is observed with the leaching experiment. The concentration of Fe, Pb, Ti and K is quite high in the stone samples from the outside.

Some results of EPMA are shown in Figures 1 and 2. For sample MA–3 some S has been found in the outer layer (10%), and it seems that NaCl crystals may be present till a depth of 500 μm. The weathering layer of MA–5 seems to be more enriched in NaCl than sample MA–3 (cfr. Table 1), till the same depth.

The enrichment factors of various elements with respect to average carbonate rock have been calculated to identify the component due to the deposition of atmospheric gases and aerosol on the stone surfaces. The following formula has been used [7]:

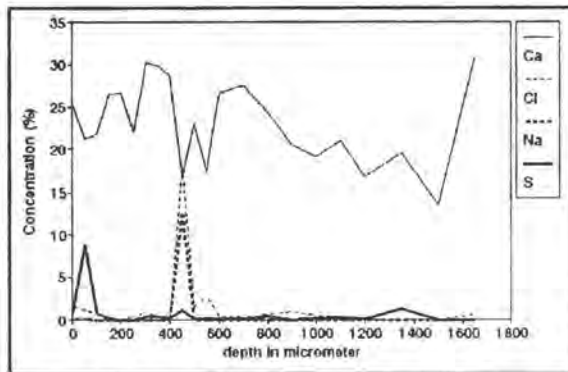$$EF \text{ carb. rock } (X) = \frac{(X/Ti)_{decay\ layer}}{(X/Ti)_{carb.\ rock}}$$
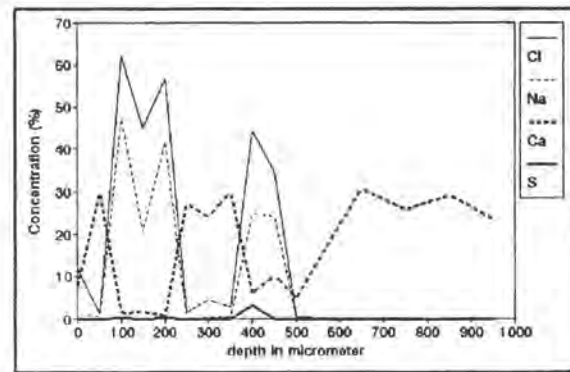
Fig. 1 Depth profile of MA–3

Fig. 2 Depth profile of MA–5.

where X and Ti are the concentrations of element X and titanium. The elemental composition of carbonate rock, reported by Mason [8] is used in the denominator. To estimate the importance of sea derived elements and soil dust on the stones, enrichment factors relative to the average sea water composition and the average soil dust composition have been determined as well, using an analogous formula, with Na as indicator element for sea water and Al as indicator element for soil dust [8]. results are presented in Table 3.

Enrichments to carbonate rock have been found for Cl, S and Na. Cl, Mg, S and K seem to originate from the sea. Ca in the crust is enriched with respect to sea water, because of the underlying limestone; the Ca content of the efflorescence seems to be influenced by sea wa-

ter. For Mg, K, Si, Mn and Fe enrichment factors to soil dust are close to 1, indicating that soil dust may be their major source.

The weathering layer of the church seems to be mostly affected by the action of sea water. At the outside of the building sea salt particles are found till a depth of 500 μm in the stone, especially in the sample from the depth of the alveolar weathering. The efflorescence sample from the inside contains mostly sulphates and chlorides, depending on the height. Enrichment factors indicate that the weathered layers are enriched mainly in Cl⁻ and Na⁺, which originate from the sea, and that soil dust could be the source of Si and Fe, but these elements are not enriched relative to the average carbonate rock composition.

Table 3 Damage layer enrichment factors.

	Cl	S	Ca	Mg	Na	K	Si	Mn	Fe	Sr	Pb
	vs. carbonate rock (and Ti as indicator element)										
MA-1-2	9300	210	0.2	0.0	2200	1.8	2.7	0.0	0.4	0.4	0.0
MA-3-5	660	3.5	0.4	0.1	440	3.3	2.1	0.1	0.6	0.7	1.8
	vs. sea water (and Na as indicator element)										
MA-1-2	0.75	3.9	2.2	0.01	1	0.2					
MA-3-5	0.75	0.43	47	0.4	1	5.4					
	vs. soil dust (and Al as indicator element)										
MA-1-2	10^5	10^4	20	0.3	350	2.1	2.6	0.6	0.4	7.3	0.0
MA-3-5	8400	180	35	1.4	68	3.8	2.0	1.0	0.5	13	14

4.2. Total deposition and aerosols

The ionic balance has been calculated to check whether the major ionic species had been determined. The calculated balance falls within the uncertainty range.

The weekly average total depositions of the ions are presented in Table 4. Ca^{2+}, Na^+ and Cl^- are the major ions in the total deposition. The pH and Ca^{2+} are quite high because of the neutralizing action of calcite particles from the monument. Roekens et al. [9] observed the same phenomenon near the cathedral of Mechelen (Belgium). In the Mediterranean the high Ca^{2+} content may also be explained by the presence of Saharan dust [10], but only this can not be the cause of the high value.

When comparing our results with results obtained in Sicily [11], it seems that we determined higher concentrations of Ca^{2+} and Cl^-, but that the SO_4^{2-} content is lower in the samples from Malta. Generally, deposition seems to be higher in winter than during summer.

In analogy to the enrichment factors, calculated for the stone samples, these factors have been determined for the total deposition samples. The total deposition samples are enriched relative to sea water in Ca^{2+}; this may be explained by calcite particles from the monument, while the other elements originate from sea water.

The relationship between two variables is considered by use of the concept of the correlation coefficient.

The variables that are included in the calculations are: the ion amounts, expressed in meq/m^2, the volume in L, TSP in mg and the meteorological parameters: temperature (T) in °C, wind speed (WS) in m/s, wind direction (WD) in ° and relative humidity (RH) in %. The correlation matrix is presented in Table 5. A high correlation is observed between Na^+, Mg^{2+} and Cl^-. The volume is correlated with the Ca^{2+} content, and also with the Cl^- and HCO_3^- content. The acidity (H^+) is correlated with the Na^+, Mg^{2+} and Cl^- content. Ca^{2+} is

Table 4 Weekly average total deposition ($\mu eq/m^2/week$) (the average volume is expressed in $l/m^2/week$).

Vol	H^+	Ca^{2+}	Mg^{2+}	Na^+	K^+	HCO_3^-	Cl^-	NO_3^-	SO_4^{2-}
7.5	1.2	6900	1000	3900	350	3200	5100	330	1500

Table 5 Correlation matrix of total deposition and meteorological data.

	Vol	TSP	H^+	Ca^{2+}	Mg^{2+}	Na^+	K^+	HCO_3^-	Cl^-	NO_3^-	SO_4^{2-}	T	WS	WD	RH
Vol	1.00														
TSP	0.07	1.00													
H^+	0.43	0.01	1.00												
Ca^{2+}	**0.76**	0.17	0.24	1.00											
Mg^{2+}	0.59	0.00	**0.65**	0.53	1.00										
Na^+	0.60	-0.02	**0.70**	0.49	**0.93**	1.00									
K^+	0.48	0.15	0.34	0.32	0.54	0.53	1.00								
HCO_3^-	**0.79**	0.39	0.04	**0.76**	0.33	0.27	0.32	1.00							
Cl^-	**0.62**	0.09	**0.72**	0.51	**0.89**	**0.96**	0.56	0.32	1.00						
NO_3^-	0.25	0.37	-0.02	0.53	0.20	0.10	0.04	**0.62**	0.15	1.00					
SO_4^{2-}	0.54	0.48	0.26	**0.68**	0.39	0.37	0.27	**0.71**	0.50	**0.74**	1.00				
T	-0.30	0.09	-0.38	-0.19	-0.36	-0.42	-0.12	0.00	-0.44	0.07	-0.27	1.00			
WS	0.21	0.15	0.28	0.19	0.33	0.33	0.37	-0.06	0.39	0.00	0.23	-0.48	1.00		
WD	-0.05	-0.13	0.28	-0.02	0.22	0.26	0.12	-0.20	0.25	-0.11	-0.06	-0.27	0.13	1.00	
RH	0.23	0.06	0.11	0.25	0.10	0.08	0.03	0.10	0.09	0.10	0.19	-0.23	0.13	-0.11	1.00

correlated with the HCO_3^- and SO_4^{2-} content. HCO_3^-, NO_3^- and SO_4^{2-} are correlated. The temperature is not significantly correlated with any ion, but all correlation coefficients are negative, which means that the lower the temperature the higher the deposition (winter rains).

Principal component analysis (PCA) is a statistical technique to reduce the dimensionality of a large data set, without loosing information. The original correlated variables are transformed into new uncorrelated variables, which are linear combinations of the original data set. Each principal component is composed of the product of a score vector and a loading vector plus an error term. The loading plot shows the correlation between the variables. If a group of variables correlate with each other and reflect the operation of a single process, the variables will be represented as a cluster in the loading plot.

Variables that are situated close to the origin of the plot do not contribute to the model. Figure 3 shows the result. The first factor is
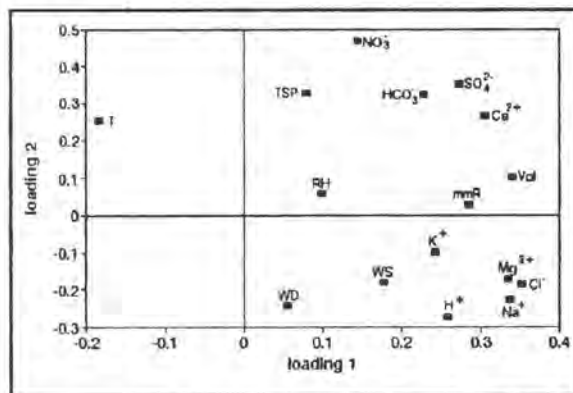
Fig. 3 Loading plot of total deposition and meteorological data.

mainly formed by the volume, Cl^-, Na^+, Mg^{2+} and Ca^{2+}. Two clusters are visible: Na^+, Mg^{2+} and Cl^- form one cluster, while HCO_3^-, SO_4^{2-} and Ca^{2+} form another cluster of variables. This implies that these elements explain most of the variance in the data matrix, but they do not reflect the action of the same source: a marine factor is acting together with the influence

of calcite particles from the monument. The second factor is mostly explained by NO_3^-. Meteorological variables (WD, WS, RH and T) explain the third and fourth factor and are thus less important to explain the variance in the data matrix. The four first factors explain 62% of the variance. The temperature seems to be negatively correlated with Cl^-, Na^+ and Mg^{2+} (the lower the temperature the higher the deposition of these elements, i.e. more breaking wave generating sea salt in winter).

The composition of the total deposition is mainly influenced by the vicinity of the sea (high Na^+, Mg^{2+} and Cl^- concentration). Ca^{2+} is correlated with HCO_3^- and SO_4^{2-}, which indicates the action of a second source (anthropogenic influence or calcite particles from the monument).

The average aerosol concentrations are given in Table 6. The concentrations of the 2 and 0.4 µm pore– size Nuclepore filter from the outside are given separately, while the sum is also presented to compare the values with the inside aerosols. Ca, Na, Cl and S are the most abundant elements in the aerosols. The inside concentration is more or less the same (or a bit higher) as the outside concentration for most elements; Ca, Fe, Al, Ti, Mn, Ni and Sr are more abundant at the outside. The concentration of the fine fraction is lower than of the coarse fraction; only K^+ is more abundant in the small particle fraction.

In comparison with the aerosol composition around the cathedral in Mechelen (Belgium) [12], it seems that the Cl and Ca concentration is higher in Malta, due to the vicinity of the sea and the higher Ca content is possibly influenced by the composition of the soil in Malta. The concentration of S, Pb, Fe, V and Ni is higher in Mechelen, due to higher anthropogenic activities. When comparing the aerosol concentrations for each month, it seems that at the inside of the building, concentrations are for all elements higher in spring than in winter and summer. At the outside of the building the trend is different for some ele-

Table 6   *Average concentration for the aerosol samples (concentrations are expressed in ng/m^3)*

	NO_3^- IC	Na^+ AES	Mg^{2+} AAS	Al XRF	Si XRF	SO_4^{2-} IC	Cl^- IC	K^+ AES	Ca XRF
in	2400	3910	382	85	585	7430	6440	2010	6100
out	1480	3110	390	216	652	6210	4550	1130	6980
out 2	1380	2770	356	186	522	5320	3730	432	5950
out 0.4	97	341	34	5.5	56	895	818	693	230

	Ti XRF	V XRF	Cr XRF	Mn XRF	Fe XRF	Ni XRF	Cu XRF	Zn XRF	Br XRF	Sr XRF	Pb XRF
in	21	5.8	20	6.2	312	4.8	16	74	55	14	115
out	41	11	7.3	8.3	399	6.0	17	47	25	17	60
out 2	36	9.0	2.7	7.1	338	4.7	11	38	14	14	40
out 0.4	0.5	0.7	3.7	0.3	15	0.6	3.7	3.8	7.4	1.7	13

ments. Na', NO_3^- and Cl concentrations are higher in spring than in summer, while for SO_4^{2-}, the concentration is higher during summer. For most elements concentrations are getting higher again at the end of the summer. Kubilay and Saydam [13] also found the maximum concentrations of anthropogenic elements in the Mediterranean during the summer season, while in November, when rain events occur, a sharp drop in concentration is measured.

The correlation coefficient has been calculated between the inside and the outside concentration for each element. Only for V, S and Ni, some correlation is observed between the inside and the outside.

It seems that the concentration inside is for most elements independent of the concentration outside, for short time intervals like one week. This may be explained by the fact that the church is rarely used nowadays [2].

The contribution of sea water and mineral dust to each element in the aerosol is assessed by means of the enrichment factors. Mg, Cl, S, Br and Sr originate mainly from the sea. Schneider [14] also observed that a part of Sr is sea salt derived. Si, Mg, Fe and Ti behave as non–enriched elements to crustal concentrations, while the other elements are enriched. For most elements, the enrichment factors are larger for the small particles than for the large particle fraction. Mg, K and Sr seem to originate from soil dust in the coarse particle fraction, while these elements are enriched to soil dust for the fine fraction.

The correlation matrices have been calculated for the aerosols inside and outside and are summarized here. At the inside, a correlation is observed between Na, Mg, Cl, K and Ca. Fe is correlated with Si and K. At the outside a correlation is observed between Na, Mg and Cl. Al, Si, K, Ca, Ti, Mn, Fe and Sr are all correlated. Pb is correlated with some metals (V, Cr, Mn, Ni, Zn). Cl is negatively correlated with the temperature and positively with the wind speed. For the coarse fraction we find a correlation between Na, Mg and Cl, while Al, Si, K, Ca, Ti, Mn, Fe and Sr form a highly correlated group of soil derived elements. In the fine fraction, a correlation between Na, Mg, Cl, NO_3^- and Ca is observed. Si is correlated with Ca, Fe, Sr, K, S and Cl, but not with Al

Table 7 Aerosol enrichment factors.

	Na	Mg	Al	Si	S	Cl	K	Ca	Ti	Fe	Br	Sr
	vs. sea water (and Na as indicator element)											
in	1	0.82	10^5	810	5.2	0.91	15	42	10^4	10^5	2.3	2.9
out	1	1.1	10^5	1100	5.6	0.81	10	60	10^5	10^5	1.3	4.6
out 2	1	1.1	10^5	1000	4.8	0.74	4.4	58	10^5	10^5	0.87	4.0
out 0.4	1	0.84	10^5	880	6.6	1.3	58	18	10^5	10^5	3.6	4.1
	vs. soil dust (and Al as indicator element)											
in	160	16	1	2.0	3100	10^4	140	430	4.5	7.8	10^4	44
out	50	6.4	1	0.88	1000	10^4	32	190	3.4	3.9	1900	22
out 2	52	6.8	1	0.82	950	10^4	14	190	3.5	3.9	1300	20
out 0.4	220	22	1	3.0	5500	10^5	760	250	1.7	5.8	10^4	85

as in the coarse fraction. Pb is correlated with Ni and V. Na, Mg and Cl, elements originated from the sea, are correlated in the coarse and the fine fraction, while Al, Si, Fe and Ti, elements derived from soil dust, are only correlated in the coarse fraction and not in the fine one. At the inside of the church marine elements are correlated, while less correlation between soil derived elements is observed.

Principal component analysis has been performed. The loading plot of the inside and outside aerosols is shown in Figures 4 and 5.

The first factor of the aerosols at the inside (Figure 4) is composed of Fe, Si, K and Ca and explains 32 % of the variance in the data matrix. The second factor is explained by Na, Cl, Mg and K. The third factor is formed by Ti, Mn, Ni and negatively by Cu, Cr and Zn, while Pb, Ti and Ni explain the fourth factor. These factors explain 64 % of the variance. For the outside aerosol samples (Figure 5) the first

factor may be explained by Mn, Fe, K, Ca, Ti, Sr, Si and Al. The second component is explained by Cl, NO_3^-, Na, Mg and Cl and the wind speed and negatively by the temperature. Ca, Na, Mg, SO_4^{2-} and Cl explain the third factor and the wind speed and amount of rain fall explain the fourth factor. The first four factors explain 65 % of the variance. PCA has been carried out for the coarse and fine fraction separately.

The first two factors are explained by the same elements as for the sum of both fractions. The first factor contains generally soil derived elements (influenced by some anthropogenic emissions), while the second factor, which explains less of the variance, is composed of marine elements. The small fraction contains less soil derived elements.

The aerosol concentration is influenced by the sea and the vicinity of the monument. The high Ca concentration is mainly due to the
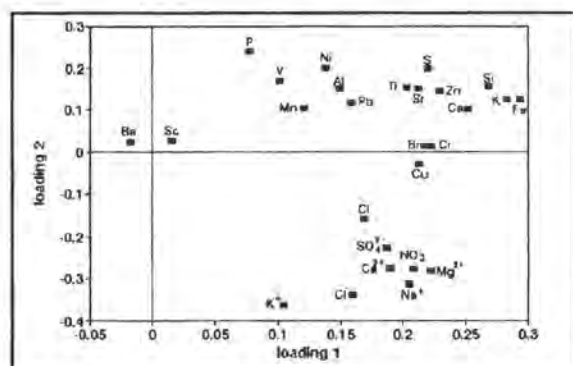
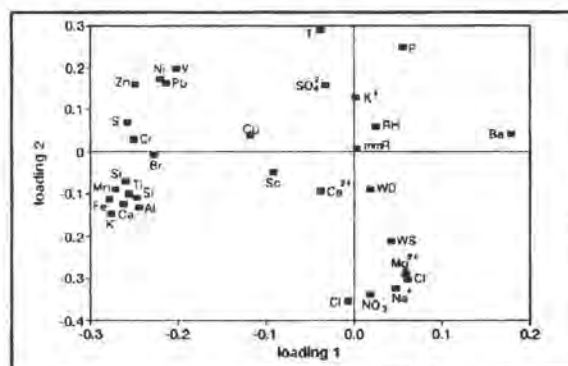*Fig. 4 Loading plot for the aerosols inside.*

Fig. 5 Loading plot for the aerosols outside.

loss of calcite particles from the church. Sea derived elements (Na and Cl) are very abundant in the aerosols. Soil derived elements (Fe, Ti, Si, Sr and Al) determine to a higher extent the aerosol composition of the coarse fraction than of the fine fraction.

The stone samples from the outside show clear enrichments in Na+ and Cl–, and a bit in SO_4^{2-}. On the inside the efflorescence is enriched in Na^+ and Cl^- as well. The total deposition contains almost only sea derived elements. The aerosol composition around the monument seems to be influenced mainly by sea salt particles and soil derived elements. Soil derived elements are abundant in the stone samples from the outside of the building. Since the analysis of the stone samples indicates mainly the influence of sea water, it can concluded that the chemical deterioration of the church is mainly caused by the sea and that anthropogenic emissions are of negligible importance.

5. Acknowledgement

6. References

1. Fitzner B., *Microstructure analysis at stone samples from Malta and Spain*. 2nd Semestrial Report: "Marine spray and polluted atmosphere as factors of damage to monuments in the Mediterranean coastal environment", Ed. Zezza F., R & D Programme in the Field of Environment, Contract No EV5V–CT92–0102, 149–177, 1993.

2. Cassar J., The Church of Santa Marija Ta'Cwerra at Siggiewi, 1st Semestrial Report: "Marine spray and polluted atmosphere as factors of damage to monuments in the Mediterranean coastal environment", Ed. Zezza F., R & D Programme in the Field of Environment, Contract No EV5V–CT92–0102, 30–35, 1993.

3. Van Espen P., Janssens K. and Nobels J., *AXIL–PC software for the analysis of complex X–ray spectra*, Chemometrics and Intelligent Laboratory Systems 1, 109–114, 1986.

4. Aires–Barros L., *Micropetrography, XRF and IR–spectroscopy of archaeological site Eleusis, church of Sta. Marija Ta'Cwerra of Malta and cathedral of Cadiz.* 2nd Semestrial Report: "Marine spray and polluted atmosphere as factors of damage to monuments in the Mediterranean coastal environment", Ed. Zezza F., R & D Programme in the Field of Environment, Contract No EV5V–CT92–0102, 88–118, 1993.

5. Fassina V., *Church of Sta. Marija Ta'Cwerra (Malta): salt efflorescence analysis by ionic chromatography.* 2nd Semestrial Report: "Marine spray and polluted atmosphere as factors of damage to monuments in the Mediterranean coastal environment", Ed. Zezza F., R & D Programme in the Field of Environment, Contract No EV5V–CT92–0102, 133–134, 1993.

6. Arnold A. and Zehnder K., *Salt weathering on monuments.* Proc. 1st International Symposium on The Conservation of Monuments in the Mediterranean Basin, Ed. F. Zezza, Grafo, Bari, 31–58, 1989.

7. Sabbioni C., *Contribution of atmospheric deposition to the formation of damage layers*, Sci. Tot. Env. 167, 49–55, 1995.

8. Mason B., Principles of Geochemistry, 3rd Ed., J. Wiley & Sons, New York, p. 329, 1966.

9. Roekens E., Komy Z., Leysen L., Veny P. and Van Grieken R., *Chemistry of precipitation near a limestone building*, Water, Air and Soil Pollution 38, 273–282, 1988.

10. Loye–Pilot M.D., Martin J.M. and Morelli J., *Influence of Saharan dust on the acidity and atmospheric input to the Mediterranean*, Nature 321, 427–428, 1986.

11. Alaimo R., Deganello S., Di Franci L., Montana G., *Caratteristiche composizionali del particolata solido atmosferico e chimismo delle acque di precipitazione nell'area urbana di Palermo.* Proc. 1st International Symposium on The Conservation of Monuments in the Mediterranean Basin, Ed. F. Zezza, Grafo, Bari, 369–377, 1989.

12. Leysen L., Roekens E. and Van Grieken R., *Air–pollution induced chemical decay of a sandy–limestone cathedral in Belgium*, Sci. Tot. Env. 78, 263–287, 1989.

13. Kubilay N. and Saydam A., *Trace elements in atmospheric particulates over the eastern Mediterranean; concentrations, sources and temporal variability*, Atmos. Environ. 29, 2289–2300, 1995.

14. Schneider B., *Source characterization for atmospheric trace metals over Kiel Bight*, Atmos. Environ. 21, 1275–1283, 1987.

Fulvio Zezza
Sandro Calogero

A neutron activation analysis study of the limestone of the Bari Cathedral
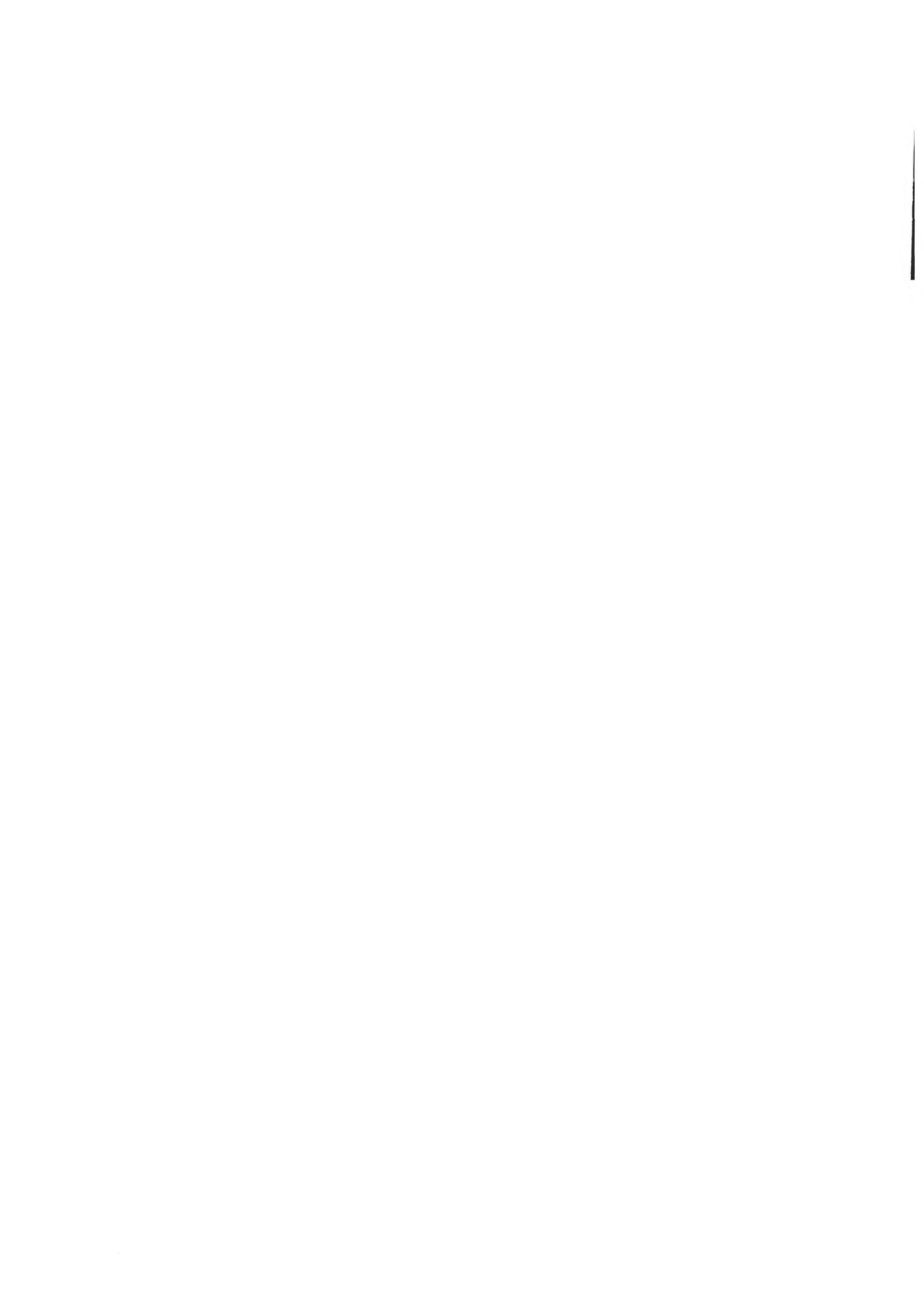
A neutron activation analysis study of the limestone of the Bari Cathedral

F. Zezza — *Istituto di Geologia Applicata e Geotecnica, Facoltà Ingegneria, Politecnico di Bari, 70125 Bari (Italy)*

S. Calogero — *Dipartimento di Chimica Fisica, Università di Venezia, 30123 Venezia (Italy)*

1. Introduction

The Bari Cathedral is one of the most important examples of Apulian Romanesque architecture [1]. It was built in 1034 by demolishing a pre–existing church, destroyed in 1156 and reconstructed from 1171 to 1292. The Cathedral is entirely built of local squared blocks of limestones, while imported white and coloured marbles have been used for columns and decorative elements. Along the centuries, many restorations were performed by using local limestones. This report attempts the identification of the origin of the limestone material employed in the Cathedral in relation to the quarrying areas present in Murge. At this end samples collected in Murge quarries (Apulia) and on the Bari Cathedral have been studied by neutron activation analysis. The eleven specimens, A1–A11, were collected in Murge in the quarrying area of building and decoration stones [2,3]. The quarries, belonging to the Cretaceous carbonate series, are shown in the map of Fig. 1. The location of the six lime-
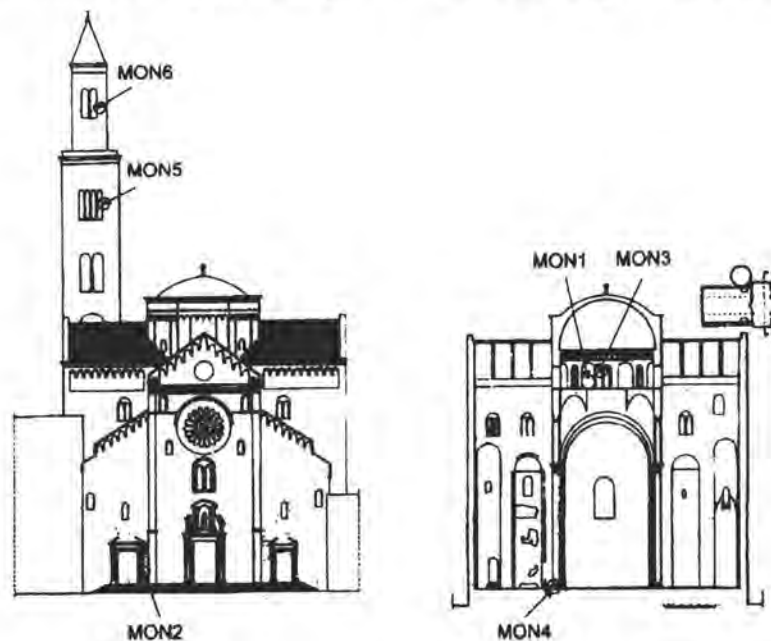
Samples from the Cathedral

MON 1 Limestone from the dome, original ashlar, XII C.
MON 2 Limestone from the right column, left portal XVII C.
MON 3 Limestone from the dome, substituted ashlar restoration 1902–1905
MON 4 Limestone from the basis of the column, apse, restoration 1921–1923
MON 5 Limestone from the bell tower (inferior part), substitution ashlar, reconstruction 1948–1952
MON 6 Limestone from the bell tower (superior part), substitution ashlar, reconstruction and restoration 1948–1952

Fig. 1 Sampling area from the Bari Cathedral.

stone specimens of the Bari Cathedral is displayed in Fig. 2. The irradiation was performed for short–living elements (Ca, Dy, K, and Na) and after two weeks irradiated again for medium–living elements (As, La, Lu, Sb, Sm, and U) and long–living elements (Ba, Co, Ce, Cr, Cs, Eu, Fe, Gd, Hf, Ho, Yb, Nd, Rb, Sb, Se, Tb, Tm, Th, and Zn). The content of these 29 elements has been used for a provenance study by multivariate and cluster analyses.

2. Results and Discussion

The provenance study was carried out by a computer assisted pattern recognition procedure [4, 5]. A stepwisediscriminant analysis program was used to identify the peculiar variables for classification purposes. The elements La, Cr, Eu, Th, and Rb shown the higher discrimination power.

The element abundance of the outcrops
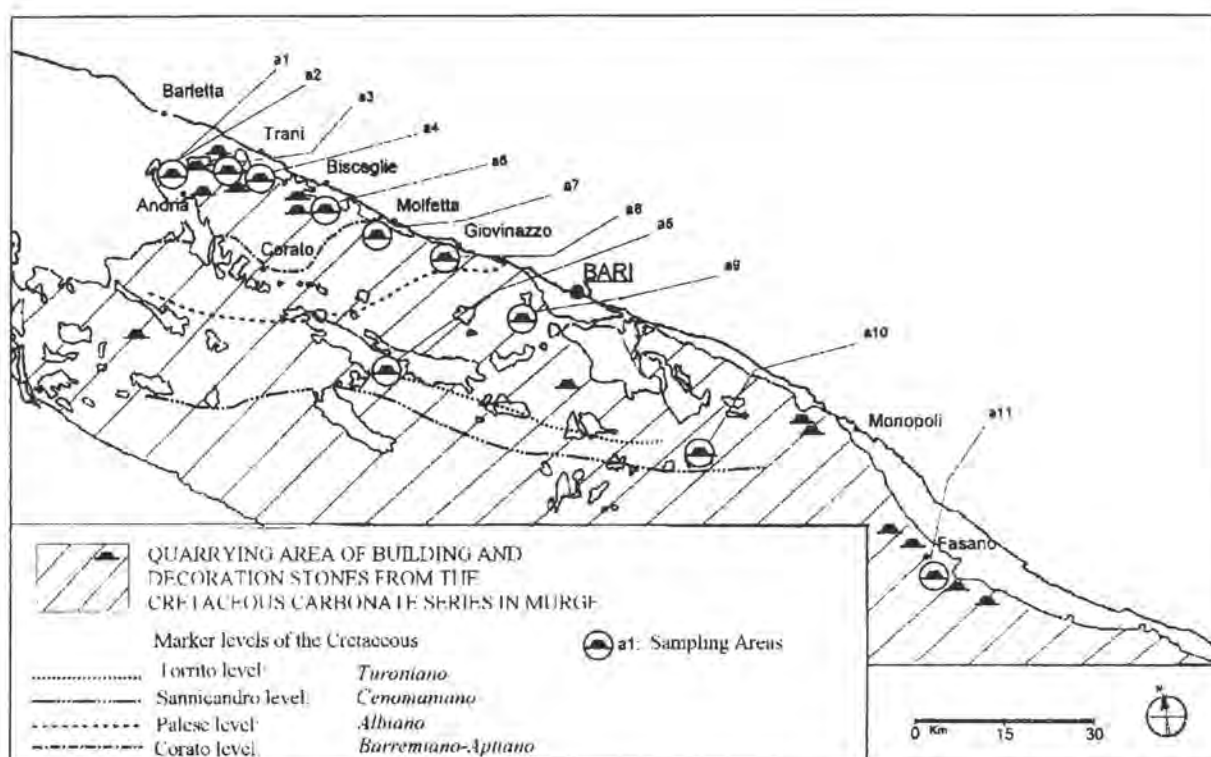
Fig. 2 Sampling area from the Apulian Murge.

were used to verify the existence of differences among the groups. In this way the eleven outcrops were separated in three groups. The discriminant variables were then used in the hierarchical cluster analysis for the samples of the quarries and of the Cathedral.

The tree dendrogram (1) indicates a partition of the outcrops in three clusters: the first contains the quarry A3; the second the quarries A8 and A7; the third cluster the remaining outcrops. All the Cathedral specimens (except

(1) *Tree Diagram by using only the content of La, Cr, Eu, Th and Rb.*
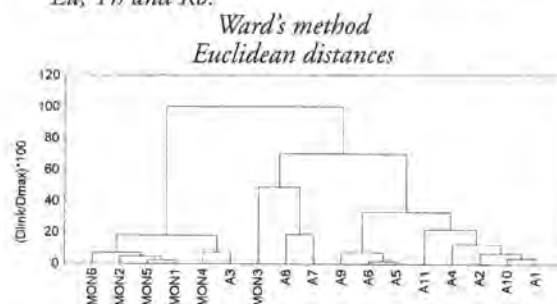
MON3) are related to A3, the quarrying area of Trani, providing a suggestion about their provenance.

The sample MON3, which belongs to a part restored in 1902–1905, is instead more similar for composition to the quarry area of Moltetta (A7) and Giovinazzo (A8). The samples A7 and A8 are different from the others for their large Fe content. The quarries belonging to the third cluster are different, inter alia, for the rare earth content.

(2) *Tree Diagram for Na and K content in ppm.*

Ward's method
Euclidean distances
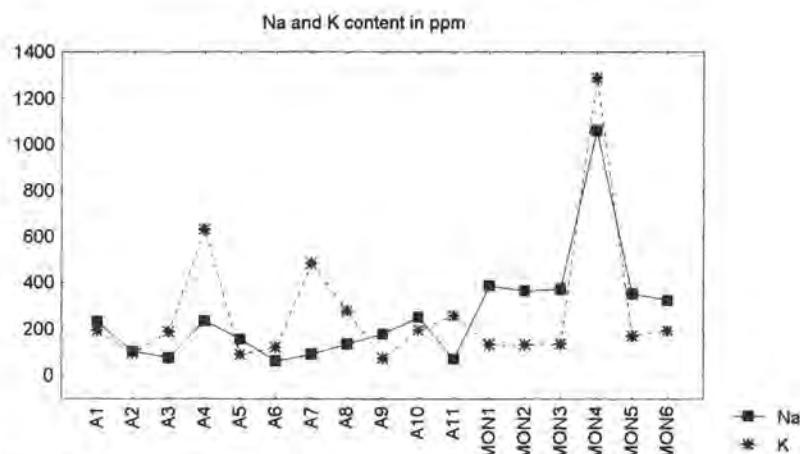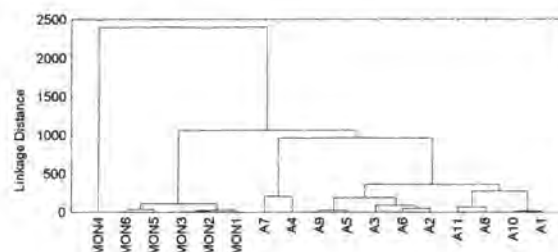
Fig. 3 Na and K content in ppm.

The dendrogram (2) shows that the Na and K elemental contents allow a good separation between the clusters containing the Cathedral specimens and the clusters containing the outcrop samples.

The Fig. 3 shows the Na content for the Cathedral specimens is larger than that found in the quarries and that the sample MON4, from the basis of the column, in front of the sea and restorated in 1921–23, displays a very high content of Na and K. This result is of great interest being related to the local weathering conditions.

3. Acknowledgements

This report has been performed according to the R&D Program in the field of Environment of EC "Marine spray and polluted at-

mosphere as factors of damage to monuments in the Mediterranean Coastal Environment" (Contract EV5V–CT92–0102).

4. References

1. E. Bertaux, L'Art dans l'Italie Meridionale, Paris, 3, 369, 471, 1904.

2. F. Zezza, Le Pietre da Costruzione della Puglia, Rassegna Tecnica Pugliese, X, n.2, 1974.

3. F. Zezza, Caratteristiche Litogeniche e Forme della Degradazione delle Pietre da Costruzione Calcaree di Origine Biochimica e Detritica, Rassegna Tecnica Pugliese, X, n.2, 1976.

4. K. Varmuza, Pattern Recognition in Chemistry, Springer Verlag, Heidelberg, 1980.

5. BMDP, Statistical Software Manual, E. J. Dixon Ed., Un. of California Press, Los Angeles, 1992.
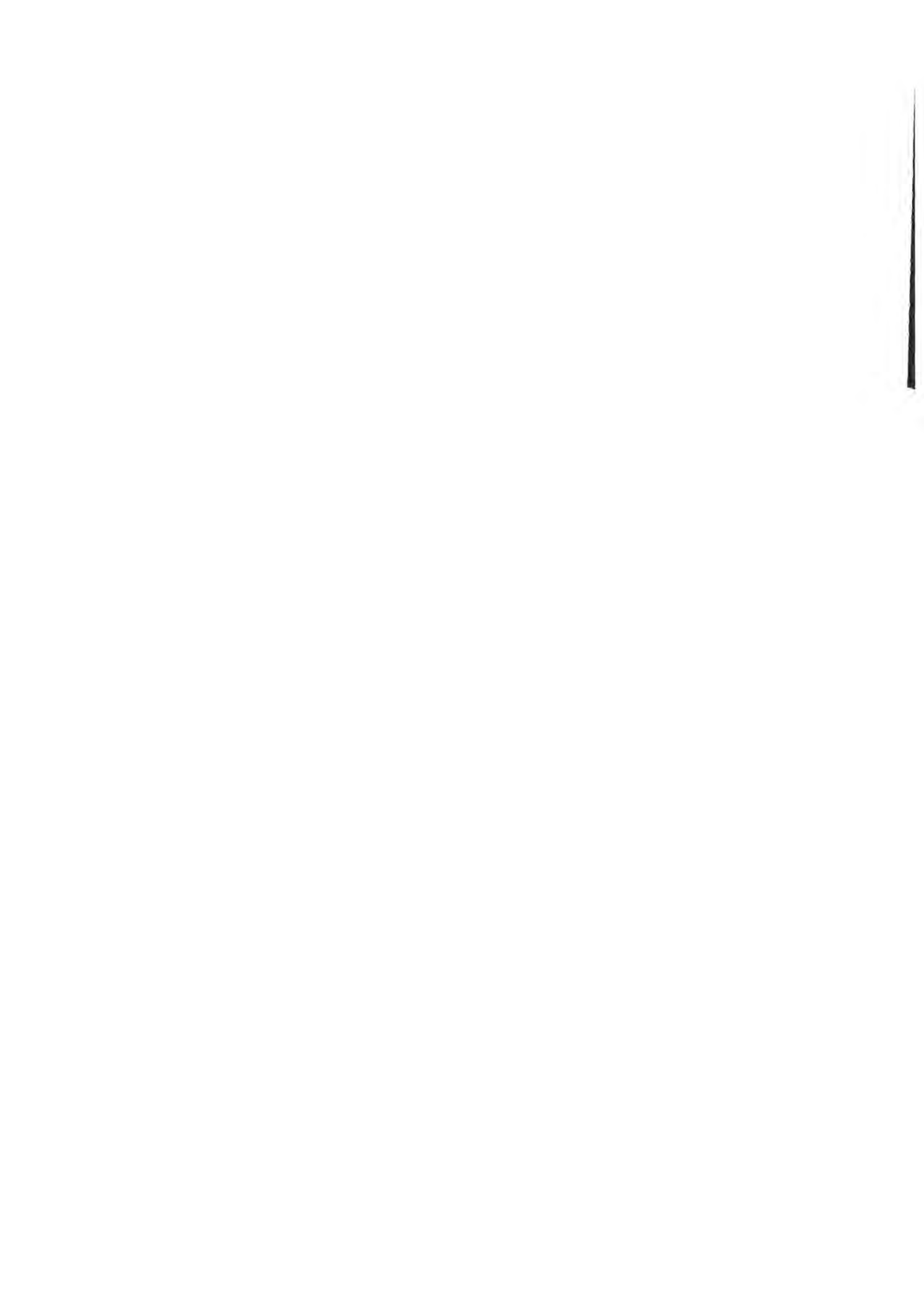
Fulvio Zezza
Karlien Torfs
René Van Grieken
Nuria García Pascua
Fabio Macrì

Study of environmental effects on deterioration of monuments: case study the Cathedral of Bari, Italy
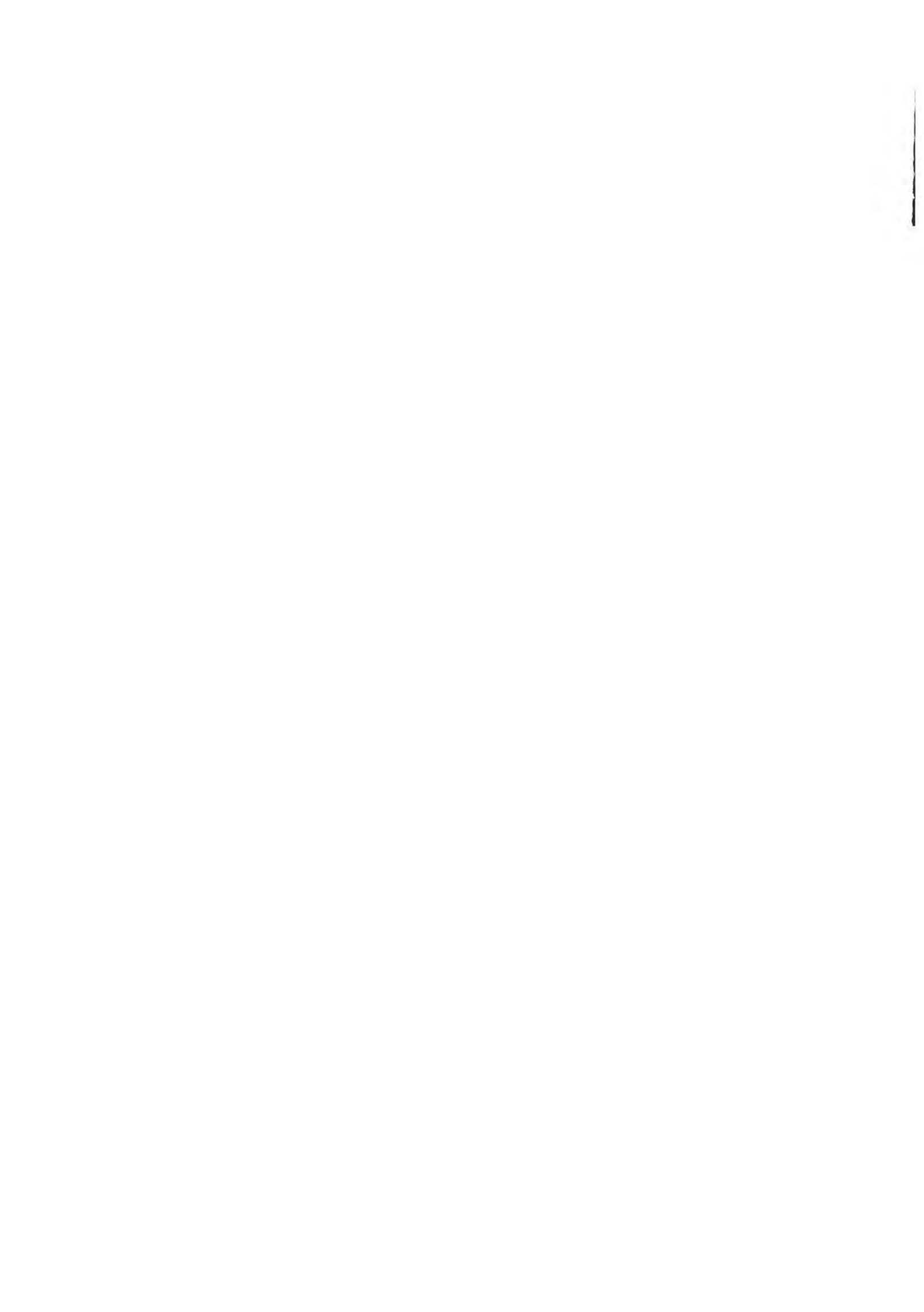
Study of environmental effects on deterioration of monuments: case study the Cathedral of Bari, Italy

F. Zezza — *Istituto di Geologia Applicata e Geotecnica, Facoltà Ingegneria Politecnico di Bari, Italy*
K. Torfs — *Istituto di Geologia Applicata e Geotecnica, Facoltà Ingegneria Politecnico di Bari, Italy*
R. Van Grieken — *Dept. of Chemistry, University of Antwerp (U.I.A.), Belgium*
N. García Pascua — *Dept. of Chemistry, University of Antwerp (U.I.A.), Belgium*
F. Macrì — *Istituto di Geologia Applicata e Geotecnica, Facoltà Ingegneria Politecnico di Bari, Italy*

Abstract

The aim of the study is to investigate the processes of stone weathering on monuments with particular reference to the Mediterranean coastal areas. Two factors are expected to be the main causes of stone weathering in southern Europe: the action of air pollution together with the influence of marine aerosols. The Cathedral of Bari (Italy), located in the central part of the southern coast of Europe, exposed to a marine environment influenced by anthropogenic activity, has been chosen to study the influence of the surrounding environment on the decay of the monument.

1. Introduction

The Cathedral of Bari is situated in the centre of the old city, at a distance of 300 metres from the sea. Since the city has been subjected to a series of foreign dominations, different influences and styles are visible in the cathedral. The building contains elements of a paleo–christian church, the cathedral built at the beginning of the 11th century by Byzantius and his successors, that was largely destroyed, the cathedral which was dedicated in 1292 and the subsequent reworkings and restorations [1].

The cathedral is constructed of limestone and marble. The limestone that is used is named "Calcare di Bari"; the stone contains more than 95% calcite [2]. The limestone shows a medium porosity, ranging from 12 to 20% [3]. The marble has a lower porosity of around 5%.

The phenomena of stone decay belong mainly to the following typologies: corrosion of the exposed surface (alveolization and crumbling), exfoliation, efflorescences, granular disaggregation, detachment, pulverization, fissuring and black crust on the external facade.

2. Sampling

The main part of the samples has been taken at the inside of the cathedral. Two flake samples with a coating layer, have been taken: *BA–1* (flake from a possibly recent block at the north–east of the cathedral) and *BA–2* (flake from a possibly original block at the east of the cathedral). Several efflorescences and powders deriving from the granular disaggregation of the limestone blocks were sampled: *BA–3* (powder from granular disaggregation of the decoration above the arches at the east side), *BA–4* (flake and powdery stone material of a capital under the arch at the south side), *BA–5* (powder from the pulverization of the decoration at the east side), *BA–6* (sub–efflorescence present in a fracture at the north–east side) and *BA–7* (white efflorescence between blocks at the north–east). Two black crust samples have been taken at the north–west side at the outside of the cathedral: *BA–LS* (black crust on limestone) and *BA–M* (black crust on a marble stone).

The total, wet and dry deposition have been collected in the upper part of the cathedral, in the terrace between the dome and the bell–tower. The total deposition is sampled by

means of a funnel, which is connected to a 1L polyethylene collection bottle. Every week a sample has been taken; therefore the funnel is rinsed with 50 mL of deionised water and this rinsing water is added to the collection bottle. 75 samples have been gathered starting from March 1994 till October 1995. The wet and dry deposition have been monitored as well by using a rain water collector, which permits to collect consecutive rain samples during a rain event. This equipment permits to collect the dry deposition by rinsing the collector bucket, which is opened during dry periods, with 50 mL of deionised water, every week. More than 250 rain water samples and 88 dry deposition samples have been collected in the period from October 1993 till October 1995.

Aerosols have been collected by pumping air through two polycarbonate filters (Nuclepore), with a pore size of 2 and 0.4 m, exposed in a filter unit in cascade geometry, at the outside of the cathedral. The volume of air that is pumped through the filters is determined by a gas volume meter. The sampling was started in February 1995 and lasted till November 1995; 22 samples have been collected.

3. Sample preparation and analysis techniques

The soluble salts in the stone are determined after dispersing some crushed powder of the stone in deionised water. The suspension is filtered and the filtrate is analyzed for the ionic content using ion chromatography (IC), atomic absorption and atomic emission spectrometry (AAS/ AES). To apply energy dispersive X–ray fluorescence (EDXRF), about one gram of the stone samples is wet–ground in a McCrone Micronizing Mill. A few millilitres of the suspension is brought on a Mylar foil, which is glued on a Teflon ring, to obtain a sample thickness of around 1 mg/cm^2. The foil is dried in an oven at a temperature of 60°C. To analyze the stone composition in depth, the sample is imbedded in a resin, cut perpendicularly to the weathered crust, and

polished without water. After carbon coating, scanning electron microscopy, coupled with energy dispersive X–ray detection (SEM–EDX) has been applied.

The total volume of the total and wet deposition sample is measured. The total deposition sample is filtered over a Whatman 41 filter. Weighing the filter before and after filtration gives the mass of the total suspended particles (TSP) in the total deposition (the filters are placed in an exsiccator before weighing because the filters are hygroscopic). The pH of the total, wet and dry deposition is measured using a pH electrode, which is calibrated with buffer solution of pH 4 and 7. The HCO_3^- content of the samples is determined by titration. HCl is added to 10 mL of the sample till the colour of the methyl–orange indicator changes from yellow to orange. The anion and cation analyses are carried out using IC/AAS/AES.

The aerosols are first analyzed by EDXRF. After EDXRF analysis, the filters are leached in exactly 25 mL of deionised water. The suspension is filtered and the soluble ions are determined by IC/AAS/ AES.

Ion chromatography (IC) is used for Cl^-, NO_3^- and SO_4^{2-} determinations; a Dionex 4000i instrument, equipped with a AS11 separator column is used; the eluent is 20 mN NaOH. Ca^{2+} and Mg^{2+} are determined by means of AAS, whereas Na^+ and K^+ are measured by AES, both by means of a Perkin Elmer 3030 spectrometer.

A Tracor Spectrace 5000 instrument is used for EDXRF. The instrument is equipped with a Si(Li) detector and a low power X–ray tube with a Rh target, controlled by an IBM computer. The X–ray spectra are accumulated for 3000 sec and analyzed using the AXIL software [4]. The calculation of the concentrations in the stone samples has been checked with soil standards: IAEA Soil 5 and BCR 142. For the aerosol samples the AXIL program calculates the concentration of the elements on the filters in g/m^2. Since the surface of the filter

Table 1   Results of IC/AAS/AES on the leachate samples (weight %)

	Cl⁻	SO_4^{2-}	NO_3^-	Ca^{2+}	Mg^{2+}	Na^+	K^+
BA-1	0.58	0.40	0.18	3.47	0.03	0.31	0.15
BA-2	4.59	2.04	3.81	5.44	0.29	3.07	2.89
BA-3	0.67	0.77	0.17	2.43	0.09	0.60	0.23
BA-4	2.52	27.1	1.48	16.7	0.20	1.98	1.15
BA-5	1.66	1.47	0.19	2.80	1.82	0.31	0.22
BA-LS	0.79	25.2	0.80	15.5	0.06	0.56	0.61
BA-M	0.97	36.1	0.28	19.9	0.10	0.65	0.36

and the volume that has been sampled are determined, the concentrations of the elements can be expressed in ng/m^3.

Micro–analysis has been performed using a JEOL–JSM 6300 Scanning Microscope, equipped with a PGT (Princeton Gamma Tech, Princeton, NJ, USA) energy dispersive X–ray detector system. The samples are excited with an electron beam of 1 nA and an electron energy of 15 keV. By recording energy dispersive X–ray spectra of subsequent small areas, perpendicular to the exposed surface, depth profiles are obtained, showing the elemental distribution through the sample, when proceeding from the outer surface layer towards the unaffected inner part. Concentrations of the elements are calculated without standards, after ZAF–correction and are expressed in weight percent.

4. Analysis of stone samples

Table 1 shows the results of the leaching experiment on the stone samples. Concentrations are expressed as weight percent of the dissolved mass of the sample. The samples do not dissolve very well in deionised water (70 to 90 % of the sample is insoluble in water). Ca^{2+} is the main cation; some Na^+ is present in samples BA–2, 3 and 4. SO_4^{2-} and Cl⁻ are the most important anions. SO_4^{2-} is the main anion in sample BA–4, while Cl⁻ is the major anion in BA–2. In the other samples SO_4^{2-} and Cl⁻ are present in the same concentration.

Aires–Barros [5] observed, contrary to our results, gypsum in sample BA–3, and no gyp-

sum in samples BA–4 and BA–5; this may be due to the small samples, maybe the coating layer, containing gypsum, was removed. In the analyzed samples from the inside of the building, no high sea salt concentrations are observed. The stone samples from outside contain high amounts of SO_4^{2-} and Ca^{2+} (gypsum), and some Cl⁻.

EDXRF analysis shows that calcium is the most important element in all samples. Some

Table 2   Results of EDXRF on the inside samples.

	BA-1	BA-2	BA-3	BA-4	BA-5	BA-6	BA-7
K (ppm)	4490	4750	3300	3070	3420	6780	1.3%
Ca (%)	41	34	39	41	34	37	19
Ti (ppm)	343	357	91	108	199	454	47
Cr (ppm)	53	N.D.	N.D.	N.D.	N.D.	N.D.	N.D.
Mn (ppm)	70	53	60	N.D.	50	98	34
Fe (ppm)	580	1630	492	770	5220	5980	1300
Ni (ppm)	N.D.	N.D.	N.D.	N.D.	7.8	N.D.	N.D.
Cu (ppm)	N.D.	9.6	5.6	11	21	22	7.5
Zn (ppm)	7.3	27	9.9	21	78	89	19
Br (ppm)	N.D.	52	N.D.	5.2	52	16	N.D.
Rb (ppm)	5.1	8.7	5.0	5.4	8.7	20	28
Sr (ppm)	191	161	131	149	161	449	807
Y (ppm)	6.8	4.9	8.0	6.3	4.9	N.D.	N.D.
Zr (ppm)	14	5.6	4.7	3.6	5.6	22	N.D.
Pb (ppm)	20	120	144	46	120	97	N.D.

Fe and K have been found as well. Low–Z elements could not be measured reliably because of the high calcium concentration. The samples from outside were only measured qualitatively, the enrichments in comparison to Ca have been calculated. The crust (black surface) of both samples is enriched in Fe in comparison with the inside (white surface). K is more present in the limestone crust than in the marble crust. Metals, like Pb, Cu, Cr, Ni, are more present in the crust than in the inside of the stone, indicating air pollution influences.

Micro–analysis has been performed on inside samples BA–1 and BA–2 in order to determine the composition in depth (Figures 1 and 2).

The thickness of the crust of BA–1

Table 3   Results of EDXRF analysis on outside samples (ratio of intensities: element to Ca).

	limestone		marble	
---	white surface	black surface	white surface	black surface
K	0.28	2.0	1.4	0.05
Ti	0.009	0.002	0.06	0.01
Fe	0.01	4.8	0.05	0.8
Zn	0.001	0.1	-	0.05
Rb	0.008	0.2	0.01	0.02
Sr	0.07	1.3	0.4	0.3
Y	0.02	0.1	0.04	0.02
Pb	-	0.4	-	0.08
Cr	-	0.07	-	0.005
Ni	-	0.08	-	0.006
Cu	-	0.07	-	0.01
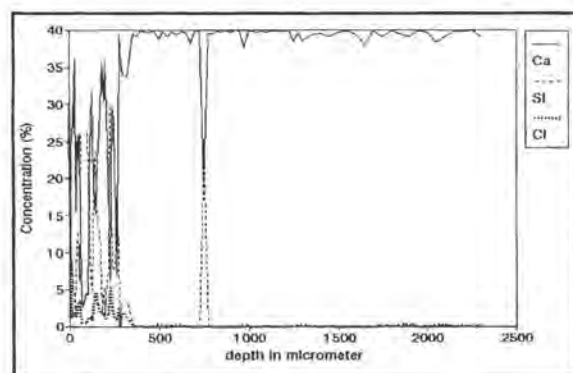
Fig. 1   Depth profile of BA–1

seems to be thicker than the crust from sample BA–2. It is of course difficult to measure the thickness of the crust, because the sections transverse to the crust are difficult to prepare because a portion of the crust may fall during the cutting process [6]. The backscattered electron image of both samples indicates that more pores are present in sample BA–2 and maybe this confirms that this sample comes from an original block, while sample BA–1 comes from a recent block [7].

Depth profiles from the samples of the outside are shown in Figures 3 and 4. In the crust some fly–ash particles are observed, originated from different burning processes. In the crust of the limestone, S is present at a high concentration (10 – 20%) till a depth of

reaches 300 µm; more deeply inside the stone almost only Ca is present. Si and Fe are present at high concentrations: 20 and 10%, respectively. The depth profile of BA–2 shows that the affected side is around 100 µm thick. One peak of K, Si and Al has been found near the surface, probably indicative for a fly–ash particle. Sulphur could not be detected in either of both samples, while the Cl concentration is quite low (a few % in the crust of BA–1). When examining the backscattered electron image of both samples, one could see that sample BA–2 is more porous and seems to be more affected than sample BA–1. Although in the sample description, it has been stated that BA–1 possibly comes from a recent and BA–2 from an original block, the crust in sample BA–1
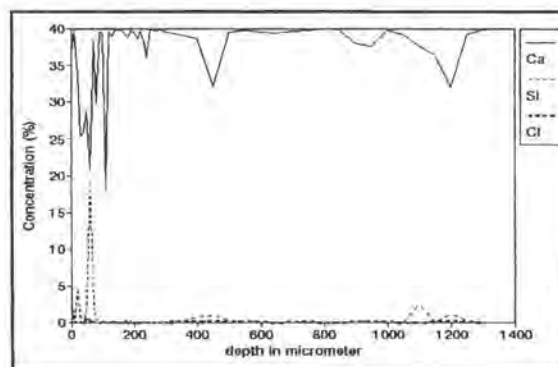
Fig. 2   Depth profile of BA–2

400 µm. Fe is clearly enriched till a depth of 200 µm (3%). Cl is present in the crust till 200 µm at a concentration level of 5%. In the marble crust S is present at the same concentration level as in the limestone, till a depth of 400 µm. Fe is present in the crust with a concentration of 5 10%, also till a depth of 300 µm. Si is more abundant in the crust on marble than on limestone.

The enrichment factors of various elements with respect to sea water have been calculated to identify the component due to the deposition of sea derived elements on the stone surfaces. The following formula has been used [8]:

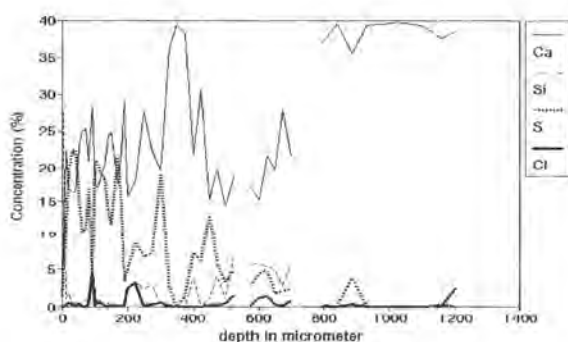$$EF_{sea\ water}(X) = \frac{(X/Na)_{stone}}{(X/Na)_{sea\ water}}$$
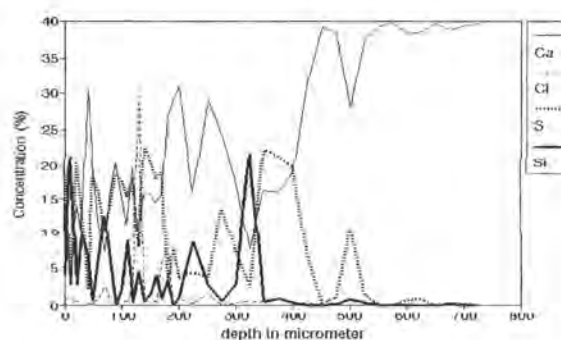
Fig. 3   Depth profile of BA–LS.

Fig. 4   Depth profile of BA–M.

where X and Na are the concentrations of element X and Na, respectively.

The results are summarized in Table 4. SO_4^{2-} and Ca^{2+} are the components with the highest enrichment factors. Ca^{2+} in the crust is of course originated from the underlying carbonate rock, while SO_4^{2-} has mainly been deposited on the surfaces as both gaseous SO_2 and sulphate particles, not originating from the sea. Cl^- seems to originate from the sea at the inside and the outside of the building, while Mg^{2+} at the inside does not seem to correspond with the ratio in sea water. Deposition of sea salt particles does not seem to be the most important source for K^+. At the outside of the building, the weathering layer seems to be caused mainly by anthropogenic emissions (high sulphate concentrations and enriched to sea water), while some influence from the sea is still present (ratio of Cl^-/Na^+ corresponds with sea water). At the inside of the building, however, the chemical analysis of the powders, efflorescences and flakes proves the major influence of sea water in the deterioration process.

5. Total, wet and dry deposition and aerosols

The average ionic balance of the depositions has been calculated. Within the uncertainty ranges, the result indicates that the most abundant ions have been determined.

The weekly average total, wet and dry deposition of the ions were calculated. Results are shown in Table 5. Ca^{2+}, Na^+ and Cl^- are the most abundant ions in the samples. The measured average volume of the wet deposition in Bari is higher than of the total deposition; this may be explained by evaporation processes, which occur less in the rain water collector, because the collector for wet deposition is closed during dry periods. The pH is quite high. This can be due to neutralization by Saharan soil dust [9] or by calcite particles from the monument [10]. Roekens et al. [10] also observed high pH values, together with a high Ca content, in total deposition samples collected near the St. Rombouts cathedral in Mechelen (Belgium). When comparing our results for Bari with those of Alaimo et al. [11] for Palermo, it seems that the concentrations we measured, are a bit lower than the results they observed, except for Ca^{2+} and H^+.

An estimation is made of the contribution of wet and dry deposition for each element (Table 6). This estimation is quite rough, because the dry deposition depends on a variety of meteorological and geographical specific factors [12] and is highly variable from week to week and from element to element [13]. Since the collector in Bari permits to collect the dry

Table 4   Enrichment factors of damage layer vs. sea salt (Na).

	Cl^-	SO_4^{2-}	Ca^{2+}	Mg^{2+}	K^+
BA-1 - BA-5	1.23	17	200	10.7	18.1
BA-LS	0.78	180	790	0.86	31.9
BA-M	0.83	220	880	1.29	16.3

Table 5 *Weekly average total, wet and dry deposition*
(μeq/m²/week) (the volume in L/m²/week)

	Vol	H⁺	Ca²⁺	Mg²⁺	Na⁺	K⁺	HCO₃⁻	Cl⁻	NO₃⁻	SO₄²⁻
total	5.8	1.0	4100	720	2300	260	4000	3100	450	1200
wet	9.9	1.5	3300	710	2700	250	2400	3100	550	1700
dry	–	0.07	1800	260	710	92	590	900	290	410

Table 6 *Estimation of dry and wet deposition (%).*

	H⁺	Ca²⁺	Mg²⁺	Na⁺	K⁺	HCO₃⁻	Cl⁻	NO₃⁻	SO₄²⁻
Wet	96	64	74	79	73	80	78	66	81
Dry	4	36	26	21	27	20	22	34	19

Table 7 *Enrichment factors of*
deposition vs. sea water (Na).

	Cl⁻	K⁺	Ca²⁺	Mg²⁺	SO₄²⁻
total	1.1	5.5	44	1.4	4.3
wet	1.0	4.7	31	1.2	5.4
dry	1.1	6.5	65	1.6	4.7

and wet deposition separately, the relative importance of these depositions could be determined. H⁺ is only caused by wet deposition, while for the other ions the wet deposition is also higher than the dry deposition, but not to such a high extent as H⁺. Smirnioudi and Siskos [14] made comparisons between the wet and dry deposition in Athens (Greece); with the exception of Ca²⁺, they found for all other elements always a larger contribution of the wet deposition than for the dry deposition. In Belgium, to the contrary, the dry and wet deposition equal each other [15], while above the North Sea the wet deposition is twice the dry deposition for heavy metals [16].

When evaluating the deposition for each month separately, it is observed that the deposition of nitrate is highest during summer, while the deposition of sulphate is highest during winter. This high NO₃⁻ deposition is due to the formation of nitrate salts and HNO₃ from nitrogen oxides by photochemical reaction [14]. The peak of sulphate corresponds to higher SO₂ levels during winter. The deposition of Ca²⁺ is quite constant during the year, while the deposition of Na⁺ and Cl⁻ seems to be higher during winter. This may be explained by higher wind velocities.

Similarly to the stone analyses, enrichment factors to sea water have been calculated for the deposition samples (Table 7).

Cl⁻ and Mg²⁺ are mainly derived by the sea, while some fraction of SO₄²⁻ and K⁺ are also originated from the sea, but other sources are present as well for these ions. Ca²⁺ is not originated from the sea; especially the dry deposition seems to be caused mainly by calcite particles from the cathedral.

The relationship between the variables is considered by use of the correlation coefficient. The variables that were included are: the deposited ion amounts, expressed in μeq/m²/week, the volume in L/week and TSP in mg/week. For the total deposition in Bari (Table 8), a correlation has been observed between Ca²⁺ and the volume, TSP is correlated with HCO₃⁻. A high correlation is observed between Na⁺, Mg²⁺ and Cl⁻, the components

Table 8 *Correlation matrix: total deposition.*

	Vol	TSP	H⁺	Ca²⁺	Mg²⁺	Na⁺	K⁺	HCO₃⁻	Cl⁻	NO₃⁻	SO₄²⁻
Vol	1.00										
TSP	0.14	1.00									
H⁺	0.52	-0.05	1.00								
Ca²⁺	**0.74**	0.24	0.32	1.00							
Mg²⁺	0.39	0.62	0.11	0.52	1.00						
Na⁺	0.36	0.63	0.11	0.47	**0.96**	1.00					
K⁺	0.33	0.50	0.08	0.49	**0.77**	**0.75**	1.00				
HCO₃⁻	0.46	**0.78**	0.17	0.53	**0.87**	**0.88**	**0.82**	1.00			
Cl⁻	0.37	0.46	0.08	0.48	**0.94**	**0.90**	**0.73**	**0.73**	1.00		
NO₃⁻	0.12	-0.15	0.03	0.19	0.11	0.09	0.28	-0.02	0.21	1.00	
SO₄²⁻	0.52	0.40	0.12	0.68	**0.82**	**0.76**	**0.75**	**0.77**	**0.89**	0.40	1.00

originating from the sea, while some correlation is observed between HCO_3^-, SO_4^{2-} and K^+. Ca^{2+} is not correlated with any other ion (except slightly with SO_4^{2-}). In the wet deposition of Bari, (Table 9) the volume, H^+ and HCO_3^- are correlated. Mg^{2+}, Na^+ and Cl^- are highly correlated; Ca^{2+} is highly correlated with SO_4^{2-}. Ca^{2+}, K^+, and SO_4^{2-} are also correlated with Mg^{2+}, Na^+ and Cl^-. NO_3^- is correlated with Ca^{2+} and SO_4^{2-}. Table 10 presents the results for the dry deposition in Bari and again a high correlation between Na^+, Mg^{2+} and Cl^- is found. Mg^{2+}, Na^+ and Cl^- are all correlated with SO_4^{2-}. H^+ is negatively correlated with the other ions. Ca^{2+} is only correlated in the wet deposition with SO_4^{2-}, while for the dry and total deposition no high correlation is observed.

Principal component analysis (PCA) has been performed on the total, wet and dry deposition. The results are almost the same for the three deposition types: the first factor is explained by Cl^-, Na^+, Mg^{2+} and by SO_4^{2-} and Ca^{2+}. Two clusters of variables are present in the loading plot, indicating the influence of two different sources: a marine component, together with the effect of anthropogenic emissions [11].

It seems that the wet deposition has, for all compounds under study, a higher contribution to the total deposition than the dry deposition. The deposition of Ca^{2+} is very high, because of the vicinity of the monument. Na^+, Mg^{2+} and Cl^- are mainly caused by the sea, while SO_4^{2-} and K^+ originate from another source. Although the Cl^- concentration is not extremely high, PCA proves the importance of sea derived elements to explain the variance in the data matrix.

Table 9   Correlation matrix: wet deposition.

	Vol	H$^+$	Ca^{2+}	Mg^{2+}	Na$^+$	K$^+$	HCO$_3^-$	Cl$^-$	NO$_3^-$	SO$_4^{2-}$
Vol	1.00									
H$^+$	**0.86**	1.00								
Ca^{2+}	0.35	0.24	1.00							
Mg^{2+}	0.43	0.30	**0.78**	1.00						
Na$^+$	0.50	0.36	**0.73**	**0.98**	1.00					
K$^+$	0.34	0.24	0.68	**0.80**	**0.79**	1.00				
HCO$_3^-$	**0.92**	**0.71**	**0.71**	0.57	0.64	0.58	1.00			
Cl$^-$	0.46	0.32	**0.75**	**0.98**	**0.96**	**0.82**	0.61	1.00		
NO$_3^-$	0.16	0.10	**0.85**	0.50	0.45	0.53	0.22	0.49	1.00	
SO$_4^{2-}$	0.33	0.22	**0.96**	**0.82**	**0.77**	**0.73**	0.59	**0.80**	**0.86**	1.00

Table 10   Correlation matrix: dry deposition

	H$^+$	Ca^{2+}	Mg^{2+}	Na$^+$	K$^+$	HCO$_3^-$	Cl$^-$	NO$_3^-$	SO$_4^{2-}$
H$^+$	1.00								
Ca^{2+}	-0.31	1.00							
Mg^{2+}	-0.18	**0.72**	1.00						
Na$^+$	-0.20	0.52	**0.91**	1.00					
K$^+$	-0.11	0.46	0.43	0.41	1.00				
HCO$_3^-$	-0.17	0.60	0.46	0.21	0.49	1.00			
Cl$^-$	-0.20	0.51	**0.89**	**0.96**	0.47	0.04	1.00		
NO$_3^-$	-0.20	0.50	0.49	0.47	0.34	0.20	0.52	1.00	
SO$_4^{2-}$	-0.18	0.63	**0.80**	**0.82**	0.53	0.25	**0.86**	0.64	1.00

The average aerosol composition is given in Table 11. The concentrations of the 2 m and 0.4 μm pore–size Nuclepore filter are given separately. Ca, SO_4^{2-}, K^+, Cl^- and Na^+ are the most abundant components. The concentrations are lower than the concentrations that Chester [17] obtained for the sea. When comparing the results with the values obtained near a cathedral in Belgium, it is obvious that the Cl^- concentration is higher in Bari, while for the other elements, lower concentrations are observed [18].

Enrichment factors versus sea water, soil dust and anthropogenic emissions have been calculated, using Na, Al and Zn as respective indicator elements. The average soil dust composition was taken from Mason [19], the average anthropogenic emissions were taken from Pacyna [20]. Table 12 presents the result for the coarse and fine fraction separately and for the sum of both fractions. Mg^{2+}, Cl^-, Br and Sr seem to originate mainly from the sea. Schneider [21] also observed that a part of Sr is sea salt derived. In the fine fraction, Ca^{2+} seems to originate from sea water as well, while for the coarse fraction, Ca^{2+} is enriched to sea water. The ratios of Si, Mg^{2+} and Ti to Al, correspond

Table 11   *Average concentration of the aerosol samples (expressed in ng/m^3).*

	NO_3^- IC	Na^+ AES	Mg^{2+} AAS	Al XRF	Si XRF	P XRF	SO_4^{2-} IC	Cl^- IC	K^+ AES	Ca XRF
2 μm	207	164	20	13	50	4.3	526	192	62	207
0.4 μm	29	81	6.3	0.3	1.0	1.6	282	157	53	6.3

	Ti XRF	V XRF	Cr XRF	Mn XRF	Fe XRF	Ni XRF	Cu XRF	Zn XRF	Br XRF	Sr XRF	Pb XRF
2 μm	1.7	0.3	1.7	4.1	45	0.4	1.2	11	1.8	0.6	5.2
0.4 μm	0	0.1	1.1	0.7	4.5	0.2	0.3	1.2	1.9	0.2	2.9

Table 12   *Enrichment factors of aerosols.*

	Na	Mg	Al	Si	SO_4^{2-}	Cl	K	Ca	Ti	Cr	Mn	Ni	Cu	Zn	Br	Sr	Pb
vs. sea water (Na as indicator element)																
2 μm	1	1.03	10^5	1700	13	0.65	11	34			10^4	10^4	1700	10^4	1.8	3.2	10^5
0.4 μm	1	0.65	10^4	70	14	1.1	19	2.1			10^4	10^5	930	10^4	3.9	2.1	10^5
2 + 0.4	1	0.90	10^5	1400	13	0.79	13	29			10^4	10^5	1700	10^4	3.1	3.5	10^5
vs. soil dust (Al as indicator element)																
2 μm	45	5.6	1	1.2	1400	10^4	30	98	2.3	55	31	33	390	1600	2300	14	2100
0.4 μm	820	65	1	0.90	10^4	10^5	930	110	0.0	1300	190	620	3800	1400	10^5	160	10^4
2 + 0.4	54	5.9	1	1.2	2000	10^4	44	98	2.3	89	35	48	480	6000	4700	18	3200
vs. anthropogenic source emissions (Zn as indicator element)																
2 μm										0.64	1.7	0.17	0.56	1			0.31
0.4 μm										3.8	2.4	0.77	1.3	1			1.5
2 + 0.4										1.0	1.7	0.23	0.64	1			0.43

with the ratio in soil dust and indicate the importance of this source. The other elements are enriched to soil dust. The extent to which these elements are enriched varies. For most elements enrichment factors are larger for the small particles than for the large particle fraction, indicating that for these elements soil dust is a more important source for the large particles than for the fine particles. Chester et al. [17] found generally lower enrichment factors to crustal material for aerosols, sampled near the Mediterranean. Pb showed an EF of 500, Zn of 100, Cu and Ni of 15, Fe and Mn around 1 – 2. For our samples the enrichment factors to crustal material are generally 10 times higher. The ratios of Cr, Mn, Ni, Cu and Pb to Zn do not vary a lot from the ratios of average anthropogenic emissions; these elements seem therefore mainly be caused by anthropogenic activities.

The correlation matrix has been calculated for the aerosols and is presented in Table 13. Na^+, Mg^{2+}, Cl^- and Br^- are highly correlated. Correlation is observed between Al and Si and Ca, Ti, V, Fe, Mn and Zn. When looking only at the coarse fraction, almost the same interrelations are found: Na^+, Mg^{2+}, and Cl^- are correlated, but are also related with Ca and Br. Al and Si are correlated with Ca, Ti, V, Mn, Fe, Ni and Zn, the same as for the sum of both fractions. Pb is correlated with the NO_3^- and SO_4^{2-} concentration. For the fine fraction, to the contrary, other correlations are observed. Na^+ and Cl^- are correlated, but no correlation with Mg^{2+} is observed. NO_3^-, SO_4^{2-} and Ca^{2+} are correlated with Mg^{2+}. Al and Si are not correlated, in contrast to the coarse fraction; Si is correlated with SO_4^{2-}, Ca^{2+}, Fe and Sr. Na^+, Mg^{2+} and Cl^- are correlated in the coarse fraction, while in the fine fraction no correlation

Table 13   Correlation matrix for Bari aerosols.

	NO_3^-	Na^+	Mg^{2+}	Al	Si	SO_4^{2-}	Cl^-	K^+	Ca	Ti	V	Cr	Mn	Fe	Ni	Cu	Zn	Br	Sr	Pb
NO_3^-	1.00																			
Na^+	0.42	1.00																		
Mg^{2+}	0.44	**0.82**	1.00																	
Al	0.23	0.19	0.36	1.00																
Si	0.29	0.16	0.37	**0.95**	1.00															
SO_4^{2-}	0.33	0.30	0.57	0.23	0.36	1.00														
Cl^-	0.26	**0.92**	**0.68**	0.11	0.10	0.13	1.00													
K^+	0.45	0.56	0.34	0.54	0.49	0.11	0.48	1.00												
Ca	0.40	0.53	0.65	**0.81**	**0.77**	0.25	0.42	0.45	1.00											
Ti	0.26	0.01	0.24	**0.92**	**0.92**	0.28	-0.07	0.48	**0.66**	1.00										
V	0.34	-0.04	0.20	**0.66**	**0.72**	0.42	-0.12	0.30	0.44	**0.77**	1.00									
Cr	-0.02	0.01	0.15	0.41	0.53	0.58	-0.07	0.00	0.41	0.36	0.39	1.00								
Mn	0.15	0.10	0.21	**0.64**	**0.70**	0.49	0.01	0.15	**0.62**	**0.63**	**0.66**	**0.77**	1.00							
Fe	0.31	0.36	0.49	**0.86**	**0.90**	0.47	0.26	0.43	**0.87**	**0.78**	**0.67**	**0.69**	**0.85**	1.00						
Ni	0.08	0.18	0.23	0.50	0.58	0.32	0.27	0.28	0.40	**0.62**	**0.66**	0.26	**0.64**	0.58	1.00					
Cu	0.38	0.59	0.66	0.54	0.57	0.51	0.47	0.41	**0.79**	0.43	0.33	0.61	0.59	**0.77**	0.34	1.00				
Zn	0.20	0.05	0.28	**0.63**	**0.74**	0.51	0.01	0.04	**0.64**	**0.64**	**0.64**	**0.64**	**0.90**	0.82	**0.68**	0.53	1.00			
Br	0.30	**0.73**	**0.64**	0.17	0.24	0.45	0.70	0.33	0.56	-0.01	-0.03	0.49	0.34	0.51	0.16	**0.79**	0.30	1.00		
Sr	0.06	-0.02	0.23	0.30	0.32	0.42	-0.10	0.03	0.31	0.33	0.21	0.45	0.27	0.32	0.12	0.45	0.23	0.33	1.00	
Pb	0.28	0.19	0.33	0.29	0.42	0.54	0.03	0.31	0.40	0.34	0.32	0.47	0.53	0.49	0.31	0.51	0.57	0.43	0.12	1.00

with Mg^{2+} is present. Al and Si are correlated in the coarse fraction, but not in the fine fraction. Since both elements originate from soil dust, this implies that less small particles originated from soil dust are present.

Principal component analysis (PCA) is a statistical technique to reduce the dimensionality of a large data set, without loosing information. The original correlated variables are transformed into new uncorrelated variables, which are linear combinations of the original data set. Each principal component is composed of the product of a score vector and a loading vector plus an error term. The loading plot shows the correlation between the variables. If a group of variables correlate with each other and reflect the operation of a single process, the variables will be represented as a cluster in the loading plot. Variables that are situated close to the origin of the plot do not contribute to the model. The loading plot of the aerosols is shown in Figure 5.

The first factor explains 32% of the variance in the data set. Ca, Fe, Zn, Si and Al form the first factor: material of terrestrial origin (except Zn), while the second factor consists of sea salt (Na, Cl, Br and negatively Sr). The first four factors explain 62% of the variance. The results can be generalized that the aerosol composition can be explained mainly by a factor, composed of terrestrial elements, while the second, less important factor, is composed of marine elements.
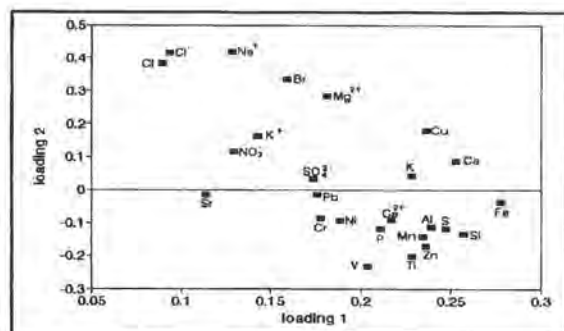
6. Conclusions

The Cathedral of Bari has been studied in relation to the surrounding atmosphere. Stone samples at the inside (flakes and powders) seem to have a chemical composition mainly influenced by the sea. At the outside of the monument black crust samples have been investigated and show the presence of fly ash particles. High sulphate concentrations indicate the influence of anthropogenic activities in the deterioration, together with sea salt. The chemical analysis of the powders from the inside of the building proves the major influence of sea water in their deterioration process.

The composition of the deposition near the monument can mainly be explained by the vicinity of the sea. Sea derived elements are highly abundant (Na^+ and Cl^-), while the deposition is influenced by calcite particles from the monument. The aerosols are composed of elements from terrestrial origin together with some sea derived elements. Especially the coarse fraction (> 2 μm) mainly originates from soil dust. Heavy metals in the aerosols are mostly caused by anthropogenic emissions. Sulphur in the aerosols and deposition originates mainly from the sea. The high sulphate content in the deterioration layer at the outside of the building must therefore be caused by gaseous SO_2.

Fig. 5   Loading plot for the aerosols outside

8. References

1. Zezza F., *The Cathedral of Bari*. 1st Semestrial Report: "Marine spray and polluted atmosphere as factors of damage to monuments in the Mediterranean coastal environment", Ed. Zezza F., R & D Programme in the Field of Environment, Contract No EV5V–CT92–0102, 25–30, 1993.

2. Galan E., *Petrographical study, XRD and chemical analysis of the samples from the Cathedral in Bari*. 2nd Semestrial Report: "Marine spray and polluted atmosphere as factors of damage to monuments in the Mediterranean coastal environment", Ed. Zezza F., R & D Programme in the Field of Environment, Contract No EV5V–CT92–0102, 124–132, 1993.

3. Fitzner B., *Microstructure analysis at limestone and mortar samples from the Bari Cathedral*. 4th Semestrial Report: "Marine spray and polluted atmosphere as factors of damage to monuments in the Mediterranean coastal environment", Ed. Zezza F., R & D Programme in the Field of Environment, Contract No EV5V–CT92–0102, 115–150, 1994.

4. Van Espen P., Janssens K. and Nobels J., AXIL–PC software for the analysis of complex X–ray spectra, Chemometrics and Intelligent Laboratory Systems 1, 109–114, 1986.

5. Aires–Barros L., *Mineropetrography, XRF and IR–spectroscopy of cathedral of Bari and archaeological site of Eleusis*. 3rd Semestrial Report: "Marine spray and polluted atmosphere as factors of damage to monuments in the Mediterranean coastal environment", Ed. Zezza F., R & D Programme in the Field of Environment, Contract No EV5V–CT92–0102, 17–27, 1994.

6. Yerrapragada S., Jaynes J., Chirra S. and Gauri K., *Rate of weathering of marble due to dry deposition of ambient sulfur and nitrogen dioxides*, Anal. Chem. 66, 655–659, 1994.

7. Van Grieken R. and Torfs K., *Cathedral of Bari and archaeological site of Eleusis: chemical analysis and micro-analysis*. 3rd Semestrial Report: "Marine spray and polluted atmosphere as factors of damage to monuments in the Mediterranean coastal environment", Ed. Zezza F., R & D Programme in the Field of Environment, Contract No EV5V–CT92–0102, 52–86, 1994.

8. Sabbioni C., *Contribution of atmospheric deposition to the formation of damage layers*, Sci. Tot. Env. 167, 49–55, 1995.

9. Loye–Pilot M.D., Martin J.M. and Morelli J., *Influence of Saharan dust on the acidity and atmospheric input to the Mediterranean*, Nature 321, 427–428, 1986.

10. Roekens E., Komy Z., Leysen L., Veny P. and Van Grieken R., *Chemistry of precipitation near a limestone building*, Water, Air and Soil Pollution 38, 273–282, 1988.

11. Alaimo R., Deganello S., Di Franci L., Montana G., *Caratteristiche composizionali del particolato solido atmosferico e chimismo delle acque di precipitazione nell'area urbana di Palermo*. Proc. 1st International Symposium on The Conservation of Monuments in the Mediterranean Basin, Ed. F. Zezza, Grafo, Bari, 369–377, 1989.

12. Hansen D.H. and Hidy G.M., *Review of questions regarding rain acidity data*, Atmos. Environ. 25B, 429–434, 1982.

13. Likens G.E., Bormann F.H., Pierce R.S., Eaton J.S. and Munn R.E., *Long–term trends in precipitation chemistry at Hubbard Brook*, New Hampshire, Atmos. Environ. 18, 2641–2647, 1984.

14. Smirnioudi V.N. and Siskos P.A., *Chemical composition of wet and dust deposition in Athens, Greece*, Atmos. Environ. 26B, 483–490, 1992.

15. Vleugels G., *Weathering of bare and treated limestone under filed–exposure conditions in Belgium: study of the runoff water from micro–catchment units*, Ph.D. dissertation, University of Antwerp, 1992.

16. Rojas C., Injuk J., Laane R. and Van Grieken R., *Dry and wet deposition fluxes of Cd, Cu, Pb and Zn into the southern Bight of the North Sea*, Atmos. Environ. 27A, 251–259, 1993.

17. Chester R., Nimmo M., Alarcon M., Saydam C., Murphy K., Sanders G. and Corcoran P., *Defining the chemical character of aerosols from the atmosphere of the Mediterranean Sea and surrounding regions*, Oceanologica Acta 16, 231–246, 1993.

18. Leysen L., Roekens E. and Van Grieken R., *Air–pollution–induced chemical decay of a sandy–limestone cathedral in Belgium*, Sci. Tot. Env. 78, 263–287, 1989.

19. Mason B., Principles of Geochemistry, 3rd Ed., p. 329, J. Wiley & Sons, New York, 1966.

20. Pacyna J., Semb A. and Hanssen J., Emissions and long-range transport of trace elements in Europe, Tellus 36B, 163–1781, 1984.

21. Schneider B., *Source characterization for atmospheric trace metals over Kiel Bight*, Atmos. Environ. 21, 1275–1283, 1987.

Fulvio Zezza
Nuria García Pascua
Fabio Macrì

Microclimate of Bari Cathedral. The influence of outdoor factors in the indoor microenvironment
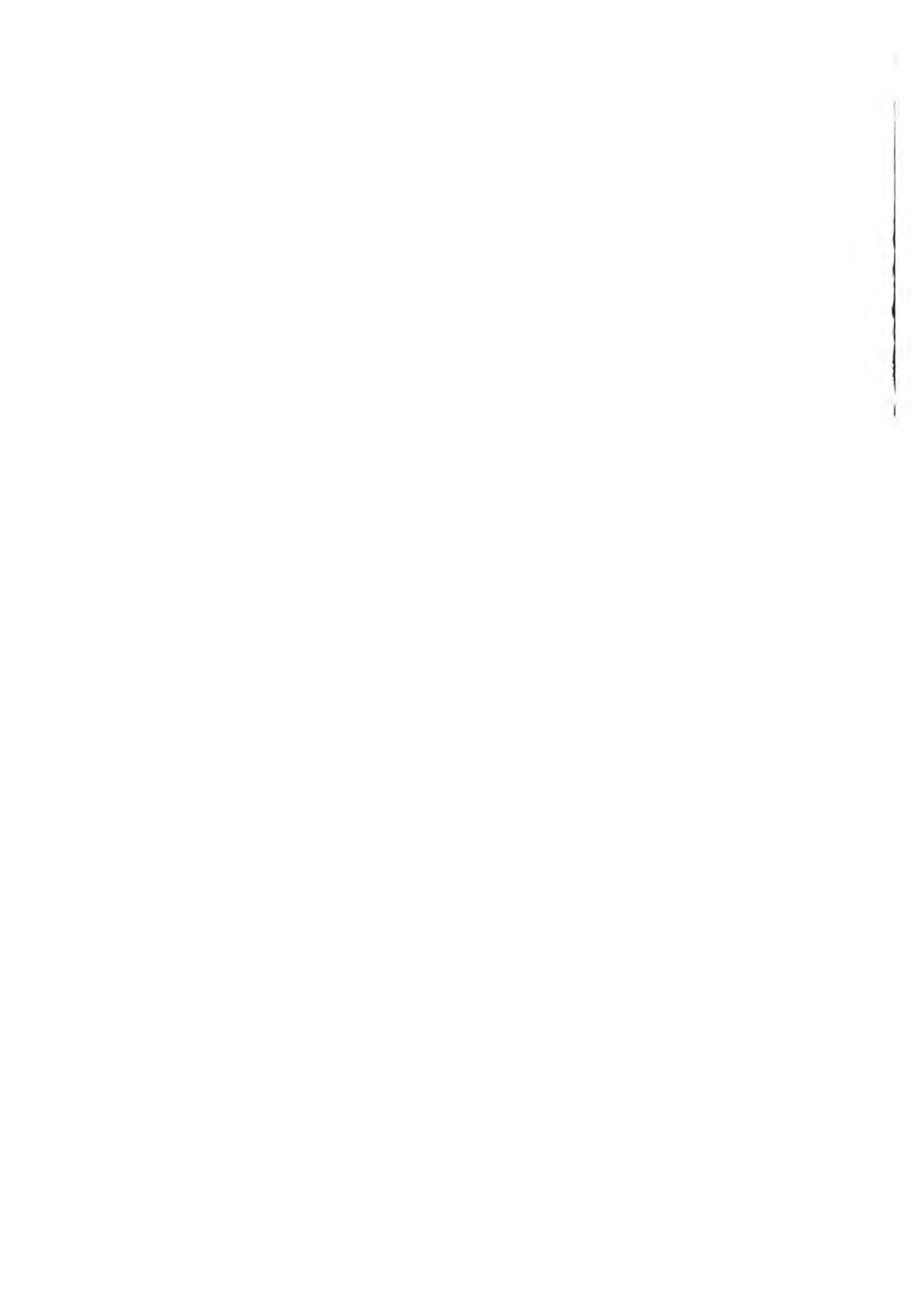
Microclimate of Bari Cathedral. The influence of outdoor factors in the indoor microenvironment

F. Zezza, N. García Pascua, F. Macrì
Istituto di Geologia Applicata e Geotecnica,
Facoltà di Ingegneria, Politecnico di Bari, Italy

1. Introduction

The environmental characteristics to which stone materials are exposed differ greatly from area to area according with the different geographic position, the action of marine aerosol and the level of atmospheric pollution.

The Cathedral of Bari (XII century), entirely built in Cretaceous limestone, is situated in the heart of the old city, at a distance of 300 meters from the sea; the orientation of the main façade is towards the north–west.

To evaluate the influence of the outdoor conditions on the indoor microclimate, strongly conditioned by the marine environment to which the Cathedral is exposed, monitoring has been carried out for a period of three years. The indoor microclimatic phenomena play, in fact, a fundamental role in favouring the conditions which permit the neo-formation soluble salts to crystallize and migrate in the stone material through microcracks and the porous system.

The aim of this work is to outline the thermo–hygrometric conditions present inside the monument which are correlated and influenced by the external environmental parameters.

2. Microenvironmental monitoring

The microenvironmental monitoring station installed inside the Cathedral (Fig. 1) has recorded continuosly (from October 1993 to November 1995) the following thermo–hygrometric parameters:

- *surface stone temperature measured on the internal walls;*

- *air temperature of the film in contact with the stone at the internal and external walls;*

- *air relative humidity of the film in contact with the stone measured at the internal and external walls.*

The indoor environmental monitoring has been completed with the seasonal monitoring (spring, summer, autumn, winter) of the condensation waters, sampled at three different heights in correspondence with the thermo–hygrometric sensors. The positioning of the sensors at different heights (Fig. 2, Tab. 1) along the vertical section of the left nave (where the weathering of the stone due to the humidity is more visible) has allowed, by the elaboration and correlation of the data, the individuation of:

- *thermo–hygrometric stratification of the air in the indoor environment;*

- *evolution in time of the relative humidity, that means the individuation of the frequency of condensation–evaporation conditions which determine the crystallization/dissolution processes of neo–formation soluble salts.*

3. Thermo–hygrometric relations between outdoor and indoor environment

The influence of the external environment parameters on the internal microclimate has been detected through the correlation between the data collected by sensors placed in the Dome and those coming from sensors on the terrace near the Dome. The standard deviation has been used to establish the variations of the
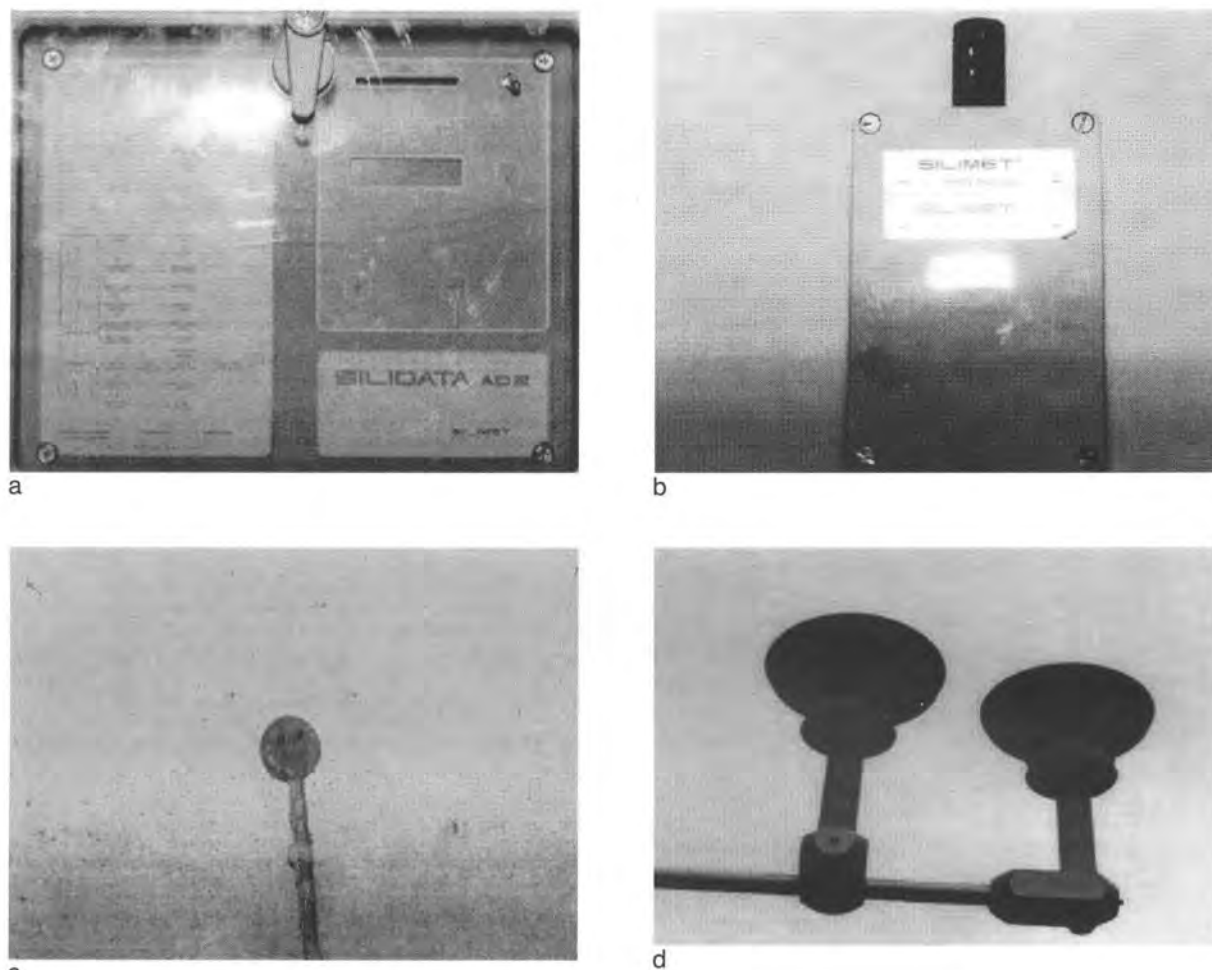
Fig. 1   Microenvironmental Monitoring Station.

a) Remote computing system; b) air temperature and air relative humidity sensor; c) surface stone temperature sensor; d) external air temperature and relative humidity sensors.

air temperature (outdoor/indoor) which directly affect the value of the relative humidity.

The values of this statistic variable has always been higher for the outdoor parameters, so that the increases or decreases of temperature are higher than in the indoor environment. Inside the monument the temperature has a more uniform trend, this means that sudden variation of relative humidity are excluded in the air film close to the stone surface, even if remarkable external variations occur. The higher variations from the standard conditions of indoor air temperature take place during the transition seasons (spring and autumn) when the outdoor temperatures increase or decrease suddenly.

The frequency histograms for the air relative humidity values are relative to each season. The more common values vary between 60% ÷ 70% and 70% ÷ 80% whether outdoor or indoor environment. The comparison of data indicates, in general, good correlations even if in some particular periods (autumn 94 and winter 95) the differences are remarkable. The equilibrium relative humidities of halite (the principal neo–formation salt present in the stone) vary in the range 75.1% ÷ 75.7% of relative humidity with temperatures from 0°C to 30°C; with reference to the recorded data it is that the main periods in which the crystallization conditions of *halite* have been verified are spring 94, summer 94, autumn 94 and
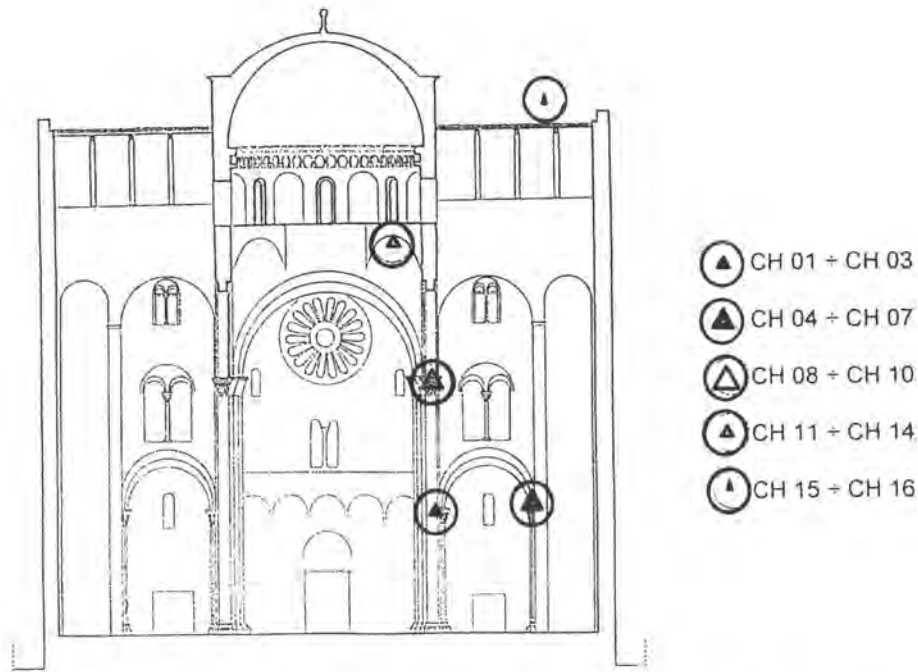
Fig. 2   Positioning of the thermo-hygrometric sensors along the vertical section of Bari Cathedral (see Table 1)

Table 1   Location of thermo-hygrometric sensors along the vertical section of Bari Cathedral

CHANNELS	LOCATION OF SENSORS	HEIGHT
CH 01	Surface stone temperature, capital of 1st order	
CH 02	Air temperature close to the capital of 1st order	8 meters
CH 03	Air relative humidity close to the capital of 1st order	
CH 04	Surface stone temperature, arcade near capital of 1st order	
CH 05	Surface stone temperature, arcade near capital of 1st order	
CH 06	Air temperature close to the arcade near capital of 1st order	8 meters
CH 07	Air relative humidity close to the arcade near capital of 1st order	
CH 08	Surface stone temperature, capital of 2nd order	
CH 09	Air temperature close to the capital of 2nd order	14.5 meters
CH 10	Air relative humidity close to the capital of 2nd order	
CH 11	Surface stone temperature, Dome	
CH 12	Surface stone temperature, Dome	
CH 13	Air temperature, Dome	24 meters
CH 14	Air relative humidity, Dome	
CH 15	External air temperature	30 meters
CH 16	External air relative humidity	

summer 95. Consequently, during autumn 93, winter 94, winter 95 and spring 95 halite is mainly in solution.

4. Thermo–hygrometric stratification of in-door air

The relationship microenvironment/stone decay can be explained taking into account the different distribution of the thermo–hygrometric parameters; weathering forms detected in the stone are not distributed in the same way along the whole section, but they are concentrated in function of the existing microclimate.

The months selected are those which present the most extreme conditions, these are January 94 and August 94; and the hours are: 7 a.m., 12 p.m. and 8 p.m. These selected data are representative of movements of the heat/cold air along the vertical section.

In winter (January 94) there is an intermediate zone (height: 14.5 m) with the highest air temperature values, while the Dome (height: 24 m) represents the coldest zone; this distribution remains constant during the whole day and it is the same for the surface stone temperature. On the contrary, in summer (August 94) the distribution is different because the Dome (24 m) represents the warmest zone (which is directly in contact with the external environment) while the lower part of the Cathedral (8 m) is the coldest.

As regards the air relative humidity (Fig. 3), in both periods (winter and summer) the highest values have been found in the lower part. The lowest values have not been always recorded in the same zone, changing in function of the season and the hour: a) in winter, during the day (7 a.m. and 12 p.m.) the dome is the zone with lowest values, while at night (8 p.m), with the decrease of the temperature, the internal air relative humidity of the Dome increases, so that the lowest zone is the one at 14.5 m; b) in August, both in the day and at night the behaviour is the same and the Dome is the zone with the lowest values of relative humidity.

On the basis of the above considerations, while in winter the values of air relative humidity are higher than 75% along the whole vertical section (*halite* is always in solution) in summer values are lower than 75%, so that *halite* is present in crystalline form.

5. Condensation waters

The sampling of the condensation waters at three different heights (8 m, 14.5 m and 24 m) allows the following considerations to be made about the distribution of the chemical compositions along the vertical section of the Cathedral.

In winter (January 94), proceeding from the lowest zone (8 m) to the highest (Dome, 24 m), the total ionic content progressively increases. In particular, this increase regards both ions of marine origin (Mg^{2+}, Na^+, Cl^-) and ions of anthropic origin (SO_4^{2-}, NO_3^-).

In summer, while for the anthropic ions (SO_4^{2-}, NO_3^-, Ca^{2+}) the highest contents are present in the condensation water of the Dome, the marine ions (Mg^{2+}, Na^+, Cl^-) are the main constituent in the lowest part of the Cathedral.

With particular reference to the variations of the chemical composition of condesation waters in the same zone, the seasonal monitoring (from winter 94 to autumn 95, Fig. 4) shows:

- *During 1994, the highest concentrations of both marine ions (Mg^{2+}, Na^+, Cl^-) and anthropic ions (SO_4^{2-}, NO_3^-, Ca^{2+}) are present in the condensation waters sampled in winter; on the contrary, in summer the concentrations clearly lower; in the transition seasons the concentration values are intermediate (spring higher than autumn). This tendency is more evident in the condensation water sampled in the Dome.*

- *In the course of 1995, the tendency is rather different: in the Dome highest contents of ma-*

WINTER
Air Relative Humidity

Fig. 3

SCALE 1 cm. = 1,045 meters

1994
Dome (heigh: 24 m)

Ca+ Mg++ Na+ K+ HCO3 Cl- SO4 NO3-
- ● Winter 94
- ▲ Spring 94
- ■ Summer 94
- ○ Autumn 94

1995
Dome (heigh: 24 m)

Ca+ Mg++ Na+ K+ HCO3 Cl- SO4 NO3-
- ● Winter 95
- ▲ Spring 95
- ■ Summer 95
- ○ Autumn 95

Capital 2nd order (heigh: 14.5 m)

Ca+ Mg++ Na+ K+ HCO3 Cl- SO4 NO3-
- ● Winter 94
- ▲ Spring 94
- ■ Summer 94
- ○ Autumn 94

Capital 2nd order (heigh: 14.5 m)

Ca+ Mg++ Na+ K+ HCO3 Cl- SO4 NO3-
- ● Winter 95
- ▲ Spring 95
- ■ Summer 95
- ○ Autumn 95

Capital 1st order (heigh: 8 m)

Ca+ Mg++ Na+ K+ HCO3- Cl- SO4-NO3-
- ● Winter 94
- ▲ Spring 94
- ■ Summer 94
- ○ Autumn 94

Capital 1st order (heigh: 8 m)

Ca+ Mg++ Na+ K+ HCO3 Cl- SO4 NO3-
- ● Winter 95
- ▲ Spring 95
- ■ Summer 95
- ○ Autumn 95

Fig. 4

DRY DEPOSITIONS

(SO4--) + (NO3-)

(Na+) + (Mg++)   (Ca++) + (K+)

(Cl-)

● Winter-94 ▲ Spring-94 ■ Summer-94 ○ Autumn 94
● Winter 95 ▲ Spring 95 ■ Summer 95

WET DEPOSITIONS

(SO4--) + (NO3-)

(Na+) + (Mg++)   (Ca++) + (K+)

(Cl-)

● Winter-94 ▲ Spring-94 ■ Summer-94 ○ Autumn 94
● Winter 95 ▲ Spring 95 ■ Summer 95

CONDENSATION WATERS

(SO4--) + (NO3-)

(Na+) + (Mg++)   (Ca++) + (K+)

(Cl-)

● Winter-94 ▲ Spring-94 ■ Summer-94 ○ Autumn 94
● Winter 95 ▲ Spring 95 ■ Summer 95

Fig. 5 Langelier–Ludwig diagrams

rine and anthropic ions characterize the condensation waters of summer, while the lowest correspond to the autumn waters: probably this is put in relation with the fact that in summer 95 a window of the Dome, exposed towards the sea, was continously semi–opened, and a series of thunderstorms have been occured in August. The trends characterizing the chemical composition of condensation waters in lower zones (8 m and 14.5 m) are very different: the highest ionic contents were found in the sample taken in spring; in the other seasons the values, even if they are affected by some variations (i.e. Mg^{2+}), remain in the whole more or less constant.

6. Wet deposition, dry deposition and condensation waters

The relationships between the chemical compositions of wet deposition, dry deposition and condensation waters have been pointed out through the modified Langelier–Ludwig diagrams (Fig. 5). The analysis of the recorded data in the period winter 1994–summer 1995 allows the following considerations:

- *The chemical nature of the wet deposition in winter is generally characterized from the prevalence of chlorides (Mg^{2+}, Na^+) on sulphates (Ca^{2+}, K^+); in summer the main trend is the opposite; in spring and autumn, even if there is a greater dispersion in the anionic contents, the anthropic cations (Ca^{2+}, K^+) are prevalent on the marine cations (Mg^{2+}, Na^+).*

- *As regards the chemical composition of dry depositions, a clear seasonal differentiation is not evident; however, almost always the dry depositions are very poor of marine cations (Mg^{2+}, Na^+).*

- *In the condensation waters, the marine anions (Cl^-) are almost always prevalent on anthropic anions (SO_4^{2-}); the cations, for their part, are principally represented by Ca^{2+} and K^+ (anthropic cations) even if in some spring and summer periods chlorides are mainly represented by NaCl and $MgCl_2$.*

References

1. Zezza F.,(Ed.), 1st Semestral Report: "Marine spray and polluted atmosphere as factors of damage to monumets in the Mediterranean coastal environment". R & D Programme in the Field of Environment. Contract n. EV5V–CT92–0102, June 1993.

2. Zezza F.,(Ed.), 2nd Semestral Report: "Marine spray and polluted atmosphere as factors of damage to monumets in the Mediterranean coastal environment". R & D Programme in the Field of Environment. Contract n. EV5V–CT92–0102, December 1993.

3. Zezza F.,(Ed.), 3rd Semestral Report: "Marine spray and polluted atmosphere as factors of damage to monumets in the Mediterranean coastal environment". R & D Programme in the Field of Environment. Contract n. EV5V–CT92–0102, June 1994.

4. Zezza F.,(Ed.), 4th Semestral Report: "Marine spray and polluted atmosphere as factors of damage to monumets in the Mediterranean coastal environment". R & D Programme in the Field of Environment. Contract n. EV5V–CT92–0102, December 1994.

CONTENTS